UTS UNIVERSITY OF TECHNOLOGY SYDNEY

Generation of genetic and non-genetic risk factor-based mouse models resembling the sporadic human Alzheimer's disease phenotype

by Kiruthika Ganesan

Thesis submitted in fulfilment of the requirements for the degree of

Doctor of Philosophy

under the supervision of Dr. Laura Bradfield
Dr. Peggy Rentsch

University of Technology Sydney
School of Life Sciences

September 2023

Certificate of original authorship:

I, Kiruthika Ganesan declare that this thesis, is submitted in fulfilment of the requirements for the award of the Doctor of Philosophy, in the school of life sciences at the University of Technology Sydney.

This thesis is wholly my own work unless otherwise reference or acknowledged. In addition, I certify that all information sources and literature used are indicated in the thesis.

This document has not been submitted for qualification at any other academic institution.

This research is supported by the Australian Government Research Training Program.

Signature:

Production Note:
Signature removed prior
to publication.

Date: 09/09/2023

Statement of the thesis format:

This thesis is written as a conventional thesis.

Acknowledgments:

This journey has been extremely challenging specifically because of COVID pandemic and CNRM centre shutdown, yet it feels immensely satisfying and rewarding to have finally reached the stage of submission.

Firstly, I would like to start by expressing my sincere gratitude to my primary supervisor, 'The amazing' Dr. Laura Bradfield, for her excellent guidance and mentorship, immense support and encouragement, throughout the tough times of this journey. The intense scientific conversations we had, helped me gain some invaluable insights in the field of behavioural neuroscience. Laura's constructive feedback has improved my research approach, critical thinking and reasoning and has especially helped me refine my writing skills. I would like to take this opportunity to specifically thank her for being a huge moral support during the initial phase of the struggle I faced, soon after shifting our lab to UTS. I feel extremely fortunate to have worked with her in my PhD and her positive influence in my life will always be remembered.

Next, I would like to extend my gratitude to Dr. Bryce Vissel, for identifying the talent in me and supporting my scholarship applications for the PhD program. He has served as a great source of scientific knowledge, and I gained valuable insights on the field of Alzheimer's disease. I extend my sincere thanks to Dr. Peggy Rentsch, my co-supervisor who played a most important role in helping me improve the quality of work during the initial stages of my PhD candidature. A special thanks to her for stimulating scientific thoughts and pushing me to gain a thorough understanding of the research question. I am extremely grateful to Dr. Sujoy Bera, and Dr. Ossama Khalaf from whom I gained a great deal of knowledge and scientific insights.

I would like to extend my thanks to Arvie and Molly for the moral support and for providing a nourishing lab environment to work in. Specifically, I thank Arvie for all his help with the experimental troubleshooting and analysis. A special appreciation and a huge thanks to Molly for helping with all the staining and mounting procedures towards the hectic end-phase of my PhD. It would not have been possible without her help and her contribution is very much appreciated. I would like to thank Nabila, for being there for me through the rough times since the starting of my candidature. All the constant support and motivation from her helped me move forward with my professional/personal life. I sincerely appreciate the time she dedicated to me, despite having a child to attend to. Her immense support will never be forgotten.

Special thanks to my friends Pavithra Suresh and Srivaishnavi Loganathan for being a constant support in every step of my life. I would like to particularly extend my thanks to Pavithra Suresh for being the ultimate source of emotional support throughout my PhD candidature. Her extra efforts to dedicate her valuable time for me, despite being miles away, is greatly appreciated. All the thought-provoking scientific conversations we had were largely helpful in my PhD journey and it would have been impossible to have come so far if not for her continuous support. Warm thanks to Srivaishnavi Loganathan, who constantly motivated me through all the scientific conversations and her huge support. Her encouragement kept me going throughout the PhD journey. The great conversations on various topics ranging from poetry to history and archaeology will always be cherished. The endless late-night conversations about family, books, movies, language, culture and travel kept me alive during hard times. The memorable moments during my trip to Munich will always remain close to heart.

I would like to particularly extend my thanks to Gokulakrishnan Sivakumar, for all the encouragement and support throughout the process of my thesis submission. The valuable and thought-provoking conversations about Tamil language and literature was insightful, contributing to a productive time off lab-work. All the discussions on various perspectives in the field of arts are highly valued and will always be remembered.

Finally, I am indebted to my parents for their immense support all through these years. They had always encouraged me to pursue my dreams and went against all odds to support me in every step of my life. I would like to especially thank them for believing in me this whole time and for standing by me in all the important decisions I made. I am deeply aware of all the sacrifices they have made in their life, purely to put me in a highly fortunate situation. I thank my brother Shiv Ram Kumar for always wishing me the best in whatever I do. All my family members including my aunt, uncle, grandmother, and grandfather have been a huge support all throughout and they will all be remembered forever.

Extended thanks to my friends from India, firstly Lekhangda Bhatnagar, who was with me through every step of my PhD application and helped me with preparing for interviews. All the life lessons learnt from the conversations with her will always be cherished. It would have been difficult to make it to this point without her constant encouragement and she was my greatest strength throughout the whole time.

Finally, a huge thanks to Vigneshwar Senthivel, for travelling with me through every step of life all these years. With his consistent support all throughout these years, I was able to refine my scientific knowledge and life skills. The endless conversations on various aspects of life in both professional and personal life has helped me shape my view of life and it will always be remembered.

Thanks to all my family and friends in Syndey including Manoj, Nirali and Aaliya, and all my well-wishers from Tamil school. Special thanks to Srivarshini Rukmani Krishnan, who served as a great source of support throughout the process of thesis submission. All your contributions are highly regarded.

Contributions to the thesis titled 'Generating genetic and non-genetic risk-factor based mouse models for the sporadic form of Alzheimer's disease':

Alexander Langdon contributed to the Figures 3.8 and 3.11 from Chapter 3 of this thesis. This included, planning and execution of the experiments, data collection, interpretation, and analysis of the obtained data. This contribution is greatly appreciated. Alexander Langdon approved the final version of these two figures and provided consent to use these figures as a part of the thesis.

Production Note:
Signature removed prior to publication.

Alexander Langdon 07/09/2023

Table of Contents:

List of Abbreviations:

AD	Alzheimer's disease
GBD	Global Burden of Dementia
Aβ	Amyloid beta
NFT	Neurofibrillary tangles
APP	Amyloid Precursor Protein
CTF	C-terminal fragment
AICD	APP Intracellular Domain
MAP	Microtubule Associated Protein
PHF	Paired Helical Filaments
PSEN	Presenilin
APOE4	Apolipoprotein E4
TREM2	Triggering Receptor Expressed on Microglia 2
LPS	Lipopolysaccharide
TBI	Traumatic Brain Injury
PAMP	Pathogen Activated Molecular Patterns
DAMP	Damage Associated Molecular Patterns
CNS	Central Nervous System
GFAP	Glial Fibrillary Astrocytic Protein

CA1	Cornu Ammonis
DG	Dentate Gyrus
EC	Entorhinal Cortex
NMDA	N-methyl D-aspartate
AMPA	α-amino-3-hydroxy-5-methyl-4-isoxazolepropionic acid
GABA	γ-aminobutyric acid
LTP	Long-term Potentiation
PSD95	Post-synaptic Density 95
ADL	Activities of Daily Living
MCI	Mild Cognitive Impairment
IADL	Instrumental Activities of Daily Life
PL	Prelimbic Cortex
MD	Mediodorsal Thalamus
pDMS	Posterior dorsomedial striatum
BLA	Basolateral amygdala
IC	Insular cortex
mOFC	medial Orbitofrontal Cortex
NAc	Nucleus Accumbens core
VTA	Ventral Tegmental Area

VStr	Ventral Striatum
DREADDs	Designer Receptors Exclusively Activated by Designer Drugs
CNO	Clozapine N-Oxide

Manuscripts/Publications from this thesis:

Modelling sporadic Alzheimer's disease in mice by combining Apolipoprotein E4 risk gene with environmental risk factors. **(Published in Frontiers in Aging Neuroscience, 27 Feb, 2024)** https://doi.org/10.3389/fnagi.2024.1357405

Hippocampal neuroinflammation causes sex-specific disruptions in instrumental conditioning, Pavlovian approach, and neuronal excitation. **(Published in Biorxiv, 20 May 2024)** https://doi.org/10.1101/2024.05.19.594460 (Submitted to Brain Behaviour and Immunity on 29-05-2024)

Towards the development of a sporadic model of Alzheimer's disease: Comparing pathologies between humanized APP and the familial J20 mouse models. **(Under review, Frontiers in Aging Neuroscience)**

Posters/Oral presentations:

Presented a poster on 'Modelling sporadic Alzheimer's disease in mice with risk factors ApoE4 and neuroinflammation' at FENS (Federation of European Neurosciences Society) at Paris, France, July 9-13, **2022**

Presented a poster on 'Lipopolysaccharide induced neuroinflammation in the dorsal hippocampus accelerates goal-directed action in female mice, facilitates Pavlovian approach in male mice' at SFN (Society for Neuroscience) at San Diego, California, November 12-16, **2022**.

Oral presentation on 'Lipopolysaccharide induced neuroinflammation in the dorsal hippocampus accelerates goal-directed action in female mice, facilitates Pavlovian approach in male mice' at ALG (Australian Learning Group) June 26-28, 2022.

Abstract:

The overall aim of the current thesis was to create a better preclinical mouse model of sporadic Alzheimer's disease (AD). Sporadic AD comprises > 95% of cases but the vast majority of preclinical AD models mimic the heritable, familial form of AD which comprise fewer than 5% of cases, which could be hampering translatability between species. The first half of this thesis employed experiments which examined several genetic and non-genetic risk factors, both individually and in combination, in an attempt to recapitulate the human sporadic AD phenotype. These attempts were largely unsuccessful, because they produced mixed behavioural effects, no evidence of neuroinflammation (i.e. no elevation in various glial cell markers), and only mild changes to dendritic spine density. Lipopolysaccharide-induced neuroinflammation was prioritized for the experiments that followed, and although systemic injections of LPS did not produce the desired cellular changes, intra-hippocampal injections of LPS produced both elevated glial cell expression and dendritic spine loss.

Once intra-hippocampal injections of LPS were established to be a potentially viable model of sporadic AD, the second half of the thesis aimed to improve the translatability of this model from a behavioural perspective, by investigating the consequences of hippocampal neuroinflammation for a behaviour that is crucial to AD diagnosis but has been almost entirely overlooked in preclinical studies: goal-directed action control. In contrast to the results reported in the first half of the thesis, in this section hippocampal neuroinflammation produced clear sex differences. First, and contrary to the expected impairment, LPS treated female mice showed an acceleration of goal-directed learning relative to controls. LPS treated males, on the other hand, did not differ from controls in their goal-directed actions but did display a facilitation of Pavlovian approach behaviour.

Although microglial and astrocytic expression was elevated in the hippocampus as a result of LPS injections in both males and females, it was only associated (positively correlated) with goal-directed control and with neuronal excitation in female mice, suggesting that these changes may have caused the accelerated action control.

Reasons for the divergence in the observed results from the hypotheses are discussed and included the relatively young age of the animals used in the current study (8 weeks to 6 months), the dosage of LPS administered, as well as the specific strains of mice that were used. Despite this divergence, however, two important implications can be drawn from the current study. First, the results are suggestive of a number of important steps that future studies should take to better model Sporadic forms of Alzheimer's, and second, these results provide valuable insights into the sex differences that result from targeted hippocampal neuroinflammation in mice, which is reflective of gender differences in human neurological conditions including Alzheimer's and depressive disorders.

INTRODUCTION
(Chapters 1 and 2)

1. Molecular and Cellular Mechanisms of Alzheimer's disease:

1.1) Alzheimer's disease:

The very first case of AD was identified by Dr. Alois Alzheimer in 1906, in a 56-year-old woman named Auguste Deter. In 1901, Auguste D. started showing symptoms like sleep disturbances, alterations in memory, aggressiveness, and progressive confusion. After her death in 1906, Alzheimer performed histopathological analysis on the autopsied brain tissue and identified abnormal protein aggregations which were later termed as plaques and neurofibrillary tangles. Together with the clinical symptoms, these findings were first reported by Alzheimer in the year 1906 at the Tubingen scientific congress. In 1910, Kraepelin named it 'Alzheimer's disease' in his 'Handbook of Psychiatry' (Hippius & Neundörfer, 2003). In the decades that followed, similar cases were diagnosed all over the world, with an exponential increase of cases in the recent years (study by Li et al, report 147.95% of increase in disease prevalence from 1990-2019 (Li et al., 2022)).

We now know that Alzheimer's disease (AD) is a neurodegenerative disorder, characterized by progressive and irreversible loss of memory and cognitive functions that interfere with the normal lifestyle of the affected individual (Hoogmartens et al., 2021). According to the GBD (Global Burden of Dementia) 2019 statistics, there are nearly 57 million people living with Alzheimer's worldwide, with this number expected to almost triple by 2050. The global VSL (Value of Statistical Life) estimated an economic burden of Alzheimer's disease related dementia as $ 2.8 trillion in 2019, with a projected increase to $ 16.9 trillion in 2050 (Nandi et al., 2022). However, due to its complex etiology, it is difficult to attain a comprehensive understanding of the features of AD, and the

development of effective treatments remains a challenge. As has been widely reported in both scientific and general media, the vast majority of treatments that were considered successful in removing AD's neuropathological features and preventing cognitive decline in mice have failed to translate to successful treatments in humans (Asher & Priefer, 2022; Kim et al., 2022; Yiannopoulou et al., 2019). Such failures have motivated researchers to rethink their methods for preclinical research, and to attempt to modify these methods in a manner that will better capture the real-world conditions of Alzheimer's disease.

It is the overall aim of the current thesis to improve upon the current preclinical models of Alzheimer's disease, with a specific view of replicating the far more frequent (≥95% of cases) sporadic types of Alzheimer's rather than the familial Alzheimer's (which is ≤5% of cases). I will achieve this overall aim through experiments completed under two sub-aims: first by testing a novel transgenic model (with sporadic AD risk factors) in conjunction with neuroinflammation, and second, by testing whether local neuroinflammation is causing the functional deficits in goal-directed action observed in individuals with Alzheimer's disease. I will introduce these two sub-aims in two separate chapters. Specifically, in Chapter 1 (the current chapter) I will review the molecular and cellular mechanisms of Alzheimer's disease, and in Chapter 2 I will review the behavioural phenotypes of Alzheimer's. These introductory chapters are followed by two empirical chapters reporting the results of 7 experiments with a view of providing a more comprehensive preclinical mouse model of Alzheimer's disease and with a long-term hope of providing a more translatable preclinical model for future studies to draw upon.

1.2) Diagnosis and staging of Alzheimer's disease:

After the first identification of Alzheimer's disease in 1906, it took decades of devoted research to properly identify the complex nature of its pathogenesis. In the year 1984, the

National Institute of Neurological and Communicative Disorders and Stroke and the Alzheimer's Disease and Related Disorders Association (NINCDS-ADRDA) proposed a clinical diagnostic criteria introducing categories of 'possible' 'probable' and 'definite' AD (McKhann et al., 1984).

Years later in 2011, the National Institute of Aging and the Alzheimer's Association (NIA-AA) conducted collaborative research that led to publication of a new set of diagnostic guidelines for dementia due to AD (McKhann et al., 2011) Mild Cognitive Impairment due to AD (Albert et al., 2011) and preclinical AD (Sperling et al., 2011). Few years after, in 2018 NIA-AA released a research framework with a major focus on amyloid beta as a core pathological marker for diagnosis of AD (Jack et al., 2018). However, this framework was purely designed for research purposes without much focus on framing it for clinical diagnostic purposes. Therefore in mid-2023, NIA-AA updated these guidelines to be suitable for both research and clinical settings, which is updated on their website currently (*Revised Criteria for Diagnosis and Staging of Alzheimer's Disease: Alzheimer's Association Workgroup*, 2023).

There is a clear distinction between diagnosis and staging criteria. Diagnosis of AD, according to the revised 2023 guidelines are carried out through imaging (such as Positron Emission Tomography (PET)) and Cerebrospinal Fluid (CSF) analysis of biomarkers. In the above-mentioned revised guidelines 2023, there are two core biomarkers proposed (for diagnosis) – Core 1 biomarkers involve - amyloid 162 PET; CSF Aβ42/40, CSF p-tau181/Aβ42, CSF t-tau/Aβ42, which are sufficient to diagnose AD and core 2 biomarkers - tau PET, pT205, MTBR-243, non-phosphorylated tau fragments, all of which cannot be used as standalone diagnostic tests for AD (*Revised Criteria for Diagnosis and Staging of Alzheimer's Disease: Alzheimer's Association Workgroup*, 2023). It is

emphasized that the Core-1 biomarkers are central for AD diagnosis as the disease is existent with the detection of these biomarkers, even though the symptoms appear way later in life. Upon diagnosis of AD, staging becomes relevant by categorising individuals according to the severity of their disease stages. There are typically two types of staging – biological (based on the neuropathological markers) and clinical (based on the cognitive severity of the disease). In this section, I will first discuss the biological staging – including the conventional staging for amyloid beta and tau, and the recent staging described in 2023 guidelines for AD. This will be followed by a discussion of clinical staging which outlines the most familiar methods used to clinically stage AD, followed by details on the clinical staging proposed in the 2023 guidelines.

1.2.1) Biological staging of Alzheimer's disease:

Conventional biological staging relied on post-mortem analyses of AD, the best examples of which are the Thal system of amyloid beta staging proposed by Dietmar R. Thal in (2002) and Braak staging for tau proposed by Braak and Braak (1991). Recent diagnosis of AD relies considerably on the amyloid and Tau-PET along with brain CSF biomarkers.

1.2.1a) Thal staging of amyloid beta:

Deposits of amyloid beta were detected using Campbell-Switzer silver staining and by anti-Aβ immunohistochemistry on post-mortem brains of AD patients. The five different staging are as follows-

Phase 1- This phase is characterized by amyloid deposits in the neocortical regions such as frontal, parietal, temporal and occipital neocortex. At this stage, the Aβ deposits were in the form of diffuse plaques in different neocortical layers – II, III, IV and V. The rest of the brain regions do not show plaque accumulation at this point.

Phase 2- In addition to the Aβ deposits in neocortical regions, during phase 2, Aβ deposits appeared in the entorhinal region, CA1 region of the hippocampus, and the insular cortex. In some other cases Aβ deposits were seen in regions such as amygdala, cingulate cortex, and presubicular region (Thal et al., 2002).

Phase 3- In phase 3, subcortical regions were affected: caudate nucleus, putamen, claustrum, basal forebrain nuclei, substantia innominata, thalamus, and hypothalamus. Aβ deposits were also found in the fascia dentata (molecular layer). In 10-45% of the cases, Aβ deposits were found in the central gray region in the midbrain, superior and the inferior colliculi, CA4 region of the hippocampus, red nucleus and the subthalamic nucleus.

Phase 4- During this phase, Aβ deposits additionally appear in substantia nigra, medulla oblongata (reticular formation) and olivary nucleus. Aβ deposits that were only present in brain regions of 10-45% of the cases mentioned in phase 3 are now present in all cases.

Phase 5- In phase 5, Aβ deposits occured in the following regions (in addition to the regions mentioned in the above phases) – the reteculotegmental nucleus of the pons, the reticular region of the pons, the pontine nuclei, central and dorsal raphe nuclei, the parabrachial nuclei, locus coerulus, and the dorsal tegmental nucleus. The cerebellum appeared to show Aβ deposits in the molecular region (Thal et al., 2002).

1.2.1b) Conventional Braak staging of tau:

In the year 1991, Braak and Braak established 6 different stages of Alzheimer's disease based on the progression of Tau pathology in the postmortem brain tissue of patients (Braak & Braak, 1991). A refined version of this staging was published in the year 2006,

clearly indicating the brain regions harbouring pathological Tau accumulation during each disease stage (Braak et al., 2006), discussed as follows.

Stage-1 – A part of the brain called the transentorhinal cortex was identified to be the earliest region of the cerebral cortex to exhibit tau pathology. Specifically, during Stage 1, this region displayed lesions and tau positive neurons, specifically in the rhinal sulcus region. At this stage, no other brain regions are involved.

Stage-2 – During stage 2, lesions are also visible in the entorhinal cortex region (adjacent to the transentorhinal cortex region). Tau positive neurons also start appearing in the Cornu Ammonis (CA) regions – CA1 and CA2 of the hippocampus, and extending to some neurites in the stratum radiatum and stratum oriens, also in the hippocampus (Braak & Braak, 1991).

Stage-3 – The entorhinal and transentorhinal regions show severe pathology with the temporal neocortex also showing acute lesions. Additionally, lesions from stage-2 become severe during this stage and the hippocampal formation is extensively affected by tau inclusions. The CA1 and CA2 regions contain many tau positive pyramidal neurons, whereas few mossy fibres from CA3 and CA4 region are showing tau deposits.

Stage-4 – Lesions from stage-3 intensified and spread to superior temporal gyrus. The subiculum started exhibiting tau positive neurons and the entorhinal and transentorhinal regions were affected to their maximum capacity. The hippocampal CA3 and CA4 mossy fibres were progressively affected, and the pathology slowly extended to mature neocortex (Braak & Braak, 1991).

Stage-5 – The peristriate region is extensively affected with lesions spreading to specific regions of the frontal, parietal, and occipital neocortex. The parastriate region at this

stage, shows occasional lesions. During this stage, layers I-IV of cortex harbour unevenly distributed tau positive neurons with layer V sparingly affected. The striate cortex/primary visual cortex begin to show signs of tau pathology.

Stage-6 – Almost all layers of neocortex are affected at this stage with the striate area, primary, and secondary neocortical regions showing severe pathology. Regions within the hippocampus (e.g. CA1/CA2, etc) appear almost indistinguishable due to progressing brain atrophy. Additionally, the entirety of the superior temporal gyrus and the transverse gyrus regions appear to be affected at this stage. Overall, the brain shrinks in size due to the cellular atrophy resulting from spreading of pathology and the severity of lesions.

1.2.1c) Biological staging according to the NIA-AA:

According to NIA-AA's revised guidelines 2023, biological staging of Alzheimer's disease is performed predominantly using amyloid and tau-PET imaging. The amyloid-PET staging has been reported to show a certain degree of variability across individuals in different studies (Mattsson et al., 2019; Palmqvist et al., 2017). However, the overall pattern of results displays early accumulation of amyloid-beta in medial neocortical region, followed by striatum, and the medial temporal regions (Enrico et al., 2020; Palmqvist et al., 2017). A 2020 study has highlighted that a specific regional measure of amyloid-PET imaging, instead of global amyloid-PET can predict which individuals with MCI will progress to AD (Pascoal et al., 2020). Another study conducted on >3000 individuals showed that amyloid staging according to region-specific abnormalities paralleled different profiles of cognitive decline in these individuals (Collij et al., 2020). Therefore amyloid-PET staging is observed to be predictive of future cognitive decline than that of progressive cognitive impairment in patients (Therriault et al., 2022).

Compared to the conventional Braak staging that was carried out in post-mortem tissue, tau-PET staging provides a real-time estimate of Tau accumulation in the brain. Additionally, tau-PET Braak staging was found to correspond well with the conventional Braak histopathological staging system (Arthur et al., 2023). Similar to amyloid-PET imaging studies, there were differences in tau accumulation in the literature, however the general pattern of accumulation started in medial temporal lobe in the earliest stages, followed by temporal neocortex, and finally primary sensory cortices (Therriault et al., 2022). Tau-PET Braak staging was found to be associated with various measures of cognitive impairment in AD individuals, highlighting the potential usefulness of this tool as a diagnostic system to help determine the individual's clinical stage (Therriault et al., 2022).

The following stages were proposed in the guidelines: **Stage A/Initial stage** – Individuals with abnormal amyloid PET with no tau PET uptake, which is denoted by (A+T-). **Stage B/Early stage** – Individuals with abnormal amyloid-PET uptake with tau-PET uptake in medial temporal region (A+T_{MTL}+). **Stage C/Intermediate stage** – Individuals with abnormal amyloid-PET uptake with moderate uptake of tau-PET in neocortical region (A+T_{MOD}+). Stage D/Advanced stage - Individuals with abnormal amyloid-PET uptake with high uptake of tau-PET in neocortical region (A+T_{HIGH}+) (*Revised Criteria for Diagnosis and Staging of Alzheimer's Disease: Alzheimer's Association Workgroup*, 2023).

1.2.2) Clinical staging of Alzheimer's disease:

Clinical staging roughly translates to clinical symptoms that occur because of biological changes happening in the individual's brain. This clinical staging would especially be applied to individuals within the AD continuum to rate the severity of the progression of

cognitive decline (Therriault et al., 2022). The following are several scales that are used to stage clinical symptoms of AD.

1.2.2a) Alzheimer's Disease Assessment Scale – Cognitive Subscale (ADAS-Cog):

ADAS-Cog scale was developed in the 1980s and has since been widely used in pharmaceutical trials to determine the cognitive ability of individuals with AD. This assessment scale uses a series of 11 tasks, some of which will be completed by the individuals, and the rest are completed by an observer scoring these individuals. The 11 tasks cover various aspects of cognition such as the recall of words, the ability to listen and act according to a given command, the individual's state of orientation by asking for the specific date and time of the year, their grasp of the spoken language, and their ability to remember details of the task instructions provided. Individuals are scored on a scale of 1-70 where a higher score corresponds to greater cognitive dysfunction (Balsis et al., 2015; Kueper et al., 2018).

1.2.2b) Mini Mental State Examination (MMSE):

Developed by Folstein et al., in 1975, the MMSE is usually employed by clinicians or researchers focusing on cognitive aging to get a quick scoring of cognitive assessments of the subjects. This test consists of a set of 30 questions that assess the individual's ability of attention to details, orientation, the ability to recall certain words mentioned to the individual during the test, to read and understand the instructions and act accordingly, to copy a geometric structure exactly as provided. The individuals will be scored from 0-30, where a low score indicates severe cognitive impairment (Folstein et al., 1975).

1.2.2c) Clinical Dementia Ratio – Sum of Boxes (CDR-SOB):

The Clinical Dementia Ratio scale is a widely used diagnostic scale for individuals with dementia due to Alzheimer's disease. CDR-SOB is an updated version of Clinical Dementia Ratio (scores 0-3) which scores individuals from 0-18 (Yang et al., 2021) on six different domains, some of which overlaps with the above mentioned tests. Domains unique to CDR-SOB involves judgement and problem-solving, community affairs, and activities of daily living scored according to the individual's self-observation and observation by the informants (O'Bryant et al., 2008). The CDR-SOB has known to reliably predict progression from MCI to AD dementia and reversion to normal cognition (Tzeng et al., 2022).

1.2.2d) Clinical staging according to the NIA-AA:

The clinical numerical staging as described by NIA-AA in 2018 (Jack et al., 2018) and revised in 2023 (*Revised Criteria for Diagnosis and Staging of Alzheimer's Disease: Alzheimer's Association Workgroup*, 2023), provides details on the progression of cognitive decline in AD.

Stage 1 (Asymptomatic) – This stage individuals are asymptomatic with only biomarker evidence for AD. As such, there are no reports of cognitive decline or behavioural symptoms occurring at this stage.

Stage 2 (Transitional decline) – Individuals showed a decline of cognitive function from the previous stage. This change from previous level of cognition is observed within 1-3 years of testing, with a persistent decline observed in the most recent six months. According to the revised 2023 guidelines (*Revised Criteria for Diagnosis and Staging of Alzheimer's Disease: Alzheimer's Association Workgroup*, 2023), individuals can be

categorized as being in stage 2, with neurobehavioural symptoms alone (like depression and anxiety), without requiring to display any cognitive changes such as memory decline (according to an addition made in the revised guidelines).

Stage 3 (Cognitive impairment with early signs of functional impairment) – At this stage, performance of cognitive tests is in the impaired/abnormal range, and accompanied by neurobehavioural symptoms. Individual's performances of daily activities are intact, however, there is a notable decline in cognitive performance that results in a delay in completing the daily activities (i.e., taking more time, being less efficient). Nevertheless, individuals manage to complete the task with no assistance from another person (*Figures and tables-Clinical criteria for staging and diagnosis for public comment draft-2*, 2023).

Stage 4 (Dementia with mild functional impairment) – Clear cognitive impairment that appears to progress with time, along with neurobehavioural symptoms. At this stage, cognitive decline affects an individual's ability to perform everyday tasks, and they often require assistance from a caregiver.

Stage 5 (Dementia with moderate functional impairment) - Extensive cognitive and behavioural impairments leading to the necessity of assistance from a caregiver to be able to perform daily activities.

Stage 6 (Dementia with severe functional impairment) – Severe cognitive impairment resulting in an inability to participate in clinical interviews. Individuals are completely dependent on caregivers for very basic activities including self-care (Jack et al., 2018) (*Figures and tables-Clinical criteria for staging and diagnosis for public comment draft-2*, 2023; *Revised Criteria for Diagnosis and Staging of Alzheimer's Disease: Alzheimer's Association Workgroup*, 2023; Souchet et al., 2023).

1.3) Pathological hallmarks of Alzheimer's Disease:

There are two major pathological hallmarks of Alzheimer's disease: extracellular amyloid plaques and intracellular hyperphosphorylated tau tangles. In this section, I will discuss these two hallmark pathologies and their effects in AD.

1.3.1) Amyloid beta peptides – how are they produced?

The human amyloid precursor protein (APP) is highly conserved (Zheng & Koo, 2011)across various species with orthologs in *Drosophila* (Rosen et al., 1989) Zebrafish (Musa et al., 2001) and Xenopus laevis (Okado & Okamoto, 1992). APP is located on chromosome 21 with approximately 639 to 770 amino acids in length (Matsui et al., 2007; Tharp & Sarkar, 2013). This protein contains an extracellular N-terminal domain and an intracellular C-terminal domain. It undergoes cleavage by α, β and γ secretases and follows either amyloidogenic or non-amyloidogenic degradation pathway (Figure 1.1). As shown in the left side of Figure 1.1, the non-amyloidogenic pathway (i.e. the one which does not lead to plaque formation) is initiated by the cleavage of APP protein by α-secretase resulting in a soluble APP-α (sAPPα) fragment and a C-terminal α (CTF-α) fragment. The CTF-α fragment is further cleaved by γ-secretase to yield a small P3 fragment and an APP intracellular C-terminal domain (AICD). The right side of Figure 1.1 shows the amyloidogenic pathway (i.e. that which leads to plaque formation), and it involves cleavage of APP protein by β-secretase which produces a sAPPβ fragment and a CTF-β fragment. This membrane bound CTF-β is then cleaved by γ-secretase to yield either Aβ40 or Aβ42 peptide which is then secreted extracellularly. Out of the two peptides, Aβ42 is considered more neurotoxic, and aggregates readily compared to Aβ40 (Scheuner et al., 1996).

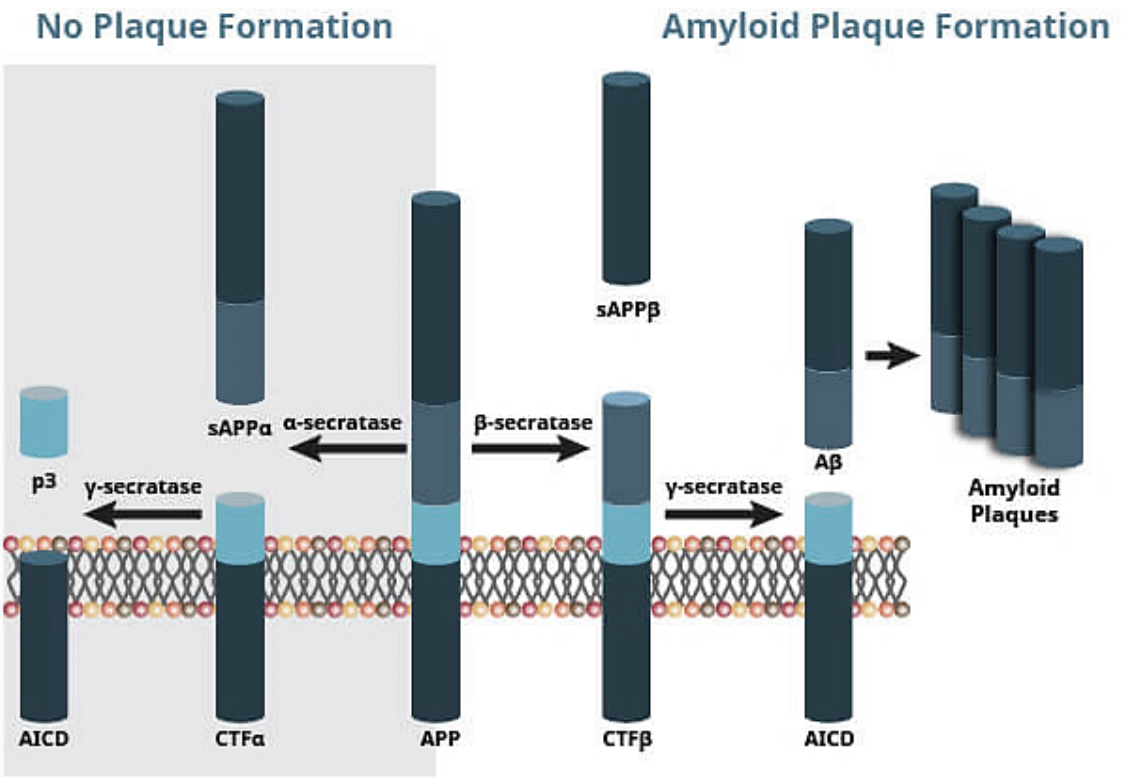

Figure 1.1: *Illustration reproduced courtesy of Cell signalling Technology, Inc. (www.cellsignal.com)*; Non-amyloidogenic (left) and Amyloidogenic (right) pathways of APP gene. Amyloid beta peptide formation as the result of β and γ secretases.

1.3.1a) Toxicity of Amyloid beta:

During the early stages of Alzheimer's disease, amyloid beta produced through the above-mentioned pathway starts aggregating exponentially both within and outside neurons (Sideris et al., 2021). These aggregated amyloid beta peptides are more commonly known as Aβ plaques, which is the first of the two of the hallmarks of AD mentioned above. The soluble form of Aβ, known as the Aβ oligomers were found to be a major cause for the loss of neuronal synapses, which are small protrusions along the dendrites of neurons that facilitate signal transduction within neurons (Crimins et al., 2013; Gauthier-Umaña et al., 2020).

Amyloid beta monomers, other than forming plaques, can accumulate into oligomers (which includes dimers, trimers, tetramers, etc.,) that can interact with receptors in the brain to initiate abnormal downstream signalling (Chen et al., 2017). For instance, Aβ oligomers can cause aberrant neuronal signal transmission by binding to different receptors at the synapse (Xia et al., 2016). Soluble Aβ oligomers were known to inhibit long-term potentiation (Origlia et al., 2008; Townsend et al., 2006) and facilitate long-term depression (Cleary et al., 2005), impairing synaptic plasticity. This is in part due to the altered endocytosis and trafficking of AMPA (α-amino-3-hydroxy-5-methyl-4-isoxazolepropionic acid), NMDA (N-methyl D-aspartate) receptors caused by soluble Aβ (Snyder et al., 2005). Both AMPA and NMDA receptors are crucial to synaptic plasticity and memory function and the imbalance in their recycling caused by Aβ oligomers results in dysfunction of synaptic plasticity.

Aβ has been reported to hamper mitochondrial activity by penetrating the mitochondrial membrane and interfering with the electron transport chain (Tillement et al., 2006). This process has been known to result in excessive reactive oxygen species (ROS) production, leading to oxidative stress (Bobba et al., 2013). However, some studies suggest that oxidative stress is a precursor to Aβ production and accumulation (Arimon et al., 2015; Leuner et al., 2012). It could be possible that Aβ both induces and gets induced by oxidative stress to partly result in neuronal degeneration (Reiss et al., 2018). Another important trigger of cytotoxicity in neurons mediated by Aβ oligomers is the dysfunction of calcium homeostasis. Aβ has been reported to induce pore formation in the membrane, which functions as Ca^{2+} sensitive ion channel, that increases calcium influx (Sepúlveda et al., 2014). In addition to this, Aβ induces calcium release from endoplasmic reticulum, resulting in increased intracellular calcium levels (Ferreiro et al., 2008). Mitochondria sequesters this cytosolic calcium to maintain calcium homeostasis in the cell. This

continuous uptake of increased calcium by mitochondria in turn leads to excessive reactive oxygen species production and apoptosis of neurons (Ferreira et al., 2015).

Aβ oligomers also interact with receptors on the glial cells to activate them and release an array of inflammatory cytokines, thereby triggering neuroinflammation in the brain (Minter et al., 2016). A 2021 study highlighted the role of Aβ in acting synergistically with cytokines to induce inflammatory profile of astrocytes. This is achieved through Aβ acting as a substitute of C1q complement component that induce astrocytic activation as a part of the inflammatory response (LaRocca et al., 2021). This is noteworthy because persistent neuroinflammation has been implicated as a key feature in Alzheimer's disease pathology. In recent years, however, parallel avenues of research emphasizing neuroinflammation-induced Aβ accumulation/toxicity have been emerging, resulting in a shift away from the conventional Aβ-induced neuroinflammation hypothesis (discussed later in the neuroinflammation section).

Outside of the above mentioned pathological events, oligomeric Aβ acts as seeds that are transferred from the affected neurons to healthy neurons via tunnelling nanotubules (TNTs) which are tube-like structures connecting neurons and mediating cell to cell communication, allowing transport of cellular compounds (Khattar et al., 2022). This process leads to the spreading of the infection and amyloid beta pathology (Ollinger et al., 2019). Thus, excessive production and aggregation of amyloid beta protein can prove to be toxic to the brain at multiple levels.

1.3.2) Tau protein and its functions:

Hyperphosphorylated Tau tangles are the second major hallmark of AD. The human Tau protein coding sequence is located on the Tau gene on chromosome 17 (Neve et al., 1986). A single Tau gene encodes for 6 different isoforms of Tau protein which varies slightly in

the composition of the N-terminal region (Goode & Feinstein, 1994). Tau is a phosphoprotein that needs to be phosphorylated at Serine and Threonine sites in order to be functional (as can be seen from figure 1.2, top)(Billingsley & Kincaid, 1997). Specifically, its function arises out of its membership to a class of Microtubule Associated Protein (MAP), that stabilizes microtubules by facilitating the assembly of tubulins into microtubules in the neurons (Weingarten et al., 1975). These microtubules help maintain the structural integrity of the neurons and enable axonal transport of proteins and other organelles from the cell body to the distal ends of the axons (Dehmelt & Halpain, 2005). It is worth noting, however, that despite the centrality of tau tangles to the neuropathology of AD it is beyond the scope of the current study and will not feature in any of the experiments in the current thesis.

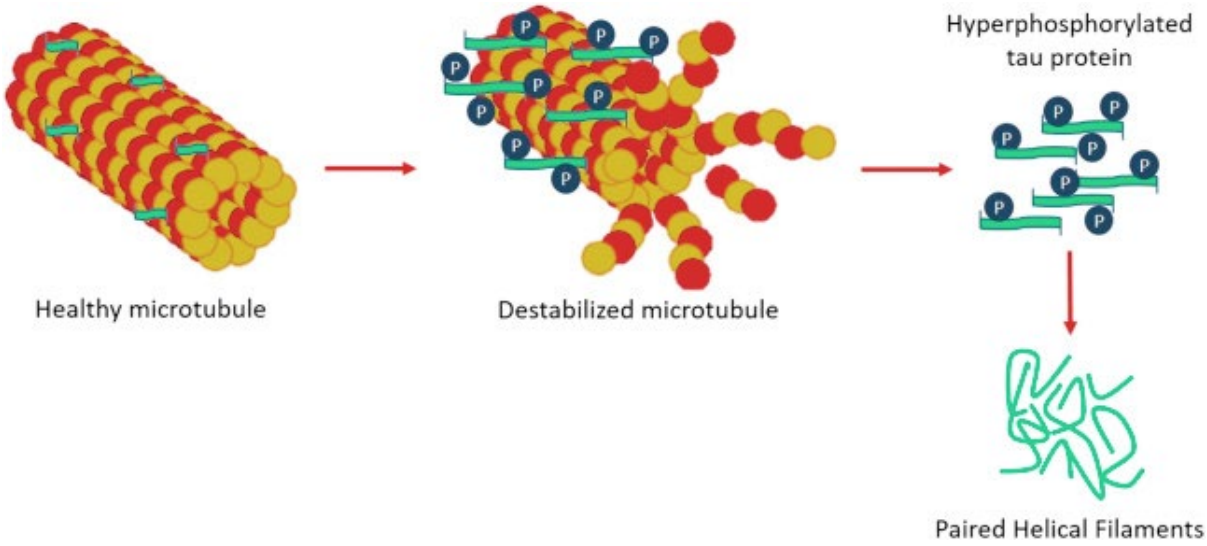

Figure 1.2: Tau hyperphosphorylation(left), Microtubule disassembly & paired helical filament formation(right);*Image adapted from Encyclopaedia of movement disorders, 2010*

1.3.2a) Hyperphosphorylated Tau and Neurofibrillary tangles in Alzheimer's disease:

Under normal conditions, there is minimal and controlled phosphorylation of Tau (Gong & Iqbal, 2008). However, in diseased conditions, Tau proteins are hyperphosphorylated

(excessive, higher than usual phosphorylation), leading to the dissociation of these proteins from the microtubules and forming insoluble aggregates (Goedert & Spillantini, 2017). These aggregates are termed as Paired Helical Filaments (PHF) which then results in Neurofibrillary Tangles formation (as described in Figure 2, right). The hyperphosphorylated Tau then sequesters other Microtubule Associated Proteins (MAP) like MAP1 and MAP2 which causes total microtubule disassembly (Alonso et al., 1997). In Alzheimer's disease, brain autopsy studies identified more than 40 phosphorylation sites on the Tau protein, which is a two-to-three-fold increase compared to the healthy brain (Blennow et al., 1995; Gong et al., 2005). Braak staging, (a method used to classify the progression of pathology in AD), is based on neurofibrillary tangle accumulation in the brain regions starting from entorhinal cortex, spreading to limbic areas and finally to the cortex (Braak et al., 2006).

Similar to Aβ, soluble forms of Tau (either hyperphosphorylated, conformationally changed or oligomeric) are known to be toxic to neurons (Kopeikina et al., 2012). Soluble tau bound to microtubules has been reported to alter the function of dynein and kinesin (i.e. motor proteins that transport cargos such as organelles and synaptic vesicles across the microtubule structure) by reversing the direction of dynein and detaching kinesin from microtubules (Dixit et al., 2008). This affects the distribution of organelles such as mitochondria (Kopeikina et al., 2011) which, in turn, extensively affects synapses because normal synaptic function is dependent on high-energy supplying mitochondria, and their depletion at synapses results in synapse loss (Kopeikina et al., 2011; Sheng & Cai, 2012)

Hyperphosphorylated tau has also been found to alter mitochondrial fission and fusion genes. This occurs because the regulation of mitochondrial size, shape function, and maintenance rely upon genes such as dynamin related protein 1 (Drp1), fission (Fis1) for

mitochondrial fission; and mitofusins 1 and 2 (Mfn1, Mfn2), optic atrophy 1 (Opa1) for mitochondrial fusion (Pérez et al., 2018), and human full-length tau has been shown to increase fusion proteins such as Opa1, Mfn1,2 in rat primary hippocampal neurons (X.-C. Li et al., 2016). Specifically, hyperphosphorylated tau was found to interact with Drp1 to result in mitochondrial fragmentation and disrupted mitochondrial function and neuronal damage in post-mortem AD tissues and 3xTg mouse model (Manczak & Reddy, 2012).

In addition to the above-mentioned intracellular toxicity of Tau, extracellularly released Tau impacts neurons by binding to certain receptors and spreading to adjacent neurons, thereby spreading Tau pathology (Medina & Avila, 2014; Zhang et al., 2021). Although a number of *in vivo* and *in vitro* studies have identified the presence of extracellular Tau (Chai et al., 2012; Kim et al., 2010), the exact mechanism through which tau is released into the extracellular environment is yet to be determined (Nickel & Rabouille, 2009). While the conventional theory states that Tau is released extracellularly following neuronal death (Simón et al., 2012), later studies have reported that neuronal activity can partly result in release of pathological tau while the neuron is still alive, in a calcium dependent manner . Aside from this, tau is also thought to be released when lysosomes carrying tau fuse with plasma membrane, as well as through vesicle mediated exosome release (Saman et al., 2012).

Extracellularly secreted Tau becomes toxic partly due to its abnormal binding to muscarine receptors M1 and M3. Specifically, in neuronal cultures tau has been reported to bind to M1 and M3 receptors in a way that results in the dysregulation of calcium homeostasis through excessive calcium influx, leading to excitotoxicity and neuronal death (Sebastián-Serrano et al., 2018; Wysocka et al., 2020). AD related pathological tau

was found to interact with muscarinic receptors (in cell cultures), causing retraction of neurites and altered neuronal connectivity (Morozova et al., 2019). Extracellular tau has also been shown to be toxic through its binding to microglial cell which stimulates phagocytosis of healthy, living neurons (Pampuscenko et al., 2023). Extracellular oligomeric tau can further impair long term potentiation and result in synaptic dysfunction and memory loss – two key features of Alzheimer's disease (Fá et al., 2016).

Aside from these factors, a major contribution of extracellularly secreted tau to the spread of Tau pathology occurs via template misfolding (Calafate et al., 2016). That is, tau is internalized through endosomes in the extracellular space, which then permeabilizes endosomal membranes to be released within the cell (Calafate et al., 2016), and causes misfolding of (otherwise) healthy tau molecules in that cell. This is one of the crucial mechanisms through which pathological tau spreads from one neuron to another (Brunello et al., 2020).

1.4) Familial and Sporadic AD – Comparison and Contrast:

As mentioned in the introduction, there are two major types of Alzheimer's disease in humans - Familial and sporadic. Clinically, these two types of Alzheimer's are indistinguishable because neuropathological features like excessive accumulation of amyloid-beta plaques and intracellular hyperphosphorylated tau tangles are evident in patients with either type of AD (Nochlin et al., 1993). What does clearly distinguish each type of AD, however, is the source of these pathological changes. That is, whereas the aetiology of Familial AD is highly definite, and patients develop amyloid beta plaques due to the inheritance of specific mutations in their genes, Sporadic AD patients have a multifactorial aetiology involving the interaction of various genetic, epigenetic, environmental and lifestyle factors. Until recently, preclinical mouse models of AD have

exclusively modelled the much rarer (<5% of cases, [22]) Familial form of AD. This also means that treatments developed in mice have been developed to treat the much rarer Familial form of AD and is a potential reason why these treatments fail to translate effectively to the clinic. Therefore, because it is the aim of the current thesis to improve preclinical mouse models of AD, the first sub-aim will do so by investigating a novel model of sporadic AD, with the long-term view that this should lead to more translatability.

In the following section, I will discuss the two major forms of AD in detail, with a focus on the differential manifestation of brain pathologies in these distinct two forms.

1.5) Familial Alzheimer's disease:

Familial Alzheimer's disease is partly caused by autosomal dominant inheritance of mutations in APP (Amyloid Precursor Protein), PSEN1 (Presenilin 1) and PSEN2 (Presenilin 2) genes (Irene Piaceri et al., 2013). Out of these, PS1 has been found to be the gene most predominantly associated with AD, with a higher percentage of Familial AD patients showing PS1 mutations compared to the other two mutations (Kelleher & Shen, 2017). The age of onset for this type of ADis typically within 30 to 60 years (Bekris et al., 2010). Although linkage studies have identified APP, PSEN1 and PSEN2 genes with pathogenic mutations that are fully heritable, there are several other rare variants that are reported to have reduced penetrance within the familial AD cohort.

1.5.1) Highly penetrant APP, PSEN1 and PSEN2 mutations:

1.5.1a) APP mutations:

As mentioned, Amyloid Precursor Protein is cleaved by different secretase enzymes to produce amyloid beta peptides. In Alzheimer's disease, mutations in the APP gene appear to occur either within the secretase cleavage sites or the transmembrane region of this

gene (mostly in exons 16 and 17 which encodes amyloid beta protein) (Bekris et al., 2010), resulting in an altered or increased production of amyloid beta peptides. The first mutation to be identified in the APP gene was the Valine to Isoleucine change at amino acid (aa) 717 (V717I), aka London mutation, in 1991 (Goate et al., 1991). Since then, other common APP mutations have been identified, including Swedish mutations K670N, M671L and Indiana mutation V717F. Today, more than 30 mutations in APP have been identified in Alzheimer's disease (AD mutation database; http://www.molgen.ua.ac.be/ADMutations/).

1.5.1b) PSEN mutations:

Presenilin genes 1 and 2 (PSEN1, PSEN2) are important for the γ-secretase activity as they form a major component of γ-secretase enzyme (specifically, they form the catalytic subunits which is one of the four subunits of γ-secretase enzyme that catalyzes chemical reactions like phosphorylation, oxidation, and so on). PSEN1 and PSEN2 are present on Chromosome 14 and Chromosome 1 respectively and are highly homologous (about 67%) (Li et al., 2000; Irene Piaceri et al., 2013). Gamma-secretase cleavage of APP gene in the amyloidogenic pathway is responsible for excessive production of amyloid-beta peptides.

To date, PSEN1 mutations remain the most common genetic cause of Familial AD and over 200 mutations in this gene have been reported in AD (http://www.molgen.ua.ac.be/ADMutations) (Kabir et al., 2020; Lanoiselée et al., 2017). These mutations are known to alter the Aβ40/Aβ42 ratio which are crucial in terms of determining the aggregation capacity of Aβ peptides – whether they form stable fibrillary aggregates (plaques) or the more toxic oligomeric aggregates (Mucke & Selkoe, 2012). In addition, previous studies have reported that PSEN1 mutations contribute to an

impairment of neurogenesis. For example, the study by Wen et al., used transgenic mice specifically expressing mutant PSEN1 in neurons and observed a decrease in survival rates of neuronal progenitor cells (Wen et al., 2004). Another study conducted on neural progenitor cell cultures with a viral expression of PSEN1 mutation reported a decrease in self-renewal and pre-mature differentiation of these neural cell populations (Veeraraghavalu et al., 2010). Together, these studies suggest that the above mentioned mutations lead to a depletion in the pool of mature neurons to replace the degenerated neurons in the context of AD (Hernández-Sapiéns et al., 2022).

PSEN2 gene has similar functions as that of PSEN1, however, the impact of PSEN2 mutations is less efficient in causing Aβ accumulation when compared to PSEN1 mutations. This was supported by a study conducted on cell lines expressing different PSEN mutations, which observed that PSEN2 mutations are less effective in processing APP, and therefore produced fewer Aβ peptides relative to PSEN1 (Bentahir et al., 2006). Hence, PSEN2 mutations are a rarer cause of familial AD compared to APP and PSEN1 mutations, with only 20 or so mutation sites for PSEN2 identified in AD (http://www.molgen.ua.ac.be/ADMutations) (I. Piaceri et al., 2013).

1.5.2) Reduced penetrant rare mutations:

Although APP, PSEN1 and PSEN2 mutations are highly penetrant, they only account for 5-10% of total Early-onset AD patients. The remaining 90-95% are largely unexplained, leaving room for rare genetic variants with various levels of penetrance (Gaël Nicolas et al., 2016). The following are some of the rare mutations that show lower penetrance (with symptoms being produced only sometimes at a detectable level) in early onset AD.

1.5.2a) Sortilin related receptor 1 (SORL1):

In 2007 (Rogaeva et al., 2007) and later in 2011 (Reitz, Cheng, et al., 2011), common variants of SORL1 were reported to be associated with risk for Alzheimer's disease. Later, rare variants of SORL1 were specifically reported to lead to a five-fold increased risk for Early-onset Alzheimer's (G. Nicolas et al., 2016). A significantly higher percentage of these rare variants were observed to be premature stop codon (PTC) mutations (Gaël Nicolas et al., 2016). Additionally, SORL1 missense variants were shown to possess a 1.5-fold increased risk in Early-onset AD patients (Alvarez-Mora et al., 2022; Verheijen et al., 2016).

SORL1 gene encodes for a protein SorLA, which is a membrane bound receptor. SorLA functions to target proteins to the endosomal/lysosomal system and aids in the process of protein trafficking from Golgi to the membranes (Schmidt et al., 2017). In the context of AD, SorLA plays an important role in APP trafficking and facilitates targeting of Aβ peptides to the lysosomes for degradation, thus reducing Aβ overproduction (Andersen et al., 2005; Caglayan et al., 2014). SORL1 variants are found to confer AD risk by binding to APP with reduced affinity, thereby interfering with proper trafficking of the protein within the cells (Cuccaro et al., 2016).

1.5.2b) ATP-binding cassette, sub-family A, member 7 (ABCA7):

Like SORL1, genome wide association studies have reported the observation of rare ABCA7 variants in ATP-binding cassette in AD patients. ATP-binding cassette functions in transferring small organic molecules, proteins, peptides between different cellular compartments in the cell (Dib et al., 2021). In the brain, ABCA7 has been reported to be expressed in neurons, astrocytes, microglia, Blood Brain Barrier (endothelial cells and pericytes). ABCA7 has been known to regulate immune response, lipid release and trafficking, as well as phagocytosis within the cell (Dib et al., 2021). Premature stop codon

variants in particular were found to be enriched in AD patients, aside from the common missense variants (Dib et al., 2021). Despite these findings, however, studies with ABCA7 are still in their early stages and further research is needed to gain a better understanding of the rare variants and their penetrance (De Roeck et al., 2017).

1.6) Sporadic Alzheimer's disease:

Sporadic Alzheimer's disease has a combination of genetic and environmental triggers. More than 95% of the total AD cases are sporadic, meaning that they are without a definitive cause, leading to an increased difficulty in understanding the disease onset and progression, simultaneously posing a challenge to creating preclinical models and drug treatments (S. Chakrabarti et al., 2015). In this section, I will review few of the crucial genetic and environmental risk factors reported to increase the incidence of Alzheimer's disease starting ApoE4, followed by TREM2, Clusterin and BIN1.

1.6.1) Genetic risk factors of sporadic AD:

Sporadic AD has a few genetic risk factors, such as the presence of ApoE4 allele, specific variants of Triggering Receptor Expressed on Microglia 2 (TREM2) gene, which have been identified through Genome Wide Association Studies. A key difference between the genetic mutations seen in familial AD and the genetic risk factors for sporadic AD is that the former ensures 100% penetrance to the next generation, whereas people with genetic risk factors like ApoE4 may or may not develop the disease. In other words, the presence of a particular mutation on PS1 genes, for example guarantees development of the disease (i.e. the mutation appears to be the cause of the disease), whereas the presence of ApoE4 only increases the risk of getting the disease but does not guarantee it.

ApoE4/E4 appears to be the greatest genetic risk factor for AD, with the presence of two alleles increasing risk of AD by approximately 15 times (Montagne et al., 2021) compared to people carrying ApoE2/E2. Other risk factors identified include TREM2, ADAM10, and PLD3, each of which appear to have a low risk for AD (≤1% of the total AD population) (Gratuze et al., 2018; Nackenoff et al., 2021), although more studies are required to fully understand the nature of these risk factors (Karch & Goate, 2015; Kim et al., 2009).

1.6.1a) Apolipoproteins and ApoE4 – structure and functions:

The Apolipoprotein E (ApoE) family of lipoproteins function as a lipid transporter in the brain (Leduc et al., 2010). Because lipids are hydrophobic, they require lipoproteins to navigate through the aqueous environments (Tulenko & Sumner, 2002), and apolipoproteins form the outer layer of these lipoproteins (as shown in Figure 1.3). Apolipoproteins facilitate the transport of cholesterol from astrocytes to neurons for maintenance. This is critical because neurons are in constant need for cholesterol to maintain homeostasis and function, making them largely dependent on astrocytes for their cholesterol requirements (Poirier et al., 1993).

In humans, there are three different isoforms of ApoE – E2, E3 and E4, however, only ApoE4 has been associated with AD risk. This is due to some inherent differences among the ApoE isoforms that underlie the pathological properties of ApoE4. One such difference is that ApoE4 carriers have overall decreased concentrations of ApoE in the brain compared to other isoform carriers, leading to less effective functioning of ApoE (Martínez-Morillo et al., 2014).

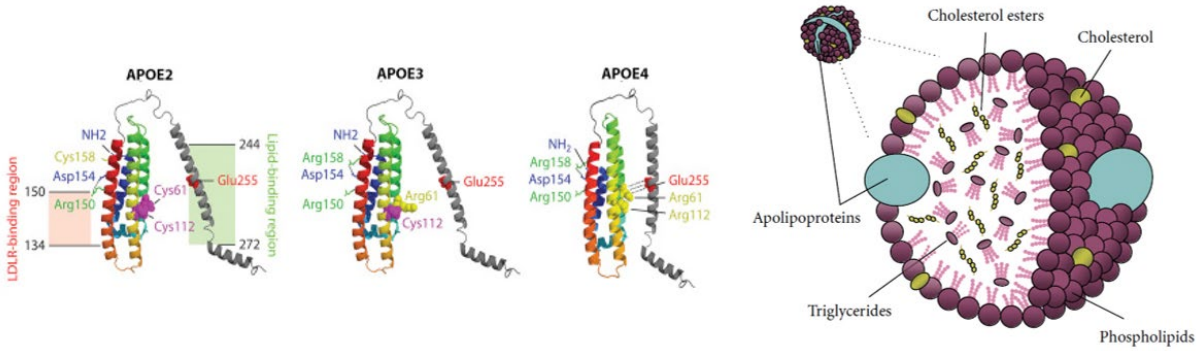

Figure 1.3: Different isoforms of ApoE (left). ApoE location on the outer lipoprotein layer (right); *Image adapted from Belloy et al., 2019; Leduc et al., 2011*.

1.6.1b) ApoE4 – altered functions:

There are several potential pathways that have been suggested by which ApoE4 increases the risk of AD. They are as follows:

Altered Aβ metabolism: The most widely accepted mechanism through which ApoE4 has been suggested to exert changes in AD is by altering Aβ metabolism in the brain. Huynh et al., (2017) in his study reported that aggregation and deposition of Aβ is increased in the presence of ApoE4, in a transgenic mouse model with simultaneous decrease in Aβ clearance. Additionally, Tai et al., (2013) observed that oligomeric Aβ levels were higher in AD transgenic mouse brain, human synaptosomes and cerebrospinal fluid by performing ELISA (Enzyme Linked Immunosorbent Assay).

Altered Lipid metabolism: ApoE4 induced cholesterol and phospholipid dysregulation in the brain highlights the role played by ApoE4 in lipid metabolism (Zhu et al., 2015). That is, ApoE4 is shown to be less effective than other isoforms in inducing cholesterol outflow/efflux, thus causing disturbances in the cholesterol levels in brain (Leduc et al., 2010; Safieh et al., 2019) resulting in increased cholesterol levels in the CNS, which is one of the risk factors associated with Alzheimer's disease (Shepardson et al., 2011; M. Wu et

al., 2022). In addition to this, abnormal cholesterol levels have been found to exert negative effects on amyloid beta aggregation and immune cell responses, thus indirectly contributing to AD progression (Feringa & van der Kant, 2021).

Alteration of neuronal integrity: ApoE4 has been found to hinder neuronal outgrowth through microtubule disassembly, thereby affecting neuronal structure and stability (Nathan et al., 1995). Neuronal expression of ApoE4 has been reported to cause axonal degeneration and disrupt axonal transport in transgenic mice expressing ApoE4, which would hinder communication between neurons (Tesseur et al., 2000). Additionally, neuronal ApoE4 has been shown to alter neural gene networks that are vital for synaptic activity and calcium signalling (Brian et al., 2022). ApoE4 has also been reported to downregulate the expression of insulin receptor, and growth factor receptors which are important for the normal functioning of neurons (Salomon-Zimri et al., 2016; N. Zhao et al., 2017). Together, therefore, these alterations can cause disturbances in the neuronal activity and cause dysfunction of the neurons.

Alteration of immune response: Epidemiological studies and human trials revealed that ApoE4 carriers express more pronounced neuroinflammation compared to the other isoform carriers (Gorelick, 2010; Reale et al., 2012). It has also been reported that neuroinflammation is more prolonged in ApoE4 mice after stimulation with any type of inflammatory triggers (Ophir et al., 2005; Passamonti et al., 2019). For example, in the study by Passamonti et al., ApoE4 mice were given intracerebroventricular Liposaccharide (LPS) injections and checked for elevation of inflammatory markers 5, 10 and 24 hours after injections. Microarray results revealed that there were elevated levels of inflammatory markers in ApoE4 mice at 10 and 24 hours timepoint compared to controls (Ophir et al., 2005). As will be reviewed in detail below, persistent

neuroinflammation causes damage to brain cells and contributes to cognitive decline as witnessed both in humans (Passamonti et al., 2019) and animal models (Luo et al., 2019) of Alzheimer's disease.

Other deleterious effects of ApoE4: In addition, the effect of ApoE4 has been constantly associated with Tau hyperphosphorylation which is a major hallmark of Alzheimer's disease. It has been found that neuronal ApoE4 directly interacts with cytoplasmic tau to induce hyperphosphorylation, eventually resulting in the formation of Neurofibrillary tangles (Harris et al., 2004). Moreover, ApoE4 disturbs mitochondrial homeostasis, leading to mitochondrial dysfunction in AD (Pires & Rego, 2023), via downregulation of the expression levels of mitochondrial respiratory complexes I, IV and V. ApoE4 contributes to Blood Brain Barrier disruption by accelerating pericytes degeneration in the brain as evident from human AD postmortem studies (Halliday et al., 2016). Therefore, ApoE4 exerts its role on multiple pathways related to AD thereby playing a predominant role as the major genetic risk factor for AD (Huang & Mahley, 2014).

1.6.1c) Triggering receptor expressed on myeloid cells 2 (TREM2) ligand and its functions:

TREM2 belongs to a family of cell surface receptors that are mostly expressed in dendritic cells, granulocytes and certain tissue-specific macrophages like osteoclasts and Kupffer cells (Gonçalves et al., 2013; Humphrey et al., 2009). In the brain, TREM2 is exclusively expressed in microglia (Forabosco et al., 2013; Neumann & Takahashi, 2007). Nevertheless, there seems to be an uncertainty regarding whether their expression is found on all or only on a particular subgroup of microglia (Schmid et al., 2002). TREM2 expressing microglia has a varied distribution in the brain with certain regions like

hippocampus, spinal cord, and the white matter showing relatively higher expression compared to other brain regions (Forabosco et al., 2013).

TREM2 has been reported to modulate the survival and proliferation of different cell types such as myeloid cells (including microglia) and dendritic cells (Saber et al., 2016). Several *in-vivo* and *in-vitro* studies have highlighted the requirement of TREM2 for microglial survival and proliferation (discussed in detail in the next section) (Masahito et al., 2015; Seno et al., 2009; Wang et al., 2016). Activation of TREM2 was shown to increase dendritic cell survival via the Extracellular-signal regulated kinase (ERK) pathway (Bouchon et al., 2001). Another prominent function of TREM2 is its regulation of neuroinflammatory signalling pathways. In primary cell cultures, for example, knockdown of TREM2 has been shown to shift the balance of inflammatory cytokines resulting in an ineffective clearance of apoptotic neurons (Takahashi et al., 2005). The modulation of cytokine profiles by TREM2 thus plays a key role in determining the phagocytic properties of microglia (Masahito et al., 2015).

TREM2 and microglia: Apart from influencing the phagocytic properties of microglia, TREM2 tightly controls the metabolism of these glial cells. A 2017 study revealed that microglia from TREM2 deficient mice show unusually low levels of ATP, glycolysis, and anabolic metabolism. These microglia were also seen to accumulate abnormal levels of autophagic vesicles, indicating a compromised energy metabolism (Ulland et al., 2017). Such metabolic disturbances in the absence of TREM2 expression in microglia is suggestive of its trophic support to microglia in extreme stressful conditions (Salter & Stevens, 2017). Interestingly, in a subset of microglia, TREM2 triggers an activation of neurodegenerative signalling through interaction with the APOE pathway, resulting in a loss of homeostatic function of microglia (Krasemann et al., 2017). With regards to the

plaque associated properties of microglia, a decrease in TREM2 has always been shown to impair the effectiveness of microglial cells in clearing the plaques in-vivo (Jay et al., 2015; Y. Wang et al., 2015b). This is mainly due to the inability of the TREM2 deficient microglia to be recruited to cluster around the plaques, for successive clearance (Y. Wang et al., 2015b; Yuan et al., 2016).

TREM2 and Aβ load: Variations in amyloid beta accumulation with regards to TREM2 results from microglial mediated phagocytosis as described in the previous section (Kleinberger et al., 2014). In-vitro studies add weight to this hypothesis as TREM2 expression increases microglial uptake of Aβ (Jiang et al., 2014). However, in-vivo studies provide mixed evidence regarding the TREM2 mediated clearance/uptake. For instance, the APPPS1-21 AD mouse model with a total deletion of TREM2 had decreased Aβ accumulation in the cortex at 3 months of age but an increased plaque load at 8 months of age,(Jay et al., 2017), whereas results from Wang et al.'s (2015) study of 5xFAD animals with TREM2 deletion reported an increase in amyloid plaques in the hippocampus but not cortical regions at the age of 8.5 months. Therefore, further studies and appropriate mouse models are required to fully understand the altered functions of TREM2 with regards to amyloid burden in-vivo.

TREM2 and Tau pathology: Although there are fewer studies linking TREM2 and tau than those exploring TREM2-Aβ interactions, the literature that is available does suggest a TREM2-tau pathology link. For example, a study conducted by Wang et al., (2015a) on a cohort of human AD patients reported a positive correlation of TREM2 mRNA levels with tau pathology specifically in the hippocampal region. Another study examined the cerebrospinal fluid of AD patients and found that soluble TREM2 positively correlated with total and phosphorylated tau in AD patients compared to control cohort (Piccio et

al., 2016). In contrast, silencing TREM2 in the brain resulted in an abnormal increase of tau pathology eventually leading to neurodegeneration and spatial learning deficits in a tau transgenic model (Jiang et al., 2018). Although these studies indicate a link, it is unclear what direction the association is in, therefore further studies are required to clarify these associations.

1.6.1d) TREM2 variants in Alzheimer's disease: Genome wide association studies have identified several rare variants of TREM2 that increase the risk of late onset AD by 2-4 fold (Gratuze et al., 2018; Guerreiro et al., 2013; Jonsson et al., 2013). Among them, the most well-studied and strongly associated variant is the R47H TREM2 variant, as confirmed through direct genotyping in a cohort of 1887 AD and 4061 control patients (Guerreiro et al., 2013). Despite its prevalence in AD, however, the R47H variant of TREM2 has be reported to be population specific: mostly limited to the Caucasian population (Murcia et al., 2013). Variants other than R47H, such as R62H, D87N, T96K, L211P and R136Q were also found to be associated with late-onset AD (Guerreiro et al., 2012). Most of the TREM2 variants appear to alter the ligand binding properties of TREM2 – R47H and R62H variants modify the phagocytic properties of TREM2 in-vitro (Kleinberger et al., 2014). In AD patients, R47H TREM2 variants were associated with higher levels of total tau and phosphorylated tau in the CSF compared to control cohorts (Cruchaga et al., 2013). Additionally, another human study reported an increase in axonal dystrophy around amyloid plaques in humans carrying R47H TREM2 variant (Yuan et al., 2016).

1.6.1e) Clusterin (CLU): Clusterin has been reported to be the third most significant risk factor for late-onset AD (Yuste-Checa et al., 2022). Clusterin shares similarities with APOJ, and is predominantly expressed in astrocytes (Foster et al., 2019). Unlike APOE4 which is heavily involved in the lipid metabolism of the brain, clusterin is known to play a notable

role at synapses (particularly excitatory synapses) (Chen et al., 2021; Fu & Ip, 2023). Two extensive genome wide association studies identified 3 important CLU variants – rs11136000, rs93318888, rs2279590 associated with AD risk. Out of these, rs11136000 was considered to be the major variant that increases susceptibility to AD (Lambert et al., 2009). In particular, exacerbated brain atrophy and greater conversion rates from MCI-AD was observed in patients with MCI carrying this variant (Carrasquillo et al., 2015). Like the R47H TREM2 variant, rs11136000 was also reported to exert these effects preferentially in the Caucasian population compared to the Asian population. This could mean that there are other, as-yet unknown variants that confer AD risk in the non-Caucasian population, and further studies are needed to determine if this is the case (Foster et al., 2019).

1.6.1f) Bridging Indicator 1 (BIN1): BIN1, also known as amphiphysin II, functions to regulate membrane dynamics, mediate protein trafficking, and facilitate endocytosis. It is also reported to play an overall important role in pre-synaptic neurotransmitter release and memory consolidation (De Rossi et al., 2020). Aside from the pre-synaptic function of BIN1, accumulating evidence suggest a role for BIN1 in cytoskeleton dynamics and therefore an interaction with Tau protein. Specifically, the BIN1 variant rs744373 is reported to confer AD risk by increasing tau loads, leading to cognitive decline (Franzmeier et al., 2019). Another recent human study pointed out how the rs744373 variant induced faster tau accumulation in the presence of amyloid beta (Franzmeier et al., 2022). Other than the rs744373 variant, p.K858R has also been shown to be associated with later-onset AD, but again, only in a specific population (Caribbean Hispanics) (Vardarajan et al., 2015).

In addition to the variants mentioned in this section, several others have been found to be associated with AD risk at various levels, with a few of them showing population specific inheritance of AD, such as Unc-5 homolog C (UNC5C) A Kinase Anchor Protein 9 (AKAP9) (Cacace et al., 2016; Hoogmartens et al., 2021).

1.6.2) Environmental risk factors of sporadic AD:

Non-genetic or environmental risk factors contribute to almost 30% of sporadic Alzheimer's disease, most of which are modifiable. According to a 2015 study, lifestyle risk factors like excessive smoking, alcohol consumption is reported to increase Alzheimer's risk by about 40% (Zhong et al., 2015). AD risk is also significantly increased with diabetes and obesity, with each contributing independently to the susceptibility of the disease (Profenno et al., 2010). Another risk factor highlighted in multiple studies is the elevated blood pressure levels, especially in midlife (Shah et al., 2012) compared to late life (Fotuhi et al., 2009; Launer, 2005; Qiu et al., 2005). There are also numerous evidence in the literature suggesting heavy metal exposure is a risk factor for Alzheimer's disease (F. Liu et al., 2022; L. Wang et al., 2020). Lead, cadmium and manganese are a few examples of metal ion neurotoxicant associated with AD pathology (Kelly M. Bakulski et al., 2020). Traumatic Brain Injury (TBI), which comprises damage to the brain via an external mechanical force of any kind, or an internal penetration of the skull and brain, has also been extensively linked with Alzheimer's Disease (Lye & Shores, 2000; Srinivasan & Brafman, 2022). Although there is no direct mechanism by which TBI results in AD, it is believed that in certain cases, TBI is followed by cognitive decline, which in the later stages of life, can develop into Alzheimer's dementia (Graham et al., 2022; W. Li et al., 2016).

A recent meta-analysis study revealed that people with insomnia are at a greater risk of developing Alzheimer's disease (Chappel-Farley et al., 2020; Sadeghmousavi et al., 2020; Shi et al., 2018). Insomnia is tightly linked with mental health disorders and people experiencing mental health issues have increased risk of developing AD. For instance, apathy, anxiety and depression are all associated with AD risk. Longitudinal studies conducted on AD patients and healthy controls have identified anxiety independently (Santabárbara et al., 2019) and in association with depression and sleep disturbances as potential risk factors for AD (Burke et al., 2018). Depression has been vastly explored in its association with AD since the early 90s (Förstl et al., 1992). Studies report that depression is one of the major predictors of progression from Mild Cognitive Impairment to Alzheimer's dementia (Palmer et al., 2010; Van der Mussele et al., 2014). As a neuropsychiatric symptom, depression continues to persist in up to 50% of patients with AD, causing increased burden to the caregivers (Chi et al., 2014; Zhao et al., 2016).

Based on the studies outlined above, it is clear that there is a diverse range of environmental risk factors for AD that, on a superficial level, appear to have little in common. One commonality they all share, however, is that in all the above-mentioned conditions, neuroinflammation appears to play an inevitable role. In the following section, I will review the process of neuroinflammation, how it's modulated by immune cells in the brain, and its predominant role in the pathology of Alzheimer's disease.

1.7) Neuroinflammation – A Key player in Alzheimer's disease:

As mentioned, neuroinflammation plays a prominent role in all the risk factors associated with Alzheimer's disease. In the context of AD, neuroinflammation is triggered through multiple pathways and has deleterious consequences for the progression of AD.

1.7.1) Neuroinflammation – An essential immune response in the brain:

Maintaining homeostasis in the brain is crucial to its normal functioning, and microglia and other immune cells help maintain homeostasis by constantly surveilling for any disturbances caused from within and outside Central Nervous System (as shown in Figure 1.4). For example, neurons undergo apoptosis (i.e. cell death) as a part of the normal developmental process, and the cellular debris is cleared from brain through the activation of inflammatory pathway (Sierra et al., 2010). In addition, external stimuli such as pathogens need to be eliminated from the brain and triggering the inflammatory response aids in the process of protecting the brain from such infections (Püntener et al., 2012). In the absence of such a response, neurons would not be able to function normally and would suffer damage, possibly even death.

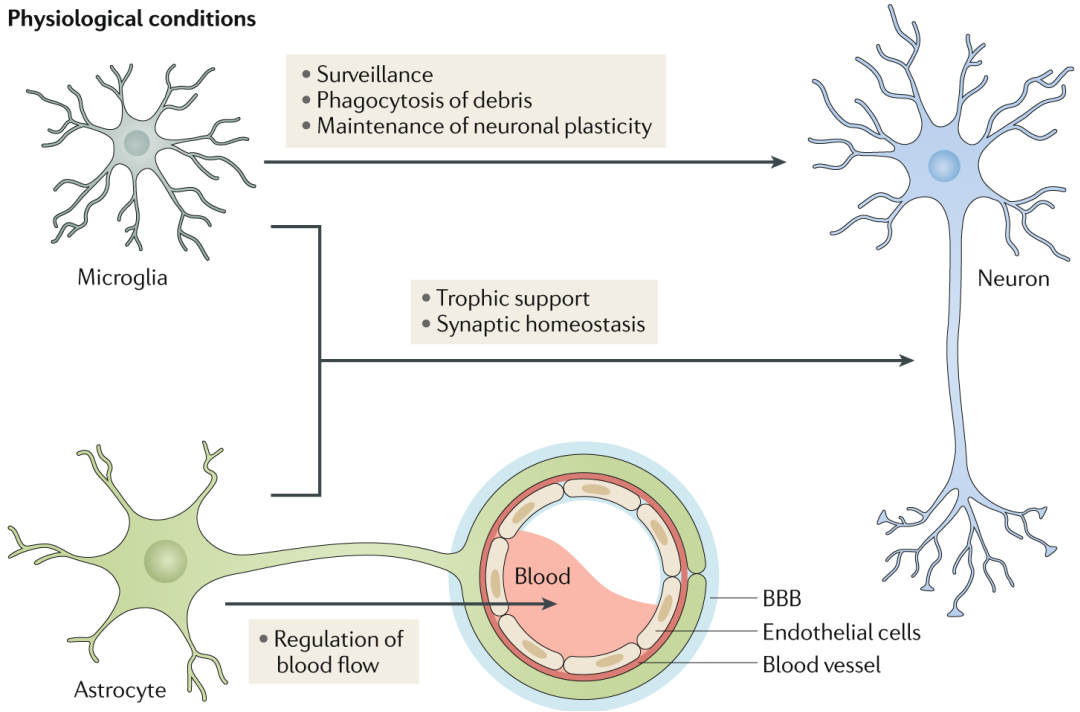

Figure 1.4: Immune cells in maintaining homeostasis of the brain under physiological conditions; microglia achieving this by constantly surveilling, phagocytosing debris, both

microglia and astrocytes providing trophic support to neurons, and astrocytes maintaining the integrity of blood brain barrier; *Image adapted from Leng et al., 2020*.

1.7.2) Immune cells of the brain:

An inflammatory response involves immune cells and secretion of inflammatory cytokines that carry-out the whole process. Originally considered immune-privileged, the brain is now known to involve a wide range of cell types: cells that are resident in the brain or can be recruited to the brain when the need arises. Here I will detail the brain's immune cells and how they orchestrate an inflammatory response.

1.7.2a) Myeloid cells:

These are cells that migrate to brain during the central nervous system development process and are widely categorized into two groups: parenchymal microglia and CNS-associated macrophages (CAMs). CAMs can also be present in the brain's border regions therefore called border-associated macrophages (Mrdjen et al., 2018). The following section describes microglia whereas CNS Associated Macrophages will be discussed in the later sections.

Microglia: Microglia are the cells of myeloid lineage that reside within the Central Nervous System. Similar to macrophages in the peripheral nervous system, microglia are a part of the immune system. During development, myeloid precursor cells migrate to the brain where they later mature to become microglia (Harry, 2013). Microglia in the brain in their surveillant state are otherwise known as 'ramified' microglia. In this state they are extensively branched and carrying out surveillance, as well as eliminating cell debris, removing excessive synapses in the developing neurons, providing trophic support to the

neurons, and undergoing a self-renewal process, as shown in Figure 1.5 (Gomez-Nicola & Perry, 2014).

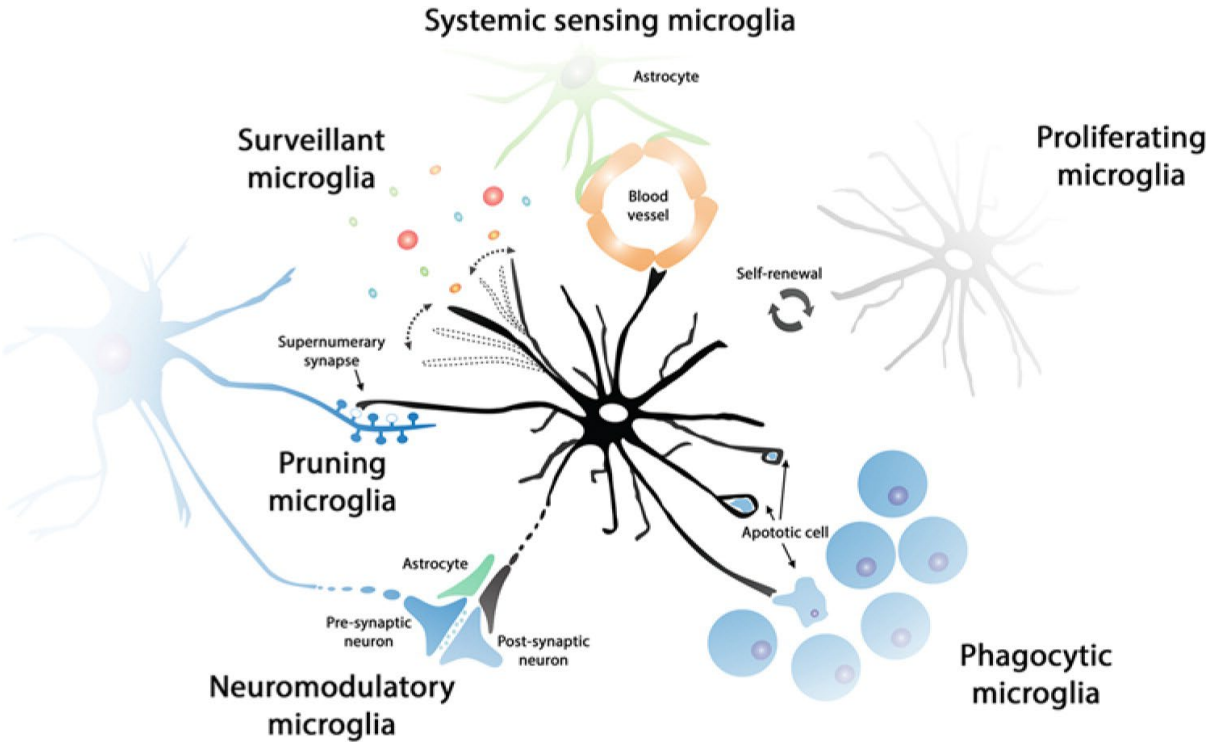

Figure 1.5: Different functional states of microglia in its surveillant form, including phagocytic action, neuromodulation, pruning synapses, self-renewal through proliferation; *Image adapted from Gomez-Nicola et al., 2014*.

Microglial cells become activated out of their surveillant state by a range of triggering molecules that trigger inflammatory response within the brain. Reactive microglia adapt a more amoeboid-like morphology by retracting all its processes. The inflammatory triggers are majorly categorized into - Pathogen Activated Molecular Patterns (PAMPs) which are molecules released by pathogens or small parts of the pathogen themselves and Damage Associated Molecular Patterns (DAMPs), which are molecules released by cells and cellular components that are of endogenous origin (Tang et al., 2012). These DAMPs and PAMPs are recognized by microglia through a set of receptors expressed on the cell surface referred to as Pattern Recognition Receptors. A major category of these

types of receptors are Toll-like receptors that recognize a vast variety of ligands, especially ligands of pathogenic origin. Amyloid beta and other misfolded proteins come under the category of Danger Associated Molecular Patterns. (Kigerl et al., 2014).

Both Danger Associated Molecular Patterns and Pathogen Associated Molecular Patterns trigger a cascade of inflammatory responses within microglia when they bind to their respective receptors, activating a series of downstream signalling mechanisms that release a series of inflammatory cytokines and chemokines. The inflammatory cytokines carry out inflammatory reactions in the brain, some well-known examples include Interferons (IFN) including IFN-α, β and γ, Tumour Necrosis Factor (TNF-α), and the Interleukin family with IL-6, IL1β. For instance, excessive production of TNF-α results in increased intracellular Aβ accumulation and tau pathology eventually leading to neuronal death in 3xtg-AD model (Janelsins et al., 2008). This is problematic because TNF-α induced Aβ has been shown to mediate deficits of learning and memory and synaptic dysfunction in AD (Tobinick, 2009).

Overexpression of IL1β has been reported to enhance tau phosphorylation and tangle formation leading to a significant decrease in LTP and synaptic plasticity, whereas blocking of IL1β signalling was seen to attenuate tau pathology and reverse the cognitive deficits in AD mouse models (Kitazawa et al., 2011). Increased levels of IL-6 were shown to be directly proportionate to increased levels of C-reactive proteins (CRP). In AD patients and mouse models, Wang et al., (2015) reported increased levels of IL-6 in the brain, cerebrospinal fluid, plasma and specifically surrounding the Aβ plaques in brain tissues. Together, these results suggest that these cytokines contribute to the pathology of AD (Wojdasiewicz et al., 2014).

Additional cytokines involved in AD neuropathology include Transforming Growth Factor- β (TGF- β), IL-4, IL10, IL-13 and several other interleukins. These cytokines are shown to support the normal functioning of the brain by regulating various neuroinflammatory processes. For example. in conditions like excitotoxicity, IL-10 has been shown to mitigate the effect in a time and dose-dependent manner (in-vitro) and provide trophic support to neurons (Zhou et al., 2009). This in turn is complemented by the effect of IL-10 in enhancing neuroplasticity by inducing LTP (in hippocampal slices) (Nenov et al., 2019). Similarly IL-4 has been reported to have a positive effect by increasing phagocytosis and proteolysis of damaged cells and proteins thereby aiding tissue repair (Balce et al., 2011). The role of TGF- β as a neurotrophic factor is well documented, not only during the phase of neuroinflammation, but also during early developmental stages of the brain as well as during neuro-regeneration (Massagué, 2012). Activins, a member of TGF- β family was reported to regulate memory processesthrough preservation of long term memory (in mouse models) (Ageta et al., 2010). These studies highlight the importance of intricate balance between different cytokines to ensure proper functioning of the brain and how this is disrupted in AD is addressed in the section later in this Chapter.

Evolving research has characterized microglia into specific subtypes based on morphological, spatial and structural analysis. One of the earliest classifications of microglial subtype appears to be the Keratan Sulphate Proteoglycan microglia (KSPG microglia) (Stratoulias et al., 2019). This subtype is classified in accordance with its ramified microglia and its expression is relatively region-specific, with high expression in hippocampus, brain stem, and olfactory bulb, and lower expression in cerebellum and cerebral cortex (Bertolotto et al., 1998).

Hox8b microglia comprise another subtype and although these are expressed throughout the brain; they are particularly concentrated in the cerebral cortex and olfactory bulb (Chen et al., 2010). The absence of this microglial subtype is accompanied by impaired grooming, anxiety, and social behaviours in rodents (De et al., 2018).

Another microglial subtype is the CD11c subtype, which can be found distributed in the primary myelinating regions of the brain: the corpus callosum and cerebellar white matter. This subtype is known to contribute to neurogenesis and myelinogenesis during brain development (Wlodarczyk et al., 2018). Accordingly, expression of CD11c is maximal during postnatal development, and decreases to less than 3% in adult mice brain.

In addition to these, there are several other microglial subtypes that are known to be associated with Alzheimer's disease (Disease Associated Microglia – DAM) and other neurodegenerative diseases (Neurodegenerative microglia – MGnD), although their status regarding whether they are harmful or protective remains unclear (Wei & Li, 2022).

Disease Associated Microglia in Alzheimer's disease were identified in 2017, through single-cell RNA sequencing. These microglia show upregulation of genes such as Axl, Apoe, Clec7a, Itgax, Galectin 3 (LGALS3), and cystatin F (CST7) and are usually not associated with acceleration of neurodegeneration (Sobue et al., 2021). Rather, the role of these microglia appears to be predominantly protective, a study that revealed that their activation resulted in the clearance of Aβ plaques (Keren-Shaul et al., 2017).

Like DAM, MGnD were reported at higher levels in several neurodegenerative diseases. MGnD polarization is triggered by increased phagocytosis of plaques and apoptotic neurons as observed in APP/PS1 mice and humans (Krasemann et al., 2017). This switch was especially activated by APOE and were associated with activation of inflammatory

genes including Axl, Itgax, Clec7a, and Apoe and a decrease of homeostatic genes including Tgfb(r), Hexb, P2ry12, and Cx3cr1. In the context of AD, restoring MGnD phenotype of microglia is assumed to play a protective role as prolonged activation of this microglial subtype is found to be deleterious (Krasemann et al., 2017; Pimenova et al., 2017). Similar to DAM and MGnD, several different subtypes of microglia such as proliferative-region associated microglia (PAM), activated response microglia (ARM) are being extensively studied in the recent years (Wei & Li, 2022).

1.7.2b) Astrocytes:

Astrocytes are the second set of immune cells in the CNS which scaffold the entire brain structure (Sofroniew & Vinters, 2010). Although not considered a part of classical immune cells in the brain, astrocytes seem to be activated during conditions like neuroinflammation (Wheeler et al., 2020) and neurodegeneration (Habib et al., 2020). Astrocytes, along with pericytes, form a close-knit layer around the blood vessels, keeping them intact, known as the blood brain barrier (Burn et al., 2021). Besides maintaining standard homeostasis in the brain, astrocytes also contribute to the formation of unique perivascular tunnels of the recently discovered glymphatic system, through which neurotoxic wastes are removed from the CNS (Jessen et al., 2015). Astrocytes also extend their support to oligodendrocytes by supplying growth factors that promote the maturation of oligodendrocytes, therefore indirectly influencing myelin maintenance (Tognatta et al., 2020). Apart from these, astrocytes serve as a rich source of energy metabolites such as glucose, lipids and amino acids which are necessary for normal functioning of neurons (as seen from Figure 1.6) (Chen et al., 2023).

The term ‘reactive astrocytes’ is often used to describe the activated version of astrocytes. One common characteristic of reactive astrocytes is the expression of ‘Glial Fibrillary

Astrocytic Protein' (GFAP), which is upregulated in the activated state of astrocytes in central nervous system (Sofroniew, 2014).

Like microglia, reactive astrocytes also express multiple receptors on their surface including Pattern Recognition Receptors and Toll-Like Receptors, which are activated through their respective ligands, to release interferons and Interferon Stimulated Genes (ISGs), which is a major innate immune response against viral infections (McNab et al., 2015). This excessive inflammatory cytokine secretion leads to the infiltration of immune cells from the periphery into the CNS (Sofroniew, 2015). This has a variety of consequences for brain function, for instance reactive astrocytes fail to regulate synaptic transmission and thus contribute to excitotoxicity (as reviewed in synapse loss section below).

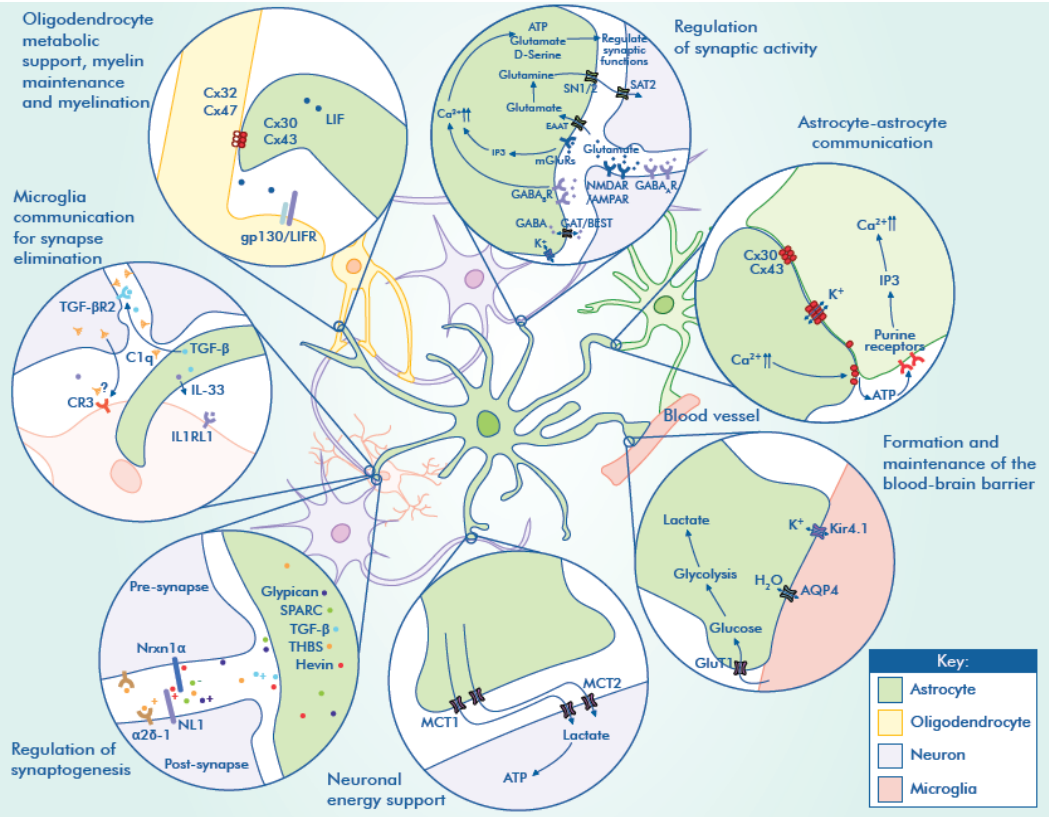

Figure 1.6: Functional diversity of astrocytes in the CNS; astrocytes providing energy support to neurons, regulating synaptogenesis, maintaining integrity of blood brain

barrier, regulating activity at the synapses, providing metabolic support to oligodendrocytes, integrating with microglia to function at the synapses; *Illustration reproduced courtesy of Novus Biologicals.*

1.7.2c) Immune cells in the immunological niches:

In addition to microglia and astrocytes, several other types of immune cells play a time-dependent role in brain development, inflammatory conditions, and healthy brain functioning. $CD4^+$ T cells are known to play a critical role in healthy brain function and abnormal T cell signalling, and depletion of these cells is met with neurological disability in animal models (Desdín-Micó et al., 2020). Likewise, $CD8^+$ T cells can infiltrate the brain during aging, which reduces the proliferation of neuronal stem cells in neurogenic niches (Dulken et al., 2019). B lymphocytes also contribute to the functioning of the brain by enhancing oligodendrocyte development from precursor cells, as observed in the early stages of murine brain development (Tanabe & Yamashita, 2018). These (and many other) immune cells are stocked in different anatomical interfaces such as the meninges, choroid plexus, and perivascular spaces. Additionally, the bone marrow of the skull supplies a varied set of immune cells to the brain when necessary (Castellani et al., 2023) which, like microglia, constantly surveil the brain for danger signal and exert control either remotely by secretion of cytokines/neurotrophic factors, or locally by infiltrating the brain (Ito et al., 2019). The meninges act as a reservoir of immune cells such as lymphocytes and Antigen Presenting Cells (APCs) such as CNS Associated Macrophages, as well as dendritic cells that present antigens to the T cells (Merlini et al., 2022). The meninges also serve as a niche for immature B cells that originally migrate from bone marrow of the skull (Schafflick et al., 2021).

There are additional immune cells in the choroid plexus. The choroid plexus forms the blood-cerebrospinal fluid-barrier, with the maximum population of macrophages, which immediately respond to any insults from the brain or peripheral immune challenge (Shipley et al., 2020). Other than macrophages, this niche holds enhanced major histocompatibility complex-II expressing APCs (Mrdjen et al., 2018) and leukocytes that migrate to CNS upon interferon signalling (Kunis et al., 2013).

Finally, perivascular spaces hold immune cells and these are the spaces surrounding small blood vessels that integrates into the brain parenchyma (Mrdjen et al., 2018). The immune cells present in this compartment are recognized as part of the innate immune system, acting as the first line of defence. Most of the cells that populate the perivascular spaces are leukocytes, perivascular CAMs, and macrophages (Mrdjen et al., 2018). Together with the brain resident microglia, all these various immune cells function to maintain homeostasis in the brain, and all are subject to alteration during aging and neurodegenerative conditions (Castellani et al., 2023).

1.7.3) Neuroinflammation – A persistent immune response:

Acute neuroinflammation is a necessary immune response to invading pathogens and toxic proteins within the brain, which usually subsides within few hours to days and is required to maintain homeostasis. When the acute inflammation does not subside within few weeks, neuroinflammation starts persisting indefinitely. This phenomenon is termed chronic neuroinflammation which typically lasts for months and sometimes over years, causing damage to the brain (as shown in figure 1.7) (Hannoodee & Nasuruddin, 2023).

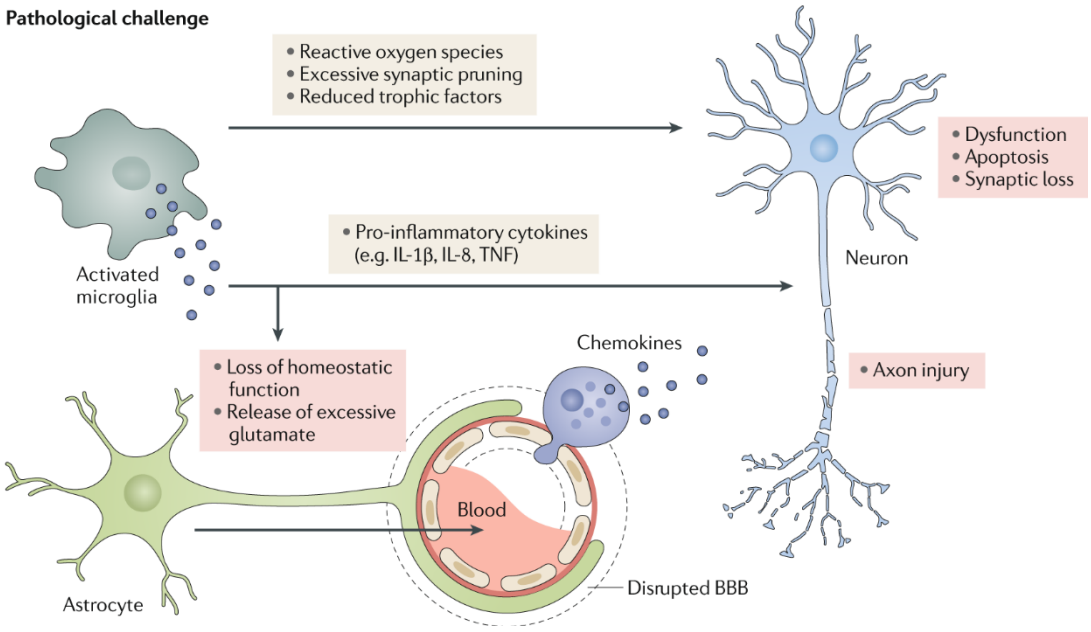

Figure 1.7: Uncontrolled neuroinflammatory response during pathological challenge, with reactive microglia and astrocytes causing dysfunction of neurons, apoptosis and synaptic loss through excessive secretion of reactive oxygen species, reduced supply of trophic factors, and excessive release of glutamate; *Image adapted from Leng et al., 2020.*

1.7.3a) Neuroinflammation and cognitive deficits in Alzheimer's disease:

There are several lines of evidence showing that neuroinflammation is a probable factor leading to cognitive deficits in Alzheimer's disease and Mild Cognitive impairment. First, a number of preclinical studies have shown that neuroinflammation underlies cognitive decline in AD-related mouse models. For example, in the APP/PS1 mouse model, neuroinflammation was found to parallel the progression of learning and memory deficits in spatial and working memory tasks (Zhu et al., 2017). A separate study found that TGCRND8 animals that were fed a whole-food diet showed spatial memory deficits that was mediated by neuroinflammation in these animals (Parrott et al., 2015). Another popular 5xFAD model demonstrated that neuroinflammation preceded synaptic loss and therefore lead to cognitive dysfunction as evidenced by poor performance on spatial and

working memory tasks. Treatment with Pomalidomide, an immunomodulatory drug, mitigated the severity of cognitive dysfunction in this AD model(Lecca et al., 2022).

Second, neuroinflammation has been found to disrupt the brain network communication and synaptic function, resulting in cognitive disturbance (Heppner et al., 2015). A study by Passamonti et al. (2019) reported that neuroinflammation (as marked by microglial reactivity), and brain functional connectivity (proposed to have resulted from abnormal microglial activity at the synapses) each had strong correlations with cognitive decline in Alzheimer's patients. These were supported by another imaging study conducted on AD patients, that reported a positive correlation between dysfunction of network structural integrity and various cognitive impairments (e.g. verbal memory, short-term memory). Microglial reactivity but not Aβ deposition was correlated with network dysfunction, associated with cognitive defects in AD patients, suggesting that neuroinflammation is more predictive of such defects than Aβ plaques (Leng et al., 2023). Several biomarker studies have suggested the same thing regarding neuroinflammation in AD. For example, glial cell and neuroinflammation markers such as YKL40, MCP1, VILIP1, sTREM2, IL-6, TGF-β were found to be specifically upregulated in AD patients (Kiraly et al., 2023). Glial cell marker such as YKL40 was further reported to be elevated in the CSF of MCI patients, which could mark the earliest traces of neuroinflammation and aid precise diagnosis of MCI to AD progression (Schmidt-Morgenroth et al., 2023).

1.7.3b) The effect of neuroinflammation on pathological markers of AD:

A third line of evidence supporting the role of neuroinflammation in AD progression comes from studies pointing out neuroinflammation that occurs as a response to amyloid-beta plaques and hyperphosphorylated Tau (Craft et al., 2006; Ismail et al., 2020). For instance, several studies report microglial reactivity in response to Aβ plaque formation

(Simard et al., 2006) which can phagocytose Aβ. Apart from phagocytosing the plaques, however, microglia have also been shown to limit plaque growth and preserve neuronal connections. This was demonstrated in a 2017 study that depleted microglia in APP/PS1 mice crossed with *CX₃CR1-iDTR* mice (i.e. a modification that allows control of microglia and myeloid cells in brain) by injecting diphtheria toxin (DT). Although there were no changes in plaque number, the size of plaques in these microglia depleted mice were increased by 13%, confirming that microglia functions to limit the plaque growth (R. Zhao et al., 2017). Similar results were reported in a 2020 study that looked at microglia's modification of plaque morphology. In a 5xFAD mouse model, microglia were found to successfully limit diffuse plaques and maintain plaques in a compact stage, highlighting the neuroprotective nature of microglia with respect to controlling amyloid plaques (Casali et al., 2020). Over longer periods of time, however, microglia become incapable of phagocytosing Aβ peptides, which contributes to the accumulation of Aβ. This was observed in the study by (Hickman et al., 2008) where microglia isolated from adult (14 months old) PS1-APP transgenic mice displayed marked decrease in Amyloid-beta scavenger receptors.

Just like microglia, astrocytes also contribute to Aβ degradation by secreting proteolytic enzymes to cleave Aβ (Nalivaeva et al., 2012). In organotypic brain culture slides, pharmacological ablation of astrocytes led to a sharp increase in amyloid beta levels, confirming the need for astrocytes in the clearance of amyloid beta (Davis et al., 2020). Although astrocytes take up aggregated amyloid beta, this disrupts the normal function of astrocytes by hampering their energy metabolism. This was indicated by swollen mitochondria and excessive fission in the astrocytes with excessive plaque accumulation (Zyśk et al., 2023).

Although astrocytes and microglia have been documented to play a vital role in clearance/modification of amyloid plaque pathology, during certain scenarios (such as chronic neuroinflammation) persistent reactivity of these cell types are associated with dysregulation of their canonical function leading to spreading of amyloid pathology. Reactive astrocytes on the other hand are reported to increase Aβ accumulation by releasing inflammatory cytokines that can trigger plaque formation (Blasko et al., 2000). A 2022 study by d' Errico et al., proved that reactive microglia contribute to spreading of Aβ pathology to the unaffected brain regions. In this study, the authors transplanted wildtype embryonic neuronal cells into the neocortex of 5xFAD mice and observed that the Aβ plaques were present in the transplanted wildtype grafts. With the help of in-vivo two photon imaging the authors demonstrated the movement of Aβ laden microglia migrating to the previously unaffected tissues, therefore being partly responsible for the spreading of Aβ plaques in the uninfected brain region (d'Errico et al., 2022).

Similarly, microglia engulf Tau oligomers under physiological conditions, but dysfunctional microglia are unable to phagocytose the aggregated Tau and are therefore thought to indirectly contribute to Tau tangle formation (Bolós et al., 2017) In a recent study, microglial reactivity has been shown to lead tau accumulation in a Braak staging dependent manner. By performing network analysis following positron emission tomography (PET) imaging for microglia and tau, it was reported that microglial reactivity and accumulation propagated in the brain regions in a manner that followed the pattern of Braak staging (Pascoal et al., 2021). A later study demonstrated that the correlation between microglial reactivity and tau accumulation was driven by Aβ burden. Particularly, the co-occurrence of Aβ, tau and microglial abnormality was seen to result in a severity of cognitive phenotype in AD patients (Wang & Xie, 2022).

Astrocytes have been shown to contribute to tau pathology propagation via vesicle secretion and tunnelling nanotubules. Astrocytes engulf tau deposits in an attempt to clear the accumulated tau and upon failing to degrade the ingested tau, astrocytes start aggregating it within the cells. Mothes et al., used FRET based seeding assay and observed that tau proteoforms are released by astrocytes and these released tau possess a higher seeding capacity compared to the ingested tau which are then eventually spread to the nearby cells (Mothes et al., 2023). Additionally, similar to the above-mentioned interplay between microglia, Aβ and tau, there exists a link between astrocytes, Aβ and tau. Evidence for this was reported in a 2011 study which stated that astrocytes are a key downstream modulator of Aβ pathology, resulting in tau phosphorylation in primary neurons (Garwood et al., 2011). A recent study by Bellaver et al., (2023) examined cognitively unimpaired individuals positive for astrocytic reactivity and reported that reactive astrocytes are important in Aβ induced worsening of tau pathology through biomarker studies. This particular finding could help in the precise identification of individuals in clinical trials who could eventually develop AD.

Activated microglia and astrocytes share common pathways that contribute to neuronal degeneration in the context of chronic neuroinflammation. Both glial cells secrete excessive amounts of inflammatory cytokines when activated, which leads to increased levels of intracellular calcium in neurons. These abnormal levels of calcium can damage mitochondria and activate caspases, eventually resulting in neuronal apoptosis (Kruman et al., 1998). Microglia and astrocytes both also secrete nitric oxide and other free radicals, high levels of which can lead to DNA and oxidative damage in neurons (Rumbaugh & Nath, 2009). As a consequence of this, mitochondrial dysfunction and calcium induced excitotoxicity occurs, which marks a major pathological feature of Alzheimer's disease (Verma et al., 2022).

A final way in which neuroinflammation can be destructive is through the sustained reactivity of microglia and astrocytes, which can lead to the loss of their homeostatic function (among other things). For example, astrocytes maintain Blood Brain Barrier integrity, and loss of this function through their consistent activation can lead to infections from the periphery spreading to the brain (Drögemüller et al., 2008). Additionally, the reduced secretion of neurotrophic factors by glial cells deprives neurons of their energy and normal functioning, resulting in degeneration. These neurotrophic factors play a crucial role in maintaining cognitive function, such that disturbances in their balance can affect higher order functions like memory and cognition, which is a well-known clinical feature of AD (De Sousa, 2022). Therefore, for all the reasons outlined above, chronic neuroinflammation can be detrimental to normal brain function, and appears to be inseparably linked to multiple features of AD pathology.

1.8) Hippocampal atrophy in Alzheimer's disease:

Brain atrophy (shrinkage) and volume loss is a common phenomenon observed in Alzheimer patients. Nevertheless, it is interesting to note that only selective regions of the brain are affected by atrophy and volume loss in Alzheimer's disease, and this remains consistent across all AD cases (Prasad, 2020). A recent study conducted by (Planche et al., 2022) depicted the chronological order in which brain region atrophy progresses throughout the entire course of Alzheimer's disease. According to this study, the progression of brain atrophy starts from the hippocampal and amygdala regions and slowly extends to cortical regions including entorhinal cortex, cingular and insular cortices. This constitutes the major reason for my focus on the hippocampal region in this study. In the following section, I will explain hippocampal anatomy, its circuitry and how degeneration of hippocampus occurs in AD. I will be primarily referring to the mouse

hippocampus in this section, but with noted references to human hippocampus in several sections.

1.8.1) Hippocampus:

The hippocampus is a brain structure within the temporal lobe that forms a part of the limbic system of the brain. The key functions of the hippocampus include memory acquisition, regulation of learning and memory, spatial navigation, and decision making (Tatu & Vuillier, 2014). The hippocampus has both efferent and afferent connections to various other parts of the brain including anterior thalamus, hypothalamus, amygdala, and entorhinal cortex.

1.8.2) Hippocampal anatomy:

In mice, the hippocampus can be divided into dorsal, medial/intermediate, and ventral parts, with the dorsal hippocampus roughly corresponding to the posterior hippocampus in humans and the ventral to the anterior hippocampus in human. The dorsal/posterior hippocampus is known to play a vital role in spatial memory and navigation in both humans and mice (Burgess et al., 2002). This is facilitated through the presence of 'place cells' in the hippocampus which enables the subject to understand its location in the given space (Moser et al., 2015). In humans, these place cells are located in hippocampus, entorhinal cortex (Whalley, 2013). In animal studies, the hippocampus has been causally linked to spatial memory in behavioural experiments like Water maze, Barnes maze and contextual fear conditioning (Holt & Maren, 1999; Kim & Fanselow, 1992; Moser et al., 1993). Specifically, these studies have found that lesioning or inactivating the hippocampus prevents animals from recalling the location of an escape platform, escape

box, or the context in which a foot shock was delivered. This function does appear to be specific to dorsal hippocampus, whereas the ventral hippocampus has been shown to be involved in processing anxiety related behavioural responses (Bannerman et al., 2004).

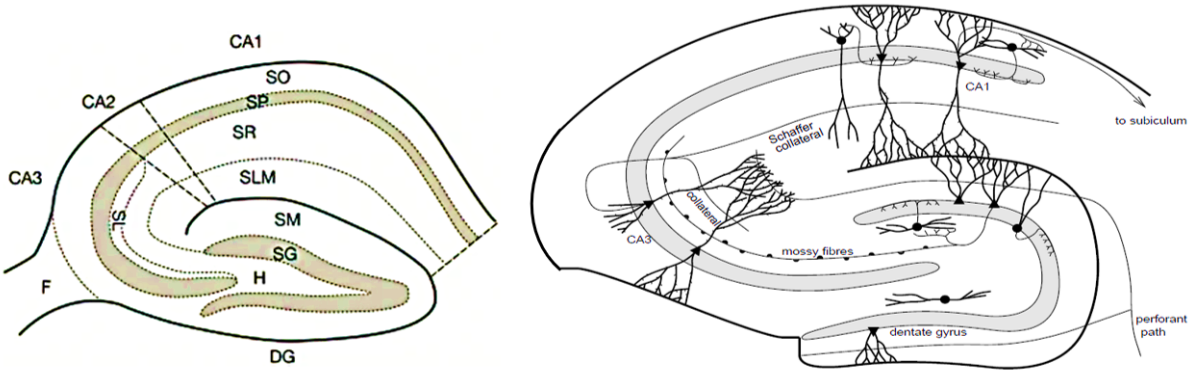

Figure 1.8: Major regions and different sublayers of the hippocampus (left); Hippocampal circuitry (right); *Images adapted from Noguchi et al., 2020, (left) Schultz et al., 1999 (right)*.

As shown in Figure 1.8, Coronal sections of the (mouse) dorsal hippocampus reveal two major sub-regions – 'Cornu Ammonis' (CA) and Dendate Gyrus (DG). CA region is further subdivided into CA1, CA2, CA3 and CA4 (Mercer & Thomson, 2017). CA1, being the largest region of hippocampus, is bordered on one side by subiculum, on the other side by CA2 region. CA2 is bordered by CA1 and CA3 on either side. CA3 region is located in close proximity to the DG region and bordered by CA2 on one side. A deep sublayer of DG is termed CA4 region (Blackstad, 1956). DG region appears to follow the CA3 region, aligned opposite the CA1 and CA2 regions.

1.8.3) Hippocampal circuitry:

The neural circuit within hippocampus is crucial for processing information and encoding memories (Lisman, 1999). The entorhinal cortex, DG, CA1, CA3 and subiculum regions of the hippocampus constitute a part of the major hippocampal circuit (Lopez-Rojas &

Kreutz, 2016). The CA regions of the hippocampus are further layered as follows – Stratum Oriens, Stratum Pyramidale, Stratum Radiatum and Stratum Lacunosum Moleculare (Li & Pleasure, 2013) (Figure 1.8, left). CA1 – CA3 regions of the hippocampus are made of pyramidal neurons and a small population of (mostly inhibitory) interneurons. Pyramidal neurons have dendritic projections that are termed apical and basal dendrites (Ho et al., 2013). Both these dendrites differ in electrical conduction and neurotrophic factors. As apical dendrites are contained within the stratum radiatum (refer to the section above), they form a major part in trisyanaptic hippocampal circuit, therefore they are crucial to learning and memory (Arikkath, 2012; Wu et al., 2015). Axonal projections from the CA3 pyramidal neurons in the ipsilateral and contralateral hippocampus are named 'Schaffer collaterals' and 'commissural fibers' respectively (Laurberg, 1979; Swanson et al., 1978). The DG is composed of granular cells and axons of these granular cells are termed 'mossy fibers'.

Axons of the layer II of Entorhinal cortex project to the DG and CA3. Mossy fibers of the DG project to stratum radiatum of CA3 region. CA3 combines these inputs from DG and EC layer II, and then sends off Schaffer collaterals to the stratum radiatum of the ipsilateral CA1 region, as well as commissural fibers to the stratum oriens of the contralateral CA1. The CA1 region then sends projections to the subiculum. Axons of the subiculum in turn mainly project to the Entorhinal Cortex (Figure 1.8, right).

1.8.4) Degeneration of hippocampus in AD:

As mentioned earlier in this section, hippocampal atrophy is evident in the very early stages of AD. It has been reported by (Frisoni et al., 2010) that the patients with early AD experience the loss of almost 15-30% of hippocampal volume. Numerous reasons for this degeneration have been identified, out of which accumulation of Aβ plaques and Tau

tangles are considered foremost. NFT accumulation starts in the Entorhinal cortex and follows Braak staging of spatio-temporal distribution (which is typically the region wise spread of neurofibrillary tangles, starting from transentorhinal cortex, to limbic regions and finally the neo-cortical regions (Braak & Braak, 1991)). Additional factors simultaneously contributing to hippocampal atrophy include chronic stress and hyperexcitability of neurons together with a reduction in neurogenic niche (Anand & Dhikav, 2012; Dhikav & Anand, 2011). Together, these factors lead to cognitive decline in individuals with AD (C. R. Jack et al., 2002).

1.9) Synapse loss in Alzheimer's disease:

Synapse loss is one of the earliest pathological changes and strongest correlations of Alzheimer's disease next to Aβ and NFTs. Loss of synapses in AD was first reported in early 90s in a study by (Sze et al., 1997), where levels of synaptophysin (a pre-synaptic marker) were decreased in post-mortem tissue taken from individuals with AD compared to healthy controls. Ever since, evidence of its correlation with cognitive decline has grown stronger. Analogous to hippocampal atrophy, synapse loss has diverse factors contributing to the initiation and advancement of this pathology in the AD brain. For instance, Aβ oligomers and its negative effects on synaptic transmission were discussed in the previous section (Aβ toxicity section). In this following section I will first introduce spines and synapses, their functional significance, followed by how synapse loss occurs in AD (i.e. major factors contributing to synapse loss).

1.9.1) Dendritic spines and synapses?

Dendritic spines are small yet dynamic protrusions along the dendrites of specific sets of neurons in the brain. They function as the receiving end of information from other neurons, thus accommodating a functional synapse at the spine head (Figure 1.10, right). The dendritic spine structure is supported by actin cytoskeleton, which facilitates it's dynamicity (continuous shape shifting according to the synaptic activity) (Koskinen et al., 2012). Spine formation and maturation consists of the following stages in the following order, each of which gives rise to different spine types – filopodium, thin, stubby, mushroom, cup-shaped or branched spines (Figure 1.9). It has been widely accepted that the mushroom spines are the most mature and stable form of spine, facilitating a functional synapse formation, whilst other types of spines receiving signals on and off, in the process of maturation into a stable spine (Nimchinsky et al., 2002).

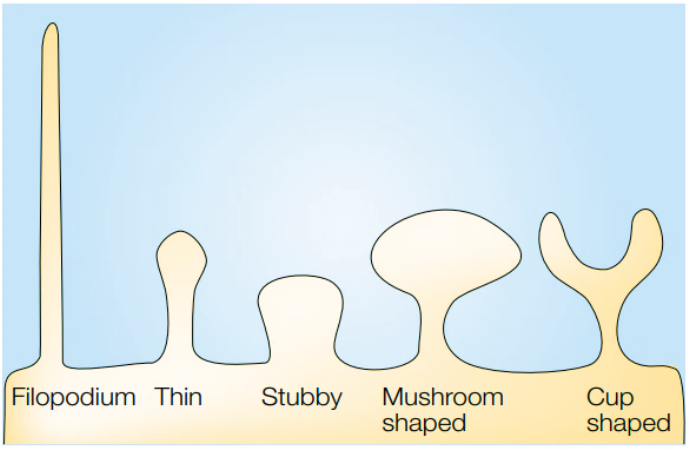

Figure 1.9: Different maturation stages of a dendritic spines starting from filopodium, thin, stubby, mushroom, and cup-shaped (from left to right); *Image adapted from Hering& Sheng, 2001*.

A synapse consists of a pre-synaptic terminal (axonal terminal from the neuron sending information) and a post-synaptic density (dendritic spine of the receiving neuron) as

shown in figure 1.10. The pre-synaptic terminal stocks the neurotransmitters in synaptic vesicles which are released into the synaptic cleft during neurotransmission. The part of the post-synaptic cell that receives this message, which for most synapses is the spine head, holds the Post-synaptic density with neurotransmitter receptors like AMPA (α-amino-3-hydroxy-5-methyl-4-isoxazolepropionic acid), NMDA (N-methyl D-aspartate) and GABA (γ-aminobutyric acid) receptors, which receive excitatory and inhibitory signals from the pre-synapse (Voglewede & Zhang, 2022). The presynaptic terminals which send signals to the spines are part of most glutamatergic neurons (i.e. excitatory neurons that release glutamate as neurotransmitter) like pyramidal neurons of the hippocampus, and some GABAergic neurons (releasing GABA as neurotransmitter, inhibitory) like Purkinje neurons, as well as some interneurons (Chiu et al., 2013; Hering & Sheng, 2001).

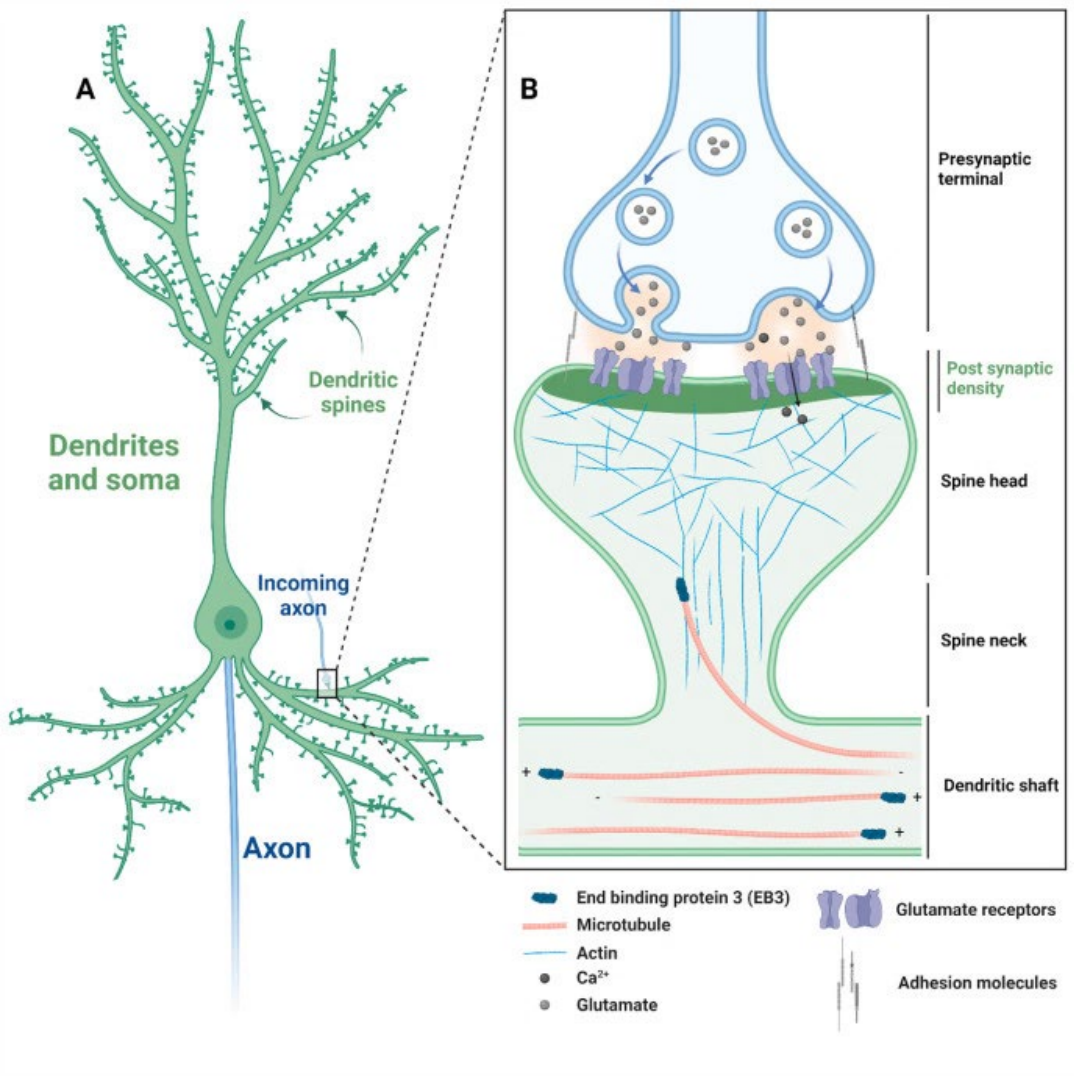

Figure 1.10: A pyramidal neuron showing dendritic spines on its dendrites (left), A functional synapse with a pre-synaptic terminal and a post-synaptic density that is residing on a spine head, which is attached to dendritic shaft through spine neck(right); *Image adapted from Voglewede and Zhang, 2022*.

1.9.2) Functional significance of dendritic spines:

As noted above, filopodia are the most abundant spine type during the initial stages (first postnatal week) of development, followed by thin, stubby, and finally mushroom spines being more prominent in the adult/fully developed brain (Fiala et al., 1998). Sustenance/stabilization of the mature spines occurs with repeated synaptic

transmission through a phenomenon called Long-term Potentiation (LTP) (Baltaci et al., 2019), and this directly corresponds to the strengthening of the synapse (Citri & Malenka, 2008). This process is crucial for learning and memory which relies on the formation of neural connections (i.e. synapses) within the brain. It has been consistently reported in the literature that the learning and memory process is directly correlated with an increase in the number of dendritic spines (Hayashi-Takagi et al., 2015; Hwang et al., 2022; Ma & Zuo, 2022; Moretti et al., 2006). For example, the study by Hwang et al., reported the strengthening of highly specific synaptic circuit during the formation of long-lasting motor memory in the mouse brain cortex. These studies indicate that the formation and stabilization of dendritic spines is essential for maintaining the integrity of adult/mature brain.

1.9.3) Mechanisms leading to loss of synapses in AD:

Although there are reports of multiple pathways and triggering mechanisms leading to synapse loss in AD, I will, here focus on the detrimental effects of activated microglia and astrocytes in synapse pathology specifically, because much of this thesis deals with looking at the glial cell expression profile in neuroinflammation and its effect on spine density. The rationale for this stems from the fact that decrease in spine density/synapse loss is evidenced in the early stages of AD (Scheff et al., 2007; Scheff et al., 2006) and has further been reported across majority of the well-known AD models (Jang et al., 2021; Salvatore Oddo et al., 2003), making it an important pathology to account for in our sporadic AD model.

Microglia play an important role in pruning synapses during the initial stages of brain development. However, it is being increasingly reported that abnormally activated microglia phagocytose neuronal synapses to a greater extent in neurodegenerative

conditions like AD (Crehan et al., 2012; Hansen et al., 2018). This is mediated through the complement pathway. Briefly, the CR3 receptor expressed by microglia recognizes the C1q ligand on apoptotic cells which can then be engulfed and cleared. These C1q ligands have been reported to be expressed on synapses, which are then recognized by the CR3 receptors on the activated microglia.

Excessive C1q-CR3 mediated synaptic phagocytosis has been shown to be detrimental in Alzheimer's disease (Stevens et al., 2007). In 2016, Hong S et al., reported that complement dependent synaptic pruning is activated in the early stages of AD brain, suggesting that microglia mediated synapse loss happens in early AD. In addition, both the expression of C1q and synapse elimination are found to occur prior to amyloid-beta accumulation in the brain, thereby highlighting synapse loss as one of the earliest pathological changes that is independent of amyloid plaque accumulation (Hong et al., 2016).

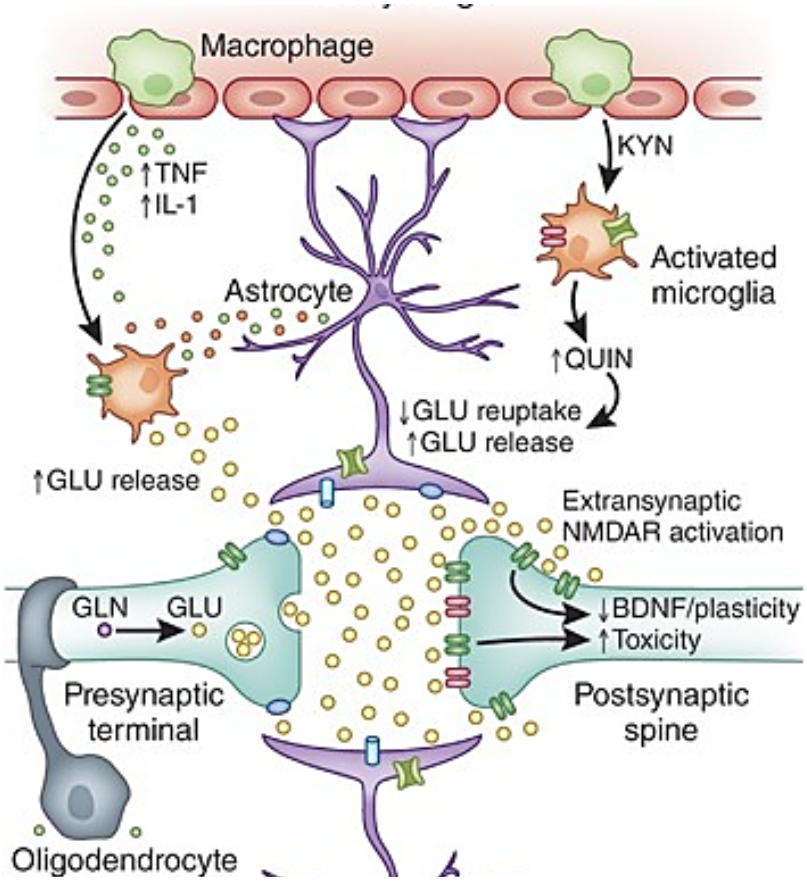

Figure 1.11: Schematic representation of a tripartite synapse – showing pre-synapse, post-synapse and an astrocytic terminal; excessive gluatamate released at the synapse where reactive astrocytes struggle to remove the glutamate released efficiently, therefore resulting in glutamate excitotoxicity; *Image adapted from Haroon et al., 2017*.

Another way in which synaptic excitotoxicity can occur is via the dysregulation of astrocytic function, as shown in Figure 1.11. Astrocytes form an integral part of synaptic transmission via the 'tripartite synapse' (Velasco et al., 2017). The tripartite synapse includes a pre-synaptic terminal, post-synapse and an astrocytic terminal which regulates neurotransmitter flow at the synapse, particularly glutamate. Glutamate is the major excitatory neurotransmitter in the brain and glutamate mediated excitotoxicity is a major cause of neuronal death in Alzheimer's disease (González-Reyes et al., 2017). At the

synapse, glutamate released by the pre-synaptic terminal stimulates the post-synapse and initiates an action potential, after which the excessive glutamate is cleared by the astrocytes which carry glutamate transporters. Glutamate is then recycled within the astrocytes and transported to neurons for the next cycle of synaptic transmission. Reactive astrocytes become less efficient at this or even fail to perform this function (Haroon et al., 2017) The resulting failure to uptake excessive glutamate by reactive astrocytes results in glutamate excitotoxicity, which is the overstimulation of glutamate receptors causing Ca2+ influx. One effect of this excessive Ca2+ influx is the activation of proteasome pathway leading to synaptic dysfunction and loss of synapses. Synapse loss is eventually followed by neuronal network degeneration leading to cognitive impairments witnessed in AD (Nanclares et al., 2021).

Now that I have reviewed the gene mutations, risk factors and neuropathological features of AD, I will move on to understand how these features have been modelled in preclinical studies. Specifically, in the following section, I will discuss some of the familial pre-clinical models and already existing sporadic models of Alzheimer's.

1.10) Mouse models of Alzheimer’s disease:

Most widely used mouse models of Alzheimer's disease are familial AD models. However, a few sporadic AD models have begun to emerge in recent years.

1.10.1) Familial AD models:

First, I will briefly review several of the popular familial AD models that exhibit mixed (combination of APP, PSEN1, MAPT) mutations or only APP mutations. The behavioural and pathophysiological features of these models are summarized in Table 1.1 below.

The 5x-FAD model is one of the most popular models in preclinical AD research. This model combines three mutations on the APP gene and two mutations on the PSEN gene, which together makes 5x-mutations (Oakley et al., 2006). The plaque deposits begin in this model at around 2 months of age, along with gliosis indicating neuroinflammation. Synapse loss occurs in this strain, as demonstrated by a reduction in expression of the pre-synaptic marker synaptophysin relative to wildtype controls by 4 months (Crouzin et al., 2013). Working memory and spatial memory deficits begin at 4-5 months age (Kimura & Ohno, 2009).

Another popular model is the 3xtg-AD model, which has a single mutation in each of the APP, PSEN, and MAPT genes (as shown in Table 1.1), therefore combining both amyloid beta and tau pathologies in a single model. Phenotypically, these animals start showing deficits in spatial and working memory by 4 months of age (Billings et al., 2005). Pathophysiological features include extracellular amyloid beta deposits by 6 months age, tau aggregations by 12 months in the cortex and hippocampal regions (S. Oddo et al., 2003).

Familial AD models – mixed gene mutations:

STRAIN	No of mutations	Aβ	Tau	Mutations-detail	Locomotor impairment	Spatial memory impairment	Synapse loss	Neuroinflammation
5xFAD	5	✓	×	APP: Swe (K670N/M671L) Flo (I716V) Lon (V717I) PSEN1: (M146L) and (L286V)	✓ 12 months	✓ 4-5 months	✓ 9 months	✓ 2 months
APP/PS1	2	✓	×	APP: Swe (K670_M671delinsNL) PSEN1: L166P	×	✓ 7 months	✓ 1 month	✓ 1.5 months
3xTg-AD	3	✓	✓	APP: Swe (K670N/M671L) PSEN1: (TM1) MAPT: (P301L)	✓ 4 months	✓ 4 months	✓ 3 months	✓ 7 months

Table 1.1: Widely used familial AD models with a combination of different gene mutations in AD preclinical research.

Strains with just the APP mutations have also been used to model Alzheimer's disease, and the features of several of these models are summarized in Table 1.2 below. One such popular model is the J20-AD model which harbours two mutations in the APP gene (Mucke et al., 2000). Neuronal loss begins at the age of 3 months for these animals, accompanied by loss of synapses around the same time, marked by decreases in pre-synaptic and post-synaptic markers (Hong et al., 2016; A. Wright et al., 2013). Spatial memory deficits in Radial arm maze and Morris water maze are observed in these animals (Cheng et al., 2007). Another model that is widely used in the field of AD is APP/PS1 (Chishti et al., 2001; Kitazawa et al., 2012), which display spatial memory deficits in water maze around 7 month age (Serneels et al., 2009) and synapse loss as early as 4 weeks (1 month) (Bittner et al., 2012). Activated microglia were found to cluster around amyloid plaques at 6 weeks of age (Radde et al., 2006). TgCRND8 is another commonly used model with two mutations in the APP gene, same as the J20 model, except that TgCRND8 (Chishti et al., 2001) uses a different promotor that results in an acceleration of AD phenotype (Chishti et al., 2001; Kitazawa et al., 2012). Therefore, onset of cognitive impairments and neuroinflammation appears much earlier in these mice compared to J20 animals as seen from Table 1.2.

MAPT mutations are known to be associated with various neurodegenerative diseases such as Frontotemporal lobular dementia and Parkinsons disease. A rare pA152T mutation of tau has been shown to increase risk in Frontotemporal dementia (FTD) and Alzheimer’s disease (Coppola et al., 2012). Similarly, recent studies have highlighted pTau-S396, pTau-T181 as pathogenic variants in Amyotrophic Lateral Sclerosis (ALS)

(Petrozziello et al., 2022). Aside from AD related mutations, other MAPT mutations in FTD, ALS and other tauopathies are listed in MAPT | ALZFORUM.

Familial AD models – only APP mutations:

STRAIN	No of mutations	Mutations-detail	Locomotor impairment	Spatial memory impairment	Synapse loss	Neuroinflammation
J20	2	APP: Swe (K670N/M671L) Indiana (V717F)	✓ 5 months	✓ 4 months	✓ 3 months	✓ 6 months
PDAPP	1	APP: Indiana (V717F)	×	✓ 3 months	×	✓ 6 months
TgCRND8	2	APP: Swe (K670N/M671L) Indiana (V717F)	×	✓ 3 months	✓ 6 months	✓ 3 months
Tg2576	1	APP: Swe (K670N/M671L)	×	✓ 6 months	✓ 4.5 months	10 months

Table 1.2: Widely used familial AD models with just APP mutations in AD preclinical research.

1.10.2) Sporadic AD models:

Apart from the familial AD models discussed above, AD research has employed a few sporadic AD models. These models do not harbour a genetic mutation related to familial AD, but rather are engineered to reflect some of the key phenotypical and pathological features of Alzheimer's disease through expression of risk factors that are linked to AD progression (Lili Zhang et al., 2019). Here I will describe several of these sporadic models, specifically those that have been generated by infusions of Aβ or tau and other drugs to mimic pathological and behaviour phenotypes of Alzheimer's disease.

1.10.2a) Aβ infused models:

Aβ infusion models are created by intracerebroventricular (i.c.v) or intrahippocampal injections of Aβ peptides including Aβ(1-40), Aβ(1-42) and Aβ(25-30) (Akhtar et al., 2022). The injection of Aβ(1-40), in particular into the cerebral ventricle of rats was found to result in enhanced levels of secretory APP which eventually was found to cause increased deposits of Aβ in the brain (Zhang et al., 2004). Intracerebroventricular injections of Aβ (25-30) injection led to deficits in novel-object recognition and fear-conditioning paradigms, that were in part due to the downregulation of cholinergic system. Specifically the downregulation of nicotinic acetylcholine receptors, which was reversed through treatment of galantamine (acetylcholinesterase inhibitor)(Wang et al., 2007). Intracerebroventricular injections of Aβ(1-42) also caused deficits in learning and memory paradigms such as Morris Water Maze and passive avoidance, and this effect was found to be mediated in part by increased oxidative stress in the brain (Shekarian et al., 2020). Several other models infused various Aβ peptides alongside other toxic drugs to mimic AD pathology, and these will be discussed later in this section.

1.10.2b) Tau infused models:

Similar to the Aβ induced models, there are several models of tau injections in rodents that model the AD phenotype (Yokoyama et al., 2022). Clavaguvera et al., (2009) used extracts from mutant P301S mice to induce tau pathology in wildtype human tau carrying animal models. This procedure resulted in development of filamentous tauopathy in the recipient mouse model. Similarly, injection of AD brain derived pathological tau into Aβ bearing models resulted in visible tau pathologies, including neuropil threads, aggregated tau in dystrophic neurites, and neurofibrillary tangles. The formation of tau pathology was found to be induced by the Aβ plaques in this animal model (He et al., 2018). A 2021

study by Saito et al., (2021) observed similar results by crossbreeding humanized MAPT expressing mice with App-KI mice. They reported a rapid cell-to-cell propagation of pathological tau as well as an accelerated tau accumulation in the presence of amyloidosis, emphasizing the importance of investigating Aβ induced tau pathology in the context of AD.

1.10.2c) Lipopolysaccharide (LPS) injection models:

LPS (which is a component of the outer wall of gram negative bacteria (Bertani & Ruiz, 2018)) is often administered to create a neuroinflammatory response (Lee et al., 2008; Zhao et al., 2019) to study the neuroinflammation related pathology of Alzheimer's disease. There have been multiple studies that performed single and repeated injections of LPS in rodents to mimic neuroinflammation observed in AD. Czerniawski J et al., (2015) reported that a single intraperitoneal (i.p.) injection of LPS 0.167mg/kg was sufficient to impair context dependent object discrimination in rats while sparing spatial memory. A higher dosage of 1mg/kg LPS i.p. injection resulted in impairments in passive avoidance and learning deficits in water maze test (Anaeigoudari et al., 2015; Anaeigoudari et al., 2016). A single intravenous injection of LPS 1mg/kg was shown to impair cognitive performance in Barnes maze and inhibitory avoidance test (Vasconcelos et al., 2014). Continuous injections of 0.75mg/kg LPS was given for 7 days to Swiss mice resulted in early-stage impairments of spatial learning and memory. Further histological investigation of hippocampus indicated neuronal degeneration in these animals receiving 0.75mg/kg LPS (Khulud A. Bahaidrah et al., 2022). Like i.p. injections, i.c.v injections of LPS (12μg) have also shown to cause spatial learning and memory deficits accompanied by a decrease in neurons and an increase in microglia in the hippocampus. This model also displayed an increase in Aβ positive cells and inflammatory cytokines like TNF-α and

nitric oxide capturing specific pathological features of Alzheimer's disease (Zhao et al., 2019).

1.10.2d) Models of genetic risk factors of AD:

The major genetic risk factor for sporadic Alzheimer's disease, ApoE4 is modelled in mice by targeted replacement of murine ApoE for human ApoE4, to create ApoE4-TR (transgenic) mice. These mice were shown to express lower levels of total ApoE4, less ApoE4 associated with lipoprotein and less lipidated compared to the ApoE3 and ApoE2 mice (Youmans et al., 2012). The ApoE4-TR mice were reported to have a leaky blood brain barrier and impaired tight junctions (Jackson et al., 2022). In addition aged ApoE4-TR animals also showed depression-like behaviour, as well as impaired glucose metabolism and mitochondria biogenesis in the hippocampus (Lin et al., 2022). Early-life stress in ApoE4-TR animals showed impairments in spatial memory, as well as decreased expression of synaptic proteins and loss of GABA-ergic neurons (Lin et al., 2016).

Another genetic risk factor for sporadic AD, TREM2, is modelled in the TREM2-NSS (normal splice site) mice. These mice are crossed with 5xFAD mice to understand the effect of TREM2 AD related pathological profiles. TREM2-NSS/5xFAD animals display dystrophic neurites, axonal damage, and reduced size and number of microglia. Aged mice of this model exhibit deficits in long-term potentiation and postsynaptic loss. Therefore, this model serves to better understand the effect of TREM2 on microglial mediated pathogenesis of AD (Tran et al., 2023).

1.10.2e) Other sporadic AD models:

In addition to these models, there are several others. For instance, the Streptozotocin induced rodent model (modelling metabolic dysfunction factor) display memory

impairments, along with pathological amyloidogenesis, tangles and inflammation (Elahi et al., 2016; Mehla et al., 2013; Rajasekar et al., 2017; Zhang et al., 2018) (refer to Table 1.3). Another well-known model, namely Senescence accelerated mouse model (which models the aging aspect), shows Aβ, Tau pathology and neurotransmitter dysfunction. Similarly, a traumatic brain injury induced model (Iwata et al., 2002; Wang et al., 2017), a metal-ion induced dysfunction (Walton & Wang, 2009) model, and few other models have been proposed as potential candidates for sporadic AD.

Overall, although these attempts at modelling the sporadic form of AD are commendable, and even necessary to advance AD research in a preclinical setting, there have been some significant disadvantages associated with these models (Zhang et al., 2020) such as poor drug absorption and absence of neuronal apoptosis, highlighting the need for discovery of new and alternate models.

Sporadic AD models:

Model	Method	Plaques	NFTs	Locomotor activity	Spatial memory impairment	Neuron loss	Neuroinflammation
Metablic damage model	ICV - streptocotozin	✓	✓	-	✓ after 2 weeks of injection	✓	✓ after 7 days of injection
TBI model	Control cortical Impact	✓	✓	-	✓ 3 days after injury	✓ After 3 days of injury	✓ after 6 months of injury
SAMP8	Senescence acceleration	-	-	-	Anxiety and depression like behavior	-	-
Aluminium neurotoxicity	Oral administration AlCl3	✓	✓	-	✓ after 6 weeks of injection	✓ after 6 weeks	✓ after 6 weeks
Acrolein induced model	Oral administration of acrolin	✓	✓	-	✓ after 8 weeks of injection	✓ after 8 weeks	✓ after 8 weeks

Table 1.3: List of sporadic AD models that have been used in preclinical research so far.

1.11) Behaviour assays used to assess anxiety and spatial memory in preclinical mouse models of Alzheimer's disease:

AD preclinical research employs numerous behavioural paradigms to assess cognitive impairments in preclinical mouse models of AD in a manner that is intended to replicate the cognitive impairments seen in individuals with AD. In this section, we will look at two of the major behavioural assays that are relevant to this thesis and are commonly employed in Alzheimer's models.

1.11.1) Anxiety measurement:

Anxiety is one of the prominent neuropsychiatric symptoms of Alzheimer's disease with a prevalence of 40% (Mendez, 2021). It is considered to be a prelude of AD, as it is witnessed in patients with Mild Cognitive Impairment and early stages of AD (Mendez, 2021).

Although anxiety is difficult to assess in rodents and is subject to limitations, such as the reduced cognitive capacity of rodents relative to humans as well as their inability to verbally express themselves, several assays have been developed to effectively measure anxiety-like behaviours in rodents. Two of the most common assays are the Open Field Test and Elevated Plus Maze test.

The open field test is performed in an open chamber; one that has walls to prevent escape but no ceiling, as seen in Figure 1.12 (left). Mice and rats naturally prefer confined spaces where, in the wild, they would be hidden from potential predators such as cats, or swooping birds (Gould et al., 2009). Exposure to an open chamber such as this therefore elicits anxiety-like behaviours from the mice, which causes them to avoid the centre of open field and try to hide in the corners or by the walls. During the test, the animals are

allowed to explore the chamber for a standard time, and their locomotor activity is assessed along with the time spent in the centre of the open field. Animals that spend longer in the centre are thought to be less anxious relative to animals who spend more time in the periphery (Gould et al., 2009).

The performance of several AD mouse models has been tested using the open field. For example, the familial AD model APP/PS1-KI was shown to be anxious in the open field test at 7 months, as these mice spent less time in the centre zone compared to the corner zone relative to wildtype controls (Webster et al., 2013). 3xTg-AD animals showed an anxiety effect that was sex-specific, with males displaying fluctuations in anxiety behaviour throughout 11 months age, whereas female 3xTg showed consistently higher anxiety-like behaviour relative to wildtypes, starting 2 months until 11 months of age. Moreover, this increase in anxiety was accompanied by the accumulation of phospho-Tau in AD relevant brain regions such as hippocampus, amygdala, and entorhinal cortex (Szabó et al., 2023) suggesting that it could be the cause.

A third model that has been shown to exhibit increased anxiety in the open field test in the TgCNRD8 model, as relative to wildtypes these animals were found to prefer to stay in the corner zone and avoid the centre zone. In this instance, behaviour was correlated with an increase in plaques, tangles, and glial cell numbers in the cortex and in hippocampal regions (Xu et al., 2023), which therefore suggested neural correlates of this anxiety. Finally, 24 month-old APP23 mice have also been shown to display increased anxiety-like behaviours by spending reduced time in the centre zone compared to corner zone (Giménez-Llort et al., 2021), although this study did not reveal the putative neural correlates of this behavioural change.

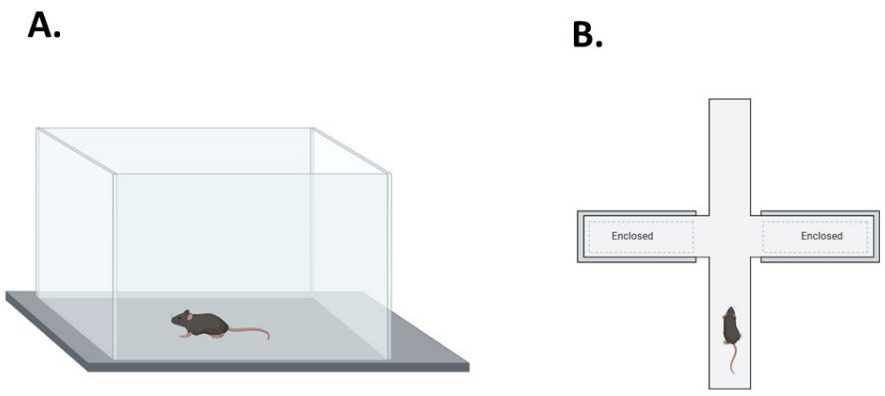

Figure 1.12: (Biorender), Schematic representation of Open Field (A) and Elevated Plus Maze (B) apparatus.

The Elevated plus Maze (refer to Figure 1.12 right) is a plus shaped maze which is placed at a certain height (usually 600-900m) from the ground level. This maze has two closed and two open arms. Anxious animals tend to spend more time in closed arms where they feel safe from falling and will typically avoid the open arms. Therefore, the time spent by the animals in open vs closed arms gives a measure of anxiety of the animal (Komada et al., 2008).

With regards to mouse models of AD, several have again been shown to exhibit anxiety-like behaviours, spending more time in the closed arms than the open arms relative to wildtypes. For instance, APP/PS1 mice show this pattern of results (Webster et al., 2013), as do 18 month old 3xTg animals. For the latter study, this behavioural deficit was paralleled by plaque accumulation in the subiculum region of the hippocampus and phospho-Tau in the CA1 region of hippocampus, with the female mice developing these pathologies more rapidly than the male mice, again highlighting a sex difference in this strain of mice (Dominic et al., 2021).

The APP$^{NL\text{-}G\text{-}F}$ model showed mixed effects when it comes to anxiety related behaviours. Whereas 8 months old APP$^{NL\text{-}G\text{-}F}$ animals were seen to spend less time in the centre of the open field chamber, thus displaying an anxiogenic profile, the same animals were seen to spend more time in the open arms compared to closed arms indicative of an anxiolytic behaviour. Although the reason for these contradictory results was not determined, the authors additionally observed increased damage to the prefrontal cortical region of the brain, which they suggested could account for the deficits seen in social and anxious behaviours (Giménez-Llort et al., 2021).

1.11.2) Spatial memory measurements:

As mentioned, people with AD experience severe impairments in spatial memory. Therefore, there are a number of different measures used in the laboratory to test spatial memory in rodents, including the Barnes Maze, and Morris Water Maze (MWM).

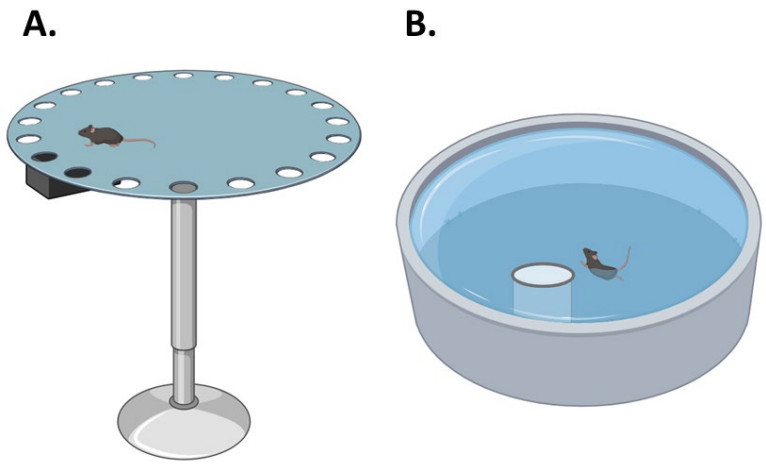

Figure 1.13: (Biorender), Schematic representation of Barnes Maze (A) and Morris Water Maze (B) apparatus. .

The Barnes maze is shown in Figure 1.13 (left) and uses a broad circular board with multiple holes on the board. Beneath one of these holes is an escape box, which the animal needs to navigate and find with the help of some visual cues. When tested, the escape box will be removed to check if the animal could remember the previous location of the box in the absence of feedback or cues. Animals with intact spatial memory will spend most of their time in or around the previous location of the box, even after it has been removed, suggesting that they are relying on their memory of the location and not external cues. Animals with impaired spatial memory tend to spend an equal amount of time in the prior location of the box as the other sections of the maze (Pitts, 2018).

The Morris water maze (shown in Figure 1.13, right) is a slight variation of this task except that it includes water into which mice are placed. During the acquisition phase, mice will learn to swim and locate a raised platform. This is a desirable outcome as mice find swimming aversive. On the test day, the platform is removed, and the time spent by animals in the quadrant where the platform was previously placed (target quadrant) is assessed to reveal whether the spatial memory of the animal is intact.

In addition to these tests, there are a few other variations of spatial memory tests including passive avoidance and contextual fear conditioning, which have an additional layer of fear encoding/memory associated with the spatial element (Ögren & Stiedl, 2010).

Most preclinical AD models showing impairments in spatial memory tests are accompanied by various pathological accumulations in the dorsal hippocampus, suggesting that this is the likely neural correlate of the deficit. For instance, 12-month old APP23 (with plaque accumulation and gliosis in the hippocampus) mice showed worse performance in the Morris water maze paradigm (i.e. longer time to learn the task, and

less time in the target quadrant on test) compared to age matched controls (Giménez-Llort et al., 2021). Several studies have found impaired performance on the Barnes maze in 3xTg mice as early as 6.5 months old, and this deficit was found to worsen with age showing a pronounced deficit in 12 months old 3xTg animals (Parachikova et al., 2010; Sterniczuk et al., 2010; Stover et al., 2015). This again was accompanied by increased amyloid plaque levels and neuroinflammation in the dorsal hippocampus. Similar to the 3xTg animal model, 5xFAD animals also show an impairment in spatial memory (Morris water maze) starting 5-6 months of age that appeared to relate to the altered expression of inflammatory markers in the hippocampus and cortical regions of these animals (Ullah et al., 2020).

A more recent study looked at cognitive deficits in APP/PS1 animals at 9 and 12 months of age and observed a significant reduction in cognitive performance in Morris water maze. This was however reversed when the animals were trained multiple times at different time points before being tested (Lonnemann et al., 2023). These findings are supported by those from a different group, who reported deficits in spatial memory of APP/PS1 mice starting at 4 months age, although dorsal hippocampal plaque pathology wasn't observed in these animals in the later time points of 6 and 12 months (suggesting an alternate source of these deficits) (Ji et al., 2023).

1.12) Interim summary:

Alzheimer's disease can be broadly classified into sporadic and familial forms. Familial AD has an early onset and accounts for a minor percentage of the cases, and sporadic AD has a late onset and accounts for a major percentage of the total cases. While familial AD has a defined set of mutations contributing to the aetiology of the disease, sporadic AD has a multifactorial aetiology. Genome wide association studies have reported ApoE4 to

be the strongest genetic risk factor for sporadic Alzheimer's, alongside TREM2, CLU, ABCA7 which are categorized low risk for AD. Environmental risk factors for AD include lifestyle risk factors like diabetes, obesity, metal ion exposure, pollution and mental health issues including depression and anxiety.

The vast majority of preclinical AD research has focused on modelling familial AD, which carries definitive gene mutations, like 5x-FAD, 3xTg, TgCRND8 and more. This has been detrimental to the understanding of the mechanisms of AD, because familial AD is present fewer than 5% of patients and these models – develop pathologies that might follow mechanisms similar to familial AD cases, not reflecting what happens in the sporadic AD cases (i.e, genetic mutations remain the source of Aβ accumulation in familial AD patients as well as familial AD models, however, there is no genetic background to the Aβ accumulation in sporadic AD cases and the mechanisms for this still remain elusive). The adverse effect of using such models is highlighted when considering a study by Van Dam and De Deyn in (2011), who listed a number of potential AD drugs that were in the pre-clinical stages of testing on familial AD models, describing their effectiveness in reversing the behavioural and pathological features of familial AD models. However, recent years of AD research has not seen a successful translation of these and other drug treatments in clinical trials (Aisen, 2019). Indeed, just 4 of the 146 drugs tested for AD was unsuccessful according to a 2019 statistics (*New Report Details the Setbacks and Challenges to Alzheimer's Research*, 2018) as shown in the Figure 1.14. This calls for a careful reconsideration of the approaches to modelling AD in pre-clinical research field. The study presented in the current thesis is therefore one such attempt to create a better preclinical model of Alzheimer's disease, specifically a sporadic model.

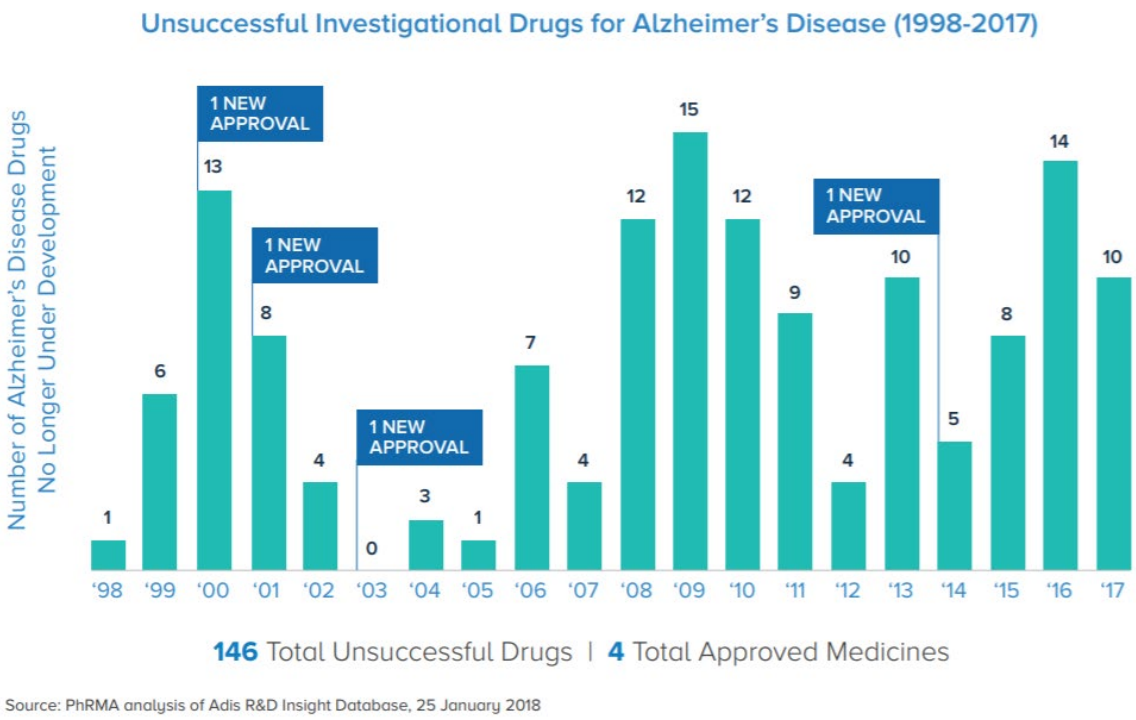

Figure 1.14: Graphical representation of success rates for Alzheimer's disease drugs; *Illustration reproduced courtesy of PhRMA.*

The question remains, however, of the best way in which to model sporadic forms of AD. Again, transgenic models can be used: several genes (e.g. APOE4) have been identified as risk factors for AD, although unlike familial AD genes, these mutations do not guarantee a diagnosis. Likewise, the human amyloid beta knock in (hAβ-KI) model carries wildtype the human amyloid beta sequence with no mutations, which can be used to determine whether this will result in the aggregation of amyloid beta plaques like that seen in human sporadic cases. Another factor that can be employed in the laboratory is neuroinflammation. Neuroinflammation, triggered through multiple pathways is being increasingly recognized as one of the central players in AD. Neuroinflammation is observed in various brain regions in Alzheimer patients, with a prominent example being the hippocampus. Because the hippocampus is crucial for learning and memory, atrophic hippocampus underlies the cognitive deficits in individuals with Alzheimer's. This

hippocampal degeneration/atrophy is characterized by loss of neurons (i.e. neurodegeneration). Neuron loss is further accompanied by the loss of synapses, which are the major sites of connection, paving way for cell-cell interactions. Collectively, these changes contribute to the progression of the observed behavioural and cognitive impairments in Alzheimer's disease.

1.13) Aim: Chapter 3

The aim of Empirical Chapter 3 of this thesis is

- To create a better sporadic AD mouse model, using a combination of genetic and non-genetic risk factors.

The first genetic risk factor I chose to employ was ApoE4, because it is the highest genetic risk factor for AD. The second risk factor I employed was human wildtype Aβ sequence (with no familial AD mutations). Each of these genetic risk factors was tested for behavioural and cellular changes alone and in combination with neuroinflammation. I also tested systemic and local neuroinflammation in the absence of these genetic factors. First, these models were investigated for locomotor and anxiety-like deficits using the open field test, as well as spatial memory deficits using the Barnes maze. Second, I investigated whether these models' produced elevations in markers associated with neuroinflammation as well as a loss in dendritic spines in the dorsal hippocampus.

2. Hippocampus and goal-directed action control in rodents as a model of activities of daily living deficits in Alzheimer's disease:

Chapter 2 provides the introduction to the experiments presented in the second empirical chapter: Chapter 4. Specifically, in the following chapter I will provide a more detailed background on the deficits in activities of daily living that are exhibited by individuals with Alzheimer's disease in addition to the behaviour deficits in spatial memory and anxiety that are discussed in Chapter 1. Furthermore, I will link these deficits to impairments in goal-directed action control – a thoroughly operationalized and well understood behaviour in the laboratory that we can study in animals to give us insights about goal-directed action in humans. Finally, I will review the neural circuits underlying these behaviours, and how this circuit interacts with that which is damaged in AD behaviour.

2.1) Activities of Daily Living (ADL) in AD:

Early diagnosis and treatment of AD could help slow its progression, keeping individuals healthier and independent for longer, which would improve the quality of life of the aging population and help mitigate the enormous healthcare costs of AD. As reviewed in Chapter-1, there are several behavioural and cognitive deficits that are central to Alzheimer's disease, such as memory loss and impaired spatial memory. These symptoms start becoming apparent in the Mild Cognitive Impairment stage, which is a prelude to dementia. In recent years, researchers have developed sensitive techniques to identify the

progression from mild cognitive impairment to Alzheimer's dementia with a view of enabling earlier diagnosis of this disorder. One such diagnostic measure is the assessment of Activities of Daily Living (ADL; (Potashman et al., 2023). Indeed, according to the 'National Institute of Ageing' clinical diagnosis criteria, a person can only be diagnosed with Alzheimer's if their cognitive deficits "are significant enough to impair a person's ability to function independently" ((NIH), 2020). Therefore, diagnostic tools like ADL scales intervene here by measuring the independent functioning of an individual, in order to determine whether an individual's disease has progressed from MCI to AD. In the following section, I will introduce ADLs, their different types, and how they are impaired at different stages of AD.

2.1.1) What are Activities of Daily Living?

Activities of Daily Living assessments are, as the name suggests, a set of tasks designed to evaluate the patient's ability to execute day-to-day activities. In addition to identifying the progression from Normal Cognition to Mild Cognitive Impairment to Alzheimer's, ADL assessments track the course of Alzheimer's development, enabling healthcare professionals to customize assistance and personal care to patients (Edemekong et al., 2023; Reisberg et al., 2001). There are two types of ADLs – basic and instrumental, and these are discussed in detail in the following section.

2.1.1a) Basic ADL:

Basic ADL assessment comprises activities that are key to an individual's independent functioning. These include measurements of 'ambulation' – an individual's ability to move around/walk and reach places within short distances independently, 'eating' – the person's ability to eat, including chewing and swallowing, maintaining personal 'hygiene' – an individual's ability to groom oneself and maintain a proper appearance and hygiene,

and ‘bathing/toileting’ – the person’s ability to use the bathroom and toilet including cleaning up after themselves. Impairments in basic ADLs are most apparent during moderate to severe stages of AD, where patients become extremely dependent on care givers for their daily activities (Edemekong et al., 2023; Marshall et al., 2012).

2.1.1b) Instrumental ADL:

Instrumental ADLs (IADLs) refer to everyday goal-directed actions that require conscious thinking, planning, and organization. Instrumental ADLs are observed in MCI and mild AD stages where patients start showing deficits in executive function and decision-making skills. There are many examples of instrumental activities of daily living. For example, transportation refers to a person’s ability to properly use transport systems and driving, and organizing alternate means of transport, there’s also shopping and meal preparation, referring to the person’s ability to shop for what’s needed and remembering step by step procedures of preparing a meal. Another such activity is house cleaning and maintenance, indicating an individual’s ability to perform necessary actions to maintain order and hygiene at home, including cleaning and doing laundry and getting essential things to keep the house functional.

Instrumental ADLs also refer to more complex activities, such as managing finances and communication. Managing finances refers to the ability to assess one’s own financial status, pay bills and manage assets, and managing communication referring to the person’s ability to appropriately communicate with others and remembering how to contact people via various modes of communication. Managing medications is also important and refers to an individual’s ability to keep track of their health conditions and take necessary medicines at the right time as directed. The most commonly used

Instrumental ADL assessments was developed by Lawton and Brody in the year 1969 which is still employed in AD diagnosis (Lawton & Brody, 1969)behaviour.

2.2) Deficits in Goal-directed action/decision-making in AD:

These activities of daily living are broadly equivalent to goal-directed actions as they have been studied in animals and humans for a number of years (Balleine & Dickinson, 1998b). As mentioned in Chapter-1, the majority of pre-clinical AD research focuses on understanding memory loss, avoidance, recognition and visual/spatial problems, without actually focusing on how these problems translate into the types of functional outcomes listed above in the activities of daily living. This is problematic because cognitive deficits such as memory loss in AD are often limiting for individuals precisely because of how they interfere with the individual's ability to perform a wide range of tasks. For example, it is of little consequence if an individual forgets what groceries they need whilst they are walking the dog, but it becomes an issue once the individual enters the shop to buy the groceries. Therefore, failing to capture this complexity at a preclinical level means that these models are failing to capture the scope of cognitive-behavioural deficits of AD. This could be contributing to problems with translatability if, for instance, treatments are tested on such models and found to be effective in treating memory loss alone but are not tested for their capacity to restore goal-directed action control. As a result, when translated, the treatment may treat only partially treat the symptoms of AD.

From this, I would suggest that simply capturing deficits in memory and visuo-spatial abilities in preclinical models of AD is not sufficient, either for understanding the full biophysiological mechanisms of the disease or for treating its full scope. Therefore, it is

the second primary aim of this thesis (addressed in Chapter 4) to better capture deficits in goal-directed action in a mouse model of AD. The nature of this model was determined by the results of Chapter 3, which demonstrated that of all the models of sporadic AD that I tested, only lipopolysaccharide injected into the dorsal hippocampus produced evidence of both elevated neuroinflammatory marker expression and significant loss of dendritic spines. I therefore tested whether mice with hippocampal neuroinflammation were also impaired in their ability to produce goal-directed actions and investigated the potential mechanisms of doing so.

Although the testing of potential treatments for these deficits is beyond the scope of the current thesis, it is hoped that the results I present will produce a deeper understanding of the neuropathological mechanisms of goal-directed deficits in AD with a view that this information might be used to test treatments in the future in a manner that will translate more effectively to humans.

2.3) Goal-directed actions:

Goal- directed action selection refers to the selection of actions that are performed with the expectation of them resulting in particular desired outcomes. For instance, a person approaching a vending machine, inserts money and presses the relevant button that delivers the exact chocolate bar that was desired by the person. In this scenario, inserting cash and pressing the button are considered actions that resulted in the chocolate bar outcome, which was the food desired. Goal-directed actions are contrasted with habits that are elicited automatically and in response to surrounding stimuli rather than in pursuit of a particular goal. For instance, when driving you might habitually take a turn that you usually take to go to work, even on the weekend when your goal was to drive to the beach. To the best of our knowledge, it is only goal-directed action control that is

affected in AD, whereas habit learning has been shown either to be intact (Eldridge et al., 2002), or to have clinically insignificant (De Wit et al., 2021) deficits relative to healthy controls.

Nevertheless, testing goal-directed actions in rodents in the laboratory does pose certain challenges. For instance, whereas an individual who presses a button for a particular chocolate bar on a vending machine can tell you that they did so with intention, rodents cannot do the same. As such, it is impossible to determine from simple observation whether a mouse might be pressing a lever in order to receive a food pellet, or whether they are doing so because they have pressed the lever so many times previously that it has become an automatic habit in the presence of the stimuli that surround the lever. Therefore, in order to distinguish between goal-directed actions from habits in the laboratory, Balleine and Dickinson stated that only goal-directed actions are motivated by both (i) the value of the outcome, and (ii) the knowledge of contingency between the action and outcome (Balleine & Dickinson, 1998a; Dickinson & Balleine, 1994). The gold standard protocol that is used in the laboratory to test whether actions conform to these criteria is known as devised 'outcome devaluation' invented by Rescorla (Colwill & Rescorla, 1985).

2.3.1) Outcome devaluation

Outcome devaluation has been described across a number of species (as reviewed below), but here I will focus on the rodent version as this is the topic of the current thesis. The rodent version of devaluation has three distinct phases. The first of these is an acquisition/learning phase during which animals are trained to press two levers that each delivering two distinct food outcomes. For example, as shown in Figure 2.1, a mouse might be taught to press a left lever for a sucrose solution and a right lever for a grain pellet (or

the opposite contingencies, counterbalanced). This is followed by a devaluation phase where the mouse is pre-fed to satiety on only one of the two outcomes (in Figure 2.1 this is shown as pellets). This pre-feeding procedure has been shown to reduce the value of the pre-fed outcome relative to the other (Balleine & Dickinson, 1998a). An analogous experience for humans might be when pizza becomes devalued after eating 4-5 slices, but ice cream is still desired. Finally, there is a test phase in which mice are given a choice between the two levers but food outcomes are not presented. When faced with such a choice, a goal-directed animal will selectively press the lever associated with the valued outcome and avoid the lever associated with the devalued outcome (in Figure 2.1 the left lever is valued and the right lever devalued).

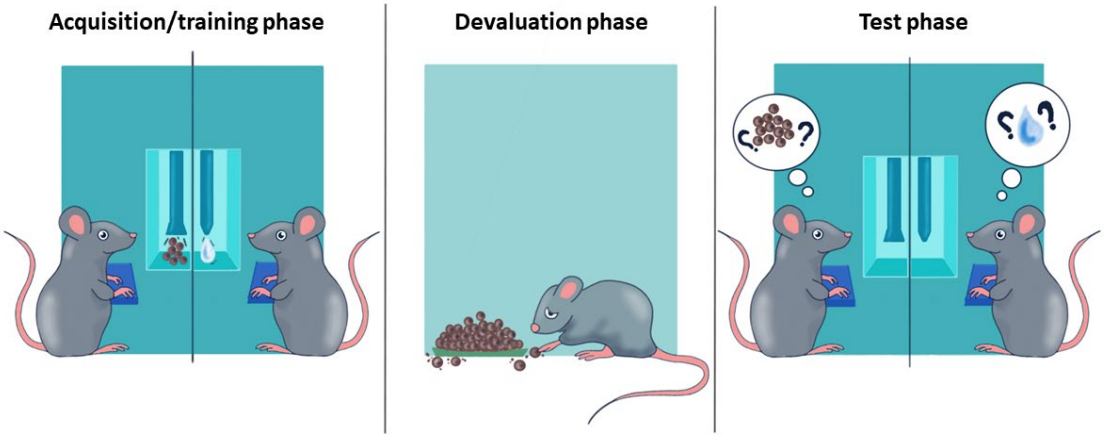

Figure 2.1: Pictorial representation of outcome devaluation procedure; acquisition phase (on the left where animals are trained to press levers), devaluation phase (where animals are devalued on one of the outcomes, usually counterbalanced), test phase (on the right, where animals are given levers, with no actual outcome being presented).

Animals that successfully perform outcome devaluation by responding selectively on the valued lever and avoiding responding on the devalued lever, demonstrate that their action is motivated by the current value of the outcome, thus fulfilling the first criterion of goal-

directed action. Moreover, because animals are tested in the absence of the food outcomes, animals must rely on their memory of which lever had earned which outcome during training in order to show this result, thus fulfilling the second criterion of goal-directed actions. Animals that show this result (Valued > Devalued) are thus acting under goal-directed control, whereas animals that press both levers equally (Valued = Devalued) are not.

2.3.2) Outcome devaluation as a model of functionality:

In order to perform outcome devaluation effectively, animals must not only have their memories intact (i.e. to remember which lever previously earned which outcome), but must also be able to integrate this with information about which outcome is currently most valuable as well as a motor command about which lever to press. In this way, outcome devaluation provides a sophisticated assessment of how memory is integrated with affective information and motivational state to produce a functional response. As reviewed above, this is precisely the type of behaviour that is impaired in individuals with AD and that has been lacking from preclinical models so far.

Although rodent models will only ever be just that – a *model* of real-world cognitive deficits, and not a faithful recapitulation of the actual cognitive/behavioural deficits observed in individuals with AD – there is reason to believe that the results from outcome devaluation studies might be both translatable to humans and predictive of cognitive deficits that occurs in various disorders and diseases. First, as well as being performed across a range of species other than mice, such as rats (Iguchi et al., 2017; Keefer et al., 2020) and monkeys (LaFlamme et al., 2022); there are a number of studies in which human versions of the outcome devaluation task has been investigated (Friedel et al.,

2014; Iain et al., 2022). In these versions, lever presses are typically replaced with button pushes, the stimuli comprise various shapes or pictures flashed upon a computer screen, food outcomes might include various types of juice, chocolates, and chips, which can be devalued by being fed to satiety, just as they are in mice. Another version of this task even replaced food with monetary outcomes (Sjoerds et al., 2016).

Second, there are now a number of findings to suggest that outcome devaluation performance is consistently impaired in a wide range of neurological disorders. For instance, people with Autism Spectrum Disorder (Alvares et al., 2016), Schizophrenia (Morris et al., 2018) and Parkinson's disease (de Wit et al., 2011) demonstrate deficits in outcome devaluation. Of particular interest is a study by Alvares et al., (2014), which reported that people with social anxiety disorder displayed impairments in goal-directed action as measured using an outcome devaluation task. Moreover, this impairment predicted individual's real-world functionality, because it correlated with their responses to cognitive-behaviour therapy. Specifically, individuals with this disorder who performed better on the outcome devaluation test were more successful in their ability to override negative/unhealthy thoughts and approaches by altering their actions, and individuals who did poorly on devaluation testing responded less well to therapy. Therefore, although outcome devaluation has yet to be tested in individuals with Alzheimer's disease, possibly due to the overwhelming focus of studies on memory deficits in particular, these examples clearly demonstrate that it does have value as a procedure both in its translatability to humans as well as its ability to predict how well those individuals function outside of the laboratory.

2.3.3) Brain Mechanisms of Goal-Directed Action

In Chapter 1 I reviewed the role of atrophy and neurodegeneration of the hippocampus in AD, as well as hippocampal anatomy and circuitry more broadly. Neuropathological features within the hippocampus (such as neuroinflammation), thus comprise an excellent candidate for the source of AD-related impairments in goal-directed action. Thus, in order to identify how deficits in goal-directed action might arise from the pathophysiological features of AD, in the following section I will review the brain regions and circuits involved in goal-directed action selection, with a particular focus on dorsal hippocampus and the structures connected to it (directly and indirectly).

2.3.4) Rodent and human brain structure homology:

It has been well documented in the literature that humans and rodents share brain structure homology between the regions associated with goal-directed action control. Functional MRI (Magnetic Resonance Imaging) in particular has been a key player in understanding the human brain structures involved in goal-directed behaviours. Such studies can be compared to lesion or inactivation studies in rodents to confirm that each brain region and/or circuit plays a causal role in producing such behaviours. A lengthy review of these studies and the degree of homology of each region within this circuit was provided by Balleine and O'Doherty (Balleine & O'Doherty, 2010). This study confirmed that there is a high degree of homology between each brain region and circuit between rodents and humans, and thus suggest the legitimacy of studying this circuit in rodents in a manner that allows us to make causal and precise implications about the consequences of disruptions to this circuit for behaviour. The following sections will therefore focus on

the brain regions and circuits underlying goal-directed action in rodents, as mice are the focus of the current thesis.

2.3.5) Neural basis of learning goal-directed actions

A simplified representation of the neural structures and circuits that underlie goal-directed action is shown in Figure 2.2.

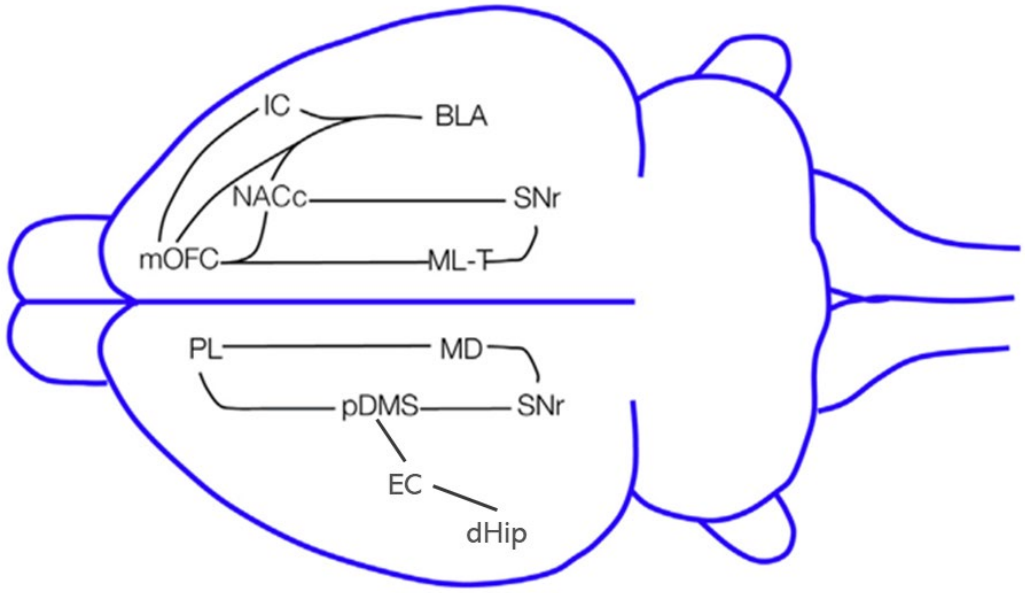

Figure 2.2:; Neural circuits involved in incentive learning and action-selection (upper hemisphere) mOFC – medial orbitofrontal cortex, NACc – nucleus accumbens core, IC – infralimbic cortex, BLA – Basolateral amygdala, SNr – substantia nigra, ML-T – mesolimbic tract, action-outcome contingency (lower hemisphere) PL – prelimbic cortex, MD – mediodorsal thalamus, pDMS – posterior dorsomedial striatum, EC – entorhinal cortex, dHip – dorsal hippocampus. *Image adapted from Bradfield and Balleine, 2017.*

In individuals with AD, it is possible that there are changes to all the brain regions such as prefrontal cortex, basolateral amygdala, and nucleus accumbens, mentioned here in the figure, however, since hippocampus is the first and extensive region to be affected in AD, we only focused on manipulations in the hippocampus for this project. As mentioned, goal-directed action selection is a complex process involving the integration of several other processes. One of these sub-processes is the learning of 'what leads to what' i.e., which action earns which outcome. With regards to action-outcome learning, three regions of the brain play an important role. They are, prelimbic cortex (PL), mediodorsal thalamus (MD), and posterior dorsomedial striatum (pDMS) (Bradfield & Balleine, 2017).

The prelimbic cortex forms a part of the medial prefrontal cortex. The mediodorsal thalamus forms part of medial thalamus and it is one of the largest nuclear structures in rodents. All four segments of the medial thalamus (medial central, lateral, and paralamellar) are distinctly connected to the prefrontal cortex (Mitchell & Chakraborty, 2013), and the mediodorsal thalamus in particular is strongly and reciprocally connected with the prelimbic cortex. The pDMS is part of the basal ganglia, and also receives inputs from the prelimbic cortex, but is not directly connected with the mediodorsal thalamus (Vandaele et al., 2019). This means that any information accrued by the mediodorsal thalamus during action-outcome learning is likely relayed to the pDMS via the prelimbic cortex.

Early evidence suggesting the involvement of the prelimbic cortex in action-outcome encoding was presented by Balleine and Dickinson (1998b) when they gave excitotoxic prelimbic lesions to rats prior to lever press training in a similar outcome devaluation paradigm to that described above. On test, sham controls demonstrated evidence of having learned goal-directed actions because they responded more on the valued relative

to the devalued lever on test. However, lesioned animals responded equally on both levers suggesting that their goal-directed actions were impaired. Later studies showed that the prelimbic cortex contributes only to the learning of action-outcome contingency but does not store these associations, because outcome devaluation was intact for animals that were given excitotoxic lesions of prelimbic cortex after lever press training but before testing (Ostlund & Balleine, 2005). Later evidence added strength to this argument, because it was found that phosphorylation of extracellular signal regulated kinase (p-ERK), a cellular activity marker, increases within 1-hour after initial lever press training, but does not increase at later timepoints, suggesting that PL is only involved in the early stages of learning (Hart & Balleine, 2016).

Pre- but not post-training excitotoxic lesions of the mediodorsal thalamus in rats also impair outcome devaluation (Corbit et al., 2003; Ostlund & Balleine, 2008). Because of these similar findings regarding mediodorsal thalamus and prelimbic cortex, as well as the fact that strong reciprocal connections exist between these structures, Bradfield et al., (2013) conducted a study to determine whether the circuit between the two structures was also necessary for learning action-outcome contingencies. They excitoxically lesioned the PL of one hemisphere and the MD of the other hemisphere, and because these structures also communicate contralaterally, they also electrolytically lesioned the part of the corpus callosum that carries these signals across the two hemispheres (Bradfield et al., 2013). Animals with sham lesions, or with the PL-MD connection intact in one hemisphere (ipsilateral controls) showed intact devaluation performance (Valued > Devalued), whereas animals with contralateral lesions and therefore no intact circuit in either hemisphere were impaired (Valued = Devalued). This suggested that interplay between these two structures is necessary for learning action-outcome contingencies.

Later studies have shown that the posterior dorsomedial striatum is also involved in learning goal-directed actions, but unlike prelimbic cortex and mediodorsal thalamus, it is also involved in storing the knowledge of those actions and their outcomes. This is because both pre and post-training lesions/inactivation of the posterior dorsomedial striatum impair outcome devaluation performance (H. H. Yin et al., 2005; Henry H. Yin et al., 2005). Altogether then, these studies indicate that the action-outcome contingency knowledge encoded in the prelimbic cortex and mediodorsal thalamus is then relayed to the posterior dorsomedial striatum where it is stored (Bradfield & Balleine, 2017).

2.3.6) Neural basis of the performance of goal-directed action:

Two regions – in addition to the posterior dorsomedial striatum - that play an important role in the performance of goal-directed actions are medial orbitofrontal cortex and the Nucleus Accumbens core in the ventral striatum (Bradfield & Balleine, 2017). Medial orbitofrontal cortex, like prelimbic, also forms a part of the prefrontal cortex (Shannon et al., 2016).

Like the prelimbic cortex and mediodorsal thalamus, pre-training excitotoxic lesions of the medial orbitofrontal cortex and nucleus accumbens core also impair performance on outcome devaluation. However, because lesions are permanent, they are present during both training and test, making it difficult to tease apart whether these structures are specifically involved in the learning that occurs during training or the selection of goal-directed actions on test. However, further testing has shown that unlike prelimbic cortex and mediodorsal thalamus, post-training inactivations of medial orbitofrontal cortex also abolish outcome devaluation performance (Bradfield et al., 2015; Bradfield et al., 2018). With regards to the nucleus accumbens core, animals with lesions of this structure were able to learn another measure of goal-directed action called contingency degradation,

suggesting that it was the performance but not the learning that was specifically impaired in these animals (Balleine et al., 2015; Corbit et al., 2001). It is notable that the medial orbitofrontal cortex projects directly and densely to the nucleus accumbens core, suggesting that the two structures likely act in concert to produce intact goal-directed action selection, although direct evidence for this hypothesis is currently lacking.

In addition to inputs from the medial orbitofrontal cortex, the Nucleus accumbens core receives inputs from the basolateral amygdala and insular cortex. Moreover, and lesion studies abolishing the connections between the nucleus accumbens core and either the of these structures (Parkes et al., 2015; Shiflett & Balleine, 2010) has decreased the animal's ability to choose the appropriate goal-directed action. From the specific results of these studies, it has been hypothesized that the changes in reward value are encoded in the basolateral amygdala, retrieved through the insular cortex, which is then aligned with information about the sensory-specific characteristics stored in the medial orbitofrontal cortex that conveys this processed information to the nucleus accumbens core to guide the performance of the right choice (Bradfield & Balleine, 2017).

2.4) The role of hippocampus in goal-direction action:

In Chapter 1 of this thesis, I looked at the anatomy and functions of hippocampus from a broader perspective of learning and memory. In the following section, I will explore hippocampal functions related to spatial decision-making, and how these fit in to the bigger picture of goal-directed action selection.

2.4.1) The interplay between OFC and hippocampus:

Hippocampus has long been appreciated for its role in 'spatial mapping': capturing a representation of the environmental cues and context to create a space map which would

facilitate navigation through that space. In 1948, Tolman established a 'cognitive map' function for hippocampus, where he proposed that hippocampus integrates the external sensory cues with the internal states of emotion/motivation to achieve a specific relevant outcome (Tolman, 1948). Recording hippocampal neuron firing (place cells firing) patterns has given some valuable insights into the versatility of hippocampal functions. Place cells are specific neuronal cells in the hippocampus that are activated when an animal enters/navigates through an environment. These cells were first described by O'Keefe (1976) and detailed place cell firing analysis has been carried out ever since, to determine the involvement of hippocampus in a range of spatial and decision-making tasks.

In accordance with Tolman's proposal of a 'cognitive map' Kennedy and Shapiro (2009) analysed place cell firing patterns and provided evidence for the influence of motivational state to perform a goal-directed action in the given context. The context here was a wooden trident box which held food and water in one of the arms and the animals were either food deprived or water deprived before the testing procedure and the animal's approach to the appropriate arm was recorded. Firing patterns were from the CA1 region of hippocampus during the animal's goal-directed action (entering arms to receive outcome). Another study by Hok et al., showed that place cell firings are clustered near the 'goal-locations' in a water-maze spatial navigation task (Hok et al., 2007). These studies suggest that not only does the hippocampus contain a cognitive map of the environment, but that information about goals and their locations is also represented here.

Additional evidence for this conclusion was provided by a study that employed a T-maze task (as seen in Figure 2.3) (Adam & Redish, 2007). In this task, rats learned through trial

and error whether turning left or turning right would result in getting a reward. During the training phase, when the rats were still figuring out the reward contingencies, they would pause before deciding to turn left or right. This pause behaviour has been termed Vicarious Trial and Error (Tolman, 1939) and is hypothesized to reflect cognition during which the rats are simulating the potential consequences of each action to be taken before choosing which action to take. Hippocampal place-cell firing patterns were observed during this phase to reveal that hippocampus is aiding this decision-making process by projecting future paths that were likely to result in reward.

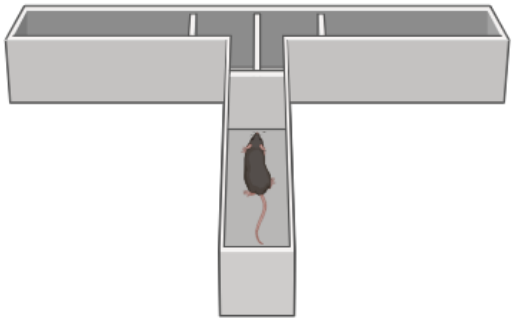

Figure 2.3: (Biorender); A representation of T-maze test.

In the previous section I highlighted the importance of orbitofrontal cortex in performing goal-directed actions. It is notable, then, that during the same T-maze task used by Adam and Redish to assess hippocampal contributions to decision-making, orbitofrontal cortical neurons responded while rats were receiving rewards in the training trials. Moreover, it was found that these same neuronal ensembles were those which were active when checked during the Vicarious Trial and Error phase (Steiner & Redish, 2012). This activation was found to occur approximately during the expected time at which the hippocampus is assessing which future course to take. These results could imply, therefore that during spatial decision-making tasks, the hippocampus evaluates the

potential courses available and sends this information to orbitofrontal cortex, which then evaluates the choices based on reward contingencies to determine the best action possible (Steiner & Redish, 2012).

This apparent synergy between the behavioural functions of the hippocampus and orbitofrontal cortex is accompanied by reports of both direct and indirect projections between the two structures (Wikenheiser & Schoenbaum, 2016). In particular, the CA1 region of the hippocampus and subiculum sends fibers to both the prelimbic and medial orbital cortices (Jay & Witter, 1991). Orbitofrontal cortex returns these projections to CA1 through indirect projections via parahippocampal structures like entorhinal cortex, perirhinal and postrhinal cortices (Witter et al., 2000). Other potential indirect pathways of communication between hippocampus and orbitofrontal cortex include the convergence of direct projections from each structure in Ventral Tegmental Area and ventral Striatum. The following figure details the connection between the above-mentioned regions (Wikenheiser & Schoenbaum, 2016).

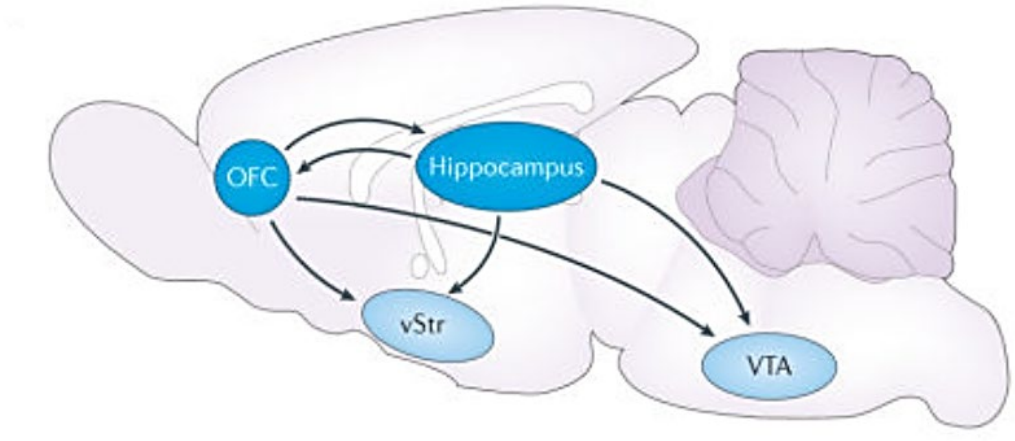

Figure 2.4: Direct and indirect connections between orbitofrontal cortex (OFC) and hippocampus; *Image adapted from Wikenheiser and Schoenbaum 2016.*

2.4.2) Hippocampal lesion studies:

In the following sections, I will review the evidence implicating the hippocampus in goal-directed actions more specifically, as opposed to spatial decision-making more generally.

The very first evidence that the dorsal hippocampus might play a role in goal-directed learning and/or action selection was provided by Corbit and Balleine. First they performed a classical outcome devaluation experiment and a second set of experiments with a slight variation made to the outcome devaluation paradigm – contingency degradation in rats (Corbit & Balleine, 2000). For the contingency degradation phase, each lever continued to earn each outcome (e.g. left lever-pellets, right lever-sucrose), but one of the outcomes was also delivered 'freely'- i.e. unearned by presses on either lever. For instance, if pellets were delivered freely, animals learned that they no longer needed to press the left lever to earn the pellets. This served to degrade the left lever-pellet contingency. However, rats still had to press the right lever to earn sucrose such that the right lever-sucrose contingency remained nondegraded. Rats that learned how to do this (i.e. respond more on the nondegraded relative to the degraded lever) thus fulfilled the second criterion of goal-directed actions: responding in accordance with the action-outcome contingency.

Electrolytic lesions were made to the dorsal hippocampus and the rats underwent outcome devaluation using a procedure similar to that described above. Here it is important to note that the lever press acquisition phase lasted 10 days (i.e. 10 lever press training sessions in total, 1 per day). Outcome devaluation performance was intact for all animals on test (Valued > Devalued), regardless of group. When tested for sensitivity to contingency degradation, however, only the sham rats demonstrated such sensitivity (Nondegraded > Degraded) whereas rats with hippocampal lesions did not (Nondegraded

= Degraded). Together, these results provided partial evidence that the dorsal hippocampus might some role in goal-directed action learning and or performance, specifically with regard to the ability to respond in accordance with changes in action-outcome contingency. With some additional research, it became apparent that damage to entorhinal cortex projections in the hippocampus had occurred in this initial study as a result of the electrolytic nature of these lesions, and that this damage specifically was responsible for the observed deficits (Corbit et al., 2002). This is because when excitotoxic lesions of the dorsal hippocampus were administered in a later study that left entorhinal projections intact, both devaluation and degradation were also found to be intact (Corbit et al., 2002).

Taken together, these studies reported limited (if any) evidence for the involvement of dorsal hippocampus in goal-direction action. However, this seemed to be at odds with the aforementioned studies of spatial learning in which hippocampal activity reflected goals (Adam & Redish, 2007; Steiner & Redish, 2012), as well as neuroimaging studies in humans (Schuck & Niv, 2019; Vikbladh et al., 2019) that indicated a role for hippocampus in goal-directed action using non-spatial tasks. One key difference between these neuroimaging studies and the rodent studies conducted above was the fact that humans are typically only trained on tasks for a short period of time (1-3 days) whereas the rodents in the studies above were lever press trained for 10 days. This is important, because the dorsal hippocampus has a well-documented role in initial learning that often becomes independent of the hippocampus over time (Bradfield et al., 2020; Schuck & Niv, 2019; Zhou et al., 2019). Therefore, learning and expression of goal-directed actions might also be temporally transient in a way that was not captured by the lesion studies that involved multiple days of training. This is explored in the next section.

2.4.3) Goal-directed actions transiently depend on dorsal hippocampus:

In 2020, (Bradfield et al., 2020)used chemogenetics to identify a transient role for dorsal hippocampus in goal-directed action. Briefly, chemogenetics refers to Designer Receptors Exclusively Activated by Designer Drugs (DREADDs), which are a genetically engineered version of G-protein coupled receptors. These designer receptors can be used to control cellular activity in a wide variety of cell types. DREADDs are typically packed within viral vectors which can then be introduced into cells using cell type specific promotors. Once integrated into the cell, the receptors can be activated with designer drugs such as Clozapine N-Oxide (CNO) (Figure 2.5). This can lead to either activation of a series of signalling cascades within the cells in case of M3 muscarine DREADD, or results in silencing the activity of the cell which is M4 muscarine DREADD (Whissell et al., 2016).

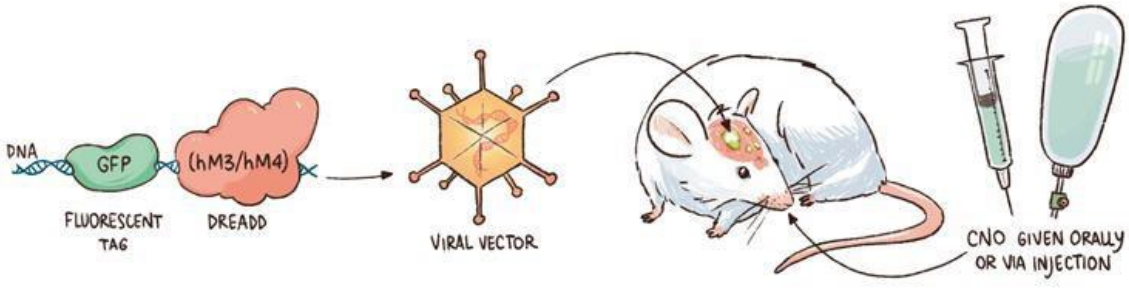

Figure 2.5: Schematic representation of DREADDs – transfection and activation in rodents; *Illustration reproduced courtesy of Claudia Flandoli/Adapted from a scheme by William Ju.*

Using M4 DREADDs, Bradfield et al, selectively silenced the dorsal hippocampus either during lever press training or test. This time, however, rather than receiving 10 days of lever press training (as in previous studies of hippocampus in goal-directed action), rats

in this study only received lever press training across 1-2 days until they reached a criterion of 20 outcomes on each lever (approx. 20% of rats did not reach this criterion and were excluded). Control animals that received vehicle injections or CNO injections paired with a non-active version of the adenovirus (i.e. AAV-hSyn-mCherry) demonstrated intact outcome devaluation (Valued > Devalued), whereas animals that received both the M4 DREADD virus and CNO injections to inactivate the dorsal hippocampus were impaired (Valued = Devalued). Moreover, animals that received transfection of the M4 DREADD localized to the CA2 region of the hippocampus were also not impaired, suggesting that it was the CA1 region specifically that moderated the effect. When the same animals were later given 4-5 additional days of lever press training and tested again, devaluation was intact for all rats, regardless of hippocampal inactivation. Together, these results suggested that the dorsal hippocampus, and likely CA1 in particular, regulates goal-directed action for a short time during/after initial learning but that goal-directed action becomes hippocampally independent after multiple days of training.

Based on these findings, (Dhungana et al., 2023) hypothesized that they might observe a similar behavioural impairment in the J20 model of Alzheimer's disease as these animals express a number of neuropathological features in their dorsal hippocampus, such as markers of neuroinflammation, amyloid plaque aggregation, and neuronal loss. Unlike rats, wildtype mice needed a minimum of 4 days of lever press training to demonstrate an intact outcome devaluation effect. When tested after these 4 days, however, wildtype mice demonstrated evidence of intact outcome devaluation (Valued > Devalued) just as control rats did in the previous study, and as expected, devaluation was impaired (Valued = Devalued) in 36 and 52 weeks old J20 mice. Again, this effect was overcome after additional lever press training, which in this study lasted for 4 days, after which all mice

they showed intact outcome devaluation (Valued > Devalued) regardless of genotype. These findings suggested that J20 mice were initially impaired in their learning/expression of goal-directed action, but that this deficit could be overcome with additional lever press training.

Interestingly, this study also provided a possible molecular mechanism underlying the hippocampal involvement in J20s. By performing a correlational analysis on the number of activated microglial cells Ionized calcium binding adapter molecule1 (Iba1) and performance on the first devaluation test that had occurred after 4 days of lever press training, Dhungana et al., found a significant negative relationship. This showed that animals with more microglial expression in their dorsal hippocampus performed more poorly on this initial test. When a similar analysis was performed with the same Iba1 expression correlated with performance on the second devaluation test (i.e. that conducted after 8 days of lever press training), no such relationship was detected. Together, these results suggested that neuroinflammation in the dorsal hippocampus might have caused the initial impairments in goal-directed action but had no impact on goal-directed action after multiple days of training.

This study is interesting for two reasons. First, it is the first demonstration of goal-directed deficits in a preclinical mouse model of AD, and second, it suggests the possibility that these outcomes could be overcome with additional training. If translatable, this could suggest that individuals with AD might also be able to overcome their impairments in everyday goal-directed activities of daily living. Nevertheless, these findings were once again detected using a familial model of AD and has not been shown in a sporadic model. This will be addressed in the current thesis.

2.5) Interim summary:

In order for individuals to progress from a diagnosis of mild cognitive impairment to Alzheimer's, the NIH states that their cognitive deficits must impair their ability to function independently ((NIH), 2020). This ability is measured by scales referred to as Activities of Daily Living (Potashman et al., 2023), with people with AD having been shown to experience difficulty performing everyday tasks and requiring additional support. In the laboratory, the ability to perform everyday tasks in a goal-directed manner is referred to as "goal-directed action" and other forms of action control (e.g. habit) have been shown to be minimally affected in AD. In both humans and animals, outcome devaluation is the gold-standard test for measuring goal-directed actions that has been shown to be predictive of real-world functionality.

As mentioned, there has only been one preclinical study investigating outcome devaluation performance in an animal model of AD, and that was performed in the J20 familial AD model. In this (Dhungana et al.,'s) study, it was found that 36- and 52-week-old J20 mice experienced initial impairments in goal-directed action control that recovered after animals were given additional training. Although interesting, these results are again subject to questions about the translatability, since familial AD represents less than 5% cases. Therefore, it is the second aim of this thesis to determine whether such results can be replicated in a sporadic model of AD, the nature of which was determined by the results of the first empirical Chapter (Chapter 3).

2.6) Aim: Chapter 4

Chapter 4 of this thesis aimed at

- To improve translatability of the identified sporadic model of Alzheimer's disease from a behavioural standpoint, by determining if it impairs goal-directed action control

To achieve this aim, the experiments reported in Chapter 4 trained sham or sporadic mice (mice with neuroinflammation in the hippocampus) to perform outcome devaluation after 4 or 8 days of training. It was expected that hippocampal neuroinflammation would impair initial goal-directed action but that performance would recover with additional training (i.e. that it would impair devaluation performance on the 4 day test but not the 8 day test). Because prior studies have identified sex differences in the abilities of male and female mice to perform goal-directed actions (Dhungana et al., 2023) I decided to separate the male and female cohorts. Once behaviour was complete, animals were culled and I then performed a series of cellular analysis, checking for glial cell and neuronal activation, and determining if these changes correlated these with the behavioural differences we observed.

RESULTS
(Chapters 3 and 4)

3. Combining major risk factors (genetic and non-genetic) to generate a sporadic AD model:

3.1) Introduction:

Preclinical AD research predominantly employs familial AD models which have a definitive genetic inheritance and differ widely from the sporadic form of AD , both in terms of the onset and progression of disease. A major concern here regarding is the fact that only ≤5% of AD patients have familial form of AD and the rest 95% of patients suffer from sporadic/late onset AD which has a complex and multifactorial aetiology (Sasanka Chakrabarti et al., 2015; Dorszewska et al., 2016; Reitz, Brayne, et al., 2011; Zetterberg & Mattsson, 2014). Preclinical familial models are therefore failing to capture the form of AD that is experienced by the vast majority of individuals, and this is likely contributing to the fact that AD treatments tested on such models are failing to translate more than 99% of the time (Cummings, 2018). For this reason, creating a sporadic preclinical model of Alzheimer's is of utmost importance to understand the disease mechanisms and develop better treatment strategies (Coronas-Samano et al., 2016; Hartantyo et al., 2020; Huynh et al., 2020; Zhang et al., 2020)

The overall aim of this Chapter is to generate a sporadic model of AD with factors that are known to be strongly associated with the sporadic form of Alzheimer's. I hypothesized that combining certain genetic and environmental risk factors that play a prominent role in the pathology of Alzheimer's would elicit similar behavioural and cellular changes in mice to that observed in patients, with the aim of facilitating a detailed understanding of the disease mechanism.

The genetic factor that I chose to model in this study is ApoE4, therefore I employed a ApoE4-KI (Knock-in) model. The environmental risk factor that was chosen for this study was neuroinflammation and I used LPS injections to model neuroinflammation. Intraperitoneal injections of LPS were given to the animals, which have been previously shown to reach the central nervous system via blood circulation (Perry, 2004). This is important because the blood brain barrier is known to exert control over the substances entering the brain, protecting brain from toxins and pathogens from the periphery (Persidsky et al., 2006). If LPS could not cross this barrier, there would be no way for it to cause pathology in the brain.

Indeed, several studies have shown that LPS exerts its effects on the brain through multiple pathways (Peng et al., 2021). For example, the paracellular pathways for LPS entry happen with the disruption of adhesion proteins thereby destroying the integrity of adherence junctions and tight junctions (Alexandrov et al., 2020; Seok et al., 2013). Endothelial cells, which form an integral part of BBB have been reported to be disrupted by LPS, by either promoting apoptosis of the cells or by reducing their proliferation (Liu et al., 2020). Death of these cells lead to increased permeability of BBB, which is further followed by entry of peripheral cytokines into the brain, triggering neuroinflammation. These infiltrating peripheral cytokines can induce microglial reactivity by binding to the toll-like receptors, thereby initiating a cascade of neuroinflammatory responses within the brain (Peng et al., 2021).

Systemic injections of LPS have been shown to increase inflammatory cytokines in the brain such as IL1β, FCγRII and microglial activation markers (Noh et al., 2014). Following a single i.p. LPS injection of 10mg/kg, brain levels of IL1β and TNFα peaked 24 hours following injection but dropped when checked 3 and 7 days after injection. IL6 on the

other hand, peaked after 24 hours of injection and stayed increased 3-9 days after injection (L. M. Wang et al., 2018). Similarly, a single LPS injection of 5mg/kg, TNFα and IL18 remained increased in frontal cortex and hippocampus 7 days after injection. Surprisingly, this study reported a sustained increase of the same cytokines for a prolonged period of 10 months', with expression extending to the cerebellum (Bossù et al., 2012). IL18 levels have also been shown to increase in the brains of AD patients (Ojala et al., 2009). These increased levels of IL18 were shown to increase APP protein levels and processing, which resulted in the excessive production of Aβ-40 (Sutinen et al., 2012). TNF-mediated neuroinflammation was also reported to result in neuronal loss in AD hippocampus. Specifically, this neuronal loss was caused by TNF mediated necroptosis, as observed in human iPSC neuronal cell cultures (Jayaraman et al., 2021).

In addition to these processes, peripheral LPS injections alter microglial cells in the hippocampus, striatum, and frontal cortical regions of the brain (Noh et al., 2014). Microglial cells immediately react to LPS, as they densely express the Toll-like receptors (TLRs) that recognize LPS, and activating these receptors leads to downstream signalling that produce inflammatory cytokines, including TNFα and IL18 (C. R. Batista et al., 2019). A single i.p. injection of LPS at 10mg/kg was found to increase microglial reactivity in the cortex of Sprague Dawley rats in a study by Wang et al., (2018). Likewise, an increase in the reactivity of microglia and astrocytes were noticed 24 hours following a single i.p. injection of LPS at 5mg/kg in C57BL6/J mice (Yang et al., 2020).

In addition to activating microglia and astrocytes, LPS administration has been seen to promote amyloid deposition. For instance, 7 days of LPS (0.5mg/kg) intraperitoneal administration was shown to increase Aβ 1-42 levels in the brain and induce AD-like neuronal degeneration (Behairi et al., 2016). APPSwe AD model mice were given chronic

LPS administration (i.e. intraperitoneal injections of 0.5mg/kg once a week for 13 weeks), which led to an increase in Aβ in the hippocampus, cortex and amygdalar regions (Sheng et al., 2003; Thygesen et al., 2018). However, a recent study gave a single LPS injection of 1mg/kg in 5xFAD mice at 6 weeks of age, before the development of Aβ plaques, to prime the microglial cells. When checked for Aβ plaque deposition 140 days later, LPS injection had resulted in increased phagocytosis of Aβ, leading to a decrease in overall plaque load. This highlighted how LPS priming of microglial before Aβ accumulation can induce an innate immune memory in microglia, which eventually improves the Aβ pathological phenotype (Yang et al., 2023).

Systemic LPS injections have also been shown to induce cognitive deficits in both WT animals. For example, a single injection of 0.5mg/kg LPS into wildtype mice before testing on the elevated plus maze was shown to affect locomotor activity of the animals and induce anxiety-like behaviour (Jiang et al., 2022). In a separate study, wildtype animals treated with LPS (i.p 5mg/kg) performed poorly relative to controls in the Morris water maze (Yang et al., 2020). In yet another study single intraperitoneal injection of 0.75mg/kg LPS were shown to induce impairment in spatial memory, specifically in the Morris water maze and passive avoidance tests. Moreover, there was a marked increase in microglial reactivity, and neuronal cell loss in the hippocampus of these animals (Zhao et al., 2019). Together, these cellular and cognitive changes induced by LPS in animal models, makes it a suitable candidate for studying AD associated phenotype in rodents (C. R. A. Batista et al., 2019).

Lastly, it is worth considering whether the neuroinflammation induced by LPS in the above studies could be considered acute or chronic. Typically, it is considered that, to model acute neuroinflammation, studies describe a single higher dosage of 5mg/kg or

more (Bossù et al., 2012; Oliveira-Lima et al., 2019; L. M. Wang et al., 2018), whereas the repeated low dosage injections of LPS either continuously (Yang et al., 2020) or at certain intervals of time (Sheng et al., 2003; Thygesen et al., 2018) is thought to model chronic neuroinflammation. Because chronic neuroinflammation is thought to be more relevant to AD pathology, in the current study I first decided to adapt a similar protocol with that of Thygesen et al., and Sheng et al., to mimic chronic neuroinflammation. Specifically, I did this by giving animals repeated LPS injections of 0.2mg/kg once a week for 17 weeks, the details of which are explained in the methods section. In later experiments I did include single injections of higher concentration LPS directly into the dorsal hippocampus. However (and as noted in the results and investigated in the general discussion) this did appear sufficient to produce a relatively long-lasting neuroinflammatory effect that persisted for up to 6 weeks following injection.

The aim of Experiment 1 of this Chapter was to validate the sensitivity of our behaviour and cellular techniques to be able to detect changes that have previously been reported in the literature, using the J20 familial model of AD. This was so that any failure to detect such changes in our future tests of novel sporadic models could not be attributed to lack of sensitivity or any other kind of methodological failure of our techniques. The behavioural tasks used included testing for locomotor activity and anxiety with the open field test, as well as spatial memory with Barnes maze test. J20 animals were expected to show enhanced locomotor activity and impaired spatial memory relative to controls. Cellular techniques included immunostaining for microglia, and astrocytes in the dorsal hippocampus, as measures of neuroinflammation, each of which were expected to be elevated in J20 animals relative to wildtype controls. Finally, I completed Golgi staining and counted dendritic spines, which were expected to be reduced for J20s relative to controls.

Following this validation, I proceeded with Experiment 2, in which I combined genetic and non-genetic risk factors of sporadic Alzheimer's disease. I employed low dosage of LPS over a prolonged period (17 weeks) to mimic chronic neuroinflammation (see figure 3.5 for reference). This environmental factor was combined with the genetic risk factor ApoE4, which is the major genetic risk factor associated with sporadic AD (A. Armstrong, 2019; Corder et al., 1993). Specifically, I tested the ApoE4-KI model for behavioural and cellular changes both on its own, and in combination with LPS injection (hereafter termed as 'ApoE4-KI + LPS'). In the same experiment, I also tested whether neuroinflammation combined with the hAβ-KI model produced behavioural and cellular changes. Unlike familial AD models that carry APP genes with familial AD mutations, the 'hAβ-KI' model was engineered to express only the wildtype form (with no mutations of any sort) of Aβ peptides that are observed in human sporadic AD cases. Because these wildtype Aβ peptides contribute to the Aβ aggregation in human sporadic AD cases, I wanted to understand whether the induced neuroinflammation in these models can act as a trigger for such an aggregation. Again, I tested this model on its own and in combination with LPS injection (referred to hereafter as 'hAβ-KI + LPS').

Unfortunately, the results of Experiment 2 were inconclusive because I observed only limited behavioural or cellular changes (if any) in any of the models tested. I hypothesized that perhaps the dosage of LPS I had chosen was too low, so in Experiment 3 I increased the dosage and frequency of LPS administration as described in Figure 3.6. However, because there were no sufficiently aged transgenic animals of either the ApoE4-KI or hAβ-KI models available, I was only able to test this in wildtype animals. Once again, however, this paradigm was only partially effective in bringing out the expected cellular changes. Therefore, in the final experiment of this chapter, Experiment 4, I tested whether LPS administered directly into the dorsal hippocampus (a brain region that has been heavily

implicated in the neuropathology of AD) was sufficient to produce the expected cellular changes. For all experiments in this section, approximately half of the animals were male, and half were female.

3.2) Methods:

3.2.1) Animals:

There were four different mice strains used in this study. The following strains were obtained from the Jackson Laboratory, Bar Harbour. 61 males and 63 females were used for this project and all mice were exactly 6 months old at the start of behavioural experiments.

(i) 37 hAβ-KI (B6J(Cg)-*App*$^{tm1.1Aduci}$/J) mice; Jax #031050 (Baglietto-Vargas et al., 2021) – This 'human Aβ knock-in' mouse strain harbours three point mutations (G→R, F→Y, R→H) in the murine APP gene, leading to the expression of human Aβ peptide sequence from the endogenous murine APP. Briefly, homologous recombination was used to introduce three mutations in the APP gene G676R (G5R), F681Y (F10Y), R684H (R13H) of embryonic stem cells. These mice are homozygous for humanized Aβ sequence.

(ii) 39 ApoE4-KI (B6(SJL)-*ApoE*$^{tm1.1(APOE*4)Adiuj}$/J) mice; Jax #027894 (Foley et al., 2022) – The 'ApoE4 knock-in' mouse expresses a humanized ApoE4 from the murine ApoE gene. Exons 2, 3 and 4 of murine ApoE was replaced by exons 2, 3, 4 and a portion of 3' UTR sequence of human ApoE4, thereby leading to the expression of human ApoE4 from endogenous murine ApoE. The C57BL/6J mouse were chosen and the ApoE gene was replaced through homologous

recombination using a targeting vector of 1.5 kb with the above-mentioned modifications in the exons. Homozygous animals are viable.

(iii) 9 hAPP-J20 (B6.Cg-*Zbtb20*$^{Tg(PDGFB-APPSwInd)20Lms}$/2Mmjax); Jax #34836 (Mucke et al., 2000) – The J20 mouse strain, is a widely used familial AD model that expresses human APP with Swedish (K670N/M671L) and Indiana (V717F) mutations. This alteration leads to the over-production of Aβ resulting in plaque pathology. The transgene expression is under control of the PGDF-β promoter. The APP gene has been inserted into mouse chromosome 16 within intron 1 of the ZBTB20 gene.

(iv) 41 C57BL/6J mice were obtained from Australian BioResources (Moss Vale, Australia).

All mice were housed at 2-5 per cage throughout the experiment and were maintained on a 12-hour light/dark cycle with food and water supply ad-libitum. All animal experiments were performed with the approval of the Garvan Institute and St. Vincent's Hospital Animal Ethics Committee under approval number 17/28 and 20/08. This was in accordance with the Australian National Health and Medical Research Council animal experimentation guideline and the local Code of Practice for the Care and Use of Animals for Scientific Purposes.

3.2.2) Experiment 1: Validating the sensitivity of our experimental procedures using an established familial mouse model of AD, the hAPP-J20 model:

Animals:

For Experiment 1, there were 6 wildtypes and 9 J20 animals.

Behavioural Procedures:

Note that for Experiments 1 and 2, the behavioural procedures were completed by an honours student, Alex Langdon. I completed all other procedures (including histology, imaging, and analysis) for these experiments. I performed all the procedures for all other experiments contained in this thesis.

i) Open Field Test (OFT):

Figure 3.1: OFT chamber used for this experiment (left), an example of how the open field is split into outer edge and centre zone for analysis (right).

Locomotor activity and anxiety in mice was assessed by using the Open Field Test (as shown in Figure 3.1). The Open Field chamber used in our study measured 273mm x 273mm with 203mm high glass walls and were placed inside a sound attenuating cubicle (MED-OFAS-MSU, MED-OFA-022, Med Associates inc.). At the start of each session, individual mice were placed in the centre of the chamber and given 10 minutes to explore it. Movement was recorded and tracked with the Activity Monitor 7 (Med Associates inc.) which uses infrared beams to detect activity inside the chamber. The total distance travelled by the animal over 10 minutes was recorded. The chamber was divided into two zones – corner zone and centre zone. The relative amount of time spent in each zone was

recorded and measured as an indicator of anxiety. As reviewed in Chapter 1, higher anxiety is typically indicated by an animal that spends more time in the corner zones and less time in the centre.

ii) Barnes Maze Test (BM):

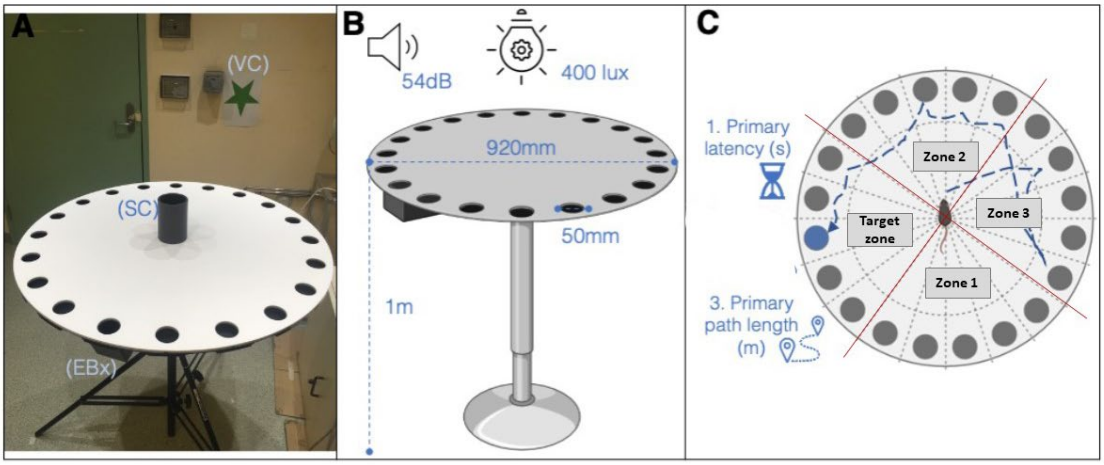

Figure 3.2: Adapted from honour's student Alexander Langdon's thesis. Photograph of the room where BM was conducted (left), Dimensions of the BM apparatus used (middle), Zone division and example of measures used for analysis (right).

Barnes Maze was used to assess spatial learning and memory in mice. A photograph of the apparatus used is shown in Figure 3.2. This apparatus was a white circular platform of 920mm diameter placed at an elevation of 1m from the ground. Along the perimeter of the platform, 20 identical holes of 50mm diameter were equally spaced. A hidden black escape box (175mm (D) x 75mm (W) x 80mm (H)) was placed beneath one of these holes while the other holes were blocked. The escape box location was signalled by visual cues, which comprised a yellow square, a green star, a blue triangle and a red circle printed on A4 sheets of paper and placed one each on the four walls of the behaviour room. Mouse

activity was recorded using ANYmaze Video Tracking System 6.33 (Stoelting Co.) with a camera (DMK 22AUC03) placed directly above the maze.

Acquisition phase (Day 1-5): Acquisition of the Barnes maze task occurred over 5 days. There were 3 training trials per day with a 35–45-minutes interval between each trial. During these trials, mice were placed at the centre of the maze in a cylindrical chamber (80mm diameter x 12.5mm height) which was left in place for 5 seconds. Mice were placed facing random directions which was rotated such that they could not use their start position as a reference to find to the escape box. The chamber was then lifted, and each mouse was given 2 minutes to explore and locate the hidden escape box. If the animal did not locate the escape box in this given time, it was manually guided (with hands) to the escape box and was given an extra 30 seconds inside the box to learn that this is the desired destination. The location of the escape box was randomly assigned for each animal prior to the experiment but remained constant for each individual mouse throughout the entire experiment. At the end of each trial, the platform was rotated and cleaned with 80% ethanol to eliminate any olfactory cues.

Probe trial (Day 6): The probe trial was conducted 24 hours after the last acquisition trial. In this trial, the hidden escape box was removed so that its hole was now undifferentiated from the other holes on the platform. Mice were again placed in the centre of the maze, then given 90 seconds to remember and locate the hole beneath which the escape box was hidden previously. Once finished, the recorded video was analysed by dividing the maze into 4 equal zones (as depicted in Figure 3.2) and the time spent by each animal in each zone was recorded and plotted. Animals with intact spatial memory should spend more time in the target zone that previously contained the escape box.

Tissue collection:

i) Tissue collection for Golgi staining:

One day after behavioural training finished, freshly extracted brains from 6 mice (3 wildtype, 3 J20) were used for Golgi staining. Mice were anaesthetized with isoflurane and cervical dislocation was carried out to extract brains. The brains were then briefly rinsed with water and immediately immersed in Golgi solution (described later in this section).

ii) Tissue preparation for histology analysis:

5 wildtype and 5 J20 animals were anaesthetized with a ketamine mixture (100 mg/kg of body weight, Mavlab) + Xylazil (20mg/kg of body weight, Troy laboratories Pty ltd) and taken for perfusion 15 minutes later. Mice were cut open from the abdominal region till the rib cage to reveal the heart. A 27G needle was used to puncture the apex of the heart and an incision was made in the right atrium. Saline was then delivered to flush the blood from blood vessels for about one minute. Next, mice were perfused with ice-cold 4% paraformaldehyde (PFA) in phosphate buffer Saline (PBS, at pH7.4) for approx. 8 minutes. Brains were carefully extracted and stored in 4% PFA overnight. The next day, brains were transferred to a 30% PBS sucrose solution where they were stored until sectioning.

Staining:

i)Golgi staining for dendritic spines:

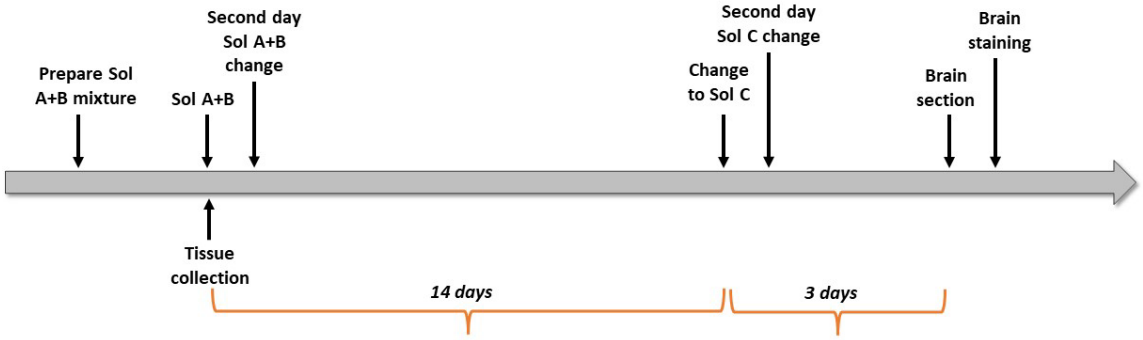

Figure 3.3: Timeline for processing tissue for Golgi staining. Collected tissues are impregnated in Golgi solution for about 18 days before it can be taken for staining.

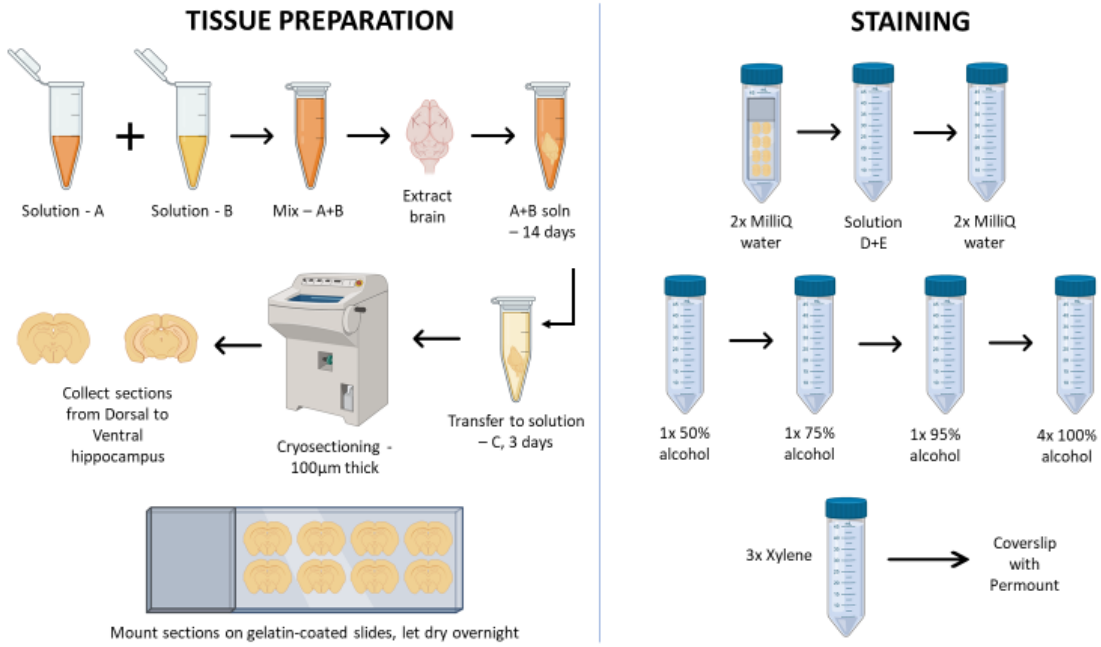

Figure 3.4: Schematic overview (made using Biorender) of the entire staining process. Solutions A, B, C, D and E are provided with the kit.

Brain Impregnation: The protocol described here was adopted from the Golgi staining kit which provided all the solutions used in this protocol (FD Rapid Golgi stain kit, PK401/401A). Throughout the process of brain impregnation, all the solutions and brains were stored in the dark, at room temperature (approx. 22 °C).

One day before the tissue collection, equal parts of Solution A and Solution B were mixed in a 5mL Eppendorf and left to sit overnight. On the day of tissue collection, freshly extracted brains were rinsed with water and immersed in A+B solution. The next day, the brains were transferred to a fresh A+B solution and stored for 14 days in solution A+B. Following this, the brains were transferred to solution C. One day later, the brains were transferred to fresh solution C and stored for a total of 3 days.

Cryosectioning: One day later, the brains were immediately and coronally sectioned at a 100 µm thickness from bregma -1.58 to -2.30 (from Paxinos brain Atlas, (Paxinos & Franklin, 2012)) and stained. The sectioned brains were first mounted on gelatin-coated slides and then stained with a series of reagents and solutions.

Staining process: Solutions were freshly prepared for staining – Solution D+E (prepared with milliQ water, Solution D: Solution E: milliQ water – 1:1:2 ratio, for example - 9ml of Sol D + 9ml of Sol E + 18ml of MilliQ ddH2O, total of 36ml), 50%, 75% and 95% alcohol solutions. Brain sections on the slides were stained in the following order:

ddH2O	- 2 times 4 minutes
Sol D+E mixture	- 1 time 10 minutes
ddH2O	- 2 times 4 minutes
50% alcohol	- 1 time 4 minutes
75% alcohol	- 1 time 4 minutes

95% alcohol - 1 time 4 minutes

100% alcohol - 4 times 4 minutes

Xylene - 3 times 4 minutes

Slides were then coverslipped using Permount (Fischer Scientific, SP15-500) and left to dry overnight.

ii) Immunostaining for microglia and astrocytes:

PFA-perfused brain sections of 40 µm thickness were cut using cryostat and stored in cryoprotectant solution. Coronal sections of brain were taken in a 1:6 ratio for the whole brain.

Once removed from cryoprotectant, sections were rinsed with 3 x 10 minutes in a PBS (pH 7.2) solution then blocked in PBS with 3% bovine serum albumin (BSA: Bovogen Biologicals, BSAS 1.0) + 0.25% Triton (Sigma Aldrich, T8787) in 1x PBS (pH 7.2) to prevent non-specific binding, for an hour at room temperature. After blocking, the sections were incubated in the following primary antibodies:

- rabbit polyclonal IBA1 (1:1000, Labome, Wako Chemicals, 019-19741),
- rabbit polyclonal GFAP (1:500, Dako Z0334),

for 72 hours at 4°C. All sections were rinsed thrice (10 minutes each) with PBS and incubated in their respective secondary antibodies:

- Donkey anti-rabbit 488 (1:500, Invitrogen, A32790),

at 4°C overnight. Subsequently sections were rinsed with PBS and counterstained with DAPI (Invitrogen, D1306) for 10 minutes at room temperature. Finally, the sections were

mounted onto SuperFrost slides (ThermoFisher Scientific, SuperFrost plus F41296SP) and coverslipped (Menzel-Glasser, #1) with 50% glycerol mounting medium (Sigma Aldrich, GG1).

Image Analysis:

i) Neurolucida:

For Golgi-stained brains, Neurolucida (MBF Biosciences) was used to analyse the number of dendritic spines. Spines were counted from CA1 region of hippocampus, bregma -1.58 to -2.30 (from Paxinos brain Atlas, (Paxinos & Franklin, 2012)). Only neurons with complete branching were chosen for analysis. Three apical and 3 basal secondary dendrites of branch orders 2-8, were chosen from four random neurons per brain. The four random neurons were chosen according to one criterion – the neurons should have a complete branching of apical and basal dendrites without any truncation of the dendritic extensions. Selected dendrites were traced at 100x magnification (Axio Imager M2), and spines were traced manually for its entire length. The tracings were then exported to Neurolucida explorer to perform spine analysis.

Under the 'Structure analysis' tab in Neurolucida explorer, 'Branched structure analyses' was chosen. The 'Segment details' tab was then used to analyse spine numbers. Spine counts were then exported to excel where spine density was calculated as the number of spines per 10µm length of the dendrite.

ii) Stereology:

For immunostained brains, Glial cells were counted using the Optical fractionator module in Stereo Investigator (MBF Biosciences). Every sixth section was taken for quantification. The region of interest was traced, and cells were quantified at 40x (Axio Imager A2) using

a counting frame of 100 µm x 100 µm and a grid size of 200 µm x 200 µm. To eliminate the possible surface irregularity, the guard zone height was set as 5 µm and the dissector height was set to 10 µm for all sections. The sampling intervals and parameters were adapted from (Stayte et al., 2015) publication where the grid size and counting frame size was adjusted according to the region of interest (in my project, the hippocampus). Sampling intervals and parameters were determined by Stayte et al., from (Gundersen & Jensen, 1987) which was followed in my project. Coefficient of error attributable to the sampling was calculated according to the publication (Gundersen & Jensen, 1987). Cell populations were estimated from the dorsal hippocampus of Bregma -1.34 to -2.30 mm based on Paxinos atlas for mouse brain (Paxinos & Franklin, 2012). To exclude the differences in traced volume, cell counts were represented as number of cells per area.

3.2.3) Experiment 2: Combining major genetic and non-genetic risk factors to create a sporadic model of AD:

Animals:

For Experiment 2, 16 wildtype Sham, 18 wildtype LPS, 15 ApoE4 Sham, 24 ApoE4 LPS, 13 hAβ Sham, 25 hAβ LPS were used.

Intraperitoneal Lipopolysaccharide (LPS) injections:

Desired LPS (LPS, *Escherichia coli* O111:B4, L3024, Sigma Aldrich) concentration – 0.2mg/kg

Working concentration – This was decided by taking the average weight of mice as 25gm. To inject 25 units to a mouse weighing 25 gm with the desired concentration of 0.2mg/kg, working concentration was decided in accordance with the following equation (Equation 1):

1) $\frac{25g*0.2mg/1000g}{0.25mL} = \frac{0.0125mg}{0.25mL} = 0.02mg/mL\ \ (working\ concentration)$

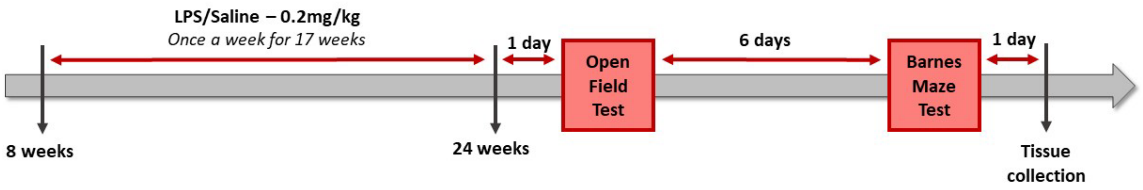

Figure 3.5: Experimental timeline for results described in Experiment 2 of this chapter.

All ApoE4-KI, hAβ-KI and C57BL/6J mice were given LPS injections of 0.2mg/kg or Saline as described in Figure 3.5. LPS injections were given once a week for a total of 17 weeks, starting at 8 weeks of age. One day after the last LPS injection, an open field test was performed. Mice then underwent other behavioural testing that is not reported here due to being beyond the scope of the current thesis. Therefore, six days after the open field test, a Barnes Maze Test was carried out. All animals were culled one day after the probe trial test of Barnes Maze. Animals were 24-25 weeks old by the time they were culled.

Behavioural Procedures:

All behavioural procedures were identical to those described for Experiment 1.

Golgi staining and immunostaining and analyses:

Mouse brains were collected one day after the last experimental procedure and were processed and analysed for Golgi or immunostaining using the same procedures described in Experiment 1.

3.2.4) Experiment 3: LPS induced neuroinflammation as a sporadic model for AD:

Animals:

For Experiment 3, 24 wildtype Sham, 24 wildtype LPS animals were used.

Behavioural Procedures:

No behavioural procedures were performed in Experiment 3.

Intraperitoneal Lipopolysaccharide (LPS) injections:

For Experiment 3, the desired concentration was 0.5mg/kg (LPS working concentration was prepared using Equation 1, with 0.5mg substituted for 0.2mg).

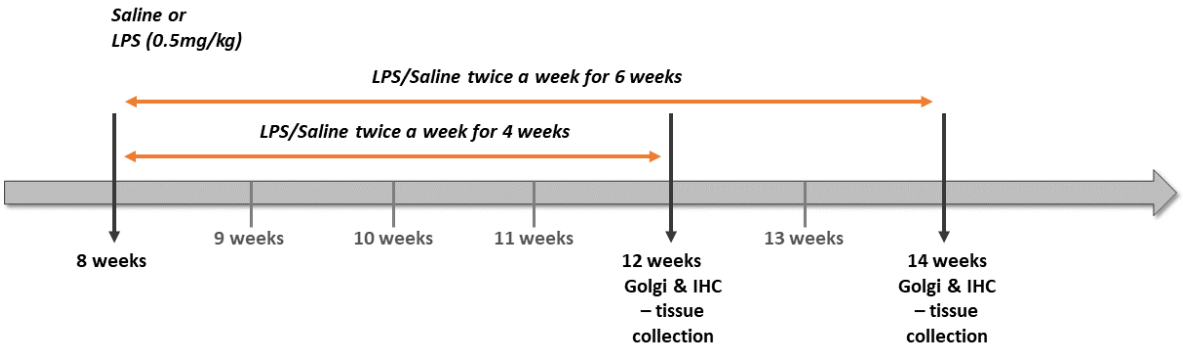

Figure 3.6: Experimental timeline for Experiment 3.

Systemic LPS injections were given to mice according to the experimental schedule in Figure 3.6. Specifically, half of the C57BL/6J mice were given LPS injections of 0.5mg/kg and half were given sterile Saline twice a week either for 4 weeks (n = 24) or for 6 weeks (n = 24). Injections started at 8 weeks of age and when 4 or 6 weeks had passed, tissue was collected for Golgi staining (n = 6 LPS/Sal) or immunostaining (n = 5 LPS/Sal). Very small 0.5ml insulin syringes were used to minimize the pain caused due to repeated injections and animal weights were recorded twice a week on the same day as injections. Animals were also monitored twice a week for any sickness caused by LPS. Specifically,

animals were check for weight loss, lethargy, pilo erection, and any wounds/infection around the site of injection. However, I did not observe weight loss or pilo erection in any of the animals, and no animals showed any infection around the injection site.

Golgi staining and immunostaining and analyses:

Mouse brains were collected one day after the last injection and were processed and analysed for Golgi or immunostaining using the same procedures described for Experiment 1.

3.2.5) Experiment 4: LPS induced neuroinflammation as a sporadic model for AD:

Animals:

For Experiment 4, 17 wildtype Sham and 15 LPS animals were used.

Intrahippocampal lipopolysaccharide injections:

LPS was freshly prepared on the day of surgery. To prepare it, 2mg of LPS was diluted in 500µl of Sham and used at a concentration of 4µg/µl. One µl of LPS or Sham was injected per hemisphere of the brain (bi-lateral injections).

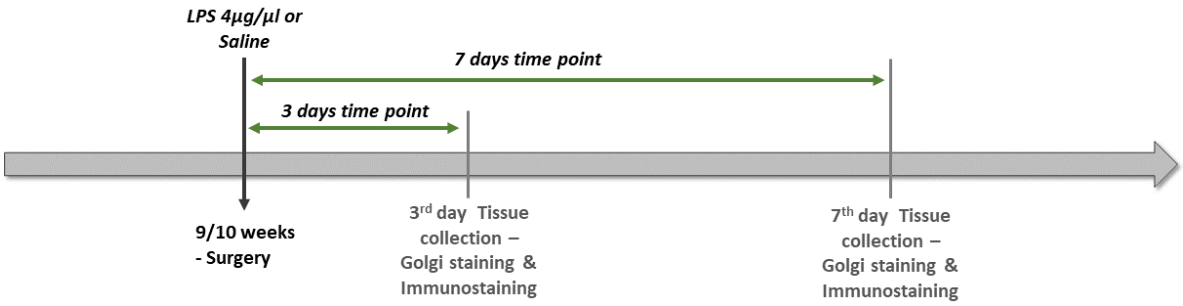

Figure 3.7: Experimental timeline for results described in 'Experiment 4' of this chapter.

C57BL/6J mice were given intrahippocampal injections of Saline and LPS bilaterally (see stereotaxic surgery section below for details). There were two timepoints – 3days and

7days after surgery, at which the tissues were collected for checking spine density and immunostaining, refer to Figure 3.7. Seventeen animals were culled at 3days timepoint and 15 animals were culled at 7days timepoint.

Stereotaxic surgery:

All tools used for the surgery were autoclaved the day before and placed in a mixture of chlorohexidine solution and purified water throughout the surgical procedure. Animals were anaesthetized with a Ketamine mixture (100 mg/kg of body weight, Mavlab) + Xylazil (20mg/kg of body weight, Troy laboratories Pty ltd).

Each mouse's head was carefully shaved to expose enough skin and fixed on a stereotaxic frame (Model 940, David KOPF Instruments). A generous amount of Betadine was applied to the shaved skin and a small amount of Bupivacaine was injected subcutaneously at the incision site to numb the area. Eye ointment (PolyVisc, Alcon) was applied to prevent the eyes from drying. A neat incision of 2cm or more was made on the skin with a scalpel blade (size 22) to expose the skull of the animal. A cotton swab, damped in H_2O_2 was used to gently dab on the skull of the animal to increase visibility of Bregma and Lambda. To make sure that the brain was level, Bregma and Lambda co-ordinates were measured, and the teeth and ear bars were adjusted until the difference between them was less than or equal to 0.05mm.

Once the skull was level, small holes were drilled (microdrill, SDR scientific, Harvard Apparatus) on either side of the skull according to the measured co-ordinates: AP(-1.8), ML(+1.5). A Hamilton syringe (10µl, 1700 series, RN syringe, 1.0µl, 7000 series, KH syringe, Neuros syringes, SDR scientific, Harvard Apparatus) filled with LPS/Sham was used to inject the desired solution (1µl per hemisphere) at DV (-1.7) at the rate of 0.2µl/minute. The syringe was then left undisturbed for 5-7 minutes post injection and

slowly retracted to make sure the liquid was contained in the area of injection. This was repeated on the other hemisphere. The animal's skin was then sutured (Dysilk, S405, 18mm, 3/8 circle, Dynek Pty Ltd) and approximately 500µl of Saline was injected sub-cutaneously to avoid animals from feeling dehydrated after surgery. Animals were closely monitored after surgery for signs of weight loss, pilo erection, hunched body posture, inflammation, gripping strength, and any infection around the surgical site. These were recorded in the monitoring sheet with a grimace scale rating of 0-2. If the animals were high on this scale, they were given Carprofen (Rimadyl, Zoetis) to ease their pain. If the animals were losing weight, special hydrogel (HydroGel, 70-01-5022 Clear H_20) was given orally.

3.2.6) Statistics:

All statistical analyses for all experiments were performed with Graphpad Prism 10.0.2. Data were assessed using one-way or two-way ANOVA or two-tailed t-tests depending on the data type, followed by *post-hoc* Bonferroni analysis where applicable. For all analysis, a p value of ≤0.05 was considered significant.

3.3) Results & Discussion:

3.3.1) Experiment 1 - Validating the sensitivity of our experimental procedures using the hAPP-J20 model:

In 'Experiment 1' of this chapter, I focused on validating the behaviour and molecular procedures we chose to employ in our study, to ensure their sensitivity before applying them to our novel sporadic AD models. This was done to confirm that our techniques were effective in case we did not detect any changes in our sporadic models going forward. I

performed this validation in a well-known familial model of AD – hAPP-J20. The behaviour experiments included Open Field Test for locomotor activity and anxiety, and Barnes Maze Test for spatial memory. Golgi staining was performed to assess spine density changes and fluorescent immunostaining to assess neuroinflammation. The J20 animals used in this study were 6 months old at the start of behavioural testing.

3.3.1a) hAPP-J20 mice demonstrate hyperactivity in the open field test and impaired spatial memory in the Barnes maze, confirming the sensitivity of our techniques to these deficits (Contributed by Alexander Langdon, honours student):

Open field test results are shown in Figure 3.8A. From this figure, it is clear that J20 animals travelled a greater distance than wildtypes, and this was supported by statistical analysis ($t=2.183$, $p=0.0480$). This suggests that J20 animals were hyperactive as hypothesized and as expected based on what has been reported in the literature (Cheng et al., 2007; Flores et al., 2018). As shown in Figure 3.8B, there was no significant difference between J20 and wildtype mice with regards to the time spent by these animals in the centre of the open field chamber ($t=0.1281$, $p=0.9000$), indicating no change in anxiety in J20 animals.

The Barnes maze results from the probe trial test are shown in Figure 3.8C, and it is clear from this figure that J20 animals performed differently to wildtype controls. The primary path length, speed and latency during acquisition did not differ between WT and J20, and these data are shown in Figure 3.8 D-G. Upon performing a repeated measures Two-way ANOVA for primary path length, there was a significant main effect of training day ($F_{(2.025, 26.32)}=7.677$, $p=0.0023$) that did not interact ($F_{(4, 52)}=0.8592$, $p=0.4946$) with genotype. Similar analysis on speed revealed a main effect of training days ($F_{(2.107, 27.40)}=3.932$, $p=0.0297$) which did not interact with genotype ($F_{(4, 52)}=1.083$, $p=0.3744$). A repeated

measures Two-way ANOVA for latency revealed a main effect of training days ($F_{(2.093, 27.21)}$ =7.776, p=0.0019) which did not interact with genotype ($F_{(4, 52)}$ =0.3636, p=0.8334). These results suggest that performance improved for all mice across days, in a manner that was equivalent between groups (suggesting that the locomotor differences observed earlier did not translate into differences in performance in the J20 mice compared to WT in our Barnes maze test).

There was, however, a significant effect on primary errors (the number of errors made by the animal before the first encounter of escape hole), as shown in Figure 3.8G, showing that J20 animals committed more errors than WTs, specifically on Day 4. This is supported by with a main effect of genotype ($F_{(1,13)}$ = 6.671, p = 0.0227). A *post hoc* analysis revealed a significant effect on training day 4 (p=0.0441). This was statistically supported by a main effect of time ($F_{(3,39)}$ = 21.38, p<0.0001) which interacted ($F_{(3,39)}$ = 3.687, p=0.0198) with genotype. The acquisition data revealed that J20 animals did not differ from wildtype animals in most tasks suggesting J20 animals learned the task as good as wildtypes albeit making more errors.

The probe test was performed on the 6th day (the next day after the last day of acquisition), the results of which are shown in figure 3.8C. A two-way ANOVA analysis revealed a significant interaction ($F_{(3,52)}$ = 4.756, p=0.0053) between genotype and time spent in different zones and a main effect of time spent in zones ($F_{(3,52)}$ = 27.58, p<0.0001). A *post hoc* analysis compared time spent in the target zone with respect to other zones and revealed that J20 animals spent significantly less time (p = 0.0153) in the target zone compared to wildtype animals, which indicated that J20 animals were unable to remember the escape box location (refer methods section for details, Figure 3.2). Together with the acquisition data, it can be seen that J20 animals show specific spatial

memory deficit, as they rely on visual cues when present, but when absent, they cannot use memory to remember the location of escape box. An alternative way of representing the same data is included in Appendix A, which shows the proximity to holes for WT and J20 animals separately. WT animals seem to spend more time in the goal box, whereas, J20 animals did not know the difference between goal box and other holes. This is in support of our probe trial data version included in main figure 3.8C. Together with the results of the open field test, these results suggested that J20 animals were hyperactive and had impaired spatial memory relative to wildtype controls.

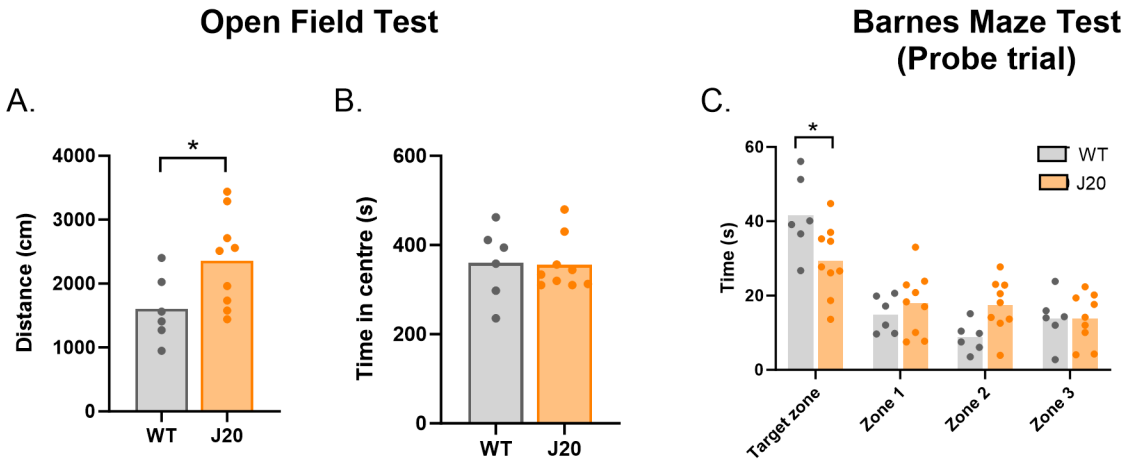

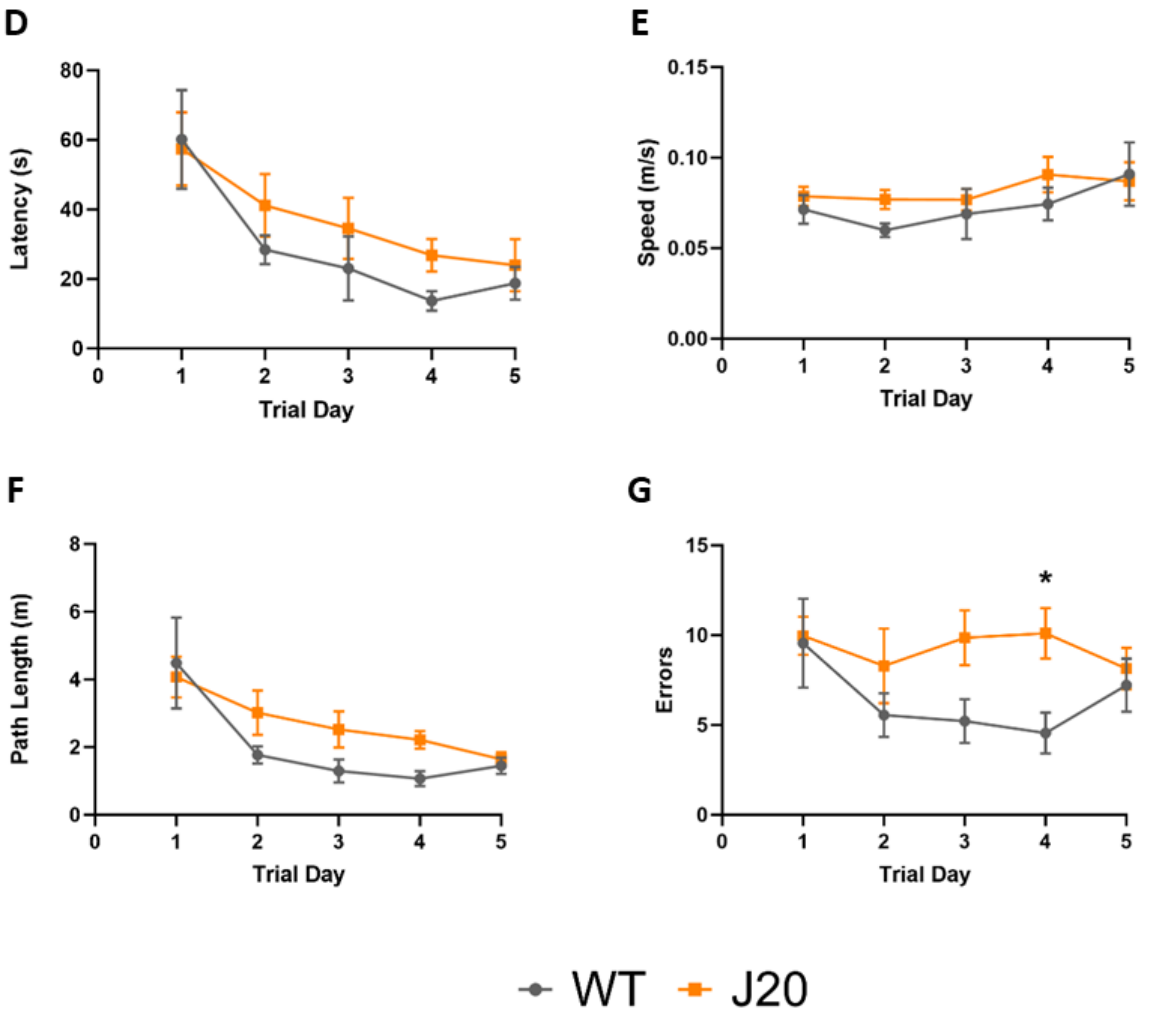

Figure 3.8: Total distance travelled by WT and J20 animals during Open field test (A), Time spent in the centre zone of Open field test (B), Time spent in target zone vs other zones in Barne's maze test on probe trial (C), Latency (D), speed (E), path length (F), and errors made by animals to reach the escape box over the 5 days of acquisition training (WT=6, J20=9; * = $p < 0.05$, All values represent the Mean ± SEM,)

3.3.1b) Reduced dendritic spine density in hAPP-J20 animals:

I wanted to determine if any alterations in neuropathology underpinned the behavioural changes observed in J20 animals. On quantifying the apical and basal dendritic spines, we observed that the apical spines were decreased in J20 animals compared to wildtype

controls (t=3.256, p=0.0028, Figure 3.9A), however the basal spine numbers remained the same between both groups (t=1.673, p=0.1047, Figure 3.9B).

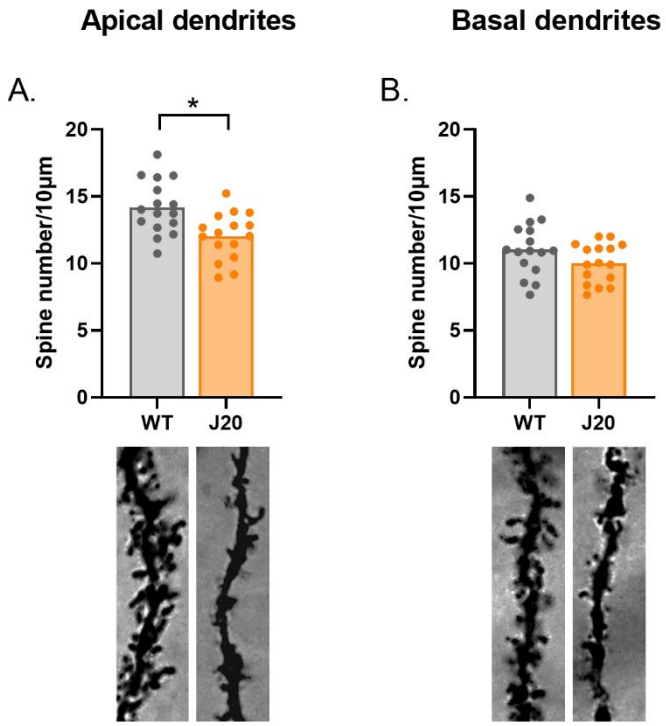

Figure 3.9: Apical dendritic spines in WT and J20 animals (A), Basal dendritic spines (B), (WT, J20, n=16 dendrites; (3 dendrites per neuron, 4 neurons per animal, 4 animals per group); p< 0.05; All values represent the Mean ± SEM)

3.3.1c) Increased astrocytic cell numbers in hAPP-J20 animals:

After observing a significant decrease in dendritic spine density, I proceeded to check for another important neuropathological marker – glial cell activation. Microglia was stained with Iba1 and astrocytes with GFAP in the dorsal hippocampus. Our J20 animals showed no differences in the number of activated microglial cells (t=0.3352, p=0.7461, Figure 3.10A), however the astrocytes cell number was significantly increased compared to the wildtype animals (t=4.679 p=0.0016, Figure 3.10B). The increase in astrocytic expression does indicate the presence of neuroinflammation in J20s, the failure to see such an

increase in microglia could be due to the small sample size (here n =5 for both WT and J20s).

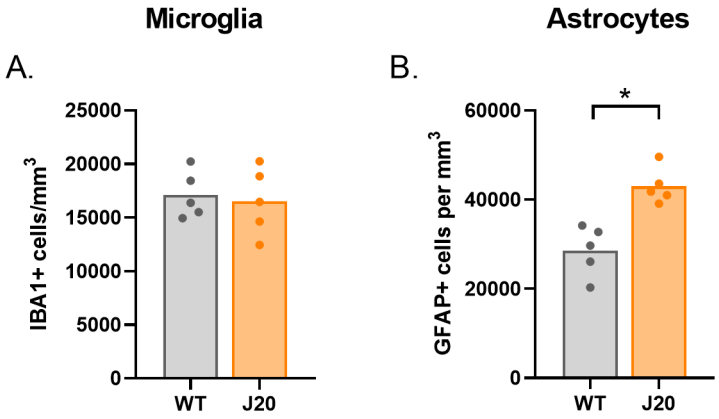

Figure 3.10: Number of Iba1+ cells (A) and GFAP+ astrocytes (B) in the dorsal hippocampus. (WT, J20, n=5; Analysis; $p<0.05$, All values represent the Mean ± SEM).

3.3.1d) Experiment 1: Discussion

The results of Experiment 1 demonstrate that our behavioural and cellular techniques were sufficiently sensitive to detect and replicate the J20 phenotype as has been previously reported in the literature. This suggested that these techniques were suitable for further testing of our novel sporadic AD models.

3.3.2) Experiment 2 – Combining major genetic and non-genetic risk factors to create a sporadic model of AD:

Following validation of our experimental techniques in Experiment 1, in Experiment 2 we used these techniques to test our sporadic mouse models of AD, which consisted of one model that combined neuroinflammation with the 'human Aβ' gene and another that combined neuroinflammation with 'human ApoE4' gene.

3.3.2a) LPS induced hypoactivity and intact spatial memory in both hAβ-KI and ApoE4-KI models (Contributed by Alexander Langdon, honours student):

Although locomotor activity is not a preclinical behaviour of AD, for some reason many studies with familial AD mouse models like J20 (Harris et al., 2010) APP/PS1 (Wang et al., 2022) and 5xFAD (Oblak et al., 2021) have reported hyperactivity. This was the first reason I investigated locomotor activity here. Second, I wanted to make sure the LPS did not affect the normal movement of animals, as I was giving multiple LPS injections and in general single LPS injection was shown to induce sickness behaviour that caused hypoactivity in animals (Biesmans et al., 2013). Finally, as I was also investigating spatial memory using Barnes maze test, in which the animal must move around to locate the escape box, it was essential to make sure that the locomotor activity did not affect test performance Open field performance of 'ApoE4-KI' and 'hAβ-KI' that received Saline and LPS is shown in Figure 3.11A. It is apparent from this figure that LPS injections alone did not alter locomotor performance in this task, however LPS-injected ApoE4-KI and hAβ-KI mice exhibited reduced locomotor activity relative to Sham controls. Indeed, statistical analysis revealed that there was a main effect of treatment ($F_{(1,104)} = 24.92$, $p<0.0001$) but no interaction with genotype. *Post-hoc* analyses demonstrated that the main effect was particularly driven by hypoactivity in the ApoE4-KI and hAβ-KI mice, because distance travelled was not different between LPS and Saline-injected wildtype controls ($p =0.1939$) but it was for ApoE4-KI ($p=0.0212$) and hAβ-KI mice ($p=0.0004$). Time spent in the centre zone of the open field is shown in Figure 3.11B, and it is clear from this figure that no groups differed on this measure. This was supported by statistical analysis which showed no interaction ($F_{(2,104)} = 1.985$, $p=0.1426$) or main effects of treatments or genotype (both Fs < 1). These results suggest that locomotor activity did, but anxiety levels did not, differ between wildtype, ApoE4-KI and hAβ-KI mice upon LPS treatment.

Barnes maze probe trial results are displayed in Figure 3.11C. From this figure, it is clear that all groups spent equal amounts of time exploring the target zone. Indeed, the two-way ANOVA analysis found a main effect of zones ($F_{(3, 416)} = 341.9$, $p<0.0001$) that did not interact with treatment or genotype (Fs < 1). Thus, we were unable to uncover evidence of any impairments in spatial learning and memory in any mice regardless of the genotype or treatment.

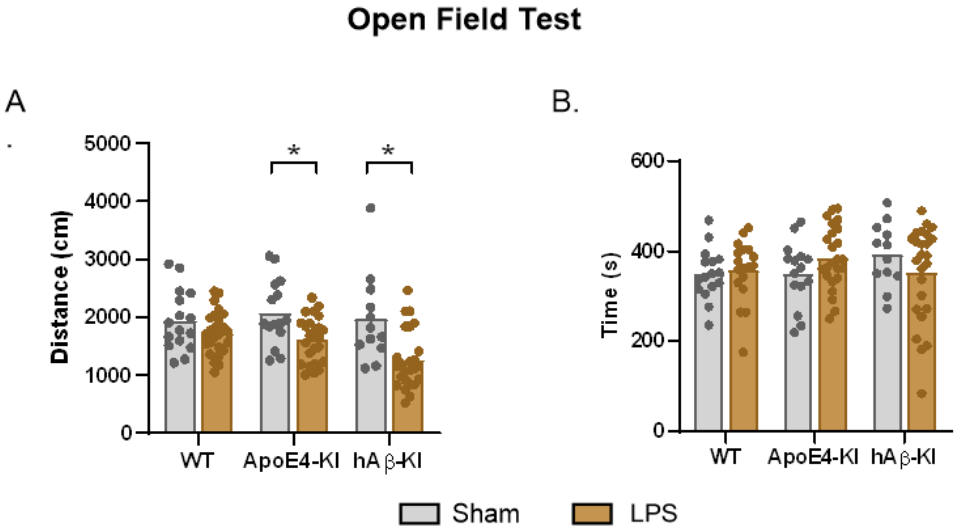

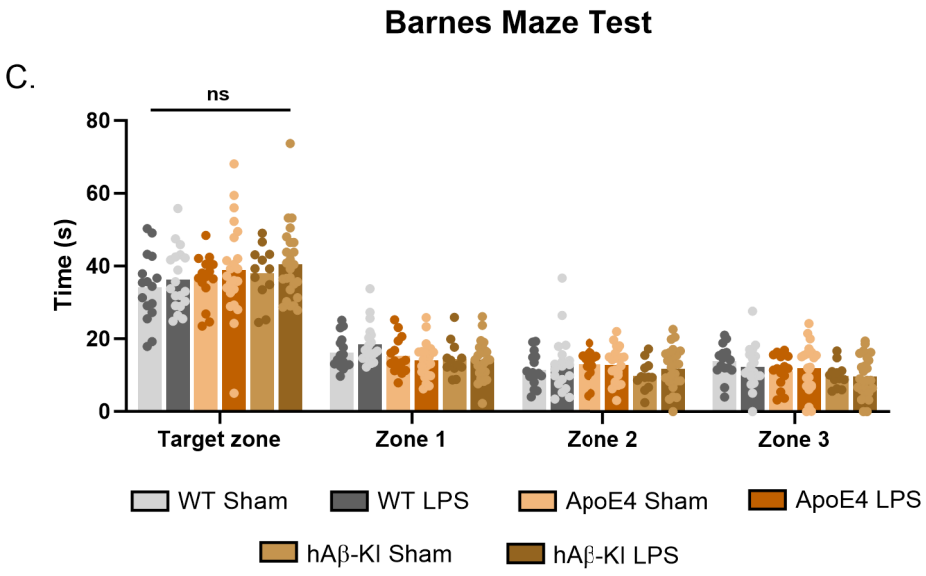

Figure 3.11: Total distance travelled by WT, WT LPS, ApoE4-KI, ApoE4-KI LPS, hAβ-KI, and hAβ-KI LPS animals (A), Time spent in the centre zone (B), Time spent in target zone vs other zones in Barnes maze test (C). (WT Sham=16, WT LPS=18, ApoE4 Sham=15, ApoE4 LPS=24, hAβ Sham=13, hAβ LPS=25; $p<0.05$ All values represent the Mean ± SEM).

3.3.2b) LPS decreased spine density in ApoE4-KI mice, but not hAβ-KI mice:

Although we did not observe a significant difference in behaviour, we wanted to check for any potential alterations at the cellular level which could result from ApoE4 or hAβ expression and/or LPS treatment. Checking for differences in apical and basal dendritic spines we observed a significant reduction in apical dendritic spines in LPS treated ApoE4-KI, but not the hAβ-KI animals. Statistical analysis revealed a significant main effect of treatment ($F_{(2, 124)} = 4.846$, $p=0.0296$) but no interaction with genotype ($F_{(2, 124)} = 3.478$, $p=0.0339$). A *post hoc* Bonferroni analysis then determined that spine density was significantly reduced for LPS-treated ApoE4-KI mice relative to Sham-treated animals of the same genotype ($p=0.0212$) (Figure 3.12A). The basal dendritic spines did not differ amongst groups (Figure 3.12B). These results suggest that neuroinflammation was successful in reducing dendritic spines in the ApoE4-KI mice but not in hAβ -KI mice or wildtypes.

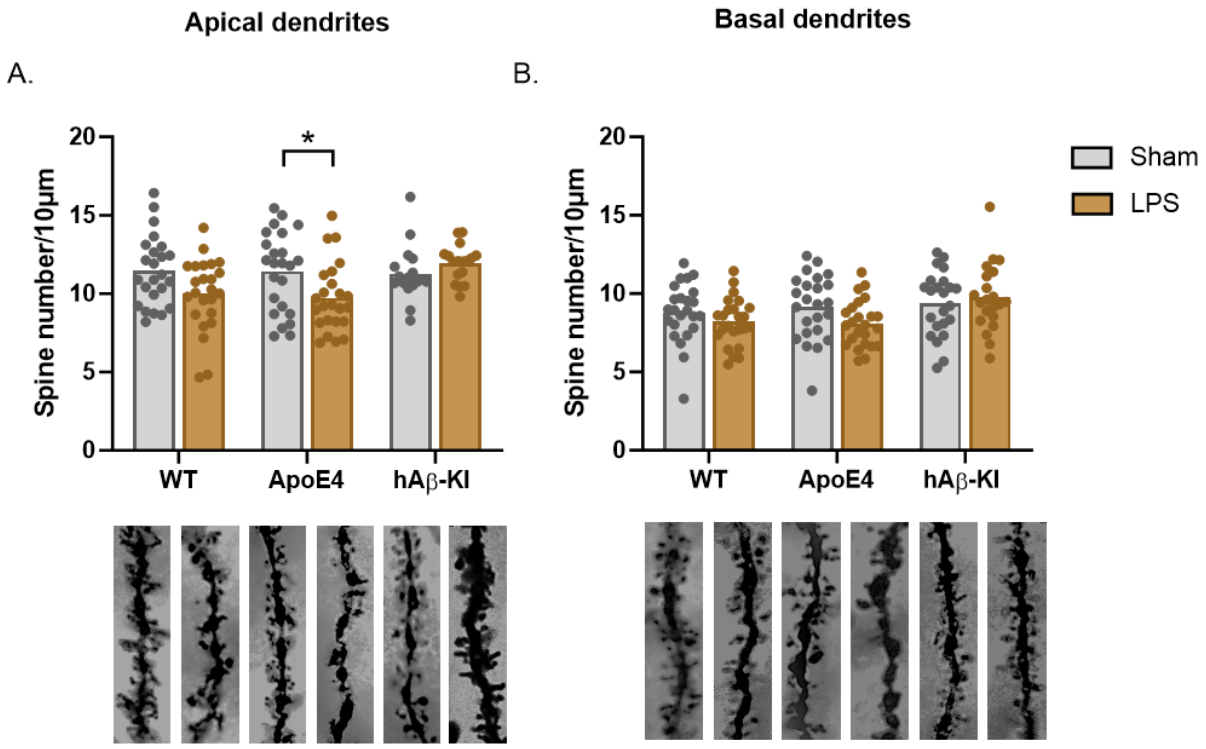

Figure 3.12: Apical dendritic spines in WT, WT LPS, ApoE4-KI, ApoE4-KI LPS, hAβ-KI and hAβ-KI LPS animals (A), Basal dendritic spines (B). (WT Sham & LPS = 24 dendrites; ApoE4 Sham & LPS = 17 dendrites, 3 dendrites per neuron, 4 neurons per animal; $p<0.05$, All values represent the Mean ± SEM).

3.3.2c) No changes in glial cell activation after LPS treatment in ApoE4-KI mice and hAβ-KI mice:

Upon checking for glial cell activation in the dorsal hippocampus of these mice, we first observed that there was no difference in the number of IBA1 positive cells, as shown in Figure 3.13. This was supported by statistical analysis because there was no main effect or interaction between genotype and treatment factors (Fs < 0.05).

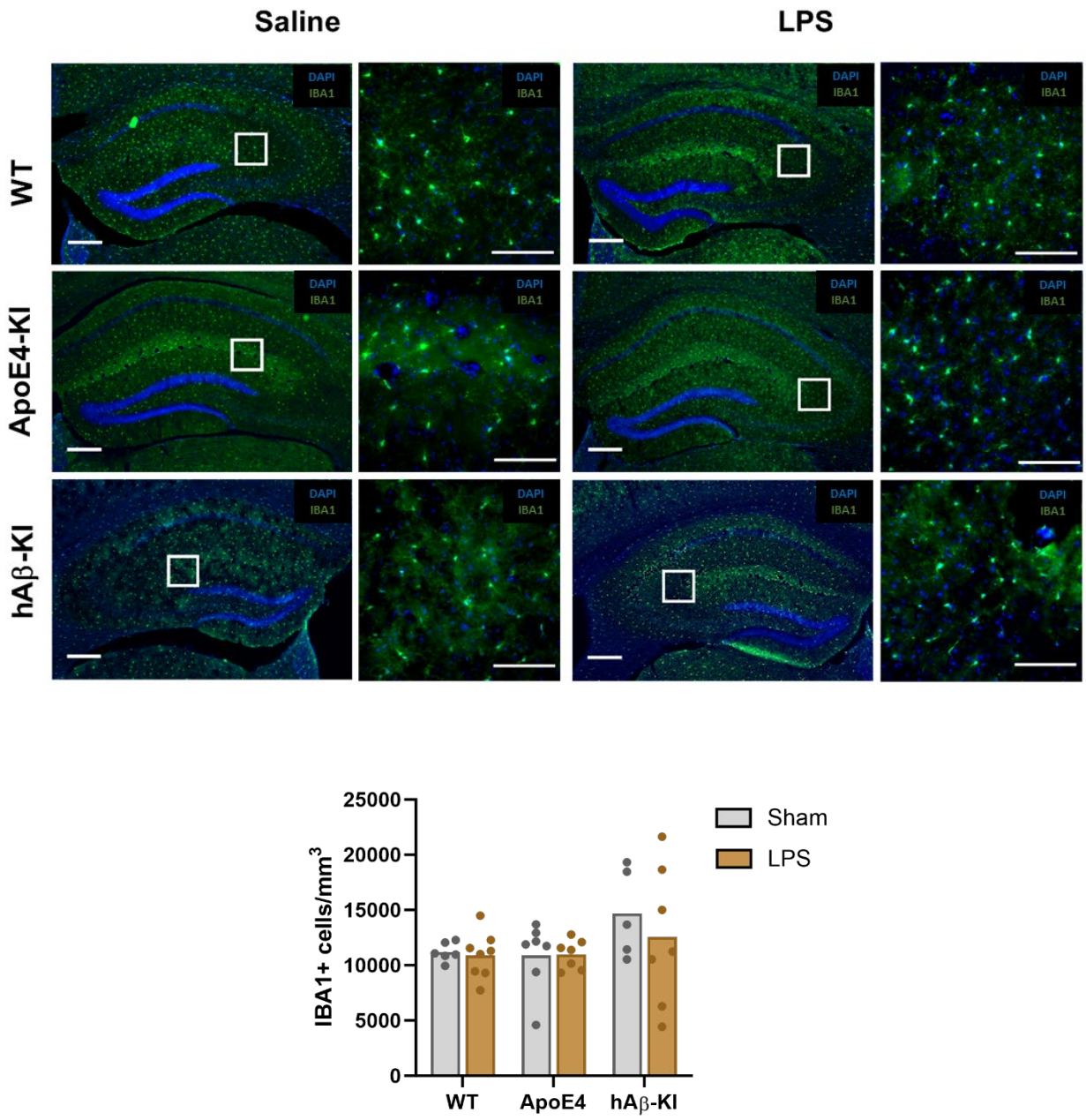

Figure 3.13: Total number of Iba1+ microglial cells (WT Sham=6, WT LPS=8, ApoE4 Sham=7, ApoE4 LPS=7, hAβ Sham=5, hAβ LPS=7, Scalebar: 20x -250µm, 40x - 100µm; All values represent the Mean ± SEM).

Similarly, GFAP positive cell numbers remained unchanged between groups as shown in Figure 3.14. This was supported by statistical analysis because there was no main effect or interaction between genotype and treatment factors (Fs < 0.3).

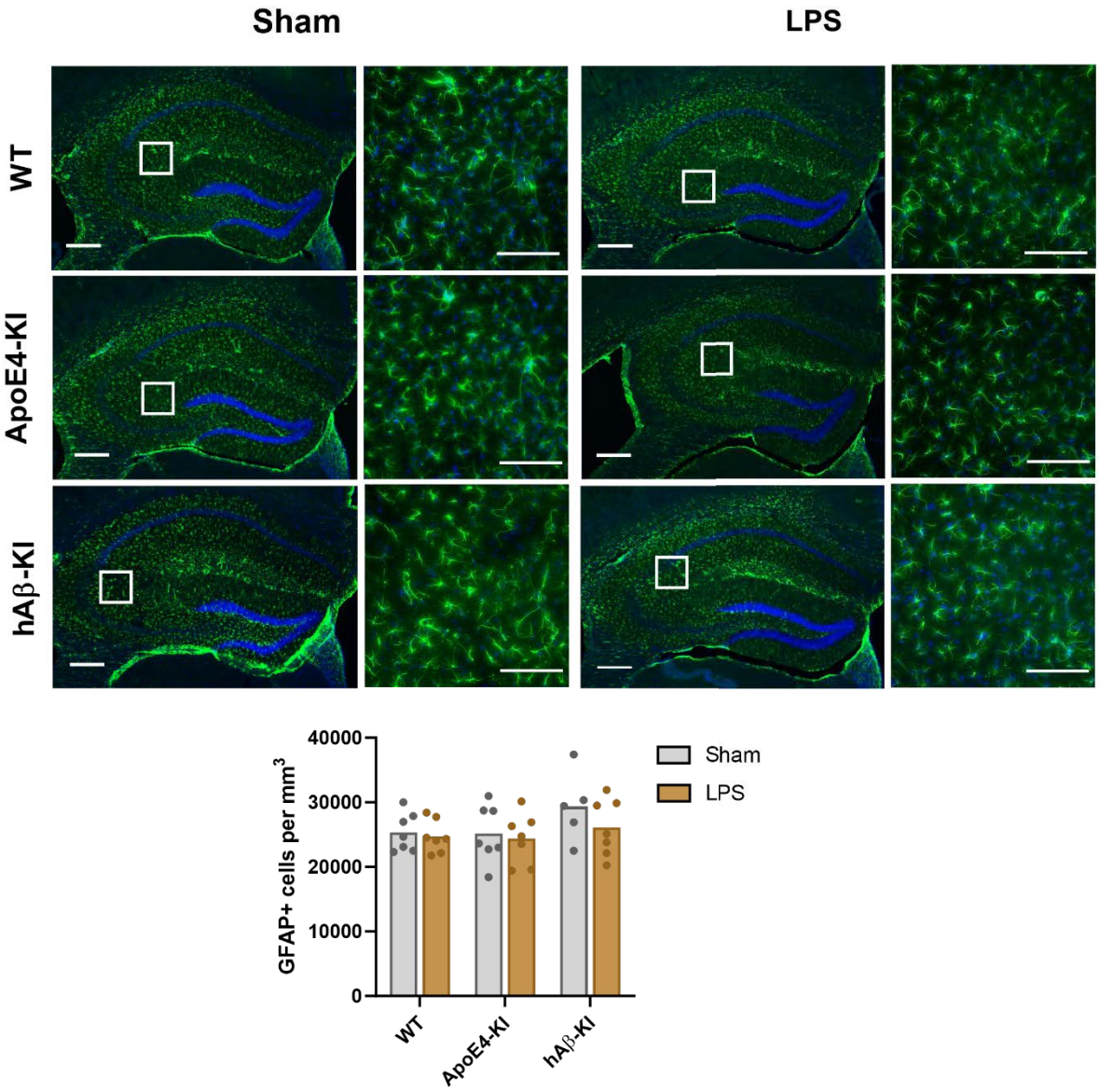

Figure 3.14: Total number of GFAP+ astrocyte cells (WT Sham=6, WT LPS=8, ApoE4 Sham=7, ApoE4 LPS=7, hAβ Sham=5, hAβ LPS=7, Scalebar: 20x -250µm, 40x - 100µm. All values represent the Mean ± SEM).

Experiment 2: Discussion

Together, the behavioural and cellular results of this experiment were somewhat inconclusive. Specifically, although I did find slight decreases in locomotor activity in LPS-treated ApoE4-KI and hAβ-KI mice, I was unable to detect any differences in anxiety or

spatial memory. Likewise, despite a decrease in spine density in LPS-treated ApoE4-KI mice, I did not see a similar decrease in hAβ-KI mice, nor did I detect increased neuroinflammation in either model.

Regarding the hypoactivity witnessed in my proposed sporadic AD model, this result could suggest that the combination of Apoe4 risk allele + LPS and hAβ genetic modification + LPS administration synergistically affected locomotor activity. This could be reflective of individuals with sporadic AD who demonstrate a reduction in activity levels (Friedland et al., 2001; Hartman et al., 2018). Interestingly, despite showing hypoactivity the ApoE4KI mice receiving LPS did not show a deficit/impairment in working memory or spatial memory relative to wildtype controls. This is interesting, because it is contradictory to what has been reported in the literature for this model, even in the absence of an LPS manipulation. For instance, a study by Rodriguez et. al., (2013) reported that young ApoE4-TR mice showed poor spatial learning in a probe trial of a Barnes Maze test. Furthermore, young (3-6 months)(G. A. Rodriguez et al., 2013), middle aged (10-13 months)(Boehm-Cagan & Michaelson, 2014; G. A. Rodriguez et al., 2013; Salomon-Zimri et al., 2014; Siegel et al., 2012) and aged (24 months)(Yin et al., 2011) ApoE4 mice have been found to exhibit deficits in acquisition learning and memory retrieval in Morris Water Maze test.

One potential reason for these contrary findings could be the choice of controls used, as most of the previous studies have compared against ApoE3 mice rather than the wildtype controls used here. Another probable reason could be the age of the animals used in our study. These two points are discussed extensively in the 'general discussion' – 'limitations and future directions' section.

The spine density changes for ApoE4+LPS animals were interesting as it could indicate a combined effect/interaction of these risk factors to result in a significant decrease of spine density. Although literature reports for a similar strain of ApoE4, the ApoE4-TR mice showed a reduced spine density without the additional neuroinflammation factor (Nwabuisi-Heath et al., 2013), I could not detect such changes in our Experiment-2. This could be because of differences in the strain, however, the combination of ApoE4 risk gene and neuroinflammation leading to a decrease in spine density could be partly attributed to the inherent effects of ApoE4 on spine density as described by (Nwabuisi-Heath et al., 2013) and discussed in the general discussion section of this chapter.

Additionally, it would be ideal to perform, a detailed analysis of spine categorizing the different types of spines like thin, stubby, or mushroom (Berry & Nedivi, 2017). This is because, according to the literature, the total number of spines could remain unchanged but there could be significant differences between certain spine types (e.g. the decrease in mushroom spines as indicated in Lin et al.,'s paper, (2017)). However, I did not have the time to carry out such a detailed analysis this in the current study. Therefore, it is indeed possible that although the total spine numbers have decreased, this decrease could have happened entirely in one specific type of spine (either thin, mushroom or stubby) which, when observed, could provide insights on the specific changes induced by LPS. Hence, future studies should consider looking at distinguishing the type of spines to better understand the effects.

We did not notice a significant difference in microglia and astrocyte cell numbers in our WT, ApoE4-KI or hAβ-KI animals treated with LPS. The results for ApoE4-KI mice, resembles the study results for this specific mouse strain published recently (Sepulveda et al., 2022). The levels of key proinflammatory cytokines such as TNF-α and IL-6

remained unchanged in APOE4-KI mice compared to controls at 6 months age, indicating that these animals do not yet show changes in inflammatory profiles. Nevertheless, results for LPS injection contradicts what has been observed in the literature in terms of brain immune cell response after LPS administration. For instance, in the study conducted by Yuangui Zu et al., (2012) a single i.c.v injection of LPS given to the ApoE4-TR mice resulted in prominent increases of both astrocytes and microglia. This difference could have resulted from the variations in the mode of LPS administration between studies, as our animals received intraperitoneal LPS injections whereas the above-mentioned study used an i.c.v injection. Likewise, LPS injections alone have been reported to increase astrocyte and microglial cell numbers in cortex and hippocampus of wildtype mice (Fernández-Calle et al., 2020; Garcia-Hernandez et al., 2022; Ryu et al., 2019; Sardari et al., 2020). This is not surprising as these studies involved a high dosage of LPS injections ranging from 1mg/kg to 10mg/kg, whereas I used a low dosage of 0.2mg/kg LPS.**3.3.3) Experiment 3 – LPS induced neuroinflammation as a sporadic model for AD:**

I hypothesized that the failure to detect any meaningful changes in behaviour or neuroinflammation in Experiment 2 was due to the very low concentration of LPS used relative to other doses that have been used to induce neuroinflammation in the literature (Khulud Abdullah Bahaidrah et al., 2022; X. Feng et al., 2021; Zhao et al., 2019). Therefore, for Experiment 3, I decided to investigate whether a higher dose of LPS (0.5mg relative to 0.2mg used in Experiment 2) would induce the desired changes in spine density and neuroinflammation. Although ideally, we would have repeated Experiment 2 in its entirety with this new, higher dose of LPS, unfortunately we did not have the requisite number of aged transgenic animals available for this, or any following studies. Therefore, we completed Experiment 3 and all following experiments in wild-type animals only, with neuroinflammation as the sole sporadic factor in our AD model. Moreover, because

previous studies have already demonstrated anxiety-like and spatial memory deficits in wildtype animals treated with this dose of LPS (Hou et al., 2014), we did not test here for behavioural deficits, but will address different behavioural deficits as a result of neuroinflammation in Chapter 4.

3.3.3a) No differences in spine density after 4 weeks LPS injections:

There were no differences in spine density in either apical (t=0.6673, p=0.5057, Figure 3.15A) or basal dendrites (t=0.5682, p=0.5708, Figure 3.15B) of animals that received 4 weeks of LPS injections relative to Sham controls.

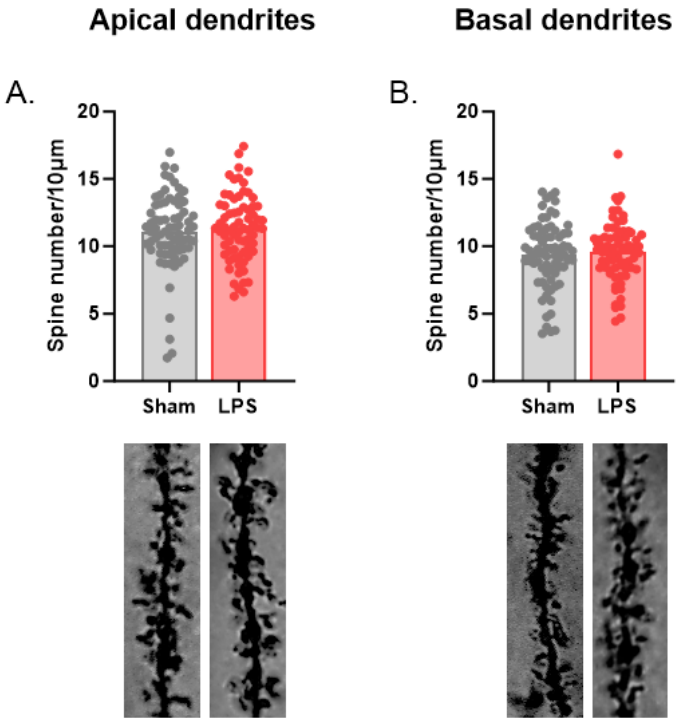

Figure 3.15: Apical dendritic spines in Sham and LPS animals (A), Basal dendritic spines (B), (Sham, LPS, n=72 dendrites; 12 dendrites randomly chosen per animal, 6 animals per group; All values represent the Mean ± SEM)

3.3.3b) Differences in glial cell population after 4 weeks LPS injections:

I next quantified the number of cells and cell intensity of both microglia and astrocytes in the dorsal hippocampus. I observed that the number of Iba1+ cells increased (t=4.387, p=0.0023, Figure 3.16A) in response to LPS injections, however, the total cell intensity of Iba1 did not change (t=1.765, p=0.1156, Figure 3.16B). This suggests that LPS caused microglia to proliferate in number but that morphological changes were not sufficiently large enough to reach significance.

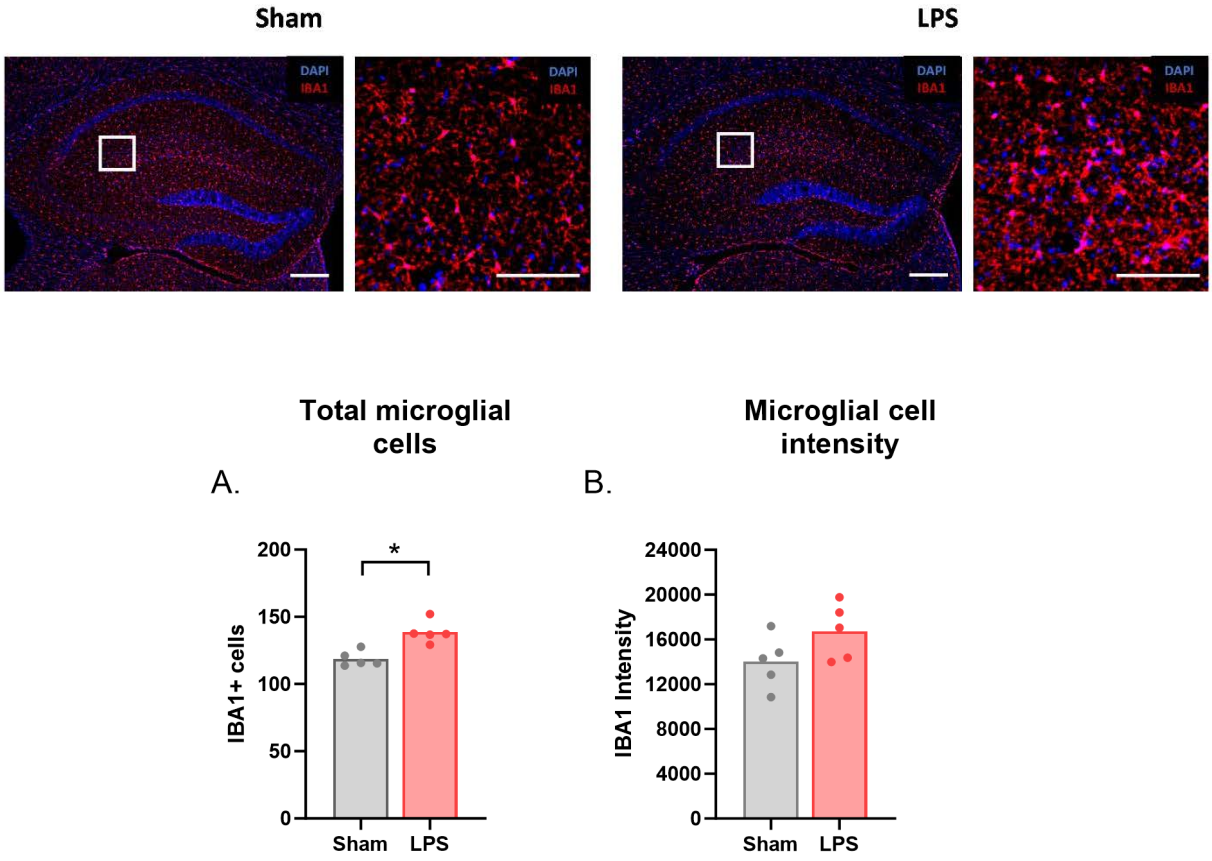

Figure 3.16: Number of Iba1+ microglial cells (A) and microglial cell intensity (B) in the dorsal hippocampus after 4 weeks LPS injections. (Sham, LPS, n=5; Scalebar: 20x -250µm, 40x - 100µm; $p<0.05$, All values represent the Mean ± SEM).

In contrast to Iba1 expression, there was no elevation in GFAP+ve cells (t=0.9506, p=0.3696, Figure 3.17A), however there was a sharp increase in the intensity of GFAP intensity in LPS-injected animals relative to Sham controls (t=5.281, p=0.0007, Figure 3.17B). This result suggests that LPS did not increase the number of astrocytic cells (at least to the threshold of significance) but did alter astrocytic morphology.

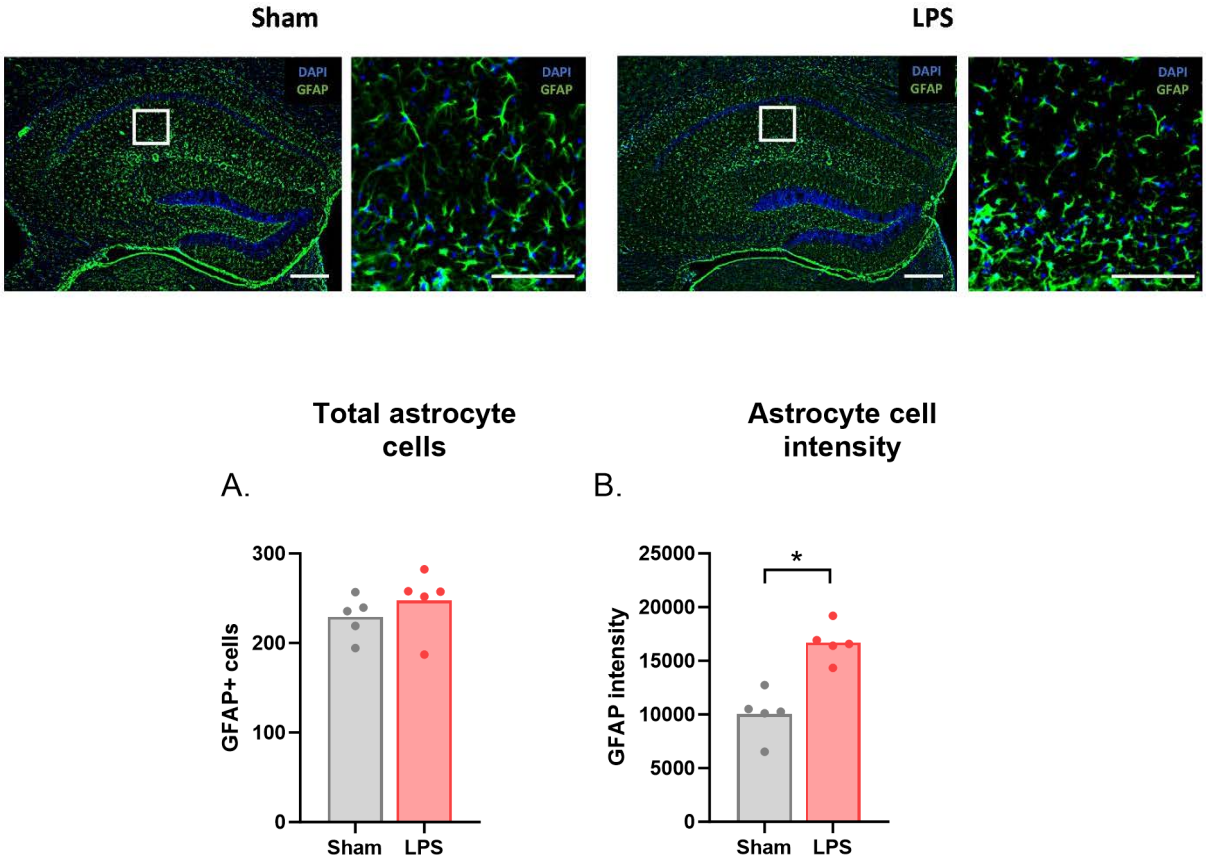

Figure 3.17: Number of GFAP+ microglial cells (A) and astrocyte cell intensity (B) in the dorsal hippocampus after 4 weeks LPS injections. (Sham, LPS, n=5; Scalebar: 20x -250µm, 40x - 100µm; p<0.05, All values represent the Mean ± SEM).

3.3.3c) No differences in spine density after 6 weeks LPS injections:

After seeing no difference in spine density after 4 weeks LPS injections, I proceeded to check for any differences in the same after 6 weeks LPS injections. I quantified apical and

basal dendritic spines, however again found no difference in both groups in animals that received LPS compared to Sham. For apical dendrites, (t=1.286, p=0.2007, Figure 3.18A), for basal dendrites, (t=0.01311, p=0.9896, Figure 3,18B).

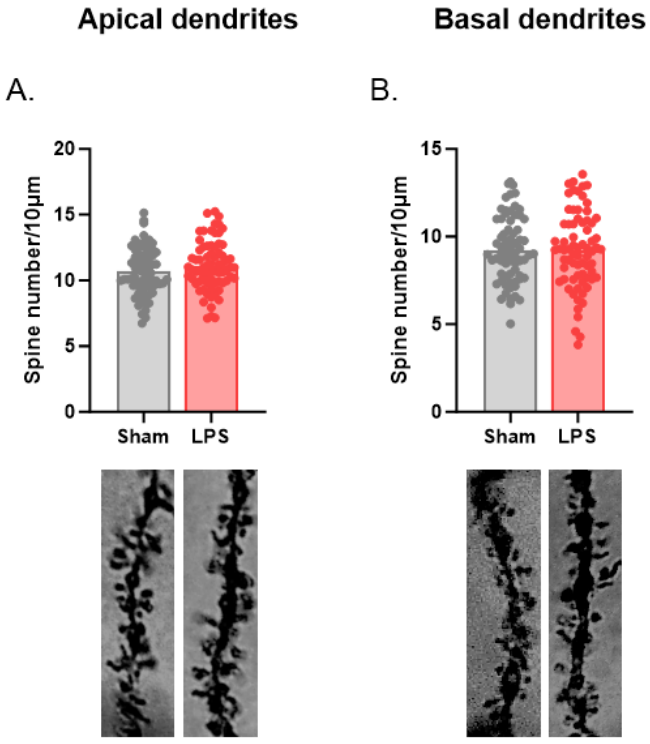

Figure 3.18: Apical dendritic spines in Sham and LPS animals (A), Basal dendritic spines (B) after 6 weeks of LPS treatment, (Sham, LPS, n=72 dendrites; 12 dendrites randomly chosen per animal, 6 animals per group; All values represent the Mean ± SEM).

3.3.3d) Differences in glial cell population after 6 weeks LPS injections:

I again quantified microglia and astrocytes population in the dorsal hippocampus for these mice. Similar to the results from mice injected for only 4 weeks, in the animals injected for 6 weeks microglial cell populations were increased because the number of Iba1+ve cells was significantly higher in LPS-injected mice relative to Sham controls,

(t=2.948, p=0.0185, Figure 3.19A). Again, however, there were no differences in IBA1+ve cell intensity (t=1.719, p=0.1240, Figure 3.19B).

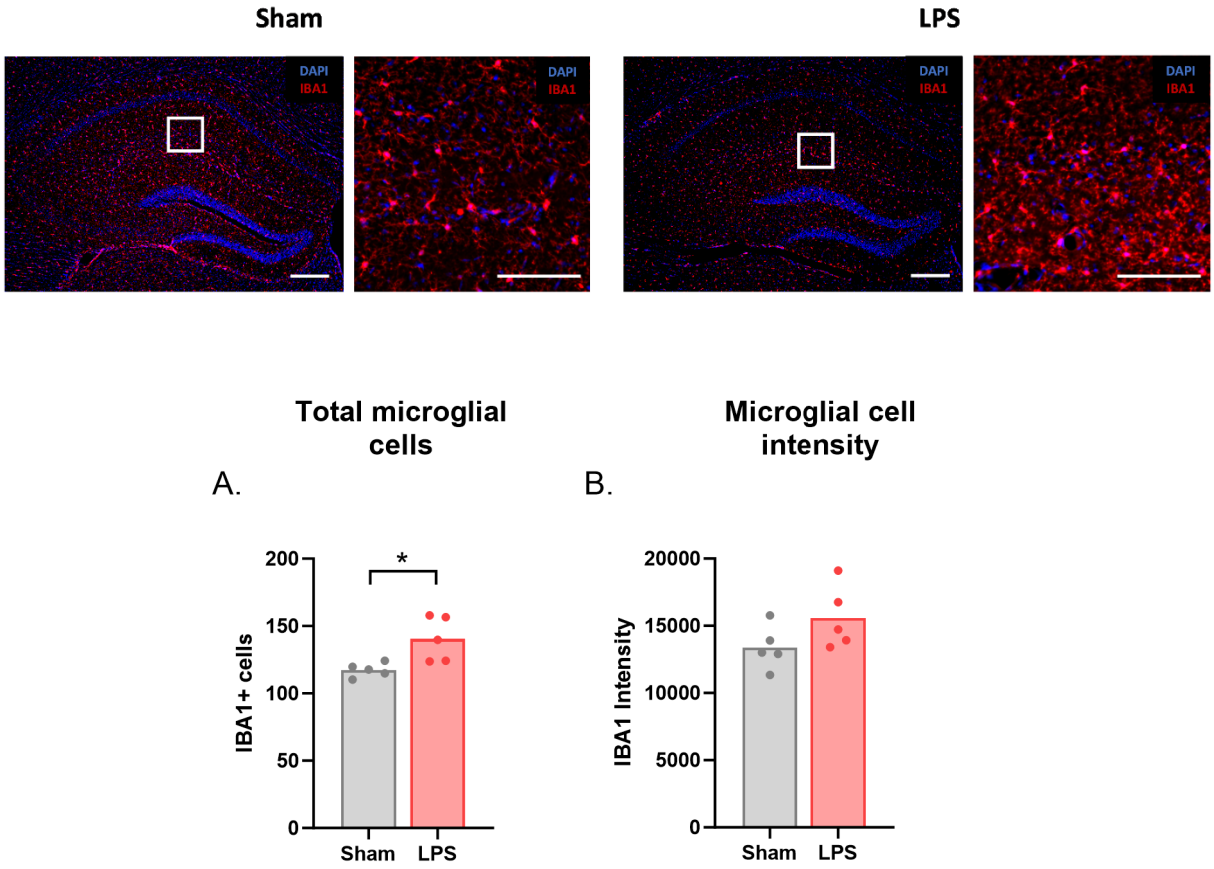

Figure 3.19: Number of Iba1+ microglial cells (A) and microglial cell intensity (B) in the dorsal hippocampus after 6 weeks LPS injections. (Sham, LPS, n=5; Scalebar: 20x -250µm, 40x - 100µm; $p<0.05$, All values represent the Mean ± SEM).

Astrocytes expression also followed the same pattern as observed for the animals injected for 4 weeks, because there were no change in the total number of astrocytes between both groups, as measured by the numbers of GFAP+ve cells (t=0.03081, p=0.9762, Figure 3.20A), however the intensity of GFAP+ cells was higher in LPS treated animals compared to Sham (t=7.429, $p<0.0001$, Figure 3.20B).

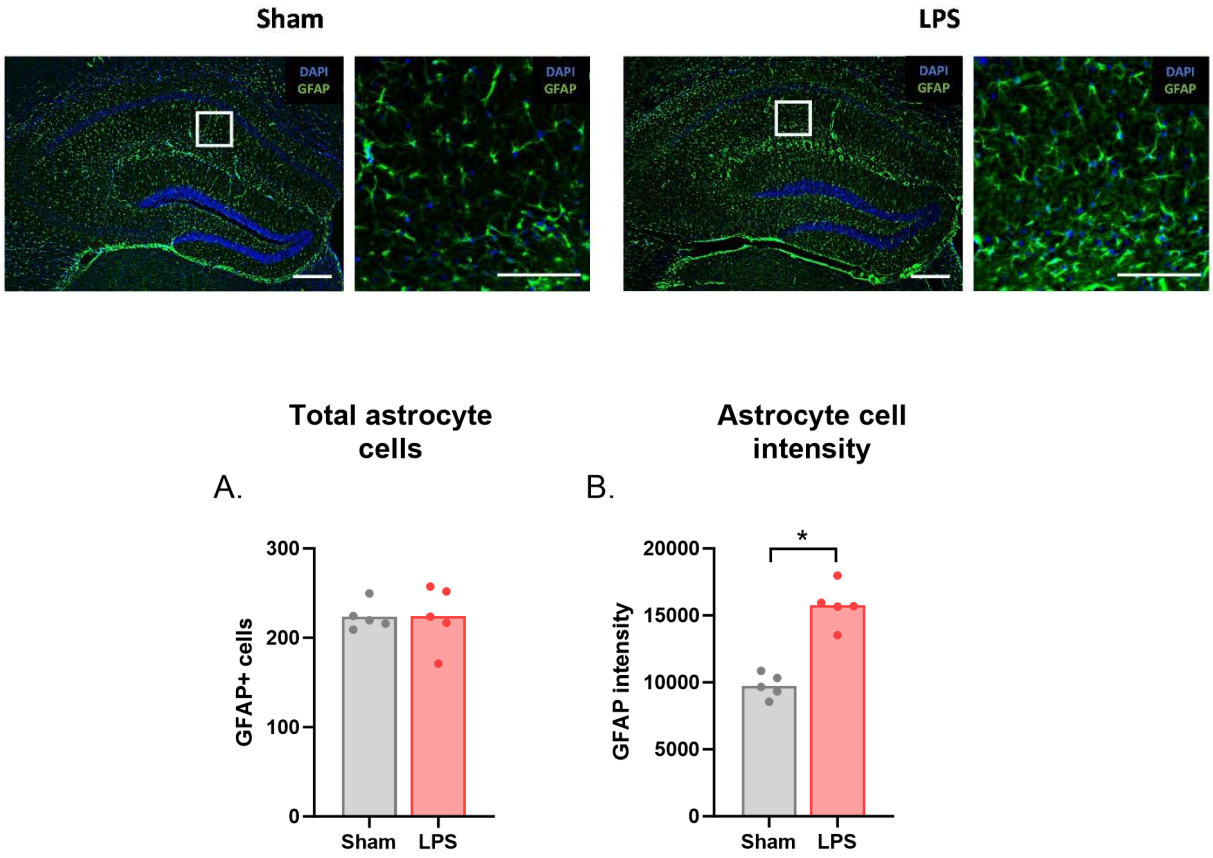

Figure 3.20: Number of GFAP+ microglial cells (A) and astrocyte cell intensity (B) in the dorsal hippocampus after 6 weeks LPS injections. (Sham, LPS, n=5; Analysis; Scalebar: 20x -250µm, 40x - 100µm; $p<0.05$, All values represent the Mean ± SEM).

3.3.3e) Experiment 3: Discussion

Overall, we did not observe a reduction in spine density after either 4 or 6 weeks of LPS injections relative to Sham controls. However, there were changes in both microglial number and astrocytic expression that indicated some success in inducing a neuroinflammatory response as a result of LPS injections.

It is curious that I observed an increase in microglial and astrocytic expression, but no similar change in spine density. The following could be potential reasons why. The failure to observe changes in spine density could be a result of the LPS dosage insufficient to

exert such long lasting influence on the spine density. Literature reports for intraperitoneal LPS induced decrease in spine density varies between studies. While a single LPS injection of 0.5mg/kg were seen to produce alterations in spine density in the CA1, CA2 and DG region of the hippocampus, there were multiple factors involved in this study, such as Trk-B agonists and surgery. Results from this study could have been a combined effect of these factors inducing changes in spine density (Zhang et al., 2014). Another study that performed single intraperitoneal injection of LPS of the same 0.5mk/kg, did not witness a change in spine density even after 28 days of injection. Significant changes in spine density started appearing only at 56 days after LPS injection (Püntener et al., 2012). A complete opposite effect i.e., increase in dendritic spines were observed upon i.p LP S injections of 0.5mg/kg in nucleus accumbens of rats (Corbit et al., 2001). This study further witnessed an increase in glial cell activation upon LPS treatment which is in line with my results here. One argument put forward by the authors was that an increase in dendritic spines occurred as a result of effects exerted by microglia and astrocytes upon activation by LPS. This was true given the literature supporting neurotrophic factors secreted by microglia (Gomes et al., 2013) and astrocytes (Iravani et al., 2012) upon activation. This could have served as a positive effect on dendritic spines in our study after each LPS injection, therefore one of the probable reasons for not witnessing a negative effect of LPS (i.e., LPS decreasing dendritic spines) on our animals. It could therefore be possible that a higher dosage of LPS is required to induce a more potent change in spine density of pyramidal neurons.

On the other hand, i.c.v. injections of LPS were found to always result in a decrease in spine density as observed in the literature (Ano et al., 2019; Ano et al., 2020). These studies could potentially provide a mechanism for central, and more direct effects of LPS on structures such as spine density in rodents. Because we ideally aimed to observe changes

in both spine density and neuroinflammatory markers, we next investigated a more localized model of hippocampal neuroinflammation in which LPS was injected directly into the hippocampus.

3.3.4) Experiment 4 – Intrahippocampal lipopolysaccharide injection:

In Experiment 4 I induced neuroinflammation specifically in the region of interest – the dorsal hippocampus - hoping to observe alterations in both spine density and neuroinflammatory markers. Dorsal hippocampal neuroinflammation is strongly associated with AD pathology (Tuppo & Arias, 2005), therefore this was our next target in our attempt to create a sporadic model of AD. Specifically, an intrahippocampal mode of injection with a concentration of 4µg/µl LPS was finalized based on the study by Huang et al., (Huang et al., 2012). Following this surgery, brains were separately collected for Golgi staining or immunostaining, at both the 3- and 7-day timepoint after surgery. These two timepoints were chosen based on the studies of (Fu et al., 2014) and (Hong et al., 2020), who showed immediate increase in inflammatory markers 2-7 days after LPS injection (systemic injections) which declined after 7 days. Based on these systemic injection studies, we expected that spine density loss and neuroinflammation markers would peak at 3 days and gradually decline after 7 days following intrahippocampal LPS surgery as well.

3.3.4a) 3 days time point: Increased glial cell activation followed by slight changes in dendritic spine density:

Brain sections were checked for reactivity of microglia (Iba1) and astrocytes (GFAP) as described previously. Figure 3.21A and B showed that microglial cell counts ($t=2.569$, $p=0.0424$) and intensity ($t=3.242$, $p=0.0176$) were significantly higher in the LPS group relative to Sham, 3 days after surgery. However, there was no change in the astrocytes cell

number (t=1.545, p=0.1733) or intensity (t=0.4587, p=0.6626) as shown in figure 3.21C and D.

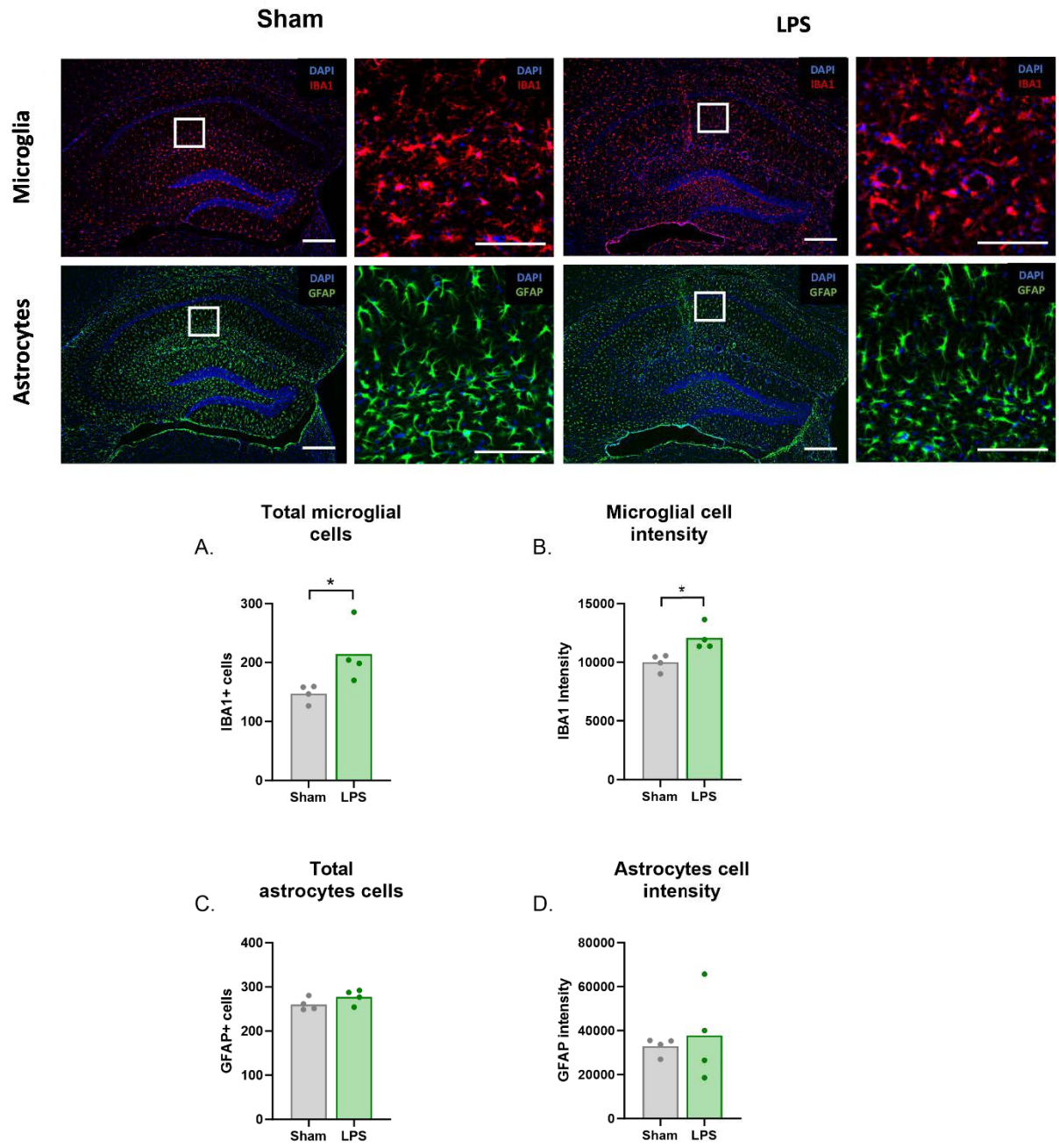

Figure 3.21: Glial cell activation 3 days after surgery. Total number of microglial cells (A) and microglial cell intensity (B) in the Sham and LPS groups. Astrocytic cell population

(C) and cell intensity (D) in both groups. (Sham, LPS, n=4; Analysis; Scalebar: 20x -250µm, 40x - 100µm; $p<0.05$, All values represent the Mean ± SEM).

After confirming glial cell activation following LPS injections, I proceeded to check for changes in dendritic spine density by performing Golgi staining. Figure 3.22 showed that there were only slight changes in spine density 3 days after LPS injections. The apical dendritic spines in the LPS group did not differ from the Sham controls which is indicated by t = 1.510, p-value of 0.1345 (Figure 3.22A). However, there was a significant increase in the basal dendritic spine density of the LPS group compared to Sham. This was confirmed by a two tailed t-test (t = 2.228, p=0.0283). Taken together, these results confirm the presence of neuroinflammation after LPS injections and suggest that the witnessed neuroinflammation is starting to impact dendritic spine density.

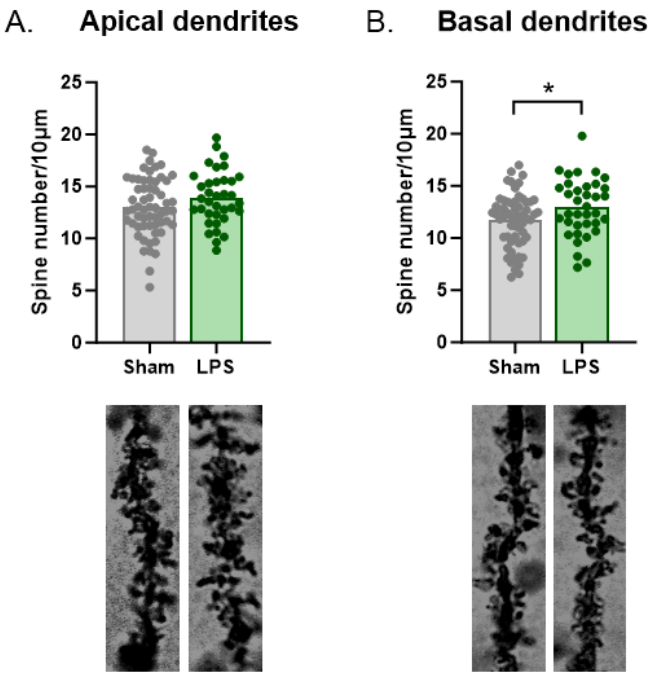

Figure 3.22: Apical dendritic spine density in Sham and LPS treated animals, 3 days after surgery (A). Dendritic spine density from basal dendrites after of Sham and LPS treated animals, 3 days after surgery (B). (Sham n=60 dendrites, LPS n=36 dendrites, 12

dendrites randomly chosen from one mouse; $p<0.05$, All values represent the Mean ± SEM).

3.3.4b) 7 day time point: Increased glial cell activation followed by decrease in dendritic spine density:

We checked for glial cell activation in our animals, 7 days after LPS surgery. Figure 3.23A and B showed that the microglial cell activation persisted 7 days after LPS injections. This was supported by a statistical analysis indicating that the microglial cell numbers ($t=4.210$, $p=0.0084$) and the intensity ($t=2.913$, $p=0.0333$) remained significantly higher in the LPS treated group relative to controls. There was an obvious change in morphology of the LPS treated microglial cells as seen from the representative images. This time, there was a change in astrocyte cell population, indicated by a significant increase in total cell counts ($t=6.717$, $p=0.0011$) but the intensity ($t=1.913$, $p=0.1193$) did not differ between Sham and LPS groups (figure 3.23C and D).

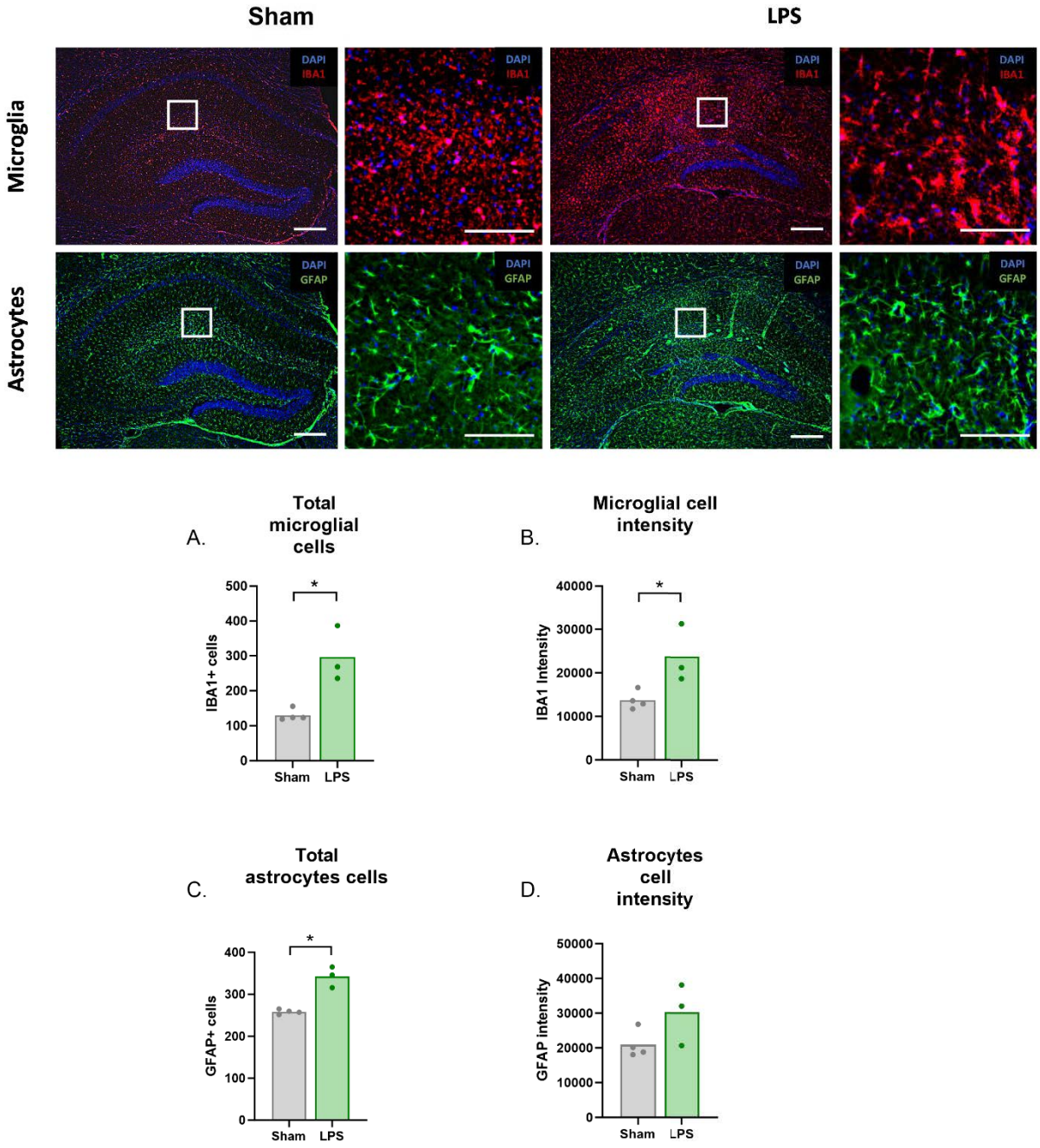

Figure 3.23: Glial cell activation 7 days after surgery. Total number of microglial cells (A) and microglial cell intensity (B) in the Sham and LPS groups. Astrocytic cell population (C) and cell intensity (D) in both groups. (Sham n=4, LPS n=3; Analysis; Scalebar: 20x - 250µm, 40x - 100µm; $p<0.05$, All values represent the Mean ± SEM).

We proceeded to check for dendritic spine density differences and found that both apical and basal dendritic spines were significantly decreased in LPS treated animals compared to Sham. This was confirmed by statistical analysis, a two tailed t-test for apical dendrites, t = 3.958, p=0.0001, (Figure 3.24A) and basal dendrites, t = 2.565, p=0.0119 (Figure 3.24B). Overall, these results confirmed that intrahippocampal LPS injections both increased glial cell numbers and decreased spine density in dorsal hippocampus.

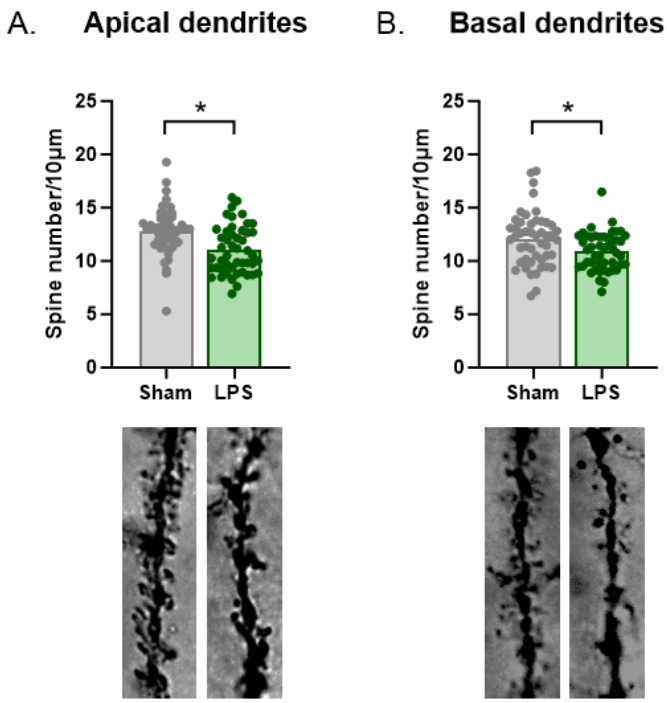

Figure 3.24: Apical dendritic spine density in Sham and LPS treated animals, 7 days after surgery (A) Basal dendritic spine density 7 days after surgery (B). (Sham, LPS n=48 dendrites, 12 dendrites randomly chosen from one mouse; $p<0.05$, All values represent the Mean ± SEM).

3.3.4c) Experiment 4: Discussion

Experiment 4 confirmed that intrahippocampal injections of LPS produced changes in glial cell activation and dendritic spine density. Increased expression of

neuroinflammatory markers was observed at both the 3- and 7-day timepoints. At the 3-day timepoint, there was an increase in dendritic spine density for the basal dendrites and no change in apical dendrites. This is consistent with previous results which have reported increases in spines in cell culture within 3 weeks after LPS treatment (Chugh et al., 2013) and 7 days after systemic LPS injections (Manabe et al., 2021). Interestingly, 7 days after LPS surgery, the glial cell activation was still higher but dendritic spine density for both apical and basal dendrites were now significantly decreased.

These results confirmed that with intrahippocampal LPS injections, there was visible neuroinflammation and loss of spines 7 days later. This is noteworthy because 7 days after surgery is the timepoint at which we would typically begin behavioural testing. This allowed us to proceed with the next step in testing our sporadic AD mouse model, which was to use this procedure in Chapter 4 to determine whether it produced cognitive-behavioural deficits in goal-directed action.

3.4) General discussion:

The overall aim of this chapter was to establish a novel sporadic model of AD. First, in Experiment 1 I validated the behavioural and cellular techniques that my proposed AD animals would be tested for. Specifically, I observed hyperactivity and impaired spatial memory in J20 animals compared to wildtype, replicating established results from the literature (Flores et al., 2018; Pozueta et al., 2013). I then checked for cellular level changes. I found that J20 animals had reduced dendritic spines compared to wildtype, and there was also a significant increase in astrocytes in J20s, but there was no difference in microglial cell numbers. In Experiment 2, I proceeded to check our proposed sporadic AD models using these now validated techniques. There was some hypoactivity observed during open field in the APOE4+LPS and hAβ-KI+LPS groups relative to the rest, but no

changes in anxiety-like behaviours and no differences in spatial memory. Moreover, glial cell assessment revealed no indication of neuroinflammation. The only change observed was a decrease in spine density in ApoE4-KI mice. Therefore, in Experiment 3, I chose to focus on a single, sporadic factor: neuroinflammation, to determine whether a higher dose would produce the desired cellular changes. After increasing the LPS concentration from 0.2mg/kg in Experiment 2 to 0.5mg/kg in Experiment 3, I did observe evidence of neuroinflammation (i.e. increased glial cell marker expression), however there was no effect on spine density. Therefore, in Experiment 4, I decided to employ a more specific and concentrated approach by administering the LPS injections locally into the dorsal hippocampus. This time, the manipulation was successful in inducing both neuroinflammation and a decrease in spine density, specifically when examined 7 days after injections. Spatial memory deficits were not tested for in Experiments 3 and 4 because these have been reliably observed previously with intra-hippocampal LPS injection. Instead, along with tests for locomotor activity and anxiety-like behaviour, I chose to dedicate the entire next chapter (Chapter 4) to investigating the consequences of intra-hippocampal LPS injections on another behaviour that is highly relevant to AD: goal-directed action control.

The results of Experiment 1 are important here for the interpretation of the following experiments, because they demonstrate that any future null effects detected in either the behaviour or the cellular analyses were not a result of problems with the methodologies or protocols used. That is, the observation that spatial memory was impaired in J20 animals confirmed results from two previous reports (Flores et al., 2018; Larson et al., 2012), and the observed reduction in spine density confirmed the findings of Pozueta J et al., (2013) as did the increase in the number of astrocytes population (Pozueta et al., 2013; A. L. Wright et al., 2013).

In Experiment 2, I observed a decrease in locomotor activity of ApoE4-KI and hAβ-KI animals treated with LPS. This is opposite to what other familial AD models (including J20) typically display in terms of locomotion, which is usually increased (Oblak et al., 2021; Wang et al., 2022). The ApoE4-KI mice that were not treated with LPS in the current study did not show a decrease in locomotor activity, which suggests that this manipulation alone was not sufficient to alter behaviour, but this alteration required a gene/environment interaction between the ApoE4-KI and neuroinflammation. This could be potentially important for our understanding of how such interactions in AD patients might be required for reductions in locomotor activity. Indeed, a 2018 genome wide association study has identified ApoE4 as one of the potent influencers of physical activity in humans (Klimentidis et al., 2018). If current results are translatable, however, they suggest that ApoE4 only causes reductions in such activity if neuroinflammation is present. Importantly, this finding could suggest that individuals expressing the ApoE4 mutation could be prevented from suffering locomotor deficits if neuroinflammation is prevented.

The failure to observe any anxiety of spatial memory deficits in Experiment 2 suggests that ApoE4-KI and hAβ-KI mice are unlikely to display such deficits, at least at 6 months of age when they were tested here, even when combined with systemic injections of 0.2mg/kg LPS to induce neuroinflammation.

Likewise, the failure to observe alterations in neuroinflammatory markers in these models is unlikely due to issues with our techniques because they were able to detect such changes in Experiment 1 as well as Experiments 3-4. This discrepancy could be a result of the difference in analysis techniques used for these experiments. The ideal methodology for all results would have been to use the stereological counting with MBF

software. This is because it provides serial section intervals and traces the hippocampal area volume, so that the software can reconstruct a hippocampal volume using the measured parameters and give us outputs in terms of cells/area. (used in Fig3.16, 3.17, 3.19-21, 3.23). The advantage of using Stereo-investigator is that the cells/area gives the total amount of cells in the reconstructed hippocampal volume (from the traced hippocampus ROI inputs). The cell counts in this case will be proportional to the hippocampal volume. The alternate method of representing just cell counts/ intensity, (such as in Fig 3.12 to 3.15, 3.18, 3.22) does not take the total hippocampal volume into account, in which case the cell counts are not proportional to this volume. Unfortunately, the shift in methodologies was unavoidable, as the laboratory I was working in moved from one institution to another and the new facility did not have stereo-investigator hardware or software. As such, the results may be slightly less reliable because the increase in cell counts observed in our case could be a direct result of an increase in glial cell numbers, or a result of comparatively bigger hippocampal size in animals of that group. However, because I made sure that the ROI stayed same throughout the sections, it is less likely that this was the case.

Experiment 2 did identify a decrease in the spine density measure in APOE4-KI+LPS animals, however, suggesting that the APOE4 mutation in combination with neuroinflammation might be a particular risk factor for loss of hippocampal spines. Whether this could probably be one of the factors underlying the hypoactivity witnessed in these animals, remain unclear. This finding is consistent with the observation that ApoE4 risk gene has been shown to have resulted in spine density decrease in primary neurons (Brodbeck et al., 2008) and in rodents (Ji et al., 2003). The failure to observe such effects in our mice could be a strain specific effect, however, our animals could have retained this effect to an extent which, in combination with the neuroinflammation factor,

resulted in an evident decrease in spine density. The role of ApoE4 in neuronal plasticity has been clear for many years now (Poirier et al., 1995). Studies suggest that ApoE4 is not as efficient as ApoE3 in the process of neuronal outgrowth stimulation and synaptic remodulation (Dumanis et al., 2009). Aged ApoE4 transgenic mice showed obvious differences in the synapse to neuron ratio (Cambon et al., 2000). One explanation for this could be an ApoE4 dependent abnormal transportation of cholesterol in the brain (Borràs et al., 2022; Jeong et al., 2019). Although neurons are able to regulate spine formation on their own, astrocyte-derived cholesterol levels have been known to play a crucial role in synaptogenesis (Mauch et al., 2001). Therefore, ApoE4 mediated abnormal cholesterol transportation could have possibly predisposed the dendritic spines for any changes triggered by LPS induced neuroinflammation in our animals.

An additional point worth noting is that the current study only tested animals were only tested for changes in locomotor activity, anxiety and spatial memory. It is possible, therefore, that other types of behavioural deficits were missed. Future studies might wish to address this by testing additional constructs, such as working memory, object recognition, and contextual fear memory to yield a complete profile of changes occurring in these animals. Recognition memory is impaired in individuals with Alzheimer's disease (Viggiano et al., 2008) and are often tested in individuals with amnestic mild cognitive impairment, in an attempt to identify individuals with potential progression to Alzheimer's disease (Ally, 2012; Goldstein et al., 2019). In rodents, recognition memory is often assessed by performing object recognition test, where rodents are checked for their ability to differentiate between a familiar and new object (Zhang et al., 2012). Similarly, fear memory is important to adapt to new threats in the environment(Hamann et al., 2002; Maturana et al., 2023) is impaired in Alzheimer's disease. Literature reports fear conditioning gradually declining in amnestic mild cognitive impairment, and individuals

with AD, compared to healthy controls, which could be an earliest marker for distinguishing AD from prodromal stages (Nasrouei et al., 2020). In rodents, fear learning and memory is assessed using fear conditioning paradigm, which is based on learning the association between a neutral cue (conditional stimulus) and an aversive cue (unconditional stimulus). Animals which learned this association would freeze to a neutral cue, even in the absence of an aversive cue in the testing session. Familiar AD models such as TgCRND8, and Tg2576 were impaired in fear conditioning by showing reduced freezing to the conditional stimulus (Hanna et al., 2012; Kishimoto et al., 2017). Checking for behavioural changes in these paradigms could enable detecting subtle changes in memory in these ApoE4-KI and hAβ-KI treated with LPS.

As expanded on in the general discussion, there could be several reasons other than methodological failure as to why I did not observe a pronounced Alzheimer's phenotype in any novel sporadic model. One important factor influencing these results must be the age at which we looked for behavioural changes. Here, the animals employed were 6 months of age which could be too soon to detect such differences, as even some of the well-known familial AD models like APP/PS1, App^{NL-G-F}/MAPT tend to start showing working and spatial memory impairments as late as 9 months of age (Malm et al., 2007; Saito et al., 2019). Likewise, recent publication on hAβ-KI mice have reported deficits in contextual fear conditioning at 10 months of age (Baglietto-Vargas et al., 2021). Future studies may therefore wish to repeat the experiments reported here with older mice. Additionally, there could be an issue with the particular strains of mice used in the current study. Most of the studies related to ApoE4 have been carried out in the ApoE4 targeted replacement mice obtained from Taconic (Baglietto-Vargas et al., 2021), while we used ApoE4-KI mice obtained from Jackson laboratory (consortium, 2018). Although these two mouse strains are almost similar in terms of gene expression pattern, there are some

subtle differences in the developmental process which could have resulted in the differential effects we see in our results. Finally, it could be that our dosage of LPS was simply too low for it to produce the expected neuroinflammatory effects, even in combination with genetic risk factors. This possibility is supported by the fact that increasing the dose in Experiments 3 and 4 was sufficient to produce evidence of neuroinflammation.

Taken together, these results suggest that intrahippocampal injections of LPS were the most effective of the various methodologies I employed to induce both neuroinflammation and decreases in spine density. As mentioned, I did not test intrahippocampally injected animals for spatial memory deficits as these have been previously reported in the literature following this manipulation. However, I did assess separate cohorts of animals that underwent this manipulation for locomotor activity and anxiety-like behaviours using the open field test, and these results are reported in Chapter 4. I chose to test this in a separate chapter so that I could do so alongside an in-depth investigation of this sporadic model of AD from a different, cognitive-behavioural perspective. In particular, I investigated whether neuroinflammation in the hippocampus could replicate the impairments observed in AD patients in their abilities to perform goal-directed action.

4. Creating a better behavioural model for sporadic Alzheimer's disease:

4.1) Introduction:

Pre-clinical AD research has largely focused on behavioural paradigms such as spatial learning and memory, working memory, object recognition memory, and associative learning tasks. Although deficits in some of these behaviours are primarily observed in Alzheimer's disease patients, functional consequences of these deficits in day-to-day life of an AD patient remains largely unaddressed in preclinical research. This is a critical oversight, because (according to the NIH)((NIH), 2020), an individual will not progress to an Alzheimer diagnosis unless they are experiencing impairments in this functionality. Additionally, the clinical staging of dementia according to NIA-AA (*Revised Criteria for Diagnosis and Staging of Alzheimer's Disease: Alzheimer's Association Workgroup*, 2023) categorizes individuals into stage 4 (dementia with mild functional impairment) only when individuals start showing a decline in activities of daily life and require assistance with certain tasks. In the following chapter, I address this by investigating whether mice with hippocampal neuroinflammation – the procedure that was demonstrated to be successful in achieving both increased neuroinflammatory markers and decreased dendritic spine density in Experiment 4 of the previous chapter – also display cognitive-behavioural deficits in goal-directed action control.

As reviewed in Chapter 2, individuals with Alzheimer's disease exhibit broad deficits in cognitive control over everyday goal-directed tasks, such as bathing, cooking, and dressing themselves. These tasks require individuals to integrate multiple underlying cognitive processes, such as memory (e.g. how much butter to add to a recipe) and motor

selection (e.g. washing themselves in the shower) to achieve a desirable goal, and could thus be considered a more complex behaviour than those typically tested in preclinical AD. Thus, it is critical that we capture these deficits in a preclinical model so that we can understand their neuropathological correlates, thus providing a more complete testing ground for future treatments. Although doing such a test is beyond the current capability of our laboratory, we are seeking out avenues in which we might be able to carry out such a study, by pairing with researchers that have access to AD patients (e.g. Prof. Bruce Brew of St. Vincent's Hospital in Sydney).

In order to evaluate goal-directed actions in animals with hippocampal neuroinflammation I used an outcome devaluation paradigm. Outcome devaluation is an extensively validated test for goal-directed action in both humans and rodent models. Although devaluation has never been tested in Alzheimer's patients directly, it has been employed in other patient populations such as individuals with Parkinson's disease (de Wit et al., 2011) and schizophrenia (Morris et al., 2018) where performance on this task was found to be predictive of real-world behavioural deficits in goal-directed actions. Given the fact that individuals with AD show multiple deficits in carrying out goal-directed activities, it would make a lot of sense for the gold standard test of goal-directed action, devaluation, to be tested in individuals with AD. The fact that it hasn't, is likely a failure of crosstalk between individuals who study goal-directed actions in the laboratory and clinicians who work with individuals with Alzheimer's disease. Another potential reason for devaluation not being tested in AD so far could be because the mainstream research has intensely focused on memory deficits, often to the detriment of other symptoms (such as depression, apathy, anxiety, and agitation, as described in a recent review; (Pless et al., 2023).

Therefore, although outcome devaluation has yet to be tested in individuals with Alzheimer's disease, possibly due to the overwhelming focus on memory deficits, these examples clearly demonstrate that it does have value as a procedure both in its translatability to humans as well as its ability to predict how well those individuals function outside of the laboratory. A final reason that devaluation may have been overlooked in AD research could be due to the hippocampal centered approach. As noted on pages 100-101, lesion studies conducted by Corbit and Balleine in (2000) and (2001) suggested that devaluation did not rely on the hippocampus and as this is the most well-studied region that is affected in AD, researchers may have thought it would also be unaffected. More recent studies have shown, however, that devaluation does rely on the hippocampus, only transiently, in the initial stages of learning (Bradfield & Balleine, 2020), which led to the demonstration that devaluation is also impaired in the J20 mouse model of AD (Dhungana et al., 2023). These studies could be used to inform the study of devaluation in people with AD.

In rodents, as described in Chapter 2, this procedure involves training them to press two levers (usually a right and left lever) for two distinct outcomes (often pellets and sucrose), then devaluing one of those outcomes by feeding it to satiety and testing whether animals will press the lever for the still-valued outcome in an extinction test.

Although this model has not been used to test people with AD, as mentioned in the previous paragraph, it has been employed in a familial mouse model of AD: the J20 model. Specifically, Dhungana et al., (2023) found that devaluation performance was impaired (Devalued = Valued) in J20 animals of either 36- or 52- weeks of age relative to age-matched wildtypes (Valued > Devalued) after 4 days of lever press training. However, performance recovered with an additional 4 days of lever press training such that

devaluation was intact (Valued > Devalued) for all animals after 8 days of lever press training, regardless of age or genotype. The distinction between performance on the 4 day and 8 day test here is interesting, because the dorsal hippocampus (and particularly the CA1 region of dorsal hippocampus) has been specifically associated with short-term and/or 'episodic' memory (Bartsch et al., 2011), which is also the type of memory loss most frequently observed in the earlier stages of Alzheimer's (Gold & Budson, 2008). Consistent with this argument, the learning and expression of goal-directed action has been argued to be reliant on episodic memory shortly after initial learning, and then dependent on semantic memory 7 days or more after this initial learning (Bradfield et al., 2020).

Following the 8-Day test, Dhungana et al., (2023) culled all animals and quantified the levels of microglial and astrocyte expression in the dorsal hippocampus. Correlational analysis revealed that the number of activated microglia in dorsal hippocampus was significantly negatively correlated with the performance of J20 animals on the 4-Day outcome devaluation test but did not correlate with performance on the 8-Day test. This suggested that dorsal hippocampal neuroinflammation was associated with poorer initial goal-directed action control. Notably, however, this correlation does not necessarily indicate that hippocampal neuroinflammation caused the observed deficits, which will be tested in the current chapter. The J20 mice in the study by Dhungana et al., had additional neuropathology, most notably Aβ plaques, as well as neuroinflammation in other parts of the brain (outside of the hippocampus). In the current chapter we are purely testing whether it is hippocampal neuroinflammation that has led to the changes in behaviour.

Dhungana et al.,'s study also found that there were sex differences in the abilities of mice, even wildtype mice, to demonstrate intact outcome devaluation performance. Moreover,

the expression of microglia and astrocytes were higher in female J20s compared to male J20s. This is noteworthy because literature reports for human Alzheimer's cases incline towards females developing the disease twice as frequently as males (Ferretti et al., 2018; Podcasy & Epperson, 2016). Therefore, in order to ensure my study was sufficiently powered to detect any differences, and in contrast to the results reported in Chapter 3, for the following chapter I separated animals by sex. Specifically, Experiment 5 of this chapter tested outcome devaluation in female animals that had received hippocampal injections of LPS. Experiment 6 of this chapter repeated the experiment with a male cohort. Dorsal hippocampal tissue from each mouse was again immunostained for microglial and astrocytic reactivity, to confirm the presence of a neuroinflammatory response and to assess any correlations with behaviour. Moreover, I assessed this tissue for levels of the immediate early gene c-Fos, which functions as an activity marker, co-localized with NeuN in order to assess whether the manipulations altered neuronal excitability in the dorsal hippocampus. This is important because only neurons possess processes long enough to make contact with the broader circuit of goal-directed action, so it is only by altering the activity of neurons that microglia and astrocytes could have any ultimate influence over behavioural responses.

4.2) Methods:

4.2.1) Animals:

A total of 97 C57BL6/J animals were used in this chapter, which was split under different experiments. All animal experiments were performed with the approval of the Garvan Institute, St. Vincent's Hospital Animal Ethics Committee and Ernst facility UTS under approval number 17/28, 20/08 and ETH21-6657. This was in accordance with the Australian National Health and Medical Research Council animal experimentation

guideline and the local Code of Practice for the Care and Use of Animals for Scientific Purposes.

4.2.2) Experiment 5: The effect of hippocampal neuroinflammation on the devaluation performance in female mice:

LPS injections and experimental schedule:

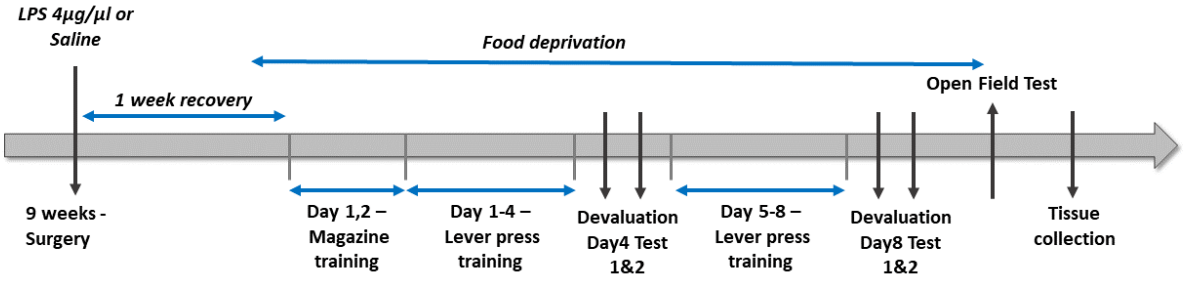

Figure 4.1: Experimental timeline for results described in Experiment 5 of this chapter.

C57BL/6J mice received bilateral hippocampal injections of Saline and LPS. Experiment 5 employed a female cohort with a total of 17 animals (9 Sham and 8 LPS). Briefly, animals underwent surgery and were given a week's recovery time after which they were food deprived for two days. This was followed by 2 days of magazine training and 4 days of lever press training, after which animals were given a devaluation test (hereafter referred to as the "4-Day devaluation test"). This was followed by 4 more days of lever press training (i.e. 8 days total lever press training) and another devaluation test, which is hereafter referred to as the "8-Day devaluation test". After this test, animals were given an open field test to check for locomotor activity and were culled within one week.

Stereotaxic surgery:

All stereotaxic surgery procedures for Experiments 5 and 6 were conducted as described for Experiment 4. Stereotaxic surgery for the DREADDs experiment was also conducted

identically, except that pAAV-GFAP-hM3D(Gq)-mCherry/ pAAV-GFAP104-mCherry was injected into the dorsal hippocampus instead of lipopolysaccharide (1µl per hemisphere) at the rate of 0.2µl/minute. For these AAV injections, 5µl aliquots were removed from the freezer and placed on ice, and only the desired amount to be injected (in this case 1µl) was taken in the syringe just before injection. All other surgical procedures were conducted identically to those previously described.

Behaviours:

i) Open Field Test (OFT):

OFT was performed identically to what was described in Experiment 1 (Chapter 3) of this thesis.

ii) Outcome devaluation:

Figure 4.2: Pictorial representation of outcome devaluation chamber.

Apparatus: The experiment was conducted in six identical Operant chambers (Med Associates). One side of the chamber wall consisted of magazine (food receptacle) in the centre and two retractable levers one on either side of the magazine delivering two different outcomes. The opposite side wall consisted of a house light for illumination and

a house fan which provided constant ~70 dB background noise. The chamber was designed to deliver pellets (BioServ Biotechnologies, 45mg grain pellets) via a pellet dispenser and sucrose solution (sucrose [white sugar, Coles] 20%+polycose [Nutricia, Polyjoule] 10%) via syringe pump to the magazine. The setup was controlled by MED-PC software which delivered pellets and sucrose, recorded the number of lever presses, outcomes, and magazine entries.

Behavioural procedures: Three days before the start of magazine training, mice were food deprived, with each mouse receiving 1.2g chow per day. This was so that mice were hungry and therefore motivated to press levers for food. The food deprivation continued for the whole experiment; however, the quantity of chow was increased to 1.4g once lever pressing behaviour had been established. Weights were continuously monitored to make sure they were kept consistent above 80% of the pre-surgery body weight.

Magazine pre-training: For two days prior to lever press training, mice received magazine training to familiarize and habituate them to the context, and to associate it with food. For this training, mice were placed in an operant chamber that was illuminated with house light, and sucrose and pellets were delivered to the animals in the magazine at random intervals around a mean of 60s. The session terminated after 30 minutes or when 20 sucrose and pellets (40 total outcomes) had been delivered. Sucrose deliveries were accompanied by a short (1 s) termination of the house light to alert mice of the delivery. Pellet deliveries make a noise and do not require an additional cue to draw attention. Levers remained retracted throughout magazine training.

***Lever-press training (Day 1-4)*:** Following magazine pre-training, animals were trained to press levers for food outcomes. Lever press training was counterbalanced so that half of the animals in each group received left lever-sucrose, right lever-pellets and the rest

received the opposite arrangement. Lever press sessions terminated after 50 minutes or when animals had earned 40 of each outcome, whichever came first. These sessions were split into four 10-minute sub-sessions (two 10-minute sessions per lever. These terminated early and mice entered time-out if 20 outcomes were earned before 10 minutes). There was a 2.5-minute time-out period in between each sub-session during which levers were retracted and the house lights turned off.

Mice were trained on a Continuous Reinforcement schedule (CRF) (Sangha et al., 2002) for the first two days during which every lever press earned an outcome. On Day 3 mice were shifted to a Random Ratio 5 (RR5) schedule (Haw, 2008) for which each lever press earned an outcome with a probability of 0.2. On Day 4, mice were further shifted to an RR10 schedule where each lever press earned an outcome with a probability of 0.1. Three to four mice progressed more slowly through the ratio increases due to low levels of lever pressing, and finished Day 4 on an RR5 rather than an RR10 schedule. Following lever-press training on Day 4, all mice were habituated to an empty cage with access to food (chow, according to the quantity mentioned earlier in this section) for approx. 50 minutes. This cage would become the context (devaluation cage) in which animals would be pre-fed to satiety on one of the outcomes to 'devalue' it prior to test on the following day.

Outcome devaluation – 4 Day Test: After Day 4 of lever press training, the first outcome devaluation test was conducted (i.e. the '4-Day Test'). Mice were randomly assigned one of the two outcomes; sucrose or pellets to be devalued. Mice were then individually placed in their devaluation cage with *ad libitum* access to one of the outcomes (i.e. 3ml of sucrose solution or 3gms of pellets) for 50 minutes which they ate until satiation. This procedure is known to reduce the value of the satiated outcome relative to the other

outcome (Balleine & Dickinson, 1998). The animals are then placed into the operant chamber for a 10-minute devaluation test where they were presented with both levers but no food outcomes were delivered (i.e. they were tested in extinction). On day 2 of the test, animals were pre-fed with the opposite outcome to that which they received on day 1 (e.g. if given pellets on day 1 they now received sucrose, and vice versa) after which they were given another 10 minute choice extinction test. Responding rates on the 'valued' and 'devalued' levers were averaged across test days.

***Lever press training (Day 5-8)*:** One day after the 4 Day devaluation test, animals were given 4 more days of lever press training, which were conducted as previously described except that animal received only one day of RR5 followed by 3 days of RR10. Four mice progressed more slowly through the ratio schedule increases due to low performance levels, so they were given 2 days of RR5 and two days of RR10 instead.

Outcome devaluation – 8 Day Test: Animals were given a second set of outcome devaluation testing the day following day 8 of lever press training (i.e. the '8 Day test'). This was conducted identically to the 4 Day test previously described.

Immunostaining:

As per all prior experiments and as previously described, within one week of completing behavioural testing mice were perfused with PFA and their brains removed, and hippocampal sections sliced on the cryostat. Sections were then taken for immunostaining.

The staining protocol was conducted in the manner described in Experiment 1 (Chapter 3) using the following primary and secondary antibodies:

primary antibodies	secondary antibodies
rabbit polyclonal iba1 (1:500,thermofischer, pa5-21274)	Donkey anti-rabbit 568 (1:500, Invtirogen, A32790)
rabbit polyclonal dsred (1:300, scientifix, 632496)	Donkey anti-rabbit 568 (1:500, Invtirogen, A32790)
rabbit polyclonal c-Fos (1:500, Synaptic systems, 226003)	Donkey anti-rabbit 568 (1:500, Invtirogen, A32790)
chicken polyclonal NeuN (1:500, Saphire bioscience, GTX00837)	Goat anti-chicken 647 (1:500, Thermofischer, A21-449)
mouse polyclonal GFAP (1:300, NE Bioloabs, GA5)	Goat anti-mouse 488 (1:500, Thermofischer, A32723)

Specifically, 4 sections per brain were stained for IBA1 and GFAP and 4 other sections per brain were separately stained for NeuN and c-Fos. The four sections were chosen from Bregma -1.34 to -2.30 mm based on Paxinos atlas for mouse brain (Paxinos & Franklin, 2012) which comprised dorsal hippocampus. 4 out of 5 good sections were chosen and damaged/torn sections were not taken into consideration. Mounting and cover slipping procedures were performed as previously described.

Image Analysis:

i) Microscopy:

Immunostained sections were imaged using a TiE2 inverted microscope under 40x magnification. Laser intensity and image capturing frames were kept consistent for all the images. Images were taken from CA1 region of the hippocampus. For c-Fos and NeuN images were additionally captured from the dentate gyrus, due to the observation that there was significant c-Fos expression there. A z-stack image covering at least 10 µm thickness of the tissue was captured, at 0.6µm/0.9µm stack interval. All images were

taken from the dorsal hippocampus which spans from Bregma -1.34 to -2.30 mm based on Paxinos atlas for mouse brain (Paxinos & Franklin, 2012). At least 7 images per brain (left and right hemispheres combined) were obtained for analysis. Most brains had 8 images from which cell numbers and intensity were counted. The images were chosen according to the number of sections containing the anatomic area – as 35-40μm thickness section with an interval of 1:6 will result in almost 5 sections of dorsal hippocampus per brain.

ii) Fiji (ImageJ):

For cell counts: The captured images were then analysed using FIJI (Fiji Is Just ImageJ). The image stack was imported to FIJI and the composite channels were first split into individual channels then these individual channels were re-stacked (i.e. merged into a single image). For the re-stacked images, the threshold was adjusted to make sure the cell bodies were all included, (count particles – 16 to infinity). Cell counts output was saved and averaged for each brain.

For intensity measurement: Following cell counts, a separate intensity measurement was performed: mean intensity was calculated for all the images and averaged for each brain. The intensity measurements were done using ImageJ, and there was a common threshold set (60,000-98,000) for within one batch while analysing using imageJ. Although this procedure is not as accurate as the stereological approach used in Chapter 3, due to the laboratory moving and no longer having stereological facilities available this shift in methods was unavoidable. However, I did take all precautions to ensure that measurements were as accurate as possible including maintaining a constant laser intensity when taking images in the microscope, which I believe could help eliminate some batch differences.***For co-localization measurement:*** Co-localization was measured

for c-Fos and NeuN only (to determine the rate of neuronal activation). The stacked images were converted into RGB colour images and made composite. The colour threshold was adjusted to select all the yellow signal (which is the colocalization of red [NeuN] and green[c-Fos]), and the percentage area of the selected signal was measured and averaged for each brain.

All graphs except for the graphs that mention cells/mm^3 did not take into account hippocampus area (in terms of volume). Rather I kept the ROI consistent (i.e, the image frame size chosen within hippocampus to perform cell counting/measure cell intensity).

4.2.7) Statistics:

All statistical analysis were performed with Graphpad Prism 8.4.3. For comparisons involving only two means, two tailed t-tests were performed. For all other analyses one-way or two-way ANOVA were conducted, followed by *post-hoc* Bonferroni analyses where applicable. For all analyses, α was set at ≤0.05.

Correlational analyses were carried out following immunohistochemical assessment, to determine whether microglial, astrocytic, and neuronal c-Fos expression was associated with behavioural performance. In order to assess correlations with devaluation performance in a manner that was not driven by differences in baseline lever pressing *per se*., I calculated a "devaluation ratio" according to the following equation:

$$SR = \frac{Lever\ press\ rate\ on\ test}{(Lever\ press\ rate\ on\ test + Lever\ press\ rate\ during\ training)}.$$

A positive score indicated intact devaluation and a score of zero or lower indicated poor devaluation performance.

4.2.3) Experiment 6: The effect of hippocampal neuroinflammation on the devaluation performance in male mice:

Experiment 6 repeated the procedures of Experiment 5 in a male cohort of mice. There was a total of 20 animals (11 Sham and 9 LPS). The experimental timeline, (surgery, behavioural procedures, and tissue collection) were conducted identically to those described for Experiment 5. The only difference was that male mice on food deprivation received slightly more chow – initially 1.3g chow per mouse, which was increased to 1.6g once lever pressing was established.

4.3) Results and Discussion:

4.3.1) Experiment 5: Hippocampal neuroinflammation accelerated devaluation performance in female mice:

Female C57BL6/J mice were given bilateral intrahippocampal injections of LPS or Saline to induce neuroinflammation and then were tested for outcome devaluation performance after either 4 or 8 days of lever press training. Hippocampal sections were then analysed for neuroinflammatory markers, neuronal markers, and c-Fos expression, and each of these markers was correlated with behavioural measures. c-Fos is an Immediate Early Gene (IEG), the expression of which indicates cellular activity (Lara Aparicio et al., 2022). Inflammation induced in the hippocampus activated microglia and astrocytes (as seen in Experiment-4); however, it was important to assess if the changes in glial cells altered neuronal activation. As reviewed in Chapter-1, neurons are a part of the trisynaptic input in the hippocampus, therefore alterations in the neuronal activation can impact changes in the brain regions that receive neuronal projections from the hippocampus. Hence

checking for c-Fos expression was crucial for our experiments. Placements for all female animals are shown in Figure 4.3.

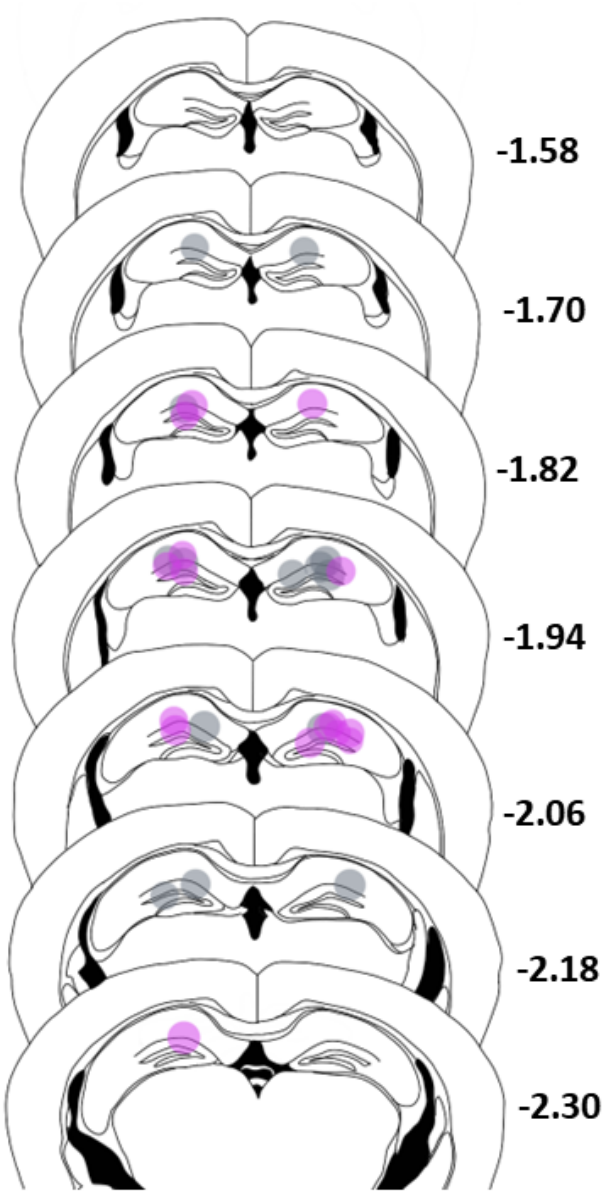

Figure 4.3: Schematic illustration of placements for female Sham (gray dots) and LPS (pink dots) groups (The numbers correspond to Bregma).

4.3.1a) Hippocampal neuroinflammation increased lever press rates but did not affect magazine entries in female mice across Days 1-4 of lever press training

Figure 4.4A shows the lever press rates for female mice during days 1-4 days of lever press training. Lever press rates were significantly higher in LPS-treated animals compared to the Sham controls, although all mice did increase lever pressing across days, indicating that they had acquired the lever press response. This was supported by a repeated measures two-way ANOVA showing a significant main effect of training days ($F_{(1.353, 20.29)}$=101.1, p<0.0001, Greenhouse-Geisser corrected for violating sphericity) indicating that mice increased lever pressing over days averaged over group. There was also a significant main effect of group ($F_{(1, 15)}$=22.59, p=0.0003), indicating that group LPS performed more lever presses averaged across days. Moreover, there was a significant group x days interaction ($F_{(3, 45)}$=21.04p<0.0001), indicating that group LPS increased lever press responding across faster than Sham. However, both Sham and LPS animals did acquire lever pressing, because there was a significant linear simple effect for each group over days: Sham, ($F_{(1,20)}$ = 15.443, p = .0001) LPS, ($F_{(1,20)}$ = 145.6, p < .001).

In contrast to lever press rates, there was no difference in the magazine entries made by LPS animals relative to Sham as shown in Figure 4.4B. This was supported by statistical analysis (repeated measures two-way ANOVA) showing only a main effect of training days ($F_{(2.299, 34.48)}$=9.717, p=0.0003), but no significant effect of group ($F_{(1, 15)}$=0.1916, p=0.6678) and no interaction ($F_{(3, 45)}$=0.2610, p=0.8531). This suggest that although magazine entries significantly decreased across days (likely due to the increase in the competitive response of lever pressing across days – i.e. mice cannot lever press and enter the magazine at the same time such that an increase in one behaviour is typically

accompanied by a decrease in the other). However, this decrease did not differ according to group.

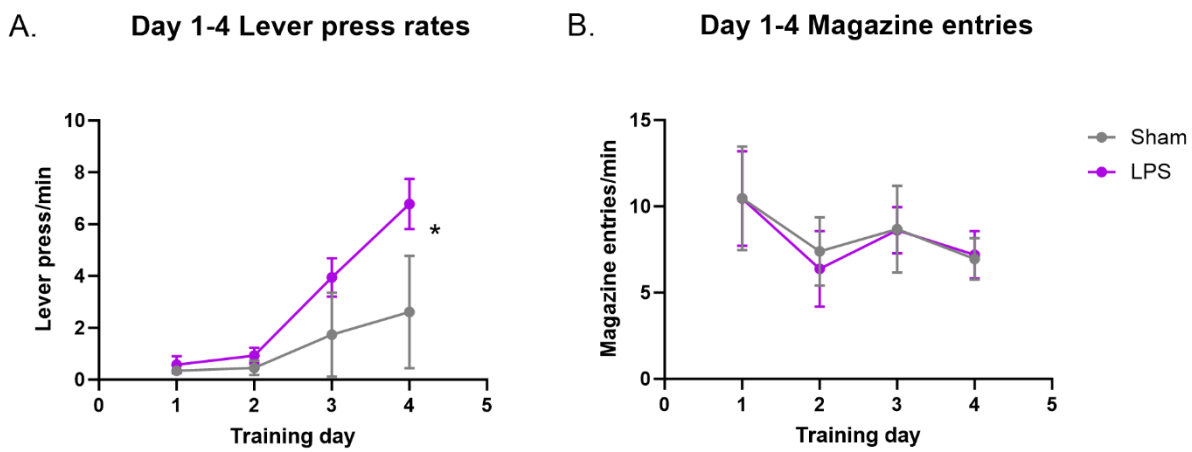

Figure 4.4: Lever press rates for females during training days 1-4 (A). Magazine entries made by mice during training days 1-4 (B) (Sham n=8, LPS, n=9; $p<0.05$; All values represent the Mean ± SEM.

4.3.1b) Hippocampal neuroinflammation accelerated goal-directed action in Day 4 devaluation test in female mice:

Lever press rates during the Day 4 devaluation test are shown in Figure 4.5A. In contrast to expectations, Sham animals did not show intact devaluation, indicated by equal responding on valued and devalued levers. However, the LPS animals were showing intact devaluation because they responded more on the valued lever compared to the devalued lever. A two-way ANOVA revealed a significant main effect of group ($F_{(1, 30)}=14.58$, $p=0.0006$) and a significant main effect of devaluation ($F_{(1, 30)}=4.740$, $p=0.0375$). In addition, there was a significant group x devaluation interaction ($F_{(1, 30)}=4.494$, $p=0.0424$). The Bonferroni *post hoc* analysis revealed the source of this interaction,

because the LPS group pressed the valued lever significantly more than the devalued lever, p = 0.0077, but Sham animals did not, F < 1.

Similar to training, magazine entries on test were equivalent between Sham and LPS groups, as indicated by a two-tailed t-test (t = 0.2477, p=0.8077, Figure 4.5B). Together, these results suggest that hippocampal neuroinflammation accelerated (rather than impaired) goal-directed action control relative to Sham animals but did not affect magazine entries.

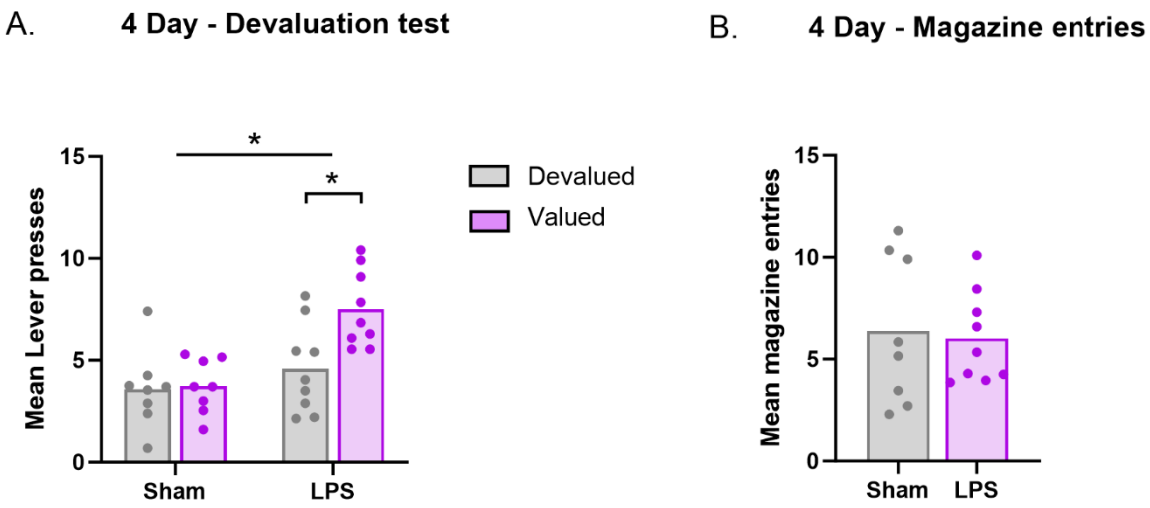

Figure 4.5: Lever presses made by Sham and LPS animals on both valued and devalued lever on the Day 4-devaluation test (A). Magazine entries made by the same animals on the Day 4-devaluation test (B). (Sham n=8, LPS, n=9; p<0.05; All values represent the Mean ± SEM).

4.3.1c) Lever press rates remained higher for female mice with neuroinflammation relative to Shams across days 5-8 of lever press training:

Consistent with days 1-4 of lever press training, LPS-treated animals maintained higher lever press rates relative to Sham across days 5-8 (Figure 4.6A). This was supported by a repeated measures two-way ANOVA that found a main effect of day ($F_{(2.045, 30.68)}$=83.52,

p<0.0001) and a main effect of group ($F_{(1, 15)}$=55.88, p<0.0001) but no day x group interaction ($F_{(3, 45)}$=1.130, p=0.3469). This suggested that although LPS animals did press the levers significantly more than Sham animals, the rate of lever press increase across days was stable for each group (i.e. LPS animals did not increase lever pressing any faster than Sham group).

As shown in Figure 4.6B, there was no difference in magazine entries made by LPS animals relevant to Shams. This was supported by statistical analysis (repeated measures two-way ANOVA) because there was no main effect of day ($F_{(1.592, 23.88)}$=2.189, p=0.1421), no main effect of group ($F_{(1, 15)}$=0.006280, p=0.9379), and no day x group interaction ($F_{(3, 45)}$=1.495, p=0.2286).

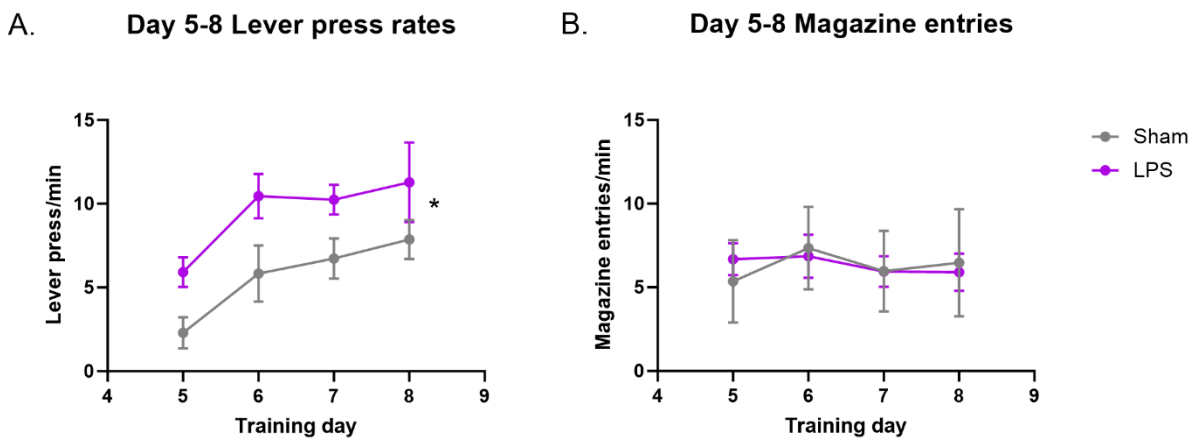

Figure 4.6: Lever press rates for females during training days 5-8 (A). Magazine entries made by mice during training days 5-8 (B) (Sham n=8, LPS, n=9; p<0.05; All values represent the Mean ± SEM).

4.3.1d) Hippocampal neuroinflammation increased lever pressing but did not affect goal-directed action in female mice on the 8 Day test:

Figure 4.7A shows the lever press rates for the Day 8 devaluation test. This time, unlike the 4-Day test, devaluation performance was intact (Valued > Devalued) for both groups, although overall lever pressing was still marginally higher for group LPS than for group Sham. This was supported by statistical analysis which found a marginally significant main effect of group, ($F_{(1, 30)}$=22.11, p=0.0571) and a significant main effect of devaluation ($F_{(1, 30)}$=22.11, p<0.0001). In contrast to the Day-4 test, however, there was no group x devaluation interaction ($F_{(1, 30)}$=0.7886, p=0.3816), suggesting that devaluation was intact for all animals, regardless of group.

Magazine entries from this test are shown in Figure 4.5B. Although from this figure it appeared as though there was a slight decrease in magazine entries made by LPS animals, this effect was not significant, as shown by a two-tailed t-test (t=1.118, p=0.2810, Figure 4.7B).

Taken together with the results of the 4-Day test, these results indicate that hippocampal neuroinflammation initially accelerated goal-directed action control in female mice, but that this effect was lost after multiple days of training when goal-directed action control was also intact for Shams. This was in spite of marginal evidence that hippocampal neuroinflammation continued to elevate the overall lever press rate on the 8-Day test but did not affect the distribution of lever presses among the valued and devalued levers which is the critical factor when determining goal-directed action control. Consistent with the 4-Day test, magazine entries on the 8-Day test again did not differ between groups.

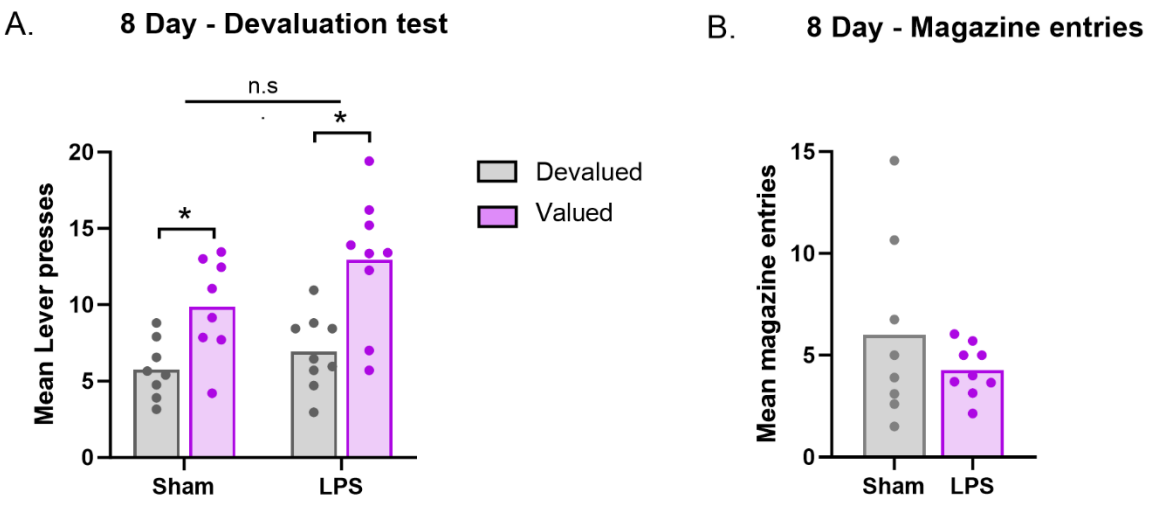

Figure 4.7: Lever presses made by Sham and LPS animals on both valued and devalued lever on the Day 8-devaluation test (A). Magazine entries made by the same animals on the Day 8-devaluation test (B). (Sham n=8, LPS, n=9; $p<0.05$; All values represent the Mean ± SEM.

4.3.1e) Hippocampal neuroinflammation did not alter locomotor activity in an Open Field Test in female mice:

The higher press rates in LPS animals relative to shams led me to speculate that the effect might be due to a general tendency towards hyperactivity in these animals, rather than a specific acceleration of goal-directed control. To assess this possibility, I conducted an open field test.

Figure 4.8A shows the total distance travelled by these animals during the 10 minutes session. As can be seen from this figure, although there appeared to be a trend towards an increase in locomotor activity in the LPS group, statistically there was no significant difference between the LPS group and Shams. This was indicated by two-tailed t-test ($t = 2.041$, $p=0.0592$). Additionally, there was no difference in the time spent by these animals in the corner zone ($t=1.427$, $p=0.1740$, Figure 4.8B) and centre zone ($t=1.427$, $p=0.1740$,

figure 4.8C). This indicated that the LPS animals were not anxious compared to the Sham controls. Overall, these results show that locomotor activity and anxiety levels were not altered by intrahippocampal injections of LPS. This suggests that the observed differences in outcome devaluation were not a result of either potential confound, but rather an indication of a specific acceleration of goal-directed control in these animals.

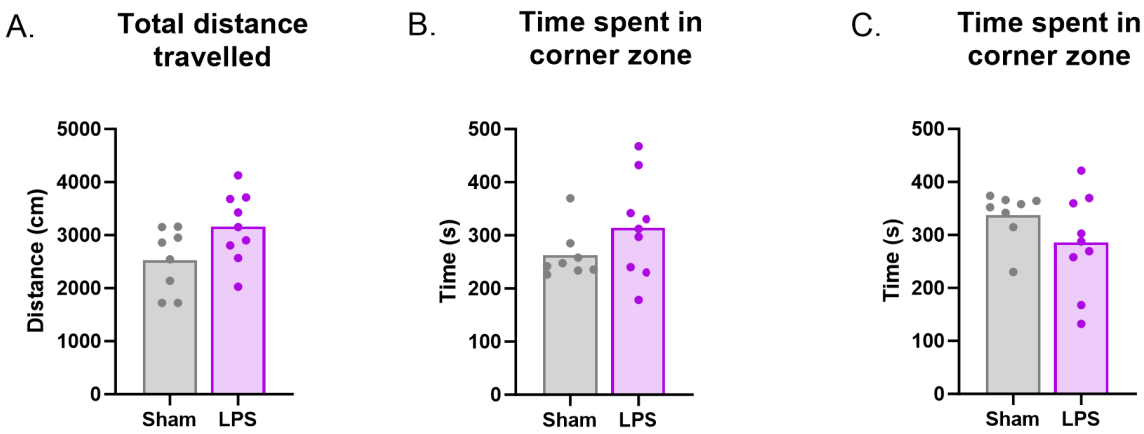

Figure 4.8: Total distance travelled by Sham and LPS animals in the open field test (A). Time spent by Sham and LPS animals in the corner zone (B) and the centre zone (C). (Sham n=8, LPS, n=9; All values represent the Mean ± SEM).

4.3.1f) Upregulation of Iba1+ microglia after LPS treatment in female mice:

The number of microglial cells in the dorsal hippocampus was increased for LPS-treated animals relative to Shams. This was supported by a two-tailed t-test ($t = 13.63$, $p<0.0001$, Figure 4.9A). This was paralleled by an increase in Iba1 intensity ($t = 3.445$, $p=0.0043$, Figure 4.9B). This confirms that the LPS injections were sufficient to produce a neuroinflammatory response in the microglia, and further shows that this response was still present after the end of behavioural testing which lasted approximately 4 weeks.

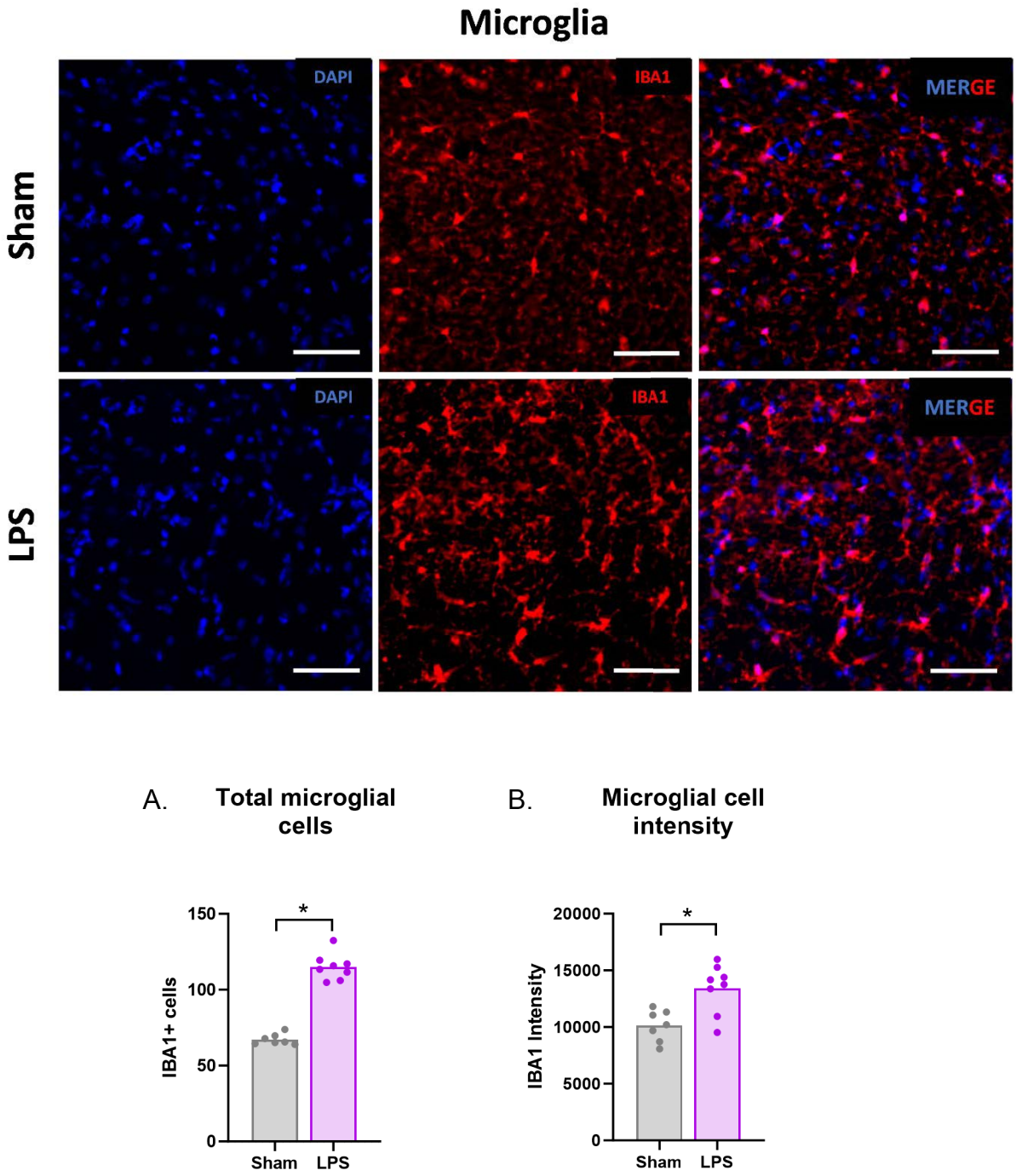

Figure 4.9: Total number of microglial cells in Sham and LPS animals (A). Microglial cell intensity in both Sham and LPS groups (B). (Sham n=7, LPS, n=8; Scalebar: 50µm; $p<0.05$; All values represent the Mean ± SEM).

4.3.1g) Upregulation of microglia correlated with devaluation on the 4 Day but not the 8 Day test, and did not correlate with magazine entries on either test:

To understand the relationship between the cellular changes and the observed behavioural differences, we performed a correlational analysis. There was a significant positive correlation between microglial cell numbers and devaluation scores from the Day 4 test. This indicated that increased number of microglial cells was associated with the better performance of female LPS animals on the Day 4 test ($r=0.6770$, $p=0.0056$) (Figure 4.10A). The same was true for microglial intensity ($r=0.6488$, $p=0.0089$) (Figure 4.10B). However, no such correlation was observed for either cell counts ($r=0.2338$, $p=0.4018$) or intensity ($r=-0.06163$, $p=0.8273$) with devaluation scores from the 8 Day test (Figures 4.10C,D).

We found no correlation of microglial cell counts or intensity on the magazine entries made by these animals on 4 Day and 8 Day devaluation test, refer to appendices.

Together, these results suggest that the upregulation of microglia in dorsal hippocampus was associated with better goal-directed control but not with Pavlovian approach behaviour (as measured by magazine entries).

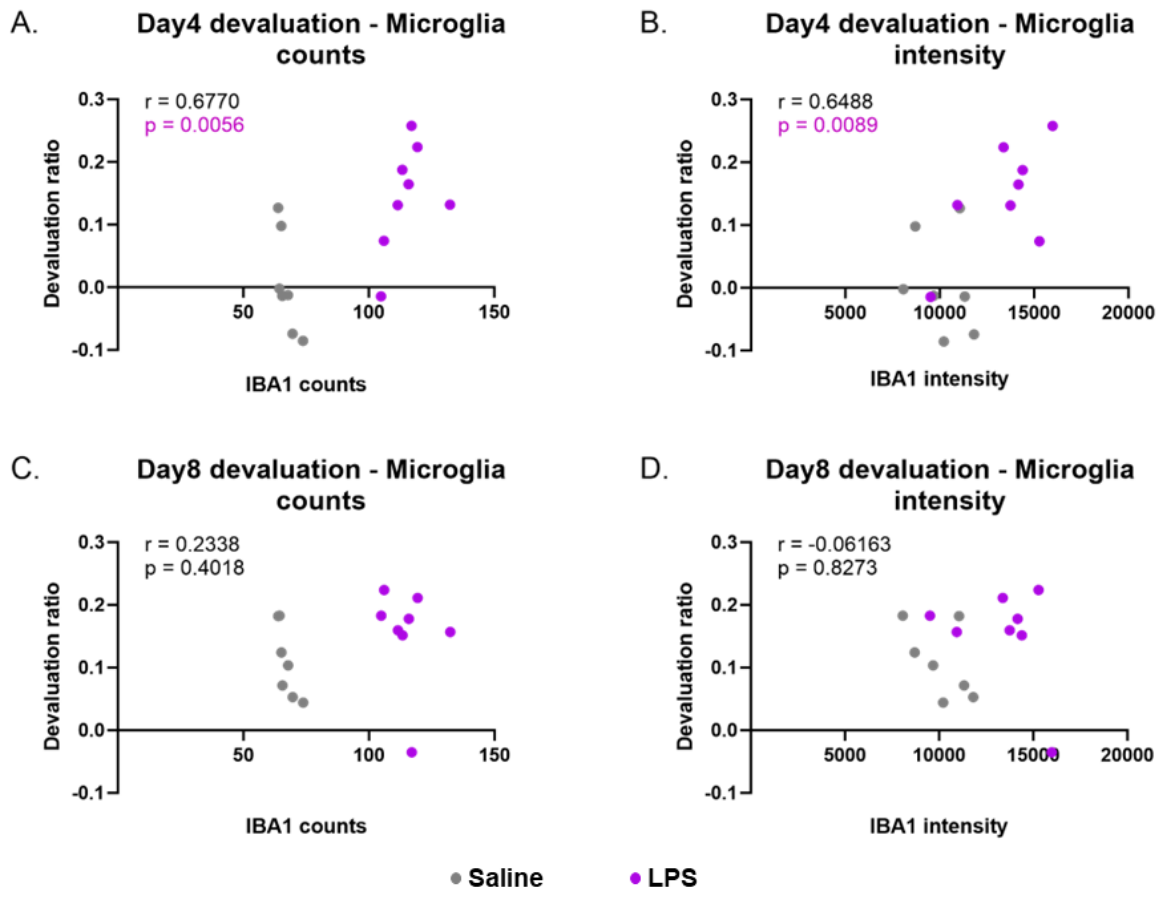

Figure 4.10: Correlation of Iba1+ cell counts with behaviour performance on the Day 4 devaluation test (A). Iba1 intensity correlation with 4-Day devaluation test performance (B). Iba1+ cell counts correlation with behaviour performance on the Day 8 devaluation test (C). Iba1 intensity correlation with 8 Day devaluation test performance (D). (Sham n=7, LPS, n=8; $p<0.05$; All values represent the Mean ± SEM).

4.3.1h) Upregulation of GFAP+ astrocytes after LPS treatment in female mice:

As shown in Figure 4.11A, there was no significant difference in the number of astrocytes in dorsal hippocampus, as observed from the equal number of GFAP+ cells in both LPS and Sham animals ($t = 1.128$, $p=0.2795$). However, as shown in Figure 4.11B, there was an increase in the intensity of GFAP+ astrocytes in the LPS group compared to the Sham group ($t = 5.053$, $p=0.0002$). Together, these results suggest that although LPS injections

did not cause the proliferation of astrocytes in dorsal hippocampus, it did cause morphological changes indicating astrocyte activation. Again, this result confirms that LPS injections were sufficient to produce a neuroinflammatory response in the astrocytes, and that this response was still present after behavioural testing.

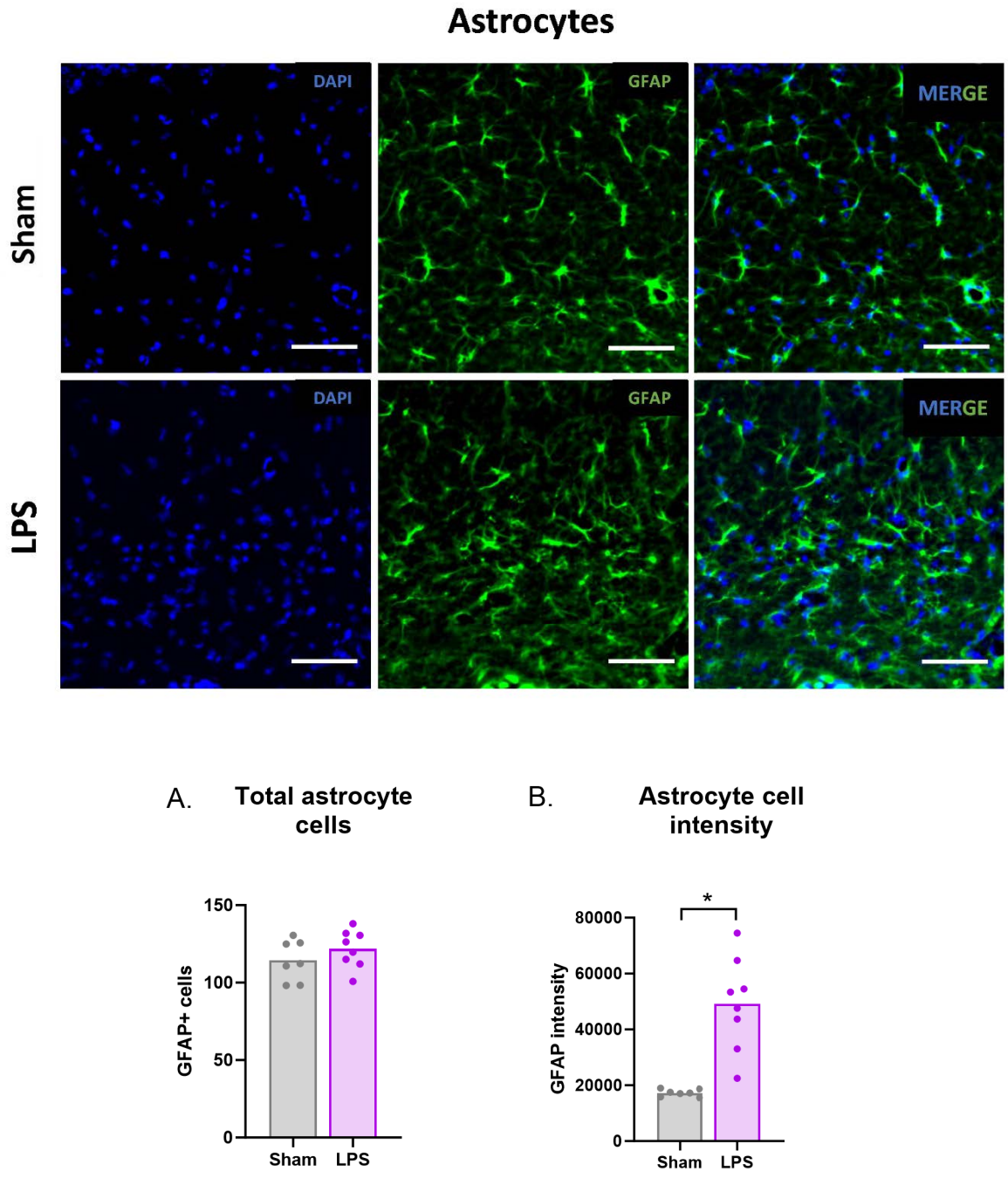

Figure 4.11: Total number of astroglial cells in Sham and LPS animals (A). Astrocytes cell intensity in both Sham and LPS groups (B). (Sham n=7, LPS, n=8; Scalebar: 50μm; $p<0.05$; All values represent the Mean ± SEM).

4.3.1i) Upregulation of astrocyte intensity correlated with devaluation on the 4 Day but not the 8 Day test, and did not correlate with magazine entries on either test:

Astrocytic cell counts did not correlate with devaluation scores of LPS-treated animals on either test (4-Day test: r=-0.06555, p=0.8165; 8-Day test: r=0.3431, p=0.2106) tests as shown in Figures 4.12A,C. However, there was a significant positive correlation between astrocytes intensity and devaluation scores from the 4-Day test (r=0.7441, p=0.0015) but not the 8 Day test (r=0.0241, p=9306), as shown in figures 4.12B,D. There were no correlations between the astrocytic cell counts/intensity with the magazine entries from either test (refer appendices).

Together, these results suggest that the upregulation of astrocytic intensity in dorsal hippocampus was associated with better goal-directed control but not with Pavlovian approach (i.e. magazine entries).

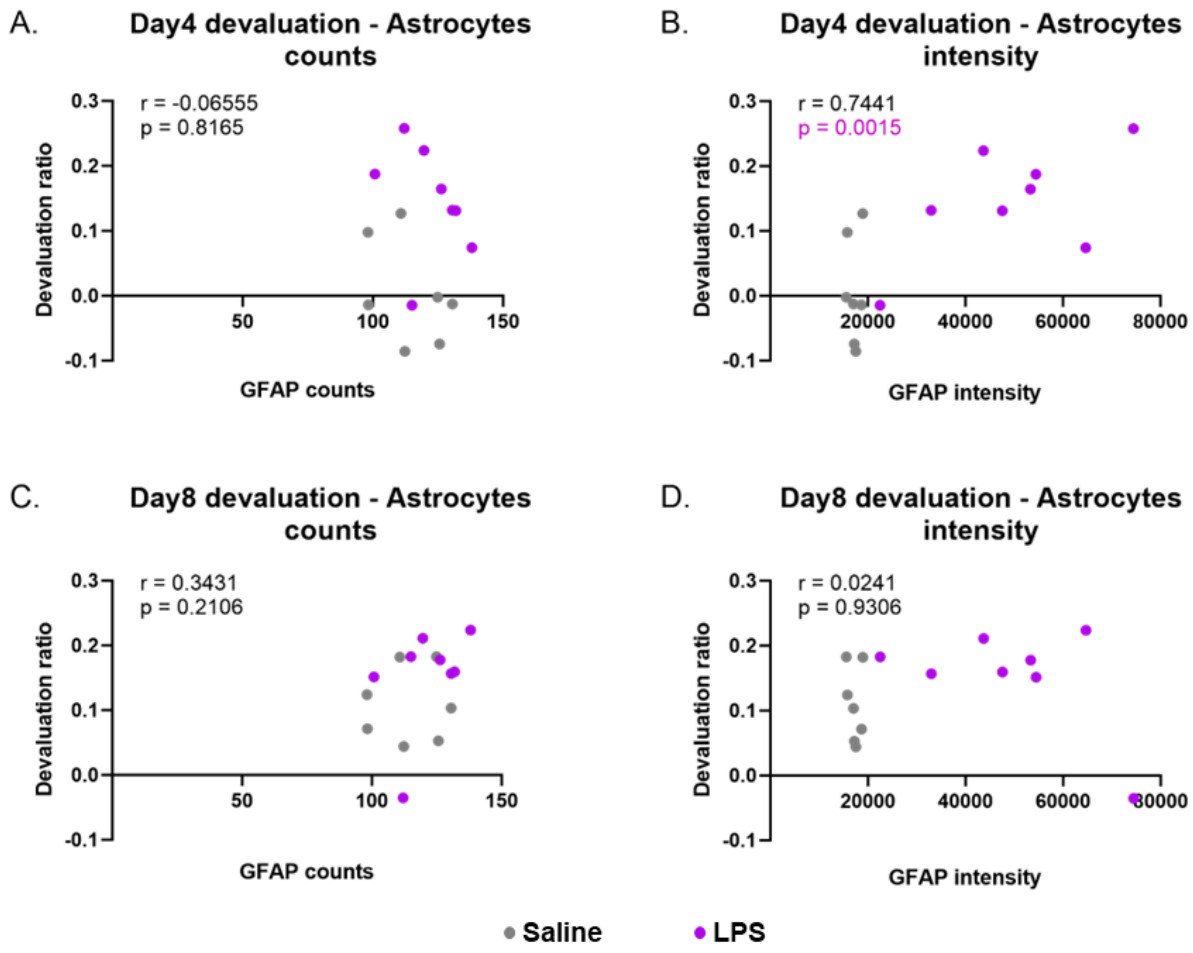

Figure 4.12: Correlation of GFAP+ cell counts with devaluation performance of animals on the Day 4 devaluation test (A), Day 8 devaluation test (C). GFAP intensity correlates with the devaluation performance on 4-Day test (B), 8-Day test (D). (Sham n=7, LPS, n=8; $p<0.05$; All values represent the Mean ± SEM).

4.3.1j) LPS treatment did not alter the NeuN+ neuronal cell population in the dorsal hippocampus of female mice:

I stained for NeuN to assess whether there was cell death of as a result of LPS injections. Although I did also measure cell counts for NeuN, it was not possible for ImageJ to recognize individual neurons regardless of how strict a threshold I set due to many cells being too close together. Although it would be ideal to perform a % area analysis after

thresholding, with threshold adjustments (as mentioned earlier) some of the cells are either completely eliminated or few cells looked clumped together and therefore I was unable to differentiate single cells. This was partly due to the issues with overexposure, even though the laser intensity was kept at minimum. As such, continuing to measure it this way appeared to result in inaccurate cell counts so that I decided to measure the intensity of the cells, which could yield some level of consistency between different sections.

NeuN positive cell intensity is shown in Figure 4.13. From this figure it is clear that NeuN intensity was similar between group LPS and group Sham in both CA1 and DG regions. This result suggests that there was no evidence of neuronal death following LPS surgeries.

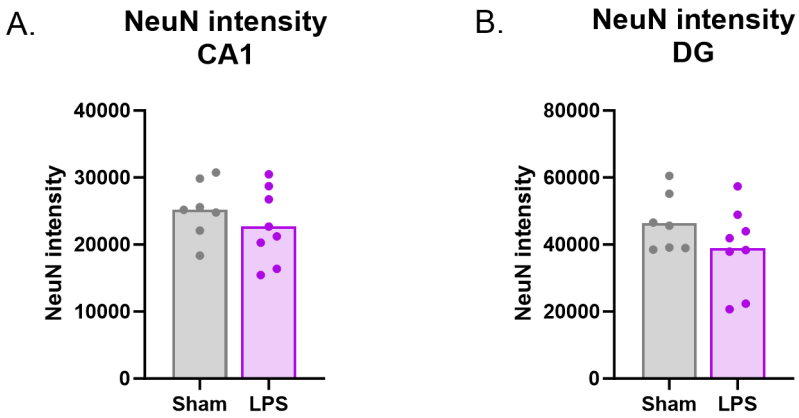

Figure 4.13: NeuN cell intensity in CA1 (A) and DG (B) regions. (Sham n=7, LPS, n=8; All values represent the Mean ± SEM).

4.3.1k) Hippocampal neuroinflammation increased the percentage of c-Fos/NeuN positive cells that expressed c-Fos in dentate gyrus in female mice:

The percentage area of NeuN colocalized with c-Fos did not differ between group LPS and group Sham in the CA1 region (Figure 4.14, t =1.528, p = 0.1506), but was significantly higher in the DG region (t = 2.916, p=0.0120), shown in Figure 4.14A,B.

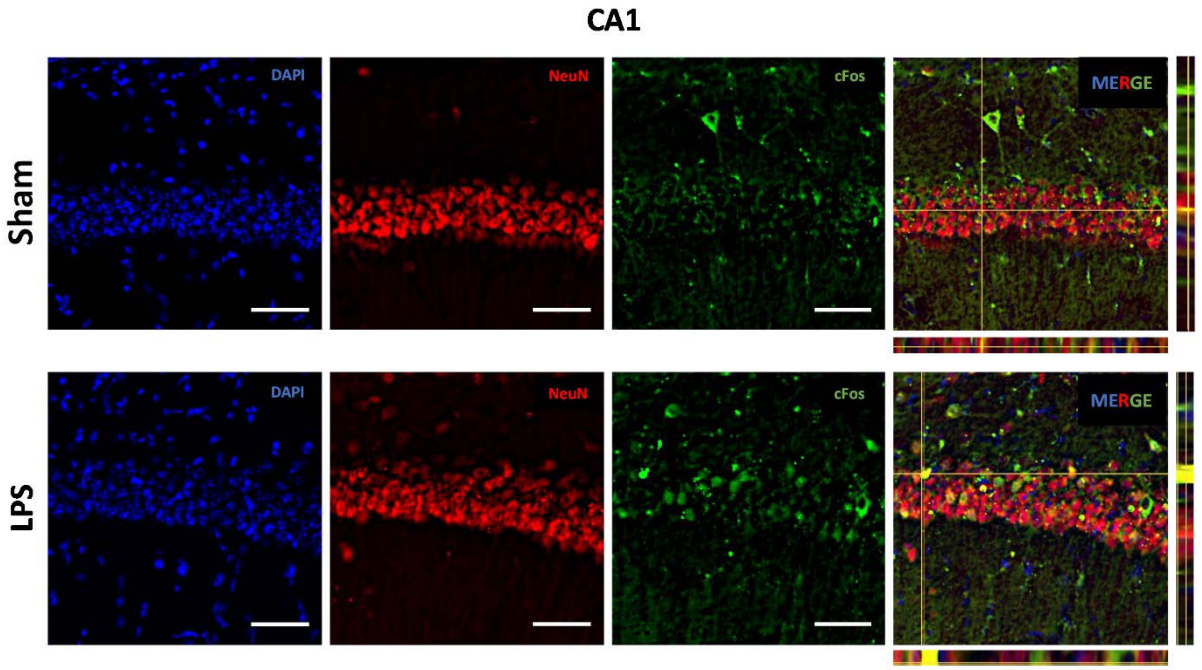
CA1
Sham
LPS
DAPI
NeuN
cFos
MERGE

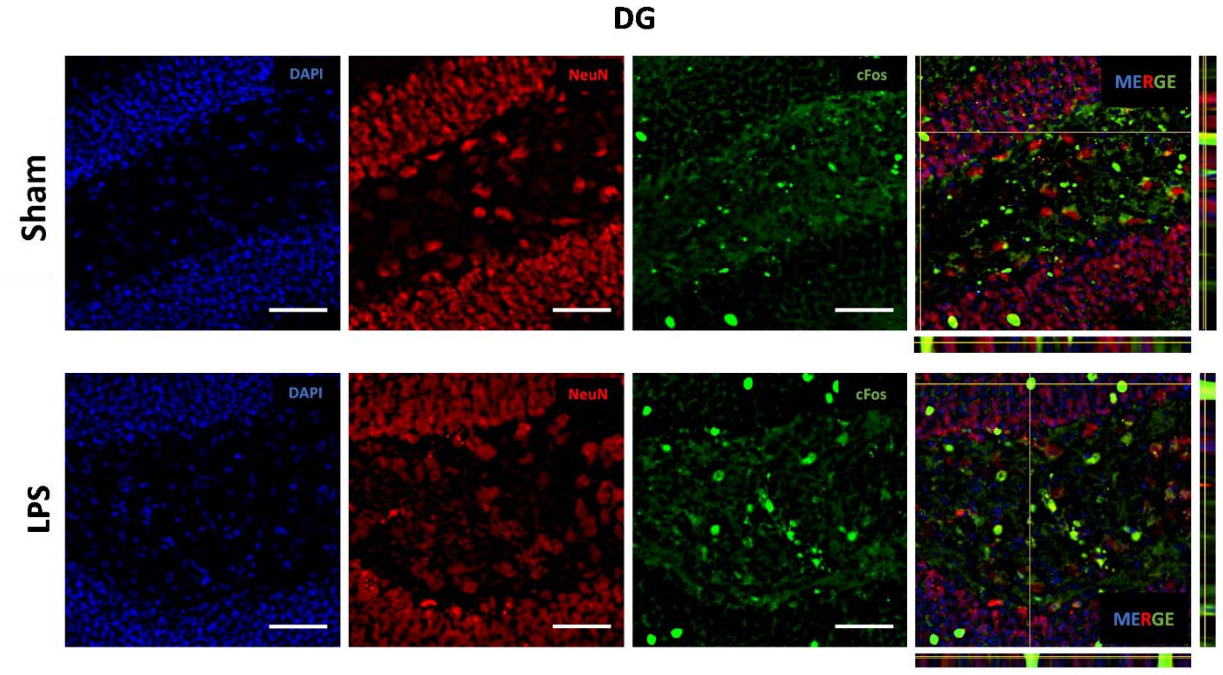
DG
Sham
LPS
DAPI
NeuN
cFos
MERGE

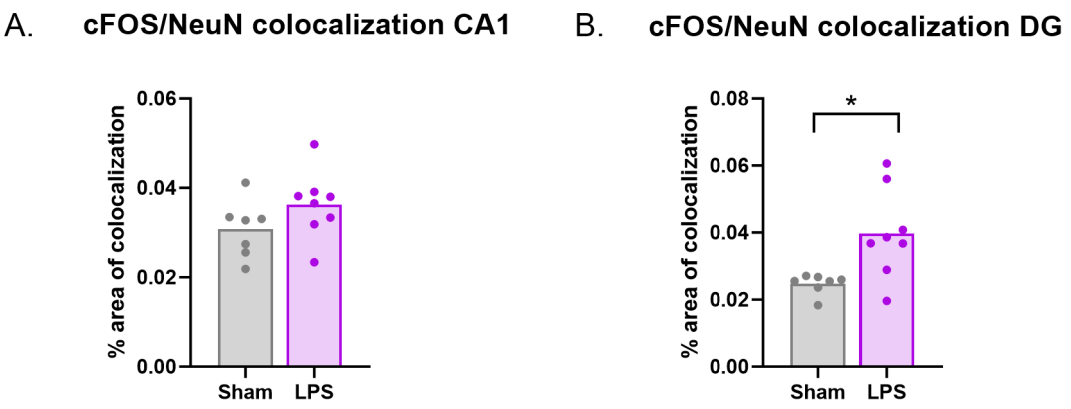

Figure 4.14: % area of co-localization of c-Fos and NeuN in CA1 (A) and DG (B) regions. (Sham n=7, LPS, n=8; Scalebar: 50µm; $p<0.05$; All values represent the Mean ± SEM).

4.3.1l) Experiment 5: Discussion

Overall, the results of Experiment 5 indicate that, in female mice, LPS was successful in causing an increase in neuroinflammatory markers (i.e. Iba1 and GFAP) in dorsal hippocampus, as well as an increase in neuronal excitation (i.e. co-localised c-Fos and NeuN) in the dentate gyrus. Behaviourally, this increase in hippocampal neuroinflammation accelerated goal-directed action control, and this acceleration was positively associated with microglial and astrocytic expression in dorsal hippocampus.

This was not the anticipated result, as I had expected LPS-induced neuroinflammation in hippocampus to impair, rather than accelerate goal-directed action. Potential reasons for this unexpected result will be expanded on in the discussion of this Chapter and in the General discussion. First, however, I wished to determine the generality of the conclusion that hippocampal neuroinflammation accelerates goal-directed control by investigating whether the same result would be obtained in male mice.

4.3.2) Experiment 6 – Hippocampal neuroinflammation facilitated Pavlovian approach behaviour but did not affect goal-directed control in male mice:

For Experiment 6, male animals (11 Sham, 9 LPS) underwent the same experimental procedures described for Experiment 5 and the results are as follows. Placements for each animal is shown in Figure 4.15.

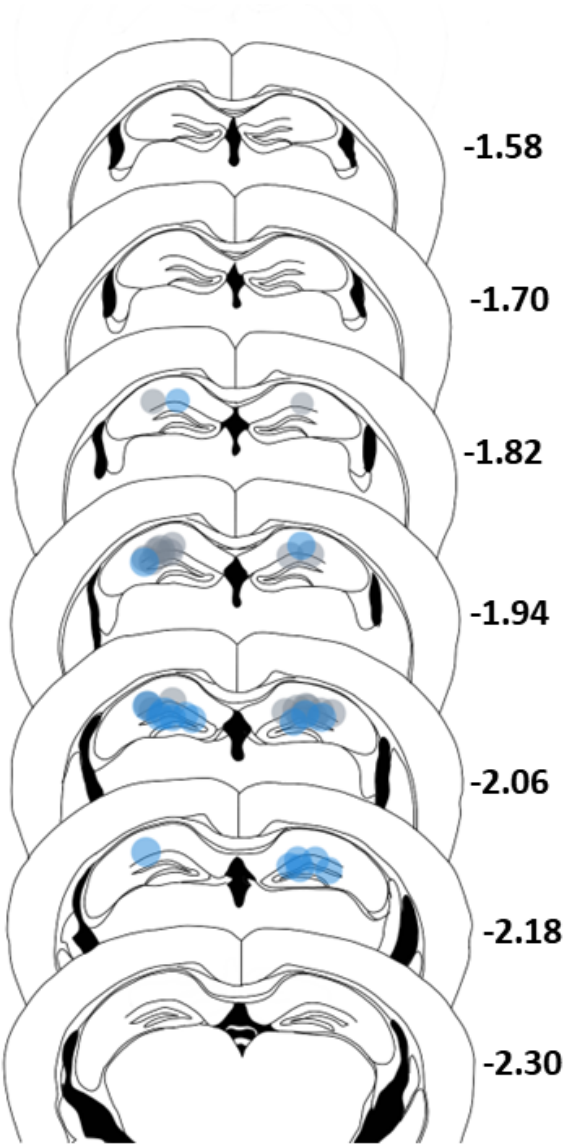

Figure 4.15: Schematic illustration of placements for male Sham (gray) and LPS (blue) groups (The numbers correspond to Bregma).

4.3.2a) Hippocampal neuroinflammation did not affect lever press rates but increased magazines entries in male mice over Days 1-4 of lever press training:

Lever press rates for Sham and LPS animals are shown in Figure 4.16A. The figure suggests that all animals, irrespective of the treatment group, learned to press levers at the same rate. This is supported by statistical analysis (repeated measures two-way ANOVA), as there was a main effect of day ($F_{(1.253, 22.56)}$=98.23, p<0.0001) but not group ($F_{(1, 18)}$=0.0005995, p=0.9807), and no significant day x group interaction ($F_{(3, 54)}$=0.8381, p=0.4842).

Figure 4.16B shows the magazine entries made by these animals over the training days 1-4. As can be seen from this figure, LPS animals made slightly more entries compared to the Sham animals. A repeated measures two-way ANOVA revealed the main effect of day ($F_{(1.927, 34.69)}$=7.535, p=0.0021) that did not interact with group ($F_{(3, 54)}$=0.05872, p=0.9811), however, the main effect of group was close to significance ($F_{(1, 18)}$=4.280, p=0.0532).

Together, these results show that lever press rates for Sham and LPS groups did not differ, however the LPS animals made more magazine entries than to Sham controls.

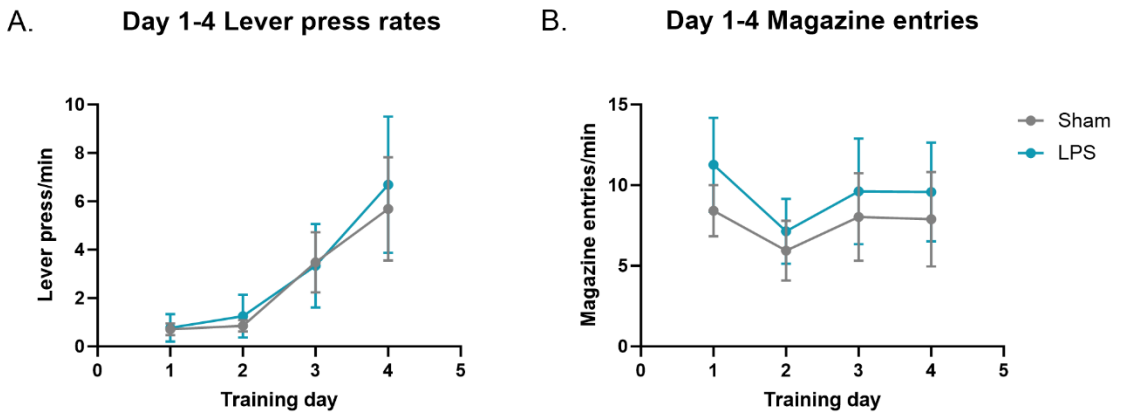

Figure 4.16: Lever press rates for males during training days 1-4 (A). Magazine entries made by mice during training days 1-4 (B) (Sham n=11, LPS, n=9; All values represent the Mean ± SEM).

4.3.2b) Hippocampal neuroinflammation did not affect goal-directed action control in male mice in the 4 Day devaluation test:

Lever press rates on the 4-Day devaluation test is shown in Figure 4.17A. As expected, the Sham animals displayed intact devaluation by responding on the valued more than the devalued lever. Surprisingly, group LPS also showed intact devaluation. These observations were supported by a Two-way ANOVA showing significant main effect of devaluation ($F_{(1, 36)}$=4.551, p=0.0398), no main effect of group ($F_{(1, 36)}$=0.1501, p=0.7007) and no significant group x devaluation interaction (F < 1).

Magazine entries elicited during the 4-Day test are shown in Figure 4.17B. From this figure it appears as though LPS animals performed more magazine entries than Shams. However, upon performing a t-test, the difference was not found to be significant (t=1.497p=0.1518).

Together, the results of the 4-day devaluation test did not produce any significant differences in either devaluation performance or magazine entries, although the latter did appear to be marginally increased in LPS animals. This suggest that, in contrast to the female mice, hippocampal neuroinflammation did not accelerate goal-directed control in male mice, although this is possibly due to the fact that Sham male mice were already showing an intact devaluation effect (Valued > Devalued) whereas Sham females in Experiment 5 were not (Valued = Devalued). Therefore, it is possible that the performance of male mice was at ceiling and no further improvements could be statistically determined.

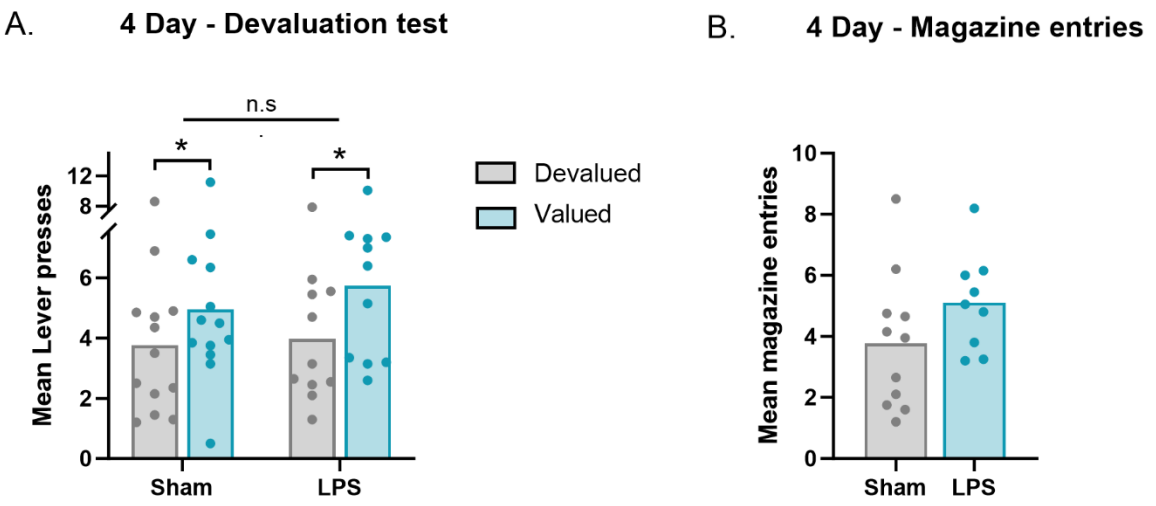

Figure 4.17: Lever presses made by Sham and LPS animals on both valued and devalued lever on the Day 4-devaluation test (A). Magazine entries made by the same animals on the Day 4-devaluation test (B). (Sham n=11, LPS, n=9; $p<0.05$; All values represent the Mean ± SEM).

4.3.2c) Hippocampal neuroinflammation did not affect lever press rates but did increase magazines entries in male mice across Days 5-8 of lever press training:

Following the 4-Day devaluation test, 4 additional days of lever press training was performed (Day 5-8). Lever press rates across days 5-8 are shown in Figure 4.18A. All animals, irrespective of their group, pressed levers at the same rate. This was supported by a repeated measures two-way ANOVA analysis showing a significant main effect of day ($F_{(1.874, 33.74)}=73.41$, $p<0.0001$) but no main effect of group ($F_{(1, 18)}=1.006$, $p=0.3291$) and no day x group interaction ($F_{(3, 54)}=0.8590$, $p=0.4680$).

Consistent with the first four days of lever press training, LPS animals again made more magazine entries than Shams during Days 5-8 (Figure 4.18B). A repeated measures two-way ANOVA revealed a significant main effect of day ($F_{(2.666, 4.99)}=9.763$, $p<0.0001$) and of group ($F_{(2.666, 4.99)}=9.763$, $p=0.0028$), although there was no significant day x group

interaction ($F_{(3, 54)}$=2.354, p=0.0822). These results suggest that LPS animals performed more magazine entries than Shams overall, but the rate at which they did so did not differ across days.

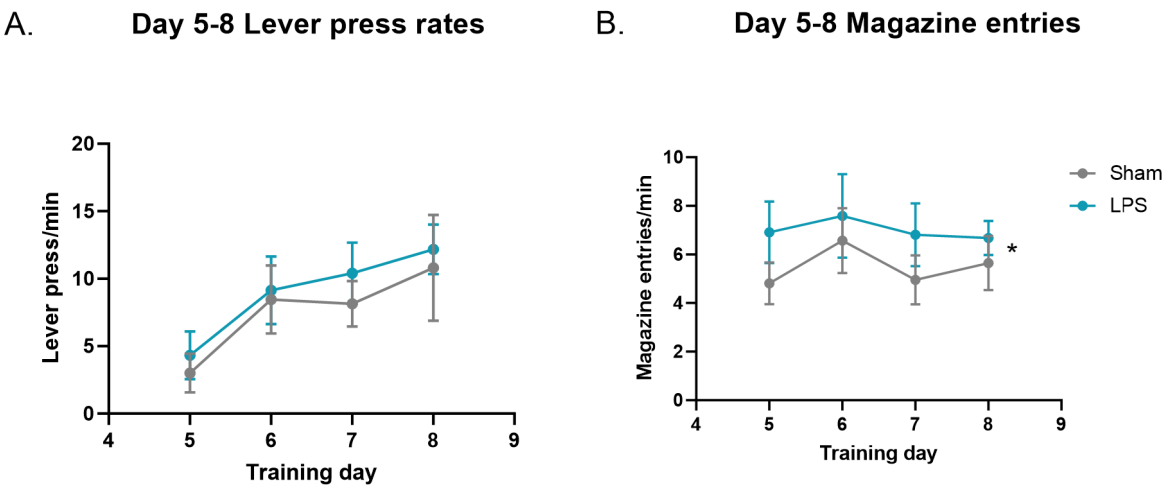

Figure 4.18: Lever press rates for males during training days 5-8 (A). Magazine entries made by mice during training days 5-8 (B) (Sham n=11, LPS, n=9; p<0.05; All values represent the Mean ± SEM).

4.3.2d) Hippocampal neuroinflammation did not affect goal-directed action control but did facilitate Pavlovian approach in male mice in the Day 8 devaluation test:

Figure 4.16 shows lever press rates during the 8-Day devaluation test. Similar to performance on the 4-Day test, devaluation was intact for both Sham and LPS animals who responded more on the valued lever versus the devalued lever (Figure 4.19A). This was supported by a two-way ANOVA which found a significant main effect of devaluation ($F_{(1, 36)}$=14.40, p=0.0005) and no main effect of group ($F_{(1, 36)}$=0.0003497, p=0.9852) as well as no significant group x devaluation interaction ($F_{(1, 36)}$=0.05546, p=0.8151).

Magazine entries from the 8-Day devaluation test are shown in Figure 4.19B. This time, the LPS treated animals made significantly more entries to the magazine relative to the Sham controls. This was indicated by the results of a t-test, t =2.536, p = 0.0207.

Overall, results from 8-Day devaluation test suggested that, in male mice, hippocampal neuroinflammation did not affect goal-directed action control, because devaluation was intact (Valued > Devalued) for both groups but did facilitate Pavlovian approach behaviour because group LPS performed more magazine entries than Shams.

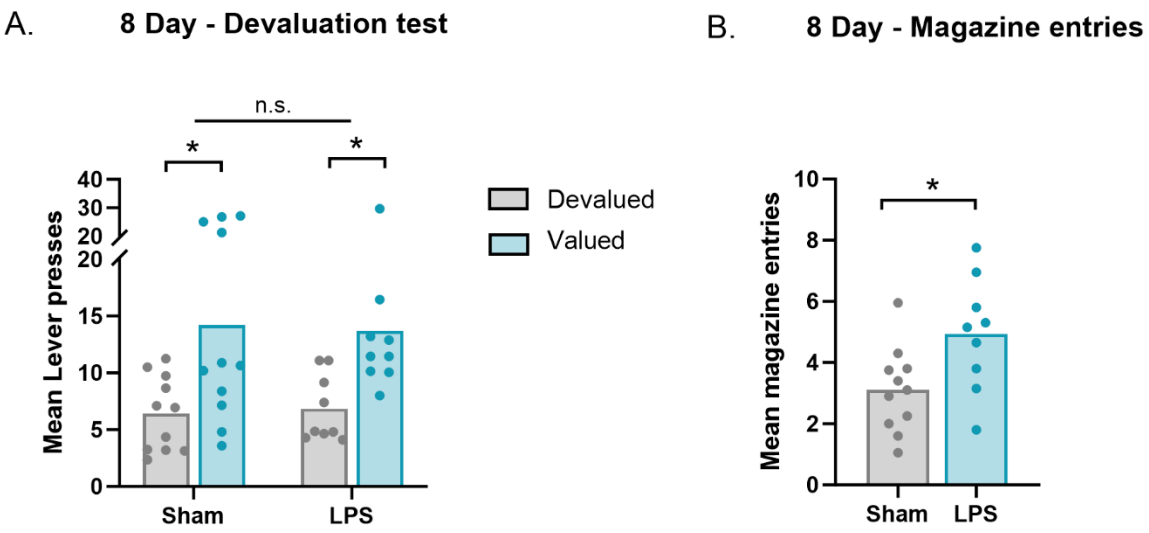

Figure 4.19: Lever presses made by Sham and LPS animals on both valued and devalued lever on the Day 8-devaluation test (A). Magazine entries made by the same animals on the Day 8-devaluation test (B). (Sham n=11, LPS, n=9; $p<0.05$; All values represent the Mean ± SEM).

4.3.2e) Hippocampal neuroinflammation did not alter locomotor activity in an Open Field Test in male mice

I next performed an open field test to determine whether the facilitation of Pavlovian approach in LPS animals was a result of an overall hyperactivity effect or differences in anxiety between groups.

Figure 4.20A shows the total distance travelled by these animals during the 10-minute test. There was no significant difference between the LPS and Sham group, which is indicated by a two-tailed t-test (t=0.8686, p=0.3965). This confirmed that the LPS animals were neither hyperactive nor hypoactive. Additionally, there was no difference in the time spent by LPS and Sham animals in the corner zone (t=0.7751, p=0.4483, Figure 4.20B) and the centre zone (t=0.7751, p=0.4483, figure 4.20C). This indicated that the LPS animals were not anxious compared to the Sham controls.

Overall, the locomotor activity and anxiety levels of the LPS treated animals remained the same as that of Sham animals. This suggests that the observed differences in magazine entries were not a result of either potential confound, but rather an indication of a specific facilitation of Pavlovian approach behaviour in these animals.

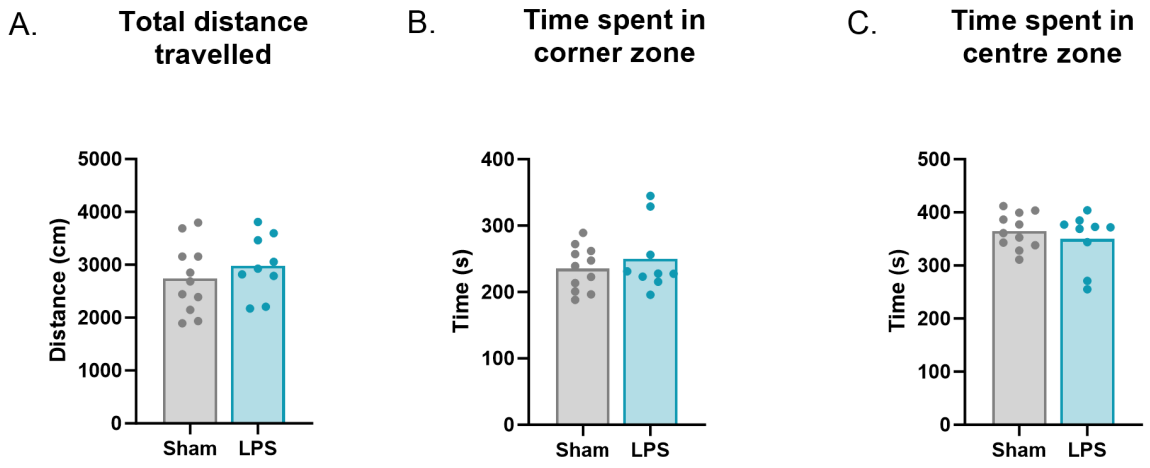

Figure 4.20: Total distance travelled by Sham and LPS animals in the open field test (A). Time spent by Sham and LPS animals in the corner zone (B) and the centre zone (C). (Sham n=11, LPS, n=9; $p<0.05$; All values represent the Mean ± SEM).

4.3.2f) Upregulation of Iba1+ microglial cells after LPS treatment:

When microglial cell numbers were quantified, I found a significant increase in the LPS group compared to the Shams ($t=9.984$, $p<0.0001$, Figure 4.21A). Additionally, microglial cell intensity was also higher in the LPS treated animals compared to the Sham animals ($t=4.403$, $p=0.0004$, Figure 4.21B). This confirmed that, similar to the females in Experiment 5, LPS was again successful in causing the proliferation of microglia in the dorsal hippocampus of male mice.

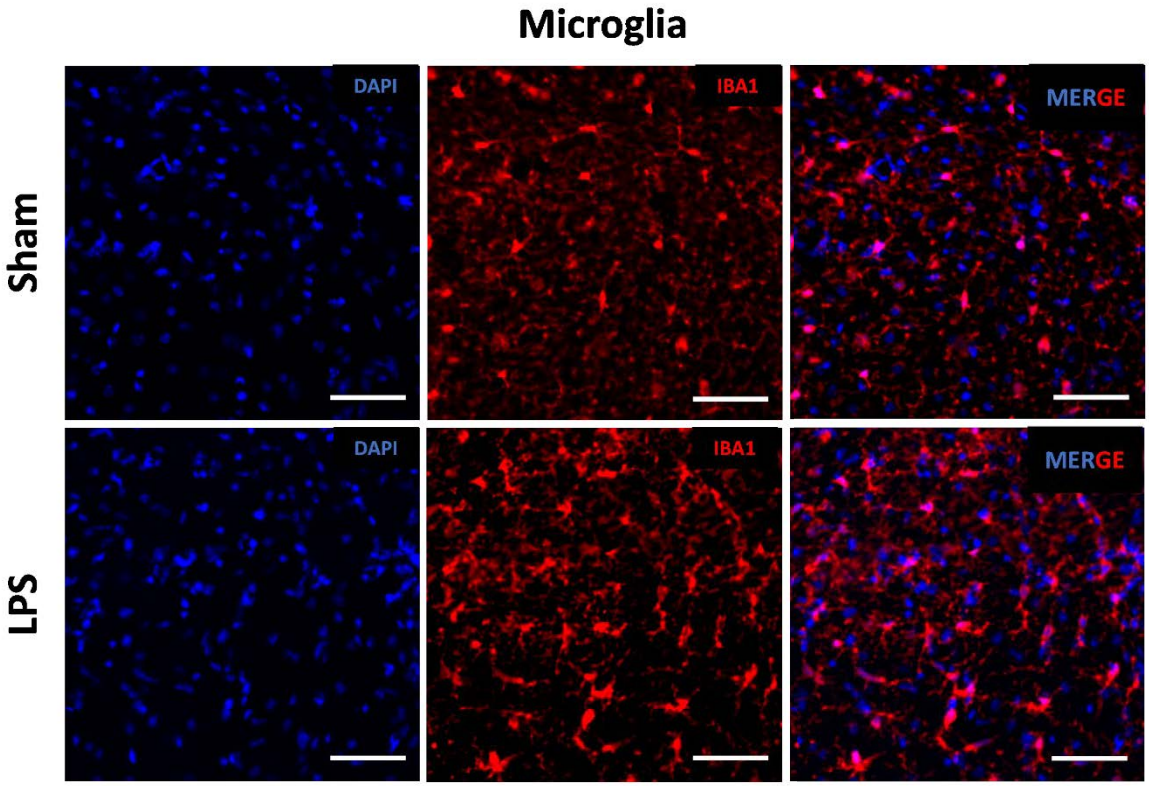

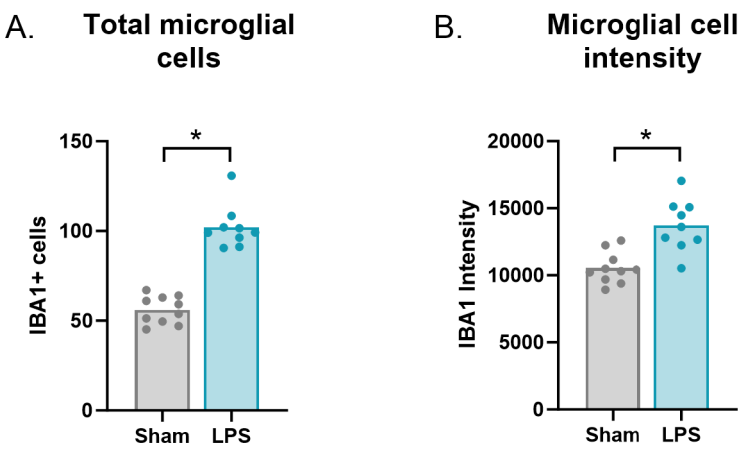

Figure 4.21: Total number of microglial cells in Sham and LPS animals (A). Microglial cell intensity in both Sham and LPS groups (B). (Sham n=10, LPS, n=9; Scalebar: 50µm; $p<0.05$; All values represent the Mean ± SEM).

4.3.2g) Increased microglial reactivity did not correlate with devaluation performance or magazine entries:

Microglial cell numbers did not correlate significantly with any behavioural measure on any test (see Appendix F for precise correlational values). Likewise, microglial intensity did not correlate with devaluation scores from either test (see Appendix F). Although microglial intensity did not correlate with magazine entries from the 4-Day devaluation test, it did marginally positively correlate with magazine entries on the Day 8 devaluation test ($p=0.0705$, $r=0.4238$, Figure 4.22D). This pattern of results is notable, because the only significant behavioural difference induced by hippocampal neuroinflammation in male mice that was observed on either test, was the increase in magazine entries on the Day 8 test, and it appears that this difference was associated with increased microglial expression in dorsal hippocampus. This suggests the possibility of a causal relationship between microglial proliferation and enhanced Pavlovian approach.

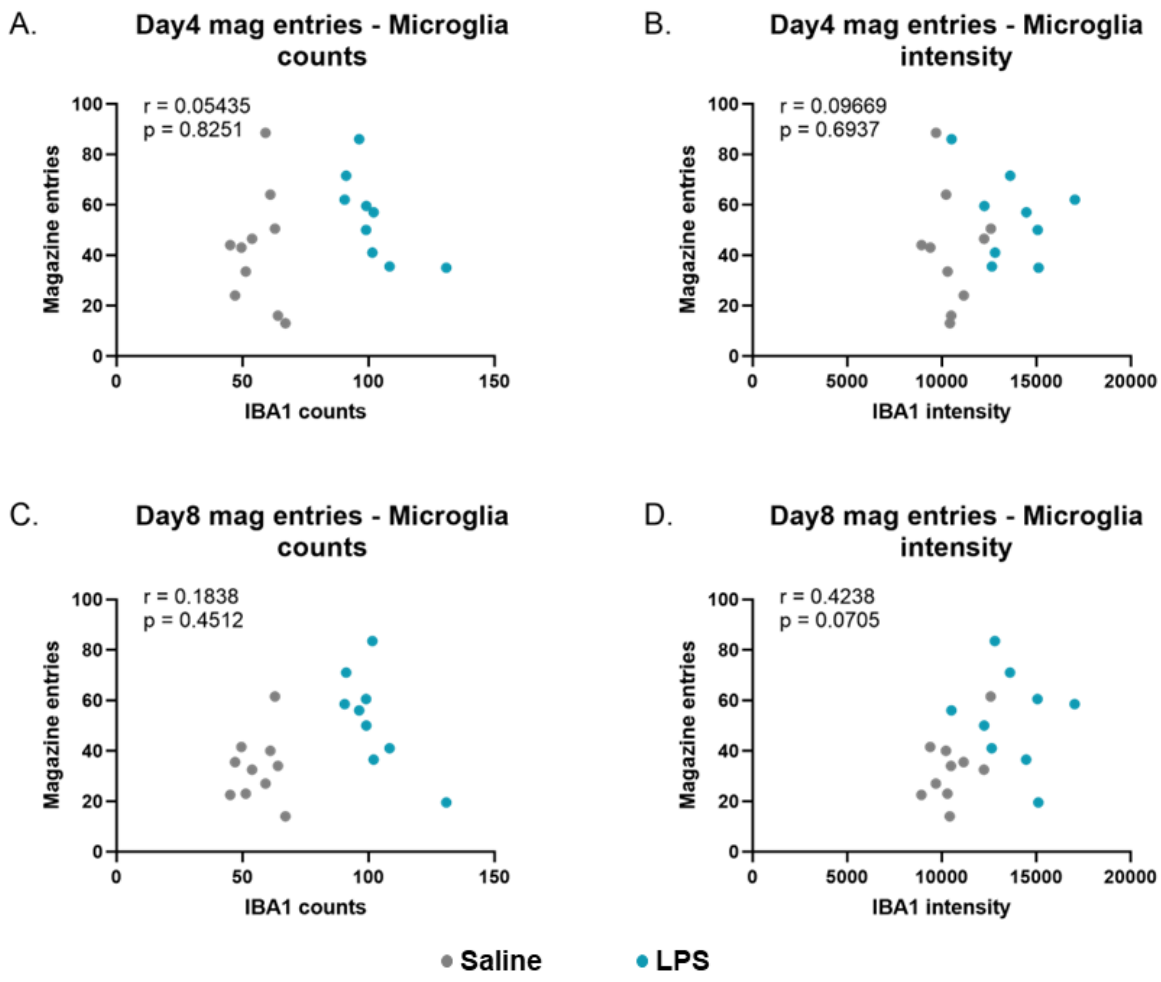

Figure 4.22: Correlation of Iba1+ cell counts with behaviour performance of males on the 4-day magazine entries (A). Iba1 intensity correlations with 4-Day magazine entries (B). Iba1+ cell counts correlation with behaviour performance on the 4-day magazine entries (C). Iba1 intensity correlation with 8-Day magazine entries (D). (Sham n=7, LPS, n=8; $p<0.05$; All values represent the Mean ± SEM).

4.3.2h) Upregulation of GFAP+ astrocytes cells after LPS treatment:

The number and intensity of GFAP+ astrocytes is shown in Figures 4.23A and B, respectively. From Figure 4.23A, it can be observed that there was no significant difference in the astrocytes cell number between LPS and Sham controls (t=0.5047, p=0.6202). However, there was an increase in the intensity of GFAP+ astrocytes in the LPS

group compared to the Sham group, which revealed that there were likely some morphological changes to the astrocytes indicating astrocyte activation (t=7.690, p<0.0001, Figure 4.23B). These results mirrored those observed in female mice and again suggested that LPS was successful in producing a neuroinflammatory response in the dorsal hippocampus that lasted for the duration of the experiment.

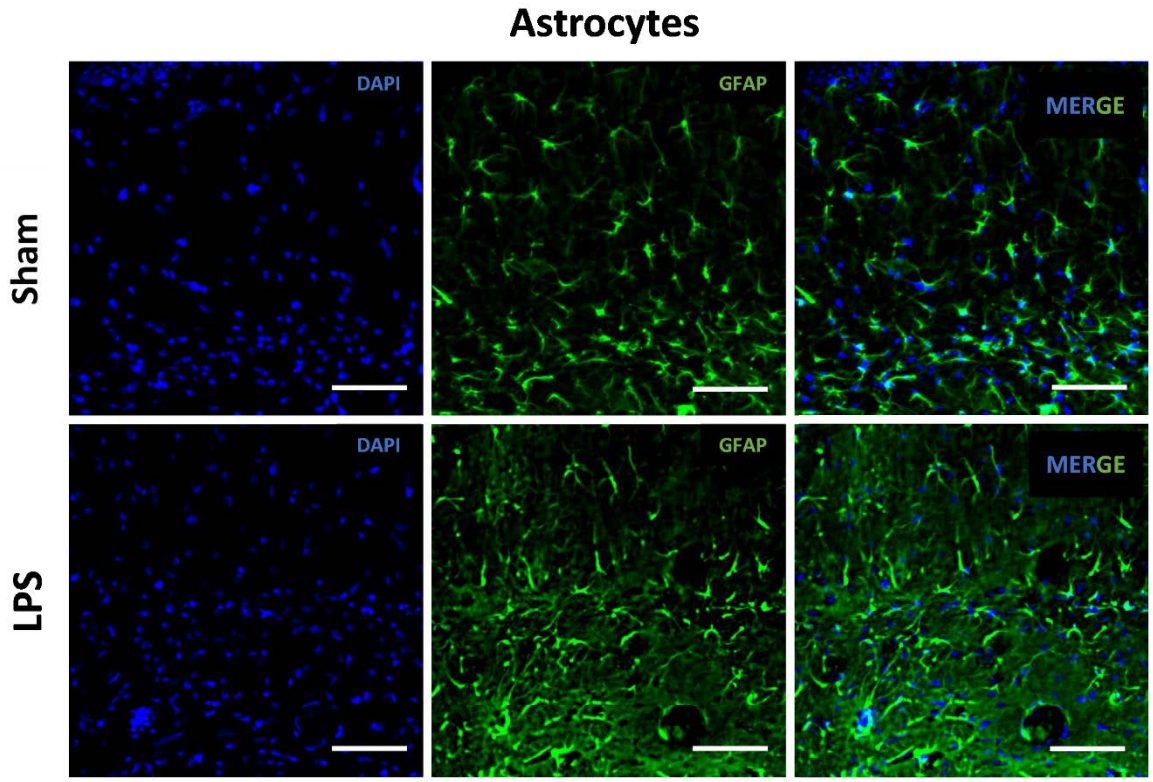

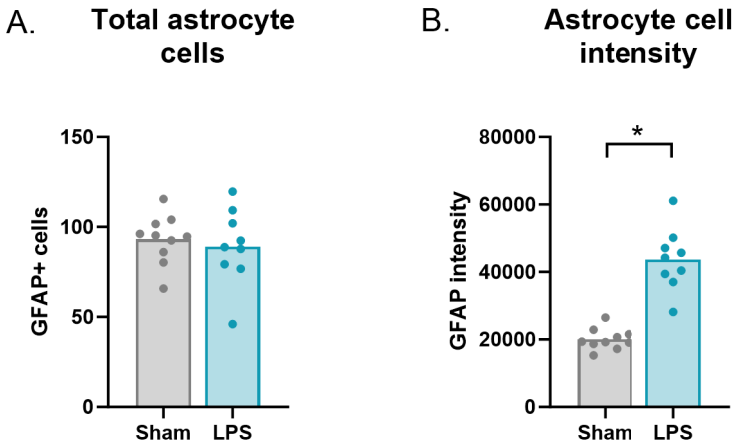

Figure 4.23: Total number of astroglial cells in Sham and LPS animals (A). Astrocytes cell intensity in both Sham and LPS groups (B). (Sham n=10, LPS, n=9; Scalebar: 50µm; $p<0.05$; All values represent the Mean ± SEM).

4.3.2i) No correlation of reactive astrocytes with the devaluation performance and magazine entries made by male animals:

Neither astrocytic cell numbers nor intensity significantly correlated with any behavioural measure on any test (see Appendix F for the specific values).

4.3.2j) No changes in NeuN activation after LPS treatment:

Figure 4.24A showed that the intensity of NeuN positive was similar between LPS treated animals and Sham controls in both the CA1 and DG regions. Therefore. the LPS treatment did not disturb neuronal cell populations.

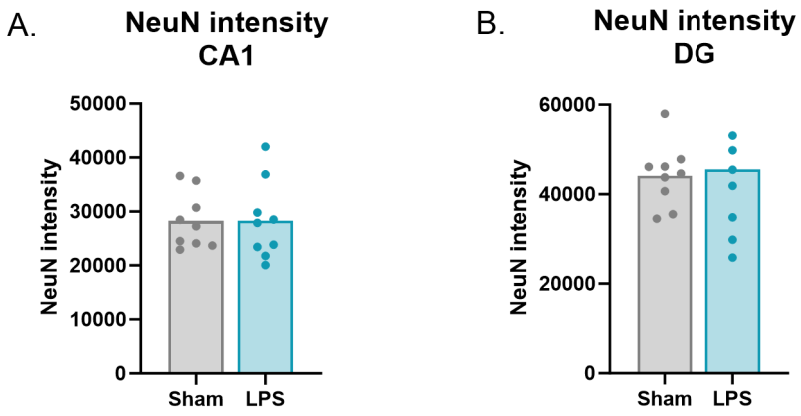

Figure 4.24: NeuN cell intensity in both Sham and LPS groups in CA1 region (A) and DG region (B). (Sham n=9, LPS, n=9; $p<0.05$; All values represent the Mean ± SEM).

4.3.2k) c-Fos colocalized with NeuN positive cells:

As shown in Figures 4.25A, LPS treatment did not affect the % area of colocalization for c-Fos and NeuN in the CA1 of male mice, which was no different from Sham controls. As

can be seen from Figure 4.25B, that there was a trend towards decreased expression of c-Fos in NeuN+ cells c-Fos in the DG of LPS animals compared to sham controls. Statistically this effect was marginal, t=2.050, p=0.0571.

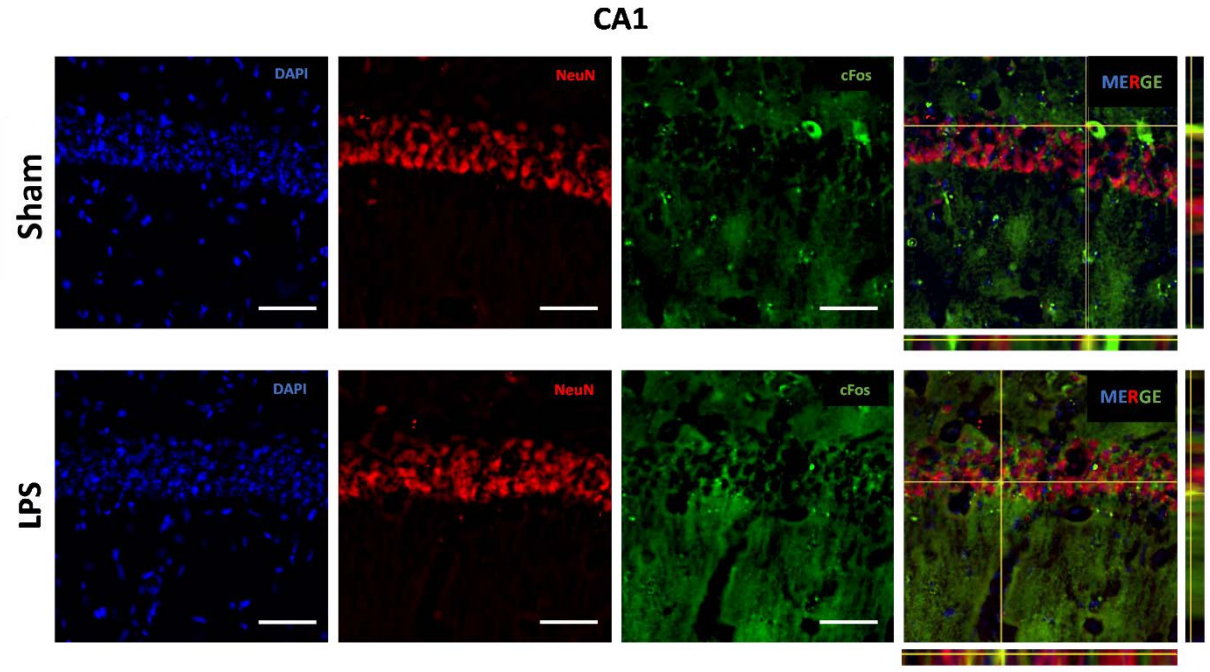

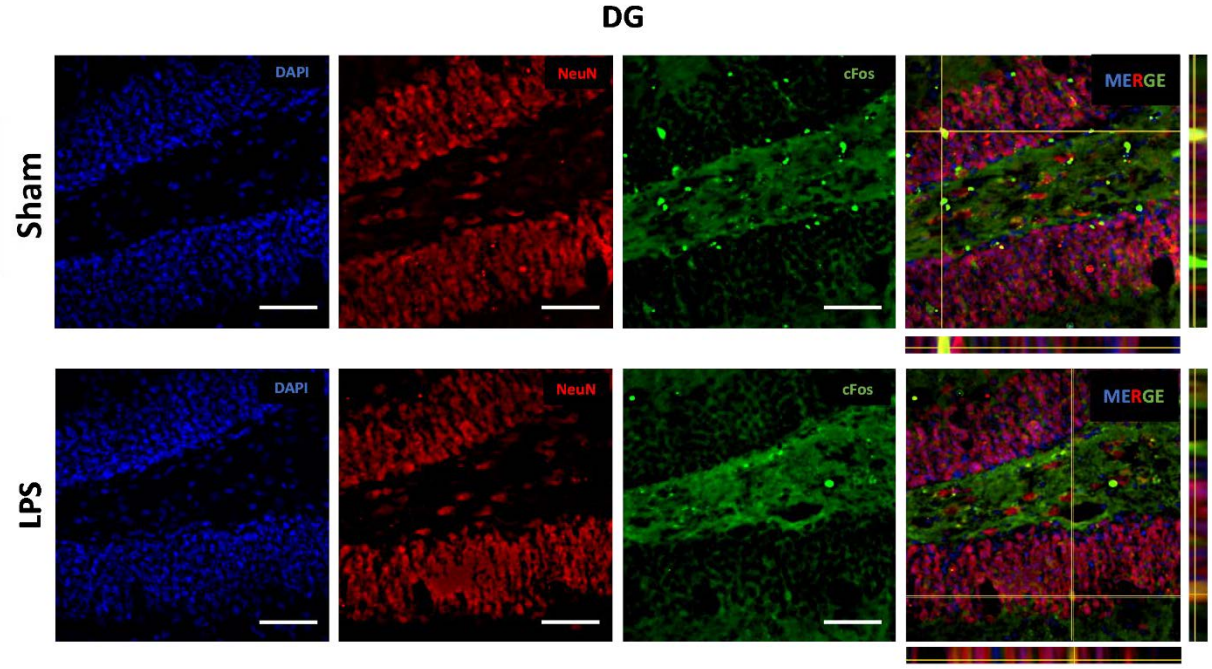

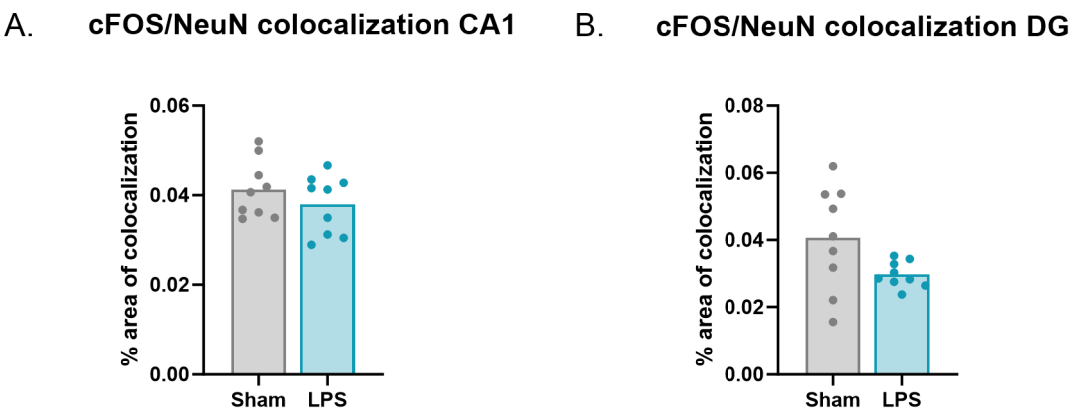

Figure 4.25: % area of co-localization of c-Fos and NeuN in CA1 (A) and DG (B) regions. (Sham n=9, LPS, n=9; Scalebar: 50µm, All values represent the Mean ± SEM).

4.3.2l) Experiment 6: Discussion

Overall, the results of Experiment 6 indicate that, in male mice, LPS was successful in causing an increase in neuroinflammatory markers (i.e. Iba1 and GFAP) in dorsal hippocampus but did not significantly affect neuronal excitation (i.e. co-localised c-Fos and NeuN). Behaviourally, this increase in hippocampal neuroinflammation did not affect goal-directed action control but did facilitate magazine entries across training and on the 8-Day test. This was unexpected, as not only did LPS-induced neuroinflammation in the hippocampus failed to impair goal-directed action, it facilitated our measure of Pavlovian approach to the food magazine – magazine entries. Post-mortem analyses of neuroinflammatory markers revealed that, in spite of the overall increase, there was no correlation with either of these markers and any behavioural measure. Moreover, neuroinflammation did not cause neuronal death (NeuN) or any differences in c-Fos expression in neurons (c-Fos colocalized with NeuN).

Together, the results of Experiment 5 and 6 were unexpected. First, Experiment 5 revealed that in female mice, hippocampal neuroinflammation accelerated goal-directed control

without affecting Pavlovian approach, whereas in Experiment 6, hippocampal neuroinflammation did not affect goal-directed control but did facilitate Pavlovian approach in male mice. To further investigate the potential mechanisms of these surprising effects, we next attempted to chemogenetically excite astrocytes specifically in both male and female mice to determine whether we could replicate the behavioural effects observed following LPS injections into dorsal hippocampus. That is, we injected the virus AAV-GFAP-hM3Dq-mCherry (n = 23 females, n =19 males) or the control virus AAV-GFAP-mCherry (n = 10 females, n = 13 males) into the dorsal hippocampus to cause astrocyte-specific transfection with the 'excitatory' hM3Dq designer receptor exclusively activated by designer drugs (DREADD). The hM3Dq receptor will not respond to any endogenous ligand but does cause cellular activation (Roth, 2016) including of astrocytes (Adamsky et al., 2018) when the animal is given an i.p. injection of the designer drug clozapine-N-oxide (CNO).

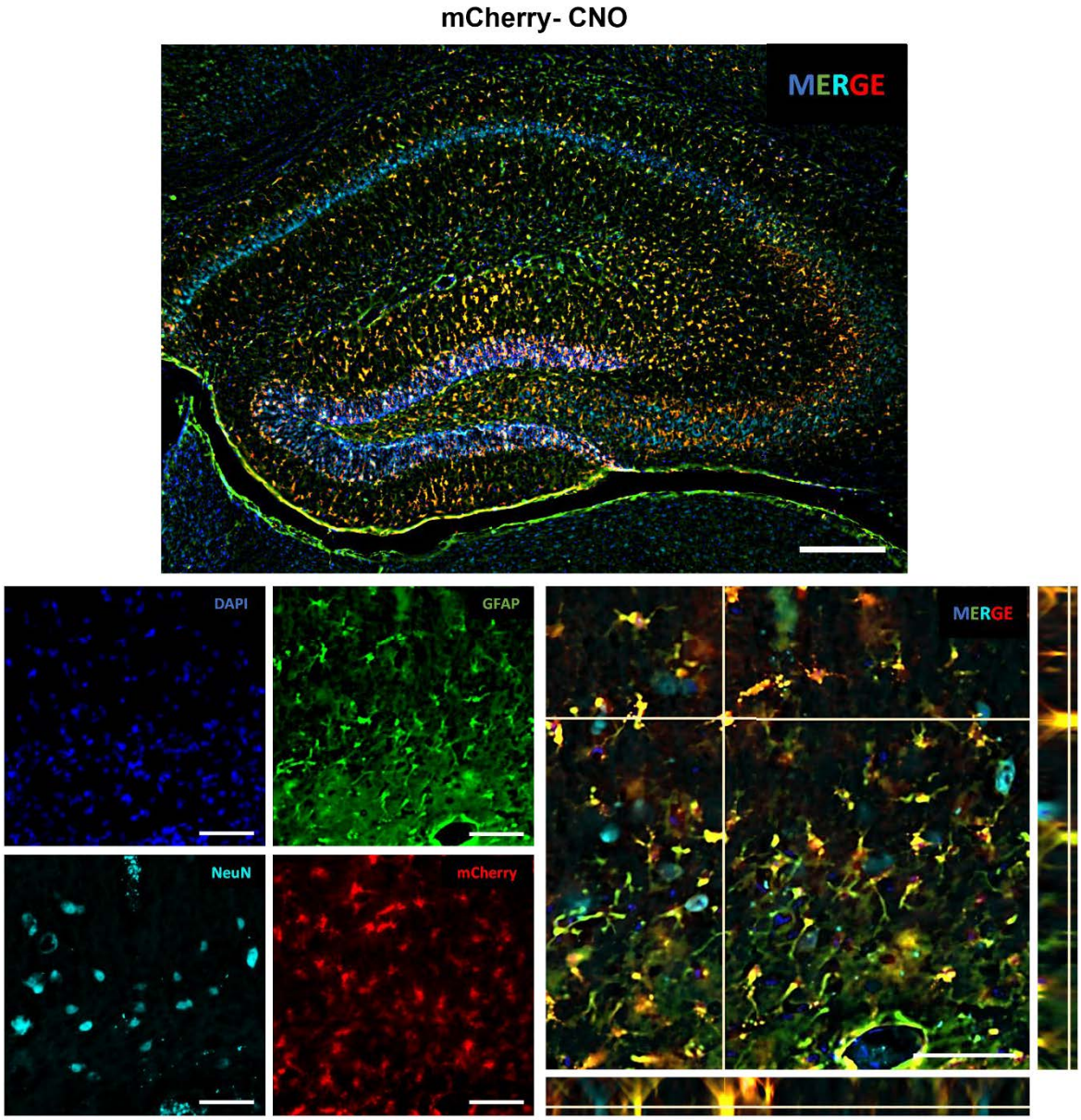

Figure 4.26: Representative image showing expression of pAAV-GFAP-hM3D(Gq)-mCherry (AAV5) – upon activation with CNO in the dorsal hippocampus area. Image on the bottom – DAPI (blue), GFAP for astrocytes (green), NeuN for neurons (cyan), mCherry – DREADDs (red). Merged images (zoomed in from the image on the top) with orthogonal views (small panel on the right and bottom) showing co-localization of astrocytes and mCherry. Image on the top was captured at a 10x magnification (Scalebar: 250µm). All other images were captured at a 40x magnification (Scalebar: 50µm).

However, the results of this experiment were only partially conclusive for two reasons: First, I observed transfection of the AAV in both astrocytes and neurons, as shown in Figure 4.27, and second, I did not observe any robust behavioural alterations.

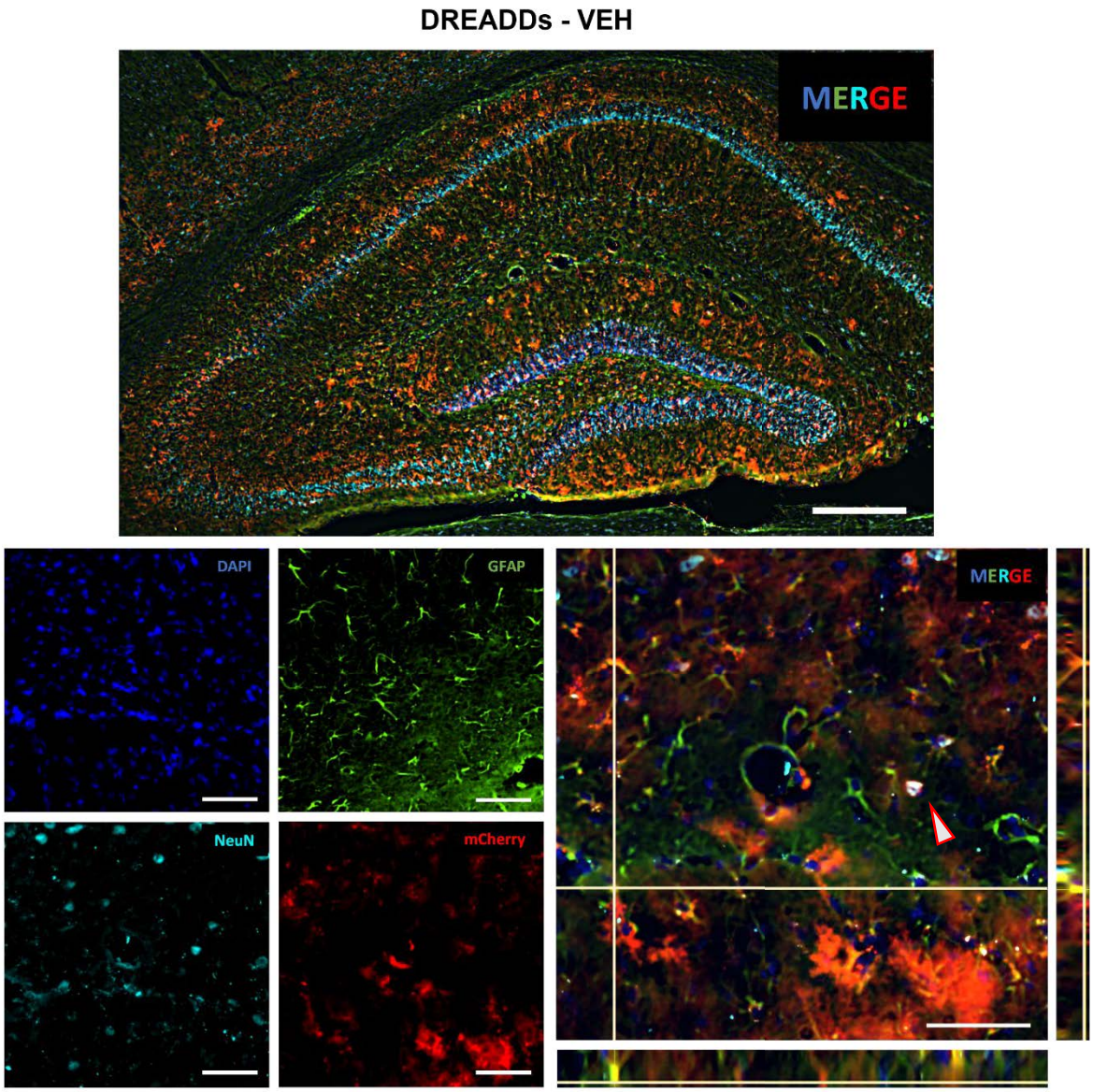

Figure 4.27: Representative image showing expression of pAAV-GFAP104-mCherry (AAV5) that received Vehicle injections in the dorsal hippocampus area. Image on the bottom – DAPI (blue), GFAP for astrocytes (green), NeuN for neurons (cyan), mCherry – DREADDs (red). Merged images (zoomed in from the image on the top) with orthogonal views (small panel on the right and bottom) showing co-localization of astrocytes and

DREADDs. Image on the top was captured at a 10x magnification (Scalebar: 250µm). All other images were captured at a 40x magnification (Scalebar: 50µm). Highlighted in white arrow is the expression of pAAV-GFAP104-mCherry (AAV5) in the neurons (stained with NeuN), confirming that the viral expression was not limited to astrocytes only.

Therefore, I am not reporting this experiment in its entirety, although the full methods and results can be found in Appendix G. Nevertheless, there was one result of interest.

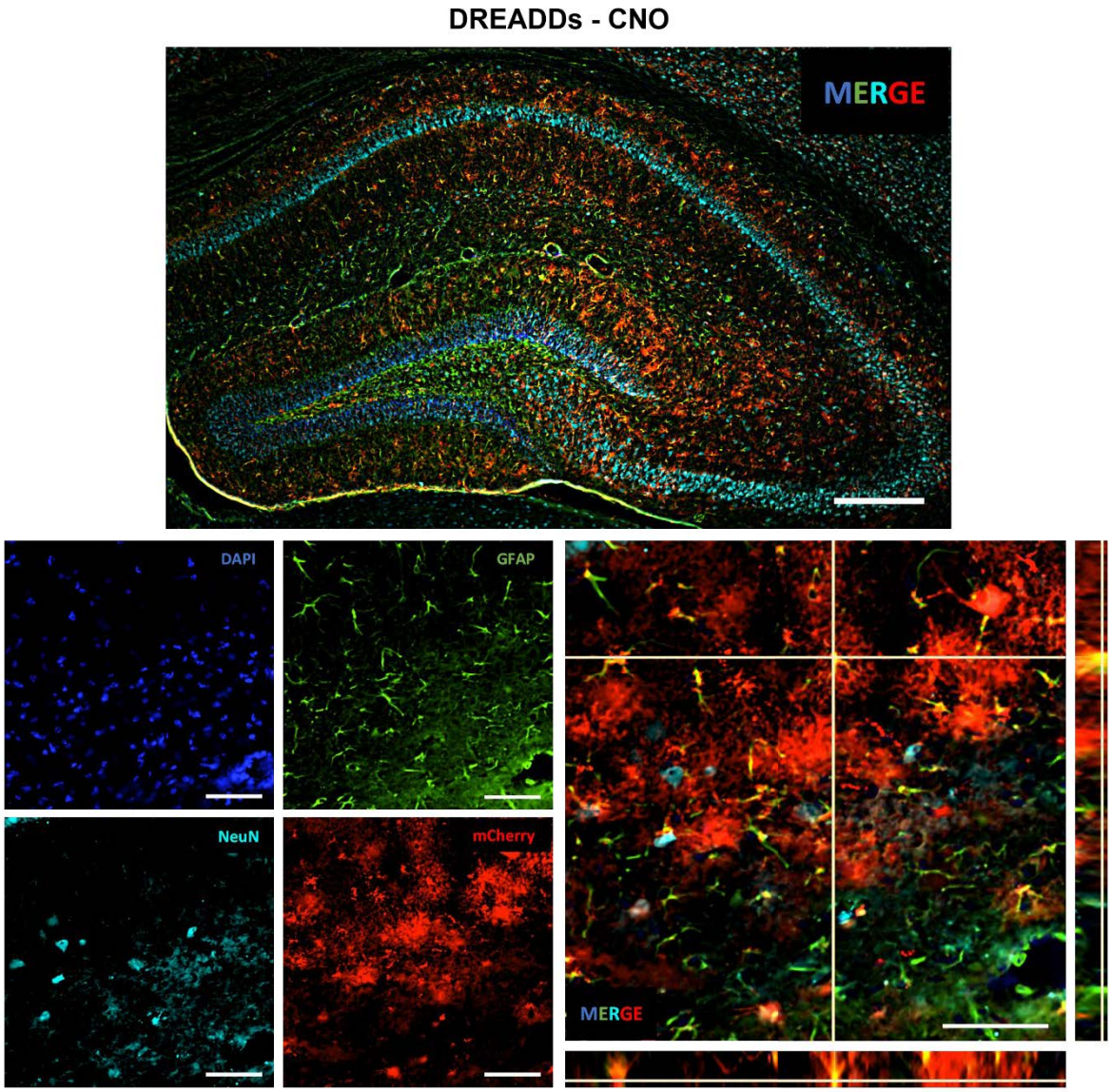

Figure 4.28: Representative image showing expression of pAAV-GFAP104-mCherry (AAV5) that received Vehicle injections in the dorsal hippocampus area. Image on the

bottom – DAPI (blue), GFAP for astrocytes (green), NeuN for neurons (cyan), mCherry – DREADDs (red). Merged images (zoomed in from the image on the top) with orthogonal views (small panel on the right and bottom) showing co-localization of astrocytes and DREADDs. Image on the top was captured at a 10x magnification (Scalebar: 250μm). All other images were captured at a 40x magnification (Scalebar: 50μm).

This is shown in Figure 4.29, and comprised partial evidence that excitation of neurons and astrocytes in the dorsal hippocampus accelerated goal-directed action control because, when averaged across mice of each sex, there was a significant simple effect of devaluation (Valued > Devalued) for the hM3Dq group that received CNO (i.e. the group in which astrocytes/neurons were excited), ($F_{(1,61)}$ = 4.369, p = 0.041), but not for either the mCherry+CNO or hM3Dq+Vehicle controls, both Fs < 1, indicating that these animals pressed each lever equally (Valued = Devalued). The reason why this evidence is only partial, is because there was no main effect of group, F < 1, no main effect of devaluation, ($F_{(1,61)}$ = 3.533, p = 0.072), and no significant group x devaluation interaction, ($F_{(1,61)}$ = 1.665, p = 0.202), suggesting that there was no basis upon which follow-up simple effects should have been assessed. No differences in magazine entries was observed ($F_{(2,59)}$ = 0.7266, p = 0.4878).

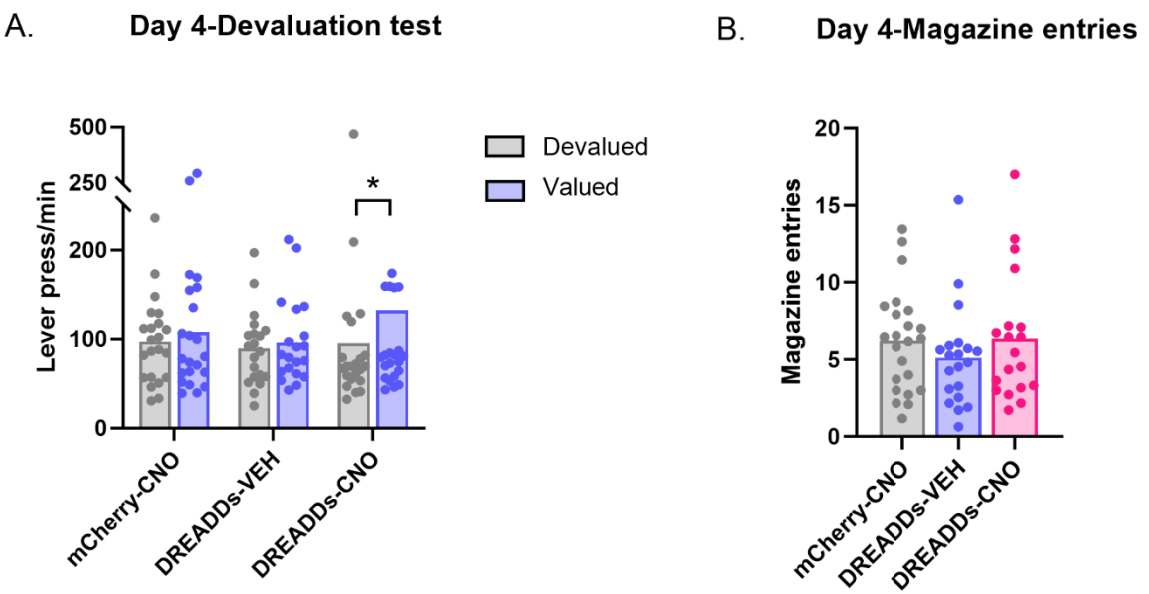

Figure 4.29: Lever press rates for all animals during day 4 devaluation test (A). Magazine entries made by mice during Day 4 devaluation test (B) (mCherry-CNO – 23, DREADDs-VEH – 20, DREADDs-CNO - 19; $p<0.05$; All values represent the Mean ± SEM).

Similar to all previous observations, however, these partial differences disappeared after 4 more days of additional lever press training, as shown in Figure 4.30, when devaluation was intact (Valued > Devalued) for all groups, regardless of neuronal/astrocytic excitation. This was supported by a main effect of devaluation ($F_{(1,118)} = 8.110$, $p = 0.0052$), no main effect of group and no group x devaluation ($F_{(2,118)} = 0.1894$, $p = 0.8277$) interaction. Again, no differences in magazine entries was observed ($F=0.2346$, $p=0.7916$).

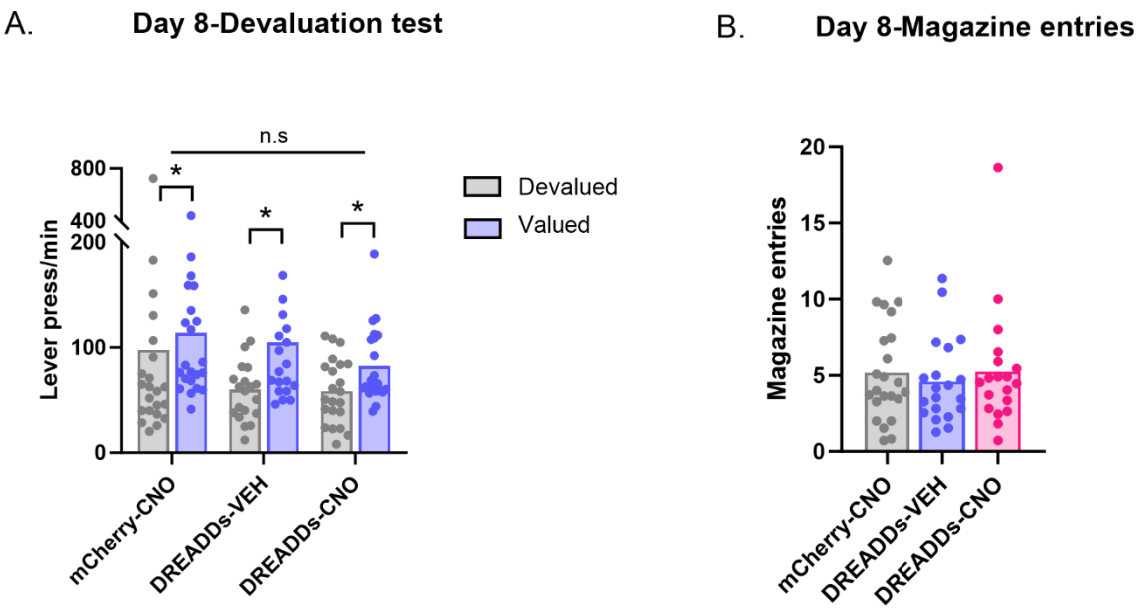

Figure 4.30: Lever press rates for all animals during day 8 devaluation test (A). Magazine entries made by mice during Day 8 devaluation test (B) (mCherry-CNO – 23, DREADDs-VEH – 20, DREADDs-CNO - 19; $p<0.05$; All values represent the Mean ± SEM).

Together, these results suggest that hippocampal neuroinflammation accelerates goal-directed action in female mice and facilitates Pavlovian approach in male mice. There is partial evidence that the acceleration of goal-directed action resulted from the excitation of astrocytes/neurons that occurred as a result of the neuroinflammatory response. These results are discussed in more detail below and in the general discussion.

4.3.3) General Discussion:

The experiments reported in this chapter aimed to investigate the behavioural consequences of the environmental factor that produced alterations in both neuroinflammation and dendritic spine density from Chapter 3: LPS injections into dorsal hippocampus. Specifically, because such injections have already been demonstrated to produce deficits in spatial memory (Hou et al., 2014), I decided to concentrate on the more complex, goal-directed actions which have recently been shown to be impaired in a

mouse model of AD (Dhungana et al., 2023). Overall, however, the results reported in this Chapter were not as anticipated. First, hippocampal neuroinflammation in female mice accelerated rather than impaired goal-directed action control. Second, hippocampal neuroinflammation in male mice did not affect goal-directed action but did facilitate Pavlovian approach behaviour (i.e. increased entries into the food magazine). Finally, I uncovered partial evidence that the acceleration in goal-directed control was a result of astrocytic and neuronal activation in the dorsal hippocampus across both male and female mice, as well as increased neuronal activity in the dentate gyrus. No differences in locomotor activity or anxiolytic responses were observed in either experiment, because LPS and Sham animals travelled equal distance and spent equal time in the centre zone of the chamber in the open field tests. This suggests that the observed behavioural changes were therefore not a result of alterations to motor ability but were specific to goal-directed action control (Experiment 5) and Pavlovian approach behaviour (Experiment 6).

As mentioned, LPS treated female animals from Experiment 5 displayed an acceleration of goal-directed learning that differed from (Dhungana et al., 2023)'s observation of impaired initial goal-directed activity in J20 animals. There are several potential reasons for these contrasting results. The LPS treated females in Experiment 5 showed significantly higher hippocampal neuroinflammation than shams, which positively correlated with devaluation performance (Figure 4.12). This suggests that, rather than impairing goal-directed action control as expected, higher rates of neuroinflammation were associated with *better* goal-directed action control. This is surprising, given that J20 animals also experience higher levels of neuroinflammation than wildtypes. However, there exists a stark contrast between the inflammation profile of J20 animals and our LPS treated animals. In J20 animals, inflammation is visible at the very early stage of 2 months

old (A. L. Wright et al., 2013). Therefore, by the time Dhungana et al., tested for goal-directed action deficits in these animals (at 9 months age), animals had experienced at least 7 months of neuroinflammation which would have induced long term changes to the glial cells and neurons. This was supported by Wright et al.,'s (2013) study showing neuronal death in 9-month-old (starting as early as 12 weeks) J20 animals. Another study reported neuronal loss in 5 months old J20 animals (Beauquis et al., 2014). This contrasts with the current study in which animals experienced behavioural testing approximately one month after LPS injection and therefore had experienced only one month of hippocampal neuroinflammation, and I did not notice any neuronal death in the current study (unaltered NeuN population, Figure 4.13, 4.24). Rather, I uncovered evidence that there was an excitation of neurons (seen in Figures 4.14, 4.25) probably resulting from changes to glial cell expression patterns. Over prolonged periods of neuronal excitation the cells can become overexcited and eventually die (Van Epps, 2006), suggesting that neuroinflammation could still be the underlying cause of behavioural changes in each study, in opposite directions.

Evidence from the literature suggest that short term acute neuroinflammation can be beneficial to neurons in different ways (Yong et al., 2019; Yong & Rivest, 2009). For instance, limited amounts of secreted IFN-γ in the brain has been shown to enhance neurogenesis in the DG region of the hippocampus of Alzheimer's disease mouse models (Baron et al., 2008). Another study of spinal cord injury in rats employed low doses of LPS stimulation and observed axonal regeneration in the corticospinal tract (Torres-Espín et al., 2018). Stimulating immune cells with TLR ligands has been shown to increase the recruitment of oligodendritic precursor cells to the lesion sites to facilitate remyelination of the neurons (Glezer et al., 2006; Setzu et al., 2006).

There is also evidence that acute/mild neuroinflammation can act partially beneficial for certain behaviours at least on novel object recognition (NOR) paradigm in wildtype mice. This study employed a lower dosage of LPS (0.3 mg/kg), which stimulated the immune system and led to a hyperexcitability of parvalbumin expressing interneurons in the medial prefrontal cortex. This excitability resulted in the recruitment of a higher proportion of PV interneurons into the neural circuitry crucial for novel object recognition specifically as shown by Feng et al., (2021). The object recognition performance remained intact in these animals highlighting the beneficial effects of acute inflammation in mediating recruitment of PV neurons to maintain functional integrity of the NOR circuit. It is possible that similar beneficial effects could underlie behavioural enhancement in our animals treated with LPS: an excitation of neurons resulting in better performance of animals on the devaluation task.

On the other hand, sustained neuroinflammation/chronic neuroinflammation for a prolonged period has been shown to be deleterious to neurons. The intrahippocampal neuroinflammation in this study can be considered sustained as the glial cell activation is observed roughly more than a month after LPS surgeries. As discussed in the 'neuroinflammation' section in Chapter 1, Aβ induced toxicity, ROS production, mitochondrial failure, neurotoxic cytokine production, impaired neurogenesis, and compromised synaptic connections are all consequences of chronic neuroinflammation on neurons (Sochocka et al., 2017). In particular, extended neuroinflammation in the brain has been associated with increase in inflammatory cytokines such as IL1-β and TNF-α, which triggers abnormal synaptic signalling (Pickering et al., 2005). Elevated levels of TNF-α is known to result in increased calcium release in primary neuronal cell cultures (Park et al., 2008) and as much as calcium is crucial for normal synaptic transmission, its dysregulation at the synapses, such as excessive calcium influx/storage has been shown

to be detrimental to dendritic spines (Higley & Sabatini, 2012). At the synapses, increased calcineurin in astrocytes induces calcium dysregulation and calcineurin activity within neurons leading to synaptic dysregulation (Sama & Norris, 2013). In a 2019 study, Jafari M et al., (2019) observed that excessive calcium accumulation at the spines acts as a signal for removal of these spines by microglial cells. Loss of synapses eventually leads to loss of neuronal connectivity, resulting in cognitive dysfunction (Sama & Norris, 2013). Should neuroinflammation persist over many months or even years, than the 4-6 weeks it was experienced here, it is possible that it would lead to synapse loss, neuronal atrophy, and impaired rather than enhanced goal-directed action control. Together, these studies suggest that hippocampal neuroinflammation in the short term might improve goal-directed action control, but when sustained over long periods it might lead to neuronal death which would impair GD control.

The LPS treated male animals from Experiment 6 showed intact goal-directed action, but a facilitation of Pavlovian approach. Such a difference is consistent with literature reports of inherent behavioural differences between male and female mice, such as in learning and memory processing (Dalla & Shors, 2009). Moreover, another study has shown that female rats were more inclined towards a Pavlovian approach behaviour, as calculated by the number of food trough entries that were increased in females compared to males (Hammerslag & Gulley, 2014). It seems less likely that LPS might have altered the metabolism to result in an increased consumption of food by these animals. As far as the literature reports, LPS causes hypometabolism in C57BL6/J mice, which is opposite to what we would be expecting with food consumption (Piirsalu et al., 2020). Additionally, our animals received a local LPS injection (intra-hippocampal) which is comparatively less likely to affect the overall metabolism as much as the peripheral LPS injections (which was performed in the above cited paper). Although it is not valid to statistically

compare between experiments, from observations of the data it appears that sham female mice in the current study were also more prone to perform magazine entries than male mice, as shown in Figure 4.31. This suggests that performance of magazine entries may have already been at ceiling in the females in Experiment 5, as there is a physical limitation on how many actions a mouse can perform per minute, leaving little room to detect any further increase over and above these levels in LPS-treated mice.

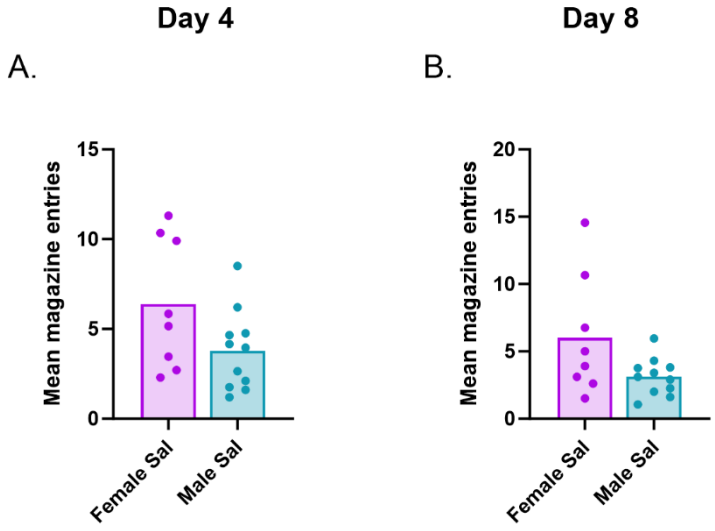

Figure 4.31: Magazine entries made by Sham females and males on the 4-Day test (A). 8-Day test (B). (All values represent the Mean±SEM).

With regards to changes in the inflammatory markers, it is of particular interest that microglial and astrocyte expression correlated very specifically with the devaluation scores from the 4-Day test and not the 8-Day test in female mice in Experiment 5, which is the only test from either experiment in which a significant difference in devaluation performance between shams and LPS-treated animals was observed. This suggests, therefore, that it could have been the reactivity of these glial cells that led to the acceleration of goal-directed action, and the fact that c-Fos/NeuN expression was also significantly increased in these mice suggests that glial activation achieved this

acceleration by causing excitation in neurons. This idea is partially supported by the results of the chemogenetic activations reported in the discussion for Experiment 6, as only the group that experienced neuronal/astrocytic excitation showed some evidence of intact goal-directed control on the 4-day test. Although it may have again been surprising that the control animals for this experiment did not show intact devaluation (particularly the males, given the results of Experiment 6), this could be due to the fact that all animals received i.p. injections each day before lever press training, which likely caused an increase in stress and reduced learning in these animals. Given these data, it will be of particular interest for future studies to determine whether there is a causal relationship between the reactivity of microglia, astrocytes, and neurons, and the acceleration of goal-directed action control.

Taken together, results of this chapter indicate that more work is needed to establish a Sporadic model of AD with better behavioural translatability. Specifically, these experiments suggest that, in mice at least, hippocampal neuroinflammation that persists for at least one month prior to behavioural testing produces an acceleration in goal-directed action control in females and a facilitation of Pavlovian approach behaviour in males. The sex differences in these cohorts are notable, however, given the fact that females are at a higher risk of developing Alzheimer's compared to the males. It is well known that women live longer than men (Baum et al., 2021) and therefore it might appear as if women are only prone to diseases like AD as they live long enough to reach the age where biological functions start to derail. However, age is not the sole factor that can account for this difference. For one thing, women typically only live 2-3 years longer than men, which is not sufficient for differential rates of degeneration to become apparent (which only becomes apparent after around 5 years or more (Mosconi et al., 2018)). Moreover, a recent study has shown that there are several other factors that place

women at a higher risk (Udeh-Momoh & Watermeyer, 2021). For instance, as noted by Fleisher et al., (2005), in female ApoE4 carriers with MCI, hippocampal volume loss is higher compared males. This is despite the similar prevalence of ApoE4 in females and males (Sundermann et al., 2018). It has also been shown that females over 60 years of age, who were a carrier of one ApoE4 allele, are four times more likely to be diagnosed with AD compared to heterozygous males (Farrer et al., 1997) although it is not entirely clear why this is the case. Next to female sex, menopausal status was the strongest correlated factor of the observed biomarker differences in AD (Rahman et al., 2020). For example, in a longitudinal study that looked for cognitive differences the peri and post-menopausal females showed poor cognitive performance and decreased hippocampal volume compared with age matched males. This was due to the following reasons i) neurodegenerative changes happening at an earlier time point(age) in females compared to males, ii) Aβ deposition being widespread (affecting more brain regions) in females compared to males and iii) certain brain regions like frontal cortex being metabolically vulnerable to aging in females during perimenopause to menopause transition compared to males(Mosconi et al., 2018).

These results could suggest that goal-directed action control in female mice could be particularly sensitive to hippocampal neuroinflammation, and whether or not it is accelerated or impaired depends on the length of time neuroinflammation is experienced. This conclusion is purely speculative, of course, and requires future studies to address it in detail.

DISCUSSION
(Chapters 5)

5. Discussion:

The overall aim of this thesis was to provide a better preclinical model of Alzheimer's disease, with a specific focus on replicating the sporadic Alzheimer's phenotype. There were two specific aims:

(i) To combine two major risk factors (genetic and non-genetic) to generate a sporadic mouse model of Alzheimer's disease.

(ii) To investigate whether the identified sporadic Alzheimer's disease model might alter goal-directed action with a view to improve translatability.

Chapter 3 corresponded to the first aim. Experiment 1 demonstrated the validity of my behavioural and molecular techniques using a well-known familial AD model – J20. That is, I successfully replicated the increase in locomotor activity in the open field test and impaired spatial memory (Barnes Maze performance), as well as the increases in glial cell activation (microglia [Iba1] and astrocytes [GFAP]) and decreased spine density that has been observed previously in J20 animals (Cheng et al., 2007; Pozueta et al., 2013). These results suggested that the techniques I employed were suitable to go forward and test the novel sporadic models in my remaining studies. Experiment 2 employed two separate transgenic models, the ApoE4-KI and hAβ-KI models, in conjunction with neuroinflammation (systemic LPS injection) to check for behaviour and pathological changes resembling sporadic AD phenotype. Although I detected reduced locomotor activity in both 'ApoE4-KI + LPS' and 'hAβ-KI + LPS' models (but not in these models without LPS), there were no spatial memory deficits in any model, and no alterations in glial cell expression. There was a slight decrease in the dendritic spine density of 'ApoE4-KI + LPS' mice relative to controls, but this alone was not sufficient to capture the broad

spectrum of deficits observed in patients with AD at a preclinical level. No differences in spine density were detected for the hAβ-KI model, with or without neuroinflammation. Because the results of Experiment 2 were not particularly promising, for my next experiment I focused on enhancing the neuroinflammation factor. Experiment 3 employed intraperitoneal LPS injections to induce neuroinflammation, but this time I increased the dosage and frequency of LPS. Although the results did show an increase in glial cell activation this time, the increase in neuroinflammation did not seem to affect spine density. Because I was ideally looking for a model that affected both glial activation and spine density, I further modified this sporadic factor into a more potent form. Hence, Experiment 4 involved LPS injection directly into the target dorsal hippocampal region. With this manipulation, I observed the cellular changes I was looking for, 7 but not 3days after LPS injections took place: increased levels of astrocyte expression (GFAP) and microglial expression (Iba1), as well as a decrease in spine density.

Moving forward, rather than test these animals for changes to spatial memory, deficits in which have already been reported using this model (Hou et al., 2014), I decided to test whether hippocampal neuroinflammation impaired goal-directed action to determine whether they might replicate the deficits in goal-directed control observed in individuals with AD (see Chapter 2 section 2.3.2 for review). Accordingly, Chapter 4 of this thesis focused on the behavioural translatability aspect, with neuroinflammation as the key sporadic AD factor. The first experiment in this chapter, Experiment 5, investigated changes to goal-directed action control in female wildtype mice that had local neuroinflammation in the dorsal hippocampus (with intra-hippocampal LPS injections). Contrary to expectations, however, rather than impairing goal-directed action control in these animals, dorsal hippocampal neuroinflammation accelerated it. Specifically, when tested on the gold standard test of goal-directed action – outcome devaluation – after 4

days of lever press training, performance was not yet intact for Sham controls (i.e. Valued = Devalued) but was for LPS-injected animals (Valued > Devalued). These differences disappeared after 4 more days of lever press training, when performance was intact for both groups on the 8-Day Devaluation Test. Pavlovian approach behaviour, measured as the number of entries made into the food magazine, was not altered by hippocampal neuroinflammation in female mice. I next proceeded to repeat the experiment in male wildtype mice, to test for the generality of the results, in Experiment 6. This time, however, goal-directed action was unaffected by hippocampal neuroinflammation, possibly because the Shams were already showing a small devaluation effect on the 4-Day test, indicating the possibility of a ceiling effect. LPS animals did, however, make more entries into the food magazine relative to Shams throughout training and testing of this experiment (with the exception of a non-significant effect on the 4-Day test), suggesting that, in males, hippocampal neuroinflammation facilitated Pavlovian approach. Importantly, hippocampal neuroinflammation did not alter locomotor activity or anxiety-like behaviours in male or female mice in either experiment. Together, these surprising results revealed that hippocampal neuroinflammation produces different behavioural profiles in male and female mice, and potential reasons for these sex differences are discussed below.

Post-mortem analyses of dorsal hippocampal tissue did provide some insight into the potential mechanisms of these behavioural alterations. Specifically, all animals were culled following the 8-Day test, and increased reactivity of microglia and astrocytes in LPS-injected animals was detected for both males and females. In females (Experiment 5), these increases correlated with a 'devaluation score' taken from the 4-Day test but not a similar score taken from the 8-Day test, indicating that higher glial activation was associated with better initial goal-directed control. In male mice (Experiment 6),

microglial and astrocytic expression did not correlate with any behavioural measure. Moreover, in female mice but not male mice there was increased in c-Fos expression in neurons in the dentate gyrus (and a trend towards a similar increase in the CA1 region). Together, these results suggest that neuroinflammation increased the reactivity of both microglia and astrocytes in the dorsal hippocampus, and in female mice this caused increased neuronal excitation in dentate gyrus, in a manner that was linked to better goal-directed action control.

Overall, these results lead to the following conclusions:

(i) Combining a genetic and non-genetic factor to create a novel sporadic AD model successfully replicated the spine density changes (only in the ApoE4-KI + LPS model) observed in individuals with AD, but none of the other behavioural or cellular changes associated with Alzheimer's.

(ii) Neuroinflammation localized to the dorsal hippocampus produced the expected increase in microglial and astrocytic markers, as well as the decrease in dendritic spine density,

(iii) Dorsal hippocampal neuroinflammation accelerated goal-directed action control and neuronal excitation in female mice in a manner that was associated with increased glial activation, and

(iv) Hippocampal neuroinflammation facilitated Pavlovian approach in male mice but does not alter neuronal excitation, and in a manner that was not associated with glial expression,

In the following sections, I will be discussing the results as two separate parts. The first half will discuss the theoretical and clinical implications, limitations, and future directions of Chapter 3 of this thesis, followed by the second half of the section which will discuss

the same for the empirical Chapter 4 of this thesis. This will be followed by a brief conclusion section summarizing the overall findings of the thesis.

5.1) Theoretical and clinical implications of combining the major genetic risk factors along with the non-genetic risk factor to create a novel model of sporadic AD:

5.1.1) Locomotor activity of the proposed sporadic AD mouse models:

The abnormal increase in locomotor activity observed in J20 animals in Experiment 1 is consistent with what has been commonly reported for J20 animals of the same age (6 months). In particular, a study by Wright et al., showed that 6 month old J20 males were hyperactive compared to WT males of the same age (2013). Two other studies (Flores et al., 2018; Harris et al., 2010) also reported hyperactivity in the open field test in J20 animals of the same age group relative to controls. Although, as mentioned, these findings were useful to the current study in validating the sensitivity of this measure to detect established changes, the consistent increase in hyperactivity in J20 animals does raise general questions about the translatability of the J20 model. That is, although hyperactivity has been reported in AD patients in some studies (Keszycki et al., 2019), it is not generally considered a core feature of the disease. Moreover, a significant subset of patients present with what might be considered the opposite of hyperactivity: apathy and fatigue (Daumas et al., 2021). Together with anxiety (a major neuropsychiatric symptom of AD), these symptoms are reported to be the early clinical manifestations of AD (Johansson et al., 2020). Here, however, the J20 animals were not anxious, as seen from the equal amount of time spent by these animals compared to wildtypes in the centre zone of the open field chamber. This result is in line with studies reporting reduced (Zussy

et al., 2022) or no anxiety in J20 animals (A. L. Wright et al., 2013). Therefore, this specific result does bring into question how closely the familial J20 model is recapitulating AD at a preclinical level, and further highlights the need for better preclinical models of sporadic forms of AD.

In Experiment 2, the WT animals that received systemic injections of LPS did not show any abnormality in their locomotor activity and anxiety. This is inconsistent with a number of studies that reported locomotor activity decrease after LPS injections in mice (Biesmans et al., 2013; Engeland et al., 2001; Hasriadi et al., 2021; Sulakhiya et al., 2016; Zhao et al., 2019). The major reason for this discrepancy in the results could be the dosage of LPS administered in these studies. For instance, Zhao et al, (2019) used LPS at a dosage of 0.75mg/kg for 7 consecutive days intraperitoneally to observe differences in locomotion. Likewise, Engeland et al., employed 3mg/kg LPS to witness a locomotor deficit. These deficits may not have been a result of neuroinflammation per se, but rather could have been the result of LPS induced sickness behaviours (Biesmans et al., 2013; Engeland et al., 2001; Hasriadi et al., 2021), because it has been shown that a single intraperitoneal injection of 1mg/kg was sufficient to induce sickness behaviour in mice that persisted for several hours according to the murine sickness score (Savage et al., 2019). Moreover, these animals, with an already existing sickness behaviour, when introduced into a novel environment were hesitant to explore the environment, thereby resulting in reduced locomotor activity (Savage et al., 2019). The behaviour of LPS-injected animals in the current study is unlikely to have been affected by sickness behaviour because of the low dose (0.2mg/kg) used, and because I did not observe any behavioural evidence of such abnormalities in my twice-weekly monitoring.

However, because this low dose was also insufficient to cause a significant increase in either microglia or astrocyte activation in post-mortem assessment, it is possible that it did not induce sufficient neuroinflammation in the wildtype animals, or that the induced inflammation was so mild that it did not translate into locomotor deficit or anxious behaviour. Another possibility is that the repeated LPS injections resulted in tolerance, which was observed by White et al., (2017) in their study on C57BL/6J mice. In that study, LPS injections of 0.25 mg/kg were intraperitoneally administered for seven consecutive days, pre-exposing the animals to LPS induced effects. These animals were exposed to LPS for the second time after another 14 days, and this time expressed decreased levels of inflammatory cytokines and Aβ relative to animals that are not pre-exposed to LPS, suggesting that the prior exposure encouraged tolerance (White et al., 2017). If animals in the current study also developed tolerance across the course of injections, this could be a reason why no decrease in locomotor activity was observed.

Literature reports for locomotor activity and anxiety in ApoE4 (with no LPS injections) mice predominantly support the lack of effect on either that I also observed in Experiment 2. For instance, Zhang et al., (2019) reported no difference in the locomotor activity of ApoE4 animals, and neither did Fang et al., (2021), even at 8 months old. Crucially, a Jackson laboratory report published specifically for the strain of mice used in the current study showed no alterations to locomotor activity of ApoE4-KI mice, even at 12 months of age (consortium, 2018). All of these results do contrast with one study, by Siegel et al., (2012), who showed that ApoE4 animals, irrespective of their age (young – 6-8 months old, old – 14-22 months old) were showing decreased locomotor activity in open field test. This could be because Siegel et al., employed only female animals, whereas the current study and other reported studies, used a combination of male and female mice. I did observe a decrease in locomotor activity, however, when I combined the ApoE4-KI

model with LPS, although this manipulation still did not produce any effects on anxiety. This partly reflects what is observed in Alzheimer's patients in terms of apathy and fatigue due to low energy levels, and therefore suggests some potential utility of the novel sporadic AD model ApoE4-KI + LPS.

There has only been one published study that I am aware of conducted on hAβ-KI mice (mostly likely due to its novelty in the field of Alzheimer's research) and it did not assess locomotor activity changes (Baglietto-Vargas et al., 2021). Therefore, it is possible that the current study could be the first to assess locomotor activity in these mice. Much like the APO4-KI model, the hAβ-KI alone did not differ from controls in either locomotor activity or anxiety, but the addition of neuroinflammation in these animals (i.e., the hAβ-KI + LPS) did significantly reduce locomotor activity. It is notable that this is the direct opposite of what is typically observed with the traditional familial models of AD, which are usually hyperactive relative to controls (Baeta-Corral & Giménez-Llort, 2015; Wang et al., 2022). However, the excessive accumulation of Aβ plaques, which hAβ-KI do not express in abundance could be one of the major driving factors for the observed hyperactivity; although why this would be the case is not entirely clear.

Nevertheless, it should also be noted that in a study involving a familial AD model (Tg2576), i.p. injections of 0.33 mg/kg LPS resulted in hypoactivity in open field test as a result of depressive-like behaviour (Knopp et al., 2022). This leaves us with two possible explanations for the hypoactivity observed in our hAβ-KI+LPS animals. First, LPS induced neuroinflammation could have opposite effects to that of endogenous neuroinflammation observed as a result of multiple pathological pathways in the case of familial AD mice. Second, the formation of amyloid beta plaques follow a slow seeding/nucleation mechanism which involves oligomeric seeds formation before maturing as Aβ plaques

(Soto et al., 2006). Baglietto-Vargas et al., (2021) only checked for levels of Aβ 40 and 42 plaques in these mice, while there exists a possibility of oligomeric Aβ formation already in these 6 months old hAβ-KI mice, which was not checked. It could be possible that these animals slowly started accumulation of oligomeric Aβ at this stage, which combined with an external LPS injection, resulted in hypoactivity in these animals, similar to the pattern observed in Tg2576 animals that received external LPS injections. The above results suggest that the ApoE4 or hAβ changes alone are not sufficient to produce deficits. Additionally, wildtype animals that received LPS also did not show altered locomotor activity. Together, these results indicate that the genetic risk factors paired with neuroinflammation to produce a more potent alteration in behaviour relative to any of these factors alone. This suggests that the ApoE4 and hAβ factors might predispose or create a particular vulnerability in these animals to the LPS induced changes. If translatable, it suggests that people with either of these genetic changes might be particularly vulnerable to behavioural changes when they experience neuroinflammation. This notion is supported by a study conducted in 2022 reported inflammation and ApoE4 risk factors were related to apathy in individuals with Alzheimer's (Azocar et al., 2022). Despite these changes, it remains unclear as to why I did not also observe changes to anxiety-like behaviour in these animals. Future studies may wish to employ different behavioural paradigms that test for anxiety-like behaviour, such as elevated plus maze test (Komada et al., 2008) or zero maze (Kulkarni et al., 2007) which may have a higher probability of capturing small changes in the behaviour of these animals.

In Experiments 5 and 6 of Chapter 4 I applied the open field test to animals who had received LPS injections in their dorsal hippocampus. I did not observe any alterations to performance in either experiment, which allowed me to rule out whether changes to

locomotor activity or anxiety at baseline could account for the differences in goal-directed action (Experiment 5) and Pavlovian approach (Experiment 6). This is discussed in the sections referring to Chapter 4 below.

5.1.2) Alterations in spatial memory of the proposed sporadic AD mouse models:

Once again, I first validated that the Barnes Maze protocol was sufficiently sensitive to detect such deficits using J20 mice. In particular, and in line with the literature reports (Flores et al., 2018; Larson et al., 2012), J20 animals in the current study (Experiment 1) were impaired in Barnes Maze spatial memory test as they spent equal time exploring all zone on the test day, indicating they did not remember the target zone (where escape box was placed).

LPS injections in wildtype animals in Experiment 2 did not result in a spatial memory deficit. This is largely inconsistent with previous reports (Khulud Abdullah Bahaidrah et al., 2022; X. Feng et al., 2021; Luo et al., 2020; Zhao et al., 2019) in which both intraperitoneal and intracerebroventricular LPS injections in WT mice were found to significantly impair working and spatial memory. In a recent 2022 study, intraperitoneal injections of 0.25 mg/kg, 0.50 mg/kg and 0.75 mg/kg each day for 7 days LPS to swiss mice and observed a severe impairment of short term and long term spatial memory deficits in both Y-maze and water maze paradigms (Khulud Abdullah Bahaidrah et al., 2022). A higher dosage of LPS 5mg/kg was given to C57BL/6J mice, which showed an obvious decrease in fear memory in both contextual and cued- fear conditioning test (Luo et al., 2020). In a study by Feng et al., (2021) single i.c.v injection of 50μg/10μl LPS in rats were seen to impair learning and memory in Y-maze and water maze tests. This inconsistency could be a result of the higher dosage (Luo et al., used 5mg/kg) and/or the different mode of LPS injections used in these previous studies. Although Bahaidrah et al.,

(2022) used a lower dosage of i.p. LPS (0.25 mg/kg), this was administered daily compared to weekly (for 17 weeks) in the current study. It is therefore possible that the schedule employed by Bahaidrah et al., produced a more intense inflammatory response, leading to deficits in spatial memory that were not observed in the current study (Khulud Abdullah Bahaidrah et al., 2022).

None of the proposed sporadic AD models in the same experiment ('ApoE4-KI', 'ApoE4-KI + LPS' 'hAβ-KI', or 'hAβ-KI + LPS') demonstrated any difference in performance from respective controls on the Barnes Maze either. Because Experiment 1 had confirmed that our protocol was sufficiently sensitive to observe such deficits, this result implied that neither the individual risk factors nor the combination of risk factors resulted in spatial memory impairments in these animals. The lack of effect in ApoE4-KI mice was somewhat surprising, given several reports of spatial memory deficits in these mice. For instance, Rodriguez et al., used the same Barnes maze test and observed spatial memory deficits in ApoE4 mice as early as 3 months (2013). Several other studies found spatial memory deficits in ApoE4 animals in a Morris water maze paradigm (Boehm-Cagan & Michaelson, 2014; Salomon-Zimri et al., 2014; Yin et al., 2011). It is possible that this inconsistency is a result of differences in the precise mouse strain used (explained in detail in the limitations section), and indeed a recent publication on the specific mouse strain employed here failed to find any deficit in spatial memory at 6 months of age (Sepulveda et al., 2022).

Again, the hAβ-KI mice have not been assessed for spatial memory deficits in any study that I am aware of, so it is not possible to compare the current results with any previous findings. However, one study did report that hAβ-KI animals were found to have no impairment in contextual fear memory when tested at 6 months old but were found to

exhibit a significant decrease at 10 months' time (Baglietto-Vargas et al., 2021). Specifically, hAβ-KI animals were found to exhibit significantly less freezing than wildtype controls when tested 24 hours after receiving a foot shock in the same context, which suggests that these animals failed to remember the context from the previous day. Although not a direct measure of spatial memory, contextual memory is closely linked (Bird & Burgess, 2008; Broadbent et al., 2004) and is also heavily dependent on hippocampus. Therefore, the lack of impairment observed in hAβ-KI mice at 6 months is consistent with the lack of spatial deficit we observed in the same mice at 6 months of age. If I were to extrapolate further, these results could imply that we might expect to see a deficit in spatial memory in hAβ-KI mice around 10 months age.

The current study is the first, to my knowledge, to test spatial memory using the combination of ApoE4-KI and hAβ-KI models with LPS, and I did not uncover any evidence here for impaired spatial memory in these models. In considering this result, it is worth briefly revisiting the open field results. This is because Barnes maze performance relies on a degree of locomotor activity, as the mouse must move towards the escape box during learning and on test, such that one might expect any change in locomotor activity to also affect Barnes maze performance. Despite both ApoE4-KI + LPS and hAβ-KI + LPS causing hypoactivity, however, this did not appear to affect the Barnes maze. Taking a closer look at the learning curve of these animals on the Barnes maze test (refer Appendix B) reveals that the ApoE4-KI + LPS and hAβ-KI + LPS animals were slower in learning the task (as indicated by decreased path length and increased latency to locate the escape box) on the first two days, but that this difference disappeared on the final day of acquisition training. The fact that any differences did not persist on test provides a clear indication that these models specifically affected locomotor activity but that their spatial memory was intact. Based on these results, it is possible that the ApoE4 and hAβ-KI

combined with LPS are not risk factors for spatial memory deficits. There are other possibilities for these results, however, including that the LPS administration regime was not sufficiently intensive to produce a deficit, or that the age of the animals (6 months) was too young. It would be interesting to revisit these models at an older age to determine whether spatial memory was still intact. Further speculations along this line are discussed in the limitations and future directions section below.

5.1.3) Dendritic spine density decreased in J20 mice, APOE-KI + LPS mice, and mice with intra-hippocampal LPS:

Consistent with previous reports (Pozueta et al., 2013), I identified a significant decrease in spine density in the dorsal hippocampus of J20 animals at 6 months of age compared to age-matched controls (Experiment 1). In Experiment 2, however, there were no changes in spine density in the LPS treated wildtype animals compared to the sham controls, which again differs from published evidence. Similar to the failure to observe behavioural changes with this manipulation, the lack of effect on spine density could be a result of comparatively higher dosages of LPS used in these studies (Huifeng et al., 2020; Y. Wang et al., 2020). LPS injections of 2.5 mg/kg i.p. for two days resulted in a significant reduction in spine density, which was rescued by astragalus (anti-inflammatory drug) injections in mice (Huifeng et al., 2020). Similarly, seven continuous days of i.p. LPS injections of 0.75 mg/kg in C57BL6/J mice resulted in a marked decrease in spine density in the pyramidal neurons of CA1 region of the dorsal hippocampus (Tyrtyshnaia et al., 2020). There is one instance in which a lower dose of LPS (0.10 mg/kg) reducing spine density in hippocampal neurons, but only when induced in young mice – at P10 as observed by Wu et al., (2022). As mentioned with regards to LPS-induced memory deficits, each of these studies either employed a higher single dosage of LPS or daily

administrations of a lower dosage of LPS than the current study. Either of this could account for the fact that a low, weekly dose of LPS in the current study did not lead to dendritic spine loss. It is also worth considering the possibility that there are unpublished studies that may have failed to find an effect of systemic LPS on dendritic spines. Indeed, such an explanation could also apply to any of the inconsistencies between current results and published studies where I have failed to reject the null hypotheses. As there is beginning to be more of a push towards publishing null effects moving forward (and indeed, I will shortly be publishing the null effects contained in the current thesis), hopefully this situation will be rectified and the effects reported in the literature will be more reflective of the actual underlying effects of certain manipulations, whether they be positive or null.

Despite the failure to observe any effect of systemic LPS alone, I did find a significant reduction in the number of apical (but not basal) spines in the CA1 region of hippocampus in the ApoE4-KI cohort that received LPS, although mice with either risk factor alone showed no differences. This was of particular interest because apical dendrites are a part of the 'tri-synaptic input' (refer to Chapter 1 section 1.8.2) which is crucial to learning and memory in the hippocampal region. If translatable, the vulnerability of these apical dendritic spines to APOE4 + LPS could suggest that this combination might have particularly been detrimental for hippocampal-dependent learning memory (although perhaps excepting spatial memory, which was found to be intact here). Indeed, the most recent studies on AD patients show an association between ApoE4 and synapse loss in these patients (Forner et al., 2021).

However, how this result integrates with prior findings is unclear because literature reports for the spine density changes in only the 'ApoE4-KI' mice remain inconsistent.

While Dumanis et al., did not observe a reduction in hippocampal spines in their ApoE4-KI mice (2009), several other studies have reported reduced dendritic arborization and spine density in ApoE4 based mouse models (Jain et al., 2013; Taxier et al., 2022). Another study by Jain et.al., reported spine density differences in 19-21 months old mice in the basal dendrites of the CA1 region of the hippocampus (2013). Again, it is possible that these discrepancies could be arising from differences in the particular strain of model used in these studies as well as the differences in age. Regarding the lack of dendritic spine loss in hAβ-KI mice, it is possible that once again age could have been a factor here. A study by Baglietto et al., (2021) showed synaptic changes (i.e. changes in the presynaptic marker synapsin, and the postsynaptic marker post-synaptic density-95 [PSD-95] in hAβ-KI mice in the absence of LPS injections at around 18 months of age. Therefore, it is possible that at 6 months of age, the mice in the current study were simply too young to observe spine loss.

Although I did not observe any spine loss in Experiment 3, despite the increase in systemic LPS dose, I did observe a significant reduction in spine density in Experiment 4, 7 days after animals had received intrahippocampal injections of LPS. This result aligns well with previous studies in which intracerebroventricular (Ano et al., 2019; Milatovic et al., 2003) injections of LPS were shown to significantly decrease dendritic spine density irrespective of the age of animals used. This pronounced effect could result from the spike of pro-inflammatory cytokines that occurs immediately following LPS injections to the brain, as assessed by (Zhao et al., 2019), and highlights the robustness of directly targeting the region of interest.

5.1.4) Glial cell activation profile in our proposed sporadic AD animals:

The increase in the number of astrocytes in J20 animals in Experiment 1 is consistent with reports that these animal models express neuroinflammation in the hippocampus which starts becoming apparent around 6 months of age (Dekens et al., 2018; A. L. Wright et al., 2013). The failure to find any increase in microglia was more surprising, given the fact that prior studies have found increases in this model (Hong et al., 2016). One reason for this discrepancy could be that the marker we stained for (Iba1) is a more generalized marker of microglial/macrophages, whereas previous studies have used markers such as CD68 that are more specific for activated microglia (Hong et al., 2016; A. Wright et al., 2013).

LPS injections in mice have previously shown to activate microglia and astrocytes irrespective of the mode of injection. A 5mg/kg LPS injection in mice has shown to shift the microglia from surveillant stage to ameboid stage (activated stage) (Jin et al., 2014). Two continuous days of LPS injections of 5mg/kg i.p. was shown to shift GFAP and Iba1 interactions, which peaked at 4 days after injection and declined after 8 days of LPS injection, indicating a wave pattern of glial cell activation induced by LPS injections (Xingi et al., 2023). Continuous injections of low dosage LPS (0.25mg/kg i.p.) for seven days have shown to increase both microglial and astrocytic cell numbers significantly compared to saline counterparts (Ifuku et al., 2012). Two days of 0.5 mg/kg LPS i.p. injection in C57BL/6J mice showed a significant increase in microglia 3 days post injection, although this did not persist when assessed 4-8 days post injection (Jung et al., 2023). Once again, therefore, the different dosages and rates of administration could account for the differences between the current and previous studies in the abilities to detect neuroinflammation.

Aside from these factors, there are two other possible reasons why we did not observe an increase in glial cells in Experiment 2. First, as observed by Xingi et al., (2023) and Jung et al., (2023) glial cells follow a pattern of expression/activation that peaks at 2-4 days after injection and returns to their normal/surveillant stage in the following days. In Experiment 2, the tissue was collected about one week following the last injection, which could have meant that any increased activation was missed (as elaborated in the limitations section). Second, as observed by White et al., (2017) there could be a possibility that these animals developed tolerance, with repeated LPS injections in our study, which resulted in a failure to observe an obvious reactivity of glial cells.

In Experiment 2, neither of the ApoE4-KI or hAβ-KI models produced an increase in glial cell numbers relative to age-matched wildtype controls, either alone or when combined with LPS injections. The finding that 6-month-old hAβ-KI animals did not show neuroinflammation in the absence of LPS is consistent with previous reports, because Baglietto-Vargas et al., (2021) also reported no evidence of neuroinflammation in hAβ-KI who were less than 18 months of age. Additionally, LPS did not by itself induce neuroinflammation in wildtype controls. This suggests that these manipulations may not have been sufficient to produce a neuroinflammatory response, or that there was a response but that it was highly variable and/or below the threshold for detection. Again, this was possibly due to the low dose of LPS used, a conclusion that is supported by the fact that increasing the dose in Experiments 3 and 4 was sufficient to produce evidence of dorsal hippocampal neuroinflammation.

The fact that the ApoE4 + LPS group did not experience a neuroinflammatory response, raises a challenge in determining why this group might have experienced a loss of dendritic spines. Because mice carrying just the 'ApoE4' factor did not show any

differences in spine density, it appears that the addition of LPS was important for dendritic spine loss, yet the addition of LPS did not significantly induce neuroinflammation in the dorsal hippocampus. One possibility is that, due to the systemic nature of LPS injections in this experiment, mice may have experienced neuroinflammation in other brain regions connected to hippocampus, and the reduction in these connections affected the number of spines. One candidate region for this could be the entorhinal cortex, which serves as a primary interface between hippocampus and other brain regions (Garcia & Buffalo, 2020; Witter et al., 2017).

Nevertheless, this null effect is surprising, because there is evidence for glial cell activation following LPS injections in ApoE4 animals. For instance, a single i.c.v injection of 1000ng LPS in ApoE4 animals was shown to increase microglia and astrocyte expression 72 hours post injection compared to ApoE3 and ApoE2 animals (Zhu et al., 2012). A single i.p. injection of 5 mg/kg LPS in ApoE4 animals was shown to increase microglial expression pattern, with a specific gene cluster increase in metabolic pathways related to oxidation-phosphorylation and glycolysis (Lee et al., 2023). A tail vein injection of 40 μg/kg was also seen to result in an increase of inflammatory cytokines in ApoE4 mice compared to ApoE3 mice, an effect which lasted 3 hours post injection (Lynch et al., 2003). Although current results are surprising in light of these studies, there are obvious differences with the dosage and mode of injections which could be the reason for not witnessing similar effects in our ApoE4-KI animals.

5.1.5) Null effects could be reflective of population effects:

In the sections above, I have given several reasons why I may have observed null effects in several of my experiments, and I give more below. These generally relate to differences in the features of the mice studied, and experimental parameters that could be altered.

There is another consideration, however, which is that the null effects I observed here are in fact reflective of the broader effects one might see in the population. For instance, 'ApoE4' is just one of the many risk factors of Alzheimer's. Just being the biggest risk factor of AD alone cannot guarantee a development of disease phenotype in rodent models, as human sporadic AD individuals harbour more than just one risk factor. Furthermore, not all the individuals who carry ApoE4 allele develop sporadic AD; only 65% of people develop sporadic Alzheimer's which leaves 35% of people unaffected. This could be the very reason for not witnessing profound changes with just the ApoE4 mice in our experiments; perhaps the majority animals in my study by chance might have fallen into the 35% of those not developing the disease. Likewise, the phenotype of the hAβ-KI model is broadly unknown due to very few studies on it. Moreover, it is a model of humans who sporadically develop amyloid plaques, and little is known about their phenotype as well, particularly in the absence of any other risk factors. Indeed, there are multiple reports of individuals who express amyloid plaques in their brain but appear cognitively normal (Mormino & Papp, 2018). Therefore, it is just as possible that humans and mice who sporadically develop plaques in the absence of multiple other risk factors do not express any of the behavioural or cellular changes I was looking for.

To account for these discrepancies, a study by Neuner et al., have described a new and reproducible set of AD mouse models: the AD-BXD models with a focus on reproducing the genetic diversity observed in human AD cases. These models were shown to display high levels of overlap with human AD at genetic, phenotypic and transcriptional levels. Future studies could consider using AD-BXD model to explore different aspects of cognitive-behavioural alterations in human AD cases along with potential drug treatments (Neuner et al., 2019). This, combined with a cellular level understanding of genetic factors i.e., cellular dissection of polygenicity (CDiP), as described in this 2023

paper (Kondo et al., 2023), would enable gaining better understanding of the disease phenotype and provide potential treatment platforms for future AD research.

5.1.6) Limitations and future directions of Chapter 3:

Overall, the results from the Chapter 3 of this thesis suggested that neither of the genetic factors (ApoE4 or hAβ) were sufficient – either alone or in conjunction with systemic injections of LPS – to reproduce a meaningful model of sporadic AD. With regards to the behaviour experiments, the fact that the animals underwent more than one behaviour test and the order of the test might be a concern. This was discussed in a recent study which compared animals that underwent a series of behaviour experiments and animals which were naïve (not tested in such a series). There were only minor effects of tested animals compared to naïve animals; for example in rotarod and hot-plate behaviours, tested animals were less active than the naïve animals (McIlwain et al., 2001). On the other hand, spatial memory test like Morris water maze performance remained unchanged between these two groups. In the same study, they looked for whether the series in which the animals were tested affected their performance and observed that the order of the behavioural experiments had minimal effect on the animal's performance on different behaviours. Additionally, this study also suggested that if the animals are to be used for such continuous behaviour experiments, it is better to start with the least invasive tests followed by invasive test later (example of an invasive test, foot shock)(McIlwain et al., 2001).

In our study, we performed Open field test first before Barnes maze test. Although it might be possible that animals might have carried over some anxiety from open field test to Barnes maze, this remained the same for all groups, thereby ruling out this factor on the results we observed. Moreover, the mice were given 5 days of acquisition training for

Barnes maze test during which time, any differences that the animals started with were faded by the end of the training days as shown in the respective Barnes maze results in Experiment 1 and 2. Since the above mentioned study clearly reported that doing a series of experiments do not affect the spatial memory performance of mice (which is similar to what we checked in our study) and our study did not have any invasive behaviour tests, it is unlikely that our animals would have been affect by either the 'variety of behaviour' factor or the 'order in which animals were tested' factor.

As noted in the sections above, the low dosage of LPS injections used here relative to previous studies, as well as the relatively younger age of the animals (6 months here versus 9-18 months in prior studies) could well account for many of these differences. In addition to these factors, however, there are other potential limitations of the current study that could be addressed in future studies to comprehensively determine the risk of each of these factors – individually and together – which I will detail in the following sections.

5.1.6a) Age factor and differences in the strain of ApoE4 animals used:

It is well known that the sporadic form of Alzheimer's disease has a late onset of 60 years and after (Rabinovici, 2019). However, since preclinical AD research administers familial AD models, these models are engineered to show robust phenotype within a short period of time to be able to study them effectively. For instance, the J20 animals start showing memory deficits as early as 3 months age (Flores et al., 2018; A. L. Wright et al., 2013) and a popular familial AD model, the 3xtg-AD shows memory impairments around 6 months of age (Roda et al., 2020). Even the most familiar non-sporadic AD model, SAMP8 (Senescence Accelerated Mouse), is developed with aging as a prominent factor and shows early memory deficits (Morley et al., 2012). In most of these models, there are

genetic manipulations specifically performed to overproduce certain proteins that are associated with Alzheimer's disease, therefore resulting in an obvious phenotype. Although our experiments displayed how (relatively) young animals with these combinations would perform, it would be ideal to look for memory deficits in these animals at a comparatively later age to see if they start showing AD like symptoms.

Another reason why the current study may have differed from prior studies in its ability to detect changes between APOE4-KI mice and wildtype controls could be due to the particular strain of APOE4-KI mice used. The majority of studies in the literature have been carried out with ApoE4-Targeted Replacement mice obtained from Taconic, developed in the year 1999 (Leung et al., 2012), whereas the ApoE4-KI mice we used in our study were obtained from Jackson Laboratory and are relatively new (generated in 2018) (consortium, 2018). Although these two mouse strains have almost identical modifications to the ApoE gene, there are some subtle differences in the developmental process which could have resulted in the differential effects we see in our results. This raises the question as to the reliability of these results and brings to light one of the biggest challenges with translatability of AD preclinical mouse models. That is, if two almost identical strains of mice are found to have different behavioural and cellular changes, then it is difficult to see how well any findings from these strains might translate to humans. One way in which this could be addressed in future research is by including a screening step with more than one (and preferably several) of the best preclinical models of AD used to test potential drugs before proceeding to clinical trials.

5.1.6b) ApoE3-KI mice as controls:

Previous studies conducted on ApoE4 animals have predominantly employed ApoE3 animals as controls rather than WT animals. In the current study, because I used both

ApoE4-KI and hAβ-KI mice in the same experiment, I used a wildtype control which was the background for generating these mice strains so that it could serve as a common control for both these mouse models. This could have hindered my ability to observe significant differences. For example, in the study by Rodriguez et.al., (2013) young ApoE4 mice (6 months) were compared against ApoE3 animals to reveal a significant reduction in spatial learning, but another study reported that young ApoE4 mice showed intact spatial memory when compared against wildtype animals, (Yin et al., 2011). This contrast could arise from the similarities that have been reported in the literature with regards to endogenous murine ApoE in the wildtype mice and humanized ApoE4 in the targeted replacement/knock-in mice. It can be seen from the literature that the lipid binding properties of murine ApoE are more similar to human ApoE4 than ApoE3 (Nguyen et al., 2014; Rajavashisth et al., 1985) and that mouse ApoE is more amyloidogenic than ApoE3 or E2 (Liao et al., 2015). Additionally, animals carrying murine ApoE performed similar to that of human ApoE4 transgenic mice in Y-maze active avoidance task (Bour et al., 2008). One other reason why future studies may wish to compare ApoE4 mice with ApoE3 and/or ApoE2 mice is that this is more reflective of human cases. Although mice do not carry different isoforms of APOE, humans carry three isoforms in which ApoE2 is considered protective, E3 to be neutral and E4 to be disease causing. Therefore, comparison of mice expressing these alleles should give us better insights on the actual mechanisms happening in AD.

5.1.6c) Quantification of inflammatory markers:

Although it would be straightforward to conclude that the LPS did not induce neuroinflammation in animals in Experiment 2, I cannot rule out the fact that LPS induced neuroinflammation was in the initial stages and required more powerful quantification

techniques to bring out changes. For example, in addition to counting the total cell numbers, adapting a more detailed method of quantification including morphological analysis like dendritic branching, measuring cell soma intensity could have made it possible to reveal any subtle changes occurring at the cellular level. Insights for this could be taken from Baglietto et al.,'s (2021) study where they found no alterations in the number of astrocytes at 22 months old hAβ-KI mice, but did observe morphological changes in these astrocytes at the same time point .

There are other possible reasons for the absence in glial cell activation in Experiment 2 upon LPS treatment. For instance, the interval between our last LPS administration and tissue collection in our study is comparatively longer (approximately two weeks) than other studies in the literature. Moreover, it is possible that I would have observed differences in other measures that were not tested here. For instance, many studies measure neuroinflammation in LPS treated animals by quantifying the serum and brain cytokine levels (Liu et al., 2017; Zhao et al., 2019). It is possible that these measures are more sensitive and would have shown changes in the current study where immunohistochemical staining for glial cell expression did not.

5.1.6d) Combining additional risk factors of sporadic AD:

As mentioned in the introduction of Chapter 3 of this thesis, there are multiple risk factors associated with AD, most of which fall under the category of lifestyle risk factors. For example high cholesterol levels in the mid-life and late life has been linked to the risk of developing AD (Popp et al., 2013). A more recent study states the link between diabetes and AD and the role of Amyloid beta in this scenario (Stanciu et al., 2020). In addition to these, heavy metal exposures like exposure to lead, manganese and cadmium has been exclusively linked to AD pathologies (K. M. Bakulski et al., 2020). Therefore, it would be

ideal to start thinking about combining several such factors in preclinical animal models to produce better sporadic AD like phenotypes.

5.2) Theoretical and clinical implications of altered goal-directed action control in female mice and altered Pavlovian approach behaviour in male mice with hippocampal neuroinflammation

The results of Chapter 3 demonstrated that out of all the potential sporadic models tested (systemic LPS injection, ApoE4-KI transgenic mice, hAβ-KI transgenic mice, ApoE4-KI + LPS, hAβ-KI + LPS, and intra-hippocampal LPS), intrahippocampal LPS was most successful in producing both i) a neuroinflammatory response, as demonstrated by the increase in markers for both astrocytes (GFAP) and microglia (IBA1), and ii) a reduction in dendritic spines in the dorsal hippocampus. On this basis, I then next decided to investigate the consequences of intrahippocampal LPS on behaviour. In particular, I investigated whether intrahippocampal LPS would alter goal-directed action control which, as discussed in Chapter 2, is a core feature of Alzheimer diagnosis that has been overlooked in preclinical models. I also once again investigated whether this manipulation altered locomotor activity and/or anxiety in open field tests, but did not repeat the Barnes maze tests, as spatial memory deficits using this manipulation have been well-established (Hou et al., 2014). The results of this investigation are reported in Chapter 4. In contrast to the results reported in Chapter 3, in which the performance and neuropathological features assessed did not differ between males and females, when assessing goal-directed action there were clear sex differences. I therefore assessed the consequences of hippocampal neuroinflammation in female and male mice separately in Experiments 5 and 6 respectively.

5.2.1) Hippocampal neuroinflammation accelerated goal-directed action control in female mice:

The first major result reported in Chapter 4 was the finding that, in female wildtype mice, hippocampal neuroinflammation accelerated goal-directed action control. That is, devaluation performance was intact for LPS-injected mice but not Shams after 4 days of lever press training, but after 8 days these differences disappeared. This specific pattern of results: an initial facilitation in performance that did not persist, is the reason why I have characterized hippocampal neuroinflammation as accelerating rather than facilitating goal-directed action control in these mice. In other words, although the shams were eventually able to demonstrate evidence of goal-directed action control, the LPS-injected mice were simply able to do so sooner. Importantly, these differences were not a result of hippocampal neuroinflammation simply increasing the locomotor activity or altering anxiety-like behaviours, because neither was affected in these mice when they were tested for open field performance.

This was not the expected result because of two major reasons. First, Marquez et al., showed LPS injected into a different brain region, the substantia nigra (SN), impaired rather than accelerated goal-directed actions in rats (2020). Second, as mentioned in previous chapters, Dhungana et al., (2023) reported initial impairments in goal-directed actions in a J20 familial AD model who experienced neuroinflammation in their dorsal hippocampus. Moreover, this neuroinflammation appeared to be related to the initial impairment in goal-directed action, because microglial reactivity (Iba1) in the hippocampus was negatively correlated with devaluation performance.

There are several differences between the current study and these previous studies that could underlie these differences in results. For example, the current study differed from

Marquez et al.,'s (2020) in the region of interest, and neuroinflammation in the substantia nigra can have a very distinct profile compared to inflammation in hippocampus, as well as exhibiting differences in its broader neural circuitry. For instance, the posterior dorsomedial striatum (pDMS) which has a central role in goal-directed actions, send direct outputs to SN (Agster & Burwell, 2013; Peak et al., 2019), but dorsal hippocampus does not, suggesting that neuroinflammation in pDMS and its efferents might impair rather than accelerate goal-directed action.

The most important difference between the current study and that of Dhungana et al., was the age and strain of animals used. Dhungana et al.,'s study featured J20 mice who were 36 and 52 weeks old, whereas I used mice that were 10 to 12 weeks old. It is well known that animals of different age express different cellular and cognitive profiles (detailed discussion in the previous sections) such that neuroinflammation in differently aged mice is likely to have different consequences for behaviour. Future studies should test this directly. Another factor to consider is that the neuropathological features expressed by J20 mice, including neuroinflammation, are not confined to the hippocampus but extend to other brain regions (Shibly et al., 2022) which could have also impacted behaviour in a different manner. A similar situation is observed in AD patients, where although the hippocampus is one of the first regions that becomes susceptible to neuropathological changes (Planche et al., 2022), it later spreads to other regions as the disease progresses, suggesting that damage to these other regions might underlie alterations in goal-directed activities of daily living.

One important difference between the current study and that of Dhungana et al is that J20 animals experience neuroinflammation that persists from 2 months of age (Wright et al., 2013) whereas neuroinflammation was induced in the current study only one week

before the start of behavioural training. Thus, at the time of testing, even the youngest 9-month-old animals in the J20 study would have experienced neuroinflammation for many months whereas animals in the current study would have experienced it for less than one month. This is critical because sustained neuroinflammation in J20 models can induce permanent changes in the brain such as neuronal death, which we did not observe in our model (refer to figures 4.13, 4.24).

The implications of this result are interesting. In one sense, hippocampal neuroinflammation could be interpreted as being beneficial in the short term, something that leads to an immediate improvement in goal-directed action control. If translatable, this could function such that if an individual has experienced any of the common causes of hippocampal neuroinflammation, such as stress, injury, or disease, it might be useful for them to be able to exert goal-directed control sooner, in order to seek out a method by which they can alleviate the adverse condition. By contrast, sustained hippocampal neuroinflammation becomes detrimental and impairs the ability to exert goal-directed control. Another way in which to interpret these findings is that the 'acceleration' I observed is in fact abnormal, not beneficial, as increased goal-directed activity can prove to be harmful in certain conditions. For instance, excessive goal-directed activity has been identified in bipolar disorders during 'mania', when patients seem to be extremely agitated, show sleep disturbances, set high ambitious standards and are self-critical in trying to achieve what is considered a far-fetched goal. This is usually followed by a phase of harsh self-judgement when such goals are not achieved (Dailey & Saadabadi, 2023; Dempsey et al., 2022).

Overall, relevance of the accelerated goal-directed action control to Alzheimer's remains hazy at this point. Future studies may wish to induce neuroinflammation for a much

longer period than that achieved here, potentially leading to neuronal death, to be relevant to AD.

5.2.2) Hippocampal neuroinflammation facilitated Pavlovian approach behaviour in male mice.

In Experiment 6, male mice with LPS-induced neuroinflammation in the hippocampus showed intact goal-directed action control, on both the 4-Day test and the 8-Day tests. Hippocampal neuroinflammation was not without a behavioural effect in these mice, however, because Pavlovian approach behaviour (i.e. entries into the food magazine) was facilitated in LPS-injected mice. Unlike the alteration in goal-directed action control observed in female mice in Experiment 5, the effect on Pavlovian approach persisted throughout the experiment as it was observed throughout the training days 1-4 and 5-8 and was present on the 8-Day test. Similar to the females, however, this change in behaviour was not a result of changes in locomotor activity or anxiety, because I detected no such differences between LPS animals and Shams on the open field test.

Nevertheless, the facilitation in magazine entries was not predicted for these animals, who were expected to show an impairment in initial goal-directed action control in line with the results reported by Dhungana et al., (2023). Again, the reason for this difference could be the same as that mentioned above for the females; differences in the age of mice used and alterations in the neuroinflammation profile in these animals. One reason why the male mice may not have showed an acceleration of goal-directed action similar to the female mice in Experiment 5 could be because of a ceiling effect. That is, sham females in Experiment 5 did not yet show an intact devaluation effect on the 4-Day test, whereas Sham males in Experiment 6 did which may have left little room to detect any improvement by LPS induced hippocampal neuroinflammation over and above the

control effect. The fact that the devaluation effect does appear to improve further by the 8-Day test for both groups however, (i.e. the difference in lever pressing on the valued relative to the devalued lever is larger on the 8-Day relative to the 4-Day test for both groups), suggests that there was room for improvement and a ceiling effect is unlikely.

Although it was not the target behaviour in the current study, the observed facilitation of Pavlovian approach by hippocampal neuroinflammation in male mice is interesting and deserves more exploration. This kind of behaviour was described by (Harris et al., 2013) albeit using a slightly different paradigm. Specifically, they tested rats on a conditioned magazine approach (Pavlovian approach) paradigm where the rats were presented with a Conditioned Stimulus (CS, such as a tone), which was followed by an Unconditioned Stimuli (US, which was food). By altering certain parameters of this paradigm, they confirmed that rats approaching the magazine during the presence of CS is performing this action in the expectation of receiving a food soon after. Thus, it can be assumed that the LPS mice in Experiment 6 were also making more entries to the magazine to check for the delivery of food, particularly on test when food outcomes were not delivered so that these mice could only rely on their memory of food being delivered there, and not on the sight or smell of the food itself. Although interesting, why exactly hippocampal inflammation might induce a facilitation in Pavlovian approach behaviour, and why specifically in males, is unclear at this point.

Just as the acceleration of goal-directed control in female mice could be construed as abnormal and disadvantageous, so could the facilitation of Pavlovian approach behaviour in male mice be viewed as an impairment. This is because increased sensitivity to Pavlovian cues (here the cues are the sight/smell of the food magazine) have been shown to promote unhealthy behaviours in populations that experience hippocampal

neuroinflammation. For example, an early study by Monti and colleagues found that college students who are heavy drinkers, when exposed to an alcohol cue, were more inclined to choose an alcoholic drink (when given a choice) (Monti et al., 1987). Another study that compared males and females reported that alcohol consumption was higher in individuals who were shown pictures of drinking compared to controls and, consistent with current findings, this effect was specific to males, not the females (Koordeman et al., 2011).

Once again, how this relates to AD is unclear. However, one study has found that Alzheimer's patients are actually benefited by cues that would trigger the associated memory, and enable them to perform in a goal-directed manner (Davis & Weisbeck, 2016), suggesting that an enhancement in this ability could potentially compensate for goal-directed deficits. Nevertheless, it would be useful for future studies to induce neuroinflammation for a longer period than that studied here and assess goal-directed action/Pavlovian approach at an older age for the employed methodologies to have more relevance to AD.

5.2.3) Significant changes in glial and neuronal cell activation patterns:

In both Experiments 5 and 6, there was a significant reactivity of microglial and astrocyte cells, as seen from the increase in number Iba1 positive cells and an increased intensity of GFAP positive cells. Neither experiment found any difference in the number of neurons, suggesting that any behavioural differences were unlikely to be a result of neuronal death (or altered neurogenesis).

In females, both the Iba1 counts and intensity and the GFAP intensity (Figure 4.9, 4.11) positively correlated with the devaluation score that was calculated based on performance on the 4-Day devaluation test. There were no significant correlations on the

8-Day test for females and no significant correlations with any behavioural measures on either test in male mice. Therefore, increased microglia and astrocyte cell number/intensity was specifically associated with better goal-directed action control on the one test in which hippocampal neuroinflammation altered performance: the 4-Day test in female mice in Experiment 5. This suggests that it is possible that the reactivity of microglia and astrocytes in this region caused the animals to have better action control.

This conclusion was partially supported by the attempt to replicate the result by chemogenetically activating astrocytes in the dorsal hippocampus. Results from the 4-Day test of this experiments showed that only the animals which had astrocytes activated in the dorsal hippocampus showed intact goal-directed action, like what was observed in the female animals. However, these results should be treated with caution because firstly, the DREADDs expression in these animals were not limited to astrocytes only (Figure 4.26), as I did find some expression in the neurons. Second, the animals did not show a sex specific effect as observed in my LPS experiments, therefore I combined results from males and females to be reported in this thesis. Third, the statistical support for this observation was only partial, because there was no group x devaluation interaction, indicating that the differential pressing on levers was not different between groups. Therefore, the result of this experiment still leaves a big question unanswered – how does hippocampal neuroinflammation differentially affect males and females with respect to goal-directed actions.

I further checked for c-Fos activation and its co-localization with neurons in the dorsal hippocampus. This was important because, although the proliferation of microglia and astrocytes appeared to be related to the acceleration of goal-directed action control (in females), these glial cells exhibit only local processes and cannot influence neurons in the

broader circuit of goal-directed action control. Moreover, the dorsal hippocampus cannot achieve goal-directed action control in isolation and must contact the broader neuronal circuit associated with this behaviour. The only way it can do so is through neuronal connections, suggesting that the reactivity of glia must have altered the activity of neurons to accelerate goal-directed action control. Indeed, there is evidence that glia can modulate neuronal activity as measured by c-Fos. For instance, a study by Liu et al., showed that selective inhibition of astrocytes reduced c-Fos activity in the CA1 region of hippocampus (Adi et al., 2019; S. Liu et al., 2022). Glial modulation also appears to have increased neuronal activity in the current study because there was a significant increase in c-Fos/NeuN signals in the DG region of dorsal hippocampus in LPS treated females.

The data from male mice in Experiment 6 was quite different from the female data because rather than being increased, the % co-localization area of c-Fos with NeuN showed a trend towards decrease in the LPS group. It is tempting to speculate that this decrease might underlie the failure to accelerate goal-directed action control in LPS treated males. The trend towards a decrease in neuronal activity as a result of neuroinflammation in male mice aligns with results from a recent study (Gan et al., 2022) that employed intraperitoneal LPS injections in male C57BL6/J mice that were 12 weeks old. These mice were the same strain and close to the age of the mice I used in Experiment 6. Gan et al., also reported a marked decrease in neuronal activation measured by reduced c-Fos expression in the dorsal hippocampus. In addition, they found no abnormal locomotor activity or anxiety in open field test, which also reflects the results of Experiment 6. Because the only behavioural change observed in male mice in the current study was the facilitation of Pavlovian approach behaviour, it is further tempting to speculate that the trend towards neuronal inhibition in these mice was what underpinned this change.

5.2.4) The broader neural circuit of goal-directed action:

As discussed in Chapter-2, unlike other brain structures such as orbitofrontal cortex, posterior dorsomedial striatum, and basolateral amygdala, which have a sustained role in goal-directed action control, the role of the dorsal hippocampus in goal-directed action is temporally transient. This suggests that any alterations to goal-directed action control that occur because of altered hippocampal function must be achieved through connections between hippocampus and these other structures within the goal-directed action control circuit. The question remains as to which connections have been affected in Experiment 5 to produce the acceleration of goal-directed action control.

A detailed polysynaptic study by Wenquin et al., (2021) gives several possibilities. Specifically, they depicted a series of indirect connections from the dorsal and ventral hippocampus to the dorsal striatum and nucleus accumbens core through mediatory structures such as dorsal subiculum, lateral septum, entorhinal cortex and prefrontal cortex. These connections are one way in which heightened neuronal activity in the dorsal hippocampus could send messages to these structures to accelerate goal-directed learning.

As mentioned in the discussion, another connection via which altered activity within the hippocampus might affect goal-directed action control is through the orbitofrontal cortex. The dorsal hippocampus is directly connected with the lateral OFC and indirectly with the medial OFC, both of which have been reported to play a role in goal-directed action selection (Bradfield et al., 2015; Parkes et al., 2020). Moreover, Wang et al, have shown that the OFC and hippocampus interact to make inferences that are critical for goal-directed action selection (2020). In the current study, therefore, as hippocampal

neuroinflammation appeared to increase neuronal activity, this could have strengthened the hippocampal-OFC connections to accelerate goal-directed action control.

5.2.5) Sex differences in behaviour: potential reasons and implications:

Experiments 5 and 6 identified clear differences in the ways in which male and female mice responded to hippocampal neuroinflammation, both regarding their behaviour and in the cellular changes identified. The behavioural differences in particular are consistent with a number of other studies that have identified sex differences in operant and Pavlovian conditioning. For instance, van Haaren et al., (1990) exposed rats to aversive stimuli such as foot shock, and found that males took some time to react whereas females reacted instantly to the same stimuli. In a different study, female rats were shown to be more active than males in open field and running wheels tasks (Beatty & Fessler, 1976). In humans, men and women have performed strikingly differently in the same tasks involving same processing elements. For instance, men were showed to perform considerably better in spatial memory related tests whereas women were better at tests involving semantic memory (Andreano & Cahill, 2009; Koss & Frick, 2017). Therefore, the identification of sex differences in the current study is not entirely surprising.

In addition, there are multiple studies demonstrating sex differences in hippocampally-dependent tasks specifically. For example, a recent study by Le et al., (2022) described how there is enhanced hippocampal LTP and hippocampally-dependent learning in prepubescent female mice which are switched as the animals become adults. On the other hand, the magnitude of LTP for male mice reached adult levels in roughly four weeks after birth, even before attaining puberty (Baudry et al., 1981; Figurov et al., 1996; Muller et al., 1989). The authors therefore suggested that fluctuations in the level of oestrogen during the transition phase to puberty made female animals less effective in learning

hippocampal associated tasks compared to males. Evidence for this can further be obtained from another study (W. Wang et al., 2018) which demonstrated the particular requirement of high oestrogen levels to successfully achieve LTP in hippocampus of the female rodents. With regards the current study, if hippocampal LTP underlies goal-directed action selection, then this could explain why our female sham animals at 4-Day devaluation tests were slower in acquiring the task than the male shams, as the age of females in Experiment 5 (which was approx. 12 weeks at the time of testing) was similar to that used in the study by Wang et al., (2-4 months old). These studies provide little insight, however, into why hippocampal neuroinflammation in male mice led to a facilitation in Pavlovian approach behaviour, although, as noted in the discussion for Chapter 4, this may not be a sex-specific effect and relatively higher levels of magazine entries in Sham females may have masked any potential increase as a result of hippocampal neuroinflammation.

5.2.6) Influence of sex hormones in the hippocampus:

Next, it is worth considering what might have caused the sex differences in behaviour and cellular expression. One key candidate is differential expression of hormones. It is now well known that both sexes carry androgen and oestrogen and the differential expression of these two hormones seem to contribute to the control of various signalling cascades within the brain (Knouff et al., 1999). Oestrogen is produced by both neurons and astrocytes in the brain and the level of oestrogen in female brain increases during puberty, fluctuates throughout menstrual cycle, and sharply decreases after menopause. As implied in the previous section, these fluctuations may well have contributed to the sex differences in the current study. In addition to this, the levels of oestrogen are reported to increase following an inflammation process, to facilitate brain repair (Gillies & McArthur,

2010; Jing et al., 2020). Therefore, if neuroinflammation generally reduces neuronal activity, which I observed some evidence for in male mice, it is possible that higher levels of oestrogen in female mice compensated and prevented this decrease. Nevertheless, this does not account for why neuronal activity was increased in females.

Oestrogen also plays an important role in increasing dendritic spine density and synaptic plasticity especially in the hippocampus. By performing hippocampal slice electrophysiology, Wang et al., (2018) showed that, in females, oestrogen receptors are highly expressed in the synapses and requires excessive oestrogen to activate these receptors to facilitate LTP formation. On the other hand, MacLusky et al., (2006) have shown that androgens mediate hippocampal synaptic plasticity, via a mechanism that is oestrogen independent. A very recent study (Chen et al., 2022) examined the synaptosome fraction for PSD-95, and found that there was an increased expression of PSD-95 mRNA after treatment with androgen, proving the neuroprotective effect of androgens on the synaptic plasticity. Moreover, stress has been shown to alter spine formation in this hippocampus in sex-dependent manner. For instance, the acute stress of intermittent tail shocks was shown to inhibit oestrogen dependent spine formation in the CA1 region of the hippocampus of female animals while showing the opposite effect enhancing spine formation in males (Shors et al., 2001).

Thus, it is possible in the current experiments (Experiments 5 and 6) that spine density was also differentially altered by LPS injection and that this underscored the behavioural differences. Unfortunately, because I could not process the tissue for both glial/neuronal cell markers and dendritic spine density (due to these techniques requiring different tissue processing methods) I cannot provide a definitive answer to this question. In addition, although I did detect a reduction in dendritic spine density with

intrahippocampal LPS injections in Experiment 4, the sample size in this experiment was too small to permit comparison between mice of different sexes.

5.2.8) Sex differences in Alzheimer's disease:

One clear result from the current study is that hippocampal neuroinflammation has different consequences for both behaviour and cellular changes in female and male mice. If translatable, this would imply that in humans, hippocampal neuroinflammation also has differential effects on behaviour and cellular mechanisms. The fact that Alzheimer's disease affects more females than males could support the notion that females are somehow particularly susceptible to neuroinflammation among other risk factors. Indeed, it is well-known that two-thirds of the people who develop AD are women, and disease progression in women has been twice as fast as men once diagnosed with MCI (Sohn et al., 2018). Notably, other conditions involving hippocampal neuroinflammation, such as major depressive disorder, are also twice as prevalent in females as in males (Albert, 2015).

As seen in the previous section, there are numerous evidence suggesting cellular level changes in male and female hippocampus with respect to sex hormones. These changes might translate into bigger behavioural differences when it comes to neurological diseases. Interestingly, there has been a term 'oestrogen hypothesis' which argues that the risk of AD in women is highly correlated with the decrease in oestrogen levels post menopause (since AD is predominantly late onset) (Rahman et al., 2019). Since oestrogen has prominent positive neuroprotective effects, a sharp decrease in brain after menopause is speculated to make the brain prone damage (Kadlecova et al., 2023; Zárate et al., 2017).

There have been some detailed studies conducted with microglia from males and females in terms of structure and expression of genes and developmental processes. It has been reported that during aging, where sex hormone levels are markedly decreased, female microglia shows more expression of inflammatory-related genes compared to males (Mangold et al., 2017). Similarly, ovariectomized rats showed increased pro-inflammatory cytokine profiles (Sárvári et al., 2012). In contrast binding of oestrogens to microglia through oestrogen receptors have been shown to be neuroprotective (Loiola et al., 2019) in cell-culture experiments. With respect to amyloid-beta, in AD patients, more amyloid plaque burden was observed in female AD patients compared to the males (Kadlecova et al., 2023). In line with this, ovariectomized female AD mice were shown to accelerate the number of activated microglia, which worsens the pathology but does not effectively clear Aβ plaques and this was reversed by oestrogen treatment in these animals (Vegeto et al., 2006). Collectively, these studies highlight the importance of oestrogen and why a decrease in its levels can be a reason behind the observed disease severity in females.

Therefore, given the sex differences detected in the current study together with those found in prior studies, as well as the fact that AD is more prevalent in females, highlights not only the necessity of including female animals in preclinical AD studies, but suggests that perhaps such preclinical studies should investigate males and females separately.

5.2.7) Limitations and future directions:

5.2.7a) Potential alterations to the inflammation paradigm:

As discussed in previous sections, although neuroinflammation in Experiment 4 did reflect AD pathology in the sense that it caused an increase in glial cell activation as well as a decrease in dendritic spine density, it is possible that the injections in Experiments

4-6 induced acute rather than chronic neuroinflammation. (Parra et al.) categorizes chronic neuroinflammation as something that lasts for months. Other studies have induced chronic neuroinflammation through continuous LPS injections for 10 weeks (Ostos et al., 2002) or slow release pellets of LPS (Droke et al., 2007). In the current study, however, my attempt to replicate chronic neuroinflammation by giving LPS over 17 weeks in Experiment 2 and 4-6 weeks in Experiment 3 was not successful in inducing glial cell activation (Experiment 2) or dendritic spine loss (Experiments 2-3). With the intrahippocampal LPS injections given in Experiments 5 and 6, glial activation was still present even when tissue was assessed approximately 1 month after a single injection, which could potentially be considered a chronic neuroinflammation paradigm. However, behavioural experiments started 1 week after LPS surgery, which according to Parra et al., would be considered the late stage of acute or early stage of sub-acute phase of neuroinflammation. Therefore, future studies may wish to leave animals for a month or two after intrahippocampal LPS injections before performing behavioural experiments. This could help translate the observed results to real-world disease conditions.

Another consideration for future studies might be to induce neuroinflammation in more than just one region of the brain. For instance, LPS injections can still be made to hippocampus, but along with another region of the brain that is already known to play a prominent role in goal-directed action pathway like medial prefrontal cortex, and posterior dorsomedial striatum. This would serve two purposes i) to understand how neuroinflammation in the hippocampus plays a role in conjunction with other regions to influence goal-directed action, and ii) to mimic real-life pathological conditions where neuroinflammation is not restricted to just the hippocampus.

5.2.7b) A deeper insight into the cellular mechanisms:

In the discussion of Chapter 4 I discussed a partially successful experiment in which I chemogenetically activated astrocytes (and neurons) in the dorsal hippocampus to accelerate goal-directed action control. One reasons why this experiment may only have been partially successful, is because the analysis of glial cell expression revealed that both astrocyte and microglial reactivity was positively associated with goal-directed action, specifically in females, specifically for the test on which goal-directed actions were accelerated. Therefore, the observed acceleration may have required the reactivity of both astrocytes and microglia, which was not captured in the chemogenetic experiment. It might be useful for future studies to chemogenetically (or otherwise) activate both astrocytes and microglia in the same animal to determine if this can successfully replicate the results of Experiment 5.

Another technique that future studies may wish to use in order to gain further insights into the roles of microglia and astrocytes in the dorsal hippocampus in goal-directed action control (and potentially Pavlovian approach) is that of fibre photometry. Unlike neurons, microglia and astrocytes do not communicate using electrical signals, but they do express calcium transients. Fibre photometry records calcium signalling, and AAVs with the correct promoter (e.g. Iba1 or GFAP or something similar) could be used to specifically record the calcium signals of microglia and astrocytes during behaviour in real time.

Finally, given the role of oestrogen and androgen in learning and memory behaviour, future studies may wish to explore this further. One way in which they could do so would be by selecting specific sets of animals according to their menopause time, and each group

given LPS injections to understand how neuroinflammation interacts with sex hormones at different stages of menopause to bring about changes in goal-directed action.

5.2.8) Conclusion:

Overall, the experiments reported in the current thesis did not produce a singular model that was a comprehensive preclinical recapitulation of the sporadic form of Alzheimer's. The first half of this study aimed to create such a model by combining genetic risk factors with neuroinflammation. However, whether investigated individually or separately, none of these models completely replicated the sporadic Alzheimer's phenotype. Intrahippocampal LPS injections were more successful in producing evidence of neuroinflammation and dendritic spine loss such that, in the second half of the thesis, I investigated the consequences of such injections for goal-directed action with a view to improving behavioural translatability. Although these experiments revealed interesting behavioural differences, with hippocampal neuroinflammation accelerating goal-directed action control in female mice and facilitating Pavlovian approach in male mice, these differences are not reflective of the cognitive-behavioural deficits observed in individuals with AD. Potential reasons why I observed this pattern of results are discussed above.

Despite the fact that the observed results were not as expected, they did produce a number of important insights. For example, to my knowledge, the current study is the first to observe sex differences as a result of hippocampal neuroinflammation. This is noteworthy, because a number of conditions and diseases, including AD, differentially affect males and females. Current results suggest that these differences in prevalence rates might be a result of hippocampal neuroinflammation affecting males and females differently, and that females might express a particular vulnerability to neurological changes as a result. Another important implication of the results from this thesis is that

creating a sporadic model of AD should take into account the multifactorial aetiology of Alzheimer's and should focus on bringing out most (if not all) of the behavioural and pathological changes together in a model. Such studies can advance our research one step closer to understanding the dysfunctional mechanisms of AD. Only if we continue to improve our preclinical models will we be able to achieve an advanced understanding of these mechanisms and potentially use them to discover new and improved treatments.

5. References:

(NIH), N. I. o. H. (2020). *Alzheimer's Disease Diagnostic Guidelines*. https://www.hhs.gov/guidance/document/alzheimers-disease-diagnostic-guidelines

A. Armstrong, R. (2019). Risk factors for Alzheimer's disease [journal article]. *Folia Neuropathologica*, *57*(2), 87-105. https://doi.org/10.5114/fn.2019.85929

Adam, J., & Redish, A. D. (2007). Neural Ensembles in CA3 Transiently Encode Paths Forward of the Animal at a Decision Point. *The Journal of Neuroscience*, *27*(45), 12176. https://doi.org/10.1523/JNEUROSCI.3761-07.2007

Adamsky, A., Kol, A., Kreisel, T., Doron, A., Ozeri-Engelhard, N., Melcer, T., Refaeli, R., Horn, H., Regev, L., Groysman, M., London, M., & Goshen, I. (2018). Astrocytic Activation Generates De Novo Neuronal Potentiation and Memory Enhancement. *Cell*, *174*(1), 59-71.e14. https://doi.org/https://doi.org/10.1016/j.cell.2018.05.002

Adi, K., Adar, A., Maya, G., Tirzah, K., Michael, L., & Inbal, G. (2019). Astrocytes Contribute to Remote Memory Formation by Modulating Hippocampal-Cortical Communication During Learning. *bioRxiv*, 682344. https://doi.org/10.1101/682344

Ageta, H., Ikegami, S., Miura, M., Masuda, M., Migishima, R., Hino, T., Takashima, N., Murayama, A., Sugino, H., & Setou, M. (2010). Activin plays a key role in the maintenance of long-term memory and late-LTP. *Learning & memory*, *17*(4), 176-185.

Agster, K. L., & Burwell, R. D. (2013). Hippocampal and subicular efferents and afferents of the perirhinal, postrhinal, and entorhinal cortices of the rat. *Behav Brain Res*, *254*, 50-64. https://doi.org/10.1016/j.bbr.2013.07.005

Aisen, P. S. (2019). Failure After Failure. What Next in AD Drug Development? *The Journal of Prevention of Alzheimer's Disease*, *6*(3), 150-150. https://doi.org/10.14283/jpad.2019.23

Akhtar, A., Gupta, S. M., Dwivedi, S., Kumar, D., Shaikh, M. F., & Negi, A. (2022). Preclinical Models for Alzheimer's Disease: Past, Present, and Future Approaches. *ACS Omega*, *7*(51), 47504-47517. https://doi.org/10.1021/acsomega.2c05609

Albert, M. S., DeKosky, S. T., Dickson, D., Dubois, B., Feldman, H. H., Fox, N. C., Gamst, A., Holtzman, D. M., Jagust, W. J., Petersen, R. C., Snyder, P. J., Carrillo, M. C., Thies, B., & Phelps, C. H. (2011). The diagnosis of mild cognitive impairment due to Alzheimer's disease: recommendations from the National Institute on Aging-Alzheimer's Association workgroups on diagnostic guidelines for Alzheimer's disease. *Alzheimers Dement*, *7*(3), 270-279. https://doi.org/10.1016/j.jalz.2011.03.008

Albert, P. R. (2015). Why is depression more prevalent in women? *J Psychiatry Neurosci*, *40*(4), 219-221. https://doi.org/10.1503/jpn.150205

Alexandrov, P. N., Hill, J. M., Zhao, Y., Bond, T., Taylor, C. M., Percy, M. E., Li, W., & Lukiw, W. J. (2020). Aluminum-induced generation of lipopolysaccharide (LPS) from the human gastrointestinal (GI)-tract microbiome-resident Bacteroides fragilis. *Journal of Inorganic Biochemistry*, *203*, 110886. https://doi.org/https://doi.org/10.1016/j.jinorgbio.2019.110886

Ally, B. A. (2012). Using Pictures and Words To Understand Recognition Memory Deterioration in Amnestic Mild Cognitive Impairment and Alzheimer's Disease: A Review. *Current Neurology and Neuroscience Reports*, *12*(6), 687-694. https://doi.org/10.1007/s11910-012-0310-7

Alonso, A. D., Grundke-Iqbal, I., Barra, H. S., & Iqbal, K. (1997). Abnormal phosphorylation of tau and the mechanism of Alzheimer neurofibrillary degeneration: sequestration of microtubule-associated proteins 1 and 2 and the disassembly of microtubules by the abnormal tau. *Proc Natl Acad Sci U S A*, *94*(1), 298-303. https://doi.org/10.1073/pnas.94.1.298

Alvares, G. A., Balleine, B. W., & Guastella, A. J. (2014). Impairments in goal-directed actions predict treatment response to cognitive-behavioral therapy in social anxiety disorder. *PLOS ONE*, *9*(4), e94778. https://doi.org/10.1371/journal.pone.0094778

Alvares, G. A., Balleine, B. W., Whittle, L., & Guastella, A. J. (2016). Reduced goal-directed action control in autism spectrum disorder. *Autism Res*, *9*(12), 1285-1293. https://doi.org/10.1002/aur.1613

Alvarez-Mora, M. I., Blanco-Palmero, V. A., Quesada-Espinosa, J. F., Arteche-Lopez, A. R., Llamas-Velasco, S., Palma Milla, C., Lezana Rosales, J. M., Gomez-Manjon, I., Hernandez-Lain, A., Jimenez Almonacid, J., Gil-Fournier, B., Ramiro-León, S., González-Sánchez, M., Herrero-San Martín, A. O., Pérez-Martínez, D. A., Gómez-Tortosa, E., Carro, E., Bartolomé, F., Gomez-Rodriguez, M. J., . . . Moreno-Garcia, M. (2022). Heterozygous and Homozygous Variants in SORL1 Gene in Alzheimer's Disease Patients: Clinical, Neuroimaging and Neuropathological Findings. *Int J Mol Sci*, *23*(8). https://doi.org/10.3390/ijms23084230

Anaeigoudari, A., Shafei, M. N., Soukhtanloo, M., Sadeghnia, H. R., Reisi, P., Beheshti, F., Mohebbati, R., Mousavi, S. M., & Hosseini, M. (2015). Lipopolysaccharide-induced memory impairment in rats is preventable using 7-nitroindazole. *Arq Neuropsiquiatr*, *73*(9), 784-790. https://doi.org/10.1590/0004-282x20150121

Anaeigoudari, A., Soukhtanloo, M., Reisi, P., Beheshti, F., & Hosseini, M. (2016). Inducible nitric oxide inhibitor aminoguanidine, ameliorates deleterious effects of lipopolysaccharide on memory and long term potentiation in rat. *Life Sci*, *158*, 22-30. https://doi.org/10.1016/j.lfs.2016.06.019

Anand, K. S., & Dhikav, V. (2012). Hippocampus in health and disease: An overview. *Ann Indian Acad Neurol*, *15*(4), 239-246. https://doi.org/10.4103/0972-2327.104323

Andersen, O. M., Reiche, J., Schmidt, V., Gotthardt, M., Spoelgen, R., Behlke, J., von Arnim, C. A. F., Breiderhoff, T., Jansen, P., Wu, X., Bales, K. R., Cappai, R., Masters, C. L., Gliemann, J., Mufson, E. J., Hyman, B. T., Paul, S. M., Nykjær, A., & Willnow, T. E. (2005). Neuronal sorting protein-related receptor sorLA/LR11 regulates processing of the amyloid precursor protein. *Proceedings of the National Academy of Sciences*, *102*(38), 13461-13466. https://doi.org/doi:10.1073/pnas.0503689102

Andreano, J. M., & Cahill, L. (2009). Sex influences on the neurobiology of learning and memory. *Learning & Memory*, *16*(4), 248-266. https://doi.org/10.1101/lm.918309

Ano, Y., Ohya, R., Kita, M., Taniguchi, Y., & Kondo, K. (2019). Theaflavins Improve Memory Impairment and Depression-Like Behavior by Regulating Microglial Activation. *Molecules*, *24*, 467. https://doi.org/10.3390/molecules24030467

Ano, Y., Ohya, R., Yamazaki, T., Takahashi, C., Taniguchi, Y., Kondo, K., Takashima, A., Uchida, K., & Nakayama, H. (2020). Hop bitter acids containing a β-carbonyl moiety prevent inflammation-induced cognitive decline via the vagus nerve and noradrenergic system. *Scientific Reports*, *10*. https://doi.org/10.1038/s41598-020-77034-w

Arikkath, J. (2012). Molecular mechanisms of dendrite morphogenesis. *Front Cell Neurosci*, *6*, 61. https://doi.org/10.3389/fncel.2012.00061

Arimon, M., Takeda, S., Post, K. L., Svirsky, S., Hyman, B. T., & Berezovska, O. (2015). Oxidative stress and lipid peroxidation are upstream of amyloid pathology. *Neurobiol Dis*, *84*, 109-119. https://doi.org/10.1016/j.nbd.2015.06.013

Arthur, C. M., Cécile, T., Joseph, T., Stijn, S., Yi-Ting, W., Jaime, F.-A., Nesrine, R., Firoza, Z. L., Marie, V., Gleb, B., Paolo, V., Kok Pin, N., Eduardo, R. Z., Marie-Christine, G., Tharick, A. P., Serge, G., & Pedro, R.-N. (2023). The Use of Tau PET to Stage Alzheimer Disease According to the Braak Staging Framework. *Journal of Nuclear Medicine*, jnumed.122.265200. https://doi.org/10.2967/jnumed.122.265200

Asher, S., & Priefer, R. (2022). Alzheimer's disease failed clinical trials. *Life Sciences*, *306*, 120861. https://doi.org/https://doi.org/10.1016/j.lfs.2022.120861

Azocar, I., Rapaport, P., Burton, A., Meisel, G., & Orgeta, V. (2022). Risk factors for apathy in Alzheimer's disease: A systematic review of longitudinal evidence. *Ageing Res Rev*, *79*, 101672. https://doi.org/10.1016/j.arr.2022.101672

Baeta-Corral, R., & Giménez-Llort, L. (2015). Persistent hyperactivity and distinctive strategy features in the Morris water maze in 3xTg-AD mice at advanced stages of disease. *Behav Neurosci*, *129*(2), 129-137. https://doi.org/10.1037/bne0000027

Baglietto-Vargas, D., Forner, S., Cai, L., Martini, A. C., Trujillo-Estrada, L., Swarup, V., Nguyen, M. M. T., Do Huynh, K., Javonillo, D. I., Tran, K. M., Phan, J., Jiang, S., Kramár, E. A., Nuñez-Diaz, C., Balderrama-Gutierrez, G., Garcia, F., Childs, J., Rodriguez-Ortiz, C. J., Garcia-Leon, J. A., . . . LaFerla, F. M. (2021). Generation of a humanized Aβ expressing mouse demonstrating aspects of Alzheimer's disease-like pathology. *Nature Communications*, *12*(1), 2421. https://doi.org/10.1038/s41467-021-22624-z

Bahaidrah, K. A., Alzahrani, N. A., Aldhahri, R. S., Mansouri, R. A., & Alghamdi, B. S. (2022). Effects of Different Lipopolysaccharide Doses on Short- and Long-Term Spatial Memory and Hippocampus Morphology in an Experimental Alzheimer’s Disease Model. *Clinical and Translational Neuroscience*, *6*(3), 20. https://www.mdpi.com/2514-183X/6/3/20

Bahaidrah, K. A., Alzahrani, N. A., Aldhahri, R. S., Mansouri, R. A., & Alghamdi, B. S. (2022). Effects of Different Lipopolysaccharide Doses on Short- and Long-Term Spatial Memory and Hippocampus Morphology in an Experimental Alzheimer's Disease Model. *Clinical and Translational Neuroscience*, *6*(3).

Bakaeva, Z., Lizunova, N., Tarzhanov, I., Boyarkin, D., Petrichuk, S., Pinelis, V., Fisenko, A., Tuzikov, A., Sharipov, R., & Surin, A. (2021). Lipopolysaccharide From E. coli Increases Glutamate-Induced Disturbances of Calcium Homeostasis, the Functional State of Mitochondria, and the Death of Cultured Cortical Neurons. *Front Mol Neurosci*, *14*, 811171. https://doi.org/10.3389/fnmol.2021.811171

Bakulski, K. M., Seo, Y. A., Hickman, R. C., Brandt, D., Vadari, H. S., Hu, H., & Park, S. K. (2020). Heavy Metals Exposure and Alzheimer's Disease and Related Dementias. *J Alzheimers Dis*, *76*(4), 1215-1242. https://doi.org/10.3233/jad-200282

Bakulski, K. M., Seo, Y. A., Hickman, R. C., Brandt, D., Vadari, H. S., Hu, H., & Park, S. K. (2020). Heavy Metals Exposure and Alzheimer's Disease and Related Dementias. *Journal of Alzheimer's Disease*, *76*, 1215-1242. https://doi.org/10.3233/JAD-200282

Balce, D. R., Li, B., Allan, E. R., Rybicka, J. M., Krohn, R. M., & Yates, R. M. (2011). Alternative activation of macrophages by IL-4 enhances the proteolytic capacity of their phagosomes through synergistic mechanisms. *Blood, The Journal of the American Society of Hematology*, *118*(15), 4199-4208.

Balleine, B. W., & Dickinson, A. (1998a). Goal-directed instrumental action: contingency and incentive learning and their cortical substrates. *Neuropharmacology*, *37*(4), 407-419. https://doi.org/https://doi.org/10.1016/S0028-3908(98)00033-1

Balleine, B. W., & Dickinson, A. (1998b). The role of incentive learning in instrumental outcome revaluation by sensory-specific satiety. *Animal Learning & Behavior*, *26*(1), 46-59. https://doi.org/10.3758/BF03199161

Balleine, B. W., Morris, R. W., & Leung, B. K. (2015). Thalamocortical integration of instrumental learning and performance and their disintegration in addiction. *Brain Res*, *1628*(Pt A), 104-116. https://doi.org/10.1016/j.brainres.2014.12.023

Balleine, B. W., & O'Doherty, J. P. (2010). Human and Rodent Homologies in Action Control: Corticostriatal Determinants of Goal-Directed and Habitual Action. *Neuropsychopharmacology*, *35*(1), 48-69. https://doi.org/10.1038/npp.2009.131

Balsis, S., Benge, J. F., Lowe, D. A., Geraci, L., & Doody, R. S. (2015). How Do Scores on the ADAS-Cog, MMSE, and CDR-SOB Correspond? *Clin Neuropsychol*, *29*(7), 1002-1009. https://doi.org/10.1080/13854046.2015.1119312

Baltaci, S. B., Mogulkoc, R., & Baltaci, A. K. (2019). Molecular Mechanisms of Early and Late LTP. *Neurochem Res*, *44*(2), 281-296. https://doi.org/10.1007/s11064-018-2695-4

Bannerman, D. M., Rawlins, J. N. P., McHugh, S. B., Deacon, R. M. J., Yee, B. K., Bast, T., Zhang, W. N., Pothuizen, H. H. J., & Feldon, J. (2004). Regional dissociations within the hippocampus—

memory and anxiety. *Neuroscience & Biobehavioral Reviews*, *28*(3), 273-283. https://doi.org/https://doi.org/10.1016/j.neubiorev.2004.03.004

Baron, R., Nemirovsky, A., Harpaz, I., Cohen, H., Owens, T., & Monsonego, A. (2008). IFN-γ enhances neurogenesis in wild-type mice and in a mouse model of Alzheimer's disease. *The FASEB Journal*, *22*(8), 2843-2852. https://doi.org/https://doi.org/10.1096/fj.08-105866

Bartsch, T., Döhring, J., Rohr, A., Jansen, O., & Deuschl, G. (2011). CA1 neurons in the human hippocampus are critical for autobiographical memory, mental time travel, and autonoetic consciousness. *Proc Natl Acad Sci U S A*, *108*(42), 17562-17567. https://doi.org/10.1073/pnas.1110266108

Batista, C. R., Gomes, G. F., Candelario-Jalil, E., Fiebich, B. L., & de Oliveira, A. C. (2019). Lipopolysaccharide-Induced Neuroinflammation as a Bridge to Understand Neurodegeneration. *International Journal of Molecular Sciences*, *20*(9).

Batista, C. R. A., Gomes, G. F., Candelario-Jalil, E., Fiebich, B. L., & de Oliveira, A. C. P. (2019). Lipopolysaccharide-Induced Neuroinflammation as a Bridge to Understand Neurodegeneration. *Int J Mol Sci*, *20*(9). https://doi.org/10.3390/ijms20092293

Baudry, M., Arst, D., Oliver, M., & Lynch, G. (1981). Development of glutamate binding sites and their regulation by calcium in rat hippocampus. *Developmental Brain Research*, *1*(1), 37-48. https://doi.org/https://doi.org/10.1016/0165-3806(81)90092-4

Baum, F., Musolino, C., Gesesew, H. A., & Popay, J. (2021). New Perspective on Why Women Live Longer Than Men: An Exploration of Power, Gender, Social Determinants, and Capitals. *Int J Environ Res Public Health*, *18*(2). https://doi.org/10.3390/ijerph18020661

Beatty, W. W., & Fessler, R. G. (1976). Ontogeny of sex differences in open-field behavior and sensitivity to electric shock in the rat. *Physiol Behav*, *16*(4), 413-417. https://doi.org/10.1016/0031-9384(76)90319-x

Beauquis, J., Vinuesa, A., Pomilio, C., Pavía, P., Galván, V., & Saravia, F. (2014). Neuronal and glial alterations, increased anxiety, and cognitive impairment before hippocampal amyloid deposition in PDAPP mice, model of Alzheimer's disease. *Hippocampus*, *24*(3), 257-269. https://doi.org/https://doi.org/10.1002/hipo.22219

Behairi, N., Belkhelfa, M., Rafa, H., Labsi, M., Deghbar, N., Bouzid, N., Mesbah-Amroun, H., & Touil-Boukoffa, C. (2016). All-trans retinoic acid (ATRA) prevents lipopolysaccharide-induced neuroinflammation, amyloidogenesis and memory impairment in aged rats. *J Neuroimmunol*, *300*, 21-29. https://doi.org/10.1016/j.jneuroim.2016.10.004

Bekris, L. M., Yu, C.-E., Bird, T. D., & Tsuang, D. W. (2010). Review Article: Genetics of Alzheimer Disease. *Journal of Geriatric Psychiatry and Neurology*, *23*(4), 213-227. https://doi.org/10.1177/0891988710383571

Bellaver, B., Povala, G., Ferreira, P. C. L., Ferrari-Souza, J. P., Leffa, D. T., Lussier, F. Z., Benedet, A. L., Ashton, N. J., Triana-Baltzer, G., Kolb, H. C., Tissot, C., Therriault, J., Servaes, S., Stevenson, J., Rahmouni, N., Lopez, O. L., Tudorascu, D. L., Villemagne, V. L., Ikonomovic, M. D., . . . Pascoal, T. A. (2023). Astrocyte reactivity influences amyloid-β effects on tau pathology in preclinical Alzheimer's disease. *Nature Medicine*, *29*(7), 1775-1781. https://doi.org/10.1038/s41591-023-02380-x

Bentahir, M., Nyabi, O., Verhamme, J., Tolia, A., Horré, K., Wiltfang, J., Esselmann, H., & De Strooper, B. (2006). Presenilin clinical mutations can affect gamma-secretase activity by different mechanisms. *J Neurochem*, *96*(3), 732-742. https://doi.org/10.1111/j.1471-4159.2005.03578.x

Berry, K. P., & Nedivi, E. (2017). Spine Dynamics: Are They All the Same? *Neuron*, *96*(1), 43-55. https://doi.org/10.1016/j.neuron.2017.08.008

Bertani, B., & Ruiz, N. (2018). Function and Biogenesis of Lipopolysaccharides. *EcoSal Plus*, *8*(1). https://doi.org/10.1128/ecosalplus.ESP-0001-2018

Bertolotto, A., Agresti, C., Castello, A., Manzardo, E., & Riccio, A. (1998). 5D4 keratan sulfate epitope identifies a subset of ramified microglia in normal central nervous system parenchyma. *J Neuroimmunol*, *85*(1), 69-77. https://doi.org/10.1016/s0165-5728(97)00251-8

Biesmans, S., Meert, T. F., Bouwknecht, J. A., Acton, P. D., Davoodi, N., De Haes, P., Kuijlaars, J., Langlois, X., Matthews, L. J. R., Ver Donck, L., Hellings, N., & Nuydens, R. (2013). Systemic Immune Activation Leads to Neuroinflammation and Sickness Behavior in Mice. *Mediators of Inflammation*, *2013*, 271359. https://doi.org/10.1155/2013/271359

Billings, L. M., Oddo, S., Green, K. N., McGaugh, J. L., & LaFerla, F. M. (2005). Intraneuronal Abeta causes the onset of early Alzheimer's disease-related cognitive deficits in transgenic mice. *Neuron*, *45*(5), 675-688. https://doi.org/10.1016/j.neuron.2005.01.040

Billingsley, M. L., & Kincaid, R. L. (1997). Regulated phosphorylation and dephosphorylation of tau protein: effects on microtubule interaction, intracellular trafficking and neurodegeneration. *Biochem J*, *323 (Pt 3)*(Pt 3), 577-591. https://doi.org/10.1042/bj3230577

Bird, C. M., & Burgess, N. (2008). The hippocampus and memory: insights from spatial processing. *Nature Reviews Neuroscience*, *9*(3), 182-194. https://doi.org/10.1038/nrn2335

Bittner, T., Burgold, S., Dorostkar, M. M., Fuhrmann, M., Wegenast-Braun, B. M., Schmidt, B., Kretzschmar, H., & Herms, J. (2012). Amyloid plaque formation precedes dendritic spine loss. *Acta Neuropathol*, *124*(6), 797-807. https://doi.org/10.1007/s00401-012-1047-8

Blackstad, T. W. (1956). Commissural connections of the hippocampal region in the rat, with special reference to their mode of termination [https://doi.org/10.1002/cne.901050305]. *Journal of Comparative Neurology*, *105*(3), 417-537. https://doi.org/https://doi.org/10.1002/cne.901050305

Blasko, I., Veerhuis, R., Stampfer-Kountchev, M., Saurwein-Teissl, M., Eikelenboom, P., & Grubeck-Loebenstein, B. (2000). Costimulatory effects of interferon-gamma and interleukin-1beta or tumor necrosis factor alpha on the synthesis of Abeta1-40 and Abeta1-42 by human astrocytes. *Neurobiol Dis*, *7*(6 Pt B), 682-689. https://doi.org/10.1006/nbdi.2000.0321

Blennow, K., Wallin, A., Ågren, H., Spenger, C., Siegfried, J., & Vanmechelen, E. (1995). Tau protein in cerebrospinal fluid: a biochemical marker for axonal degeneration in Alzheimer disease? *Molecular and chemical neuropathology*, *26*, 231-245.

Bobba, A., Amadoro, G., Valenti, D., Corsetti, V., Lassandro, R., & Atlante, A. (2013). Mitochondrial respiratory chain Complexes I and IV are impaired by β-amyloid via direct interaction and through Complex I-dependent ROS production, respectively. *Mitochondrion*, *13*(4), 298-311. https://doi.org/10.1016/j.mito.2013.03.008

Boehm-Cagan, A., & Michaelson, D. M. (2014). Reversal of apoE4-Driven Brain Pathology and Behavioral Deficits by Bexarotene. *The Journal of Neuroscience*, *34*(21), 7293. https://doi.org/10.1523/JNEUROSCI.5198-13.2014

Bolós, M., Llorens-Martín, M., Perea, J. R., Jurado-Arjona, J., Rábano, A., Hernández, F., & Avila, J. (2017). Absence of CX3CR1 impairs the internalization of Tau by microglia. *Molecular Neurodegeneration*, *12*(1), 59. https://doi.org/10.1186/s13024-017-0200-1

Borràs, C., Mercer, A., Sirisi, S., Alcolea, D., Escolà-Gil, J. C., Blanco-Vaca, F., & Tondo, M. (2022). HDL-like-Mediated Cell Cholesterol Trafficking in the Central Nervous System and Alzheimer's Disease Pathogenesis. *International Journal of Molecular Sciences*, *23*(16).

Bossù, P., Cutuli, D., Palladino, I., Caporali, P., Angelucci, F., Laricchiuta, D., Gelfo, F., De Bartolo, P., Caltagirone, C., & Petrosini, L. (2012). A single intraperitoneal injection of endotoxin in rats induces long-lasting modifications in behavior and brain protein levels of TNF-α and IL-18. *J Neuroinflammation*, *9*, 101. https://doi.org/10.1186/1742-2094-9-101

Bouchon, A., Hernández-Munain, C., Cella, M., & Colonna, M. (2001). A Dap12-Mediated Pathway Regulates Expression of Cc Chemokine Receptor 7 and Maturation of Human Dendritic Cells. *Journal of Experimental Medicine*, *194*(8), 1111-1122. https://doi.org/10.1084/jem.194.8.1111

Bour, A., Grootendorst, J., Vogel, E., Kelche, C., Dodart, J.-C., Bales, K., Moreau, P.-H., Sullivan, P. M., & Mathis, C. (2008). Middle-aged human apoE4 targeted-replacement mice show retention deficits on a wide range of spatial memory tasks. *Behavioural brain research*, *193*(2), 174-182. https://doi.org/https://doi.org/10.1016/j.bbr.2008.05.008

Braak, H., Alafuzoff, I., Arzberger, T., Kretzschmar, H., & Del Tredici, K. (2006). Staging of Alzheimer disease-associated neurofibrillary pathology using paraffin sections and immunocytochemistry. *Acta Neuropathol*, *112*(4), 389-404. https://doi.org/10.1007/s00401-006-0127-z

Braak, H., & Braak, E. (1991). Neuropathological stageing of Alzheimer-related changes. *Acta Neuropathol*, *82*(4), 239-259. https://doi.org/10.1007/bf00308809

Bradfield, L., Hart, G., & Balleine, B. (2013). The role of the anterior, mediodorsal, and parafascicular thalamus in instrumental conditioning [Review]. *Frontiers in Systems Neuroscience*, *7*. https://doi.org/10.3389/fnsys.2013.00051

Bradfield, L. A., & Balleine, B. W. (2017). Chapter 6 - The Learning and Motivational Processes Controlling Goal-Directed Action and Their Neural Bases. In J.-C. Dreher & L. Tremblay (Eds.), *Decision Neuroscience* (pp. 71-80). Academic Press. https://doi.org/https://doi.org/10.1016/B978-0-12-805308-9.00006-3

Bradfield, L. A., Dezfouli, A., van Holstein, M., Chieng, B., & Balleine, B. W. (2015). Medial Orbitofrontal Cortex Mediates Outcome Retrieval in Partially Observable Task Situations. *Neuron*, *88*(6), 1268-1280. https://doi.org/10.1016/j.neuron.2015.10.044

Bradfield, L. A., Hart, G., & Balleine, B. W. (2018). Inferring action-dependent outcome representations depends on anterior but not posterior medial orbitofrontal cortex. *Neurobiol Learn Mem*, *155*, 463-473. https://doi.org/10.1016/j.nlm.2018.09.008

Bradfield, L. A., Leung, B. K., Boldt, S., Liang, S., & Balleine, B. W. (2020). Goal-directed actions transiently depend on dorsal hippocampus. *Nat Neurosci*, *23*(10), 1194-1197. https://doi.org/10.1038/s41593-020-0693-8

Brian, P. G., Kelly, A. Z., Yanxia, H., Seo Yeon, Y., Patrick, A., & Yadong, H. (2022). Early and lifelong effects of APOE4 on neuronal gene expression networks relevant to Alzheimer's disease. *bioRxiv*, 2022.2006.2016.496371. https://doi.org/10.1101/2022.06.16.496371

Broadbent, N. J., Squire, L. R., & Clark, R. E. (2004). Spatial memory, recognition memory, and the hippocampus. *Proceedings of the National Academy of Sciences*, *101*(40), 14515-14520. https://doi.org/doi:10.1073/pnas.0406344101

Brodbeck, J., Balestra, M. E., Saunders, A. M., Roses, A. D., Mahley, R. W., & Huang, Y. (2008). Rosiglitazone increases dendritic spine density and rescues spine loss caused by apolipoprotein E4 in primary cortical neurons. *Proc Natl Acad Sci U S A*, *105*(4), 1343-1346. https://doi.org/10.1073/pnas.0709906104

Brunello, C. A., Merezhko, M., Uronen, R.-L., & Huttunen, H. J. (2020). Mechanisms of secretion and spreading of pathological tau protein. *Cellular and Molecular Life Sciences*, *77*(9), 1721-1744. https://doi.org/10.1007/s00018-019-03349-1

Burgess, N., Maguire, E. A., & O'Keefe, J. (2002). The Human Hippocampus and Spatial and Episodic Memory. *Neuron*, *35*(4), 625-641. https://doi.org/10.1016/S0896-6273(02)00830-9

Burke, S. L., Cadet, T., Alcide, A., O'Driscoll, J., & Maramaldi, P. (2018). Psychosocial risk factors and Alzheimer's disease: the associative effect of depression, sleep disturbance, and anxiety. *Aging Ment Health*, *22*(12), 1577-1584. https://doi.org/10.1080/13607863.2017.1387760

Burn, L., Gutowski, N., Whatmore, J., Giamas, G., & Pranjol, M. Z. I. (2021). The role of astrocytes in brain metastasis at the interface of circulating tumour cells and the blood brain barrier. *FBL*, *26*(9), 590-601. https://doi.org/10.52586/4969

C. R. Jack, Jr., Dickson, D. W., Parisi, J. E., Xu, Y. C., Cha, R. H., O'Brien, P. C., Edland, S. D., Smith, G. E., Boeve, B. F., Tangalos, E. G., Kokmen, E., & Petersen, R. C. (2002). Antemortem MRI findings correlate with hippocampal neuropathology in typical aging and dementia. *Neurology*, *58*(5), 750. https://doi.org/10.1212/WNL.58.5.750

Cacace, R., Sleegers, K., & Van Broeckhoven, C. (2016). Molecular genetics of early-onset Alzheimer's disease revisited. *Alzheimer's & Dementia*, *12*(6), 733-748. https://doi.org/https://doi.org/10.1016/j.jalz.2016.01.012

Caglayan, S., Takagi-Niidome, S., Liao, F., Carlo, A.-S., Schmidt, V., Burgert, T., Kitago, Y., Füchtbauer, E.-M., Füchtbauer, A., Holtzman, D. M., Takagi, J., & Willnow, T. E. (2014). Lysosomal Sorting of Amyloid-β by the SORLA Receptor Is Impaired by a Familial Alzheimer's Disease Mutation. *Science Translational Medicine*, *6*(223), 223ra220-223ra220. https://doi.org/doi:10.1126/scitranslmed.3007747

Calafate, S., Flavin, W., Verstreken, P., & Moechars, D. (2016). Loss of Bin1 Promotes the Propagation of Tau Pathology. *Cell Reports*, *17*(4), 931-940. https://doi.org/10.1016/j.celrep.2016.09.063

Cambon, K., Davies, H. A., & Stewart, M. G. (2000). Synaptic loss is accompanied by an increase in synaptic area in the dentate gyrus of aged human apolipoprotein E4 transgenic mice [Article]. *Neuroscience*, *97*(4), 685-692. https://doi.org/10.1016/S0306-4522(00)00065-8

Carrasquillo, M. M., Crook, J. E., Pedraza, O., Thomas, C. S., Pankratz, V. S., Allen, M., Nguyen, T., Malphrus, K. G., Ma, L., Bisceglio, G. D., Roberts, R. O., Lucas, J. A., Smith, G. E., Ivnik, R. J., Machulda, M. M., Graff-Radford, N. R., Petersen, R. C., Younkin, S. G., & Ertekin-Taner, N. (2015). Late-onset Alzheimer's risk variants in memory decline, incident mild cognitive impairment, and Alzheimer's disease. *Neurobiol Aging*, *36*(1), 60-67. https://doi.org/10.1016/j.neurobiolaging.2014.07.042

Casali, B. T., MacPherson, K. P., Reed-Geaghan, E. G., & Landreth, G. E. (2020). Microglia depletion rapidly and reversibly alters amyloid pathology by modification of plaque compaction and morphologies. *Neurobiology of Disease*, *142*, 104956. https://doi.org/https://doi.org/10.1016/j.nbd.2020.104956

Castellani, G., Croese, T., Peralta Ramos, J. M., & Schwartz, M. (2023). Transforming the understanding of brain immunity. *Science*, *380*(6640), eabo7649. https://doi.org/10.1126/science.abo7649

Chai, X., Dage, J. L., & Citron, M. (2012). Constitutive secretion of tau protein by an unconventional mechanism. *Neurobiol Dis*, *48*(3), 356-366. https://doi.org/10.1016/j.nbd.2012.05.021

Chakrabarti, S., Khemka, V. K., Banerjee, A., Chatterjee, G., Ganguly, A., & Biswas, A. (2015). Metabolic Risk Factors of Sporadic Alzheimer's Disease: Implications in the Pathology, Pathogenesis and Treatment. *Aging and disease*, *6*(4), 282-299. https://doi.org/10.14336/AD.2014.002

Chakrabarti, S., Khemka, V. K., Banerjee, A., Chatterjee, G., Ganguly, A., & Biswas, A. (2015). Metabolic Risk Factors of Sporadic Alzheimer's Disease: Implications in the Pathology, Pathogenesis and Treatment. *Aging Dis*, *6*(4), 282-299. https://doi.org/10.14336/ad.2014.002

Chappel-Farley, M. G., Lui, K. K., Dave, A., Chen, I. Y., & Mander, B. A. (2020). Candidate mechanisms linking insomnia disorder to Alzheimer's disease risk. *Current Opinion in Behavioral Sciences*, *33*, 92-98. https://doi.org/https://doi.org/10.1016/j.cobeha.2020.01.010

Chen, F., Swartzlander, D. B., Ghosh, A., Fryer, J. D., Wang, B., & Zheng, H. (2021). Clusterin secreted from astrocyte promotes excitatory synaptic transmission and ameliorates Alzheimer's disease neuropathology. *Molecular Neurodegeneration*, *16*(1), 5. https://doi.org/10.1186/s13024-021-00426-7

Chen, G.-f., Xu, T.-h., Yan, Y., Zhou, Y.-r., Jiang, Y., Melcher, K., & Xu, H. E. (2017). Amyloid beta: structure, biology and structure-based therapeutic development. *Acta Pharmacologica Sinica*, *38*(9), 1205-1235. https://doi.org/10.1038/aps.2017.28

Chen, H., Qiao, D., Si, Y., He, Z., Zhang, B., Wang, C., Zhang, Y., Wang, X., Shi, Y., Cui, C., Cui, H., & Li, S. (2022). Effects of membrane androgen receptor binding on synaptic plasticity in primary hippocampal neurons. *Molecular and Cellular Endocrinology*, *554*, 111711. https://doi.org/https://doi.org/10.1016/j.mce.2022.111711

Chen, S. K., Tvrdik, P., Peden, E., Cho, S., Wu, S., Spangrude, G., & Capecchi, M. R. (2010). Hematopoietic origin of pathological grooming in Hoxb8 mutant mice. *Cell*, *141*(5), 775-785. https://doi.org/10.1016/j.cell.2010.03.055

Chen, Z., Yuan, Z., Yang, S., Zhu, Y., Xue, M., Zhang, J., & Leng, L. (2023). Brain Energy Metabolism: Astrocytes in Neurodegenerative Diseases. *CNS Neuroscience & Therapeutics*, *29*(1), 24-36. https://doi.org/https://doi.org/10.1111/cns.13982

Cheng, I. H., Scearce-Levie, K., Legleiter, J., Palop, J. J., Gerstein, H., Bien-Ly, N., Puoliväli, J., Lesné, S., Ashe, K. H., Muchowski, P. J., & Mucke, L. (2007). Accelerating amyloid-beta fibrillization reduces oligomer levels and functional deficits in Alzheimer disease mouse models. *J Biol Chem*, *282*(33), 23818-23828. https://doi.org/10.1074/jbc.M701078200

Chi, S., Yu, J.-T., Tan, M.-S., & Tan, L. (2014). Depression in Alzheimer's Disease: Epidemiology, Mechanisms, and Management. *Journal of Alzheimer's Disease*, *42*, 739-755. https://doi.org/10.3233/JAD-140324

Chishti, M. A., Yang, D. S., Janus, C., Phinney, A. L., Horne, P., Pearson, J., Strome, R., Zuker, N., Loukides, J., French, J., Turner, S., Lozza, G., Grilli, M., Kunicki, S., Morissette, C., Paquette, J., Gervais, F., Bergeron, C., Fraser, P. E., . . . Westaway, D. (2001). Early-onset amyloid deposition and cognitive deficits in transgenic mice expressing a double mutant form of amyloid precursor protein 695. *J Biol Chem*, *276*(24), 21562-21570. https://doi.org/10.1074/jbc.M100710200

Chiu, C. Q., Lur, G., Morse, T. M., Carnevale, N. T., Ellis-Davies, G. C., & Higley, M. J. (2013). Compartmentalization of GABAergic inhibition by dendritic spines. *Science*, *340*(6133), 759-762. https://doi.org/10.1126/science.1234274

Chugh, D., Nilsson, P., Afjei, A., Bakochi, A., & Ekdahl, C. (2013). Brain Inflammation Induces Post-Synaptic Changes During Early Synapse Formation in Adult-Born Hippocampal Neurons. *Experimental neurology*, *250*. https://doi.org/10.1016/j.expneurol.2013.09.005

Chung, W. S., Allen, N. J., & Eroglu, C. (2015). Astrocytes Control Synapse Formation, Function, and Elimination. *Cold Spring Harb Perspect Biol*, *7*(9), a020370. https://doi.org/10.1101/cshperspect.a020370

Citri, A., & Malenka, R. C. (2008). Synaptic Plasticity: Multiple Forms, Functions, and Mechanisms. *Neuropsychopharmacology*, *33*(1), 18-41. https://doi.org/10.1038/sj.npp.1301559

Clavaguera, F., Bolmont, T., Crowther, R. A., Abramowski, D., Frank, S., Probst, A., Fraser, G., Stalder, A. K., Beibel, M., Staufenbiel, M., Jucker, M., Goedert, M., & Tolnay, M. (2009). Transmission and spreading of tauopathy in transgenic mouse brain. *Nat Cell Biol*, *11*(7), 909-913. https://doi.org/10.1038/ncb1901

Cleary, J. P., Walsh, D. M., Hofmeister, J. J., Shankar, G. M., Kuskowski, M. A., Selkoe, D. J., & Ashe, K. H. (2005). Natural oligomers of the amyloid-beta protein specifically disrupt cognitive function. *Nat Neurosci*, *8*(1), 79-84. https://doi.org/10.1038/nn1372

Collij, L. E., Heeman, F., Salvadó, G., Ingala, S., Altomare, D., de Wilde, A., Konijnenberg, E., van Buchem, M., Yaqub, M., Markiewicz, P., Golla, S. S. V., Wottschel, V., Wink, A. M., Visser, P. J., Teunissen, C. E., Lammertsma, A. A., Scheltens, P., van der Flier, W. M., Boellaard, R., . . . Vilor-Tejedor, N. (2020). Multitracer model for staging cortical amyloid deposition using PET imaging. *Neurology*, *95*(11), e1538-e1553. https://doi.org/10.1212/WNL.0000000000010256

Colwill, R. M., & Rescorla, R. A. (1985). Postconditioning devaluation of a reinforcer affects instrumental responding. *Journal of Experimental Psychology: Animal Behavior Processes*, *11*(1), 120-132. https://doi.org/10.1037/0097-7403.11.1.120

consortium, H. W. o. b. o. t. M.-A. (2018). Characterizing the APOE4/Trem2R47H Mouse Model for Late Onset Alzheimer's Disease. *MODEL-AD Model oragnism develeptment and evaluation for Late-Onset Alzheimer's disease*. https://cpb-us-w2.wpmucdn.com/sites.jax.org/dist/4/9/files/2018/07/APOE4-trem2-model-1_sjsr-edits2-GRH-v2-min.pdf

Coppola, G., Chinnathambi, S., Lee, J. J., Dombroski, B. A., Baker, M. C., Soto-Ortolaza, A. I., Lee, S. E., Klein, E., Huang, A. Y., Sears, R., Lane, J. R., Karydas, A. M., Kenet, R. O., Biernat, J., Wang, L. S., Cotman, C. W., Decarli, C. S., Levey, A. I., Ringman, J. M., . . . Geschwind, D. H. (2012). Evidence for a role of the rare p.A152T variant in MAPT in increasing the risk for FTD-spectrum and Alzheimer's diseases. *Hum Mol Genet*, *21*(15), 3500-3512. https://doi.org/10.1093/hmg/dds161

Corbit, L. H., & Balleine, B. W. (2000). The role of the hippocampus in instrumental conditioning. *J Neurosci*, *20*(11), 4233-4239. https://doi.org/10.1523/jneurosci.20-11-04233.2000

Corbit, L. H., Muir, J. L., & Balleine, B. W. (2001). The role of the nucleus accumbens in instrumental conditioning: Evidence of a functional dissociation between accumbens core and shell. *J Neurosci*, *21*(9), 3251-3260. https://doi.org/10.1523/jneurosci.21-09-03251.2001

Corbit, L. H., Muir, J. L., & Balleine, B. W. (2003). Lesions of mediodorsal thalamus and anterior thalamic nuclei produce dissociable effects on instrumental conditioning in rats. *European Journal of Neuroscience*, *18*(5), 1286-1294. https://doi.org/https://doi.org/10.1046/j.1460-9568.2003.02833.x

Corbit, L. H., Ostlund, S. B., & Balleine, B. W. (2002). Sensitivity to instrumental contingency degradation is mediated by the entorhinal cortex and its efferents via the dorsal hippocampus. *J Neurosci*, *22*(24), 10976-10984. https://doi.org/10.1523/jneurosci.22-24-10976.2002

Corder, E. H., Saunders, A. M., Strittmatter, W. J., Schmechel, D. E., Gaskell, P. C., Small, G. W., Roses, A. D., Haines, J. L., & Pericak-Vance, M. A. (1993). Gene dose of apolipoprotein E type 4 allele and the risk of Alzheimer's disease in late onset families. *Science*, *261*(5123), 921-923. https://doi.org/10.1126/science.8346443

Coronas-Samano, G., Baker, K. L., Tan, W. J., Ivanova, A. V., & Verhagen, J. V. (2016). Fus1 KO Mouse As a Model of Oxidative Stress-Mediated Sporadic Alzheimer's Disease: Circadian Disruption and Long-Term Spatial and Olfactory Memory Impairments. *Front Aging Neurosci*, *8*, 268. https://doi.org/10.3389/fnagi.2016.00268

Craft, J. M., Watterson, D. M., & Van Eldik, L. J. (2006). Human amyloid beta-induced neuroinflammation is an early event in neurodegeneration. *Glia*, *53*(5), 484-490. https://doi.org/10.1002/glia.20306

Crehan, H., Hardy, J., & Pocock, J. (2012). Microglia, Alzheimer's disease, and complement. *Int J Alzheimers Dis*, *2012*, 983640. https://doi.org/10.1155/2012/983640

Crimins, J. L., Pooler, A., Polydoro, M., Luebke, J. I., & Spires-Jones, T. L. (2013). The intersection of amyloid beta and tau in glutamatergic synaptic dysfunction and collapse in Alzheimer's disease. *Ageing Research Reviews*, *12*(3), 757-763. https://doi.org/https://doi.org/10.1016/j.arr.2013.03.002

Crouzin, N., Baranger, K., Cavalier, M., Marchalant, Y., Cohen-Solal, C., Roman, F. S., Khrestchatisky, M., Rivera, S., Féron, F., & Vignes, M. (2013). Area-specific alterations of synaptic plasticity in the 5XFAD mouse model of Alzheimer's disease: dissociation between somatosensory cortex and hippocampus. *PLOS ONE*, *8*(9), e74667. https://doi.org/10.1371/journal.pone.0074667

Cruchaga, C., Kauwe, John S. K., Harari, O., Jin, Sheng C., Cai, Y., Karch, Celeste M., Benitez, Bruno A., Jeng, Amanda T., Skorupa, T., Carrell, D., Bertelsen, S., Bailey, M., McKean, D., Shulman, Joshua M., De Jager, Philip L., Chibnik, L., Bennett, David A., Arnold, Steve E., Harold, D., . . . Goate, Alison M. (2013). GWAS of Cerebrospinal Fluid Tau Levels Identifies Risk Variants for Alzheimer’s Disease. *Neuron*, *78*(2), 256-268. https://doi.org/10.1016/j.neuron.2013.02.026

Cuccaro, M. L., Carney, R. M., Zhang, Y., Bohm, C., Kunkle, B. W., Vardarajan, B. N., Whitehead, P. L., Cukier, H. N., Mayeux, R., St. George-Hyslop, P., & Pericak-Vance, M. A. (2016). SORL1 mutations in early- and late-onset Alzheimer disease. *Neurology Genetics*, *2*(6), e116. https://doi.org/doi:10.1212/NXG.0000000000000116

Cummings, J. (2018). Lessons Learned from Alzheimer Disease: Clinical Trials with Negative Outcomes. *Clin Transl Sci*, *11*(2), 147-152. https://doi.org/10.1111/cts.12491

Czerniawski, J., Miyashita, T., Lewandowski, G., & Guzowski, J. F. (2015). Systemic lipopolysaccharide administration impairs retrieval of context-object discrimination, but not spatial, memory: Evidence for selective disruption of specific hippocampus-dependent memory functions during acute neuroinflammation. *Brain Behav Immun*, *44*, 159-166. https://doi.org/10.1016/j.bbi.2014.09.014

d'Errico, P., Ziegler-Waldkirch, S., Aires, V., Hoffmann, P., Mezö, C., Erny, D., Monasor, L. S., Liebscher, S., Ravi, V. M., Joseph, K., Schnell, O., Kierdorf, K., Staszewski, O., Tahirovic, S., Prinz, M., & Meyer-Luehmann, M. (2022). Microglia contribute to the propagation of Aβ into unaffected brain tissue. *Nature Neuroscience*, *25*(1), 20-25. https://doi.org/10.1038/s41593-021-00951-0

Dailey, M. W., & Saadabadi, A. (2023). Mania. In *StatPearls*. StatPearls Publishing

Dalla, C., & Shors, T. J. (2009). Sex differences in learning processes of classical and operant conditioning. *Physiol Behav*, *97*(2), 229-238. https://doi.org/10.1016/j.physbeh.2009.02.035

Daumas, L., Manera, V., Robert, P., & Zory, R. (2021). Associations between apathy and fatigue in patients with neurocognitive disorders. *Alzheimer's & Dementia*, *17*(S6), e057472. https://doi.org/https://doi.org/10.1002/alz.057472

Davis, N., Mota, B. C., Stead, L., Palmer, E. O. C., Lombardero, L., Rodriguez-Puertas, R., de Paola, V., Barnes, S. J., & Sastre, M. (2020). Ablation of astrocytes affects Aβ degradation, microglia activation and synaptic connectivity in an ex vivo model of Alzheimer's disease. *Alzheimer's & Dementia*, *16*(S3), e047419. https://doi.org/https://doi.org/10.1002/alz.047419

Davis, R., & Weisbeck, C. (2016). Creating a Supportive Environment Using Cues for Wayfinding in Dementia. *J Gerontol Nurs*, *42*(3), 36-44. https://doi.org/10.3928/00989134-20160212-07

De Roeck, A., Van den Bossche, T., van der Zee, J., Verheijen, J., De Coster, W., Van Dongen, J., Dillen, L., Baradaran-Heravi, Y., Heeman, B., Sanchez-Valle, R., Lladó, A., Nacmias, B., Sorbi, S., Gelpi, E., Grau-Rivera, O., Gómez-Tortosa, E., Pastor, P., Ortega-Cubero, S., Pastor, M. A., . . . Sleegers, K. (2017). Deleterious ABCA7 mutations and transcript rescue mechanisms in early onset Alzheimer's disease. *Acta Neuropathol*, *134*(3), 475-487. https://doi.org/10.1007/s00401-017-1714-x

De Rossi, P., Nomura, T., Andrew, R. J., Masse, N. Y., Sampathkumar, V., Musial, T. F., Sudwarts, A., Recupero, A. J., Le Metayer, T., Hansen, M. T., Shim, H.-N., Krause, S. V., Freedman, D. J., Bindokas, V. P., Kasthuri, N., Nicholson, D. A., Contractor, A., & Thinakaran, G. (2020). Neuronal BIN1 Regulates Presynaptic Neurotransmitter Release and Memory Consolidation. *Cell Reports*, *30*(10), 3520-3535.e3527. https://doi.org/10.1016/j.celrep.2020.02.026

De, S., Van Deren, D., Peden, E., Hockin, M., Boulet, A., Titen, S., & Capecchi, M. R. (2018). Two distinct ontogenies confer heterogeneity to mouse brain microglia. *Development*, *145*(13). https://doi.org/10.1242/dev.152306

De Sousa, R. A. L. (2022). Reactive gliosis in Alzheimer's disease: a crucial role for cognitive impairment and memory loss. *Metabolic Brain Disease*, *37*(4), 851-857. https://doi.org/10.1007/s11011-022-00953-2

De Wit, L., Marsiske, M., O'Shea, D., Kessels, R. P. C., Kurasz, A. M., DeFeis, B., Schaefer, N., & Smith, G. E. (2021). Procedural Learning in Individuals with Amnestic Mild Cognitive Impairment and Alzheimer's Dementia: a Systematic Review and Meta-analysis. *Neuropsychol Rev*, *31*(1), 103-114. https://doi.org/10.1007/s11065-020-09449-1

de Wit, S., Barker, R. A., Dickinson, A. D., & Cools, R. (2011). Habitual versus goal-directed action control in Parkinson disease. *J Cogn Neurosci*, *23*(5), 1218-1229. https://doi.org/10.1162/jocn.2010.21514

Dehmelt, L., & Halpain, S. (2005). The MAP2/Tau family of microtubule-associated proteins. *Genome Biol*, *6*(1), 204. https://doi.org/10.1186/gb-2004-6-1-204

Dekens, D. W., Naudé, P. J. W., Keijser, J. N., Boerema, A. S., De Deyn, P. P., & Eisel, U. L. M. (2018). Lipocalin 2 contributes to brain iron dysregulation but does not affect cognition, plaque load, and glial activation in the J20 Alzheimer mouse model. *Journal of Neuroinflammation*, *15*(1), 330. https://doi.org/10.1186/s12974-018-1372-5

Dempsey, R. C., Eardley, K., & Dodd, A. L. (2022). The role of tenacious versus flexible goal pursuit in the vulnerability to bipolar disorder. *Current Psychology*, *41*(4), 2382-2389. https://doi.org/10.1007/s12144-020-00748-7

Desdín-Micó, G., Soto-Heredero, G., Aranda, J. F., Oller, J., Carrasco, E., Gabandé-Rodríguez, E., Blanco, E. M., Alfranca, A., Cussó, L., Desco, M., Ibañez, B., Gortazar, A. R., Fernández-Marcos, P., Navarro, M. N., Hernaez, B., Alcamí, A., Baixauli, F., & Mittelbrunn, M. (2020). T cells with dysfunctional mitochondria induce multimorbidity and premature senescence. *Science*, *368*(6497), 1371-1376. https://doi.org/10.1126/science.aax0860

Dhikav, V., & Anand, K. (2011). Potential predictors of hippocampal atrophy in Alzheimer's disease. *Drugs Aging*, *28*(1), 1-11. https://doi.org/10.2165/11586390-000000000-00000

Dhungana, A., Becchi, S., Leake, J., Morris, G., Avgan, N., Balleine, B. W., Vissel, B., & Bradfield, L. A. (2023). Goal-Directed Action Is Initially Impaired in a hAPP-J20 Mouse Model of Alzheimer's Disease. *eNeuro*, *10*(2). https://doi.org/10.1523/eneuro.0363-22.2023

Dib, S., Pahnke, J., & Gosselet, F. (2021). Role of ABCA7 in Human Health and in Alzheimer's Disease. *Int J Mol Sci*, *22*(9). https://doi.org/10.3390/ijms22094603

Dickinson, A., & Balleine, B. (1994). Motivational control of goal-directed action. *Animal Learning & Behavior*, *22*(1), 1-18. https://doi.org/10.3758/BF03199951

Dixit, R., Ross, J. L., Goldman, Y. E., & Holzbaur, E. L. (2008). Differential regulation of dynein and kinesin motor proteins by tau. *Science*, *319*(5866), 1086-1089. https://doi.org/10.1126/science.1152993

Dominic, I. J., Kristine, M. T., Jimmy, P., Edna, H., Enikö, A. K., Celia da, C., Stefania, F., Shimako, K., Jonathan, N., Crystal, E. B., Michelle, H., Dina, P. M., Narges, R., Joshua, A. A., Ali, M., Marcelo, A. W., Andrea, J. T., Grant, R. M., Kim, N. G., & Frank, M. L. (2021). Systematic phenotyping and characterization of the 3xTg-AD mouse model of Alzheimer's Disease. *bioRxiv*, 2021.2010.2001.462640. https://doi.org/10.1101/2021.10.01.462640

Dorszewska, J., Prendecki, M., Oczkowska, A., Dezor, M., & Kozubski, W. (2016). Molecular Basis of Familial and Sporadic Alzheimer's Disease. *Current Alzheimer Research*, *13*(9), 952-963. https://doi.org/http://dx.doi.org/10.2174/1567205013666160314150501

Drögemüller, K., Helmuth, U., Brunn, A., Sakowicz-Burkiewicz, M., Gutmann, D. H., Mueller, W., Deckert, M., & Schlüter, D. (2008). Astrocyte gp130 expression is critical for the control of Toxoplasma encephalitis. *J Immunol*, *181*(4), 2683-2693. https://doi.org/10.4049/jimmunol.181.4.2683

Droke, E. A., Hager, K. A., Lerner, M. R., Lightfoot, S. A., Stoecker, B. J., Brackett, D. J., & Smith, B. J. (2007). Soy isoflavones avert chronic inflammation-induced bone loss and vascular disease. *Journal of Inflammation*, *4*(1), 1-12.

Dulken, B. W., Buckley, M. T., Navarro Negredo, P., Saligrama, N., Cayrol, R., Leeman, D. S., George, B. M., Boutet, S. C., Hebestreit, K., Pluvinage, J. V., Wyss-Coray, T., Weissman, I. L., Vogel, H., Davis, M. M., & Brunet, A. (2019). Single-cell analysis reveals T cell infiltration in old neurogenic niches. *Nature*, *571*(7764), 205-210. https://doi.org/10.1038/s41586-019-1362-5

Dumanis, S. B., Tesoriero, J. A., Babus, L. W., Nguyen, M. T., Trotter, J. H., Ladu, M. J., Weeber, E. J., Turner, R. S., Xu, B., Rebeck, G. W., & Hoe, H. S. (2009). ApoE4 decreases spine density and dendritic complexity in cortical neurons in vivo. *J Neurosci*, *29*(48), 15317-15322. https://doi.org/10.1523/jneurosci.4026-09.2009

Edemekong, P. F., Bomgaars, D. L., Sukumaran, S., & Schoo, C. (2023). Activities of Daily Living. In *StatPearls*. StatPearls Publishing

Elahi, M., Hasan, Z., Motoi, Y., Matsumoto, S. E., Ishiguro, K., & Hattori, N. (2016). Region-Specific Vulnerability to Oxidative Stress, Neuroinflammation, and Tau Hyperphosphorylation in Experimental Diabetes Mellitus Mice. *Journal of Alzheimer's disease : JAD*, *51*(4), 1209-1224. https://doi.org/10.3233/jad-150820

Eldridge, L. L., Masterman, D., & Knowlton, B. J. (2002). Intact implicit habit learning in Alzheimer's disease. *Behav Neurosci*, *116*(4), 722-726.

Engeland, C. G., Nielsen, D. V., Kavaliers, M., & Ossenkopp, K. P. (2001). Locomotor activity changes following lipopolysaccharide treatment in mice: a multivariate assessment of behavioral tolerance. *Physiol Behav*, *72*(4), 481-491. https://doi.org/10.1016/s0031-9384(00)00436-4

Enrico, F., Lyduine, C., Isadora Lopes, A., Christopher, B., & Gill, F. (2020). The Spatial-Temporal Ordering of Amyloid Pathology and Opportunities for PET Imaging. *Journal of Nuclear Medicine*, *61*(2), 166. https://doi.org/10.2967/jnumed.119.235879

Fá, M., Puzzo, D., Piacentini, R., Staniszewski, A., Zhang, H., Baltrons, M. A., Li Puma, D. D., Chatterjee, I., Li, J., Saeed, F., Berman, H. L., Ripoli, C., Gulisano, W., Gonzalez, J., Tian, H., Costa, J. A., Lopez, P., Davidowitz, E., Yu, W. H., . . . Arancio, O. (2016). Extracellular Tau Oligomers Produce An Immediate Impairment of LTP and Memory. *Scientific Reports*, *6*(1), 19393. https://doi.org/10.1038/srep19393

Fang, W., Xiao, N., Zeng, G., Bi, D., Dai, X., Mi, X., Ye, Q., Chen, X., & Zhang, J. (2021). APOE4 genotype exacerbates the depression-like behavior of mice during aging through ATP decline. *Translational Psychiatry*, *11*(1), 507. https://doi.org/10.1038/s41398-021-01631-0

Farrer, L. A., Cupples, L. A., Haines, J. L., Hyman, B., Kukull, W. A., Mayeux, R., Myers, R. H., Pericak-Vance, M. A., Risch, N., & van Duijn, C. M. (1997). Effects of Age, Sex, and Ethnicity on the Association Between Apolipoprotein E Genotype and Alzheimer Disease: A Meta-analysis. *JAMA*, *278*(16), 1349-1356. https://doi.org/10.1001/jama.1997.03550160069041

Feng, X.-Y., Hu, H.-D., Chen, J., Long, C., Yang, L., & Wang, L. (2021). Acute neuroinflammation increases excitability of prefrontal parvalbumin interneurons and their functional recruitment during novel object recognition. *Brain, Behavior, and Immunity*, *98*, 48-58. https://doi.org/https://doi.org/10.1016/j.bbi.2021.08.216

Feng, X., Hu, J., Zhan, F., Luo, D., Hua, F., & Xu, G. (2021). MicroRNA-138-5p Regulates Hippocampal Neuroinflammation and Cognitive Impairment by NLRP3/Caspase-1 Signaling Pathway in Rats. *Journal of Inflammation Research*, *Volume 14*, 1125-1143. https://doi.org/10.2147/JIR.S304461

Feringa, F. M., & van der Kant, R. (2021). Cholesterol and Alzheimer's Disease; From Risk Genes to Pathological Effects [Review]. *Frontiers in Aging Neuroscience*, *13*. https://doi.org/10.3389/fnagi.2021.690372

Fernández-Calle, R., Galán-Llario, M., Gramage, E., Zapatería, B., Vicente-Rodríguez, M., Zapico, J. M., de Pascual-Teresa, B., Ramos, A., Ramos-Álvarez, M. P., Uribarri, M., Ferrer-Alcón, M., & Herradón, G. (2020). Role of RPTPβ/ζ in neuroinflammation and microglia-neuron communication. *Sci Rep*, *10*(1), 20259. https://doi.org/10.1038/s41598-020-76415-5

Ferreira, I. L., Ferreiro, E., Schmidt, J., Cardoso, J. M., Pereira, C. M., Carvalho, A. L., Oliveira, C. R., & Rego, A. C. (2015). Aβ and NMDAR activation cause mitochondrial dysfunction involving ER calcium release. *Neurobiol Aging*, *36*(2), 680-692. https://doi.org/10.1016/j.neurobiolaging.2014.09.006

Ferreiro, E., Oliveira, C. R., & Pereira, C. M. F. (2008). The release of calcium from the endoplasmic reticulum induced by amyloid-beta and prion peptides activates the mitochondrial apoptotic pathway. *Neurobiol Dis*, *30*(3), 331-342. https://doi.org/10.1016/j.nbd.2008.02.003

Ferretti, M. T., Iulita, M. F., Cavedo, E., Chiesa, P. A., Schumacher Dimech, A., Santuccione Chadha, A., Baracchi, F., Girouard, H., Misoch, S., Giacobini, E., Depypere, H., Hampel, H., for the Women's Brain, P., & the Alzheimer Precision Medicine, I. (2018). Sex differences in Alzheimer disease — the gateway to precision medicine. *Nature Reviews Neurology*, *14*(8), 457-469. https://doi.org/10.1038/s41582-018-0032-9

Fiala, J. C., Feinberg, M., Popov, V., & Harris, K. M. (1998). Synaptogenesis via dendritic filopodia in developing hippocampal area CA1. *J Neurosci*, *18*(21), 8900-8911. https://doi.org/10.1523/jneurosci.18-21-08900.1998

Figures and tables-Clinical criteria for staging and diagnosis for public comment draft-2. (2023). https://alz.org/media/Documents/scientific-conferences/Figures-and-Tables-Clinical-Criteria-for-Staging-and-Diagnosis-for-Public-Comment-Draft-2.pdf?_gl=1*1iwox7g*_ga*OTY2MDk5MzY0LjE3MDY0OTQ2NzU.*_ga_QSFTKCEH7C*MTcxMjA0MzgyNy4zLjEuMTcxMjA0Mzg3NC4xMy4wLjA.*_ga_9JTEWVX24V*MTcxMjA0MzgyNy4zLjEuMTcxMjA0Mzg3NC4xMy4wLjA.

Figurov, A., Pozzo-Miller, L. D., Olafsson, P., Wang, T., & Lu, B. (1996). Regulation of synaptic responses to high-frequency stimulation and LTP by neurotrophins in the hippocampus. *Nature*, *381*(6584), 706-709. https://doi.org/10.1038/381706a0

Flores, J., Noël, A., Foveau, B., Lynham, J., Lecrux, C., & LeBlanc, A. C. (2018). Caspase-1 inhibition alleviates cognitive impairment and neuropathology in an Alzheimer's disease mouse model. *Nature Communications*, *9*(1), 3916. https://doi.org/10.1038/s41467-018-06449-x

Foley, K. E., Hewes, A. A., Garceau, D. T., Kotredes, K. P., Carter, G. W., Sasner, M., & Howell, G. R. (2022). The APOE (ε3/ε4) Genotype Drives Distinct Gene Signatures in the Cortex of Young Mice. *Front Aging Neurosci*, *14*, 838436. https://doi.org/10.3389/fnagi.2022.838436

Folstein, M. F., Folstein, S. E., & McHugh, P. R. (1975). "Mini-mental state": A practical method for grading the cognitive state of patients for the clinician. *Journal of Psychiatric Research*, *12*(3), 189-198. https://doi.org/https://doi.org/10.1016/0022-3956(75)90026-6

Forabosco, P., Ramasamy, A., Trabzuni, D., Walker, R., Smith, C., Bras, J., Levine, A. P., Hardy, J., Pocock, J. M., Guerreiro, R., Weale, M. E., & Ryten, M. (2013). Insights into TREM2 biology by network analysis of human brain gene expression data. *Neurobiology of Aging*, *34*(12), 2699-2714. https://doi.org/https://doi.org/10.1016/j.neurobiolaging.2013.05.001

Forner, S., Kawauchi, S., Balderrama-Gutierrez, G., Kramár, E. A., Matheos, D. P., Phan, J., Javonillo, D. I., Tran, K. M., Hingco, E., da Cunha, C., Rezaie, N., Alcantara, J. A., Baglietto-Vargas, D., Jansen, C., Neumann, J., Wood, M. A., MacGregor, G. R., Mortazavi, A., Tenner, A. J., . . . Green, K. N. (2021). Systematic phenotyping and characterization of the 5xFAD mouse model of Alzheimer's disease. *Scientific Data*, *8*(1), 270. https://doi.org/10.1038/s41597-021-01054-y

Förstl, H., Burns, A., Luthert, P., Cairns, N., Lantos, P., & Levy, R. (1992). Clinical and neuropathological correlates of depression in Alzheimer's disease. *Psychological Medicine*, *22*(4), 877-884. https://doi.org/10.1017/S0033291700038459

Foster, E. M., Dangla-Valls, A., Lovestone, S., Ribe, E. M., & Buckley, N. J. (2019). Clusterin in Alzheimer's Disease: Mechanisms, Genetics, and Lessons From Other Pathologies [Review]. *Frontiers in Neuroscience*, *13*. https://doi.org/10.3389/fnins.2019.00164

Fotuhi, M., Hachinski, V., & Whitehouse, P. J. (2009). Changing perspectives regarding late-life dementia. *Nature Reviews Neurology*, *5*(12), 649-658. https://doi.org/10.1038/nrneurol.2009.175

Franzmeier, N., Ossenkoppele, R., Brendel, M., Rubinski, A., Smith, R., Kumar, A., Mattsson-Carlgren, N., Strandberg, O., Duering, M., Buerger, K., Dichgans, M., Hansson, O., Ewers, M., for the Alzheimer's Disease Neuroimaging Initiative, & the Swedish Bio, F. s. (2022). The BIN1 rs744373 Alzheimer's disease risk SNP is associated with faster Aβ-associated tau accumulation and cognitive decline. *Alzheimer's & Dementia*, *18*(1), 103-115. https://doi.org/https://doi.org/10.1002/alz.12371

Franzmeier, N., Rubinski, A., Neitzel, J., Kim, Y., Damm, A., Na, D. L., Kim, H. J., Lyoo, C. H., Cho, H., Finsterwalder, S., Duering, M., Seo, S. W., & Ewers, M. (2019). Functional connectivity associated with tau levels in ageing, Alzheimer's, and small vessel disease. *Brain*, *142*(4), 1093-1107. https://doi.org/10.1093/brain/awz026

Friedel, E., Koch, S. P., Wendt, J., Heinz, A., Deserno, L., & Schlagenhauf, F. (2014). Devaluation and sequential decisions: linking goal-directed and model-based behavior [Original Research]. *Frontiers in Human Neuroscience*, *8*. https://doi.org/10.3389/fnhum.2014.00587

Friedland, R. P., Fritsch, T., Smyth, K. A., Koss, E., Lerner, A. J., Chen, C. H., Petot, G. J., & Debanne, S. M. (2001). Patients with Alzheimer's disease have reduced activities in midlife compared with healthy control-group members. *Proc Natl Acad Sci U S A*, *98*(6), 3440-3445. https://doi.org/10.1073/pnas.061002998

Frisoni, G. B., Fox, N. C., Jack, C. R., Jr., Scheltens, P., & Thompson, P. M. (2010). The clinical use of structural MRI in Alzheimer disease. *Nat Rev Neurol*, *6*(2), 67-77. https://doi.org/10.1038/nrneurol.2009.215

Fu, H., Yang, T., Xiao, W., Fan, L., Wu, Y., Terrando, N., & Wang, T. (2014). Prolonged Neuroinflammation after Lipopolysaccharide Exposure in Aged Rats. *PLOS ONE*, *9*, e106331. https://doi.org/10.1371/journal.pone.0106331

Fu, W.-Y., & Ip, N. Y. (2023). The role of genetic risk factors of Alzheimer's disease in synaptic dysfunction. *Seminars in Cell & Developmental Biology*, *139*, 3-12. https://doi.org/https://doi.org/10.1016/j.semcdb.2022.07.011

Gan, Y.-L., Wang, C.-Y., He, R.-H., Hsu, P.-C., Yeh, H.-H., Hsieh, T.-H., Lin, H.-C., Cheng, M.-Y., Jeng, C.-J., Huang, M.-C., & Lee, Y.-H. (2022). FKBP51 mediates resilience to inflammation-induced anxiety through regulation of glutamic acid decarboxylase 65 expression in mouse hippocampus. *Journal of Neuroinflammation*, *19*(1), 152. https://doi.org/10.1186/s12974-022-02517-8

Garcia-Hernandez, R., Cerdán Cerdá, A., Trouve Carpena, A., Drakesmith, M., Koller, K., Jones, D. K., Canals, S., & De Santis, S. (2022). Mapping microglia and astrocyte activation in vivo using diffusion MRI. *Science Advances*, *8*(21), eabq2923. https://doi.org/doi:10.1126/sciadv.abq2923

Garcia, A. D., & Buffalo, E. A. (2020). Anatomy and Function of the Primate Entorhinal Cortex. *Annu Rev Vis Sci*, *6*, 411-432. https://doi.org/10.1146/annurev-vision-030320-041115

Garwood, C. J., Pooler, A. M., Atherton, J., Hanger, D. P., & Noble, W. (2011). Astrocytes are important mediators of Aβ-induced neurotoxicity and tau phosphorylation in primary culture. *Cell Death Dis*, *2*(6), e167. https://doi.org/10.1038/cddis.2011.50

Gauthier-Umaña, C., Muñoz-Cabrera, J., Valderrama, M., Múnera, A., & Nava-Mesa, M. O. (2020). Acute Effects of Two Different Species of Amyloid-β on Oscillatory Activity and Synaptic Plasticity in the Commissural CA3-CA1 Circuit of the Hippocampus. *Neural Plasticity*, *2020*, 8869526. https://doi.org/10.1155/2020/8869526

Gillies, G. E., & McArthur, S. (2010). Estrogen actions in the brain and the basis for differential action in men and women: a case for sex-specific medicines. *Pharmacol Rev*, *62*(2), 155-198. https://doi.org/10.1124/pr.109.002071

Giménez-Llort, L., Marin-Pardo, D., Marazuela, P., & Hernández-Guillamón, M. (2021). Survival Bias and Crosstalk between Chronological and Behavioral Age: Age- and Genotype-Sensitivity Tests Define Behavioral Signatures in Middle-Aged, Old, and Long-Lived Mice with Normal and AD-Associated Aging. *Biomedicines*, *9*(6). https://doi.org/10.3390/biomedicines9060636

Glezer, I., Lapointe, A., & Rivest, S. (2006). Innate immunity triggers oligodendrocyte progenitor reactivity and confines damages to brain injuries. *Faseb j*, *20*(6), 750-752. https://doi.org/10.1096/fj.05-5234fje

Goate, A., Chartier-Harlin, M. C., Mullan, M., Brown, J., Crawford, F., Fidani, L., Giuffra, L., Haynes, A., Irving, N., James, L., & et al. (1991). Segregation of a missense mutation in the amyloid precursor protein gene with familial Alzheimer's disease. *Nature*, *349*(6311), 704-706. https://doi.org/10.1038/349704a0

Goedert, M., & Spillantini, M. G. (2017). Propagation of Tau aggregates. *Mol Brain*, *10*(1), 18. https://doi.org/10.1186/s13041-017-0298-7

Gold, C. A., & Budson, A. E. (2008). Memory loss in Alzheimer's disease: implications for development of therapeutics. *Expert Rev Neurother*, *8*(12), 1879-1891. https://doi.org/10.1586/14737175.8.12.1879

Goldstein, F. C., Loring, D. W., Thomas, T., Saleh, S., & Hajjar, I. (2019). Recognition Memory Performance as a Cognitive Marker of Prodromal Alzheimer's Disease. *J Alzheimers Dis*, *72*(2), 507-514. https://doi.org/10.3233/jad-190468

Gomes, C., Ferreira, R., George, J., Sanches, R., Rodrigues, D. I., Gonçalves, N., & Cunha, R. A. (2013). Activation of microglial cells triggers a release of brain-derived neurotrophic factor (BDNF) inducing their proliferation in an adenosine A2A receptor-dependent manner: A2A receptor blockade prevents BDNF release and proliferation of microglia. *J Neuroinflammation*, *10*, 16. https://doi.org/10.1186/1742-2094-10-16

Gomez-Nicola, D., & Perry, V. H. (2014). Microglial Dynamics and Role in the Healthy and Diseased Brain: A Paradigm of Functional Plasticity. *The Neuroscientist*, *21*(2), 169-184. https://doi.org/10.1177/1073858414530512

Gonçalves, L. A., Rodrigues-Duarte, L., Rodo, J., Vieira de Moraes, L., Marques, I., & Penha-Gonçalves, C. (2013). TREM2 governs Kupffer cell activation and explains belr1 genetic resistance to malaria liver stage infection. *Proceedings of the National Academy of Sciences*, *110*(48), 19531-19536. https://doi.org/doi:10.1073/pnas.1306873110

Gong, C. X., & Iqbal, K. (2008). Hyperphosphorylation of microtubule-associated protein tau: a promising therapeutic target for Alzheimer disease. *Curr Med Chem*, *15*(23), 2321-2328. https://doi.org/10.2174/092986708785909111

Gong, C. X., Liu, F., Grundke-Iqbal, I., & Iqbal, K. (2005). Post-translational modifications of tau protein in Alzheimer's disease. *J Neural Transm (Vienna)*, *112*(6), 813-838. https://doi.org/10.1007/s00702-004-0221-0

González-Reyes, R. E., Nava-Mesa, M. O., Vargas-Sánchez, K., Ariza-Salamanca, D., & Mora-Muñoz, L. (2017). Involvement of Astrocytes in Alzheimer's Disease from a Neuroinflammatory and Oxidative Stress Perspective [Review]. *Frontiers in Molecular Neuroscience*, *10*. https://doi.org/10.3389/fnmol.2017.00427

Goode, B. L., & Feinstein, S. C. (1994). Identification of a novel microtubule binding and assembly domain in the developmentally regulated inter-repeat region of tau. *The Journal of cell biology*, *124*(5), 769-782.

Gorelick, P. B. (2010). Role of inflammation in cognitive impairment: results of observational epidemiological studies and clinical trials. *Ann N Y Acad Sci*, *1207*, 155-162. https://doi.org/10.1111/j.1749-6632.2010.05726.x

Gould, T. D., Dao, D. T., & Kovacsics, C. E. (2009). The Open Field Test. In T. D. Gould (Ed.), *Mood and Anxiety Related Phenotypes in Mice: Characterization Using Behavioral Tests* (pp. 1-20). Humana Press. https://doi.org/10.1007/978-1-60761-303-9_1

Graham, A., Livingston, G., Purnell, L., & Huntley, J. (2022). Mild Traumatic Brain Injuries and Future Risk of Developing Alzheimer's Disease: Systematic Review and Meta-Analysis. *Journal of Alzheimer's Disease*, *87*, 969-979. https://doi.org/10.3233/JAD-220069

Gratuze, M., Leyns, C. E. G., & Holtzman, D. M. (2018). New insights into the role of TREM2 in Alzheimer's disease. *Molecular Neurodegeneration*, *13*(1), 66. https://doi.org/10.1186/s13024-018-0298-9

Guerreiro, R., Wojtas, A., Bras, J., Carrasquillo, M., Rogaeva, E., Majounie, E., Cruchaga, C., Sassi, C., Kauwe, J. S., Younkin, S., Hazrati, L., Collinge, J., Pocock, J., Lashley, T., Williams, J., Lambert, J. C., Amouyel, P., Goate, A., Rademakers, R., . . . Hardy, J. (2013). TREM2 variants in Alzheimer's disease. *N Engl J Med*, *368*(2), 117-127. https://doi.org/10.1056/NEJMoa1211851

Guerreiro, R., Wojtas, A., Bras, J., Carrasquillo, M., Rogaeva, E., Majounie, E., Cruchaga, C., Sassi, C., Kauwe, J. S. K., Younkin, S., Hazrati, L., Collinge, J., Pocock, J., Lashley, T., Williams, J., Lambert, J.-C., Amouyel, P., Goate, A., Rademakers, R., . . . Hardy, J. (2012). TREM2 Variants in

Alzheimer's Disease. *New England Journal of Medicine*, *368*(2), 117-127. https://doi.org/10.1056/NEJMoa1211851

Gundersen, H. J., & Jensen, E. B. (1987). The efficiency of systematic sampling in stereology and its prediction. *J Microsc*, *147*(Pt 3), 229-263. https://doi.org/10.1111/j.1365-2818.1987.tb02837.x

Habib, N., McCabe, C., Medina, S., Varshavsky, M., Kitsberg, D., Dvir-Szternfeld, R., Green, G., Dionne, D., Nguyen, L., Marshall, J. L., Chen, F., Zhang, F., Kaplan, T., Regev, A., & Schwartz, M. (2020). Disease-associated astrocytes in Alzheimer's disease and aging. *Nat Neurosci*, *23*(6), 701-706. https://doi.org/10.1038/s41593-020-0624-8

Halliday, M. R., Rege, S. V., Ma, Q., Zhao, Z., Miller, C. A., Winkler, E. A., & Zlokovic, B. V. (2016). Accelerated pericyte degeneration and blood-brain barrier breakdown in apolipoprotein E4 carriers with Alzheimer's disease. *J Cereb Blood Flow Metab*, *36*(1), 216-227. https://doi.org/10.1038/jcbfm.2015.44

Hamann, S., Monarch, E. S., & Goldstein, F. C. (2002). Impaired fear conditioning in Alzheimer's disease. *Neuropsychologia*, *40*(8), 1187-1195. https://doi.org/https://doi.org/10.1016/S0028-3932(01)00223-8

Hammerslag, L. R., & Gulley, J. M. (2014). Age and sex differences in reward behavior in adolescent and adult rats. *Dev Psychobiol*, *56*(4), 611-621. https://doi.org/10.1002/dev.21127

Hanna, A., Iremonger, K., Das, P., Dickson, D., Golde, T., & Janus, C. (2012). Age-related increase in amyloid plaque burden is associated with impairment in conditioned fear memory in CRND8 mouse model of amyloidosis. *Alzheimer's Research & Therapy*, *4*(3), 21. https://doi.org/10.1186/alzrt124

Hannoodee, S., & Nasuruddin, D. N. (2023). Acute Inflammatory Response. In *StatPearls*. StatPearls Publishing

Hansen, D. V., Hanson, J. E., & Sheng, M. (2018). Microglia in Alzheimer's disease. *J Cell Biol*, *217*(2), 459-472. https://doi.org/10.1083/jcb.201709069

Haroon, E., Miller, A. H., & Sanacora, G. (2017). Inflammation, Glutamate, and Glia: A Trio of Trouble in Mood Disorders. *Neuropsychopharmacology*, *42*(1), 193-215. https://doi.org/10.1038/npp.2016.199

Harris, F. M., Brecht, W. J., Xu, Q., Mahley, R. W., & Huang, Y. (2004). Increased tau phosphorylation in apolipoprotein E4 transgenic mice is associated with activation of extracellular signal-regulated kinase: modulation by zinc. *J Biol Chem*, *279*(43), 44795-44801. https://doi.org/10.1074/jbc.M408127200

Harris, J. A., Andrew, B. J., & Kwok, D. (2013). Magazine approach during a signal for food depends on Pavlovian, not instrumental, conditioning [Post-print]. http://hdl.handle.net/2123/9069

Harris, J. A., Devidze, N., Halabisky, B., Lo, I., Thwin, M. T., Yu, G. Q., Bredesen, D. E., Masliah, E., & Mucke, L. (2010). Many neuronal and behavioral impairments in transgenic mouse models of Alzheimer's disease are independent of caspase cleavage of the amyloid precursor protein. *J Neurosci*, *30*(1), 372-381. https://doi.org/10.1523/jneurosci.5341-09.2010

Harry, G. J. (2013). Microglia during development and aging. *Pharmacol Ther*, *139*(3), 313-326. https://doi.org/10.1016/j.pharmthera.2013.04.013

Hart, G., & Balleine, B. W. (2016). Consolidation of Goal-Directed Action Depends on MAPK/ERK Signaling in Rodent Prelimbic Cortex. *J Neurosci*, *36*(47), 11974-11986. https://doi.org/10.1523/jneurosci.1772-16.2016

Hartantyo, R. Y., Hidayat, M. R. M., Azzam, A. B., & mulyati, m. (2020). Animal model for sporadic dementia of Alzheimer's type (SDAT) using streptozotocin and lipopolysaccharide combinations in rats [β-amyloid; lipopolysaccharide; memory; sporadic dementia; streptozotocin;]. *2020*, *52*(3). https://doi.org/10.19106/JMedSci005203202003

Hartman, Y. A. W., Karssemeijer, E. G. A., van Diepen, L. A. M., Olde Rikkert, M. G. M., & Thijssen, D. H. J. (2018). Dementia Patients Are More Sedentary and Less Physically Active than Age- and

Sex-Matched Cognitively Healthy Older Adults. *Dement Geriatr Cogn Disord*, *46*(1-2), 81-89. https://doi.org/10.1159/000491995

Hasriadi, Dasuni Wasana, P. W., Vajragupta, O., Rojsitthisak, P., & Towiwat, P. (2021). Automated home-cage monitoring as a potential measure of sickness behaviors and pain-like behaviors in LPS-treated mice. *PLOS ONE*, *16*(8), e0256706. https://doi.org/10.1371/journal.pone.0256706

Haw, J. (2008). Random-ratio schedules of reinforcement: The role of early wins and unreinforced trials. *Journal of Gambling Issues*, *21*, 56-67. https://doi.org/10.4309/jgi.2008.21.6

Hayashi-Takagi, A., Yagishita, S., Nakamura, M., Shirai, F., Wu, Y. I., Loshbaugh, A. L., Kuhlman, B., Hahn, K. M., & Kasai, H. (2015). Labelling and optical erasure of synaptic memory traces in the motor cortex. *Nature*, *525*(7569), 333-338. https://doi.org/10.1038/nature15257

He, Z., Guo, J. L., McBride, J. D., Narasimhan, S., Kim, H., Changolkar, L., Zhang, B., Gathagan, R. J., Yue, C., Dengler, C., Stieber, A., Nitla, M., Coulter, D. A., Abel, T., Brunden, K. R., Trojanowski, J. Q., & Lee, V. M. (2018). Amyloid-β plaques enhance Alzheimer's brain tau-seeded pathologies by facilitating neuritic plaque tau aggregation. *Nat Med*, *24*(1), 29-38. https://doi.org/10.1038/nm.4443

Heppner, F. L., Ransohoff, R. M., & Becher, B. (2015). Immune attack: the role of inflammation in Alzheimer disease. *Nat Rev Neurosci*, *16*(6), 358-372. https://doi.org/10.1038/nrn3880

Hering, H., & Sheng, M. (2001). Dentritic spines : structure, dynamics and regulation. *Nature Reviews Neuroscience*, *2*(12), 880-888. https://doi.org/10.1038/35104061

Hernández-Sapiéns, M. A., Reza-Zaldívar, E. E., Márquez-Aguirre, A. L., Gómez-Pinedo, U., Matias-Guiu, J., Cevallos, R. R., Mateos-Díaz, J. C., Sánchez-González, V. J., & Canales-Aguirre, A. A. (2022). Presenilin mutations and their impact on neuronal differentiation in Alzheimer's disease. *Neural Regeneration Research*, *17*(1), 31-37. https://doi.org/10.4103/1673-5374.313016

Hickman, S. E., Allison, E. K., & El Khoury, J. (2008). Microglial dysfunction and defective beta-amyloid clearance pathways in aging Alzheimer's disease mice. *J Neurosci*, *28*(33), 8354-8360. https://doi.org/10.1523/jneurosci.0616-08.2008

Higley, M. J., & Sabatini, B. L. (2012). Calcium signaling in dendritic spines. *Cold Spring Harb Perspect Biol*, *4*(4), a005686. https://doi.org/10.1101/cshperspect.a005686

Hippius, H., & Neundörfer, G. (2003). The discovery of Alzheimer's disease. *Dialogues Clin Neurosci*, *5*(1), 101-108. https://doi.org/10.31887/DCNS.2003.5.1/hhippius

Ho, N. F., Hooker, J. M., Sahay, A., Holt, D. J., & Roffman, J. L. (2013). In vivo imaging of adult human hippocampal neurogenesis: progress, pitfalls and promise. *Molecular Psychiatry*, *18*(4), 404-416. https://doi.org/10.1038/mp.2013.8

Hok, V., Lenck-Santini, P. P., Roux, S., Save, E., Muller, R. U., & Poucet, B. (2007). Goal-related activity in hippocampal place cells. *J Neurosci*, *27*(3), 472-482. https://doi.org/10.1523/jneurosci.2864-06.2007

Holt, W., & Maren, S. (1999). Muscimol inactivation of the dorsal hippocampus impairs contextual retrieval of fear memory. *J Neurosci*, *19*(20), 9054-9062. https://doi.org/10.1523/jneurosci.19-20-09054.1999

Hong, J., Yoon, D., Nam, Y., Seo, D., Kim, J.-H., Kim, M. S., Lee, T. Y., Kim, K. S., Ko, P.-W., Lee, H.-W., Suk, K., & Kim, S. R. (2020). Lipopolysaccharide administration for a mouse model of cerebellar ataxia with neuroinflammation. *Scientific Reports*, *10*(1), 13337. https://doi.org/10.1038/s41598-020-70390-7

Hong, S., Beja-Glasser, V. F., Nfonoyim, B. M., Frouin, A., Li, S., Ramakrishnan, S., Merry, K. M., Shi, Q., Rosenthal, A., Barres, B. A., Lemere, C. A., Selkoe, D. J., & Stevens, B. (2016). Complement and microglia mediate early synapse loss in Alzheimer mouse models. *Science*, *352*(6286), 712-716. https://doi.org/10.1126/science.aad8373

Hoogmartens, J., Cacace, R., & Van Broeckhoven, C. (2021). Insight into the genetic etiology of Alzheimer's disease: A comprehensive review of the role of rare variants. *Alzheimer's &*

Dementia: Diagnosis, Assessment & Disease Monitoring, *13*(1), e12155. https://doi.org/https://doi.org/10.1002/dad2.12155

Hou, Y., Xie, G., Miao, F., Ding, L., Mou, Y., Wang, L., Su, G., Chen, G., Yang, J., & Wu, C. (2014). Pterostilbene attenuates lipopolysaccharide-induced learning and memory impairment possibly via inhibiting microglia activation and protecting neuronal injury in mice. *Progress in Neuro-Psychopharmacology and Biological Psychiatry*, *54*, 92-102. https://doi.org/https://doi.org/10.1016/j.pnpbp.2014.03.015

Huang, H.-J., Chen, Y.-H., Liang, K.-C., Jheng, Y.-S., Jhao, J.-J., Su, M.-T., Lee-Chen, G.-J., & Hsieh-Li, H. M. (2012). Exendin-4 Protected against Cognitive Dysfunction in Hyperglycemic Mice Receiving an Intrahippocampal Lipopolysaccharide Injection. *PLOS ONE*, *7*(7), e39656. https://doi.org/10.1371/journal.pone.0039656

Huang, Y., & Mahley, R. W. (2014). Apolipoprotein E: Structure and function in lipid metabolism, neurobiology, and Alzheimer's diseases. *Neurobiology of Disease*, *72*, 3-12. https://doi.org/https://doi.org/10.1016/j.nbd.2014.08.025

Huifeng, Z., Liu, K., Jiang, R., Wan, G., Zou, L., Zhu, X., Ren, Q., Wan, D., Cheng, F., & Feng, S. (2020). *Astragalus injection ameliorate Lipopolysaccaride-induced mice cognitive decline via relieving acute neuroinflammation and BBB damage as well as up-regulating BDNF-CREB pathway in chronic stage*. https://doi.org/10.21203/rs.2.19795/v1

Humphrey, M. B., Daws, M. R., Spusta, S. C., Niemi, E. C., Torchia, J. A., Lanier, L. L., Seaman, W. E., & Nakamura, M. C. (2009). TREM2, a DAP12-Associated Receptor, Regulates Osteoclast Differentiation and Function*. *Journal of Bone and Mineral Research*, *21*(2), 237-245. https://doi.org/10.1359/jbmr.051016

Huynh, K. D., Nguyen, M. M. T., Cheung, A., Tran, J. P., Nuñez-Diaz, C., Forner, S., Martini, A. C., Trujillo-Estrada, L., Da Cunha, C., Shahnawaz, M., Soto, C., Moreno-Gonzalez, I., Gutierrez, A., LaFerla, F., & Baglietto-Vargas, D. (2020). Amyloid propagation in a sporadic model of Alzheimer's disease. *Alzheimer's & Dementia*, *16*(S2), e045657. https://doi.org/https://doi.org/10.1002/alz.045657

Huynh, T. V., Davis, A. A., Ulrich, J. D., & Holtzman, D. M. (2017). Apolipoprotein E and Alzheimer's disease: the influence of apolipoprotein E on amyloid-β and other amyloidogenic proteins. *J Lipid Res*, *58*(5), 824-836. https://doi.org/10.1194/jlr.R075481

Hwang, F.-J., Roth, R. H., Wu, Y.-W., Sun, Y., Kwon, D. K., Liu, Y., & Ding, J. B. (2022). Motor learning selectively strengthens cortical and striatal synapses of motor engram neurons. *Neuron*, *110*(17), 2790-2801.e2795. https://doi.org/10.1016/j.neuron.2022.06.006

Iain, E. P., Richard, W. M., Kristi, R. G., Stephanie, Q., Felicity, W., Margo, O. B., Philip, L. H., & Bernard, W. B. (2022). The motivational determinants of human action, their neural bases and functional impact in adolescents with OCD. *medRxiv*, 2022.2003.2019.22272645. https://doi.org/10.1101/2022.03.19.22272645

Ifuku, M., Katafuchi, T., Mawatari, S., Noda, M., Miake, K., Sugiyama, M., & Fujino, T. (2012). Anti-inflammatory/anti-amyloidogenic effects of plasmalogens in lipopolysaccharide-induced neuroinflammation in adult mice. *Journal of Neuroinflammation*, *9*, 197. https://doi.org/10.1186/1742-2094-9-197

Iguchi, Y., Lin, Z., Nishikawa, H., Minabe, Y., & Toda, S. (2017). Identification of an unconventional process of instrumental learning characteristically initiated with outcome devaluation-insensitivity and generalized action selection. *Scientific Reports*, *7*(1), 43307. https://doi.org/10.1038/srep43307

Iravani, M. M., Sadeghian, M., Leung, C. C., Jenner, P., & Rose, S. (2012). Lipopolysaccharide-induced nigral inflammation leads to increased IL-1β tissue content and expression of astrocytic glial cell line-derived neurotrophic factor. *Neurosci Lett*, *510*(2), 138-142. https://doi.org/10.1016/j.neulet.2012.01.022

Ismail, R., Parbo, P., Madsen, L. S., Hansen, A. K., Hansen, K. V., Schaldemose, J. L., Kjeldsen, P. L., Stokholm, M. G., Gottrup, H., Eskildsen, S. F., & Brooks, D. J. (2020). The relationships

between neuroinflammation, beta-amyloid and tau deposition in Alzheimer's disease: a longitudinal PET study. *Journal of Neuroinflammation*, *17*(1), 151. https://doi.org/10.1186/s12974-020-01820-6

Ito, M., Komai, K., Mise-Omata, S., Iizuka-Koga, M., Noguchi, Y., Kondo, T., Sakai, R., Matsuo, K., Nakayama, T., Yoshie, O., Nakatsukasa, H., Chikuma, S., Shichita, T., & Yoshimura, A. (2019). Brain regulatory T cells suppress astrogliosis and potentiate neurological recovery. *Nature*, *565*(7738), 246-250. https://doi.org/10.1038/s41586-018-0824-5

Iwata, A., Chen, X. H., McIntosh, T. K., Browne, K. D., & Smith, D. H. (2002). Long-term accumulation of amyloid-beta in axons following brain trauma without persistent upregulation of amyloid precursor protein genes. *J Neuropathol Exp Neurol*, *61*(12), 1056-1068. https://doi.org/10.1093/jnen/61.12.1056

Jack, C. R., Bennett, D. A., Blennow, K., Carrillo, M. C., Dunn, B., Haeberlein, S. B., Holtzman, D. M., Jagust, W., Jessen, F., Karlawish, J., Liu, E., Molinuevo, J. L., Montine, T., Phelps, C., Rankin, K. P., Rowe, C. C., Scheltens, P., Siemers, E., Snyder, H. M., . . . Silverberg, N. (2018). NIA-AA Research Framework: Toward a biological definition of Alzheimer's disease. *Alzheimer's & Dementia*, *14*(4), 535-562. https://doi.org/https://doi.org/10.1016/j.jalz.2018.02.018

Jackson, R. J., Meltzer, J. C., Nguyen, H., Commins, C., Bennett, R. E., Hudry, E., & Hyman, B. T. (2022). APOE4 derived from astrocytes leads to blood–brain barrier impairment. *Brain*, *145*(10), 3582-3593. https://doi.org/10.1093/brain/awab478

Jafari, M., Schumacher, A.-M., Snaidero, N., Neziraj, T., Gavilanes, E., Jürgens, T., Weidinger, J., Schmidt, S., Beltrán, E., Hagan, N., Woodworth, L., Ofengeim, D., Gans, J., Wolf, F., Kreutzfeldt, M., Portugues, R., Merkler, D., Misgeld, T., & Kerschensteiner, M. (2019). *Localized calcium accumulations prime synapses for phagocyte removal in cortical neuroinflammation*. https://doi.org/10.1101/758193

Jain, S., Yoon, S. Y., Leung, L., Knoferle, J., & Huang, Y. (2013). Cellular Source-Specific Effects of Apolipoprotein (Apo) E4 on Dendrite Arborization and Dendritic Spine Development. *PLOS ONE*, *8*(3), e59478. https://doi.org/10.1371/journal.pone.0059478

Janelsins, M. C., Mastrangelo, M. A., Park, K. M., Sudol, K. L., Narrow, W. C., Oddo, S., LaFerla, F. M., Callahan, L. M., Federoff, H. J., & Bowers, W. J. (2008). Chronic neuron-specific tumor necrosis factor-alpha expression enhances the local inflammatory environment ultimately leading to neuronal death in 3xTg-AD mice. *Am J Pathol*, *173*(6), 1768-1782. https://doi.org/10.2353/ajpath.2008.080528

Jang, Y. N., Jang, H., Kim, G. H., Noh, J. E., Chang, K. A., & Lee, K. J. (2021). RAPGEF2 mediates oligomeric Aβ-induced synaptic loss and cognitive dysfunction in the 3xTg-AD mouse model of Alzheimer's disease. *Neuropathol Appl Neurobiol*, *47*(5), 625-639. https://doi.org/10.1111/nan.12686

Jay, T. M., & Witter, M. P. (1991). Distribution of hippocampal CA1 and subicular efferents in the prefrontal cortex of the rat studied by means of anterograde transport of Phaseolus vulgaris-leucoagglutinin. *J Comp Neurol*, *313*(4), 574-586. https://doi.org/10.1002/cne.903130404

Jay, T. R., Hirsch, A. M., Broihier, M. L., Miller, C. M., Neilson, L. E., Ransohoff, R. M., Lamb, B. T., & Landreth, G. E. (2017). Disease Progression-Dependent Effects of TREM2 Deficiency in a Mouse Model of Alzheimer's Disease. *J Neurosci*, *37*(3), 637-647. https://doi.org/10.1523/jneurosci.2110-16.2016

Jay, T. R., Miller, C. M., Cheng, P. J., Graham, L. C., Bemiller, S., Broihier, M. L., Xu, G., Margevicius, D., Karlo, J. C., Sousa, G. L., Cotleur, A. C., Butovsky, O., Bekris, L., Staugaitis, S. M., Leverenz, J. B., Pimplikar, S. W., Landreth, G. E., Howell, G. R., Ransohoff, R. M., & Lamb, B. T. (2015). TREM2 deficiency eliminates TREM2+ inflammatory macrophages and ameliorates pathology in Alzheimer's disease mouse models. *Journal of Experimental Medicine*, *212*(3), 287-295. https://doi.org/10.1084/jem.20142322

Jayaraman, A., Htike, T. T., James, R., Picon, C., & Reynolds, R. (2021). TNF-mediated neuroinflammation is linked to neuronal necroptosis in Alzheimer's disease hippocampus.

Acta Neuropathologica Communications, *9*(1), 159. https://doi.org/10.1186/s40478-021-01264-w

Jeong, W., Hyein, L., Cho, S., & Seo, J. (2019). ApoE4-Induced Cholesterol Dysregulation and Its Brain Cell Type-Specific Implications in the Pathogenesis of Alzheimer's Disease. *Molecules and cells*, *42*. https://doi.org/10.14348/molcells.2019.0200

Jessen, N. A., Munk, A. S., Lundgaard, I., & Nedergaard, M. (2015). The Glymphatic System: A Beginner's Guide. *Neurochem Res*, *40*(12), 2583-2599. https://doi.org/10.1007/s11064-015-1581-6

Ji, Q., Yang, Y., Xiong, Y., Zhang, Y.-J., Jiang, J., Zhou, L.-P., Du, X.-H., Wang, C.-X., & Zhu, Z.-R. (2023). Blockade of adenosine A2A receptors reverses early spatial memory defects in the APP/PS1 mouse model of Alzheimer's disease by promoting synaptic plasticity of adult-born granule cells. *Alzheimer's Research & Therapy*, *15*. https://doi.org/10.1186/s13195-023-01337-z

Ji, Y., Gong, Y., Gan, W., Beach, T., Holtzman, D. M., & Wisniewski, T. (2003). Apolipoprotein E isoform-specific regulation of dendritic spine morphology in apolipoprotein E transgenic mice and Alzheimer's disease patients. *Neuroscience*, *122*(2), 305-315. https://doi.org/https://doi.org/10.1016/j.neuroscience.2003.08.007

Jiang, J., Tang, B., Wang, L., Huo, Q., Tan, S., Misrani, A., Han, Y., Li, H., Hu, H., Wang, J., Cheng, T., Tabassum, S., Chen, M., Xie, W., Long, C., & Yang, L. (2022). Systemic LPS-induced microglial activation results in increased GABAergic tone: A mechanism of protection against neuroinflammation in the medial prefrontal cortex in mice. *Brain, Behavior, and Immunity*, *99*, 53-69. https://doi.org/https://doi.org/10.1016/j.bbi.2021.09.017

Jiang, T., Tan, L., Zhu, X.-C., Zhang, Q.-Q., Cao, L., Tan, M.-S., Gu, L.-Z., Wang, H.-F., Ding, Z.-Z., Zhang, Y.-D., & Yu, J.-T. (2014). Upregulation of TREM2 Ameliorates Neuropathology and Rescues Spatial Cognitive Impairment in a Transgenic Mouse Model of Alzheimer's Disease. *Neuropsychopharmacology*, *39*(13), 2949-2962. https://doi.org/10.1038/npp.2014.164

Jiang, Y., Li, Z., Ma, H., Cao, X., Liu, F., Tian, A., Sun, X., Li, X., & Wang, J. (2018). Upregulation of TREM2 Ameliorates Neuroinflammatory Responses and Improves Cognitive Deficits Triggered by Surgical Trauma in Appswe/PS1dE9 Mice. *Cellular Physiology and Biochemistry*, *46*(4), 1398-1411. https://doi.org/10.1159/000489155

Jin, M., Jang, E., & Suk, K. (2014). Lipocalin-2 Acts as a Neuroinflammatogen in Lipopolysaccharide-injected Mice. *Experimental neurobiology*, *23*, 155-162. https://doi.org/10.5607/en.2014.23.2.155

Jing, W., Gangadhara, R. S., Yujiao, L., Uday, P. P., Fulei, T., Karah, M. G., Pornjittra, L. M., Rajeshwar, R. T., Ratna, K. V., & Darrell, W. B. (2020). Astrocyte-Derived Estrogen Regulates Reactive Astrogliosis and is Neuroprotective following Ischemic Brain Injury. *The Journal of Neuroscience*, *40*(50), 9751. https://doi.org/10.1523/JNEUROSCI.0888-20.2020

Johansson, M., Stomrud, E., Lindberg, O., Westman, E., Johansson, P. M., van Westen, D., Mattsson, N., & Hansson, O. (2020). Apathy and anxiety are early markers of Alzheimer's disease. *Neurobiol Aging*, *85*, 74-82. https://doi.org/10.1016/j.neurobiolaging.2019.10.008

Jonsson, T., Stefansson, H., Steinberg, S., Jonsdottir, I., Jonsson, P. V., Snaedal, J., Bjornsson, S., Huttenlocher, J., Levey, A. I., Lah, J. J., Rujescu, D., Hampel, H., Giegling, I., Andreassen, O. A., Engedal, K., Ulstein, I., Djurovic, S., Ibrahim-Verbaas, C., Hofman, A., . . . Stefansson, K. (2013). Variant of TREM2 Associated with the Risk of Alzheimer's Disease. *New England Journal of Medicine*, *368*(2), 107-116. https://doi.org/doi:10.1056/NEJMoa1211103

Jung, H., Lee, D., You, H., Lee, M., Kim, H., Cheong, E., & Um, J. W. (2023). LPS induces microglial activation and GABAergic synaptic deficits in the hippocampus accompanied by prolonged cognitive impairment. *Scientific Reports*, *13*(1), 6547. https://doi.org/10.1038/s41598-023-32798-9

Kabir, M. T., Uddin, M. S., Setu, J. R., Ashraf, G. M., Bin-Jumah, M. N., & Abdel-Daim, M. M. (2020). Exploring the Role of PSEN Mutations in the Pathogenesis of Alzheimer's Disease. *Neurotox Res*, *38*(4), 833-849. https://doi.org/10.1007/s12640-020-00232-x

Kadlecova, M., Freude, K., & Haukedal, H. (2023). Complexity of Sex Differences and Their Impact on Alzheimer’s Disease. *Biomedicines*, *11*(5), 1261. https://www.mdpi.com/2227-9059/11/5/1261

Karch, C. M., & Goate, A. M. (2015). Alzheimer's Disease Risk Genes and Mechanisms of Disease Pathogenesis. *Biological Psychiatry*, *77*(1), 43-51. https://doi.org/https://doi.org/10.1016/j.biopsych.2014.05.006

Keefer, S. E., Bacharach, S. Z., Kochli, D. E., Chabot, J. M., & Calu, D. J. (2020). Effects of Limited and Extended Pavlovian Training on Devaluation Sensitivity of Sign- and Goal-Tracking Rats [Original Research]. *Frontiers in Behavioral Neuroscience*, *14*. https://doi.org/10.3389/fnbeh.2020.00003

Kelleher, R. J., 3rd, & Shen, J. (2017). Presenilin-1 mutations and Alzheimer's disease. *Proc Natl Acad Sci U S A*, *114*(4), 629-631. https://doi.org/10.1073/pnas.1619574114

Kennedy, P. J., & Shapiro, M. L. (2009). Motivational states activate distinct hippocampal representations to guide goal-directed behaviors. *Proc Natl Acad Sci U S A*, *106*(26), 10805-10810. https://doi.org/10.1073/pnas.0903259106

Keren-Shaul, H., Spinrad, A., Weiner, A., Matcovitch-Natan, O., Dvir-Szternfeld, R., Ulland, T. K., David, E., Baruch, K., Lara-Astaiso, D., Toth, B., Itzkovitz, S., Colonna, M., Schwartz, M., & Amit, I. (2017). A Unique Microglia Type Associated with Restricting Development of Alzheimer’s Disease. *Cell*, *169*(7), 1276-1290.e1217. https://doi.org/10.1016/j.cell.2017.05.018

Keszycki, R. M., Fisher, D. W., & Dong, H. (2019). The Hyperactivity–Impulsivity–Irritiability–Disinhibition–Aggression–Agitation Domain in Alzheimer's Disease: Current Management and Future Directions [Review]. *Frontiers in Pharmacology*, *10*. https://doi.org/10.3389/fphar.2019.01109

Khattar, K. E., Safi, J., Rodriguez, A. M., & Vignais, M. L. (2022). Intercellular Communication in the Brain through Tunneling Nanotubes. *Cancers (Basel)*, *14*(5). https://doi.org/10.3390/cancers14051207

Kigerl, K. A., de Rivero Vaccari, J. P., Dietrich, W. D., Popovich, P. G., & Keane, R. W. (2014). Pattern recognition receptors and central nervous system repair. *Exp Neurol*, *258*, 5-16. https://doi.org/10.1016/j.expneurol.2014.01.001

Kim, C. K., Lee, Y. R., Ong, L., Gold, M., Kalali, A., & Sarkar, J. (2022). Alzheimer's Disease: Key Insights from Two Decades of Clinical Trial Failures. *J Alzheimers Dis*, *87*(1), 83-100. https://doi.org/10.3233/jad-215699

Kim, J. J., & Fanselow, M. S. (1992). Modality-specific retrograde amnesia of fear. *Science*, *256*(5057), 675-677. https://doi.org/10.1126/science.1585183

Kim, M., Suh, J., Romano, D., Truong, M. H., Mullin, K., Hooli, B., Norton, D., Tesco, G., Elliott, K., Wagner, S. L., Moir, R. D., Becker, K. D., & Tanzi, R. E. (2009). Potential late-onset Alzheimer's disease-associated mutations in the ADAM10 gene attenuate α-secretase activity. *Human Molecular Genetics*, *18*(20), 3987-3996. https://doi.org/10.1093/hmg/ddp323

Kim, W., Lee, S., & Hall, G. F. (2010). Secretion of human tau fragments resembling CSF-tau in Alzheimer's disease is modulated by the presence of the exon 2 insert. *FEBS Lett*, *584*(14), 3085-3088. https://doi.org/10.1016/j.febslet.2010.05.042

Kimura, R., & Ohno, M. (2009). Impairments in remote memory stabilization precede hippocampal synaptic and cognitive failures in 5XFAD Alzheimer mouse model. *Neurobiol Dis*, *33*(2), 229-235. https://doi.org/10.1016/j.nbd.2008.10.006

Kiraly, M., Foss, J. F., & Giordano, T. (2023). Neuroinflammation, Its Role in Alzheimer's Disease and Therapeutic Strategies. *The Journal of Prevention of Alzheimer's Disease*, *10*(4), 686-698. https://doi.org/10.14283/jpad.2023.109

Kishimoto, Y., Fukumoto, K., Nagai, M., Mizuguchi, A., & Kobashi, Y. (2017). Early Contextual Fear Memory Deficits in a Double-Transgenic Amyloid-β Precursor Protein/Presenilin 2 Mouse

Model of Alzheimer's Disease. *Int J Alzheimers Dis*, *2017*, 8584205. https://doi.org/10.1155/2017/8584205

Kitazawa, M., Cheng, D., Tsukamoto, M. R., Koike, M. A., Wes, P. D., Vasilevko, V., Cribbs, D. H., & LaFerla, F. M. (2011). Blocking IL-1 signaling rescues cognition, attenuates tau pathology, and restores neuronal β-catenin pathway function in an Alzheimer's disease model. *J Immunol*, *187*(12), 6539-6549. https://doi.org/10.4049/jimmunol.1100620

Kitazawa, M., Medeiros, R., & Laferla, F. M. (2012). Transgenic mouse models of Alzheimer disease: developing a better model as a tool for therapeutic interventions. *Curr Pharm Des*, *18*(8), 1131-1147. https://doi.org/10.2174/138161212799315786

Kleinberger, G., Yamanishi, Y., Suárez-Calvet, M., Czirr, E., Lohmann, E., Cuyvers, E., Struyfs, H., Pettkus, N., Wenninger-Weinzierl, A., Mazaheri, F., Tahirovic, S., Lleó, A., Alcolea, D., Fortea, J., Willem, M., Lammich, S., Molinuevo, J. L., Sánchez-Valle, R., Antonell, A., . . . Haass, C. (2014). TREM2 mutations implicated in neurodegeneration impair cell surface transport and phagocytosis. *Science Translational Medicine*, *6*(243), 243ra286-243ra286. https://doi.org/10.1126/scitranslmed.3009093

Klimentidis, Y. C., Raichlen, D. A., Bea, J., Garcia, D. O., Wineinger, N. E., Mandarino, L. J., Alexander, G. E., Chen, Z., & Going, S. B. (2018). Genome-wide association study of habitual physical activity in over 377,000 UK Biobank participants identifies multiple variants including CADM2 and APOE. *Int J Obes (Lond)*, *42*(6), 1161-1176. https://doi.org/10.1038/s41366-018-0120-3

Knopp, R. C., Baumann, K. K., Wilson, M. L., Banks, W. A., & Erickson, M. A. (2022). Amyloid Beta Pathology Exacerbates Weight Loss and Brain Cytokine Responses following Low-Dose Lipopolysaccharide in Aged Female Tg2576 Mice. *International Journal of Molecular Sciences*, *23*(4).

Knouff, C., Hinsdale, M. E., Mezdour, H., Altenburg, M. K., Watanabe, M., Quarfordt, S. H., Sullivan, P. M., & Maeda, N. (1999). Apo E structure determines VLDL clearance and atherosclerosis risk in mice. *The Journal of clinical investigation*, *103*(11), 1579-1586. https://doi.org/10.1172/jci6172

Komada, M., Takao, K., & Miyakawa, T. (2008). Elevated plus maze for mice. *J Vis Exp*(22). https://doi.org/10.3791/1088

Kondo, T., Yada, Y., Ikeuchi, T., & Inoue, H. (2023). CDiP technology for reverse engineering of sporadic Alzheimer's disease. *Journal of Human Genetics*, *68*(3), 231-235. https://doi.org/10.1038/s10038-022-01047-8

Koordeman, R., Anschutz, D. J., van Baaren, R. B., & Engels, R. C. (2011). Effects of alcohol portrayals in movies on actual alcohol consumption: an observational experimental study. *Addiction*, *106*(3), 547-554.

Kopeikina, K. J., Carlson, G. A., Pitstick, R., Ludvigson, A. E., Peters, A., Luebke, J. I., Koffie, R. M., Frosch, M. P., Hyman, B. T., & Spires-Jones, T. L. (2011). Tau Accumulation Causes Mitochondrial Distribution Deficits in Neurons in a Mouse Model of Tauopathy and in Human Alzheimer's Disease Brain. *The American Journal of Pathology*, *179*(4), 2071-2082. https://doi.org/10.1016/j.ajpath.2011.07.004

Kopeikina, K. J., Hyman, B. T., & Spires-Jones, T. L. (2012). Soluble forms of tau are toxic in Alzheimer's disease. *Transl Neurosci*, *3*(3), 223-233. https://doi.org/10.2478/s13380-012-0032-y

Koskinen, M., Bertling, E., & Hotulainen, P. (2012). Chapter three - Methods to Measure Actin Treadmilling Rate in Dendritic Spines. In P. M. Conn (Ed.), *Methods in Enzymology* (Vol. 505, pp. 47-58). Academic Press. https://doi.org/https://doi.org/10.1016/B978-0-12-388448-0.00011-5

Koss, W. A., & Frick, K. M. (2017). Sex differences in hippocampal function. *Journal of Neuroscience Research*, *95*(1-2), 539-562. https://doi.org/https://doi.org/10.1002/jnr.23864

Krasemann, S., Madore, C., Cialic, R., Baufeld, C., Calcagno, N., El Fatimy, R., Beckers, L., O'Loughlin, E., Xu, Y., Fanek, Z., Greco, D. J., Smith, S. T., Tweet, G., Humulock, Z., Zrzavy, T., Conde-Sanroman, P., Gacias, M., Weng, Z., Chen, H., . . . Butovsky, O. (2017). The TREM2-APOE

Pathway Drives the Transcriptional Phenotype of Dysfunctional Microglia in Neurodegenerative Diseases. *Immunity*, *47*(3), 566-581.e569. https://doi.org/https://doi.org/10.1016/j.immuni.2017.08.008

Kruman, I. I., Nath, A., & Mattson, M. P. (1998). HIV-1 Protein Tat Induces Apoptosis of Hippocampal Neurons by a Mechanism Involving Caspase Activation, Calcium Overload, and Oxidative Stress. *Experimental Neurology*, *154*(2), 276-288. https://doi.org/https://doi.org/10.1006/exnr.1998.6958

Kueper, J. K., Speechley, M., & Montero-Odasso, M. (2018). The Alzheimer's Disease Assessment Scale-Cognitive Subscale (ADAS-Cog): Modifications and Responsiveness in Pre-Dementia Populations. A Narrative Review. *J Alzheimers Dis*, *63*(2), 423-444. https://doi.org/10.3233/jad-170991

Kulkarni, S. K., Singh, K., & Bishnoi, M. (2007). Elevated zero maze: a paradigm to evaluate antianxiety effects of drugs. *Methods Find Exp Clin Pharmacol*, *29*(5), 343-348. https://doi.org/10.1358/mf.2007.29.5.1117557

Kunis, G., Baruch, K., Rosenzweig, N., Kertser, A., Miller, O., Berkutzki, T., & Schwartz, M. (2013). IFN-γ-dependent activation of the brain's choroid plexus for CNS immune surveillance and repair. *Brain*, *136*(Pt 11), 3427-3440. https://doi.org/10.1093/brain/awt259

LaFlamme, E. M., Ahmed, F., Forcelli, P. A., & Malkova, L. (2022). Macaques fail to develop habit responses during extended training on a reinforcer devaluation task. *Behav Neurosci*, *136*(2), 159-171. https://doi.org/10.1037/bne0000503

Lambert, J. C., Heath, S., Even, G., Campion, D., Sleegers, K., Hiltunen, M., Combarros, O., Zelenika, D., Bullido, M. J., Tavernier, B., Letenneur, L., Bettens, K., Berr, C., Pasquier, F., Fiévet, N., Barberger-Gateau, P., Engelborghs, S., De Deyn, P., Mateo, I., . . . Amouyel, P. (2009). Genome-wide association study identifies variants at CLU and CR1 associated with Alzheimer's disease. *Nat Genet*, *41*(10), 1094-1099. https://doi.org/10.1038/ng.439

Lanoiselée, H. M., Nicolas, G., Wallon, D., Rovelet-Lecrux, A., Lacour, M., Rousseau, S., Richard, A. C., Pasquier, F., Rollin-Sillaire, A., Martinaud, O., Quillard-Muraine, M., de la Sayette, V., Boutoleau-Bretonniere, C., Etcharry-Bouyx, F., Chauviré, V., Sarazin, M., le Ber, I., Epelbaum, S., Jonveaux, T., . . . Campion, D. (2017). APP, PSEN1, and PSEN2 mutations in early-onset Alzheimer disease: A genetic screening study of familial and sporadic cases. *PLoS Med*, *14*(3), e1002270. https://doi.org/10.1371/journal.pmed.1002270

Lara Aparicio, S. Y., Laureani Fierro, Á. D., Aranda Abreu, G. E., Toledo Cárdenas, R., García Hernández, L. I., Coria Ávila, G. A., Rojas Durán, F., Aguilar, M. E., Manzo Denes, J., Chi-Castañeda, L. D., & Pérez Estudillo, C. A. (2022). Current Opinion on the Use of c-Fos in Neuroscience. *NeuroSci*, *3*(4), 687-702.

LaRocca, T. J., Cavalier, A. N., Roberts, C. M., Lemieux, M. R., Ramesh, P., Garcia, M. A., & Link, C. D. (2021). Amyloid beta acts synergistically as a pro-inflammatory cytokine. *Neurobiology of Disease*, *159*, 105493. https://doi.org/https://doi.org/10.1016/j.nbd.2021.105493

Larson, M. E., Sherman, M. A., Greimel, S., Kuskowski, M., Schneider, J. A., Bennett, D. A., & Lesné, S. E. (2012). Soluble α-synuclein is a novel modulator of Alzheimer's disease pathophysiology. *J Neurosci*, *32*(30), 10253-10266. https://doi.org/10.1523/jneurosci.0581-12.2012

Launer, L. J. (2005). The epidemiologic study of dementia: a life-long quest? *Neurobiology of Aging*, *26*(3), 335-340. https://doi.org/https://doi.org/10.1016/j.neurobiolaging.2004.03.016

Laurberg, S. (1979). Commissural and intrinsic connections of the rat hippocampus [https://doi.org/10.1002/cne.901840405]. *Journal of Comparative Neurology*, *184*(4), 685-708. https://doi.org/https://doi.org/10.1002/cne.901840405

Lawton, M. P., & Brody, E. M. (1969). Assessment of Older People: Self-Maintaining and Instrumental Activities of Daily Living1. *The Gerontologist*, *9*(3_Part_1), 179-186. https://doi.org/10.1093/geront/9.3_Part_1.179

Le, A. A., Lauterborn, J. C., Jia, Y., Wang, W., Cox, C. D., Gall, C. M., & Lynch, G. (2022). Prepubescent female rodents have enhanced hippocampal LTP and learning relative to males, reversing in

adulthood as inhibition increases. *Nature Neuroscience*, *25*(2), 180-190. https://doi.org/10.1038/s41593-021-01001-5

Lecca, D., Jung, Y. J., Scerba, M. T., Hwang, I., Kim, Y. K., Kim, S., Modrow, S., Tweedie, D., Hsueh, S.-C., Liu, D., Luo, W., Glotfelty, E., Li, Y., Wang, J.-Y., Luo, Y., Hoffer, B. J., Kim, D. S., McDevitt, R. A., & Greig, N. H. (2022). Role of chronic neuroinflammation in neuroplasticity and cognitive function: A hypothesis. *Alzheimer's & Dementia*, *18*(11), 2327-2340. https://doi.org/https://doi.org/10.1002/alz.12610

Leduc, V., Jasmin-Bélanger, S., & Poirier, J. (2010). APOE and cholesterol homeostasis in Alzheimer's disease. *Trends in Molecular Medicine*, *16*(10), 469-477. https://doi.org/https://doi.org/10.1016/j.molmed.2010.07.008

Lee, J. W., Lee, Y. K., Yuk, D. Y., Choi, D. Y., Ban, S. B., Oh, K. W., & Hong, J. T. (2008). Neuro-inflammation induced by lipopolysaccharide causes cognitive impairment through enhancement of beta-amyloid generation. *Journal of Neuroinflammation*, *5*(1), 37. https://doi.org/10.1186/1742-2094-5-37

Lee, S., Devanney, N. A., Golden, L. R., Smith, C. T., Schwartz, J. L., Walsh, A. E., Clarke, H. A., Goulding, D. S., Allenger, E. J., Morillo-Segovia, G., Friday, C. M., Gorman, A. A., Hawkinson, T. R., MacLean, S. M., Williams, H. C., Sun, R. C., Morganti, J. M., & Johnson, L. A. (2023). APOE modulates microglial immunometabolism in response to age, amyloid pathology, and inflammatory challenge. *Cell Reports*, *42*(3), 112196. https://doi.org/https://doi.org/10.1016/j.celrep.2023.112196

Leng, F., Hinz, R., Gentleman, S., Hampshire, A., Dani, M., Brooks, D. J., & Edison, P. (2023). Neuroinflammation is independently associated with brain network dysfunction in Alzheimer's disease. *Molecular Psychiatry*, *28*(3), 1303-1311. https://doi.org/10.1038/s41380-022-01878-z

Leuner, K., Schütt, T., Kurz, C., Eckert, S. H., Schiller, C., Occhipinti, A., Mai, S., Jendrach, M., Eckert, G. P., Kruse, S. E., Palmiter, R. D., Brandt, U., Dröse, S., Wittig, I., Willem, M., Haass, C., Reichert, A. S., & Müller, W. E. (2012). Mitochondrion-derived reactive oxygen species lead to enhanced amyloid beta formation. *Antioxid Redox Signal*, *16*(12), 1421-1433. https://doi.org/10.1089/ars.2011.4173

Leung, L., Andrews-Zwilling, Y., Yoon, S., Jain, S., Ring, K., Dai, J., Mü, M., Tong, L., Walker, D., & Huang, Y. (2012). Apolipoprotein E4 Causes Age- and Sex-Dependent Impairments of Hilar GABAergic Interneurons and Learning and Memory Deficits in Mice. *PLOS ONE*, *7*, e53569. https://doi.org/10.1371/journal.pone.0053569

Li, G., & Pleasure, S. J. (2013). Chapter 18 - Migration in the Hippocampus. In J. L. R. Rubenstein & P. Rakic (Eds.), *Cellular Migration and Formation of Neuronal Connections* (pp. 331-343). Academic Press. https://doi.org/https://doi.org/10.1016/B978-0-12-397266-8.00029-6

Li, W., Risacher, S. L., McAllister, T. W., & Saykin, A. J. (2016). Traumatic brain injury and age at onset of cognitive impairment in older adults. *Journal of Neurology*, *263*(7), 1280-1285. https://doi.org/10.1007/s00415-016-8093-4

Li, X.-C., Hu, Y., Wang, Z.-h., Luo, Y., Zhang, Y., Liu, X.-P., Feng, Q., Wang, Q., Ye, K., Liu, G.-P., & Wang, J.-Z. (2016). Human wild-type full-length tau accumulation disrupts mitochondrial dynamics and the functions via increasing mitofusins. *Scientific Reports*, *6*(1), 24756. https://doi.org/10.1038/srep24756

Li, X., Feng, X., Sun, X., Hou, N., Han, F., & Liu, Y. (2022). Global, regional, and national burden of Alzheimer's disease and other dementias, 1990-2019. *Front Aging Neurosci*, *14*, 937486. https://doi.org/10.3389/fnagi.2022.937486

Li, Y.-M., Xu, M., Lai, M.-T., Huang, Q., Castro, J. L., DiMuzio-Mower, J., Harrison, T., Lellis, C., Nadin, A. J., Neduvelil, J. G., Register, R. B., Sardana, M. K., Shearman, M. S., Smith, A. L., Shi, X.-p., Yin, K.-c., Shafer, J. A., & Gardell, S. J. (2000). Photoactivated γ-secretase inhibitors directed to the active site covalently label presenilin 1. *Nature*, *405*, 689-694.

Liao, F., Zhang, T. J., Jiang, H., Lefton, K. B., Robinson, G. O., Vassar, R., Sullivan, P. M., & Holtzman, D. M. (2015). Murine versus human apolipoprotein E4: differential facilitation of and co-localization in cerebral amyloid angiopathy and amyloid plaques in APP transgenic mouse models. *Acta Neuropathologica Communications*, *3*(1), 70. https://doi.org/10.1186/s40478-015-0250-y

Lin, L.-y., Zhang, J., Dai, X.-m., Xiao, N.-a., Wu, X.-l., Wei, Z., Fang, W.-t., Zhu, Y.-g., & Chen, X.-c. (2016). Early-life stress leads to impaired spatial learning and memory in middle-aged ApoE4-TR mice. *Molecular Neurodegeneration*, *11*(1), 51. https://doi.org/10.1186/s13024-016-0107-2

Lin, L., Lo, L. H.-Y., Lyu, Q., & Lai, K.-O. (2017). Determination of dendritic spine morphology by the striatin scaffold protein STRN4 through interaction with the phosphatase PP2A. *Journal of Biological Chemistry*, *292*(23), 9451-9464. https://doi.org/https://doi.org/10.1074/jbc.M116.772442

Lin, Y., Dai, X., Zhang, J., & Chen, X. (2022). Metformin alleviates the depression-like behaviors of elderly apoE4 mice via improving glucose metabolism and mitochondrial biogenesis. *Behavioural Brain Research*, *423*, 113772. https://doi.org/https://doi.org/10.1016/j.bbr.2022.113772

Lisman, J. E. (1999). Relating Hippocampal Circuitry to Function: Recall of Memory Sequences by Reciprocal Dentate–CA3 Interactions. *Neuron*, *22*(2), 233-242. https://doi.org/10.1016/S0896-6273(00)81085-5

Liu, F., Zhang, Z., Zhang, L., Meng, R.-N., Gao, J., Jin, M., Li, M., & Wang, X.-P. (2022). Effect of metal ions on Alzheimer's disease [https://doi.org/10.1002/brb3.2527]. *Brain and Behavior*, *12*(3), e2527. https://doi.org/https://doi.org/10.1002/brb3.2527

Liu, J., Wang, J., Luo, H., Li, Z., Zhong, T.-Y., Tang, J., & Jiang, Y. (2017). Screening cytokine/chemokine profiles in serum and organs from an endotoxic shock mouse model by LiquiChip. *Science China. Life sciences*, *60*. https://doi.org/10.1007/s11427-016-9016-6

Liu, L., Zhang, H., Shi, Y., & Pan, L. (2020). Prostaglandin E1 Improves Cerebral Microcirculation Through Activation of Endothelial NOS and GRPCH1. *Journal of Molecular Neuroscience*, *70*(12), 2041-2048. https://doi.org/10.1007/s12031-020-01610-y

Liu, S., Wong, H. Y., Xie, L., Iqbal, Z., Lei, Z., Fu, Z., Lam, Y. Y., Ramkrishnan, A. S., & Li, Y. (2022). Astrocytes in CA1 modulate schema establishment in the hippocampal-cortical neuron network. *BMC Biology*, *20*(1), 250. https://doi.org/10.1186/s12915-022-01445-6

Loiola, R. A., Wickstead, E. S., Solito, E., & McArthur, S. (2019). Estrogen Promotes Pro-resolving Microglial Behavior and Phagocytic Cell Clearance Through the Actions of Annexin A1. *Front Endocrinol (Lausanne)*, *10*, 420. https://doi.org/10.3389/fendo.2019.00420

Lonnemann, N., Korte, M., & Hosseini, S. (2023). Repeated performance of spatial memory tasks ameliorates cognitive decline in APP/PS1 mice. *Behav Brain Res*, *438*, 114218. https://doi.org/10.1016/j.bbr.2022.114218

Lopez-Rojas, J., & Kreutz, M. (2016). Mature Granule Cells of the Dentate Gyrus - Passive Bystanders or Principal Performers in Hippocampal Function? *Neuroscience and biobehavioral reviews*, *64*. https://doi.org/10.1016/j.neubiorev.2016.02.021

Luo, H., Xiang, Y., Qu, X., Liu, H., Liu, C., Li, G., Han, L., & Qin, X. (2019). Apelin-13 Suppresses Neuroinflammation Against Cognitive Deficit in a Streptozotocin-Induced Rat Model of Alzheimer's Disease Through Activation of BDNF-TrkB Signaling Pathway [Original Research]. *Frontiers in Pharmacology*, *10*. https://doi.org/10.3389/fphar.2019.00395

Luo, R.-Y., Luo, C., Zhong, F., Shen, W.-Y., Li, H., Hu, Z., & Dai, R.-P. (2020). ProBDNF promotes sepsis-associated encephalopathy in mice by dampening the immune activity of meningeal CD4+ T cells. *Journal of Neuroinflammation*, *17*. https://doi.org/10.1186/s12974-020-01850-0

Lye, T. C., & Shores, E. A. (2000). Traumatic Brain Injury as a Risk Factor for Alzheimer's Disease: A Review. *Neuropsychology Review*, *10*(2), 115-129. https://doi.org/10.1023/A:1009068804787

Lynch, J. R., Tang, W., Wang, H., Vitek, M. P., Bennett, E. R., Sullivan, P. M., Warner, D. S., & Laskowitz, D. T. (2003). APOE Genotype and an ApoE-mimetic Peptide Modify the Systemic and Central

Nervous System Inflammatory Response*. *Journal of Biological Chemistry*, *278*(49), 48529-48533. https://doi.org/https://doi.org/10.1074/jbc.M306923200

Ma, S., & Zuo, Y. (2022). Synaptic modifications in learning and memory – A dendritic spine story. *Seminars in Cell & Developmental Biology*, *125*, 84-90. https://doi.org/https://doi.org/10.1016/j.semcdb.2021.05.015

MacLusky, N. J., Hajszan, T., Prange-Kiel, J., & Leranth, C. (2006). Androgen modulation of hippocampal synaptic plasticity. *Neuroscience*, *138*(3), 957-965. https://doi.org/10.1016/j.neuroscience.2005.12.054

Malm, T. M., Iivonen, H., Goldsteins, G., Keksa-Goldsteine, V., Ahtoniemi, T., Kanninen, K., Salminen, A., Auriola, S., Van Groen, T., Tanila, H., & Koistinaho, J. (2007). Pyrrolidine dithiocarbamate activates Akt and improves spatial learning in APP/PS1 mice without affecting beta-amyloid burden. *J Neurosci*, *27*(14), 3712-3721. https://doi.org/10.1523/jneurosci.0059-07.2007

Manabe, T., Rácz, I., Schwartz, S., Oberle, L., Santarelli, F., Emmrich, J. V., Neher, J. J., & Heneka, M. T. (2021). Systemic inflammation induced the delayed reduction of excitatory synapses in the CA3 during ageing [https://doi.org/10.1111/jnc.15491]. *Journal of Neurochemistry*, *159*(3), 525-542. https://doi.org/https://doi.org/10.1111/jnc.15491

Manczak, M., & Reddy, P. H. (2012). Abnormal interaction between the mitochondrial fission protein Drp1 and hyperphosphorylated tau in Alzheimer's disease neurons: implications for mitochondrial dysfunction and neuronal damage. *Human Molecular Genetics*, *21*(11), 2538-2547. https://doi.org/10.1093/hmg/dds072

Mangold, C. A., Wronowski, B., Du, M., Masser, D. R., Hadad, N., Bixler, G. V., Brucklacher, R. M., Ford, M. M., Sonntag, W. E., & Freeman, W. M. (2017). Sexually divergent induction of microglial-associated neuroinflammation with hippocampal aging. *Journal of Neuroinflammation*, *14*(1), 141. https://doi.org/10.1186/s12974-017-0920-8

Márquez, I., Muñoz, M. F., Ayala, A., López, J. C., Vargas, J. P., & Díaz, E. (2020). Effects on goal directed behavior and habit in two animal models of Parkinson's disease. *Neurobiology of Learning and Memory*, *169*, 107190. https://doi.org/https://doi.org/10.1016/j.nlm.2020.107190

Marshall, G. A., Amariglio, R. E., Sperling, R. A., & Rentz, D. M. (2012). Activities of daily living: where do they fit in the diagnosis of Alzheimer's disease? *Neurodegenerative Disease Management*, *2*(5), 483-491. https://doi.org/10.2217/nmt.12.55

Martínez-Morillo, E., Hansson, O., Atagi, Y., Bu, G., Minthon, L., Diamandis, E. P., & Nielsen, H. M. (2014). Total apolipoprotein E levels and specific isoform composition in cerebrospinal fluid and plasma from Alzheimer's disease patients and controls. *Acta Neuropathol*, *127*(5), 633-643. https://doi.org/10.1007/s00401-014-1266-2

Masahito, K., Rachid, K., Tiina, K., Cyrus, C., Jong Youl, K., Christine, L. H., Mary, C. N., & Midori, A. Y. (2015). Triggering Receptor Expressed on Myeloid Cells 2 (TREM2) Deficiency Attenuates Phagocytic Activities of Microglia and Exacerbates Ischemic Damage in Experimental Stroke. *The Journal of Neuroscience*, *35*(8), 3384. https://doi.org/10.1523/JNEUROSCI.2620-14.2015

Massagué, J. (2012). TGFβ signalling in context. *Nature reviews Molecular cell biology*, *13*(10), 616-630.

Matsui, T., Ingelsson, M., Fukumoto, H., Ramasamy, K., Kowa, H., Frosch, M. P., Irizarry, M. C., & Hyman, B. T. (2007). Expression of APP pathway mRNAs and proteins in Alzheimer's disease. *Brain Res*, *1161*, 116-123. https://doi.org/10.1016/j.brainres.2007.05.050

Mattsson, N., Palmqvist, S., Stomrud, E., Vogel, J., & Hansson, O. (2019). Staging β-Amyloid Pathology With Amyloid Positron Emission Tomography. *JAMA Neurology*, *76*(11), 1319-1329. https://doi.org/10.1001/jamaneurol.2019.2214

Maturana, W., Lobo, I., Landeira-Fernandez, J., & Mograbi, D. C. (2023). Nondeclarative associative learning in Alzheimer's disease: An overview of eyeblink, fear, and other emotion-based conditioning. *Physiology & Behavior*, *268*, 114250. https://doi.org/https://doi.org/10.1016/j.physbeh.2023.114250

Mauch, D. H., Nägler, K., Schumacher, S., Göritz, C., Müller, E.-C., Otto, A., & Pfrieger, F. W. (2001). CNS Synaptogenesis Promoted by Glia-Derived Cholesterol. *Science*, *294*(5545), 1354-1357. https://doi.org/10.1126/science.294.5545.1354

McIlwain, K. L., Merriweather, M. Y., Yuva-Paylor, L. A., & Paylor, R. (2001). The use of behavioral test batteries: Effects of training history. *Physiology & Behavior*, *73*(5), 705-717. https://doi.org/https://doi.org/10.1016/S0031-9384(01)00528-5

McKhann, G., Drachman, D., Folstein, M., Katzman, R., Price, D., & Stadlan, E. M. (1984). Clinical diagnosis of Alzheimer's disease. *Neurology*, *34*(7), 939-939. https://doi.org/10.1212/WNL.34.7.939

McKhann, G. M., Knopman, D. S., Chertkow, H., Hyman, B. T., Jack, C. R., Jr., Kawas, C. H., Klunk, W. E., Koroshetz, W. J., Manly, J. J., Mayeux, R., Mohs, R. C., Morris, J. C., Rossor, M. N., Scheltens, P., Carrillo, M. C., Thies, B., Weintraub, S., & Phelps, C. H. (2011). The diagnosis of dementia due to Alzheimer's disease: recommendations from the National Institute on Aging-Alzheimer's Association workgroups on diagnostic guidelines for Alzheimer's disease. *Alzheimers Dement*, *7*(3), 263-269. https://doi.org/10.1016/j.jalz.2011.03.005

McNab, F., Mayer-Barber, K., Sher, A., Wack, A., & O'Garra, A. (2015). Type I interferons in infectious disease. *Nat Rev Immunol*, *15*(2), 87-103. https://doi.org/10.1038/nri3787

Medina, M., & Avila, J. (2014). The role of extracellular Tau in the spreading of neurofibrillary pathology [Review]. *Frontiers in Cellular Neuroscience*, *8*. https://doi.org/10.3389/fncel.2014.00113

Mehla, J., Pahuja, M., & Gupta, Y. K. (2013). Streptozotocin-induced sporadic Alzheimer's disease: selection of appropriate dose. *Journal of Alzheimer's disease : JAD*, *33*(1), 17-21. https://doi.org/10.3233/jad-2012-120958

Mendez, M. F. (2021). The Relationship Between Anxiety and Alzheimer's Disease. *J Alzheimers Dis Rep*, *5*(1), 171-177. https://doi.org/10.3233/adr-210294

Mercer, A., & Thomson, A. M. (2017). Cornu Ammonis Regions–Antecedents of Cortical Layers? [Review]. *Frontiers in Neuroanatomy*, *11*. https://doi.org/10.3389/fnana.2017.00083

Merlini, A., Haberl, M., Strauß, J., Hildebrand, L., Genc, N., Franz, J., Chilov, D., Alitalo, K., Flügel-Koch, C., Stadelmann, C., Flügel, A., & Odoardi, F. (2022). Distinct roles of the meningeal layers in CNS autoimmunity. *Nat Neurosci*, *25*(7), 887-899. https://doi.org/10.1038/s41593-022-01108-3

Milatovic, D., Zaja-Milatovic, S., Montine, K. S., Horner, P. J., & Montine, T. J. (2003). Pharmacologic suppression of neuronal oxidative damage and dendritic degeneration following direct activation of glial innate immunity in mouse cerebrum. *Journal of Neurochemistry*, *87*(6), 1518-1526. https://doi.org/https://doi.org/10.1046/j.1471-4159.2003.02120.x

Minter, M. R., Taylor, J. M., & Crack, P. J. (2016). The contribution of neuroinflammation to amyloid toxicity in Alzheimer's disease. *Journal of Neurochemistry*, *136*(3), 457-474. https://doi.org/https://doi.org/10.1111/jnc.13411

Mitchell, A. S., & Chakraborty, S. (2013). What does the mediodorsal thalamus do? *Front Syst Neurosci*, *7*, 37. https://doi.org/10.3389/fnsys.2013.00037

Montagne, A., Nikolakopoulou, A. M., Huuskonen, M. T., Sagare, A. P., Lawson, E. J., Lazic, D., Rege, S. V., Grond, A., Zuniga, E., Barnes, S. R., Prince, J., Sagare, M., Hsu, C.-J., LaDu, M. J., Jacobs, R. E., & Zlokovic, B. V. (2021). APOE4 accelerates advanced-stage vascular and neurodegenerative disorder in old Alzheimer's mice via cyclophilin A independently of amyloid-β. *Nature Aging*, *1*(6), 506-520. https://doi.org/10.1038/s43587-021-00073-z

Monti, P. M., Binkoff, J. A., Abrams, D. B., Zwick, W. R., Nirenberg, T. D., & Liepman, M. R. (1987). Reactivity of alcoholics and nonalcoholics to drinking cues. *Journal of abnormal psychology*, *96*(2), 122.

Moretti, P., Levenson, J. M., Battaglia, F., Atkinson, R., Teague, R., Antalffy, B., Armstrong, D., Arancio, O., Sweatt, J. D., & Zoghbi, H. Y. (2006). Learning and memory and synaptic plasticity are

impaired in a mouse model of Rett syndrome. *J Neurosci*, *26*(1), 319-327. https://doi.org/10.1523/jneurosci.2623-05.2006

Morley, J. E., Armbrecht, H. J., Farr, S. A., & Kumar, V. B. (2012). The senescence accelerated mouse (SAMP8) as a model for oxidative stress and Alzheimer's disease. *Biochimica et Biophysica Acta (BBA) - Molecular Basis of Disease*, *1822*(5), 650-656. https://doi.org/https://doi.org/10.1016/j.bbadis.2011.11.015

Mormino, E. C., & Papp, K. V. (2018). Amyloid Accumulation and Cognitive Decline in Clinically Normal Older Individuals: Implications for Aging and Early Alzheimer's Disease. *J Alzheimers Dis*, *64*(s1), S633-s646. https://doi.org/10.3233/jad-179928

Morozova, V., Cohen, L. S., Makki, A. E.-H., Shur, A., Pilar, G., El Idrissi, A., & Alonso, A. D. (2019). Normal and Pathological Tau Uptake Mediated by M1/M3 Muscarinic Receptors Promotes Opposite Neuronal Changes [Original Research]. *Frontiers in Cellular Neuroscience*, *13*. https://doi.org/10.3389/fncel.2019.00403

Morris, R. W., Cyrzon, C., Green, M. J., Le Pelley, M. E., & Balleine, B. W. (2018). Impairments in action–outcome learning in schizophrenia. *Translational Psychiatry*, *8*(1), 54. https://doi.org/10.1038/s41398-018-0103-0

Mosconi, L., Rahman, A., Diaz, I., Wu, X., Scheyer, O., Hristov, H. W., Vallabhajosula, S., Isaacson, R. S., de Leon, M. J., & Brinton, R. D. (2018). Increased Alzheimer's risk during the menopause transition: a 3-year longitudinal brain imaging study. *PLOS ONE*, *13*(12), e0207885.

Moser, E., Moser, M. B., & Andersen, P. (1993). Spatial learning impairment parallels the magnitude of dorsal hippocampal lesions, but is hardly present following ventral lesions. *J Neurosci*, *13*(9), 3916-3925. https://doi.org/10.1523/jneurosci.13-09-03916.1993

Moser, M. B., Rowland, D. C., & Moser, E. I. (2015). Place cells, grid cells, and memory. *Cold Spring Harb Perspect Biol*, *7*(2), a021808. https://doi.org/10.1101/cshperspect.a021808

Mothes, T., Portal, B., Konstantinidis, E., Eltom, K., Libard, S., Streubel-Gallasch, L., Ingelsson, M., Rostami, J., Lindskog, M., & Erlandsson, A. (2023). Astrocytic uptake of neuronal corpses promotes cell-to-cell spreading of tau pathology. *Acta Neuropathologica Communications*, *11*(1), 97. https://doi.org/10.1186/s40478-023-01589-8

Mrdjen, D., Pavlovic, A., Hartmann, F. J., Schreiner, B., Utz, S. G., Leung, B. P., Lelios, I., Heppner, F. L., Kipnis, J., Merkler, D., Greter, M., & Becher, B. (2018). High-Dimensional Single-Cell Mapping of Central Nervous System Immune Cells Reveals Distinct Myeloid Subsets in Health, Aging, and Disease. *Immunity*, *48*(3), 599. https://doi.org/10.1016/j.immuni.2018.02.014

Mucke, L., Masliah, E., Yu, G. Q., Mallory, M., Rockenstein, E. M., Tatsuno, G., Hu, K., Kholodenko, D., Johnson-Wood, K., & McConlogue, L. (2000). High-level neuronal expression of abeta 1-42 in wild-type human amyloid protein precursor transgenic mice: synaptotoxicity without plaque formation. *J Neurosci*, *20*(11), 4050-4058. https://doi.org/10.1523/jneurosci.20-11-04050.2000

Mucke, L., & Selkoe, D. J. (2012). Neurotoxicity of amyloid β-protein: synaptic and network dysfunction. *Cold Spring Harb Perspect Med*, *2*(7), a006338. https://doi.org/10.1101/cshperspect.a006338

Muller, D., Oliver, M., & Lynch, G. (1989). Developmental changes in synaptic properties in hippocampus of neonatal rats. *Developmental Brain Research*, *49*(1), 105-114. https://doi.org/https://doi.org/10.1016/0165-3806(89)90063-1

Murcia, J. D. G., Schmutz, C., Munger, C., Perkes, A., Gustin, A., Peterson, M., Ebbert, M. T., Norton, M. C., Tschanz, J. T., & Munger, R. G. (2013). Assessment of TREM2 rs75932628 association with Alzheimer's disease in a population-based sample: the Cache County Study. *Neurobiology of Aging*, *34*(12), 2889. e2811-2889. e2813.

Musa, A., Lehrach, H., & Russo, V. A. (2001). Distinct expression patterns of two zebrafish homologues of the human APP gene during embryonic development. *Dev Genes Evol*, *211*(11), 563-567. https://doi.org/10.1007/s00427-001-0189-9

Nackenoff, A. G., Hohman, T. J., Neuner, S. M., Akers, C. S., Weitzel, N. C., Shostak, A., Ferguson, S. M., Mobley, B., Bennett, D. A., Schneider, J. A., Jefferson, A. L., Kaczorowski, C. C., & Schrag, M. S. (2021). PLD3 is a neuronal lysosomal phospholipase D associated with β-amyloid plaques and cognitive function in Alzheimer's disease. *PLOS Genetics*, *17*(4), e1009406. https://doi.org/10.1371/journal.pgen.1009406

Nalivaeva, N. N., Beckett, C., Belyaev, N. D., & Turner, A. J. (2012). Are amyloid-degrading enzymes viable therapeutic targets in Alzheimer's disease? *J Neurochem*, *120 Suppl 1*, 167-185. https://doi.org/10.1111/j.1471-4159.2011.07510.x

Nanclares, C., Baraibar, A. M., Araque, A., & Kofuji, P. (2021). Dysregulation of Astrocyte–Neuronal Communication in Alzheimer's Disease. *International Journal of Molecular Sciences*, *22*(15).

Nandi, A., Counts, N., Chen, S., Seligman, B., Tortorice, D., Vigo, D., & Bloom, D. E. (2022). Global and regional projections of the economic burden of Alzheimer's disease and related dementias from 2019 to 2050: A value of statistical life approach. *eClinicalMedicine*, *51*. https://doi.org/10.1016/j.eclinm.2022.101580

Nasrouei, S., Rattel, J. A., Liedlgruber, M., Marksteiner, J., & Wilhelm, F. H. (2020). Fear acquisition and extinction deficits in amnestic mild cognitive impairment and early Alzheimer's disease. *Neurobiol Aging*, *87*, 26-34. https://doi.org/10.1016/j.neurobiolaging.2019.11.003

Nathan, B. P., Chang, K.-C., Bellosta, S., Brisch, E., Ge, N., Mahley, R. W., & Pitas, R. E. (1995). The Inhibitory Effect of Apolipoprotein E4 on Neurite Outgrowth Is Associated with Microtubule Depolymerization (∗). *Journal of Biological Chemistry*, *270*(34), 19791-19799. https://doi.org/https://doi.org/10.1074/jbc.270.34.19791

Nenov, M. N., Malkov, A. E., Konakov, M. V., & Levin, S. G. (2019). Interleukin-10 and transforming growth factor-β1 facilitate long-term potentiation in CA1 region of hippocampus. *Biochemical and Biophysical Research Communications*, *518*(3), 486-491.

Neumann, H., & Takahashi, K. (2007). Essential role of the microglial triggering receptor expressed on myeloid cells-2 (TREM2) for central nervous tissue immune homeostasis. *Journal of Neuroimmunology*, *184*(1), 92-99. https://doi.org/https://doi.org/10.1016/j.jneuroim.2006.11.032

Neuner, S. M., Heuer, S. E., Huentelman, M. J., O'Connell, K. M. S., & Kaczorowski, C. C. (2019). Harnessing Genetic Complexity to Enhance Translatability of Alzheimer's Disease Mouse Models: A Path toward Precision Medicine. *Neuron*, *101*(3), 399-411.e395. https://doi.org/10.1016/j.neuron.2018.11.040

Neve, R., Harris, P., Kosik, K., Kurnit, D., & Donlon, T. (1986). Identification of cDNA clones for the human microtubule-associated protein tau and Abbkürzungsverzeichnis 56 chromosomal localization of the genes for tau and microtubule-associated protein 2. *Brain Res*, *387*, 271-280.

New Report Details the Setbacks and Challenges to Alzheimer's Research. (2018). Pharmaceutical Research and Manufacturers of America.

Nguyen, D., Dhanasekaran, P., Nickel, M., Mizuguchi, C., Watanabe, M., Saito, H., Phillips, M. C., & Lund-Katz, S. (2014). Influence of Domain Stability on the Properties of Human Apolipoprotein E3 and E4 and Mouse Apolipoprotein E. *Biochemistry*, *53*(24), 4025-4033. https://doi.org/10.1021/bi500340z

Nickel, W., & Rabouille, C. (2009). Mechanisms of regulated unconventional protein secretion. *Nat Rev Mol Cell Biol*, *10*(2), 148-155. https://doi.org/10.1038/nrm2617

Nicolas, G., Charbonnier, C., & Campion, D. (2016). From Common to Rare Variants: The Genetic Component of Alzheimer Disease. *Human Heredity*, *81*(3), 129-141. https://doi.org/10.1159/000452256

Nicolas, G., Charbonnier, C., Wallon, D., Quenez, O., Bellenguez, C., Grenier-Boley, B., Rousseau, S., Richard, A. C., Rovelet-Lecrux, A., Le Guennec, K., Bacq, D., Garnier, J. G., Olaso, R., Boland, A., Meyer, V., Deleuze, J. F., Amouyel, P., Munter, H. M., Bourque, G., . . . Campion, D. (2016).

SORL1 rare variants: a major risk factor for familial early-onset Alzheimer's disease. *Mol Psychiatry*, *21*(6), 831-836. https://doi.org/10.1038/mp.2015.121

Nimchinsky, E. A., Sabatini, B. L., & Svoboda, K. (2002). Structure and function of dendritic spines. *Annu Rev Physiol*, *64*, 313-353. https://doi.org/10.1146/annurev.physiol.64.081501.160008

Nochlin, D., van Belle, G., Bird, T. D., & Sumi, S. M. (1993). Comparison of the severity of neuropathologic changes in familial and sporadic Alzheimer's disease. *Alzheimer Dis Assoc Disord*, *7*(4), 212-222.

Noh, H., Jeon, J., & Seo, H. (2014). Systemic injection of LPS induces region-specific neuroinflammation and mitochondrial dysfunction in normal mouse brain. *Neurochemistry International*, *69*, 35-40. https://doi.org/https://doi.org/10.1016/j.neuint.2014.02.008

Nwabuisi-Heath, E., Rebeck, G. W., LaDu, M. J., & Yu, C. (2013). ApoE4 Delays Dendritic Spine Formation during Neuron Development and Accelerates Loss of Mature Spines in Vitro. *ASN Neuro*, *6*(1), AN20130043. https://doi.org/10.1042/AN20130043

O'Keefe, J. (1976). Place units in the hippocampus of the freely moving rat. *Exp Neurol*, *51*(1), 78-109. https://doi.org/10.1016/0014-4886(76)90055-8

O'Bryant, S. E., Waring, S. C., Cullum, C. M., Hall, J., Lacritz, L., Massman, P. J., Lupo, P. J., Reisch, J. S., Doody, R., & Consortium, T. A. s. R. (2008). Staging Dementia Using Clinical Dementia Rating Scale Sum of Boxes Scores: A Texas Alzheimer's Research Consortium Study. *Archives of Neurology*, *65*(8), 1091-1095. https://doi.org/10.1001/archneur.65.8.1091

Oakley, H., Cole, S. L., Logan, S., Maus, E., Shao, P., Craft, J., Guillozet-Bongaarts, A., Ohno, M., Disterhoft, J., Van Eldik, L., Berry, R., & Vassar, R. (2006). Intraneuronal beta-amyloid aggregates, neurodegeneration, and neuron loss in transgenic mice with five familial Alzheimer's disease mutations: potential factors in amyloid plaque formation. *J Neurosci*, *26*(40), 10129-10140. https://doi.org/10.1523/jneurosci.1202-06.2006

Oblak, A. L., Lin, P. B., Kotredes, K. P., Pandey, R. S., Garceau, D., Williams, H. M., Uyar, A., O'Rourke, R., O'Rourke, S., Ingraham, C., Bednarczyk, D., Belanger, M., Cope, Z. A., Little, G. J., Williams, S.-P. G., Ash, C., Bleckert, A., Ragan, T., Logsdon, B. A., . . . Lamb, B. T. (2021). Comprehensive Evaluation of the 5XFAD Mouse Model for Preclinical Testing Applications: A MODEL-AD Study [Original Research]. *Frontiers in Aging Neuroscience*, *13*. https://doi.org/10.3389/fnagi.2021.713726

Oddo, S., Caccamo, A., Shepherd, J. D., Murphy, M. P., Golde, T. E., Kayed, R., Metherate, R., Mattson, M. P., Akbari, Y., & LaFerla, F. M. (2003). Triple-transgenic model of Alzheimer's disease with plaques and tangles: intracellular Abeta and synaptic dysfunction. *Neuron*, *39*(3), 409-421. https://doi.org/10.1016/s0896-6273(03)00434-3

Oddo, S., Caccamo, A., Shepherd, J. D., Murphy, M. P., Golde, T. E., Kayed, R., Metherate, R., Mattson, M. P., Akbari, Y., & LaFerla, F. M. (2003). Triple-Transgenic Model of Alzheimer's Disease with Plaques and Tangles: Intracellular Aβ and Synaptic Dysfunction. *Neuron*, *39*(3), 409-421. https://doi.org/https://doi.org/10.1016/S0896-6273(03)00434-3

Ögren, S. O., & Stiedl, O. (2010). Passive Avoidance. In I. P. Stolerman (Ed.), *Encyclopedia of Psychopharmacology* (pp. 960-967). Springer Berlin Heidelberg. https://doi.org/10.1007/978-3-540-68706-1_160

Ojala, J., Alafuzoff, I., Herukka, S. K., van Groen, T., Tanila, H., & Pirttilä, T. (2009). Expression of interleukin-18 is increased in the brains of Alzheimer's disease patients. *Neurobiol Aging*, *30*(2), 198-209. https://doi.org/10.1016/j.neurobiolaging.2007.06.006

Okado, H., & Okamoto, H. (1992). A Xenopus homologue of the human beta-amyloid precursor protein: developmental regulation of its gene expression. *Biochem Biophys Res Commun*, *189*(3), 1561-1568. https://doi.org/10.1016/0006-291x(92)90254-i

Oliveira-Lima, O. C., Carvalho-Tavares, J., Rodrigues, M. F., Gomez, M. V., Oliveira, A. C. P., Resende, R. R., Gomez, R. S., Vaz, B. G., & Pinto, M. C. X. (2019). Lipid dynamics in LPS-induced neuroinflammation by DESI-MS imaging. *Brain, Behavior, and Immunity*, *79*, 186-194. https://doi.org/https://doi.org/10.1016/j.bbi.2019.01.029

Ollinger, K., Kagedal, K., & Nath, S. (2019). Amyloid-β induced membrane damage instigates tunnelling nanotubes and direct cell-to-cell transfer. *bioRxiv*, 655340. https://doi.org/10.1101/655340

Ophir, G., Amariglio, N., Jacob-Hirsch, J., Elkon, R., Rechavi, G., & Michaelson, D. M. (2005). Apolipoprotein E4 enhances brain inflammation by modulation of the NF-kappaB signaling cascade. *Neurobiol Dis*, *20*(3), 709-718. https://doi.org/10.1016/j.nbd.2005.05.002

Origlia, N., Righi, M., Capsoni, S., Cattaneo, A., Fang, F., Stern, D. M., Chen, J. X., Schmidt, A. M., Arancio, O., Yan, S. D., & Domenici, L. (2008). Receptor for advanced glycation end product-dependent activation of p38 mitogen-activated protein kinase contributes to amyloid-beta-mediated cortical synaptic dysfunction. *J Neurosci*, *28*(13), 3521-3530. https://doi.org/10.1523/jneurosci.0204-08.2008

Ostlund, S. B., & Balleine, B. W. (2005). Lesions of medial prefrontal cortex disrupt the acquisition but not the expression of goal-directed learning. *J Neurosci*, *25*(34), 7763-7770. https://doi.org/10.1523/jneurosci.1921-05.2005

Ostlund, S. B., & Balleine, B. W. (2008). Differential involvement of the basolateral amygdala and mediodorsal thalamus in instrumental action selection. *J Neurosci*, *28*(17), 4398-4405. https://doi.org/10.1523/jneurosci.5472-07.2008

Ostos, M. A., Recalde, D., Zakin, M. M., & Scott-Algara, D. (2002). Implication of natural killer T cells in atherosclerosis development during a LPS-induced chronic inflammation. *FEBS Letters*, *519*(1), 23-29. https://doi.org/https://doi.org/10.1016/S0014-5793(02)02692-3

Palmer, K., Di Iulio, F., Varsi, A. E., Gianni, W., Sancesario, G., Caltagirone, C., & Spalletta, G. (2010). Neuropsychiatric Predictors of Progression from Amnestic-Mild Cognitive Impairment to Alzheimer's Disease: The Role of Depression and Apathy. *Journal of Alzheimer's Disease*, *20*, 175-183. https://doi.org/10.3233/JAD-2010-1352

Palmqvist, S., Schöll, M., Strandberg, O., Mattsson, N., Stomrud, E., Zetterberg, H., Blennow, K., Landau, S., Jagust, W., & Hansson, O. (2017). Earliest accumulation of β-amyloid occurs within the default-mode network and concurrently affects brain connectivity [Article]. *Nature Communications*, *8*(1), Article 1214. https://doi.org/10.1038/s41467-017-01150-x

Pampuscenko, K., Morkuniene, R., Krasauskas, L., Smirnovas, V., Brown, G. C., & Borutaite, V. (2023). Extracellular tau stimulates phagocytosis of living neurons by activated microglia via Toll-like 4 receptor–NLRP3 inflammasome–caspase-1 signalling axis. *Scientific Reports*, *13*(1), 10813. https://doi.org/10.1038/s41598-023-37887-3

Parachikova, A., Vasilevko, V., Cribbs, D. H., LaFerla, F. M., & Green, K. N. (2010). Reductions in Amyloid-β-Derived Neuroinflammation, with Minocycline, Restore Cognition but do not Significantly Affect Tau Hyperphosphorylation. *Journal of Alzheimer's Disease*, *21*, 527-542. https://doi.org/10.3233/JAD-2010-100204

Park, K. M., Yule, D. I., & Bowers, W. J. (2008). Tumor necrosis factor-alpha potentiates intraneuronal Ca2+ signaling via regulation of the inositol 1,4,5-trisphosphate receptor. *J Biol Chem*, *283*(48), 33069-33079. https://doi.org/10.1074/jbc.M802209200

Parkes, S. L., Bradfield, L. A., & Balleine, B. W. (2015). Interaction of insular cortex and ventral striatum mediates the effect of incentive memory on choice between goal-directed actions. *J Neurosci*, *35*(16), 6464-6471. https://doi.org/10.1523/jneurosci.4153-14.2015

Parra, M. A., Abrahams, S., Fabi, K., Logie, R., Luzzi, S., & Sala, S. D. (2009). Short-term memory binding deficits in Alzheimer's disease. *Brain*, *132*(4), 1057-1066. https://doi.org/10.1093/brain/awp036

Parrott, M. D., Winocur, G., Bazinet, R. P., Ma, D. W. L., & Greenwood, C. E. (2015). Whole-food diet worsened cognitive dysfunction in an Alzheimer's disease mouse model. *Neurobiology of Aging*, *36*(1), 90-99. https://doi.org/https://doi.org/10.1016/j.neurobiolaging.2014.08.013

Pascoal, T. A., Benedet, A. L., Ashton, N. J., Kang, M. S., Therriault, J., Chamoun, M., Savard, M., Lussier, F. Z., Tissot, C., Karikari, T. K., Ottoy, J., Mathotaarachchi, S., Stevenson, J., Massarweh, G., Schöll, M., de Leon, M. J., Soucy, J.-P., Edison, P., Blennow, K., . . . Rosa-Neto,

P. (2021). Microglial activation and tau propagate jointly across Braak stages. *Nature Medicine*, *27*(9), 1592-1599. https://doi.org/10.1038/s41591-021-01456-w

Pascoal, T. A., Therriault, J., Mathotaarachchi, S., Kang, M. S., Shin, M., Benedet, A. L., Chamoun, M., Tissot, C., Lussier, F., Mohaddes, S., Soucy, J. P., Massarweh, G., Gauthier, S., & Rosa-Neto, P. (2020). Topographical distribution of Aβ predicts progression to dementia in Aβ positive mild cognitive impairment [Article]. *Alzheimer's and Dementia: Diagnosis, Assessment and Disease Monitoring*, *12*(1), Article e12037. https://doi.org/10.1002/dad2.12037

Passamonti, L., Tsvetanov, K. A., Jones, P. S., Bevan-Jones, W. R., Arnold, R., Borchert, R. J., Mak, E., Su, L., J.T, O., Brien, & Rowe, J. B. (2019). Neuroinflammation and Functional Connectivity in Alzheimer's Disease: Interactive Influences on Cognitive Performance. *The Journal of Neuroscience*, *39*(36), 7218. https://doi.org/10.1523/JNEUROSCI.2574-18.2019

Paxinos, G., & Franklin, K. B. J. (2012). *Paxinos and Franklin's the Mouse Brain in Stereotaxic Coordinates*. Elsevier Science. https://books.google.com.au/books?id=8RJZLwEACAAJ

Peak, J., Hart, G., & Balleine, B. W. (2019). From learning to action: the integration of dorsal striatal input and output pathways in instrumental conditioning. *Eur J Neurosci*, *49*(5), 658-671. https://doi.org/10.1111/ejn.13964

Peng, X., Luo, Z., He, S., Zhang, L., & Li, Y. (2021). Blood-Brain Barrier Disruption by Lipopolysaccharide and Sepsis-Associated Encephalopathy [Review]. *Frontiers in Cellular and Infection Microbiology*, *11*. https://doi.org/10.3389/fcimb.2021.768108

Pérez, M. J., Jara, C., & Quintanilla, R. A. (2018). Contribution of Tau Pathology to Mitochondrial Impairment in Neurodegeneration [Review]. *Frontiers in Neuroscience*, *12*. https://doi.org/10.3389/fnins.2018.00441

Perry, V. H. (2004). The influence of systemic inflammation on inflammation in the brain: implications for chronic neurodegenerative disease. *Brain Behav Immun*, *18*(5), 407-413. https://doi.org/10.1016/j.bbi.2004.01.004

Persidsky, Y., Ramirez, S. H., Haorah, J., & Kanmogne, G. D. (2006). Blood-brain barrier: structural components and function under physiologic and pathologic conditions. *J Neuroimmune Pharmacol*, *1*(3), 223-236. https://doi.org/10.1007/s11481-006-9025-3

Petrozziello, T., Amaral, A. C., Dujardin, S., Farhan, S. M. K., Chan, J., Trombetta, B. A., Kivisäkk, P., Mills, A. N., Bordt, E. A., Kim, S. E., Dooley, P. M., Commins, C., Connors, T. R., Oakley, D. H., Ghosal, A., Gomez-Isla, T., Hyman, B. T., Arnold, S. E., Spires-Jones, T., . . . Sadri-Vakili, G. (2022). Novel genetic variants in MAPT and alterations in tau phosphorylation in amyotrophic lateral sclerosis post-mortem motor cortex and cerebrospinal fluid. *Brain Pathol*, *32*(2), e13035. https://doi.org/10.1111/bpa.13035

Piaceri, I., Nacmias, B., & Sorbi, S. (2013). Genetics of familial and sporadic Alzheimer's disease. *Front Biosci (Elite Ed)*, *5*(1), 167-177. https://doi.org/10.2741/e605

Piaceri, I., Nacmias, B., & Sorbi, S. (2013). Genetics of familial and sporadic Alzheimer’s disease. *FBE*, *5*(1), 167-177. https://doi.org/10.2741/e605

Piccio, L., Deming, Y., Del-Águila, J. L., Ghezzi, L., Holtzman, D. M., Fagan, A. M., Fenoglio, C., Galimberti, D., Borroni, B., & Cruchaga, C. (2016). Cerebrospinal fluid soluble TREM2 is higher in Alzheimer disease and associated with mutation status. *Acta Neuropathologica*, *131*(6), 925-933. https://doi.org/10.1007/s00401-016-1533-5

Pickering, M., Cumiskey, D., & O'Connor, J. J. (2005). Actions of TNF-alpha on glutamatergic synaptic transmission in the central nervous system. *Exp Physiol*, *90*(5), 663-670. https://doi.org/10.1113/expphysiol.2005.030734

Piirsalu, M., Taalberg, E., Lilleväli, K., Tian, L., Zilmer, M., & Vasar, E. (2020). Treatment With Lipopolysaccharide Induces Distinct Changes in Metabolite Profile and Body Weight in 129Sv and Bl6 Mouse Strains. *Front Pharmacol*, *11*, 371. https://doi.org/10.3389/fphar.2020.00371

Pimenova, A. A., Marcora, E., & Goate, A. M. (2017). A Tale of Two Genes: Microglial Apoe and Trem2. *Immunity*, *47*(3), 398-400. https://doi.org/https://doi.org/10.1016/j.immuni.2017.08.015

Pires, M., & Rego, A. C. (2023). Apoe4 and Alzheimer’s Disease Pathogenesis—Mitochondrial Deregulation and Targeted Therapeutic Strategies. *International Journal of Molecular Sciences*, *24*(1).

Pitts, M. W. (2018). Barnes Maze Procedure for Spatial Learning and Memory in Mice. *Bio Protoc*, *8*(5). https://doi.org/10.21769/bioprotoc.2744

Planche, V., Manjon, J. V., Mansencal, B., Lanuza, E., Tourdias, T., Catheline, G., & Coupé, P. (2022). Structural progression of Alzheimer's disease over decades: the MRI staging scheme. *Brain Communications*, *4*(3). https://doi.org/10.1093/braincomms/fcac109

Pless, A., Ware, D., Saggu, S., Rehman, H., Morgan, J., & Wang, Q. (2023). Understanding neuropsychiatric symptoms in Alzheimer's disease: challenges and advances in diagnosis and treatment [Review]. *Frontiers in Neuroscience*, *17*. https://doi.org/10.3389/fnins.2023.1263771

Podcasy, J. L., & Epperson, C. N. (2016). Considering sex and gender in Alzheimer disease and other dementias. *Dialogues Clin Neurosci*, *18*(4), 437-446. https://doi.org/10.31887/DCNS.2016.18.4/cepperson

Poirier, J., Baccichet, A., Dea, D., & Gauthier, S. (1993). Cholesterol synthesis and lipoprotein reuptake during synaptic remodelling in hippocampus in adult rats. *Neuroscience*, *55*(1), 81-90. https://doi.org/https://doi.org/10.1016/0306-4522(93)90456-P

Poirier, J., Minnich, A., & Davignon, J. (1995). Apolipoprotein E, synaptic plasticity and Alzheimer's disease. *Annals of medicine*, *27*(6), 663-670.

Popp, J., Meichsner, S., Kölsch, H., Lewczuk, P., Maier, W., Kornhuber, J., Jessen, F., & Lütjohann, D. (2013). Cerebral and extracerebral cholesterol metabolism and CSF markers of Alzheimer's disease. *Biochemical Pharmacology*, *86*(1), 37-42. https://doi.org/https://doi.org/10.1016/j.bcp.2012.12.007

Potashman, M., Pang, M., Tahir, M., Shahraz, S., Dichter, S., Perneczky, R., & Nolte, S. (2023). Psychometric properties of the Alzheimer's Disease Cooperative Study – Activities of Daily Living for Mild Cognitive Impairment (ADCS-MCI-ADL) scale: a post hoc analysis of the ADCS ADC-008 trial. *BMC Geriatrics*, *23*(1), 124. https://doi.org/10.1186/s12877-022-03527-0

Pozueta, J., Lefort, R., Ribe, E. M., Troy, C. M., Arancio, O., & Shelanski, M. (2013). Caspase-2 is required for dendritic spine and behavioural alterations in J20 APP transgenic mice. *Nature Communications*, *4*(1), 1939. https://doi.org/10.1038/ncomms2927

Prasad, A. (2020). Essentials of Anatomy as Related to Alzheimers disease: A Review. *Journal of Alzheimers Disease & Parkinsonism*.

Profenno, L. A., Porsteinsson, A. P., & Faraone, S. V. (2010). Meta-Analysis of Alzheimer's Disease Risk with Obesity, Diabetes, and Related Disorders. *Biological Psychiatry*, *67*(6), 505-512. https://doi.org/https://doi.org/10.1016/j.biopsych.2009.02.013

Püntener, U., Booth, S. G., Perry, V. H., & Teeling, J. L. (2012). Long-term impact of systemic bacterial infection on the cerebral vasculature and microglia. *Journal of Neuroinflammation*, *9*(1), 146. https://doi.org/10.1186/1742-2094-9-146

Qiu, C., Winblad, B., & Fratiglioni, L. (2005). The age-dependent relation of blood pressure to cognitive function and dementia. *The Lancet Neurology*, *4*(8), 487-499. https://doi.org/https://doi.org/10.1016/S1474-4422(05)70141-1

Qu, D., Ye, Z., Zhang, W., Dai, B., Chen, G., Wang, L., Shao, X., Xiang, A., Lu, Z., & Shi, J. (2022). Cyanidin Chloride Improves LPS-Induced Depression-Like Behavior in Mice by Ameliorating Hippocampal Inflammation and Excitotoxicity. *ACS Chemical Neuroscience*, *13*(21), 3023-3033. https://doi.org/10.1021/acschemneuro.2c00087

Rabinovici, G. D. (2019). Late-onset Alzheimer Disease. *Continuum (Minneap Minn)*, *25*(1), 14-33. https://doi.org/10.1212/con.0000000000000700

Radde, R., Bolmont, T., Kaeser, S. A., Coomaraswamy, J., Lindau, D., Stoltze, L., Calhoun, M. E., Jäggi, F., Wolburg, H., Gengler, S., Haass, C., Ghetti, B., Czech, C., Hölscher, C., Mathews, P. M., &

Jucker, M. (2006). Abeta42-driven cerebral amyloidosis in transgenic mice reveals early and robust pathology. *EMBO Rep*, *7*(9), 940-946. https://doi.org/10.1038/sj.embor.7400784

Rahman, A., Jackson, H., Hristov, H., Isaacson, R. S., Saif, N., Shetty, T., Etingin, O., Henchcliffe, C., Brinton, R. D., & Mosconi, L. (2019). Sex and Gender Driven Modifiers of Alzheimer's: The Role for Estrogenic Control Across Age, Race, Medical, and Lifestyle Risks [Review]. *Frontiers in Aging Neuroscience*, *11*. https://doi.org/10.3389/fnagi.2019.00315

Rahman, A., Schelbaum, E., Hoffman, K., Diaz, I., Hristov, H., Andrews, R., Jett, S., Jackson, H., Lee, A., & Sarva, H. (2020). Sex-driven modifiers of Alzheimer risk: a multimodality brain imaging study. *Neurology*, *95*(2), e166-e178.

Rajasekar, N., Nath, C., Hanif, K., & Shukla, R. (2017). Intranasal Insulin Administration Ameliorates Streptozotocin (ICV)-Induced Insulin Receptor Dysfunction, Neuroinflammation, Amyloidogenesis, and Memory Impairment in Rats. *Mol Neurobiol*, *54*(8), 6507-6522. https://doi.org/10.1007/s12035-016-0169-8

Rajavashisth, T. B., Kaptein, J. S., Reue, K. L., & Lusis, A. J. (1985). Evolution of apolipoprotein E: mouse sequence and evidence for an 11-nucleotide ancestral unit. *Proceedings of the National Academy of Sciences*, *82*(23), 8085-8089. https://doi.org/doi:10.1073/pnas.82.23.8085

Reale, M., Kamal, M. A., Velluto, L., Gambi, D., Di Nicola, M., & Greig, N. H. (2012). Relationship between inflammatory mediators, Aβ levels and ApoE genotype in Alzheimer disease. *Curr Alzheimer Res*, *9*(4), 447-457. https://doi.org/10.2174/156720512800492549

Reisberg, B., Finkel, S., Overall, J., Schmidt-Gollas, N., Kanowski, S., Lehfeld, H., Hulla, F., Sclan, S. G., Wilms, H.-U., Heininger, K., Hindmarch, I., Stemmler, M., Poon, L., Kluger, A., Cooler, C., Bergener, M., Hugonot-Diener, L., Robert, P. H., & Erzigkeit, H. (2001). The Alzheimer's Disease Activities of Daily Living International Scale (ADL-IS). *International Psychogeriatrics*, *13*(2), 163-181. https://doi.org/10.1017/S1041610201007566

Reiss, A. B., Arain, H. A., Stecker, M. M., Siegart, N. M., & Kasselman, L. J. (2018). Amyloid toxicity in Alzheimer's disease. *29*(6), 613-627. https://doi.org/doi:10.1515/revneuro-2017-0063 (Reviews in the Neurosciences)

Reitz, C., Brayne, C., & Mayeux, R. (2011). Epidemiology of Alzheimer disease. *Nat Rev Neurol*, *7*(3), 137-152. https://doi.org/10.1038/nrneurol.2011.2

Reitz, C., Cheng, R., Rogaeva, E., Lee, J. H., Tokuhiro, S., Zou, F., Bettens, K., Sleegers, K., Tan, E. K., Kimura, R., Shibata, N., Arai, H., Kamboh, M. I., Prince, J. A., Maier, W., Riemenschneider, M., Owen, M., Harold, D., Hollingworth, P., . . . Mayeux, R. (2011). Meta-analysis of the association between variants in SORL1 and Alzheimer disease. *Arch Neurol*, *68*(1), 99-106. https://doi.org/10.1001/archneurol.2010.346

Revised Criteria for Diagnosis and Staging of Alzheimer's Disease: Alzheimer's Association Workgroup. (2023). https://alz.org/media/Documents/scientific-conferences/Clinical-Criteria-for-Staging-and-Diagnosis-for-Public-Comment-Draft-2.pdf?_gl=1*4q0whj*_ga*OTY2MDk5MzY0LjE3MDY0OTQ2NzU.*_ga_QSFTKCEH7C*MTcxMjA0MzgyNy4zLjEuMTcxMjA0Mzg3NC4xMy4wLjA.*_ga_9JTEWVX24V*MTcxMjA0MzgyNy4zLjEuMTcxMjA0Mzg3NC4xMy4wLjA.

Roda, A. R., Esquerda-Canals, G., Martí-Clúa, J., & Villegas, S. (2020). Cognitive Impairment in the 3xTg-AD Mouse Model of Alzheimer's Disease is Affected by Aβ-ImmunoTherapy and Cognitive Stimulation. *Pharmaceutics*, *12*(10). https://doi.org/10.3390/pharmaceutics12100944

Rodriguez, G. A., Burns, M. P., Weeber, E. J., & Rebeck, G. W. (2013). Young APOE4 targeted replacement mice exhibit poor spatial learning and memory, with reduced dendritic spine density in the medial entorhinal cortex. *Learning & Memory*, *20*(5), 256-266. https://doi.org/10.1101/lm.030031.112

Rodriguez, G. A., Burns, M. P., Weeber, E. J., & Rebeck, G. W. (2013). Young APOE4 targeted replacement mice exhibit poor spatial learning and memory, with reduced dendritic spine

density in the medial entorhinal cortex. *Learn Mem*, *20*(5), 256-266. https://doi.org/10.1101/lm.030031.112

Rogaeva, E., Meng, Y., Lee, J. H., Gu, Y., Kawarai, T., Zou, F., Katayama, T., Baldwin, C. T., Cheng, R., Hasegawa, H., Chen, F., Shibata, N., Lunetta, K. L., Pardossi-Piquard, R., Bohm, C., Wakutani, Y., Cupples, L. A., Cuenco, K. T., Green, R. C., . . . St George-Hyslop, P. (2007). The neuronal sortilin-related receptor SORL1 is genetically associated with Alzheimer disease. *Nat Genet*, *39*(2), 168-177. https://doi.org/10.1038/ng1943

Rosen, D. R., Martin-Morris, L., Luo, L. Q., & White, K. (1989). A Drosophila gene encoding a protein resembling the human beta-amyloid protein precursor. *Proc Natl Acad Sci U S A*, *86*(7), 2478-2482. https://doi.org/10.1073/pnas.86.7.2478

Roth, B. L. (2016). DREADDs for Neuroscientists. *Neuron*, *89*(4), 683-694. https://doi.org/10.1016/j.neuron.2016.01.040

Rumbaugh, J. A., & Nath, A. (2009). Neuronal Cell Death and Inflammation. In M. D. Binder, N. Hirokawa, & U. Windhorst (Eds.), *Encyclopedia of Neuroscience* (pp. 2772-2776). Springer Berlin Heidelberg. https://doi.org/10.1007/978-3-540-29678-2_3910

Ryu, K.-Y., Lee, H.-j., Woo, H., Kang, R.-J., Han, K.-M., Park, H., Lee, S. M., Lee, J.-Y., Jeong, Y. J., Nam, H.-W., Nam, Y., & Hoe, H.-S. (2019). Dasatinib regulates LPS-induced microglial and astrocytic neuroinflammatory responses by inhibiting AKT/STAT3 signaling. *Journal of Neuroinflammation*, *16*(1), 190. https://doi.org/10.1186/s12974-019-1561-x

Saber, M., Kokiko-Cochran, O., Puntambekar, S. S., Lathia, J. D., & Lamb, B. T. (2016). Triggering Receptor Expressed on Myeloid Cells 2 Deficiency Alters Acute Macrophage Distribution and Improves Recovery after Traumatic Brain Injury. *Journal of Neurotrauma*, *34*(2), 423-435. https://doi.org/10.1089/neu.2016.4401

Sadeghmousavi, S., Eskian, M., Rahmani, F., & Rezaei, N. (2020). The effect of insomnia on development of Alzheimer's disease. *Journal of Neuroinflammation*, *17*(1), 289. https://doi.org/10.1186/s12974-020-01960-9

Safieh, M., Korczyn, A. D., & Michaelson, D. M. (2019). ApoE4: an emerging therapeutic target for Alzheimer's disease. *BMC Medicine*, *17*(1), 64. https://doi.org/10.1186/s12916-019-1299-4

Saito, T., Mihira, N., Matsuba, Y., Sasaguri, H., Hashimoto, S., Narasimhan, S., Zhang, B., Murayama, S., Higuchi, M., Lee, V. M. Y., Trojanowski, J. Q., & Saido, T. C. (2019). Humanization of the entire murine Mapt gene provides a murine model of pathological human tau propagation. *J Biol Chem*, *294*(34), 12754-12765. https://doi.org/10.1074/jbc.RA119.009487

Salomon-Zimri, S., Boehm-Cagan, A., Liraz, O., & Michaelson, D. M. (2014). Hippocampus-Related Cognitive Impairments in Young apoE4 Targeted Replacement Mice. *Neurodegenerative Diseases*, *13*(2-3), 86-92. https://doi.org/10.1159/000354777

Salomon-Zimri, S., Glat, M. J., Barhum, Y., Luz, I., Boehm-Cagan, A., Liraz, O., Ben-Zur, T., Offen, D., & Michaelson, D. M. (2016). Reversal of ApoE4-Driven Brain Pathology by Vascular Endothelial Growth Factor Treatment. *J Alzheimers Dis*, *53*(4), 1443-1458. https://doi.org/10.3233/jad-160182

Salter, M. W., & Stevens, B. (2017). Microglia emerge as central players in brain disease. *Nat Med*, *23*(9), 1018-1027. https://doi.org/10.1038/nm.4397

Sama, D. M., & Norris, C. M. (2013). Calcium dysregulation and neuroinflammation: discrete and integrated mechanisms for age-related synaptic dysfunction. *Ageing Res Rev*, *12*(4), 982-995. https://doi.org/10.1016/j.arr.2013.05.008

Saman, S., Kim, W., Raya, M., Visnick, Y., Miro, S., Saman, S., Jackson, B., McKee, A. C., Alvarez, V. E., Lee, N. C., & Hall, G. F. (2012). Exosome-associated tau is secreted in tauopathy models and is selectively phosphorylated in cerebrospinal fluid in early Alzheimer disease. *J Biol Chem*, *287*(6), 3842-3849. https://doi.org/10.1074/jbc.M111.277061

Sangha, S., McComb, C., Scheibenstock, A., Johannes, C., & Lukowiak, K. (2002). The effects of continuous versus partial reinforcement schedules on associative learning, memory and

extinction in Lymnaea stagnalis. *J Exp Biol*, *205*(Pt 8), 1171-1178. https://doi.org/10.1242/jeb.205.8.1171

Santabárbara, J., Villagrasa, B., López-Antón, R., Olaya, B., Bueno-Notivol, J., de la Cámara, C., Gracia-García, P., Lobo, E., & Lobo, A. (2019). Clinically relevant anxiety and risk of Alzheimer's disease in an elderly community sample: 4.5 years of follow-up. *J Affect Disord*, *250*, 16-20. https://doi.org/10.1016/j.jad.2019.02.050

Sardari, M., Dzyubenko, E., Schmermund, B., Yin, D., Qi, Y., Kleinschnitz, C., & Hermann, D. M. (2020). Dose-Dependent Microglial and Astrocytic Responses Associated With Post-ischemic Neuroprotection After Lipopolysaccharide-Induced Sepsis-Like State in Mice [Brief Research Report]. *Frontiers in Cellular Neuroscience*, *14*. https://doi.org/10.3389/fncel.2020.00026

Sárvári, M., Hrabovszky, E., Kalló, I., Solymosi, N., Likó, I., Berchtold, N., Cotman, C., & Liposits, Z. (2012). Menopause leads to elevated expression of macrophage-associated genes in the aging frontal cortex: rat and human studies identify strikingly similar changes. *Journal of Neuroinflammation*, *9*(1), 264. https://doi.org/10.1186/1742-2094-9-264

Savage, J. C., St-Pierre, M.-K., Hui, C. W., & Tremblay, M.-E. (2019). Microglial Ultrastructure in the Hippocampus of a Lipopolysaccharide-Induced Sickness Mouse Model [Original Research]. *Frontiers in Neuroscience*, *13*. https://doi.org/10.3389/fnins.2019.01340

Schafflick, D., Wolbert, J., Heming, M., Thomas, C., Hartlehnert, M., Börsch, A. L., Ricci, A., Martín-Salamanca, S., Li, X., Lu, I. N., Pawlak, M., Minnerup, J., Strecker, J. K., Seidenbecher, T., Meuth, S. G., Hidalgo, A., Liesz, A., Wiendl, H., & Meyer Zu Horste, G. (2021). Single-cell profiling of CNS border compartment leukocytes reveals that B cells and their progenitors reside in non-diseased meninges. *Nat Neurosci*, *24*(9), 1225-1234. https://doi.org/10.1038/s41593-021-00880-y

Scheff, S. W., Price, D. A., Schmitt, F. A., DeKosky, S. T., & Mufson, E. J. (2007). Synaptic alterations in CA1 in mild Alzheimer disease and mild cognitive impairment. *Neurology*, *68*(18), 1501-1508. https://doi.org/10.1212/01.wnl.0000260698.46517.8f

Scheff, S. W., Price, D. A., Schmitt, F. A., & Mufson, E. J. (2006). Hippocampal synaptic loss in early Alzheimer's disease and mild cognitive impairment. *Neurobiol Aging*, *27*(10), 1372-1384. https://doi.org/10.1016/j.neurobiolaging.2005.09.012

Scheuner, D., Eckman, C., Jensen, M., Song, X., Citron, M., Suzuki, N., Bird, T. D., Hardy, J., Hutton, M., Kukull, W., Larson, E., Levy-Lahad, L., Viitanen, M., Peskind, E., Poorkaj, P., Schellenberg, G., Tanzi, R., Wasco, W., Lannfelt, L., . . . Younkin, S. (1996). Secreted amyloid β–protein similar to that in the senile plaques of Alzheimer's disease is increased in vivo by the presenilin 1 and 2 and APP mutations linked to familial Alzheimer's disease. *Nature Medicine*, *2*(8), 864-870. https://doi.org/10.1038/nm0896-864

Schmid, C. D., Sautkulis, L. N., Danielson, P. E., Cooper, J., Hasel, K. W., Hilbush, B. S., Sutcliffe, J. G., & Carson, M. J. (2002). Heterogeneous expression of the triggering receptor expressed on myeloid cells-2 on adult murine microglia. *Journal of Neurochemistry*, *83*(6), 1309-1320. https://doi.org/https://doi.org/10.1046/j.1471-4159.2002.01243.x

Schmidt-Morgenroth, I., Michaud, P., Gasparini, F., & Avrameas, A. (2023). Central and Peripheral Inflammation in Mild Cognitive Impairment in the Context of Alzheimer's Disease. *International Journal of Molecular Sciences*, *24*(13).

Schmidt, V., Subkhangulova, A., & Willnow, T. E. (2017). Sorting receptor SORLA: cellular mechanisms and implications for disease. *Cellular and Molecular Life Sciences*, *74*(8), 1475-1483. https://doi.org/10.1007/s00018-016-2410-z

Schuck, N. W., & Niv, Y. (2019). Sequential replay of nonspatial task states in the human hippocampus. *Science*, *364*(6447), eaaw5181. https://doi.org/10.1126/science.aaw5181

Sebastián-Serrano, Á., de Diego-García, L., & Díaz-Hernández, M. (2018). The Neurotoxic Role of Extracellular Tau Protein. *Int J Mol Sci*, *19*(4). https://doi.org/10.3390/ijms19040998

Seno, H., Miyoshi, H., Brown, S. L., Geske, M. J., Colonna, M., & Stappenbeck, T. S. (2009). Efficient colonic mucosal wound repair requires Trem2 signaling. *Proceedings of the National Academy of Sciences*, *106*(1), 256-261. https://doi.org/10.1073/pnas.0803343106

Seok, S. M., Kim, J. M., Park, T. Y., Baik, E. J., & Lee, S. H. (2013). Fructose-1,6-bisphosphate ameliorates lipopolysaccharide-induced dysfunction of blood–brain barrier. *Archives of Pharmacal Research*, *36*(9), 1149-1159. https://doi.org/10.1007/s12272-013-0129-z

Sepúlveda, F. J., Fierro, H., Fernandez, E., Castillo, C., Peoples, R. W., Opazo, C., & Aguayo, L. G. (2014). Nature of the neurotoxic membrane actions of amyloid-β on hippocampal neurons in Alzheimer's disease. *Neurobiol Aging*, *35*(3), 472-481. https://doi.org/10.1016/j.neurobiolaging.2013.08.035

Sepulveda, J., Luo, N., Nelson, M., Ng, C. A. S., & Rebeck, George W. (2022). Independent APOE4 knock-in mouse models display reduced brain APOE protein, altered neuroinflammation, and simplification of dendritic spines. *Journal of Neurochemistry*, *163*(3), 247-259. https://doi.org/https://doi.org/10.1111/jnc.15665

Serneels, L., Van Biervliet, J., Craessaerts, K., Dejaegere, T., Horré, K., Van Houtvin, T., Esselmann, H., Paul, S., Schäfer, M. K., Berezovska, O., Hyman, B. T., Sprangers, B., Sciot, R., Moons, L., Jucker, M., Yang, Z., May, P. C., Karran, E., Wiltfang, J., . . . De Strooper, B. (2009). gamma-Secretase heterogeneity in the Aph1 subunit: relevance for Alzheimer's disease. *Science*, *324*(5927), 639-642. https://doi.org/10.1126/science.1171176

Setzu, A., Lathia, J. D., Zhao, C., Wells, K., Rao, M. S., Ffrench-Constant, C., & Franklin, R. J. (2006). Inflammation stimulates myelination by transplanted oligodendrocyte precursor cells. *Glia*, *54*(4), 297-303. https://doi.org/10.1002/glia.20371

Shah, N. S., Vidal, J.-S., Masaki, K., Petrovitch, H., Ross, G. W., Tilley, C., DeMattos, R. B., Tracy, R. P., White, L. R., & Launer, L. J. (2012). Midlife Blood Pressure, Plasma β-Amyloid, and the Risk for Alzheimer Disease. *Hypertension*, *59*(4), 780-786. https://doi.org/10.1161/HYPERTENSIONAHA.111.178962

Shannon, L. G., Kelsey, S. Z., Amanda, G. A., & Jane, R. T. (2016). The Medial Orbitofrontal Cortex Regulates Sensitivity to Outcome Value. *The Journal of Neuroscience*, *36*(16), 4600. https://doi.org/10.1523/JNEUROSCI.4253-15.2016

Shekarian, M., Komaki, A., Shahidi, S., Sarihi, A., Salehi, I., & Raoufi, S. (2020). The protective and therapeutic effects of vinpocetine, a PDE1 inhibitor, on oxidative stress and learning and memory impairment induced by an intracerebroventricular (ICV) injection of amyloid beta (aβ) peptide. *Behavioural Brain Research*, *383*, 112512. https://doi.org/https://doi.org/10.1016/j.bbr.2020.112512

Sheng, J. G., Bora, S. H., Xu, G., Borchelt, D. R., Price, D. L., & Koliatsos, V. E. (2003). Lipopolysaccharide-induced-neuroinflammation increases intracellular accumulation of amyloid precursor protein and amyloid beta peptide in APPswe transgenic mice. *Neurobiol Dis*, *14*(1), 133-145. https://doi.org/10.1016/s0969-9961(03)00069-x

Sheng, Z. H., & Cai, Q. (2012). Mitochondrial transport in neurons: impact on synaptic homeostasis and neurodegeneration. *Nat Rev Neurosci*, *13*(2), 77-93. https://doi.org/10.1038/nrn3156

Shepardson, N. E., Shankar, G. M., & Selkoe, D. J. (2011). Cholesterol level and statin use in Alzheimer disease: I. Review of epidemiological and preclinical studies. *Arch Neurol*, *68*(10), 1239-1244. https://doi.org/10.1001/archneurol.2011.203

Shi, L., Chen, S.-J., Ma, M.-Y., Bao, Y.-P., Han, Y., Wang, Y.-M., Shi, J., Vitiello, M. V., & Lu, L. (2018). Sleep disturbances increase the risk of dementia: A systematic review and meta-analysis. *Sleep Medicine Reviews*, *40*, 4-16. https://doi.org/https://doi.org/10.1016/j.smrv.2017.06.010

Shibly, A. Z., Sheikh, A. M., Michikawa, M., Tabassum, S., Azad, A. K., Zhou, X., Zhang, Y., Yano, S., & Nagai, A. (2022). Analysis of Cerebral Small Vessel Changes in AD Model Mice. *Biomedicines*, *11*(1). https://doi.org/10.3390/biomedicines11010050

Shiflett, M. W., & Balleine, B. W. (2010). At the limbic-motor interface: disconnection of basolateral amygdala from nucleus accumbens core and shell reveals dissociable components of incentive motivation. *Eur J Neurosci*, *32*(10), 1735-1743. https://doi.org/10.1111/j.1460-9568.2010.07439.x

Shipley, F. B., Dani, N., Xu, H., Deister, C., Cui, J., Head, J. P., Sadegh, C., Fame, R. M., Shannon, M. L., Flores, V. I., Kishkovich, T., Jang, E., Klein, E. M., Goldey, G. J., He, K., Zhang, Y., Holtzman, M. J., Kirchhausen, T., Wyart, C., . . . Lehtinen, M. K. (2020). Tracking Calcium Dynamics and Immune Surveillance at the Choroid Plexus Blood-Cerebrospinal Fluid Interface. *Neuron*, *108*(4), 623-639.e610. https://doi.org/10.1016/j.neuron.2020.08.024

Shors, T. J., Chua, C., & Falduto, J. (2001). Sex differences and opposite effects of stress on dendritic spine density in the male versus female hippocampus. *J Neurosci*, *21*(16), 6292-6297. https://doi.org/10.1523/jneurosci.21-16-06292.2001

Sideris, D. I., Danial, J. S. H., Emin, D., Ruggeri, F. S., Xia, Z., Zhang, Y. P., Lobanova, E., Dakin, H., De, S., Miller, A., Sang, J. C., Knowles, T. P. J., Vendruscolo, M., Fraser, G., Crowther, D., & Klenerman, D. (2021). Soluble amyloid beta-containing aggregates are present throughout the brain at early stages of Alzheimer's disease. *Brain Communications*, *3*(3), fcab147. https://doi.org/10.1093/braincomms/fcab147

Siegel, J. A., Haley, G. E., & Raber, J. (2012). Apolipoprotein E isoform-dependent effects on anxiety and cognition in female TR mice. *Neurobiol Aging*, *33*(2), 345-358. https://doi.org/10.1016/j.neurobiolaging.2010.03.002

Sierra, A., Encinas, J. M., Deudero, J. J. P., Chancey, J. H., Enikolopov, G., Overstreet-Wadiche, L. S., Tsirka, S. E., & Maletic-Savatic, M. (2010). Microglia Shape Adult Hippocampal Neurogenesis through Apoptosis-Coupled Phagocytosis. *Cell Stem Cell*, *7*(4), 483-495. https://doi.org/https://doi.org/10.1016/j.stem.2010.08.014

Simard, A. R., Soulet, D., Gowing, G., Julien, J. P., & Rivest, S. (2006). Bone marrow-derived microglia play a critical role in restricting senile plaque formation in Alzheimer's disease. *Neuron*, *49*(4), 489-502. https://doi.org/10.1016/j.neuron.2006.01.022

Simón, D., García-García, E., Royo, F., Falcón-Pérez, J. M., & Avila, J. (2012). Proteostasis of tau. Tau overexpression results in its secretion via membrane vesicles. *FEBS Lett*, *586*(1), 47-54. https://doi.org/10.1016/j.febslet.2011.11.022

Sjoerds, Z., Dietrich, A., Deserno, L., de Wit, S., Villringer, A., Heinze, H.-J., Schlagenhauf, F., & Horstmann, A. (2016). Slips of Action and Sequential Decisions: A Cross-Validation Study of Tasks Assessing Habitual and Goal-Directed Action Control [Original Research]. *Frontiers in Behavioral Neuroscience*, *10*. https://doi.org/10.3389/fnbeh.2016.00234

Snyder, E. M., Nong, Y., Almeida, C. G., Paul, S., Moran, T., Choi, E. Y., Nairn, A. C., Salter, M. W., Lombroso, P. J., Gouras, G. K., & Greengard, P. (2005). Regulation of NMDA receptor trafficking by amyloid-beta. *Nat Neurosci*, *8*(8), 1051-1058. https://doi.org/10.1038/nn1503

Sobue, A., Komine, O., Hara, Y., Endo, F., Mizoguchi, H., Watanabe, S., Murayama, S., Saito, T., Saido, T. C., Sahara, N., Higuchi, M., Ogi, T., & Yamanaka, K. (2021). Microglial gene signature reveals loss of homeostatic microglia associated with neurodegeneration of Alzheimer's disease. *Acta Neuropathol Commun*, *9*(1), 1. https://doi.org/10.1186/s40478-020-01099-x

Sochocka, M., Diniz, B. S., & Leszek, J. (2017). Inflammatory Response in the CNS: Friend or Foe? *Mol Neurobiol*, *54*(10), 8071-8089. https://doi.org/10.1007/s12035-016-0297-1

Sofroniew, M. V. (2014). Astrogliosis. *Cold Spring Harb Perspect Biol*, *7*(2), a020420. https://doi.org/10.1101/cshperspect.a020420

Sofroniew, M. V. (2015). Astrocyte barriers to neurotoxic inflammation. *Nat Rev Neurosci*, *16*(5), 249-263. https://doi.org/10.1038/nrn3898

Sofroniew, M. V., & Vinters, H. V. (2010). Astrocytes: biology and pathology. *Acta Neuropathol*, *119*(1), 7-35. https://doi.org/10.1007/s00401-009-0619-8

Sohn, D., Shpanskaya, K., Lucas, J. E., Petrella, J. R., Saykin, A. J., Tanzi, R. E., Samatova, N. F., & Doraiswamy, P. M. (2018). Sex Differences in Cognitive Decline in Subjects with High

Likelihood of Mild Cognitive Impairment due to Alzheimer's disease. *Sci Rep*, *8*(1), 7490. https://doi.org/10.1038/s41598-018-25377-w

Soto, C., Estrada, L., & Castilla, J. (2006). Amyloids, prions and the inherent infectious nature of misfolded protein aggregates. *Trends Biochem Sci*, *31*(3), 150-155. https://doi.org/10.1016/j.tibs.2006.01.002

Souchet, B., Michaïl, A., Billoir, B., & Braudeau, J. (2023). Biological Diagnosis of Alzheimer's Disease Based on Amyloid Status: An Illustration of Confirmation Bias in Medical Research? *International Journal of Molecular Sciences*, *24*(24).

Sperling, R. A., Aisen, P. S., Beckett, L. A., Bennett, D. A., Craft, S., Fagan, A. M., Iwatsubo, T., Jack Jr, C. R., Kaye, J., Montine, T. J., Park, D. C., Reiman, E. M., Rowe, C. C., Siemers, E., Stern, Y., Yaffe, K., Carrillo, M. C., Thies, B., Morrison-Bogorad, M., . . . Phelps, C. H. (2011). Toward defining the preclinical stages of Alzheimer's disease: Recommendations from the National Institute on Aging-Alzheimer's Association workgroups on diagnostic guidelines for Alzheimer's disease. *Alzheimer's & Dementia*, *7*(3), 280-292. https://doi.org/https://doi.org/10.1016/j.jalz.2011.03.003

Srinivasan, G., & Brafman, D. A. (2022). The Emergence of Model Systems to Investigate the Link Between Traumatic Brain Injury and Alzheimer's Disease [Review]. *Frontiers in Aging Neuroscience*, *13*. https://doi.org/10.3389/fnagi.2021.813544

Stanciu, G. D., Bild, V., Ababei, D. C., Rusu, R. N., Cobzaru, A., Paduraru, L., & Bulea, D. (2020). Link Between Diabetes and Alzheimer's Disease due to the Shared Amyloid Aggregation and Deposition Involving both Neurodegenerative Changes and Neurovascular Damages. *J Clin Med*, *9*(6). https://doi.org/10.3390/jcm9061713

Stayte, S., Rentsch, P., Li, K. M., & Vissel, B. (2015). Activin A Protects Midbrain Neurons in the 6-Hydroxydopamine Mouse Model of Parkinson's Disease. *PLOS ONE*, *10*(4), e0124325. https://doi.org/10.1371/journal.pone.0124325

Steiner, A., & Redish, A. D. (2012). The Road Not Taken: Neural Correlates of Decision Making in Orbitofrontal Cortex [Original Research]. *Frontiers in Neuroscience*, *6*. https://doi.org/10.3389/fnins.2012.00131

Sterniczuk, R., Antle, M. C., Laferla, F. M., & Dyck, R. H. (2010). Characterization of the 3xTg-AD mouse model of Alzheimer's disease: part 2. Behavioral and cognitive changes. *Brain Res*, *1348*, 149-155. https://doi.org/10.1016/j.brainres.2010.06.011

Stevens, B., Allen, N. J., Vazquez, L. E., Howell, G. R., Christopherson, K. S., Nouri, N., Micheva, K. D., Mehalow, A. K., Huberman, A. D., Stafford, B., Sher, A., Litke, Alan M., Lambris, J. D., Smith, S. J., John, S. W. M., & Barres, B. A. (2007). The Classical Complement Cascade Mediates CNS Synapse Elimination. *Cell*, *131*(6), 1164-1178. https://doi.org/10.1016/j.cell.2007.10.036

Stover, K. R., Campbell, M. A., Van Winssen, C. M., & Brown, R. E. (2015). Early detection of cognitive deficits in the 3xTg-AD mouse model of Alzheimer's disease. *Behavioural Brain Research*, *289*, 29-38. https://doi.org/https://doi.org/10.1016/j.bbr.2015.04.012

Stratoulias, V., Venero, J. L., Tremblay, M., & Joseph, B. (2019). Microglial subtypes: diversity within the microglial community. *Embo j*, *38*(17), e101997. https://doi.org/10.15252/embj.2019101997

Sulakhiya, K., Keshavlal, G. P., Bezbaruah, B. B., Dwivedi, S., Gurjar, S. S., Munde, N., Jangra, A., Lahkar, M., & Gogoi, R. (2016). Lipopolysaccharide induced anxiety- and depressive-like behaviour in mice are prevented by chronic pre-treatment of esculetin. *Neuroscience Letters*, *611*, 106-111. https://doi.org/https://doi.org/10.1016/j.neulet.2015.11.031

Sundermann, E. E., Tran, M., Maki, P. M., Bondi, M. W., & Alzheimer's Disease Neuroimaging, I. (2018). Sex differences in the association between apolipoprotein E ε4 allele and Alzheimer's disease markers. *Alzheimer's & Dementia: Diagnosis, Assessment & Disease Monitoring*, *10*(1), 438-447. https://doi.org/https://doi.org/10.1016/j.dadm.2018.06.004

Sutinen, E. M., Pirttilä, T., Anderson, G., Salminen, A., & Ojala, J. O. (2012). Pro-inflammatory interleukin-18 increases Alzheimer's disease-associated amyloid-β production in human

neuron-like cells. *Journal of Neuroinflammation*, *9*(1), 199. https://doi.org/10.1186/1742-2094-9-199

Swanson, L. W., Wyss, J. M., & Cowan, W. M. (1978). An autoradiographic study of the organization of intrahippocampal association pathways in the rat [https://doi.org/10.1002/cne.901810402]. *Journal of Comparative Neurology*, *181*(4), 681-715. https://doi.org/https://doi.org/10.1002/cne.901810402

Szabó, A., Farkas, S., Fazekas, C., Correia, P., Chaves, T., Sipos, E., Makkai, B., Török, B., & Zelena, D. (2023). Temporal Appearance of Enhanced Innate Anxiety in Alzheimer Model Mice. *Biomedicines*, *11*(2). https://doi.org/10.3390/biomedicines11020262

Sze, C.-I., Troncoso, J. C., Kawas, C., Mouton, P., Price, D. L., & Martin, L. J. (1997). Loss of the Presynaptic Vesicle Protein Synaptophysin in Hippocampus Correlates with Cognitive Decline in Alzheimer Disease. *Journal of Neuropathology & Experimental Neurology*, *56*(8), 933-944. https://doi.org/10.1097/00005072-199708000-00011

Tai, L. M., Bilousova, T., Jungbauer, L., Roeske, S. K., Youmans, K. L., Yu, C., Poon, W. W., Cornwell, L. B., Miller, C. A., Vinters, H. V., Van Eldik, L. J., Fardo, D. W., Estus, S., Bu, G., Gylys, K. H., & Ladu, M. J. (2013). Levels of soluble apolipoprotein E/amyloid-β (Aβ) complex are reduced and oligomeric Aβ increased with APOE4 and Alzheimer disease in a transgenic mouse model and human samples. *J Biol Chem*, *288*(8), 5914-5926. https://doi.org/10.1074/jbc.M112.442103

Takahashi, K., Rochford, C. D. P., & Neumann, H. (2005). Clearance of apoptotic neurons without inflammation by microglial triggering receptor expressed on myeloid cells-2. *Journal of Experimental Medicine*, *201*(4), 647-657. https://doi.org/10.1084/jem.20041611

Tanabe, S., & Yamashita, T. (2018). B-1a lymphocytes promote oligodendrogenesis during brain development. *Nat Neurosci*, *21*(4), 506-516. https://doi.org/10.1038/s41593-018-0106-4

Tang, D., Kang, R., Coyne, C. B., Zeh, H. J., & Lotze, M. T. (2012). PAMPs and DAMPs: signal 0s that spur autophagy and immunity. *Immunol Rev*, *249*(1), 158-175. https://doi.org/10.1111/j.1600-065X.2012.01146.x

Tatu, L., & Vuillier, F. (2014). Structure and Vascularization of the Human Hippocampus. In *The Hippocampus in Clinical Neuroscience* (Vol. 34, pp. 0). S.Karger AG. https://doi.org/10.1159/000356440

Taxier, L. R., Philippi, S. M., York, J. M., LaDu, M. J., & Frick, K. M. (2022). The detrimental effects of APOE4 on risk for Alzheimer's disease may result from altered dendritic spine density, synaptic proteins, and estrogen receptor alpha. *Neurobiology of Aging*, *112*, 74-86. https://doi.org/https://doi.org/10.1016/j.neurobiolaging.2021.12.006

Tesseur, I., Van Dorpe, J., Bruynseels, K., Bronfman, F., Sciot, R., Van Lommel, A., & Van Leuven, F. (2000). Prominent Axonopathy and Disruption of Axonal Transport in Transgenic Mice Expressing Human Apolipoprotein E4 in Neurons of Brain and Spinal Cord. *The American Journal of Pathology*, *157*(5), 1495-1510. https://doi.org/https://doi.org/10.1016/S0002-9440(10)64788-8

Thal, D. R., Rüb, U., Orantes, M., & Braak, H. (2002). Phases of Aβ-deposition in the human brain and its relevance for the development of AD. *Neurology*, *58*(12), 1791-1800. https://doi.org/10.1212/WNL.58.12.1791

Tharp, W. G., & Sarkar, I. N. (2013). Origins of amyloid-β. *BMC Genomics*, *14*, 290. https://doi.org/10.1186/1471-2164-14-290

Therriault, J., Zimmer, E. R., Benedet, A. L., Pascoal, T. A., Gauthier, S., & Rosa-Neto, P. (2022). Staging of Alzheimer's disease: past, present, and future perspectives. *Trends in Molecular Medicine*, *28*(9), 726-741. https://doi.org/https://doi.org/10.1016/j.molmed.2022.05.008

Thygesen, C., Ilkjær, L., Kempf, S. J., Hemdrup, A. L., von Linstow, C. U., Babcock, A. A., Darvesh, S., Larsen, M. R., & Finsen, B. (2018). Diverse Protein Profiles in CNS Myeloid Cells and CNS Tissue From Lipopolysaccharide- and Vehicle-Injected APP(SWE)/PS1(ΔE9) Transgenic Mice

Implicate Cathepsin Z in Alzheimer's Disease. *Front Cell Neurosci*, *12*, 397. https://doi.org/10.3389/fncel.2018.00397

Tillement, L., Lecanu, L., Yao, W., Greeson, J., & Papadopoulos, V. (2006). The spirostenol (22R, 25R)-20alpha-spirost-5-en-3beta-yl hexanoate blocks mitochondrial uptake of Abeta in neuronal cells and prevents Abeta-induced impairment of mitochondrial function. *Steroids*, *71*(8), 725-735. https://doi.org/10.1016/j.steroids.2006.05.003

Tobinick, E. (2009). Tumour necrosis factor modulation for treatment of Alzheimer's disease: rationale and current evidence. *CNS Drugs*, *23*(9), 713-725. https://doi.org/10.2165/11310810-000000000-00000

Tognatta, R., Karl, M. T., Fyffe-Maricich, S. L., Popratiloff, A., Garrison, E. D., Schenck, J. K., Abu-Rub, M., & Miller, R. H. (2020). Astrocytes Are Required for Oligodendrocyte Survival and Maintenance of Myelin Compaction and Integrity [Original Research]. *Frontiers in Cellular Neuroscience*, *14*. https://doi.org/10.3389/fncel.2020.00074

Tolman, E. C. (1939). Prediction of vicarious trial and error by means of the schematic sowbug. *Psychological Review*, *46*, 318-336. https://doi.org/10.1037/h0057054

Tolman, E. C. (1948). Cognitive maps in rats and men. *Psychol Rev*, *55*(4), 189-208. https://doi.org/10.1037/h0061626

Torres-Espín, A., Forero, J., Fenrich, K. K., Lucas-Osma, A. M., Krajacic, A., Schmidt, E., Vavrek, R., Raposo, P., Bennett, D. J., Popovich, P. G., & Fouad, K. (2018). Eliciting inflammation enables successful rehabilitative training in chronic spinal cord injury. *Brain*, *141*(7), 1946-1962. https://doi.org/10.1093/brain/awy128

Townsend, M., Shankar, G. M., Mehta, T., Walsh, D. M., & Selkoe, D. J. (2006). Effects of secreted oligomers of amyloid beta-protein on hippocampal synaptic plasticity: a potent role for trimers. *J Physiol*, *572*(Pt 2), 477-492. https://doi.org/10.1113/jphysiol.2005.103754

Tran, K. M., Kawauchi, S., Kramár, E. A., Rezaie, N., Liang, H. Y., Sakr, J. S., Gomez-Arboledas, A., Arreola, M. A., Cunha, C. D., Phan, J., Wang, S., Collins, S., Walker, A., Shi, K. X., Neumann, J., Filimban, G., Shi, Z., Milinkeviciute, G., Javonillo, D. I., . . . Green, K. N. (2023). A Trem2(R47H) mouse model without cryptic splicing drives age- and disease-dependent tissue damage and synaptic loss in response to plaques. *Mol Neurodegener*, *18*(1), 12. https://doi.org/10.1186/s13024-023-00598-4

Tulenko, T. N., & Sumner, A. E. (2002). The physiology of lipoproteins. *Journal of Nuclear Cardiology*, *9*(6), 638-649. https://doi.org/10.1067/mnc.2002.128959

Tuppo, E. E., & Arias, H. R. (2005). The role of inflammation in Alzheimer's disease. *The International Journal of Biochemistry & Cell Biology*, *37*(2), 289-305. https://doi.org/https://doi.org/10.1016/j.biocel.2004.07.009

Tyrtyshnaia, A., Bondar, A., Konovalova, S., Sultanov, R., & Manzhulo, I. (2020). N-Docosahexanoylethanolamine Reduces Microglial Activation and Improves Hippocampal Plasticity in a Murine Model of Neuroinflammation. *International Journal of Molecular Sciences*, *21*(24).

Tzeng, R.-C., Yang, Y.-W., Hsu, K.-C., Chang, H.-T., & Chiu, P.-Y. (2022). Sum of boxes of the clinical dementia rating scale highly predicts conversion or reversion in predementia stages [Original Research]. *Frontiers in Aging Neuroscience*, *14*. https://doi.org/10.3389/fnagi.2022.1021792

Udeh-Momoh, C., & Watermeyer, T. (2021). Female specific risk factors for the development of Alzheimer's disease neuropathology and cognitive impairment: Call for a precision medicine approach. *Ageing Research Reviews*, *71*, 101459. https://doi.org/https://doi.org/10.1016/j.arr.2021.101459

Ullah, R., Ali, G., Ahmad, N., Akram, M., Kumari, G., Amin, M. U., & Umar, M. N. (2020). Attenuation of Spatial Memory in 5xFAD Mice by Halting Cholinesterases, Oxidative Stress and Neuroinflammation Using a Cyclopentanone Derivative. *Pharmaceuticals (Basel)*, *13*(10). https://doi.org/10.3390/ph13100318

Ulland, T. K., Song, W. M., Huang, S. C., Ulrich, J. D., Sergushichev, A., Beatty, W. L., Loboda, A. A., Zhou, Y., Cairns, N. J., Kambal, A., Loginicheva, E., Gilfillan, S., Cella, M., Virgin, H. W., Unanue, E. R., Wang, Y., Artyomov, M. N., Holtzman, D. M., & Colonna, M. (2017). TREM2 Maintains Microglial Metabolic Fitness in Alzheimer's Disease. *Cell*, *170*(4), 649-663.e613. https://doi.org/10.1016/j.cell.2017.07.023

Van Dam, D., & De Deyn, P. P. (2011). Animal models in the drug discovery pipeline for Alzheimer's disease. *Br J Pharmacol*, *164*(4), 1285-1300. https://doi.org/10.1111/j.1476-5381.2011.01299.x

Van der Mussele, S., Fransen, E., Struyfs, H., Luyckx, J., Mariën, P., Saerens, J., Somers, N., Goeman, J., De Deyn, P. P., & Engelborghs, S. (2014). Depression in Mild Cognitive Impairment is associated with Progression to Alzheimer's Disease: A Longitudinal Study. *Journal of Alzheimer's Disease*, *42*, 1239-1250. https://doi.org/10.3233/JAD-140405

Van Epps, H. L. (2006). *Dying of excitement*. J Exp Med. 2006 Mar 20;203(3):484. doi: 10.1084/jem.2033iti4.

van Haaren, F., van Hest, A., & Heinsbroek, R. P. W. (1990). Behavioral differences between male and female rats: Effects of gonadal hormones on learning and memory. *Neuroscience & Biobehavioral Reviews*, *14*(1), 23-33. https://doi.org/https://doi.org/10.1016/S0149-7634(05)80157-5

Vandaele, Y., Mahajan, N. R., Ottenheimer, D. J., Richard, J. M., Mysore, S. P., & Janak, P. H. (2019). Distinct recruitment of dorsomedial and dorsolateral striatum erodes with extended training. *eLife*, *8*, e49536. https://doi.org/10.7554/eLife.49536

Vardarajan, B. N., Ghani, M., Kahn, A., Sheikh, S., Sato, C., Barral, S., Lee, J. H., Cheng, R., Reitz, C., Lantigua, R., Reyes-Dumeyer, D., Medrano, M., Jimenez-Velazquez, I. Z., Rogaeva, E., St George-Hyslop, P., & Mayeux, R. (2015). Rare coding mutations identified by sequencing of Alzheimer disease genome-wide association studies loci. *Ann Neurol*, *78*(3), 487-498. https://doi.org/10.1002/ana.24466

Vasconcelos, A. R., Yshii, L. M., Viel, T. A., Buck, H. S., Mattson, M. P., Scavone, C., & Kawamoto, E. M. (2014). Intermittent fasting attenuates lipopolysaccharide-induced neuroinflammation and memory impairment. *J Neuroinflammation*, *11*, 85. https://doi.org/10.1186/1742-2094-11-85

Veeraraghavalu, K., Choi, S. H., Zhang, X., & Sisodia, S. S. (2010). Presenilin 1 mutants impair the self-renewal and differentiation of adult murine subventricular zone-neuronal progenitors via cell-autonomous mechanisms involving notch signaling. *J Neurosci*, *30*(20), 6903-6915. https://doi.org/10.1523/jneurosci.0527-10.2010

Vegeto, E., Belcredito, S., Ghisletti, S., Meda, C., Etteri, S., & Maggi, A. (2006). The Endogenous Estrogen Status Regulates Microglia Reactivity in Animal Models of Neuroinflammation. *Endocrinology*, *147*(5), 2263-2272. https://doi.org/10.1210/en.2005-1330

Velasco, M., Rojas-Quintero, J., Chávez-Castillo, M., Rojas, M., Bautista, J., Martínez, M. S., Salazar, J., Mendoza, R. M., & Bermúdez, V. (2017). Excitotoxicity: An Organized Crime at The Cellular Level. *Journal of Neurology and Neuroscience*, *8*.

Verheijen, J., Van den Bossche, T., van der Zee, J., Engelborghs, S., Sanchez-Valle, R., Lladó, A., Graff, C., Thonberg, H., Pastor, P., Ortega-Cubero, S., Pastor, M. A., Benussi, L., Ghidoni, R., Binetti, G., Clarimon, J., Lleó, A., Fortea, J., de Mendonça, A., Martins, M., . . . Sleegers, K. (2016). A comprehensive study of the genetic impact of rare variants in SORL1 in European early-onset Alzheimer's disease. *Acta Neuropathol*, *132*(2), 213-224. https://doi.org/10.1007/s00401-016-1566-9

Verma, M., Lizama, B. N., & Chu, C. T. (2022). Excitotoxicity, calcium and mitochondria: a triad in synaptic neurodegeneration. *Translational Neurodegeneration*, *11*(1), 3. https://doi.org/10.1186/s40035-021-00278-7

Viggiano, M. P., Galli, G., Righi, S., Brancati, C., Gori, G., & Cincotta, M. (2008). Visual Recognition Memory in Alzheimer's Disease: Repetition-Lag Effects. *Experimental aging research*, *34*, 267-281. https://doi.org/10.1080/03610730802070241

Vikbladh, O. M., Meager, M. R., King, J., Blackmon, K., Devinsky, O., Shohamy, D., Burgess, N., & Daw, N. D. (2019). Hippocampal Contributions to Model-Based Planning and Spatial Memory. *Neuron*, *102*(3), 683-693.e684. https://doi.org/10.1016/j.neuron.2019.02.014

Voglewede, M. M., & Zhang, H. (2022). Polarity proteins: Shaping dendritic spines and memory. *Developmental Biology*, *488*, 68-73. https://doi.org/https://doi.org/10.1016/j.ydbio.2022.05.007

Walton, J. R., & Wang, M. X. (2009). APP expression, distribution and accumulation are altered by aluminum in a rodent model for Alzheimer's disease. *J Inorg Biochem*, *103*(11), 1548-1554. https://doi.org/10.1016/j.jinorgbio.2009.07.027

Wang, D., Noda, Y., Zhou, Y., Mouri, A., Mizoguchi, H., Nitta, A., Chen, W., & Nabeshima, T. (2007). The Allosteric Potentiation of Nicotinic Acetylcholine Receptors by Galantamine Ameliorates the Cognitive Dysfunction in Beta Amyloid25–35 I.c.v.-Injected Mice: Involvement of Dopaminergic Systems. *Neuropsychopharmacology*, *32*(6), 1261-1271. https://doi.org/10.1038/sj.npp.1301256

Wang, L., Yin, Y.-L., Liu, X.-Z., Shen, P., Zheng, Y.-G., Lan, X.-R., Lu, C.-B., & Wang, J.-Z. (2020). Current understanding of metal ions in the pathogenesis of Alzheimer's disease. *Translational Neurodegeneration*, *9*(1), 10. https://doi.org/10.1186/s40035-020-00189-z

Wang, L. M., Wu, Q., Kirk, R. A., Horn, K. P., Ebada Salem, A. H., Hoffman, J. M., Yap, J. T., Sonnen, J. A., Towner, R. A., Bozza, F. A., Rodrigues, R. S., & Morton, K. A. (2018). Lipopolysaccharide endotoxemia induces amyloid-β and p-tau formation in the rat brain. *Am J Nucl Med Mol Imaging*, *8*(2), 86-99.

Wang, Q., & Xie, C. (2022). Microglia activation linking amyloid-β drive tau spatial propagation in Alzheimer's disease. *Front Neurosci*, *16*, 951128. https://doi.org/10.3389/fnins.2022.951128

Wang, T., Chen, Y., Zou, Y., Pang, Y., He, X., Chen, Y., Liu, Y., Feng, W., Zhang, Y., Li, Q., Shi, J., Ding, F., Marshall, C., Gao, J., & Xiao, M. (2022). Locomotor Hyperactivity in the Early-Stage Alzheimer's Disease-like Pathology of APP/PS1 Mice: Associated with Impaired Polarization of Astrocyte Aquaporin 4. *Aging Dis*, *13*(5), 1504-1522. https://doi.org/10.14336/ad.2022.0219

Wang, W., Le, A. A., Hou, B., Lauterborn, J. C., Cox, C. D., Levin, E. R., Lynch, G., & Gall, C. M. (2018). Memory-Related Synaptic Plasticity Is Sexually Dimorphic in Rodent Hippocampus. *J Neurosci*, *38*(37), 7935-7951. https://doi.org/10.1523/jneurosci.0801-18.2018

Wang, W. Y., Tan, M. S., Yu, J. T., & Tan, L. (2015). Role of pro-inflammatory cytokines released from microglia in Alzheimer's disease. *Ann Transl Med*, *3*(10), 136. https://doi.org/10.3978/j.issn.2305-5839.2015.03.49

Wang, Y., Cella, M., Mallinson, K., Ulrich, Jason D., Young, Katherine L., Robinette, Michelle L., Gilfillan, S., Krishnan, Gokul M., Sudhakar, S., Zinselmeyer, Bernd H., Holtzman, David M., Cirrito, John R., & Colonna, M. (2015a). TREM2 Lipid Sensing Sustains the Microglial Response in an Alzheimer’s Disease Model. *Cell*, *160*(6), 1061-1071. https://doi.org/10.1016/j.cell.2015.01.049

Wang, Y., Cella, M., Mallinson, K., Ulrich, Jason D., Young, Katherine L., Robinette, Michelle L., Gilfillan, S., Krishnan, Gokul M., Sudhakar, S., Zinselmeyer, Bernd H., Holtzman, David M., Cirrito, John R., & Colonna, M. (2015b). TREM2 Lipid Sensing Sustains the Microglial Response in an Alzheimer's Disease Model. *Cell*, *160*(6), 1061-1071. https://doi.org/https://doi.org/10.1016/j.cell.2015.01.049

Wang, Y., Hall, R. A., Lee, M., Kamgar-Parsi, A., Bi, X., & Baudry, M. (2017). The tyrosine phosphatase PTPN13/FAP-1 links calpain-2, TBI and tau tyrosine phosphorylation. *Sci Rep*, *7*(1), 11771. https://doi.org/10.1038/s41598-017-12236-3

Wang, Y., Ulland, T. K., Ulrich, J. D., Song, W., Tzaferis, J. A., Hole, J. T., Yuan, P., Mahan, T. E., Shi, Y., Gilfillan, S., Cella, M., Grutzendler, J., DeMattos, R. B., Cirrito, J. R., Holtzman, D. M., &

Colonna, M. (2016). TREM2-mediated early microglial response limits diffusion and toxicity of amyloid plaques. *Journal of Experimental Medicine*, *213*(5), 667-675. https://doi.org/10.1084/jem.20151948

Wang, Y., Wei, H., Tong, J., Ji, M., & Yang, J. (2020). pSynGAP1 disturbance-mediated hippocampal oscillation network impairment might contribute to long-term neurobehavioral abnormities in sepsis survivors. *Aging*, *12*(22), 23146-23164. https://doi.org/10.18632/aging.104080

Webster, S. J., Bachstetter, A. D., & Van Eldik, L. J. (2013). Comprehensive behavioral characterization of an APP/PS-1 double knock-in mouse model of Alzheimer's disease. *Alzheimer's Research & Therapy*, *5*(3), 28. https://doi.org/10.1186/alzrt182

Wei, Y., & Li, X. (2022). Different phenotypes of microglia in animal models of Alzheimer disease. *Immun Ageing*, *19*(1), 44. https://doi.org/10.1186/s12979-022-00300-0

Weingarten, M. D., Lockwood, A. H., Hwo, S.-Y., & Kirschner, M. W. (1975). A protein factor essential for microtubule assembly. *Proceedings of the National Academy of Sciences*, *72*(5), 1858-1862.

Wen, P. H., Hof, P. R., Chen, X., Gluck, K., Austin, G., Younkin, S. G., Younkin, L. H., DeGasperi, R., Gama Sosa, M. A., Robakis, N. K., Haroutunian, V., & Elder, G. A. (2004). The presenilin-1 familial Alzheimer disease mutant P117L impairs neurogenesis in the hippocampus of adult mice. *Experimental Neurology*, *188*(2), 224-237. https://doi.org/https://doi.org/10.1016/j.expneurol.2004.04.002

Wenqin Rita, D., Elizabeth, L., Jun, G., Yuh-tarng, C., So Jung, O., Aspen, S., Ying, L., Hassana, K. O., & Wei, X. (2021). Hippocampus-striatum wiring diagram revealed by directed stepwise polysynaptic tracing. *bioRxiv*, 2021.2010.2012.464132. https://doi.org/10.1101/2021.10.12.464132

Whalley, K. (2013). Humans are on the grid. *Nature Reviews Neuroscience*, *14*(10), 667-667. https://doi.org/10.1038/nrn3588

Wheeler, M. A., Clark, I. C., Tjon, E. C., Li, Z., Zandee, S. E. J., Couturier, C. P., Watson, B. R., Scalisi, G., Alkwai, S., Rothhammer, V., Rotem, A., Heyman, J. A., Thaploo, S., Sanmarco, L. M., Ragoussis, J., Weitz, D. A., Petrecca, K., Moffitt, J. R., Becher, B., . . . Quintana, F. J. (2020). MAFG-driven astrocytes promote CNS inflammation. *Nature*, *578*(7796), 593-599. https://doi.org/10.1038/s41586-020-1999-0

Whissell, P. D., Tohyama, S., & Martin, L. J. (2016). The Use of DREADDs to Deconstruct Behavior [Review]. *Frontiers in Genetics*, *7*. https://doi.org/10.3389/fgene.2016.00070

White, J. D., Peterman, J. L., Hardy, A., Eimerbrink, M. J., Paulhus, K. C., Thompson, M. A., Chumley, M. J., & Boehm, G. W. (2017). Prior exposure to repeated peripheral LPS injections prevents further accumulation of hippocampal beta-amyloid. *Brain, Behavior, and Immunity*, *66*, e12-e13. https://doi.org/https://doi.org/10.1016/j.bbi.2017.07.056

Wikenheiser, A. M., & Schoenbaum, G. (2016). Over the river, through the woods: cognitive maps in the hippocampus and orbitofrontal cortex. *Nat Rev Neurosci*, *17*(8), 513-523. https://doi.org/10.1038/nrn.2016.56

Witter, M. P., Doan, T. P., Jacobsen, B., Nilssen, E. S., & Ohara, S. (2017). Architecture of the Entorhinal Cortex A Review of Entorhinal Anatomy in Rodents with Some Comparative Notes. *Front Syst Neurosci*, *11*, 46. https://doi.org/10.3389/fnsys.2017.00046

Witter, M. P., Naber, P. A., van Haeften, T., Machielsen, W. C., Rombouts, S. A., Barkhof, F., Scheltens, P., & Lopes da Silva, F. H. (2000). Cortico-hippocampal communication by way of parallel parahippocampal-subicular pathways. *Hippocampus*, *10*(4), 398-410. https://doi.org/10.1002/1098-1063(2000)10:4<398::Aid-hipo6>3.0.Co;2-k

Wlodarczyk, A., Benmamar-Badel, A., Cédile, O., Jensen, K. N., Kramer, I., Elsborg, N. B., & Owens, T. (2018). CSF1R Stimulation Promotes Increased Neuroprotection by CD11c+ Microglia in EAE. *Front Cell Neurosci*, *12*, 523. https://doi.org/10.3389/fncel.2018.00523

Wojdasiewicz, P., Poniatowski, Ł. A., & Szukiewicz, D. (2014). The Role of Inflammatory and Anti-Inflammatory Cytokines in the Pathogenesis of Osteoarthritis. *Mediators of Inflammation*, *2014*, 561459. https://doi.org/10.1155/2014/561459

Wright, A., Zinn, R., Voraberger, B., Konen, L., Beynon, S., Tan, R., Clark, I., Cowley, A., & Vissel, B. (2013). Neuroinflammation and Neuronal Loss Precede Aβ Plaque Deposition in the hAPP-J20 Mouse Model of Alzheimer's Disease. *PLOS ONE*, *8*, e59586. https://doi.org/10.1371/journal.pone.0059586

Wright, A. L., Zinn, R., Hohensinn, B., Konen, L. M., Beynon, S. B., Tan, R. P., Clark, I. A., Abdipranoto, A., & Vissel, B. (2013). Neuroinflammation and Neuronal Loss Precede Aβ Plaque Deposition in the hAPP-J20 Mouse Model of Alzheimer's Disease. *PLOS ONE*, *8*(4), e59586. https://doi.org/10.1371/journal.pone.0059586

Wu, M., Zhai, Y., Liang, X., Chen, W., Lin, R., Ma, L., Huang, Y., Zhao, D., Liang, Y., Zhao, W., Fang, J., Fang, S., Chen, Y., Wang, Q., & Li, W. (2022). Connecting the Dots Between Hypercholesterolemia and Alzheimer's Disease: A Potential Mechanism Based on 27-Hydroxycholesterol. *Front Neurosci*, *16*, 842814. https://doi.org/10.3389/fnins.2022.842814

Wu, X.-m., Ji, M.-h., Yin, X.-y., Gu, H.-w., Zhu, T.-t., Wang, R.-z., Yang, J.-j., & Shen, J.-c. (2022). Reduced inhibition underlies early life LPS exposure induced-cognitive impairment: Prevention by environmental enrichment. *International Immunopharmacology*, *108*, 108724. https://doi.org/https://doi.org/10.1016/j.intimp.2022.108724

Wu, Y. K., Fujishima, K., & Kengaku, M. (2015). Differentiation of apical and basal dendrites in pyramidal cells and granule cells in dissociated hippocampal cultures. *PLOS ONE*, *10*(2), e0118482. https://doi.org/10.1371/journal.pone.0118482

Wysocka, A., Palasz, E., Steczkowska, M., & Niewiadomska, G. (2020). Dangerous Liaisons: Tau Interaction with Muscarinic Receptors. *Curr Alzheimer Res*, *17*(3), 224-237. https://doi.org/10.2174/1567205017666200424134311

Xia, M., Cheng, X., Yi, R., Gao, D., & Xiong, J. (2016). The Binding Receptors of Aβ: an Alternative Therapeutic Target for Alzheimer's Disease. *Molecular Neurobiology*, *53*(1), 455-471. https://doi.org/10.1007/s12035-014-8994-0

Xingi, E., Koutsoudaki, P. N., Thanou, I., Phan, M.-S., Margariti, M., Scheller, A., Tinevez, J.-Y., Kirchhoff, F., & Thomaidou, D. (2023). LPS-Induced Systemic Inflammation Affects the Dynamic Interactions of Astrocytes and Microglia with the Vasculature of the Mouse Brain Cortex. *Cells*, *12*(10).

Xu, Q.-Q., Su, Z.-R., Yang, W., Zhong, M., Xian, Y.-F., & Lin, Z.-X. (2023). Patchouli alcohol attenuates the cognitive deficits in a transgenic mouse model of Alzheimer's disease via modulating neuropathology and gut microbiota through suppressing C/EBPβ/AEP pathway. *Journal of Neuroinflammation*, *20*(1), 19. https://doi.org/10.1186/s12974-023-02704-1

Yang, L., Zhou, R., Tong, Y., Chen, P., Shen, Y., Miao, S., & Liu, X. (2020). Neuroprotection by dihydrotestosterone in LPS-induced neuroinflammation. *Neurobiology of Disease*, *140*, 104814. https://doi.org/https://doi.org/10.1016/j.nbd.2020.104814

Yang, Y.-W., Hsu, K.-C., Wei, C.-Y., Tzeng, R.-C., & Chiu, P.-Y. (2021). Operational Determination of Subjective Cognitive Decline, Mild Cognitive Impairment, and Dementia Using Sum of Boxes of the Clinical Dementia Rating Scale [Original Research]. *Frontiers in Aging Neuroscience*, *13*. https://doi.org/10.3389/fnagi.2021.705782

Yang, Y., García-Cruzado, M., Zeng, H., Camprubí-Ferrer, L., Bahatyrevich-Kharitonik, B., Bachiller, S., & Deierborg, T. (2023). LPS priming before plaque deposition impedes microglial activation and restrains Aβ pathology in the 5xFAD mouse model of Alzheimer's disease. *Brain, Behavior, and Immunity*, *113*, 228-247. https://doi.org/https://doi.org/10.1016/j.bbi.2023.07.006

Yiannopoulou, K. G., Anastasiou, A. I., Zachariou, V., & Pelidou, S. H. (2019). Reasons for Failed Trials of Disease-Modifying Treatments for Alzheimer Disease and Their Contribution in Recent Research. *Biomedicines*, *7*(4). https://doi.org/10.3390/biomedicines7040097

Yin, H. H., Knowlton, B. J., & Balleine, B. W. (2005). Blockade of NMDA receptors in the dorsomedial striatum prevents action-outcome learning in instrumental conditioning. *Eur J Neurosci*, *22*(2), 505-512. https://doi.org/10.1111/j.1460-9568.2005.04219.x

Yin, H. H., Ostlund, S. B., Knowlton, B. J., & Balleine, B. W. (2005). The role of the dorsomedial striatum in instrumental conditioning [https://doi.org/10.1111/j.1460-9568.2005.04218.x]. *European Journal of Neuroscience*, *22*(2), 513-523. https://doi.org/https://doi.org/10.1111/j.1460-9568.2005.04218.x

Yin, J. X., Turner, G. H., Lin, H. J., Coons, S. W., & Shi, J. (2011). Deficits in spatial learning and memory is associated with hippocampal volume loss in aged apolipoprotein E4 mice. *J Alzheimers Dis*, *27*(1), 89-98. https://doi.org/10.3233/jad-2011-110479

Yokoyama, M., Kobayashi, H., Tatsumi, L., & Tomita, T. (2022). Mouse Models of Alzheimer's Disease. *Front Mol Neurosci*, *15*, 912995. https://doi.org/10.3389/fnmol.2022.912995

Yong, H. Y. F., Rawji, K. S., Ghorbani, S., Xue, M., & Yong, V. W. (2019). The benefits of neuroinflammation for the repair of the injured central nervous system. *Cellular & Molecular Immunology*, *16*(6), 540-546. https://doi.org/10.1038/s41423-019-0223-3

Yong, V. W., & Rivest, S. (2009). Taking Advantage of the Systemic Immune System to Cure Brain Diseases. *Neuron*, *64*(1), 55-60. https://doi.org/https://doi.org/10.1016/j.neuron.2009.09.035

Youmans, K. L., Tai, L. M., Nwabuisi-Heath, E., Jungbauer, L., Kanekiyo, T., Gan, M., Kim, J., Eimer, W. A., Estus, S., Rebeck, G. W., Weeber, E. J., Bu, G., Yu, C., & Ladu, M. J. (2012). APOE4-specific changes in Aβ accumulation in a new transgenic mouse model of Alzheimer disease. *J Biol Chem*, *287*(50), 41774-41786. https://doi.org/10.1074/jbc.M112.407957

Yuan, P., Condello, C., Keene, C. D., Wang, Y., Bird, Thomas D., Paul, Steven M., Luo, W., Colonna, M., Baddeley, D., & Grutzendler, J. (2016). TREM2 Haplodeficiency in Mice and Humans Impairs the Microglia Barrier Function Leading to Decreased Amyloid Compaction and Severe Axonal Dystrophy. *Neuron*, *90*(4), 724-739. https://doi.org/https://doi.org/10.1016/j.neuron.2016.05.003

Yuste-Checa, P., Bracher, A., & Hartl, F. U. (2022). The chaperone Clusterin in neurodegeneration−friend or foe? *BioEssays*, *44*(7), 2100287. https://doi.org/https://doi.org/10.1002/bies.202100287

Zárate, S., Stevnsner, T., & Gredilla, R. (2017). Role of Estrogen and Other Sex Hormones in Brain Aging. Neuroprotection and DNA Repair [Review]. *Frontiers in Aging Neuroscience*, *9*. https://doi.org/10.3389/fnagi.2017.00430

Zetterberg, H., & Mattsson, N. (2014). Understanding the cause of sporadic Alzheimer's disease. *Expert Review of Neurotherapeutics*, *14*(6), 621-630. https://doi.org/10.1586/14737175.2014.915740

Zhang, H., Cao, Y., Ma, L., Wei, Y., & Li, H. (2021). Possible Mechanisms of Tau Spread and Toxicity in Alzheimer's Disease. *Front Cell Dev Biol*, *9*, 707268. https://doi.org/10.3389/fcell.2021.707268

Zhang, H. Y., Yan, H., & Tang, X. C. (2004). Huperzine A enhances the level of secretory amyloid precursor protein and protein kinase C-α in intracerebroventricular β-amyloid-(1–40) infused rats and human embryonic kidney 293 Swedish mutant cells. *Neuroscience Letters*, *360*(1-2), 21-24.

Zhang, J.-C., Wu, J., Fujita, Y., Yao, W., Ren, Q., Yang, C., Li, S., Shirayama, Y., & Hashimoto, K. (2014). Antidepressant Effects of TrkB Ligands on Depression-Like Behavior and Dendritic Changes in Mice After Inflammation. *International Journal of Neuropsychopharmacology*, *18*. https://doi.org/10.1093/ijnp/pyu077

Zhang, L., Chen, C., Mak, M. S., Lu, J., Wu, Z., Chen, Q., Han, Y., Li, Y., & Pi, R. (2020). Advance of sporadic Alzheimer's disease animal models. *Medicinal Research Reviews*, *40*(1), 431-458. https://doi.org/https://doi.org/10.1002/med.21624

Zhang, L., Chen, C., Mak, S., Lu, J., Wu, Z., Chen, Q., Han, Y., Li, Y., & Pi, R. (2019). Advance of sporadic Alzheimer's disease animal models. *Medicinal Research Reviews*, *40*. https://doi.org/10.1002/med.21624

Zhang, L., Wang, H., Abel, G., Storm, D., & Xia, Z. (2019). The Effects of Gene-Environment Interactions Between Cadmium Exposure and Apolipoprotein E4 on Memory in a Mouse Model of Alzheimer's Disease. *Toxicological sciences : an official journal of the Society of Toxicology*, *173*. https://doi.org/10.1093/toxsci/kfz218

Zhang, R., Xue, G., Wang, S., Zhang, L., Shi, C., & Xie, X. (2012). Novel object recognition as a facile behavior test for evaluating drug effects in AβPP/PS1 Alzheimer's disease mouse model. *J Alzheimers Dis*, *31*(4), 801-812. https://doi.org/10.3233/jad-2012-120151

Zhang, Y., Ding, R., Wang, S., Ren, Z., Xu, L., Zhang, X., Zhao, J., Ding, Y., Wu, Y., & Gong, Y. (2018). Effect of intraperitoneal or intracerebroventricular injection of streptozotocin on learning and memory in mice. *Experimental and therapeutic medicine*, *16*(3), 2375-2380. https://doi.org/10.3892/etm.2018.6487

Zhao, J., Bi, W., Xiao, S., Lan, X., Cheng, X., Zhang, J., Lu, D., Wei, W., Wang, Y., Li, H., Fu, Y., & Zhu, L. (2019). Neuroinflammation induced by lipopolysaccharide causes cognitive impairment in mice. *Scientific Reports*, *9*(1), 5790. https://doi.org/10.1038/s41598-019-42286-8

Zhao, N., Liu, C. C., Van Ingelgom, A. J., Martens, Y. A., Linares, C., Knight, J. A., Painter, M. M., Sullivan, P. M., & Bu, G. (2017). Apolipoprotein E4 Impairs Neuronal Insulin Signaling by Trapping Insulin Receptor in the Endosomes. *Neuron*, *96*(1), 115-129.e115. https://doi.org/10.1016/j.neuron.2017.09.003

Zhao, Q.-F., Tan, L., Wang, H.-F., Jiang, T., Tan, M.-S., Tan, L., Xu, W., Li, J.-Q., Wang, J., Lai, T.-J., & Yu, J.-T. (2016). The prevalence of neuropsychiatric symptoms in Alzheimer's disease: Systematic review and meta-analysis. *Journal of Affective Disorders*, *190*, 264-271. https://doi.org/https://doi.org/10.1016/j.jad.2015.09.069

Zhao, R., Hu, W., Tsai, J., Li, W., & Gan, W. B. (2017). Microglia limit the expansion of β-amyloid plaques in a mouse model of Alzheimer's disease. *Mol Neurodegener*, *12*(1), 47. https://doi.org/10.1186/s13024-017-0188-6

Zheng, H., & Koo, E. H. (2011). Biology and pathophysiology of the amyloid precursor protein. *Molecular Neurodegeneration*, *6*(1), 27. https://doi.org/10.1186/1750-1326-6-27

Zhong, G., Wang, Y., Zhang, Y., Guo, J. J., & Zhao, Y. (2015). Smoking Is Associated with an Increased Risk of Dementia: A Meta-Analysis of Prospective Cohort Studies with Investigation of Potential Effect Modifiers. *PLOS ONE*, *10*(3), e0118333. https://doi.org/10.1371/journal.pone.0118333

Zhou, J., Montesinos-Cartagena, M., Wikenheiser, A. M., Gardner, M. P. H., Niv, Y., & Schoenbaum, G. (2019). Complementary Task Structure Representations in Hippocampus and Orbitofrontal Cortex during an Odor Sequence Task. *Current Biology*, *29*(20), 3402-3409.e3403. https://doi.org/10.1016/j.cub.2019.08.040

Zhou, Z., Peng, X., Insolera, R., Fink, D. J., & Mata, M. (2009). Interleukin-10 provides direct trophic support to neurons. *Journal of neurochemistry*, *110*(5), 1617-1627.

Zhu, L., Zhong, M., Elder, G. A., Sano, M., Holtzman, D. M., Gandy, S., Cardozo, C., Haroutunian, V., Robakis, N. K., & Cai, D. (2015). Phospholipid dysregulation contributes to ApoE4-associated cognitive deficits in Alzheimer's disease pathogenesis. *Proc Natl Acad Sci U S A*, *112*(38), 11965-11970. https://doi.org/10.1073/pnas.1510011112

Zhu, S., Wang, J., Zhang, Y., He, J., Kong, J., Wang, J.-F., & Li, X.-M. (2017). The role of neuroinflammation and amyloid in cognitive impairment in an APP/PS1 transgenic mouse model of Alzheimer's disease. *CNS Neuroscience & Therapeutics*, *23*(4), 310-320. https://doi.org/https://doi.org/10.1111/cns.12677

Zhu, Y., Nwabuisi-Heath, E., Dumanis, S. B., Tai, L. M., Yu, C., Rebeck, G. W., & Ladu, M. J. (2012). APOE genotype alters glial activation and loss of synaptic markers in mice. *Glia*, *60*(4), 559-569. https://doi.org/https://doi.org/10.1002/glia.22289

Zussy, C., John, R., Urgin, T., Otaegui, L., Vigor, C., Acar, N., Canet, G., Vitalis, M., Morin, F., Planel, E., Oger, C., Durand, T., Rajshree, S. L., Givalois, L., Devarajan, P. V., & Desrumaux, C. (2022). Intranasal Administration of Nanovectorized Docosahexaenoic Acid (DHA) Improves Cognitive Function in Two Complementary Mouse Models of Alzheimer’s Disease. *Antioxidants*, *11*(5).

Zyśk, M., Beretta, C., Naia, L., Dakhel, A., Påvénius, L., Brismar, H., Lindskog, M., Ankarcrona, M., & Erlandsson, A. (2023). Amyloid-β accumulation in human astrocytes induces mitochondrial disruption and changed energy metabolism. *Journal of Neuroinflammation*, *20*(1), 43. https://doi.org/10.1186/s12974-023-02722-z

7. Appendices:

Appendix A: Experiment 1: Validating the sensitivity of our experimental procedures using the hAPP-J20 model:

Open field test:

Total distance travelled			Time spent in centre	
WT	J20		WT	J20
2400.411	2510.994		358.3	430.3
1409.095	3287.752		297.6	310.2
946.692	3436.839		411.35	344.1
1563.268	1578.682		394.25	479.85
1272.716	1961.779		462.2	356.05
2023.617	2710.709		235.8	333.55
	2557.69			310.45
	1441.575			312.85
	1734.783			319.8

Total distance travelled

Unpaired t test	
Table Analyzed	OFT Distance Travelled
Column B	J20
vs.	vs.
Column A	WT
Unpaired t test	
P value	0.0480
P value summary	*
Significantly different (P < 0.05)?	Yes
One- or two-tailed P value?	Two-tailed
t, df	t=2.183, df=13
How big is the difference?	
Mean of column A	1603
Mean of column B	2358
Difference between means (B - A) ± SEM	755.2 ± 345.9
95% confidence interval	7.902 to 1503
R squared (eta squared)	0.2683
F test to compare variances	
F, DFn, Dfd	1.890, 8, 5
P value	0.5009
P value summary	ns
Significantly different (P < 0.05)?	No
Data analyzed	
Sample size, column A	6
Sample size, column B	9

Time spent in centre

Unpaired t test	
Table Analyzed	OFT Time in Centre
Column B	J20
vs.	vs.
Column A	WT
Unpaired t test	
P value	0.9000
P value summary	ns
Significantly different (P < 0.05)?	No
One- or two-tailed P value?	Two-tailed
t, df	t=0.1281, df=13
How big is the difference?	
Mean of column A	359.9
Mean of column B	355.2
Difference between means (B - A) ± SEM	-4.678 ± 36.52
95% confidence interval	-83.58 to 74.22
R squared (eta squared)	0.001260
F test to compare variances	
F, DFn, Dfd	1.863, 5, 8
P value	0.4140
P value summary	ns
Significantly different (P < 0.05)?	No
Data analyzed	
Sample size, column A	6
Sample size, column B	9

Barnes maze test:

	WT						J20								
Target zon	40.1	26.7	36.6	51.3	56.1	39.1	26.1	44.8	27.7	34.6	35.3	37	26.6	13.6	18.7
Zone 1	9.8	19.9	12.1	9.7	20.6	17.2	17	23.9	20.8	7.5	18.3	7.7	10.1	33	22.9
Zone 2	7.5	10.4	15.1	9.8	3.5	6.1	18.1	3.9	22.8	23	12.6	14.1	20.5	13.7	27.7
Zone 3	14	23.8	12	14.3	2.8	15.9	17.6	12	4.1	4.3	10.1	14.2	22.4	20.2	19.4

Two- way ANOVA

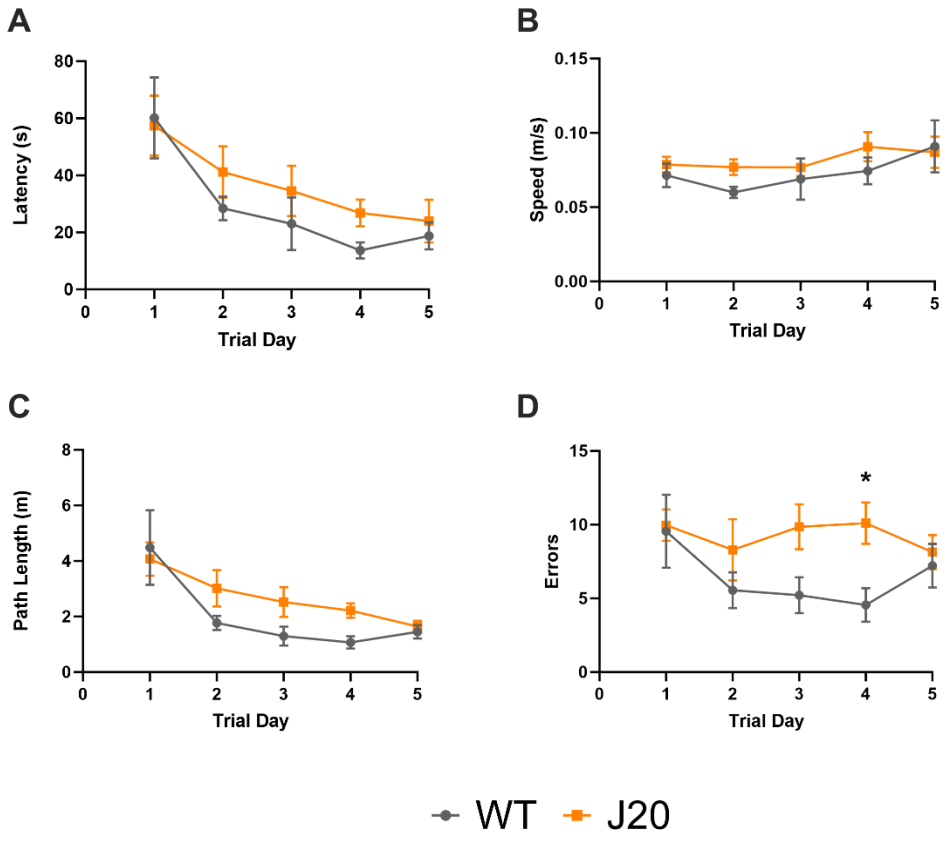

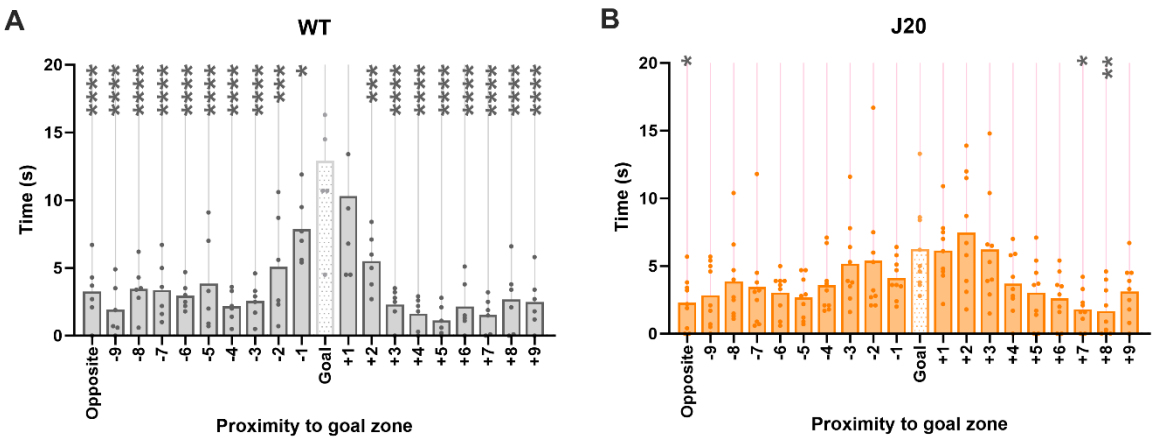

ANOVA results | Multiple comparisons

2way ANOVA
ANOVA results

1	Table Analyzed	Probe-data-redone				
2						
3	**Two-way ANOVA**	Ordinary				
4	Alpha	0.05				
5						
6	**Source of Variation**	**% of total variation**	**P value**	**P value summary**	**Significant?**	
7	Interaction	10.21	0.0053	**	Yes	
8	Zones	59.19	<0.0001	****	Yes	
9	Genotype	0.003775	0.9424	ns	No	
10						
11	**ANOVA table**	**SS (Type III)**	**DF**	**MS**	**F (DFn, DFd)**	**P value**
12	Interaction	843.9	3	281.3	F (3, 52) = 4.756	P=0.0053
13	Zones	4894	3	1631	F (3, 52) = 27.58	P<0.0001
14	Genotype	0.3121	1	0.3121	F (1, 52) = 0.005277	P=0.9424
15	Residual	3075	52	59.14		
16						
17	**Difference between column means**					
18	Predicted (LS) mean of WT	19.77				
19	Predicted (LS) mean of J20	19.62				
20	Difference between predicted means	0.1472				
21	SE of difference	2.027				
22	95% CI of difference	-3.919 to 4.214				
23						
24	**Data summary**					
25	Number of columns (Genotype)	2				
26	Number of rows (Zones)	4				
27	Number of values	60				
28						

ANOVA results | Multiple comparisons

2way ANOVA
Multiple comparisons

Compare each cell mean with the other cell mean in that row								
Number of families	1							
Number of comparisons per family	4							
Alpha	0.05							
Bonferroni's multiple comparisons test	**Predicted (LS) mean diff.**	**95.00% CI of diff.**	**Below threshold?**	**Summary**	**Adjusted P Value**			
WT - J20								
Target zone	12.27	1.784 to 22.76	Yes	*	0.0153			
Zone 1	-3.028	-13.52 to 7.460	No	ns	>0.9999			
Zone 2	-8.644	-19.13 to 1.843	No	ns	0.1507			
Zone 3	-0.01111	-10.50 to 10.48	No	ns	>0.9999			
Test details	**Predicted (LS) mean 1**	**Predicted (LS) mean 2**	**Predicted (LS) mean diff.**	**SE of diff.**	**N1**	**N2**	**t**	**DF**
WT - J20								
Target zone	41.65	29.38	12.27	4.053	6	9	3.028	52.00
Zone 1	14.88	17.91	-3.028	4.053	6	9	0.7470	52.00
Zone 2	8.733	17.38	-8.644	4.053	6	9	2.133	52.00
Zone 3	13.80	13.81	-0.01111	4.053	6	9	0.002741	52.00

Dendritic spines:

Apical dendrites

WT	J20
10.74316	13.54332
12.67597	13.88249
11.85151	12.00269

Basal dendrites

WT	J20
10.04416	8.137909
8.370935	11.10914
11.01938	9.905228

12.17444	12.81925	7.658504	12.00418
13.02748	9.965857	12.53987	8.137909
16.42239	12.288	11.63629	11.10914
13.13958	10.46288	10.86251	9.905228
14.02662	12.84915	9.52712	12.00418
13.7274	12.68213	10.94332	10.04416
14.48297	15.22595	8.560537	8.370935
16.59956	13.78709	10.83299	11.01938
15.47685	12.04373	13.095	7.658504
13.73224	8.944377	12.44859	8.944377
16.56325	11.3873	14.89792	11.3873
14.40297	9.167734	10.95563	9.167734
18.12843	11.44528	13.27942	11.44528

Apical dendrites

Tabular results

Unpaired t test
Tabular results

1	Table Analyzed	Apical spines
2		
3	Column B	J20
4	vs.	vs.
5	Column A	WT
6		
7	**Unpaired t test**	
8	P value	0.0028
9	P value summary	**
10	Significantly different (P < 0.05)?	Yes
11	One- or two-tailed P value?	Two-tailed
12	t, df	t=3.256, df=30
13		
14	**How big is the difference?**	
15	Mean of column A	14.20
16	Mean of column B	12.03
17	Difference between means (B - A) ± SEM	-2.167 ± 0.6656
18	95% confidence interval	-3.527 to -0.8080
19	R squared (eta squared)	0.2611
20		
21	**F test to compare variances**	
22	F, DFn, Dfd	1.312, 15, 15
23	P value	0.6060
24	P value summary	ns
25	Significantly different (P < 0.05)?	No
26		
27	**Data analyzed**	
28	Sample size, column A	16
29	Sample size, column B	16
30		

Unpaired t test

1	Table Analyzed	Basal spines
2		
3	Column B	J20
4	vs.	vs.
5	Column A	WT
6		
7	**Unpaired t test**	
8	P value	0.1047
9	P value summary	ns
10	Significantly different (P < 0.05)?	No
11	One- or two-tailed P value?	Two-tailed
12	t, df	t=1.673, df=30
13		
14	**How big is the difference?**	
15	Mean of column A	11.04
16	Mean of column B	10.02
17	Difference between means (B - A) ± SEM	-1.020 ± 0.6097
18	95% confidence interval	-2.265 to 0.2251
19	R squared (eta squared)	0.08534
20		
21	**F test to compare variances**	
22	F, DFn, Dfd	1.751, 15, 15
23	P value	0.2892
24	P value summary	ns
25	Significantly different (P < 0.05)?	No
26		
27	**Data analyzed**	
28	Sample size, column A	16
29	Sample size, column B	16
30		

Glial cells:

Microglia

WT	J20
18437.11	18843.64
14952.11	20239.41
15504.89	16455.83
16374.02	12457.27
20229.04	14633.19

Apparatus

WT	J20
26131.17	41815.33
20319.02	41029.95
29723.93	43640.7
34249.63	49601.21
32790.22	39147.21

Tabular results

Unpaired t test
Tabular results

1	Table Analyzed	Iba1
2		
3	Column B	J20
4	vs.	vs.
5	Column A	WT
6		
7	**Unpaired t test**	
8	P value	0.7461
9	P value summary	ns
10	Significantly different (P < 0.05)?	No
11	One- or two-tailed P value?	Two-tailed
12	t, df	t=0.3352, df=8
13		
14	**How big is the difference?**	
15	Mean of column A	17099
16	Mean of column B	16526
17	Difference between means (B - A) ± SEM	-573.6 ± 1711
18	95% confidence interval	-4520 to 3373
19	R squared (eta squared)	0.01385
20		
21	**F test to compare variances**	
22	F, DFn, Dfd	2.040, 4, 4
23	P value	0.5068
24	P value summary	ns
25	Significantly different (P < 0.05)?	No
26		
27	**Data analyzed**	
28	Sample size, column A	5
29	Sample size, column B	5
30		

Tabular results

Unpaired t test
Tabular results

1	Table Analyzed	GFAP
2		
3	Column B	J20
4	vs.	vs.
5	Column A	WT
6		
7	**Unpaired t test**	
8	P value	0.0016
9	P value summary	**
10	Significantly different (P < 0.05)?	Yes
11	One- or two-tailed P value?	Two-tailed
12	t, df	t=4.679, df=8
13		
14	**How big is the difference?**	
15	Mean of column A	28643
16	Mean of column B	43047
17	Difference between means (B - A) ± SEM	14404 ± 3078
18	95% confidence interval	7306 to 21502
19	R squared (eta squared)	0.7324
20		
21	**F test to compare variances**	
22	F, DFn, Dfd	1.956, 4, 4
23	P value	0.5317
24	P value summary	ns
25	Significantly different (P < 0.05)?	No
26		
27	**Data analyzed**	
28	Sample size, column A	5
29	Sample size, column B	5
30		

Appendix B: Experiment 2 – Combining major genetic and non-genetic risk factors to create a sporadic model of AD:

Open Field test:

Total distance travelled:

										WT															
Saline	2852.741	1900.78	1506.854	1722.351	1474.026	1769.198	2916.707	1272.267	1591.667	1661.012	2028.875	1989.461	2447.587	2290.055	2414.002	1210.245									
LPS	1048.985	1564.276	1425.449	1828.863	1332.442	1358.136	1701.474	1763.985	1533.337	2055.728	1479.583	1166.782	1812.267	1743.944	2137.049	1700.232	1911.272	1551.41							
														E4											
Saline	1248.967	1741.65	2627.298	1885.56	3011.263	1869.902	3056.384	2566.574	1287.291	1833.501	2301.997	2387.452	1899.996	1944.015	1411.764										
LPS	1842.504	1893.806	1002.853	1229.28	1179.701	2103.447	2021.189	2191.571	1378.795	1481.707	1451.863	1091.445	1037.135	1553.61	1815.438	1776.636	1144.66	1643.305	2095.764	2339.1	1686.832	1894.838	1744.895	1188.472	
														hAPP											
Saline	1655.142	2481.96	3884.748	1814.718	1621.502	1465.868	1120.651	2655.316	1156.974	2003.253	2172.325	1527.487													
LPS	912.2974	2100.601	2107.868	2459.992	1302.02	1835.956	842.905	747.0549	1266.105	837.3471	520.3773	627.9649	1158.258	1833.576	1893.621	1063.713	1148.333	1411.945	820.6126	1106.777	968.75	1198.37	925.8652	1076.988	1233.043

ANOVA results | Multiple comparisons

2way ANOVA
ANOVA results

1	Table Analyzed	Open Field Test Distance				
2						
3	**Two-way ANOVA**	Ordinary				
4	Alpha	0.05				
5						
6	**Source of Variation**	**% of total variation**	**P value**	**P value**	**Significant**	
7	Interaction	1.783	0.2925	ns	No	
8	Treatment	17.85	<0.0001	****	Yes	
9	Genotype	2.807	0.1461	ns	No	
10						
11	**ANOVA table**	**SS (Type III)**	**DF**	**MS**	**F (DFn, DF**	**P value**
12	Interaction	630252	2	315126	F (2, 104) =	P=0.2925
13	Treatment	6311295	1	6311295	F (1, 104) =	P<0.0001
14	Genotype	992537	2	496269	F (2, 104) =	P=0.1461
15	Residual	26343934	104	253307		
16						
17	**Difference between row means**					
18	Predicted (LS) mean of Saline	1992				
19	Predicted (LS) mean of LPS	1497				
20	Difference between predicted means	495.2				
21	SE of difference	99.21				
22	95% CI of difference	298.5 to 692.0				
23						
24	**Data summary**					
25	Number of columns (Genotype)	3				
26	Number of rows (Treatment)	2				
27	Number of values	110				

ANOVA results | Multiple comparisons

2way ANOVA
Multiple comparisons

1	Compare each cell mean with the other cell mean in that column								
2									
3	Number of families	1							
4	Number of comparisons per family	3							
5	Alpha	0.05							
6									
7	**Bonferroni's multiple comparisons test**	**Predicted (LS) mean diff.**	**95.00% CI of diff.**	**Below threshold?**	**Summary**	**Adjusted P Value**			
8									
9	Saline - LPS								
10	WT	323.0	-97.81 to 743.8	No	ns	0.1939			
11	E4	455.4	52.28 to 858.5	Yes	*	0.0212			
12	hAPP	707.3	277.2 to 1137	Yes	***	0.0004			
13									
14									
15	**Test details**	**Predicted (LS) mean 1**	**Predicted (LS) mean 2**	**Predicted (LS) mean diff.**	**SE of diff.**	**N1**	**N2**	**t**	**DF**
16									
17	Saline - LPS								
18	WT	1940	1618	323.0	172.9	16	18	1.868	104.0
19	E4	2072	1616	455.4	165.7	15	24	2.749	104.0
20	hAPP	1963	1256	707.3	176.8	12	25	4.002	104.0
21									

Time spent in centre:

	WT																										
Saline	336.65	321.1	315.2	430.75	343.4	375.8	304.95	352.7	276.45	377.05	329.5	381.85	235.9	350.35	393.55	468.85											
LPS	316	451.95	416.35	403.9	175.9	343.15	264.05	362.65	365.55	396.25	359.1	440.5	387.7	264.95	377.4	404.45	329.6	368.1									
	APOE4-KI																										
Saline	256.3	325.6	322.3	219.6	363.85	350.8	388.35	383.2	234.1	402.8	381.5	378.95	332.5	465.35	451.35												
LPS	361.3	439.65	266.85	461.95	494.6	449.75	417.55	382.05	477.85	425.75	340.35	310.9	469.85	382.4	332.1	360.4	250.35	292.1	345.5	363.9	373.4	361.7	408.05	491.55			
	hAβ-KI																										
Saline	350.15	452.6	382	353.85	299.15	471.9	507.45	418.4	272.95	436.05	345.15	414.4															
LPS	379.05	416.45	392.55	427.45	270.55	437.2	444.65	489.05	415.5	204.8	190.15	84.05	272.05	441.25	337.3	254.8	361.35	460.35	181.95	372.2	421	302.15	427.5	453.35	390		

2way ANOVA					
Table Analyzed	Open Field Test Time in Centre				
Two-way ANOVA	Ordinary				
Alpha	0.05				
Source of Variation	**% of total variation**	**P value**	**P value summary**	**Significant?**	
Interaction	3.639	0.1426	ns	No	
Treatment	0.006606	0.9325	ns	No	
Genotype	1.024	0.5738	ns	No	
ANOVA table	**SS (Type III)**	**DF**	**MS**	**F (DFn, DFd)**	**P value**
Interaction	24112	2	12056	F (2, 104) = 1.985	P=0.1426
Treatment	43.76	1	43.76	F (1, 104) = 0.007204	P=0.9325
Genotype	6786	2	3393	F (2, 104) = 0.5585	P=0.5738
Residual	631768	104	6075		
Difference between row means					
Predicted (LS) mean of Saline	364.0				
Predicted (LS) mean of LPS	365.3				
Difference between predicted means	-1.304				
SE of difference	15.36				
95% CI of difference	-31.77 to 29.16				
Data summary					
Number of columns (Genotype)	3				
Number of rows (Treatment)	2				
Number of values	110				

Barnes Maze learning curve:

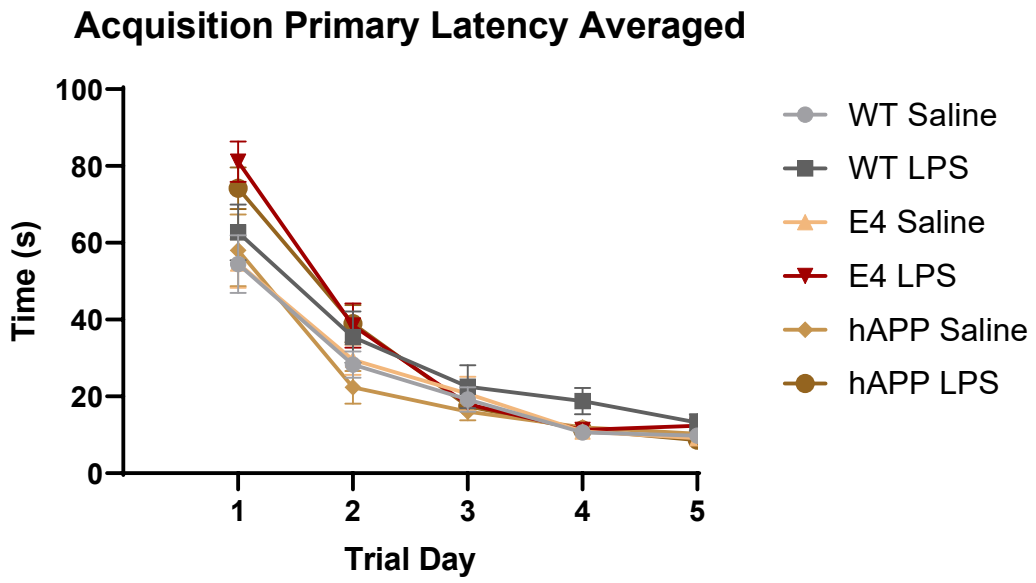

Acquisition Primary Path Length Averaged

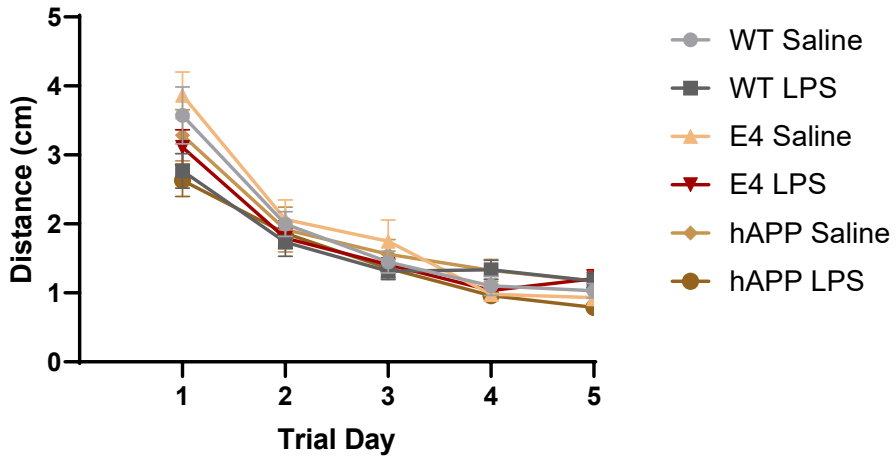

Acquisition Primary Average Speed Averaged

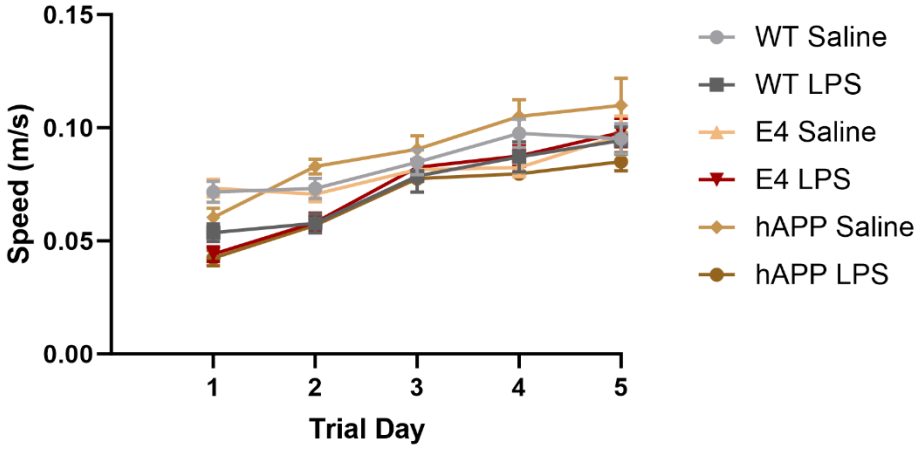

Acquisition Primary Errors Averaged

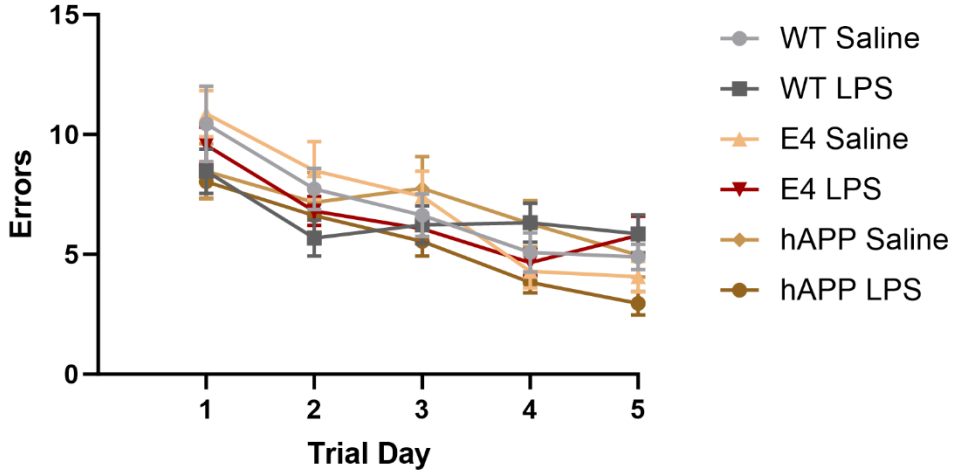

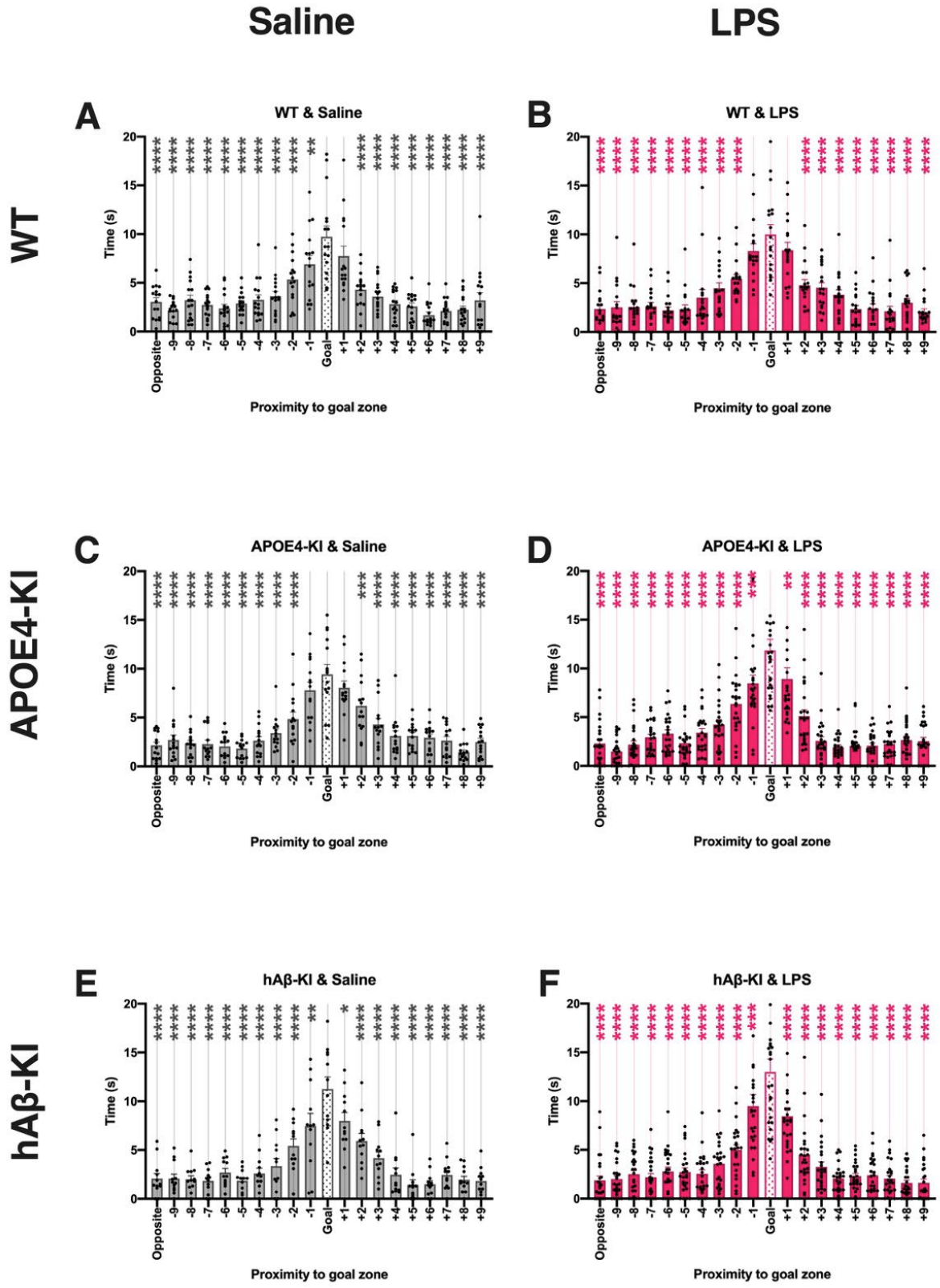

Spine density:

Apical dendrites

	Sham																						
WT	16.42736	9.219472	8.739054	10.89129	8.639904	13.65483	10.77797	11.91673	11.21828	10.43052	12.63849	12.44238	10.36245	10.89863	13.13161	14.60487	9.066137	8.858182	12.35992	9.949783	15.53034	12.14271	13.01111	8.203682
ApoE4	11.79159	11.05355	10.845	11.94867	14.38887	14.45397	13.87173	12.61561	9.196936	13.93109	13.14924	12.11133	7.292781	7.816665	8.714287	12.57248	11.93922	8.060999	7.348486	8.710073	15.01416	12.14197	15.45324	9.727215
hAβ-KI	11.10225	10.76855	10.68731	8.933391	10.53554	10.33757	12.4606	8.294705	12.23853	11.04618	11.34568	13.78222	16.17122	10.77381	10.89958	10.68439	11.73136							
	LPS																							
WT	10.93407	12.01346	14.20022	10.03116	12.85112	10.06057	11.8983	10.28046	9.640009	4.652406	11.7521	11.7521	7.911544	8.672082	4.848064	9.808365	9.598576	8.139208	11.32281	10.76025	8.776516	11.80333	10.92339	7.167288
ApoE4	8.146347	10.07768	13.59472	8.97358	9.13274	14.97841	11.42262	10.63117	6.867027	8.304883	7.066987	6.945706	11.19857	9.835904	7.25222	9.299603	13.51916	9.715272	8.22507	10.01359	8.231506	9.23256	9.065212	11.95556
hAβ-KI	12.10313	11.37843	11.23124	10.44608	12.06354	12.27399	12.44175	12.52619	13.24524	9.826846	10.55316	12.40821	10.48466	13.89843	13.92652	12.0669	12.0615							

ANOVA results | Multiple comparisons

2way ANOVA
ANOVA results

1	Table Analyzed	ApoE4 and hAPP-apical				
2						
3	**Two-way ANOVA**	Ordinary				
4	Alpha	0.05				
5						
6	**Source of Variation**	**% of total variation**	**P value**	**P value summary**	**Significant?**	
7	Interaction	4.858	0.0339	*	Yes	
8	Genotype	3.607	0.0796	ns	No	
9	Treatment	3.384	0.0296	*	Yes	
10						
11	**ANOVA table**	**SS (Type III)**	**DF**	**MS**	**F (DFn, DFd)**	**P value**
12	Interaction	31.61	2	15.80	F (2, 124) = 3.478	P=0.0339
13	Genotype	23.47	2	11.74	F (2, 124) = 2.583	P=0.0796
14	Treatment	22.02	1	22.02	F (1, 124) = 4.846	P=0.0296
15	Residual	563.4	124	4.544		
16						
17	**Difference between column means**					
18	Predicted (LS) mean of Sham	11.39				
19	Predicted (LS) mean of LPS	10.56				
20	Difference between predicted means	0.8340				
21	SE of difference	0.3789				
22	95% CI of difference	0.08416 to 1.584				
23						
24	**Data summary**					
25	Number of columns (Treatment)	2				
26	Number of rows (Genotype)	3				
27	Number of values	130				

Basal dendrites:

	Sham																						
WT	6.829434	8.964418	5.938077	11.2126	7.296349	8.601097	9.450496	8.57372	9.540653	10.07979	8.56601	8.021216	7.344098	8.996888	10.49973	10.98534	9.640559	8.93242	7.815638	10.97576	9.703697	8.299335	11.93421	3.288039
ApoE4	7.668153	9.635052	7.025415	7.106957	12.04563	10.04156	10.50921	12.40263	6.535391	10.55503	11.50194	10.34054	3.801482	8.480624	8.675871	8.220864	9.331459	10.82009	6.63668	7.488842	9.427946	10.98564	9.136127	11.24229
hAβ-KI	9.21959	5.254352	8.096128	11.94859	5.669285	10.19738	10.05891	10.31815	10.39226	7.919394	8.470044	6.911112	12.63169	10.40505	7.288309	8.342911	7.323084	11.68311	12.33135	10.39692	10.84968	8.87255	10.77484	
	LPS																						
WT	9.539901	6.491997	10.08721	7.782934	11.43827	10.72132	9.568955	7.370772	9.096412	5.891845	8.523256	8.608536	7.736179	8.585226	5.485356	8.532393	7.859676	5.955687	7.588592	7.68591	9.016136	8.950949	7.939425	6.41671
ApoE4	6.630967	8.542314	11.36048	8.789155	8.196955	8.534676	7.549714	10.52177	7.971505	6.397246	6.716751	6.634015	7.766978	6.767913	8.493419	7.135201	9.464956	10.29184	5.835488	9.116547	5.701247	8.009512	7.400468	9.745529
hAβ-KI	7.368599	11.74853	9.803771	11.39655	9.46958	9.606735	6.777492	9.916583	8.883616	9.300338	8.276765	5.881553	9.430195	10.36113	12.19862	15.53504	9.13423	11.10372	12.13475	7.946261	8.54504			

ANOVA results | Multiple comparisons

2way ANOVA
ANOVA results

1	Table Analyzed	ApoE4 and hAPP-basal				
2						
3	**Two-way ANOVA**	Ordinary				
4	Alpha	0.05				
5						
6	**Source of Variation**	**% of total variation**	**P value**	**P value summary**	**Significant?**	
7	Interaction	2.491	0.1615	ns	No	
8	Genotype	5.876	0.0146	*	Yes	
9	Treatment	1.275	0.1712	ns	No	
10						
11	**ANOVA table**	**SS (Type III)**	**DF**	**MS**	**F (DFn, DFd)**	**P value**
12	Interaction	12.89	2	6.443	F (2, 134) = 1.848	P=0.1615
13	Genotype	30.40	2	15.20	F (2, 134) = 4.360	P=0.0146
14	Treatment	6.597	1	6.597	F (1, 134) = 1.892	P=0.1712
15	Residual	467.2	134	3.486		
16						
17	**Difference between column means**					
18	Predicted (LS) mean of Sham	9.109				
19	Predicted (LS) mean of LPS	8.674				
20	Difference between predicted means	0.4347				
21	SE of difference	0.3160				
22	95% CI of difference	-0.1903 to 1.060				
23						
24	**Data summary**					
25	Number of columns (Treatment)	2				
26	Number of rows (Genotype)	3				
27	Number of values	140				
28						

Microglial cells:

	Sham								
WT	9939.494	12045.66	10962.71	10833.63	11076.12	12285.87			
ApoE4	9393.014	11744.82	4586.519	13702.84	12154.95	11891.33	12932.11		
hAβ-KI	11437.06	10537.72	19327.99	18472.14	13673.1				
	LPS								
WT	9298.344	11549.06	11003.35	9441.934	14481.6	12280.1	7744.684	11305.59	
ApoE4	11570.67	9549.268	10153.72		12788.75	12085.42	11384.52	9316.07	
hAβ-KI	21639.15	15019.1	18656.57	10524.01	6289.783	4427.419	11244.87		

ANOVA results | Multiple comparisons

2way ANOVA
ANOVA results

1	Table Analyzed	ApoE4 and hAPP-Iba1				
2						
3	**Two-way ANOVA**	Ordinary				
4	Alpha	0.05				
5						
6	**Source of Variation**	**% of total variation**	**P value**	**P value summary**	**Significant?**	
7	Interaction	1.856	0.6962	ns	No	
8	Genotype	12.10	0.1073	ns	No	
9	Treatment	1.323	0.4751	ns	No	
10						
11	**ANOVA table**	**SS (Type III)**	**DF**	**MS**	**F (DFn, DFd)**	**P value**
12	Interaction	8680939	2	4340470	F (2, 34) = 0.3660	P=0.6962
13	Genotype	56580260	2	28290130	F (2, 34) = 2.386	P=0.1073
14	Treatment	6185658	1	6185658	F (1, 34) = 0.5216	P=0.4751
15	Residual	403200579	34	11858841		
16						
17	**Difference between column means**					
18	Predicted (LS) mean of Sham	12265				
19	Predicted (LS) mean of LPS	11470				
20	Difference between predicted means	795.3				
21	SE of difference	1101				
22	95% CI of difference	-1443 to 3033				
23						
24	**Data summary**					
25	Number of columns (Treatment)	2				
26	Number of rows (Genotype)	3				
27	Number of values	40				
28						

Astrocyte cells:

	Sham								
WT	26991.58	24698.57	23128.02		22316.55	22532.35	27870.09	30026.31	
ApoE4	22763.42	30985.5	28676.6	23026	28740.44	18420.83	23654.17		
hAβ-KI	29454.72	22516.59	37431.29	30365.67	26925.78				
	LPS								
WT	21796.65	24084.33	27740.89	28409.79	24348.91	22155.97	24534.79		
ApoE4	26912.77	26311.51	30149.82	23536.93	19590.92	19430.75	24761.62		
hAβ-KI	31916.12	29891.18	29513.44	20256.98	22161.64	23811.85	25120.21		

ANOVA results | Multiple comparisons

2way ANOVA
ANOVA results

1	Table Analyzed	ApoE4 and hAPP-GFAP				
2						
3	**Two-way ANOVA**	Ordinary				
4	Alpha	0.05				
5						
6	**Source of Variation**	**% of total variation**	**P value**	**P value summary**	**Significant?**	
7	Interaction	2.109	0.6618	ns	No	
8	genotype	10.45	0.1417	ns	No	
9	Treatment	3.840	0.2258	ns	No	
10						
11	**ANOVA table**	**SS (Type III)**	**DF**	**MS**	**F (DFn, DFd)**	**P value**
12	Interaction	13157364	2	6578682	F (2, 34) = 0.4179	P=0.6618
13	genotype	65195172	2	32597586	F (2, 34) = 2.070	P=0.1417
14	Treatment	23963092	1	23963092	F (1, 34) = 1.522	P=0.2258
15	Residual	535295135	34	15743975		
16						
17	**Difference between column means**					
18	Predicted (LS) mean of Sham	26629				
19	Predicted (LS) mean of LPS	25068				
20	Difference between predicted means	1560				
21	SE of difference	1265				
22	95% CI of difference	-1010 to 4130				
23						
24	**Data summary**					
25	Number of columns (Treatment)	2				
26	Number of rows (genotype)	3				
27	Number of values	40				
28						

Appendix C: Experiment 3 – LPS induced neuroinflammation as a sporadic model for AD:

4 weeks – Spine density – Apical:

Saline	LPS
11.46132	12.48109
13.16443	12.4012
13.6722	8.315223
13.06373	13.70768
8.716496	10.38175
12.05826	11.41726
15.80236	9.90364
11.71676	7.325262
13.68907	9.222406
14.32507	6.60066
8.814887	10.22495
10.39298	9.626274
16.97752	13.61128
9.844322	11.34578
11.20845	15.07607
10.06416	11.32168
11.97227	9.118541
15.30432	12.98157

14.76015	8.818342
10.6052	12.96296
13.83227	14.07324
10.49331	9.39775
14.10915	12.7081
13.32353	12.89134
15.15581	11.37656
12.15749	7.210318
10.1728	13.54982
15.94486	12.33703
10.87903	12.06244
11.97687	11.60957
9.388646	14.73022
13.08305	15.55761
12.47254	16.88297
14.19538	17.4305
10.54438	11.99066
11.09862	13.88318
9.806556	12.55055
9.092264	15.84835
9.738453	10.53505
8.715672	11.71132
8.509604	11.22591
9.696646	11.33866
10.78462	8.920607
6.931391	11.46268
9.440324	6.299213
9.897018	13.99365
4.673405	9.757585
3.106997	12.12121
13.27067	13.82875
8.798544	11.16695
10.34942	10.11416
9.156977	10.85374
12.26277	10.84689
10.07962	11.92966
1.729344	14.98724
2.06335	9.663503
11.55647	10.81666
11.43647	10.47766
13.55014	11.78514
10.47814	13.0968
10.28668	6.835161
11.91615	7.291327
11.8116	11.11267
11.067	8.167162
12.54299	9.560043
11.40018	8.014155

10.92462	10.3855
11.39538	13.01494
13.37458	8.614272
10.07912	15.31079
9.479156	9.259259
11.36204	11.08116

	Unpaired t test	
1	Table Analyzed	Males&Females
2		
3	Column B	LPS
4	vs.	vs.
5	Column A	Saline
6		
7	**Unpaired t test**	
8	P value	0.5057
9	P value summary	ns
10	Significantly different (P < 0.05)?	No
11	One- or two-tailed P value?	Two-tailed
12	t, df	t=0.6673, df=142
13		
14	**How big is the difference?**	
15	Mean of column A	11.07
16	Mean of column B	11.37
17	Difference between means (B - A) ± SEM	0.2959 ± 0.4435
18	95% confidence interval	-0.5808 to 1.173
19	R squared (eta squared)	0.003126
20		
21	**F test to compare variances**	
22	F, DFn, Dfd	1.330, 71, 71
23	P value	0.2317
24	P value summary	ns
25	Significantly different (P < 0.05)?	No
26		
27	**Data analyzed**	
28	Sample size, column A	72
29	Sample size, column B	72
30		

4 weeks spine density – Basal

Saline	LPS
9.856533	9.997437
12.60433	10.67812
13.57354	12.2997
14.01654	13.36796
7.338158	13.6021
10.32613	10.68577
9.677865	8.603521
13.0246	10.59118
8.733019	9.755617
9.930092	11.12724
9.904836	10.48951
14.04543	10.26666
10.69561	9.921551
10.68134	11.37599
12.44317	9.822155

12.1575	10.65762
8.882521	9.130226
11.17679	7.698608
11.33001	8.460788
11.58301	10.15228
11.21466	9.825778
9.837178	4.448681
9.80893	9.948686
9.110933	9.485095
11.49425	13.70051
11.40413	8.414963
13.78275	11.82526
10.67777	11.11981
11.50592	7.224257
11.08838	7.045434
13.35726	9.534884
6.764943	8.972058
10.03344	12.16759
10.71895	16.83393
8.629738	10.48057
9.255688	10.56277
7.319486	9.913259
4.012841	8.914305
4.760458	7.995297
7.508879	12.66187
9.418808	8.429206
9.455614	9.140768
8.012018	11.37563
8.384734	8.407994
8.917714	5.45405
8.476629	8.305137
3.679592	4.697942
3.52952	7.8125
8.971872	9.576555
12.12838	10.57692
8.973905	11.01686
9.66417	8.874054
10.76994	9.895547
7.027747	8.775857
3.761393	12.67553
4.97476	8.224425
9.975984	9.530428
10.94643	5.655616
6.953668	11.91827
9.774609	10.07651
7.199273	6.071362
8.919418	11.15521
8.735181	10.86342

5.961521	8.904302
6.365327	5.557722
8.473579	6.750617
10.96684	7.788415
5.976722	6.824829
8.015717	8.336565
8.308605	10.04111
9.3224	9.82047
9.392167	9.331539

	Unpaired t test	
1	Table Analyzed	Males&Females-Basa
2		
3	Column B	LPS
4	vs.	vs.
5	Column A	Saline
6		
7	**Unpaired t test**	
8	P value	0.5708
9	P value summary	ns
10	Significantly different (P < 0.05)?	No
11	One- or two-tailed P value?	Two-tailed
12	t, df	t=0.5682, df=142
13		
14	**How big is the difference?**	
15	Mean of column A	9.385
16	Mean of column B	9.606
17	Difference between means (B - A) ± SEM	0.2211 ± 0.3892
18	95% confidence interval	-0.5483 to 0.9906
19	R squared (eta squared)	0.002268
20		
21	**F test to compare variances**	
22	F, DFn, Dfd	1.300, 71, 71
23	P value	0.2709
24	P value summary	ns
25	Significantly different (P < 0.05)?	No
26		
27	**Data analyzed**	
28	Sample size, column A	72
29	Sample size, column B	72

4 weeks – microglia:

Iba1 cell counts

Saline	LPS
121	137.2
115.4	137.6
113.8	129.2
115.8	152.1
127.8	136.8

Iba1 intensity

Saline	LPS
10841.07	19774.35
17180.71	14374
14822.74	13993.22
12855.69	18417.48
14310.63	17042.76

	Unpaired t test	
1	Table Analyzed	Iba1-cell counts
2		
3	Column B	LPS
4	vs.	vs.
5	Column A	Saline
6		
7	**Unpaired t test**	
8	P value	0.0023
9	P value summary	**
10	Significantly different (P < 0.05)?	Yes
11	One- or two-tailed P value?	Two-tailed
12	t, df	t=4.387, df=8
13		
14	**How big is the difference?**	
15	Mean of column A	118.8
16	Mean of column B	138.6
17	Difference between means (B - A) ± SEM	19.82 ± 4.518
18	95% confidence interval	9.402 to 30.24
19	R squared (eta squared)	0.7064
20		
21	**F test to compare variances**	
22	F, DFn, Dfd	2.107, 4, 4
23	P value	0.4882
24	P value summary	ns
25	Significantly different (P < 0.05)?	No
26		
27	**Data analyzed**	
28	Sample size, column A	5
29	Sample size, column B	5
30		

	Unpaired t test	
1	Table Analyzed	Iba1-Intensity
2		
3	Column B	LPS
4	vs.	vs.
5	Column A	Saline
6		
7	**Unpaired t test**	
8	P value	0.1156
9	P value summary	ns
10	Significantly different (P < 0.05)?	No
11	One- or two-tailed P value?	Two-tailed
12	t, df	t=1.765, df=8
13		
14	**How big is the difference?**	
15	Mean of column A	14002
16	Mean of column B	16720
17	Difference between means (B - A) ± SEM	2718 ± 1540
18	95% confidence interval	-833.1 to 6269
19	R squared (eta squared)	0.2803
20		
21	**F test to compare variances**	
22	F, DFn, Dfd	1.139, 4, 4
23	P value	0.9029
24	P value summary	ns
25	Significantly different (P < 0.05)?	No
26		
27	**Data analyzed**	
28	Sample size, column A	5
29	Sample size, column B	5

4 weeks – astrocytes:

Saline	LPS
219.2	282.4
239.6	257.9
256.8	187
194.3	251.8
235.6	257.4

Saline	LPS
6525.274	16929.1
10250.71	14344.49
12734.86	19195.26
10513.82	16567.31
10111.05	16403.29

Unpaired t test	
Table Analyzed	GFAP-cell counts
Column B	LPS
vs.	vs.
Column A	Saline
Unpaired t test	
P value	0.3696
P value summary	ns
Significantly different (P < 0.05)?	No
One- or two-tailed P value?	Two-tailed
t, df	t=0.9506, df=8
How big is the difference?	
Mean of column A	229.1
Mean of column B	247.3
Difference between means (B - A) ± SEM	18.20 ± 19.15
95% confidence interval	-25.95 to 62.35
R squared (eta squared)	0.1015
F test to compare variances	
F, DFn, Dfd	2.289, 4, 4
P value	0.4421
P value summary	ns
Significantly different (P < 0.05)?	No
Data analyzed	
Sample size, column A	5
Sample size, column B	5

Unpaired t test	
Table Analyzed	GFAP-Intensity
Column B	LPS
vs.	vs.
Column A	Saline
Unpaired t test	
P value	0.0007
P value summary	***
Significantly different (P < 0.05)?	Yes
One- or two-tailed P value?	Two-tailed
t, df	t=5.281, df=8
How big is the difference?	
Mean of column A	10027
Mean of column B	16688
Difference between means (B - A) ± SEM	6661 ± 1261
95% confidence interval	3752 to 9569
R squared (eta squared)	0.7771
F test to compare variances	
F, DFn, Dfd	1.667, 4, 4
P value	0.6328
P value summary	ns
Significantly different (P < 0.05)?	No
Data analyzed	
Sample size, column A	5
Sample size, column B	5

6 weeks – spine density:

Apical dendrites:

Saline	LPS
9.786918	10.6445
14.56497	14.27328
9.749671	11.75619
9.119497	11.7935
11.89163	12.78453
11.22525	9.206318
12.14698	10.28529
9.982083	11.0018
12.81041	13.7595
13.42883	13.63257
10.96224	12.11417
10.24053	10.33344
13.08576	7.273226
11.75666	13.08315
12.61511	9.815951
13.08467	12.03353
12.59869	13.79513
10.57968	12.56163
12.36591	13.96648

12.4489	7.158315
9.609326	10.67487
11.02318	15.23841
12.00403	12.30371
11.19701	11.01462
8.634868	12.65119
10.09483	9.325916
11.77024	10.8202
10.1365	10.7177
9.180709	14.30323
9.065436	9.23494
8.898237	7.934055
11.21742	11.64852
9.708738	12.72094
6.74747	10.70916
10.02848	11.2582
9.412756	9.919878
8.095311	8.364035
9.995404	10.16727
10.32195	8.961681
11.51719	15.10679
9.0151	10.77795
10.80466	9.982384
12.57709	11.57824
15.14429	7.118704
14.36163	8.84454
12.04819	10.13368
9.697733	12.55821
12.96853	11.0327
8.458739	10.99565
9.955202	12.63212
7.702393	10.09931
7.443082	8.512708
10.0821	14.86794
9.644789	10.29336
12.80113	8.726366
12.34999	10.57896
8.251676	11.28494
8.280849	11.69176
11.52436	11.21915
10.08843	9.268795
10.77122	11.55446
9.422368	9.774183
12.63597	13.62984
10.63032	11.85932
8.752155	11.58078
10.75569	13.77832
11.84629	9.785933

12.84625	10.69372
7.172572	11.195
10.05025	10.60633
11.33546	9.754738
9.785846	9.928211

	Unpaired t test	
1	Table Analyzed	Males&Females_dendrites
2		
3	Column B	LPS
4	vs.	vs.
5	Column A	Saline
6		
7	**Unpaired t test**	
8	P value	0.2007
9	P value summary	ns
10	Significantly different (P < 0.05)?	No
11	One- or two-tailed P value?	Two-tailed
12	t, df	t=1.286, df=142
13		
14	**How big is the difference?**	
15	Mean of column A	10.73
16	Mean of column B	11.12
17	Difference between means (B - A) ± SEM	0.3941 ± 0.3066
18	95% confidence interval	-0.2119 to 1.000
19	R squared (eta squared)	0.01151
20		
21	**F test to compare variances**	
22	F, DFn, Dfd	1.096, 71, 71
23	P value	0.7013
24	P value summary	ns
25	Significantly different (P < 0.05)?	No
26		
27	**Data analyzed**	
28	Sample size, column A	72
29	Sample size, column B	72

6 weeks – basal dendrites:

Saline	LPS
8.98511	8.393595
9.824199	12.5937
9.022261	8.886027
9.425878	9.902971
9.343094	11.527
7.577193	6.206756
8.509064	6.719226
10.90023	11.01833
7.703191	10.72223
8.473168	10.77383
7.290833	9.7423
8.124577	9.244724
11.55975	11.05599
11.47896	10.91728
9.405729	9.736466

8.947545	8.996089
9.704455	7.425743
11.00939	9.341429
13.01669	8.501201
12.94252	10.79806
11.21606	8.357839
11.01015	7.673789
8.679871	9.291052
12.48581	7.403581
7.742935	7.873311
8.642973	9.368836
8.622017	9.310788
6.425703	11.46132
8.662175	8.697642
9.069256	7.010058
7.441059	7.57251
11.0244	11.55357
7.876271	8.911212
7.216495	9.276621
9.763618	8.491947
6.383287	9.555607
8.792406	7.555673
9.305105	6.73788
11.31313	3.828409
10.39004	6.381282
10.38175	7.652338
8.622699	7.572526
13.1257	9.693053
9.621048	10.37133
7.163324	11.9248
9.971671	8.023409
11.58301	10.70429
11.23268	9.238139
9.085403	12.86618
8.750384	12.65432
8.879418	12.32128
6.5979	13.02143
6.16277	10.72468
7.376599	13.13659
5.030656	13.555
12.41296	12.48571
8.62069	9.495604
6.758881	12.93373
6.425143	9.152381
10.13628	9.377143
7.640879	8.654496
8.886133	4.599816
7.769337	11.53443

7.883879	7.791972
9.847311	8.468777
7.084614	7.048936
11.47192	7.098765
11.74436	4.278787
9.606373	9.967475
12.24162	5.41257
10.17087	8.233533
7.402032	5.865103

	Unpaired t test	
1	Table Analyzed	Males&Females-Basa
2		
3	Column B	LPS
4	vs.	vs.
5	Column A	Saline
6		
7	**Unpaired t test**	
8	P value	0.9896
9	P value summary	ns
10	Significantly different (P < 0.05)?	No
11	One- or two-tailed P value?	Two-tailed
12	t, df	t=0.01311, df=142
13		
14	**How big is the difference?**	
15	Mean of column A	9.236
16	Mean of column B	9.232
17	Difference between means (B - A) ± SEM	-0.004450 ± 0.3395
18	95% confidence interval	-0.6755 to 0.6666
19	R squared (eta squared)	1.210e-006
20		
21	**F test to compare variances**	
22	F, DFn, Dfd	1.423, 71, 71
23	P value	0.1393
24	P value summary	ns
25	Significantly different (P < 0.05)?	No
26		
27	**Data analyzed**	
28	Sample size, column A	72
29	Sample size, column B	72
30		

6 weeks – Iba1:

Iba1 cell counts

Saline	LPS
117.8	123.7

Iba1 intensity

Saline	LPS
13902.8	13918.44

119.75	157.9	12904.88	13407.2
110.2	139.7	11334.58	16752.41
124.3	124.2	13014.36	14727.46
114.9	156.5	15782.55	19107.66

GFAP cell counts

Saline	LPS
209.1	257.3
219.5	216.9
249.5	171.1
224.4	251.9
215.8	223.7

GFAP intensity

Saline	LPS
10861.18	15664.47
10323.14	13523.95
8556.184	15937.21
9319.727	15696.93
9651.281	17971.7

	Unpaired t test	
1	Table Analyzed	Iba1-Cell counts
2		
3	Column B	LPS
4	vs.	vs.
5	Column A	Saline
6		
7	**Unpaired t test**	
8	P value	0.0185
9	P value summary	*
10	Significantly different (P < 0.05)?	Yes
11	One- or two-tailed P value?	Two-tailed
12	t, df	t=2.948, df=8
13		
14	**How big is the difference?**	
15	Mean of column A	117.4
16	Mean of column B	140.4
17	Difference between means (B - A) ± SEM	23.01 ± 7.806
18	95% confidence interval	5.009 to 41.01
19	R squared (eta squared)	0.5206
20		
21	**F test to compare variances**	
22	F, DFn, Dfd	9.941, 4, 4
23	P value	0.0471
24	P value summary	*
25	Significantly different (P < 0.05)?	Yes
26		
27	**Data analyzed**	
28	Sample size, column A	5
29	Sample size, column B	5

	Unpaired t test	
1	Table Analyzed	Iba1-Intensity
2		
3	Column B	LPS
4	vs.	vs.
5	Column A	Saline
6		
7	**Unpaired t test**	
8	P value	0.1240
9	P value summary	ns
10	Significantly different (P < 0.05)?	No
11	One- or two-tailed P value?	Two-tailed
12	t, df	t=1.719, df=8
13		
14	**How big is the difference?**	
15	Mean of column A	13388
16	Mean of column B	15583
17	Difference between means (B - A) ± SEM	2195 ± 1277
18	95% confidence interval	-750.0 to 5140
19	R squared (eta squared)	0.2697
20		
21	**F test to compare variances**	
22	F, DFn, Dfd	2.080, 4, 4
23	P value	0.4955
24	P value summary	ns
25	Significantly different (P < 0.05)?	No
26		
27	**Data analyzed**	
28	Sample size, column A	5
29	Sample size, column B	5

	Unpaired t test	
1	Table Analyzed	GFAP-Cell counts
2		
3	Column B	LPS
4	vs.	vs.
5	Column A	Saline
6		
7	**Unpaired t test**	
8	P value	0.9762
9	P value summary	ns
10	Significantly different (P < 0.05)?	No
11	One- or two-tailed P value?	Two-tailed
12	t, df	t=0.03081, df=8
13		
14	**How big is the difference?**	
15	Mean of column A	223.7
16	Mean of column B	224.2
17	Difference between means (B - A) ± SEM	0.5200 ± 16.88
18	95% confidence interval	-38.39 to 39.43
19	R squared (eta squared)	0.0001187
20		
21	**F test to compare variances**	
22	F, DFn, Dfd	4.937, 4, 4
23	P value	0.1511
24	P value summary	ns
25	Significantly different (P < 0.05)?	No
26		
27	**Data analyzed**	
28	Sample size, column A	5
29	Sample size, column B	5

	Unpaired t test	
1	Table Analyzed	GFAP-Intensity
2		
3	Column B	LPS
4	vs.	vs.
5	Column A	Saline
6		
7	**Unpaired t test**	
8	P value	<0.0001
9	P value summary	****
10	Significantly different (P < 0.05)?	Yes
11	One- or two-tailed P value?	Two-tailed
12	t, df	t=7.429, df=8
13		
14	**How big is the difference?**	
15	Mean of column A	9742
16	Mean of column B	15759
17	Difference between means (B - A) ± SEM	6017 ± 809.9
18	95% confidence interval	4149 to 7884
19	R squared (eta squared)	0.8734
20		
21	**F test to compare variances**	
22	F, DFn, Dfd	3.122, 4, 4
23	P value	0.2961
24	P value summary	ns
25	Significantly different (P < 0.05)?	No
26		
27	**Data analyzed**	
28	Sample size, column A	5
29	Sample size, column B	5
30		

Appendix D: Experiment 4 – Intrahippocampal lipopolysaccharide injection:

Glial cell activation

Iba1 cell counts

Saline	LPS
146.625	204.125
159	169.5
126.25	198.3333
158	285.5714

Iba1 intensity

Saline	LPS
10446.4	11366.58
9009.138	11920.69
10549.58	11361.28
9948.459	13633.4

GFAP cell counts

Saline	LPS
248.875	292.25
261.4	254.125
251.125	276.6667
280.4286	287.5714

GFAP intensity

Saline	LPS
26991.24	18582.36
33702.33	26468.51
35288.71	65669.89
35486.16	40042.92

Tabular results

Unpaired t test
Tabular results

1	Table Analyzed	3 days-Microglia-counts
2		
3	Column B	LPS
4	vs.	vs.
5	Column A	Saline
6		
7	**Unpaired t test**	
8	P value	0.0424
9	P value summary	*
10	Significantly different (P < 0.05)?	Yes
11	One- or two-tailed P value?	Two-tailed
12	t, df	t=2.569, df=6
13		
14	**How big is the difference?**	
15	Mean of column A	147.5
16	Mean of column B	214.4
17	Difference between means (B - A) ± SEM	66.91 ± 26.04
18	95% confidence interval	3.185 to 130.6
19	R squared (eta squared)	0.5238
20		
21	**F test to compare variances**	
22	F, DFn, Dfd	10.72, 3, 3
23	P value	0.0825
24	P value summary	ns
25	Significantly different (P < 0.05)?	No
26		
27	**Data analyzed**	
28	Sample size, column A	4

Tabular results

Unpaired t test
Tabular results

1	Table Analyzed	3 days-Microglia-intensity
2		
3	Column B	LPS
4	vs.	vs.
5	Column A	Saline
6		
7	**Unpaired t test**	
8	P value	0.0176
9	P value summary	*
10	Significantly different (P < 0.05)?	Yes
11	One- or two-tailed P value?	Two-tailed
12	t, df	t=3.242, df=6
13		
14	**How big is the difference?**	
15	Mean of column A	9988
16	Mean of column B	12070
17	Difference between means (B - A) ± SEM	2082 ± 642.2
18	95% confidence interval	510.7 to 3653
19	R squared (eta squared)	0.6366
20		
21	**F test to compare variances**	
22	F, DFn, Dfd	2.332, 3, 3
23	P value	0.5049
24	P value summary	ns
25	Significantly different (P < 0.05)?	No
26		
27	**Data analyzed**	
28	Sample size, column A	4

Tabular results

Unpaired t test
Tabular results

1	Table Analyzed	3 days-Astrocytes-counts
2		
3	Column B	LPS
4	vs.	vs.
5	Column A	Saline
6		
7	**Unpaired t test**	
8	P value	0.1733
9	P value summary	ns
10	Significantly different (P < 0.05)?	No
11	One- or two-tailed P value?	Two-tailed
12	t, df	t=1.545, df=6
13		
14	**How big is the difference?**	
15	Mean of column A	260.5
16	Mean of column B	277.7
17	Difference between means (B - A) ± SEM	17.20 ± 11.13
18	95% confidence interval	-10.04 to 44.43
19	R squared (eta squared)	0.2846
20		
21	**F test to compare variances**	
22	F, DFn, Dfd	1.395, 3, 3
23	P value	0.7912
24	P value summary	ns
25	Significantly different (P < 0.05)?	No
26		
27	**Data analyzed**	
28	Sample size, column A	4

Tabular results

Unpaired t test
Tabular results

1	Table Analyzed	3 days-Astrocytes-intensity
2		
3	Column B	LPS
4	vs.	vs.
5	Column A	Saline
6		
7	**Unpaired t test**	
8	P value	0.6626
9	P value summary	ns
10	Significantly different (P < 0.05)?	No
11	One- or two-tailed P value?	Two-tailed
12	t, df	t=0.4587, df=6
13		
14	**How big is the difference?**	
15	Mean of column A	32867
16	Mean of column B	37691
17	Difference between means (B - A) ± SEM	4824 ± 10517
18	95% confidence interval	-20911 to 30559
19	R squared (eta squared)	0.03387
20		
21	**F test to compare variances**	
22	F, DFn, Dfd	26.68, 3, 3
23	P value	0.0231
24	P value summary	*
25	Significantly different (P < 0.05)?	Yes
26		
27	**Data analyzed**	
28	Sample size, column A	4

3 days dendritic spine density:

Apical dendrites

Saline	LPS
16.88482	12.94688
11.10499	12.78881
12.10955	19.68

Basal dendrites

Saline	LPS
8.047945	19.80594
11.21398	16.3375
15.41782	14.94444

14.63184	17.90965	12.2905	14.78076
10.58022	14.98744	10.08493	14.83235
8.53229	16.85998	7.424261	15.20717
9.695291	15.4321	9.531928	10.08455
13.04959	17.30808	6.959861	14.55889
13.39829	15.51429	11.01296	16.37427
8.78697	13.84311	7.664437	9.595404
11.96449	14.40623	11.17568	7.205453
12.62789	8.865871	8.680883	10.31357
15.88967	10.15792	10.11789	12.32366
11.43947	9.637244	13.78751	13.95973
10.51193	13.52182	11.83093	7.666099
11.24379	11.4207	12.44536	14.13374
13.7225	10.61732	13.47936	14.23027
18.50236	12.38031	14.02743	14.02806
13.72213	12.27554	13.53503	11.4573
11.22295	12.62992	8.062891	11.39102
14.1759	11.93154	14.81606	11.24598
16.47435	11.47748	17.00872	12.39276
12.65277	12.78232	12.81431	11.84551
11.76471	13.382	12.04642	13.60612
16.79919	15.59089	16.05868	15.23589
15.75543	14.25774	13.47987	12.28899
11.314	15.91876	12.09098	11.91264
15.8881	15.30945	13.77783	16.15115
17.09402	13.1161	12.42642	13.04284
11.66748	10.4547	12.01814	10.40541
12.7957	18.81804	11.47186	11.57626
13.51075	16.00366	12.77778	16.51755
12.97114	16.99614	15.55158	15.806
12.37196	14.15195	12.49802	12.30738
15.55716	14.10313	13.34512	10.68501
12.07082	12.83385	9.692473	8.263243
13.93779		10.60369	
5.326442		6.60385	
14.73214		10.18213	
6.873306		13.64208	
8.784773		8.132285	
12.13219		11.75189	
12.77432		15.30376	
15.44349		12.69991	
17.47212		12.76876	
14.78133		13.0528	
11.55252		12.98152	
18.22135		13.66799	
10.2297		12.27089	
11.30881		9.058824	
9.795045		8.194405	

9.53125	6.260729
14.84047	13.43922
12.63248	12.23278
16.09303	11.88033
15.70317	12.06581
15.58029	9.708738
15.62187	16.3876
13.03328	10.1468

Unpaired t test

1	Table Analyzed	3 days-Apical dendrites
2		
3	Column B	LPS
4	vs.	vs.
5	Column A	Saline
6		
7	**Unpaired t test**	
8	P value	0.1345
9	P value summary	ns
10	Significantly different (P < 0.05)?	No
11	One- or two-tailed P value?	Two-tailed
12	t, df	t=1.510, df=93
13		
14	**How big is the difference?**	
15	Mean of column A	13.03
16	Mean of column B	13.90
17	Difference between means (B - A) ± SEM	0.8656 ± 0.5733
18	95% confidence interval	-0.2728 to 2.004
19	R squared (eta squared)	0.02393
20		
21	**F test to compare variances**	
22	F, DFn, Dfd	1.176, 58, 35
23	P value	0.6150
24	P value summary	ns
25	Significantly different (P < 0.05)?	No
26		
27	**Data analyzed**	
28	Sample size, column A	59
29	Sample size, column B	36
30		

Unpaired t test

1	Table Analyzed	3 days-Basal dendrites
2		
3	Column B	LPS
4	vs.	vs.
5	Column A	Saline
6		
7	**Unpaired t test**	
8	P value	0.0283
9	P value summary	*
10	Significantly different (P < 0.05)?	Yes
11	One- or two-tailed P value?	Two-tailed
12	t, df	t=2.228, df=93
13		
14	**How big is the difference?**	
15	Mean of column A	11.72
16	Mean of column B	12.96
17	Difference between means (B - A) ± SEM	1.235 ± 0.5543
18	95% confidence interval	0.1341 to 2.336
19	R squared (eta squared)	0.05066
20		
21	**F test to compare variances**	
22	F, DFn, Dfd	1.174, 35, 58
23	P value	0.5781
24	P value summary	ns
25	Significantly different (P < 0.05)?	No
26		
27	**Data analyzed**	
28	Sample size, column A	59
29	Sample size, column B	36

7 days glial cells:

Iba1 cell counts

Saline	LPS
155.5	386.25
123.375	268.6
118.875	235.5
123	

Iba1 intensity

Saline	LPS
16605.78	21261.47
11730.08	31343.54
12887.76	18700.1
13591.52	

GFAP cell counts

Saline	LPS
251.5	365
257.125	315.7
265.25	346.3
259.875	

GFAP intensity

Saline	LPS
26831.5	38135.75
18058.07	20703.58
20130.72	32083.33
18792.07	

Tabular results

Unpaired t test
Tabular results

1	Table Analyzed	7 days-Microglia-counts
2		
3	Column B	LPS
4	vs.	vs.
5	Column A	Saline
6		
7	**Unpaired t test**	
8	P value	0.0084
9	P value summary	**
10	Significantly different (P < 0.05)?	Yes
11	One- or two-tailed P value?	Two-tailed
12	t, df	t=4.210, df=5
13		
14	**How big is the difference?**	
15	Mean of column A	130.2
16	Mean of column B	296.8
17	Difference between means (B - A) ± SEM	166.6 ± 39.57
18	95% confidence interval	64.88 to 268.3
19	R squared (eta squared)	0.7800
20		
21	**F test to compare variances**	
22	F, DFn, Dfd	21.73, 2, 3
23	P value	0.0328
24	P value summary	*
25	Significantly different (P < 0.05)?	Yes
26		
27	**Data analyzed**	
28	Sample size, column A	4

Tabular results

Unpaired t test
Tabular results

1	Table Analyzed	7 days-Microglia-intensity
2		
3	Column B	LPS
4	vs.	vs.
5	Column A	Saline
6		
7	**Unpaired t test**	
8	P value	0.0333
9	P value summary	*
10	Significantly different (P < 0.05)?	Yes
11	One- or two-tailed P value?	Two-tailed
12	t, df	t=2.913, df=5
13		
14	**How big is the difference?**	
15	Mean of column A	13704
16	Mean of column B	23768
17	Difference between means (B - A) ± SEM	10065 ± 3456
18	95% confidence interval	1182 to 18947
19	R squared (eta squared)	0.6292
20		
21	**F test to compare variances**	
22	F, DFn, Dfd	10.31, 2, 3
23	P value	0.0905
24	P value summary	ns
25	Significantly different (P < 0.05)?	No
26		
27	**Data analyzed**	
28	Sample size, column A	4

Tabular results

Unpaired t test
Tabular results

1	Table Analyzed	7 days-Astrocytes-counts
2		
3	Column B	LPS
4	vs.	vs.
5	Column A	Saline
6		
7	**Unpaired t test**	
8	P value	0.0011
9	P value summary	**
10	Significantly different (P < 0.05)?	Yes
11	One- or two-tailed P value?	Two-tailed
12	t, df	t=6.717, df=5
13		
14	**How big is the difference?**	
15	Mean of column A	258.4
16	Mean of column B	342.3
17	Difference between means (B - A) ± SEM	83.90 ± 12.49
18	95% confidence interval	51.79 to 116.0
19	R squared (eta squared)	0.9002
20		
21	**F test to compare variances**	
22	F, DFn, Dfd	18.90, 2, 3
23	P value	0.0399
24	P value summary	*
25	Significantly different (P < 0.05)?	Yes
26		
27	**Data analyzed**	
28	Sample size, column A	4

Tabular results

Unpaired t test
Tabular results

1	Table Analyzed	7 days-Astrocytes-intensity
2		
3	Column B	LPS
4	vs.	vs.
5	Column A	Saline
6		
7	**Unpaired t test**	
8	P value	0.1139
9	P value summary	ns
10	Significantly different (P < 0.05)?	No
11	One- or two-tailed P value?	Two-tailed
12	t, df	t=1.913, df=5
13		
14	**How big is the difference?**	
15	Mean of column A	20953
16	Mean of column B	30308
17	Difference between means (B - A) ± SEM	9354 ± 4890
18	95% confidence interval	-3215 to 21924
19	R squared (eta squared)	0.4226
20		
21	**F test to compare variances**	
22	F, DFn, Dfd	4.867, 2, 3
23	P value	0.2287
24	P value summary	ns
25	Significantly different (P < 0.05)?	No
26		
27	**Data analyzed**	
28	Sample size, column A	4

7 days spine density:

Apical dendrites

Saline	LPS
13.00236	14.40253
14.52037	8.445946
12.04013	13.52637

Basal dendrites

Saline	LPS
14.3494	10.48011
12.36197	9.19908
13.89103	12.26405

11.28801	9.759073	10.16176	9.894459
5.29435	13.20215	8.728092	12.38635
12.86633	10.25172	9.440813	10.75616
16.57892	13.52539	12.68743	11.98992
12.59227	12.45512	10.15351	16.49537
12.76813	15.64496	9.864527	9.451953
13.66999	9.415882	12.81738	12.33368
11.58966	11.98312	12.43846	8.165686
13.1548	11.17925	12.4067	9.120521
14.49753	12.78042	14.66037	9.004114
9.151481	14.18359	8.778173	12.1915
13.33864	12.99293	12.62323	10.53336
14.46305	8.942944	18.27635	13.16431
13.03049	15.97374	17.37181	9.700548
13.17973	15.09637	6.715229	12.25678
17.37772	12.66262	10.48314	11.25492
11.52687	12.87193	13.47056	7.113985
10.09096	8.705975	11.67846	9.880096
11.21002	10.04108	9.320175	13.65876
12.9644	12.15412	11.24744	12.77845
12.65512	9.363606	11.16784	9.837678
13.29056	8.673321	13.10375	8.005822
19.28883	8.279376	18.44293	9.100364
13.81827	8.848037	13.80858	9.676488
14.00707	9.370315	12.32864	12.7508
12.03758	9.822647	12.0398	9.156627
15.16684	7.616279	14.60896	9.520426
15.78245	8.80345	13.62338	11.83691
13.38306	9.863878	12.65626	8.9468
11.96172	10.02147	13.71186	9.870276
14.31745	8.469125	13.37409	12.35251
12.36343	6.932788	16.36249	8.884917
15.06339	9.818412	11.45194	9.759358
12.87341	8.805297	12.76117	11.93747
14.13541	12.68843	9.885764	11.33144
12.44407	12.16844	11.99587	11.21465
13.29629	11.92619	10.50539	12.21374
13.0039	10.99628	13.64024	12.66406
11.2582	9.225092	11.33855	11.05821
8.841259	14.40434	7.175014	11.75088
13.53725	10.52632	13.08411	10.46711
10.70464	11.26874	9.385314	11.4229
11.54401	10.49501	9.395973	12.39472
11.75999	11.44781	9.106639	11.42041
9.852217	9.662751	10.5687	12.79613

Unpaired t test	
Table Analyzed	7 days-Apical dendrites
Column B	LPS
vs.	vs.
Column A	Saline
Unpaired t test	
P value	0.0001
P value summary	***
Significantly different (P < 0.05)?	Yes
One- or two-tailed P value?	Two-tailed
t, df	t=3.958, df=94
How big is the difference?	
Mean of column A	12.85
Mean of column B	11.04
Difference between means (B - A) ± SEM	-1.810 ± 0.4573
95% confidence interval	-2.718 to -0.9022
R squared (eta squared)	0.1429
F test to compare variances	
F, DFn, Dfd	1.001, 47, 47
P value	0.9984
P value summary	ns
Significantly different (P < 0.05)?	No
Data analyzed	
Sample size, column A	48
Sample size, column B	48

Unpaired t test	
Table Analyzed	7 days-Basal dendrites
Column B	LPS
vs.	vs.
Column A	Saline
Unpaired t test	
P value	0.0119
P value summary	*
Significantly different (P < 0.05)?	Yes
One- or two-tailed P value?	Two-tailed
t, df	t=2.565, df=94
How big is the difference?	
Mean of column A	12.07
Mean of column B	10.93
Difference between means (B - A) ± SEM	-1.146 ± 0.4468
95% confidence interval	-2.033 to -0.2588
R squared (eta squared)	0.06540
F test to compare variances	
F, DFn, Dfd	2.101, 47, 47
P value	0.0123
P value summary	*
Significantly different (P < 0.05)?	Yes
Data analyzed	
Sample size, column A	48
Sample size, column B	48

Appendix E: Experiment 5: Hippocampal neuroinflammation accelerated devaluation performance in female mice:

Lever press - Acquisition

Row Labi	Average of Average LI	Average of Average LP	Average of Average LP	Average of Average LP	Average of Average LP	Average of Average LP	Average of Average LP	Average of Average LP	rate8
LPS	**0.580555556**	**0.933045457**	**3.944444444**	**6.777777778**	**5.914295758**	**10.45277778**	**10.24059859**	**11.28001486**	
661	0.475	1.025	2.5	5.5	5.625	9.65	8.675	12.08453757	
683	0.65	0.625	3.65	6.45	5.075	10.55	10.575	6.893305439	
684	0.925	1.1	4.825	8.15	6.354078744	10.575	10.7681173	12.4145469	
688	0.525	0.95	4.975	7.675	6.925	11.375	11.425	14.46203019	
709	1.075	1.322409116	3.725	6.225	7.475837321	10.75	10.65	14.44076858	
720	0.15	0.375	3.55	6.3	4.65	9.3	9.275	9.95	
729	0.25	0.85	3.825	6.925	5.526124197	11.675	10.27604167	10.49421112	
730	0.3	0.875	4.125	5.775	5.55	7.925	9.55	10.35	
731	0.875	1.275	4.325	8	6.047621564	12.275	10.97122834	10.43073394	
Sal	**0.34375**	**0.45**	**1.740625**	**2.6125**	**2.295877901**	**5.8375**	**6.73125**	**7.865625**	
655	0.15	0.3	1.025	1.775	2.1	4.9	6.65	8.475	
660	0.275	0.275	0.3	0.8	1.202741514	7.35	6.975	9.05	
682	0.175	0.125	0.225	0.75	1.839281693	6.9	8.5	9.25	
686	0.6	1.05	4.025	3.075	2.45	4.1	5.45	6.425	
710	0.45	0.575	3.35	4.95	3.525	6.5	6.875	7.35	
722	0.325	0.375	1.475	2.025	3.05	8.3	8.25	8.875	
723	0.2	0.35	0.1	0.875	1	3.475	5.25	6.65	
728	0.575	0.55	3.425	6.65	3.2	5.175	5.9	6.85	
Grand Tota	**0.469117647**	**0.705729948**	**2.907352941**	**4.817647059**	**4.211510884**	**8.280882353**	**8.58914043**	**9.673243162**	

ANOVA results | Multiple comparisons

2way ANOVA
ANOVA results

Table Analyzed	Lever press rates Day1-4				
Two-way RM ANOVA	Matching: Stacked				
Assume sphericity?	No				
Alpha	0.05				
Source of Variation	**% of total variation**	**P value**	**P value summary**	**Significant?**	**Geisser-Greenhouse's epsilon**
Training days x Treatment	11.23	<0.0001	****	Yes	
Training days	53.98	<0.0001	****	Yes	0.4509
Treatment	14.21	0.0003	***	Yes	
Subject	9.436	0.0005	***	Yes	
ANOVA table	**SS**	**DF**	**MS**	**F (DFn, DFd)**	**P value**
Training days x Treatment	42.07	3	14.02	F (3, 45) = 21.04	P<0.0001
Training days	202.1	3	67.38	F (1.353, 20.29) = 101.1	P<0.0001
Treatment	53.21	1	53.21	F (1, 15) = 22.59	P=0.0003
Subject	35.33	15	2.356	F (15, 45) = 3.534	P=0.0005
Residual	29.99	45	0.6665		
Difference between column means					
Mean of Saline	1.287				
Mean of LPS	3.059				
Difference between means	-1.772				
SE of difference	0.3729				
95% CI of difference	-2.567 to -0.9775				
Data summary					
Number of columns (Treatment)	2				
Number of rows (Training days)	4				
Number of subjects (Subject)	17				
Number of missing values	0				

ANOVA results | Multiple comparisons

2way ANOVA
Multiple comparisons

Compare each cell mean with the other ce								
Number of families	1							
Number of comparisons per family	4							
Alpha	0.05							
Bonferroni's multiple comparisons test	**Mean Diff**	**95.00% CI of diff.**	**Below threshold?**	**Summary**	**Adjusted P Value**			
Saline - LPS								
Row 1	-0.2368	-0.6007 to 0.1271	No	ns	0.3262			
Row 2	-0.4830	-0.8847 to -0.08141	Yes	*	0.0155			
Row 3	-2.204	-4.114 to -0.2938	Yes	*	0.0230			
Row 4	-4.165	-6.720 to -1.611	Yes	**	0.0025			
Test details	**Mean 1**	**Mean 2**	**Mean Diff.**	**SE of diff.**	**N1**	**N2**	**t**	**DF**
Saline - LPS								
Row 1	0.3438	0.5806	-0.2368	0.1252	8	9	1.892	12.68
Row 2	0.4500	0.9330	-0.4830	0.1415	8	9	3.414	14.94
Row 3	1.741	3.944	-2.204	0.6228	8	9	3.539	9.574
Row 4	2.613	6.778	-4.165	0.8304	8	9	5.016	9.445

Magazine entries rate

Row Labels	Average of Mag rate	Average of Mag rate2	Average of Mag rate3	Average of Mag rate4	Average of Mag rate5	Average of Mag rate6	Average of Mag rate7	Average of Mag rate8
LPS	**10.65333333**	**6.305**	**8.64**	**7.503333333**	**7.053333333**	**7.083333333**	**6.45**	**5.886666667**
661	7.4	3.62	7.6	9.28	6.98	6.14	5.84	7.5
683	9.48	7.16	7.52	5.7	5.7	6.58	5.06	4.98
684	6.7	6.12	10.28	7.22	7.16	7.88	6.76	7.2
685	10.76	7.9	8.34	9.18	8.1	7.3	10.56	6.56
687	12.14	5.1	8.74	8.4	8.96	8.12	6.68	6.26
688	10.16	7.58	9.98	6.46	7.96	7.52	5.88	5.56
709	10.86	5.56	8.4	7.18	5.42	6.42	7.64	7.3
719	10.78	5.18	9.08	7.68	7.48	7.92	6.64	4.72
720	12.18	11.04	6.82	5.48	6.16	6.12	5.58	4.72
729	13.24	3.94	8.76	8.56	5.68	5.88	4.72	5.66
730	15.22	5.72	7.68	6.22	7.3	5.48	5.42	5.3
731	8.92	6.74	10.48	8.68	7.74	9.64	6.62	4.88
Sal	**10.274**	**7.05**	**8.57**	**6.7**	**5.354**	**6.904**	**5.888**	**6.146**
655	9.74	5.76	10.4	7.1	3.96	5.9	3.88	4.7
656	5.58	3.54	7.78	4.94	6	5.5	6.44	5.88
660	6.12	7.56	10.8	6.34	4.22	7.58	5.62	7.12
682	10.44	7.24	6.24	8.34	4.9	10.66	6.28	6.26
686	10.76	8.56	11.5	8.8	9.7	10.5	8.22	7.68
710	7.22	6.64	6.88	7.56	4.58	4.22	3.4	3.76
722	10.44	4.02	6.5	6.02	8.66	8.2	5.74	5.36
723	14.18	8.88	11.3	5.4	4.16	7.34	10.54	13.46
724	13.38	7.86	8.52	6.42	4.68	4.82	4.66	3.8
728	14.88	10.44	5.78	6.08	2.68	4.32	4.1	3.44
Grand Total	**10.48090909**	**6.643636364**	**8.608181818**	**7.138181818**	**6.280909091**	**7.001818182**	**6.194545455**	**6.004545455**

ANOVA results | Multiple comparisons

2way ANOVA
ANOVA results

	Source of Variation	% of total variation	P value	P value summary	Significant?	Geisser-Greenhouse's epsilon
8	Training days x Treatment	0.8976	0.8531	ns	No	
9	Training days	33.42	0.0003	***	Yes	0.7663
10	Treatment	0.1732	0.6678	ns	No	
11	Subject	13.56	0.6827	ns	No	
12						
13	**ANOVA table**	**SS**	**DF**	**MS**	**F (DFn, DFd)**	**P value**
14	Training days x Treatment	3.779	3	1.260	F (3, 45) = 0.2610	P=0.8531
15	Training days	140.7	3	46.90	F (2.299, 34.48) = 9.719	P=0.0003
16	Treatment	0.7294	1	0.7294	F (1, 15) = 0.1916	P=0.6678
17	Subject	57.10	15	3.807	F (15, 45) = 0.7888	P=0.6827
18	Residual	217.2	45	4.826		
19						
20	**Difference between column means**					
21	Mean of Saline	8.373				
22	Mean of LPS	8.165				
23	Difference between means	0.2075				
24	SE of difference	0.4740				
25	95% CI of difference	-0.8029 to 1.218				
26						
27	**Data summary**					
28	Number of columns (Treatment)	2				
29	Number of rows (Training days)	4				
30	Number of subjects (Subject)	17				
31	Number of missing values	0				
32						

4-day Devaluation test

Row Labels	Average of Mag	Average of Dev Lev	Average of Val Lever
LPS	**64.94444444**	**46.94444444**	**75.11111111**
661	51.5	22	55.5
683	41	21.5	55.5
684	42	74.5	104
688	68	54	68.5
709	79	40.5	78.5
720	45	29	91
729	60	81.5	99

730	88	35	61
731	110	64.5	63
Sal	**68.5**	**35.8125**	**36.1875**
655	28	37	20
660	60.5	42.5	37
682	55	37.5	25.5
686	107	24	51.5
710	42	74	53
722	111	29	37
723	120.5	7	16
728	24	35.5	49.5
Grand Total	**66.61764706**	**41.70588235**	**56.79411765**

ANOVA results | Multiple comparisons

2way ANOVA
ANOVA results

1	Table Analyzed	Day 4 devaluation				
2						
3	**Two-way ANOVA**	Ordinary				
4	Alpha	0.05				
5						
6	**Source of Variation**	**% of total variation**	**P value**	**P value summary**	**Significant?**	
7	Interaction	8.263	0.0424	*	Yes	
8	Treatment	26.80	0.0006	***	Yes	
9	Outcome values	8.715	0.0375	*	Yes	
10						
11	**ANOVA table**	**SS (Type III)**	**DF**	**MS**	**F (DFn, DFd)**	**P value**
12	Interaction	1636	1	1636	F (1, 30) = 4.494	P=0.0424
13	Treatment	5306	1	5306	F (1, 30) = 14.58	P=0.0006
14	Outcome values	1725	1	1725	F (1, 30) = 4.740	P=0.0375
15	Residual	10918	30	363.9		
16						
17	**Difference between column means**					
18	Predicted (LS) mean of Devalued	41.38				
19	Predicted (LS) mean of Valued	55.65				
20	Difference between predicted means	-14.27				
21	SE of difference	6.555				
22	95% CI of difference	-27.66 to -0.8843				
23						
24	**Difference between row means**					
25	Predicted (LS) mean of Saline	36.00				
26	Predicted (LS) mean of LPS	61.03				
27	Difference between predicted means	-25.03				
28	SE of difference	6.555				
29	95% CI of difference	-38.41 to -11.64				

Magazine entries:

Tabular results

Unpaired t test
Tabular results

1	Table Analyzed	Magazine comparison Day4
2		
3	Column B	Male Sal
4	vs.	vs.
5	Column A	Female Sal
6		
7	**Unpaired t test**	
8	P value	0.0699
9	P value summary	ns
10	Significantly different (P < 0.05)?	No
11	One- or two-tailed P value?	Two-tailed
12	t, df	t=1.934, df=17
13		
14	**How big is the difference?**	
15	Mean of column A	6.375
16	Mean of column B	3.773
17	Difference between means (B - A) ± SEM	-2.602 ± 1.346
18	95% confidence interval	-5.441 to 0.2366
19	R squared (eta squared)	0.1803
20		
21	**F test to compare variances**	
22	F, DFn, Dfd	2.675, 7, 10
23	P value	0.1542
24	P value summary	ns
25	Significantly different (P < 0.05)?	No
26		
27	**Data analyzed**	
28	Sample size, column A	8
29	Sample size, column B	11

Day 5-8 Lever-press training:

ANOVA results | Multiple comparisons

2way ANOVA
ANOVA results

6						
7	**Source of Variation**	**% of total variation**	**P value**	**P value summary**	**Significant?**	**Geisser-Greenhouse's epsilon**
8	Training days x Treatment	0.5997	0.3469	ns	No	
9	Training days	44.31	<0.0001	****	Yes	0.6817
10	Treatment	37.02	<0.0001	****	Yes	
11	Subject	9.939	0.0003	***	Yes	
12						
13	**ANOVA table**	**SS**	**DF**	**MS**	**F (DFn, DFd)**	**P value**
14	Training days x Treatment	3.940	3	1.313	F (3, 45) = 1.130	P=0.3469
15	Training days	291.2	3	97.05	F (2.045, 30.68) = 83.52	P<0.0001
16	Treatment	243.3	1	243.3	F (1, 15) = 55.88	P<0.0001
17	Subject	65.30	15	4.353	F (15, 45) = 3.746	P=0.0003
18	Residual	52.29	45	1.162		
19						
20	**Difference between column means**					
21	Mean of Saline	5.683				
22	Mean of LPS	9.472				
23	Difference between means	-3.789				
24	SE of difference	0.5069				
25	95% CI of difference	-4.870 to -2.709				
26						
27	**Data summary**					
28	Number of columns (Treatment)	2				
29	Number of rows (Training days)	4				
30	Number of subjects (Subject)	17				
31	Number of missing values	0				
32						

Day 5-8 magazine entries:

ANOVA results | Multiple comparisons

2way ANOVA
ANOVA results

Source of Variation	**% of total variation**	**P value**	**P value summary**	**Significant?**	**Geisser-Greenhouse's epsilon**
Training days x Treatment	3.765	0.2286	ns	No	
Training days	5.512	0.1421	ns	No	0.5306
Treatment	0.02226	0.9379	ns	No	
Subject	53.17	<0.0001	****	Yes	
ANOVA table	**SS**	**DF**	**MS**	**F (DFn, DFd)**	**P value**
Training days x Treatment	9.728	3	3.243	F (3, 45) = 1.495	P=0.2286
Training days	14.24	3	4.747	F (1.592, 23.88) = 2.189	P=0.1421
Treatment	0.05751	1	0.05751	F (1, 15) = 0.006280	P=0.9379
Subject	137.4	15	9.158	F (15, 45) = 4.223	P<0.0001
Residual	97.58	45	2.168		
Difference between column means					
Mean of Saline	6.286				
Mean of LPS	6.344				
Difference between means	-0.05826				
SE of difference	0.7352				
95% CI of difference	-1.625 to 1.509				
Data summary					
Number of columns (Treatment)	2				
Number of rows (Training days)	4				
Number of subjects (Subject)	17				
Number of missing values	0				

Day-8 devaluation test:

Row Labels	Average of Mag Entries	Average of Deval Lever	Average of Val Lever
LPS	**4.266666667**	**6.933333333**	**12.93333333**
661	5	6.45	13.9
683	3.65	8.45	7
684	4	2.95	5.7
688	3.15	5.7	16.2
709	5	5.95	13.4
720	3.7	8.8	19.4
729	5.7	8.45	13.35
730	6.05	4.7	15.2
731	2.15	10.95	12.25
Sal	**6.00625**	**5.7625**	**9.85625**
655	3.9	8.8	13
660	1.5	3.15	4.2
682	6.75	5.4	7.85
686	10.65	4.75	9.15
710	3.1	7.9	12.45
722	5	3.9	13.45
723	14.55	5.65	7.7
728	2.6	6.55	11.05
Grand Total	**5.085294118**	**6.382352941**	**11.48529412**

ANOVA results | Multiple comparisons

2way ANOVA
ANOVA results

Table Analyzed	Day_8_devaluation_placements				
Two-way ANOVA	Ordinary				
Alpha	0.05				
Source of Variation	**% of total variation**	**P value**	**P value summary**	**Significant?**	
Interaction	1.374	0.3816	ns	No	
Treatment	6.824	0.0571	ns	No	
Devaluation factor	38.53	<0.0001	****	Yes	
ANOVA table	**SS (Type III)**	**DF**	**MS**	**F (DFn, DFd)**	**P value**
Interaction	7.695	1	7.695	F (1, 30) = 0.7886	P=0.3816
Treatment	38.21	1	38.21	F (1, 30) = 3.916	P=0.0571
Devaluation factor	215.8	1	215.8	F (1, 30) = 22.11	P<0.0001
Residual	292.7	30	9.758		
Difference between column means					
Predicted (LS) mean of Devalued	6.348				
Predicted (LS) mean of Valued	11.39				
Difference between predicted means	-5.047				
SE of difference	1.073				
95% CI of difference	-7.239 to -2.855				
Difference between row means					
Predicted (LS) mean of Saline	7.809				
Predicted (LS) mean of LPS	9.933				
Difference between predicted means	-2.124				
SE of difference	1.073				
95% CI of difference	-4.316 to 0.06801				

ANOVA results | Multiple comparisons

2way ANOVA
Multiple comparisons

Compare each cell mean with the other cell mean in that rov								
Number of families	1							
Number of comparisons per family	2							
Alpha	0.05							
Bonferroni's multiple comparisons test	**Predicted (LS) mean diff.**	**95.00% CI of diff.**	**Below threshold?**	**Summary**	**Adjusted P Valu**			
Devalued - Valued								
Saline	-4.094	-7.779 to -0.4084	Yes	*	0.0273			
LPS	-6.000	-9.475 to -2.525	Yes	***	0.0006			
Test details	**Predicted (LS) mean 1**	**Predicted (LS) mean 2**	**Predicted (LS) mean diff.**	**SE of diff.**	**N1**	**N2**	**t**	**DF**
Devalued - Valued								
Saline	5.763	9.856	-4.094	1.562	8	8	2.621	30.00
LPS	6.933	12.93	-6.000	1.473	9	9	4.075	30.00

Day 8 magazine entries:

Tabular results

	Unpaired t test Tabular results	
1	Table Analyzed	Test day8 magazine entries
2		
3	Column B	LPS
4	vs.	vs.
5	Column A	Sham
6		
7	**Unpaired t test**	
8	P value	0.2810
9	P value summary	ns
10	Significantly different (P < 0.05)?	No
11	One- or two-tailed P value?	Two-tailed
12	t, df	t=1.118, df=15
13		
14	**How big is the difference?**	
15	Mean of column A	6.006
16	Mean of column B	4.267
17	Difference between means (B - A) ± SEM	-1.740 ± 1.556
18	95% confidence interval	-5.055 to 1.576
19	R squared (eta squared)	0.07696
20		
21	**F test to compare variances**	
22	F, DFn, Dfd	12.57, 7, 8
23	P value	0.0019
24	P value summary	**
25	Significantly different (P < 0.05)?	Yes
26		
27	**Data analyzed**	
28	Sample size, column A	8

Open Field test:

Total distance travelled		Time spent in centre zone		Time spent in corner zone	
Saline	LPS	Saline	LPS	Saline	LPS
3152.129	4126.763	226	342	374	258
2952.68	2900.032	258.05	312.4	341.95	287.6
3158.486	3428.908	285.15	297.45	314.85	302.55
2859.452	3152.919	235.55	230.05	364.45	369.95
2545.797	3711.468	247.7	330.75	352.3	269.25
1722.172	3682.794	369.75	240.15	230.25	359.85
1723.558	2567.541	241.9	467.55	358.1	132.45
2139.884	2026.721	233.9	178.45	366.1	421.55
	2805.027		432.25		167.75

	Unpaired t test	
1	Table Analyzed	Total distance travelled
2		
3	Column B	LPS
4	vs.	vs.
5	Column A	Saline
6		
7	**Unpaired t test**	
8	P value	0.0592
9	P value summary	ns
10	Significantly different (P < 0.05)?	No
11	One- or two-tailed P value?	Two-tailed
12	t, df	t=2.041, df=15
13		
14	**How big is the difference?**	
15	Mean of column A	2532
16	Mean of column B	3156
17	Difference between means (B - A) ± SEM	624.0 ± 305.7
18	95% confidence interval	-27.60 to 1276
19	R squared (eta squared)	0.2174
20		
21	**F test to compare variances**	
22	F, DFn, Dfd	1.183, 8, 7
23	P value	0.8376
24	P value summary	ns
25	Significantly different (P < 0.05)?	No
26		
27	**Data analyzed**	
28	Sample size, column A	8
29	Sample size, column B	9

	Unpaired t test	
1	Table Analyzed	Time spent in corner zone
2		
3	Column B	LPS
4	vs.	vs.
5	Column A	Saline
6		
7	**Unpaired t test**	
8	P value	0.1740
9	P value summary	ns
10	Significantly different (P < 0.05)?	No
11	One- or two-tailed P value?	Two-tailed
12	t, df	t=1.427, df=15
13		
14	**How big is the difference?**	
15	Mean of column A	262.3
16	Mean of column B	314.6
17	Difference between means (B - A) ± SEM	52.31 ± 36.65
18	95% confidence interval	-25.80 to 130.4
19	R squared (eta squared)	0.1196
20		
21	**F test to compare variances**	
22	F, DFn, Dfd	3.925, 8, 7
23	P value	0.0880
24	P value summary	ns
25	Significantly different (P < 0.05)?	No
26		
27	**Data analyzed**	
28	Sample size, column A	8
29	Sample size, column B	9

	Unpaired t test	
1	Table Analyzed	Time spent in centre zone
2		
3	Column B	LPS
4	vs.	vs.
5	Column A	Saline
6		
7	**Unpaired t test**	
8	P value	0.1740
9	P value summary	ns
10	Significantly different (P < 0.05)?	No
11	One- or two-tailed P value?	Two-tailed
12	t, df	t=1.427, df=15
13		
14	**How big is the difference?**	
15	Mean of column A	337.8
16	Mean of column B	285.4
17	Difference between means (B - A) ± SEM	-52.31 ± 36.65
18	95% confidence interval	-130.4 to 25.80
19	R squared (eta squared)	0.1196
20		
21	**F test to compare variances**	
22	F, DFn, Dfd	3.925, 8, 7
23	P value	0.0880
24	P value summary	ns
25	Significantly different (P < 0.05)?	No
26		
27	**Data analyzed**	
28	Sample size, column A	8
29	Sample size, column B	9

Microglia cell counts and intensity:

Microglia cell counts

Saline	LPS
73.77778	119.375
65.5	117
69.625	106
63.875	113.375
64.375	115.8571
67.75	132.375
65.125	111.5714
	104.8571

Microglia intensity

Saline	LPS
10213.49	13382.62
11332	15981.02
11811.94	15277.92
11057.45	14398.17
8075.152	14175.39
9686.155	13754.56
8706.926	10943.86
	9516.894

Unpaired t test	
Table Analyzed	Iba1-counts
Column B	LPS
vs.	vs.
Column A	Saline
Unpaired t test	
P value	<0.0001
P value summary	****
Significantly different (P < 0.05)?	Yes
One- or two-tailed P value?	Two-tailed
t, df	t=13.63, df=13
How big is the difference?	
Mean of column A	67.15
Mean of column B	115.1
Difference between means (B - A) ± SEM	47.90 ± 3.515
95% confidence interval	40.31 to 55.50
R squared (eta squared)	0.9346
F test to compare variances	
F, DFn, Dfd	5.936, 7, 6
P value	0.0453
P value summary	*
Significantly different (P < 0.05)?	Yes
Data analyzed	
Sample size, column A	7
Sample size, column B	8

Unpaired t test	
Table Analyzed	Iba1-intensity
Column B	LPS
vs.	vs.
Column A	Saline
Unpaired t test	
P value	0.0043
P value summary	**
Significantly different (P < 0.05)?	Yes
One- or two-tailed P value?	Two-tailed
t, df	t=3.445, df=13
How big is the difference?	
Mean of column A	10126
Mean of column B	13429
Difference between means (B - A) ± SEM	3303 ± 958.6
95% confidence interval	1232 to 5374
R squared (eta squared)	0.4773
F test to compare variances	
F, DFn, Dfd	2.443, 7, 6
P value	0.2966
P value summary	ns
Significantly different (P < 0.05)?	No
Data analyzed	
Sample size, column A	7
Sample size, column B	8

Day-4 microglia and devaluation correlation:

IBA1 counts	Devaluation ratio
106	0.074024396
115.8571429	0.164461355
64.375	-0.002272861
65.125	0.09771614
111.5714286	0.131098269
104.8571429	-0.014340477
73.77777778	-0.085492037
65.5	-0.013948766
119.375	0.22371547
132.375	0.131726138
67.75	-0.012632146
69.625	-0.074016221
117	0.257969003
113.375	0.187636617
63.875	0.126854137

IBA1 intensity	Devaluation ratio
15277.92	0.074024396
14175.39	0.164461355
8075.152	-0.002272861
8706.926	0.09771614
13754.56	0.131098269
9516.894	-0.014340477
10213.49	-0.085492037
11332	-0.013948766
13382.62	0.22371547
10943.86	0.131726138
9686.155	-0.012632146
11811.94	-0.074016221
15981.02	0.257969003
14398.17	0.187636617
11057.45	0.126854137

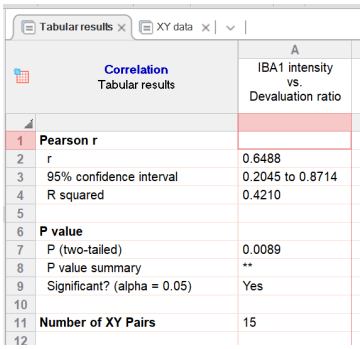

Tabular results | XY data

	Correlation Tabular results	A IBA1 intensity vs. Devaluation ratio
1	**Pearson r**	
2	r	0.6488
3	95% confidence interval	0.2045 to 0.8714
4	R squared	0.4210
5		
6	**P value**	
7	P (two-tailed)	0.0089
8	P value summary	**
9	Significant? (alpha = 0.05)	Yes
10		
11	**Number of XY Pairs**	15
12		

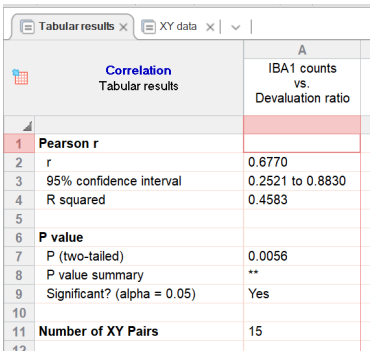

Tabular results | XY data

	Correlation Tabular results	A IBA1 counts vs. Devaluation ratio
1	**Pearson r**	
2	r	0.6770
3	95% confidence interval	0.2521 to 0.8830
4	R squared	0.4583
5		
6	**P value**	
7	P (two-tailed)	0.0056
8	P value summary	**
9	Significant? (alpha = 0.05)	Yes
10		
11	**Number of XY Pairs**	15
12		

Day-4 Microglial and magazine entries correlation:

IBA1 counts	Magazine entries
106	68
115.8571429	79
64.375	42
65.125	24
111.5714286	60
104.8571429	110
73.77777778	28
65.5	60.5
119.375	51.5
132.375	45
67.75	120.5
69.625	55
117	41
113.375	42
63.875	107

IBA1 intensity	Magazine entries
15277.92	68
14175.39	79
8075.152	42
8706.926	24
13754.56	60
9516.894	110
10213.49	28
11332	60.5
13382.62	51.5
10943.86	45
9686.155	120.5
11811.94	55
15981.02	41
14398.17	42
11057.45	107

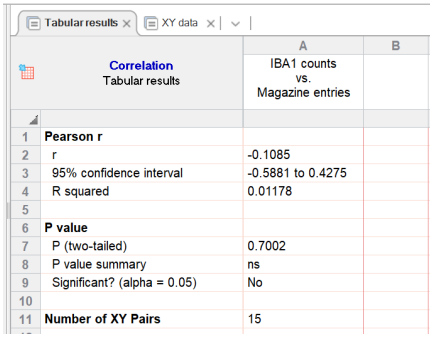

Tabular results | XY data

	Correlation Tabular results	A IBA1 counts vs. Magazine entries	B
1	**Pearson r**		
2	r	-0.1085	
3	95% confidence interval	-0.5881 to 0.4275	
4	R squared	0.01178	
5			
6	**P value**		
7	P (two-tailed)	0.7002	
8	P value summary	ns	
9	Significant? (alpha = 0.05)	No	
10			
11	**Number of XY Pairs**	15	
12			

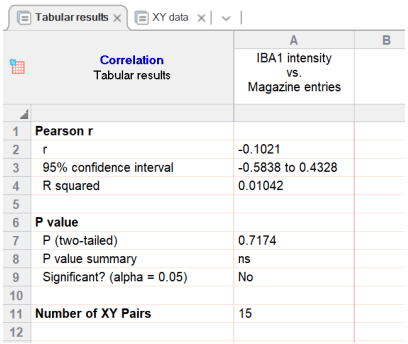

Tabular results | XY data

	Correlation Tabular results	A IBA1 intensity vs. Magazine entries	B
1	**Pearson r**		
2	r	-0.1021	
3	95% confidence interval	-0.5838 to 0.4328	
4	R squared	0.01042	
5			
6	**P value**		
7	P (two-tailed)	0.7174	
8	P value summary	ns	
9	Significant? (alpha = 0.05)	No	
10			
11	**Number of XY Pairs**	15	
12			

Day-8 Microglia and devaluation correlation:

IBA1 counts	Devaluation ratio
106	0.223883477
115.8571429	0.177966756
64.375	0.18266778
65.125	0.12407055
111.5714286	0.159577627
104.8571429	0.182682398

IBA1 intensity	Devaluation ratio
15277.92	0.223883477
14175.39	0.177966756
8075.152	0.18266778
8706.926	0.12407055
13754.56	0.159577627
9516.894	0.182682398

73.77777778	0.04402134	10213.49	0.04402134
65.5	0.071662479	11332	0.071662479
119.375	0.211204603	13382.62	0.211204603
132.375	0.156921853	10943.86	0.156921853
67.75	0.103608668	9686.155	0.103608668
69.625	0.052962999	11811.94	0.052962999
117	-0.035302945	15981.02	-0.035302945
113.375	0.15141805	14398.17	0.15141805
63.875	0.182191092	11057.45	0.182191092

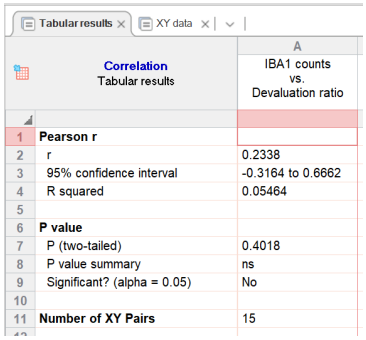

Correlation Tabular results	A IBA1 counts vs. Devaluation ratio
Pearson r	
r	0.2338
95% confidence interval	-0.3164 to 0.6662
R squared	0.05464
P value	
P (two-tailed)	0.4018
P value summary	ns
Significant? (alpha = 0.05)	No
Number of XY Pairs	15

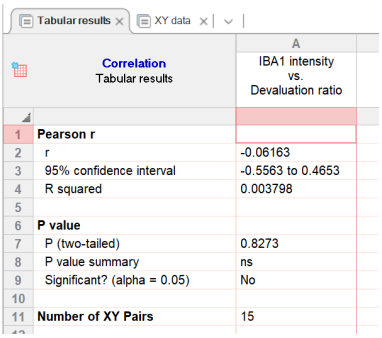

Correlation Tabular results	A IBA1 intensity vs. Devaluation ratio
Pearson r	
r	-0.06163
95% confidence interval	-0.5563 to 0.4653
R squared	0.003798
P value	
P (two-tailed)	0.8273
P value summary	ns
Significant? (alpha = 0.05)	No
Number of XY Pairs	15

Day 8 – microglia and magazine entries correlation:

IBA1 counts	Magazine entries
106	34
115.8571429	52.5
64.375	33.5
65.125	30
111.5714286	57
104.8571429	25.5
73.77777778	43
65.5	19.5
119.375	51
132.375	39
67.75	151
69.625	73
117	39.5
113.375	43
63.875	110.5

IBA1 intensity	Magazine entries
15277.92	34
14175.39	52.5
8075.152	33.5
8706.926	30
13754.56	57
9516.894	25.5
10213.49	43
11332	19.5
13382.62	51
10943.86	39
9686.155	151
11811.94	73
15981.02	39.5
14398.17	43
11057.45	110.5

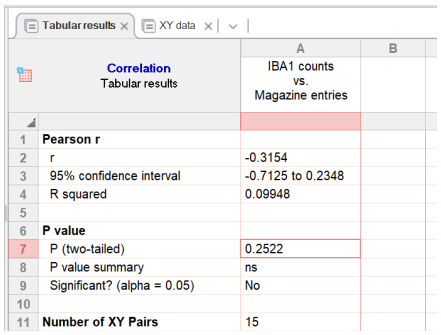

Correlation Tabular results	A IBA1 counts vs. Magazine entries	B
Pearson r		
r	-0.3154	
95% confidence interval	-0.7125 to 0.2348	
R squared	0.09948	
P value		
P (two-tailed)	0.2522	
P value summary	ns	
Significant? (alpha = 0.05)	No	
Number of XY Pairs	15	

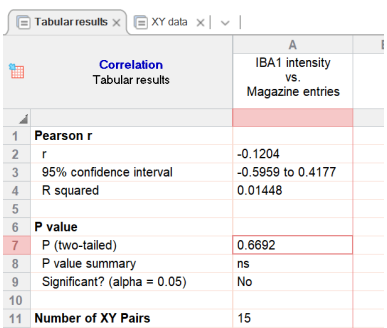

Correlation Tabular results	A IBA1 intensity vs. Magazine entries
Pearson r	
r	-0.1204
95% confidence interval	-0.5959 to 0.4177
R squared	0.01448
P value	
P (two-tailed)	0.6692
P value summary	ns
Significant? (alpha = 0.05)	No
Number of XY Pairs	15

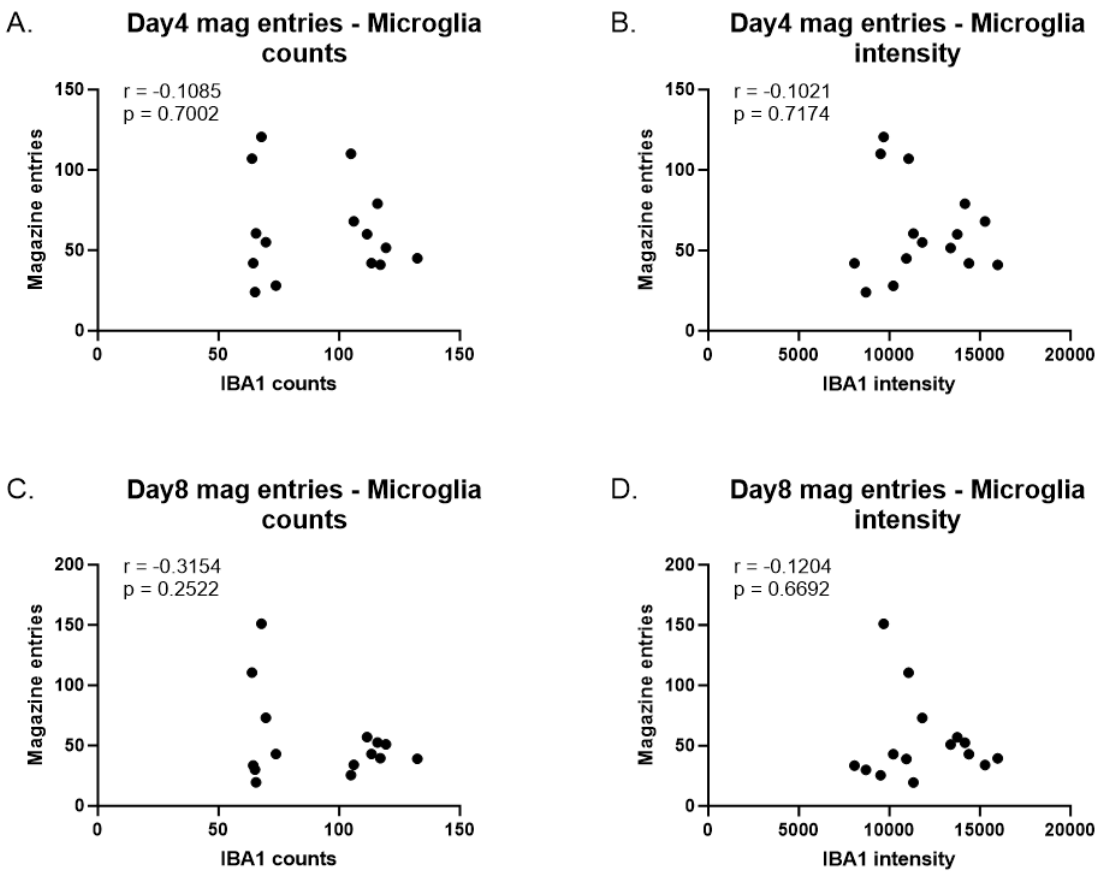

Astrocytes – cell counts and intensity:

Saline	LPS
112.3333	119.625
98.25	112
125.625	138
110.75	100.75
124.875	126.2857
130.5	130.5
98.125	131.8571
	115

Saline	LPS
17516.79	43704.11
18681.99	74482.46
17231.54	64677.89
18970.27	54473.54
15583.54	53345.92
17050.03	33021.19
15802.48	47586.31
	22495.71

Unpaired t test	
Table Analyzed	GFAP-counts
Column B	LPS
vs.	vs.
Column A	Saline
Unpaired t test	
P value	0.2795
P value summary	ns
Significantly different (P < 0.05)?	No
One- or two-tailed P value?	Two-tailed
t, df	t=1.128, df=13
How big is the difference?	
Mean of column A	114.4
Mean of column B	121.8
Difference between means (B - A) ± SEM	7.401 ± 6.559
95% confidence interval	-6.768 to 21.57
R squared (eta squared)	0.08921
F test to compare variances	
F, DFn, Dfd	1.154, 6, 7
P value	0.8445
P value summary	ns
Significantly different (P < 0.05)?	No
Data analyzed	
Sample size, column A	7
Sample size, column B	8

Unpaired t test	
Table Analyzed	GFAP-intensity
Column B	LPS
vs.	vs.
Column A	Saline
Unpaired t test	
P value	0.0002
P value summary	***
Significantly different (P < 0.05)?	Yes
One- or two-tailed P value?	Two-tailed
t, df	t=5.053, df=13
How big is the difference?	
Mean of column A	17262
Mean of column B	49223
Difference between means (B - A) ± SEM	31961 ± 6325
95% confidence interval	18297 to 45625
R squared (eta squared)	0.6627
F test to compare variances	
F, DFn, Dfd	165.7, 7, 6
P value	<0.0001
P value summary	****
Significantly different (P < 0.05)?	Yes
Data analyzed	
Sample size, column A	7
Sample size, column B	8

Day 4 – astrocytes devaluation correlation:

GFAP counts	Devaluation ratio
138	0.074024396
126.2857143	0.164461355
124.875	-0.002272861
98.125	0.09771614
131.8571429	0.131098269
115	-0.014340477
112.3333333	-0.085492037
98.25	-0.013948766
119.625	0.22371547
130.5	0.131726138
130.5	-0.012632146
125.625	-0.074016221
112	0.257969003
100.75	0.187636617
110.75	0.126854137

GFAP intensity	Devaluation ratio
64677.89	0.074024396
53345.92	0.164461355
15583.54	-0.002272861
15802.48	0.09771614
47586.31	0.131098269
22495.71	-0.014340477
17516.79	-0.085492037
18681.99	-0.013948766
43704.11	0.22371547
33021.19	0.131726138
17050.03	-0.012632146
17231.54	-0.074016221
74482.46	0.257969003
54473.54	0.187636617
18970.27	0.126854137

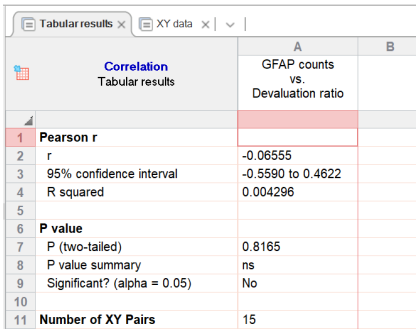

Tabular results | XY data

	Correlation Tabular results	A GFAP counts vs. Devaluation ratio	B
1	**Pearson r**		
2	r	-0.06555	
3	95% confidence interval	-0.5590 to 0.4622	
4	R squared	0.004296	
5			
6	**P value**		
7	P (two-tailed)	0.8165	
8	P value summary	ns	
9	Significant? (alpha = 0.05)	No	
10			
11	**Number of XY Pairs**	15	

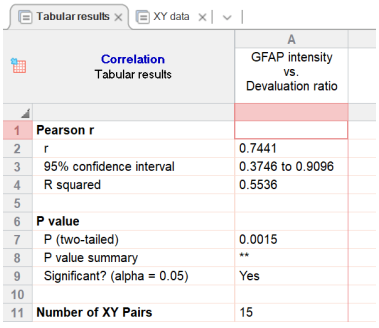

Tabular results | XY data

	Correlation Tabular results	A GFAP intensity vs. Devaluation ratio
1	**Pearson r**	
2	r	0.7441
3	95% confidence interval	0.3746 to 0.9096
4	R squared	0.5536
5		
6	**P value**	
7	P (two-tailed)	0.0015
8	P value summary	**
9	Significant? (alpha = 0.05)	Yes
10		
11	**Number of XY Pairs**	15

Day 4 - Astrocytes – magazine entries correlation:

GFAP counts	Magazine entries
138	68
126.2857143	79
124.875	42
98.125	24
131.8571429	60
115	110
112.3333333	28
98.25	60.5
119.625	51.5
130.5	45
130.5	120.5
125.625	55
112	41
100.75	42
110.75	107

GFAP intensity	Magazine entries
64677.89	68
53345.92	79
15583.54	42
15802.48	24
47586.31	60
22495.71	110
17516.79	28
18681.99	60.5
43704.11	51.5
33021.19	45
17050.03	120.5
17231.54	55
74482.46	41
54473.54	42
18970.27	107

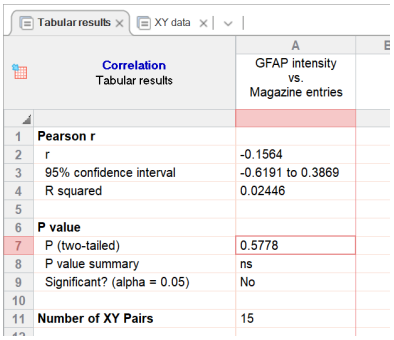

Tabular results | XY data

	Correlation Tabular results	A GFAP intensity vs. Magazine entries
1	**Pearson r**	
2	r	-0.1564
3	95% confidence interval	-0.6191 to 0.3869
4	R squared	0.02446
5		
6	**P value**	
7	P (two-tailed)	0.5778
8	P value summary	ns
9	Significant? (alpha = 0.05)	No
10		
11	**Number of XY Pairs**	15

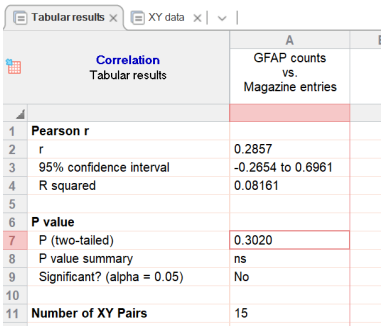

Tabular results | XY data

	Correlation Tabular results	A GFAP counts vs. Magazine entries
1	**Pearson r**	
2	r	0.2857
3	95% confidence interval	-0.2654 to 0.6961
4	R squared	0.08161
5		
6	**P value**	
7	P (two-tailed)	0.3020
8	P value summary	ns
9	Significant? (alpha = 0.05)	No
10		
11	**Number of XY Pairs**	15

Day 8 Astrocytes – devaluation correlation:

GFAP counts	Devaluation ratio
138	0.223883477
126.2857143	0.177966756
124.875	0.18266778
98.125	0.12407055
131.8571429	0.159577627

GFAP intensity	Devaluation ratio
64677.89	0.223883477
53345.92	0.177966756
15583.54	0.18266778
15802.48	0.12407055
47586.31	0.159577627

115	0.182682398	22495.71	0.182682398
112.3333333	0.04402134	17516.79	0.04402134
98.25	0.071662479	18681.99	0.071662479
119.625	0.211204603	43704.11	0.211204603
130.5	0.156921853	33021.19	0.156921853
130.5	0.103608668	17050.03	0.103608668
125.625	0.052962999	17231.54	0.052962999
112	-0.035302945	74482.46	-0.035302945
100.75	0.15141805	54473.54	0.15141805
110.75	0.182191092	18970.27	0.182191092

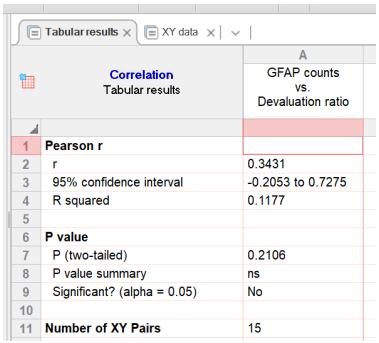

Tabular results | XY data

	Correlation Tabular results	A GFAP counts vs. Devaluation ratio
1	**Pearson r**	
2	r	0.3431
3	95% confidence interval	-0.2053 to 0.7275
4	R squared	0.1177
5		
6	**P value**	
7	P (two-tailed)	0.2106
8	P value summary	ns
9	Significant? (alpha = 0.05)	No
10		
11	**Number of XY Pairs**	15

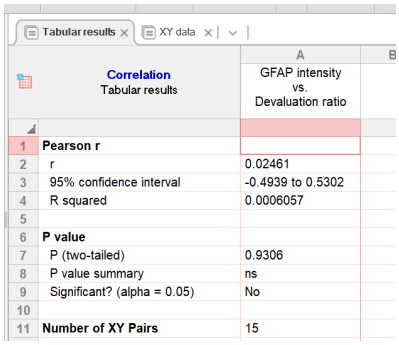

Tabular results | XY data

	Correlation Tabular results	A GFAP intensity vs. Devaluation ratio
1	**Pearson r**	
2	r	0.02461
3	95% confidence interval	-0.4939 to 0.5302
4	R squared	0.0006057
5		
6	**P value**	
7	P (two-tailed)	0.9306
8	P value summary	ns
9	Significant? (alpha = 0.05)	No
10		
11	**Number of XY Pairs**	15

Day 8 Astrocytes – magazine entries correlation:

GFAP counts	Magazine entries	GFAP intensity	Magazine entries
138	34	64677.89	34
126.2857143	52.5	53345.92	52.5
124.875	33.5	15583.54	33.5
98.125	30	15802.48	30
131.8571429	57	47586.31	57
115	25.5	22495.71	25.5
112.3333333	43	17516.79	43
98.25	19.5	18681.99	19.5
119.625	51	43704.11	51
130.5	39	33021.19	39
130.5	151	17050.03	151
125.625	73	17231.54	73
112	39.5	74482.46	39.5
100.75	43	54473.54	43
110.75	110.5	18970.27	110.5

Tabular results | XY data

	Correlation Tabular results	A GFAP counts vs. Magazine entries
1	**Pearson r**	
2	r	0.2925
3	95% confidence interval	-0.2585 to 0.6999
4	R squared	0.08557
5		
6	**P value**	
7	P (two-tailed)	0.2901
8	P value summary	ns
9	Significant? (alpha = 0.05)	No
10		
11	**Number of XY Pairs**	15

Tabular results | XY data

	Correlation Tabular results	A GFAP intensity vs. Magazine entries	B
1	**Pearson r**		
2	r	-0.2408	
3	95% confidence interval	-0.6704 to 0.3096	
4	R squared	0.05800	
5			
6	**P value**		
7	P (two-tailed)	0.3872	
8	P value summary	ns	
9	Significant? (alpha = 0.05)	No	
10			
11	**Number of XY Pairs**	15	

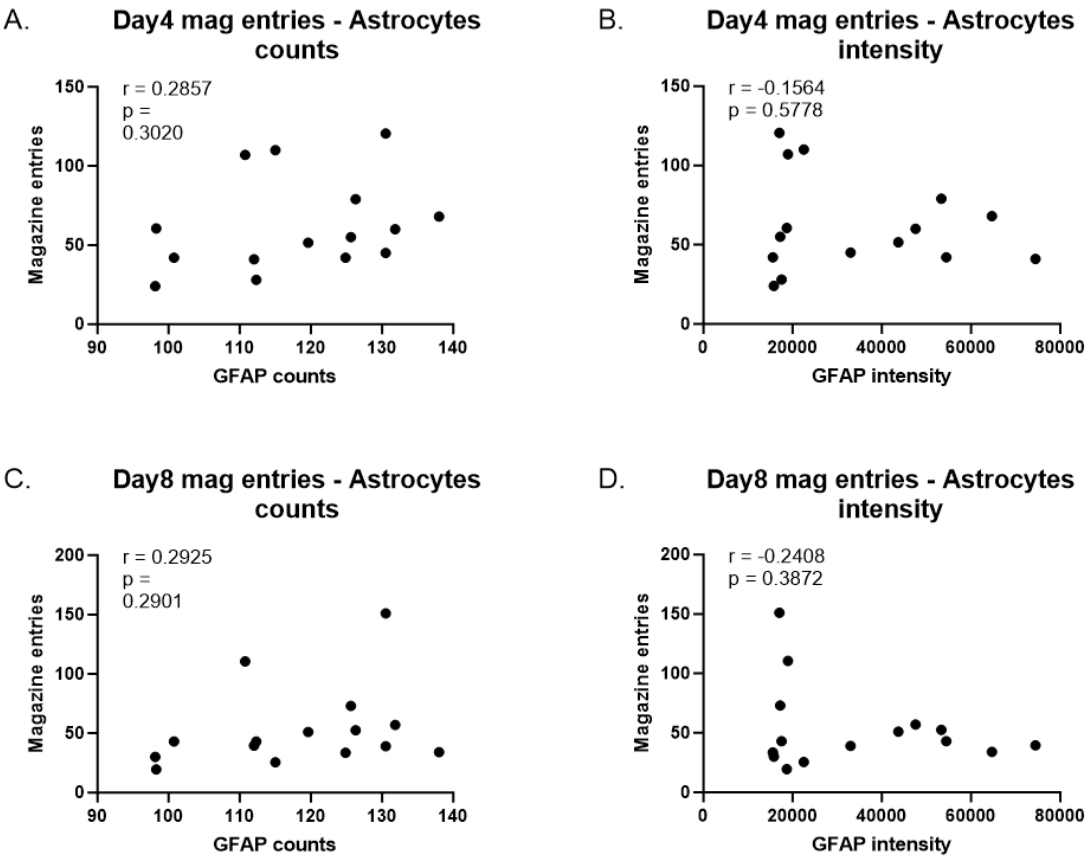

c-Fos expression:

c-Fos counts CA1		c-Fos intensity CA1		c-Fos counts DG		c-Fos intensity DG	
Saline	LPS	Saline	LPS	Saline	LPS	Saline	LPS
76	92.625	13510.73	8766.192	50.875	104.75	10928.66	8589.288
72	119.8571	9222.416	11756.7	57	96.14286	8672.692	8523.112
104.25	106	11719.76	9827.006	78.57143	77.42857	10557.48	12397.64
90.16667	79	9780.342	9399.691	49	87.625	9072.278	7489.289
77.625	96	10327.78	7279.833	89.5	105.375	9163.037	7699.448
110.875	147.875	10467.57	9281.403	80.75	96.5	10206.95	9296.409
97.125	130.875	11930.51	10723.25	74.625	112.625	10169.81	11111.64
	108.625		10722.2		107.75		10793.37

Mann-Whitney test	
Table Analyzed	cFOS-counts CA1
Column B	LPS
vs.	vs.
Column A	Saline
Mann Whitney test	
P value	0.0721
Exact or approximate P value?	Exact
P value summary	ns
Significantly different (P < 0.05)?	No
One- or two-tailed P value?	Two-tailed
Sum of ranks in column A,B	40 , 80
Mann-Whitney U	12
Difference between medians	
Median of column A	90.17, n=7
Median of column B	107.3, n=8
Difference: Actual	17.15
Difference: Hodges-Lehmann	19.23

Mann-Whitney test	
Table Analyzed	cFOS-intensity CA1
Column B	LPS
vs.	vs.
Column A	Saline
Mann Whitney test	
P value	0.2319
Exact or approximate P value?	Exact
P value summary	ns
Significantly different (P < 0.05)?	No
One- or two-tailed P value?	Two-tailed
Sum of ranks in column A,B	67 , 53
Mann-Whitney U	17
Difference between medians	
Median of column A	10468, n=7
Median of column B	9613, n=8
Difference: Actual	-854.2
Difference: Hodges-Lehmann	-1057

Mann-Whitney test	
Table Analyzed	cFOS-counts DG
Column B	LPS
vs.	vs.
Column A	Saline
Mann Whitney test	
P value	0.0037
Exact or approximate P value?	Exact
P value summary	**
Significantly different (P < 0.05)?	Yes
One- or two-tailed P value?	Two-tailed
Sum of ranks in column A,B	32 , 88
Mann-Whitney U	4
Difference between medians	
Median of column A	74.63, n=7
Median of column B	100.6, n=8
Difference: Actual	26.00
Difference: Hodges-Lehmann	28.80

Mann-Whitney test	
Table Analyzed	cFOS-intensity DG
Column B	LPS
vs.	vs.
Column A	Saline
Mann Whitney test	
P value	0.6126
Exact or approximate P value?	Exact
P value summary	ns
Significantly different (P < 0.05)?	No
One- or two-tailed P value?	Two-tailed
Sum of ranks in column A,B	61 , 59
Mann-Whitney U	23
Difference between medians	
Median of column A	10170, n=7
Median of column B	8943, n=8
Difference: Actual	-1227
Difference: Hodges-Lehmann	-561.5

A. **cFOS cells CA1**

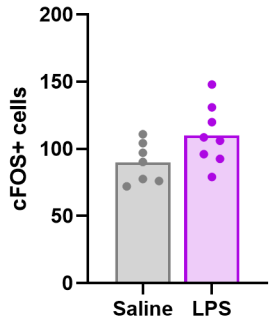

B. **cFOS intensity CA1**

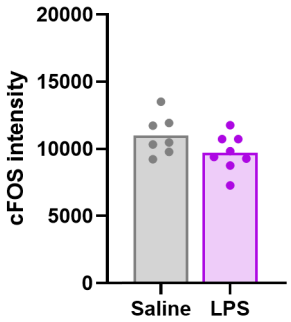

C. **cFOS cells DG**

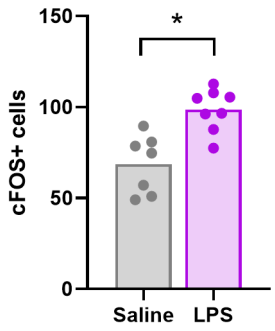

D. **cFOS intensity DG**

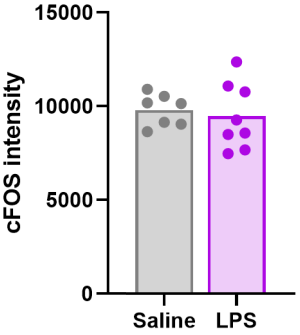

NeuN expression:

NeuN intensity CA1

Saline	LPS
25174.97	21210.79
22093.46	26749.68
30738.89	28712.52
29849.09	16395.63
18339.97	15464.68
24788.56	30480.58
25585.09	20280.02
	22684.57

NeuN intensity DG

Saline	LPS
46541.18	37921.31
38478.05	48907.3
55150.66	57396.76
60506.92	22379.86
38962.87	20697.72
45662.91	41883.35
39075.87	43944.51
	38341.71

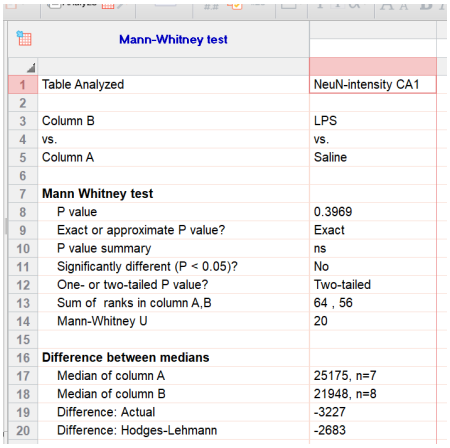

	Mann-Whitney test	
1	Table Analyzed	NeuN-intensity CA1
2		
3	Column B	LPS
4	vs.	vs.
5	Column A	Saline
6		
7	**Mann Whitney test**	
8	P value	0.3969
9	Exact or approximate P value?	Exact
10	P value summary	ns
11	Significantly different (P < 0.05)?	No
12	One- or two-tailed P value?	Two-tailed
13	Sum of ranks in column A,B	64 , 56
14	Mann-Whitney U	20
15		
16	**Difference between medians**	
17	Median of column A	25175, n=7
18	Median of column B	21948, n=8
19	Difference: Actual	-3227
20	Difference: Hodges-Lehmann	-2683

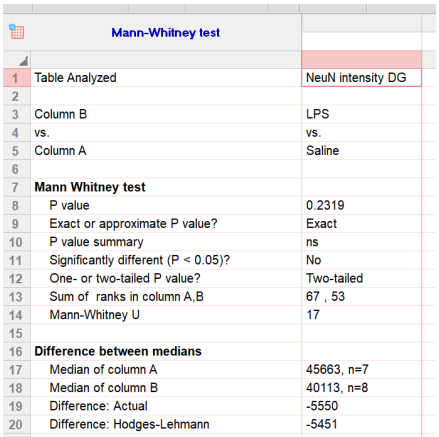

	Mann-Whitney test	
1	Table Analyzed	NeuN intensity DG
2		
3	Column B	LPS
4	vs.	vs.
5	Column A	Saline
6		
7	**Mann Whitney test**	
8	P value	0.2319
9	Exact or approximate P value?	Exact
10	P value summary	ns
11	Significantly different (P < 0.05)?	No
12	One- or two-tailed P value?	Two-tailed
13	Sum of ranks in column A,B	67 , 53
14	Mann-Whitney U	17
15		
16	**Difference between medians**	
17	Median of column A	45663, n=7
18	Median of column B	40113, n=8
19	Difference: Actual	-5550
20	Difference: Hodges-Lehmann	-5451

c-Fos/NeuN co-localisation:

c-Fos/NeuN CA1

Saline	LPS
0.027401	0.036562
0.025586	0.038164
0.021871	0.023369
0.03305	0.03189
0.041161	0.039124
0.033491	0.049775
0.032793	0.038005
	0.033375

c-Fos/NeuN DG

Saline	LPS
0.025518	0.028898
0.027117	0.036765
0.018372	0.036821
0.023664	0.019644
0.025942	0.056029
0.026741	0.060645
0.025573	0.040836
	0.038635

Unpaired t test	
Table Analyzed	cFOS coloc CA1
Column B	LPS
vs.	vs.
Column A	Saline
Unpaired t test	
P value	0.1506
P value summary	ns
Significantly different (P < 0.05)?	No
One- or two-tailed P value?	Two-tailed
t, df	t=1.528, df=13
How big is the difference?	
Mean of column A	0.03076
Mean of column B	0.03628
Difference between means (B - A) ± SEM	0.005518 ± 0.003612
95% confidence interval	-0.002286 to 0.01332
R squared (eta squared)	0.1522
F test to compare variances	
F, DFn, Dfd	1.385, 7, 6
P value	0.7073
P value summary	ns
Significantly different (P < 0.05)?	No
Data analyzed	
Sample size, column A	7
Sample size, column B	8

Unpaired t test	
Table Analyzed	cFOS coloc DG
Column B	LPS
vs.	vs.
Column A	Saline
Unpaired t test	
P value	0.0120
P value summary	*
Significantly different (P < 0.05)?	Yes
One- or two-tailed P value?	Two-tailed
t, df	t=2.916, df=13
How big is the difference?	
Mean of column A	0.02470
Mean of column B	0.03978
Difference between means (B - A) ± SEM	0.01508 ± 0.005171
95% confidence interval	0.003910 to 0.02625
R squared (eta squared)	0.3955
F test to compare variances	
F, DFn, Dfd	19.70, 7, 6
P value	0.0019
P value summary	**
Significantly different (P < 0.05)?	Yes
Data analyzed	
Sample size, column A	7
Sample size, column B	8

Appendix F: Experiment 6 – Hippocampal neuroinflammation facilitated Pavlovian approach behaviour but did not affect goal-directed control in male mice

Day 1-4 lever press:

Row Labels	Average of Average LP rate	Average of Average LP rate2	Average of Average LP rate3	Average of Average LP rate4	Average of Average LP rate5	Average of Average LP rate6	Average of Average LP rate7	Average of Average LP rate8
LPS	**0.861663869**	**1.306930246**	**3.1**	**6.047342995**	**4.061372461**	**8.692515935**	**10.13090295**	**12.17428458**
784	0.325	0.225	0.7	3.975	4.425	10.37950712	9.75	14.54439502
818	0.475	0.85	2.425	6.05	0.65	4.8	7.25	10.12526911
820	1.3	1.91134912	1.725	1.925	4.15	8.3	12.5	12.175
822	0.175	0.45	0.625	3.5	2.375	5.45	6.3	9.4
824	1.435126582	2.134080512	5.1	7.475	4.475	9.086393089	9.7	13.39252412
828	0.3	0.4	3.275	5.025	4.495548654	9.411646122	10.99391691	11.26643546
836	1.787577117	3.212121212	3.775	7.65	4.325	9.35	10.2	13.69196482
845	1.307271118	1.467487359	5.075	8.15	4.075	8.325	10.44813665	13.42332301
846	0.65	1.112334014	5.2	10.67608696	7.581803491	13.13009709	14.03607299	11.54964971
Sal	**0.709090909**	**0.873502004**	**3.727272727**	**6.052272727**	**3.233675495**	**8.690391409**	**8.330216497**	**11.37315469**
785	0.65	1.075	3.35	7.15	3.375	9.3	8.625	7.85
786	0.35	0.654911839	2.5	3.575	2.125	2.85	4.75	5.1
789	0.775	0.953610206	3.85	6	2.85	9.910913706	7.8	8.175
790	1	0.975	5.5	7.875	4.875	12.8833918	10.16845742	10.94775132
791	0.4	0.55	2.975	5.05	2.4	10.3	8.1	15.12011188
795	0.575	0.8	3.3	4.5	3.1	9.5	9.95	12.225
797	0.65	0.575	1.925	3.25	1.15	5.5	8.175	10.625
798	1.15	1	3.85	6.175	3.05	8.25	8.213924051	17.78007881
838	0.425	1.275	4.525	9.2	6.620430443	9.675	8.9	16.64536882
839	0.95	1.025	4.75	7.875	2.5	9.35	6.05	7.775
844	0.875	0.725	4.475	5.925	3.525	8.075	10.9	12.86139076
(blank)								
(blank)								
Grand Total	**0.777748741**	**1.068544713**	**3.445**	**6.050054348**	**3.606139129**	**8.691347446**	**9.140525401**	**11.73366314**

ANOVA results | Multiple comparisons

2way ANOVA
ANOVA results

1	Table Analyzed	Lever press rates Day1-				
2						
3	**Two-way RM ANOVA**	Matching: Stacked				
4	Assume sphericity?	No				
5	Alpha	0.05				
6						
7	**Source of Variation**	**% of total variation**	**P value**	**P value summary**	**Significant?**	**Geisser-Greenhouse's epsilon**
8	Training days x Treatment	0.5880	0.4842	ns	No	
9	Training days	69.75	<0.0001	****	Yes	0.4178
10	Treatment	0.0005194	0.9807	ns	No	
11	Subject	15.60	0.0001	***	Yes	
12						
13	**ANOVA table**	**SS**	**DF**	**MS**	**F (DFn, DFd)**	**P value**
14	Training days x Treatment	2.990	3	0.9968	F (3, 54) = 0.8281	P=0.4842
15	Training days	354.7	3	118.2	F (1.253, 22.56) = 98.23	P<0.0001
16	Treatment	0.002642	1	0.002642	F (1, 18) = 0.0005995	P=0.9807
17	Subject	79.31	18	4.406	F (18, 54) = 3.660	P=0.0001
18	Residual	65.00	54	1.204		
19						
20	**Difference between column means**					
21	Mean of Saline	2.841				
22	Mean of LPS	2.829				
23	Difference between means	0.01155				
24	SE of difference	0.4717				
25	95% CI of difference	-0.9795 to 1.003				
26						
27	**Data summary**					
28	Number of columns (Treatment)	2				

Day 1-4- Magazine entries

Row Labels	Average of Mag rate	Average of Mag rate2	Average of Mag rate3	Average of Mag rate4	Average of Mag rate5	Average of Mag rate6	Average of Mag rate7	Average of Mag rate8
LPS	**10.47111111**	**7.086666667**	**9.72**	**9.753333333**	**7.12**	**7.795555556**	**6.926666667**	**6.866666667**
784	12.12	12.08	9.32	6.76	5.04	7.4	6.92	7.3
818	9.66	7.12	6.36	9.58	7.66	7.4	7.78	6.78
820	9.1	7.24	16.34	15.42	9.1	11.88	9.46	7.52
822	10.2	4.72	6.06	4.94	5.58	6.58	6.1	6.52
824	8.46	5.6	7.66	9.52	6.96	6.22	5.54	6.3
828	9.4	6.9	7.94	7.06	6.42	5.92	4.6	6.74
836	9.7	6.7	14.88	12.36	7.02	7.96	7.56	6.92
845	8.86	6.56	10.38	9.1	8.38	7.5	6.84	7.74
846	16.74	6.86	8.54	13.04	7.92	9.3	7.54	5.98
Sal	**8.489090909**	**5.681818182**	**8.103636364**	**7.985454545**	**4.965454545**	**6.754545455**	**5.209090909**	**5.894545455**
785	6.98	4.94	8.04	7.6	6.42	9.5	6.62	7.68
786	9.88	6.96	5.22	6.3	3.92	4.92	4.96	4.6
789	6.62	5.04	9.62	10.64	5.14	7.46	4.3	5.82
790	9.24	3.4	6.56	7.58	5.14	6.68	4.32	5.06
791	8.3	7.58	5.64	7.22	4.7	6.32	5.98	7.44
795	10.84	4.48	9.74	8.24	3.62	7	5.08	5.16
797	7	7	7.36	4.9	5.16	6.4	4.36	4.74
798	5.96	4.88	8.6	5.56	5.48	6.66	5.38	6.06
838	10.02	5.92	7.94	8.4	4.64	7.8	4.7	6.58
839	7.88	4.84	5.04	5.54	4.34	4.76	4.88	5.76
844	10.66	7.46	15.38	15.86	6.06	6.8	6.72	5.94
Grand Total	**9.381**	**6.314**	**8.831**	**8.781**	**5.935**	**7.223**	**5.982**	**6.332**

ANOVA results | Multiple comparisons

2way ANOVA
ANOVA results

1	Table Analyzed	Magazine entries Day1-4				
2						
3	**Two-way RM ANOVA**	Matching: Stacked				
4	Assume sphericity?	No				
5	Alpha	0.05				
6						
7	**Source of Variation**	**% of total variation**	**P value**	**P value summary**	**Significant?**	**Geisser-Greenhouse's epsilon**
8	Training days x Treatment	0.1298	0.9811	ns	No	
9	Training days	16.66	0.0021	**	Yes	0.6424
10	Treatment	8.358	0.0532	ns	No	
11	Subject	35.15	0.0030	**	Yes	
12						
13	**ANOVA table**	**SS**	**DF**	**MS**	**F (DFn, DFd)**	**P value**
14	Training days x Treatment	0.8813	3	0.2938	F (3, 54) = 0.05872	P=0.9811
15	Training days	113.1	3	37.70	F (1.927, 34.69) = 7.535	P=0.0021
16	Treatment	56.74	1	56.74	F (1, 18) = 4.280	P=0.0532
17	Subject	238.6	18	13.26	F (18, 54) = 2.650	P=0.0030
18	Residual	270.2	54	5.003		
19						
20	**Difference between column means**					
21	Mean of Saline	7.565				
22	Mean of LPS	9.258				
23	Difference between means	-1.693				
24	SE of difference	0.8182				
25	95% CI of difference	-3.412 to 0.02626				
26						
27	**Data summary**					
28	Number of columns (Treatment)	2				

Day-4 devaluation test:

Row Labels	Average of Mag Entries	Average of Deval Lever	Average of Val Lever
LPS	**5.1**	**3.588888889**	**5.372222222**
784	6	7.85	7
818	6.15	3.15	3.35
820	5.05	1.3	2.6
822	3.25	2.1	3.2
824	4.8	2.65	5.15
828	8.2	2.45	3.15
836	5.45	5.55	6.4
845	3.8	2.55	7.4
846	3.2	4.7	10.1
Sal	**3.772727273**	**4.086363636**	**5.445454545**
785	4.75	4.9	7.45
786	4.15	1.2	6.6
789	1.2	1.45	3.75
790	1.75	6.9	3.45
791	1.6	3.5	4.5
795	2.65	4.85	4.6
797	3.95	4.7	5.05
798	2.1	4.35	6.35
838	4.65	8.6	3.15
839	6.2	2.35	11.15
844	8.5	2.15	3.85
Grand Total	**4.37**	**3.8625**	**5.4125**

ANOVA results | Multiple comparisons

2way ANOVA
ANOVA results

1	Table Analyzed	Day4 devaluation				
2						
3	**Two-way ANOVA**	Ordinary				
4	Alpha	0.05				
5						
6	**Source of Variation**	**% of total variation**	**P value**	**P value summary**	**Significant?**	
7	Interaction	0.2038	0.7750	ns	No	
8	Treatment	0.3688	0.7007	ns	No	
9	outcome value	11.18	0.0398	*	Yes	
10						
11	**ANOVA table**	**SS (Type III)**	**DF**	**MS**	**F (DFn, DFd)**	**P value**
12	Interaction	0.4455	1	0.4455	F (1, 36) = 0.08296	P=0.7750
13	Treatment	0.8061	1	0.8061	F (1, 36) = 0.1501	P=0.7007
14	outcome value	24.44	1	24.44	F (1, 36) = 4.551	P=0.0398
15	Residual	193.3	36	5.370		
16						
17	**Difference between column means**					
18	Predicted (LS) mean of Devalued	3.838				
19	Predicted (LS) mean of Valued	5.409				
20	Difference between predicted means	-1.571				
21	SE of difference	0.7365				
22	95% CI of difference	-3.065 to -0.07756				
23						
24	**Difference between row means**					
25	Predicted (LS) mean of Saline	4.766				
26	Predicted (LS) mean of LPS	4.481				
27	Difference between predicted means	0.2854				
28	SE of difference	0.7365				

Day 4 – magazine entries:

Saline	LPS
4.75	6
4.15	6.15
1.2	5.05
1.75	3.25
1.6	4.8
2.65	8.2
3.95	5.45
2.1	3.8
4.65	3.2
6.2	
8.5	

	Unpaired t test	
1	Table Analyzed	Day4 magazine entries
2		
3	Column B	LPS
4	vs.	vs.
5	Column A	Saline
6		
7	**Unpaired t test**	
8	P value	0.1518
9	P value summary	ns
10	Significantly different (P < 0.05)?	No
11	One- or two-tailed P value?	Two-tailed
12	t, df	t=1.497, df=18
13		
14	**How big is the difference?**	
15	Mean of column A	3.773
16	Mean of column B	5.100
17	Difference between means (B - A) ± SEM	1.327 ± 0.8869
18	95% confidence interval	-0.5361 to 3.191
19	R squared (eta squared)	0.1107
20		
21	**F test to compare variances**	
22	F, DFn, Dfd	1.940, 10, 8
23	P value	0.3594
24	P value summary	ns
25	Significantly different (P < 0.05)?	No
26		
27	**Data analyzed**	
28	Sample size, column A	11
29	Sample size, column B	9

Day 5-8 leverpress training:

ANOVA results | Multiple comparisons

2way ANOVA
ANOVA results

Source of Variation	% of total variation	P value	P value summary	Significant?	Geisser-Greenhouse's epsilon
Training days x Treatment	0.7023	0.4680	ns	No	
Training days	60.02	<0.0001	****	Yes	0.6248
Treatment	1.272	0.3291	ns	No	
Subject	22.76	<0.0001	****	Yes	

ANOVA table	SS	DF	MS	F (DFn, DFd)	P value
Training days x Treatment	8.045	3	2.682	F (3, 54) = 0.8590	P=0.4680
Training days	687.6	3	229.2	F (1.874, 33.74) = 73.41	P<0.0001
Treatment	14.57	1	14.57	F (1, 18) = 1.006	P=0.3291
Subject	260.7	18	14.48	F (18, 54) = 4.639	P<0.0001
Residual	168.6	54	3.122		

Difference between column means	
Mean of Saline	7.907
Mean of LPS	8.765
Difference between means	-0.8579
SE of difference	0.8553
95% CI of difference	-2.655 to 0.9389

Data summary	
Number of columns (Treatment)	2
Number of rows (Training days)	4
Number of subjects (Subject)	20
Number of missing values	0

Day 5-8 magazine entries:

ANOVA results | Multiple comparisons

2way ANOVA
ANOVA results

Source of Variation	% of total variation	P value	P value summary	Significant?	Geisser-Greenhouse's epsilon
Training days x Treatment	2.798	0.0822	ns	No	
Training days	11.60	<0.0001	****	Yes	0.8888
Treatment	25.19	0.0028	**	Yes	
Subject	38.05	<0.0001	****	Yes	

ANOVA table	SS	DF	MS	F (DFn, DFd)	P value
Training days x Treatment	4.761	3	1.587	F (3, 54) = 2.354	P=0.0822
Training days	19.74	3	6.581	F (2.666, 47.99) = 9.763	P<0.0001
Treatment	42.86	1	42.86	F (1, 18) = 11.92	P=0.0028
Subject	64.73	18	3.596	F (18, 54) = 5.335	P<0.0001
Residual	36.40	54	0.6741		

Difference between column means	
Mean of Saline	5.706
Mean of LPS	7.177
Difference between means	-1.471
SE of difference	0.4262
95% CI of difference	-2.367 to -0.5759

Data summary	
Number of columns (Treatment)	2
Number of rows (Training days)	4
Number of subjects (Subject)	20
Number of missing values	0

Row Labels	Average of Mag Entries	Average of Deval Lever	Average of Val Lever
LPS	**4.927777778**	**6.827777778**	**13.7**
784	5.3	9.15	11.45
818	5.8	4.85	16.45
820	3.15	11.1	10.15
822	1.8	4.65	11.45
824	6.95	11.1	12.9
828	5.15	7.4	8
836	4.65	4.8	29.65
845	7.75	4.3	13.2
846	3.8	4.1	10.05
Sal	**3.1**	**6.409090909**	**14.19090909**
785	5.95	4.35	10.65
786	2	2.35	3.6
789	1.05	3.15	21.35

790	3.4	8.65	10.9
791	3.1	3.25	25.05
795	1.6	10.5	8.4
797	3.8	9.75	10.2
798	4.3	3.2	27.2
838	2.9	11.25	7.15
839	3.75	6.95	4.8
844	2.25	7.1	26.8
Grand Total	**3.9225**	**6.5975**	**13.97**

ANOVA results | Multiple comparisons

2way ANOVA
ANOVA results

1	Table Analyzed	Day8 devaluation				
2						
3	**Two-way ANOVA**	Ordinary				
4	Alpha	0.05				
5						
6	**Source of Variation**	**% of total variation**	**P value**	**P value summary**	**Significant?**	
7	Interaction	0.1092	0.8151	ns	No	
8	Treatment	0.0006886	0.9852	ns	No	
9	outcome value	28.35	0.0005	***	Yes	
10						
11	**ANOVA table**	**SS (Type III)**	**DF**	**MS**	**F (DFn, DFd)**	**P value**
12	Interaction	2.048	1	2.048	F (1, 36) = 0.05546	P=0.8151
13	Treatment	0.01291	1	0.01291	F (1, 36) = 0.0003497	P=0.9852
14	outcome value	531.5	1	531.5	F (1, 36) = 14.40	P=0.0005
15	Residual	1329	36	36.92		
16						
17	**Difference between column means**					
18	Predicted (LS) mean of Devalued	6.618				
19	Predicted (LS) mean of Valued	13.95				
20	Difference between predicted means	-7.327				
21	SE of difference	1.931				
22	95% CI of difference	-11.24 to -3.411				
23						
24	**Difference between row means**					
25	Predicted (LS) mean of Saline	10.30				
26	Predicted (LS) mean of LPS	10.26				
27	Difference between predicted means	0.03611				
28	SE of difference	1.931				

Day 8 magazine entries:

Saline	LPS
5.95	5.3
2	5.8
1.05	3.15
3.4	1.8
3.1	6.95
1.6	5.15
3.8	4.65
4.3	7.75
2.9	3.8
3.75	
2.25	

	Unpaired t test	
1	Table Analyzed	Day8 magazine entries
2		
3	Column B	LPS
4	vs.	vs.
5	Column A	Saline
6		
7	**Unpaired t test**	
8	P value	0.0207
9	P value summary	*
10	Significantly different (P < 0.05)?	Yes
11	One- or two-tailed P value?	Two-tailed
12	t, df	t=2.536, df=18
13		
14	**How big is the difference?**	
15	Mean of column A	3.100
16	Mean of column B	4.928
17	Difference between means (B - A) ± SEM	1.828 ± 0.7207
18	95% confidence interval	0.3135 to 3.342
19	R squared (eta squared)	0.2632
20		
21	**F test to compare variances**	
22	F, DFn, Dfd	1.797, 8, 10
23	P value	0.3800
24	P value summary	ns
25	Significantly different (P < 0.05)?	No
26		
27	**Data analyzed**	
28	Sample size, column A	11
29	Sample size, column B	9

Open field test:

Total distance travelled

Saline	LPS
3157.716	2791.465
3689.327	3056.808
2851.001	2173.848
2686.047	2817.779
2387.946	3598.226
3799.749	2925.962
3154.317	3812.468
2146.478	3464.85
2444.799	2206.505
1893.159	
1936.847	

Time spent in centre zone

Saline	LPS
213.6	215.35
272	195.95
200.7	223.05
257	344.85
289.15	227.95
247.45	227.5
239.05	231.25
222.75	328.8
196.65	256.2
188.05	
261.7	

Time spent in corner zone

Saline	LPS
386.4	384.65
328	404.05
399.3	376.95
343	255.15
310.85	372.05
352.55	372.5
360.95	368.75
377.25	271.2
403.35	343.8
411.95	
338.3	

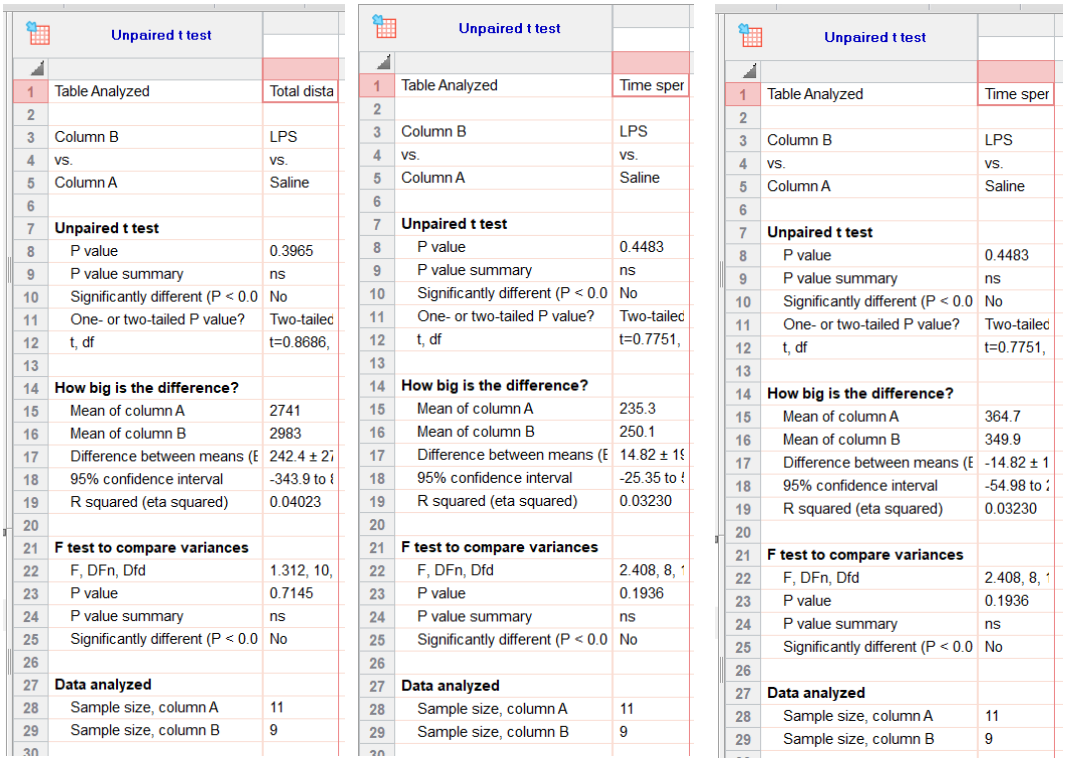

Unpaired t test		
1	Table Analyzed	Total dista
2		
3	Column B	LPS
4	vs.	vs.
5	Column A	Saline
6		
7	**Unpaired t test**	
8	P value	0.3965
9	P value summary	ns
10	Significantly different (P < 0.0	No
11	One- or two-tailed P value?	Two-tailed
12	t, df	t=0.8686,
13		
14	**How big is the difference?**	
15	Mean of column A	2741
16	Mean of column B	2983
17	Difference between means (E	242.4 ± 27
18	95% confidence interval	-343.9 to 8
19	R squared (eta squared)	0.04023
20		
21	**F test to compare variances**	
22	F, DFn, Dfd	1.312, 10,
23	P value	0.7145
24	P value summary	ns
25	Significantly different (P < 0.0	No
26		
27	**Data analyzed**	
28	Sample size, column A	11
29	Sample size, column B	9

Unpaired t test		
1	Table Analyzed	Time sper
2		
3	Column B	LPS
4	vs.	vs.
5	Column A	Saline
6		
7	**Unpaired t test**	
8	P value	0.4483
9	P value summary	ns
10	Significantly different (P < 0.0	No
11	One- or two-tailed P value?	Two-tailed
12	t, df	t=0.7751,
13		
14	**How big is the difference?**	
15	Mean of column A	235.3
16	Mean of column B	250.1
17	Difference between means (E	14.82 ± 19
18	95% confidence interval	-25.35 to 5
19	R squared (eta squared)	0.03230
20		
21	**F test to compare variances**	
22	F, DFn, Dfd	2.408, 8, 1
23	P value	0.1936
24	P value summary	ns
25	Significantly different (P < 0.0	No
26		
27	**Data analyzed**	
28	Sample size, column A	11
29	Sample size, column B	9

Unpaired t test		
1	Table Analyzed	Time sper
2		
3	Column B	LPS
4	vs.	vs.
5	Column A	Saline
6		
7	**Unpaired t test**	
8	P value	0.4483
9	P value summary	ns
10	Significantly different (P < 0.0	No
11	One- or two-tailed P value?	Two-tailed
12	t, df	t=0.7751,
13		
14	**How big is the difference?**	
15	Mean of column A	364.7
16	Mean of column B	349.9
17	Difference between means (E	-14.82 ± 1
18	95% confidence interval	-54.98 to 2
19	R squared (eta squared)	0.03230
20		
21	**F test to compare variances**	
22	F, DFn, Dfd	2.408, 8, 1
23	P value	0.1936
24	P value summary	ns
25	Significantly different (P < 0.0	No
26		
27	**Data analyzed**	
28	Sample size, column A	11
29	Sample size, column B	9

Microglial cell expression:

Microglia cell counts

Saline	LPS
62.875	90.5
45.125	91.125
67	102
47	130.8571
64	99
51.28571	96.25
49.5	99.125
53.83333	101.5
61	108.375
59.125	

Microglia intensity

Saline	LPS
12596.24	17034.66
8930.583	13615.61
10430.02	14468.73
11163	15120.96
10499.04	15073.81
10310.05	10522.01
9390.636	12249.01
12239.41	12812.92
10223.46	12651.04
9691.651	

Unpaired t test	
Table Analyzed	Iba1-coun
Column B	LPS
vs.	vs.
Column A	Saline
Unpaired t test	
P value	<0.0001
P value summary	****
Significantly different (P < 0.0	Yes
One- or two-tailed P value?	Two-tailed
t, df	t=9.984, d
How big is the difference?	
Mean of column A	56.07
Mean of column B	102.1
Difference between means (E	46.01 ± 4.
95% confidence interval	36.29 to 5
R squared (eta squared)	0.8543
F test to compare variances	
F, DFn, Dfd	2.468, 8, 9
P value	0.2003
P value summary	ns
Significantly different (P < 0.0	No
Data analyzed	
Sample size, column A	10
Sample size, column B	9

Unpaired t test	
Table Analyzed	Iba1-inten
Column B	LPS
vs.	vs.
Column A	Saline
Unpaired t test	
P value	0.0004
P value summary	***
Significantly different (P < 0.0	Yes
One- or two-tailed P value?	Two-tailed
t, df	t=4.403, d
How big is the difference?	
Mean of column A	10547
Mean of column B	13728
Difference between means (E	3180 ± 72
95% confidence interval	1656 to 47
R squared (eta squared)	0.5328
F test to compare variances	
F, DFn, Dfd	2.717, 8, 9
P value	0.1580
P value summary	ns
Significantly different (P < 0.0	No
Data analyzed	
Sample size, column A	10
Sample size, column B	9

Day-4 microglia and devaluation correlation:

IBA1 counts	Devaluation ratio
91.125	-0.014478625
102	0.173251266
130.8571429	0.101603234
53.83333333	-0.092529234
61	0.316525517
59.125	0.130274889
101.5	0.241358677
108.375	0.209994252
99	0.26391097
96.25	0.036967693
99.125	0.080602496
90.5	0.074609061
62.875	0.06176002
45.125	0.200819531
67	0.058902281
47	-0.047298326
64	0.111910948
51.28571429	0.131286579
49.5	0.008135582

IBA1 intensity	Devaluation ratio
13615.61	-0.014478625
14468.73	0.173251266
15120.96	0.101603234
12239.41	-0.092529234
10223.46	0.316525517
9691.651	0.130274889
12812.92	0.241358677
12651.04	0.209994252
15073.81	0.26391097
10522.01	0.036967693
12249.01	0.080602496
17034.66	0.074609061
12596.24	0.06176002
8930.583	0.200819531
10430.02	0.058902281
11163	-0.047298326
10499.04	0.111910948
10310.05	0.131286579
9390.636	0.008135582

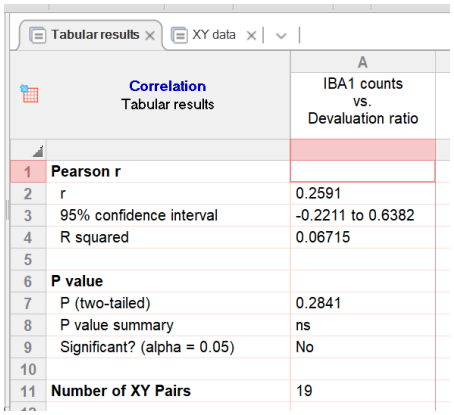

Correlation Tabular results	A IBA1 counts vs. Devaluation ratio
Pearson r	
r	0.2591
95% confidence interval	-0.2211 to 0.6382
R squared	0.06715
P value	
P (two-tailed)	0.2841
P value summary	ns
Significant? (alpha = 0.05)	No
Number of XY Pairs	19

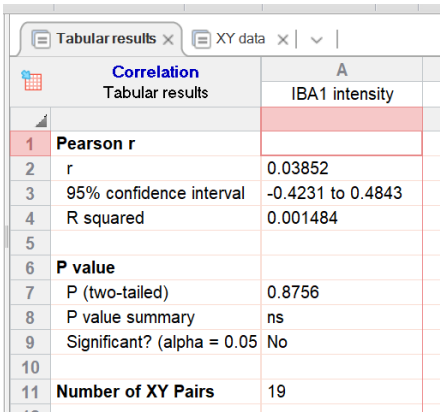

Correlation Tabular results	A IBA1 intensity
Pearson r	
r	0.03852
95% confidence interval	-0.4231 to 0.4843
R squared	0.001484
P value	
P (two-tailed)	0.8756
P value summary	ns
Significant? (alpha = 0.05	No
Number of XY Pairs	19

Day 4 – microglia and magazine entries correlation:

IBA1 counts	Magazine entries
43	71.5
102	57
130.8571429	35
53.83333333	46.5
61	64
59.125	88.5
101.5	41
108.375	35.5
99	50
96.25	86
99.125	59.5
90.5	62
62.875	50.5
45.125	44
67	13
47	24
64	16
51.28571429	33.5
49.5	43

IBA1 intensity	Magazine entries
13615.61	71.5
14468.73	57
15120.96	35
12239.41	46.5
10223.46	64
9691.651	88.5
12812.92	41
12651.04	35.5
15073.81	50
10522.01	86
12249.01	59.5
17034.66	62
12596.24	50.5
8930.583	44
10430.02	13
11163	24
10499.04	16
10310.05	33.5
9390.636	43

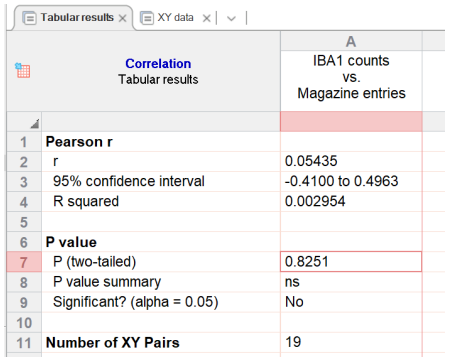

Correlation Tabular results	A IBA1 counts vs. Magazine entries
Pearson r	
r	0.05435
95% confidence interval	-0.4100 to 0.4963
R squared	0.002954
P value	
P (two-tailed)	0.8251
P value summary	ns
Significant? (alpha = 0.05)	No
Number of XY Pairs	19

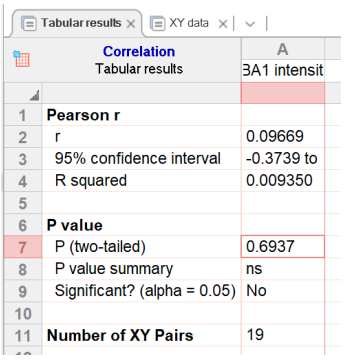

Correlation Tabular results	A 3A1 intensit
Pearson r	
r	0.09669
95% confidence interval	-0.3739 to
R squared	0.009350
P value	
P (two-tailed)	0.6937
P value summary	ns
Significant? (alpha = 0.05)	No
Number of XY Pairs	19

Day 8 – microglia and devaluation correlation:

IBA1 counts	Devaluation ratio

IBA1 intensity	Devaluation ratio

91.125	0.185777521	13615.61	0.185777521
102	-0.005004853	14468.73	-0.005004853
130.8571429	0.104825661	15120.96	0.104825661
53.83333333	-0.003425579	12239.41	-0.003425579
61	0.011355519	10223.46	0.011355519
59.125	0.311403943	9691.651	0.311403943
101.5	0.192894942	12812.92	0.192894942
108.375	0.108748198	12651.04	0.108748198
99	0.108409181	15073.81	0.108409181
96.25	0.021380108	10522.01	0.021380108
99.125	0.331418963	12249.01	0.331418963
90.5	0.09258178	17034.66	0.09258178
62.875	0.154256126	12596.24	0.154256126
45.125	0.03454085	8930.583	0.03454085
67	0.227865157	10430.02	0.227865157
47	0.134799505	11163	0.134799505
64	0.310066527	10499.04	0.310066527
51.28571429	0.024525852	10310.05	0.024525852
49.5	0.104147617	9390.636	0.104147617

Tabular results | XY data

	Correlation Tabular results	A IBA1 counts vs. Devaluation ratio
1	**Pearson r**	
2	r	0.05533
3	95% confidence interval	-0.4092 to 0.4971
4	R squared	0.003062
5		
6	**P value**	
7	P (two-tailed)	0.8220
8	P value summary	ns
9	Significant? (alpha = 0.05)	No
10		
11	**Number of XY Pairs**	19

Tabular results | XY data

	Correlation Tabular results	A IBA1 intensity
1	**Pearson r**	
2	r	-0.1020
3	95% confidence interval	-0.5316 to 0.3693
4	R squared	0.01041
5		
6	**P value**	
7	P (two-tailed)	0.6777
8	P value summary	ns
9	Significant? (alpha = 0.05)	No
10		
11	**Number of XY Pairs**	19

Day 8 – microglia and magazine entries correlation:

IBA1 counts	Magazine entries
41.5	71
102	36.5
130.8571429	19.5
53.83333333	32.5
61	40
59.125	27
101.5	83.5
108.375	41
99	60.5
96.25	56
99.125	50
90.5	58.5
62.875	61.5
45.125	22.5

IBA1 intensity	Magazine entries
13615.61	71
14468.73	36.5
15120.96	19.5
12239.41	32.5
10223.46	40
9691.651	27
12812.92	83.5
12651.04	41
15073.81	60.5
10522.01	56
12249.01	50
17034.66	58.5
12596.24	61.5
8930.583	22.5

67	14	10430.02	14
47	35.5	11163	35.5
64	34	10499.04	34
51.28571429	23	10310.05	23
49.5	41.5	9390.636	41.5

Tabular results | XY data

	Correlation Tabular results	A IBA1 counts vs. Magazine entries
1	**Pearson r**	
2	r	0.1838
3	95% confidence interval	-0.2950 to 0.5889
4	R squared	0.03379
5		
6	**P value**	
7	P (two-tailed)	0.4512
8	P value summary	ns
9	Significant? (alpha = 0.05)	No
10		
11	**Number of XY Pairs**	19

Tabular results | XY data

	Correlation Tabular results	A 3A1 intensit
1	**Pearson r**	
2	r	0.4238
3	95% confidence interval	-0.03760 t
4	R squared	0.1796
5		
6	**P value**	
7	P (two-tailed)	0.0705
8	P value summary	ns
9	Significant? (alpha = 0.05)	No
10		
11	**Number of XY Pairs**	19

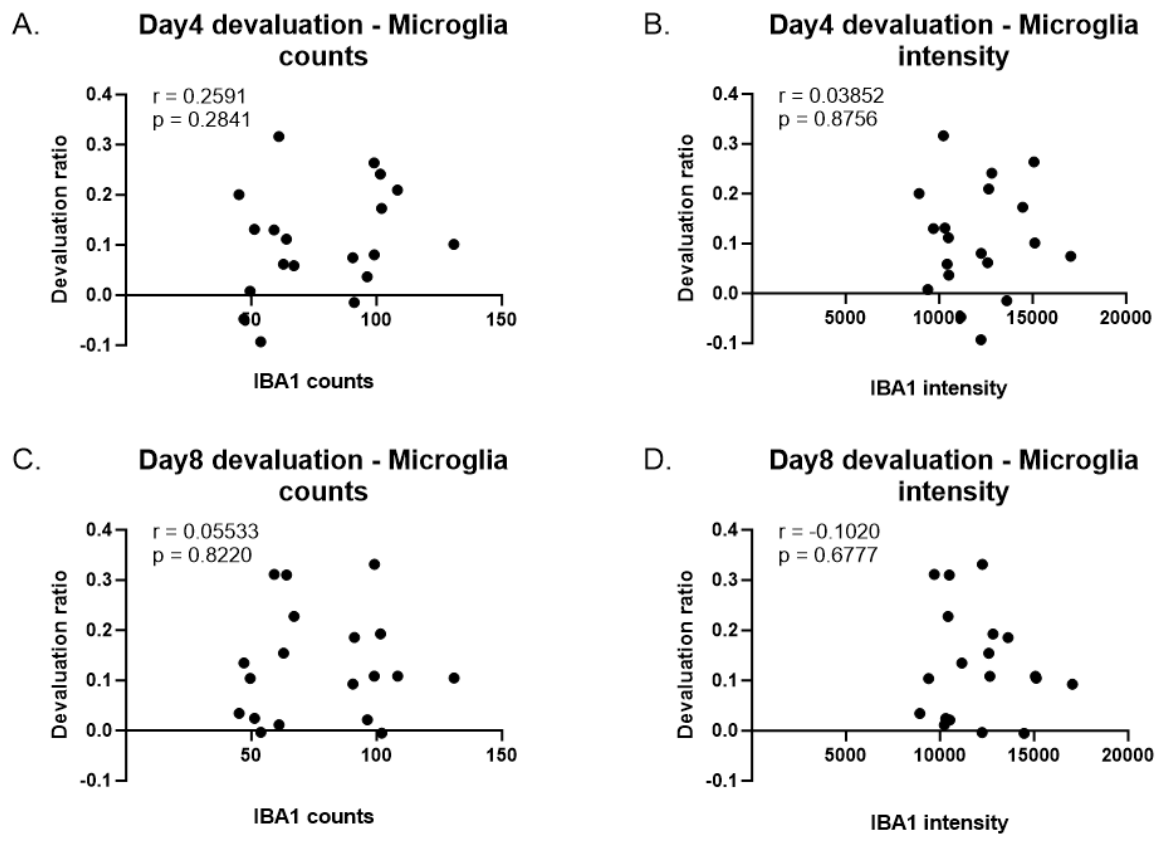

GFAP expression:

Saline	LPS
104	46
101.625	102
115.5	109.25
96.125	119.7143
95.25	88.75

Saline	LPS
26511.84	50147.07
18715.12	44205.16
19114.28	40463.05
15293.88	61095.99
22904.42	47068.13

92.57143	92.375	19384.62	37033.67
65.83333	79.25	21590.78	45691
80.33333	87.75	17212.96	28183.87
86	76.75	20680.02	39420.01
94.625		19241.13	

Unpaired t test

1	Table Analyzed	GFAP-counts
2		
3	Column B	LPS
4	vs.	vs.
5	Column A	Saline
6		
7	**Unpaired t test**	
8	P value	0.6202
9	P value summary	ns
10	Significantly different (P < 0.05)?	No
11	One- or two-tailed P value?	Two-tailed
12	t, df	t=0.5047, df=17
13		
14	**How big is the difference?**	
15	Mean of column A	93.19
16	Mean of column B	89.09
17	Difference between means (B - A) ± SEM	-4.093 ± 8.110
18	95% confidence interval	-21.20 to 13.02
19	R squared (eta squared)	0.01476
20		
21	**F test to compare variances**	
22	F, DFn, Dfd	2.450, 8, 9
23	P value	0.2038
24	P value summary	ns
25	Significantly different (P < 0.05)?	No
26		
27	**Data analyzed**	
28	Sample size, column A	10
29	Sample size, column B	9

Unpaired t test

1	Table Analyzed	GFAP-intensity
2		
3	Column B	LPS
4	vs.	vs.
5	Column A	Saline
6		
7	**Unpaired t test**	
8	P value	<0.0001
9	P value summary	****
10	Significantly different (P < 0.05)	Yes
11	One- or two-tailed P value?	Two-tailed
12	t, df	t=7.690, df=17
13		
14	**How big is the difference?**	
15	Mean of column A	20065
16	Mean of column B	43701
17	Difference between means (B -	23636 ± 3074
18	95% confidence interval	17151 to 30121
19	R squared (eta squared)	0.7767
20		
21	**F test to compare variances**	
22	F, DFn, Dfd	8.703, 8, 9
23	P value	0.0039
24	P value summary	**
25	Significantly different (P < 0.05)	Yes
26		
27	**Data analyzed**	
28	Sample size, column A	10
29	Sample size, column B	9

Day 4 – astrocytes devaluation correlation:

GFAP counts	Devaluation ratio
102	-0.014478625
109.25	0.173251266
119.7142857	0.101603234
80.33333333	-0.092529234
86	0.316525517
94.625	0.130274889
87.75	0.241358677
76.75	0.209994252
88.75	0.26391097
92.375	0.036967693
79.25	0.080602496
46	0.074609061
104	0.06176002
101.625	0.200819531
115.5	0.058902281
96.125	-0.047298326
95.25	0.111910948
92.57142857	0.131286579

GFAP intensity	Devaluation ratio
44205.16	-0.014478625
40463.05	0.173251266
61095.99	0.101603234
17212.96	-0.092529234
20680.02	0.316525517
19241.13	0.130274889
28183.87	0.241358677
39420.01	0.209994252
47068.13	0.26391097
37033.67	0.036967693
45691	0.080602496
50147.07	0.074609061
26511.84	0.06176002
18715.12	0.200819531
19114.28	0.058902281
15293.88	-0.047298326
22904.42	0.111910948
19384.62	0.131286579

65.83333333	0.008135582	21590.78	0.008135582

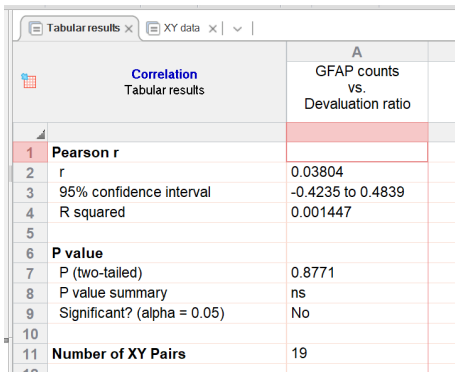

Correlation Tabular results	A GFAP counts vs. Devaluation ratio
Pearson r	
r	0.03804
95% confidence interval	-0.4235 to 0.4839
R squared	0.001447
P value	
P (two-tailed)	0.8771
P value summary	ns
Significant? (alpha = 0.05)	No
Number of XY Pairs	19

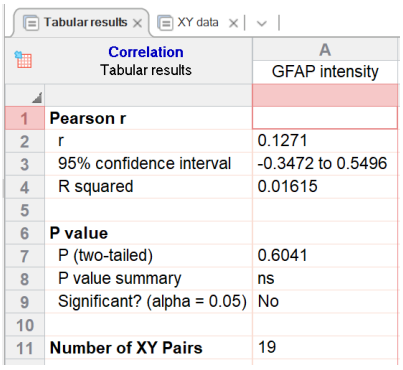

Correlation Tabular results	A GFAP intensity
Pearson r	
r	0.1271
95% confidence interval	-0.3472 to 0.5496
R squared	0.01615
P value	
P (two-tailed)	0.6041
P value summary	ns
Significant? (alpha = 0.05)	No
Number of XY Pairs	19

Day 4 - astrocytes magazine entries correlation:

GFAP counts	Magazine entries
102	71.5
109.25	57
119.7142857	35
80.33333333	46.5
86	64
94.625	88.5
87.75	41
76.75	35.5
88.75	50
92.375	86
79.25	59.5
46	62
104	50.5
101.625	44
115.5	13
96.125	24
95.25	16
92.57142857	33.5
65.83333333	43

GFAP intensity	Magazine entries
44205.16	71.5
40463.05	57
61095.99	35
17212.96	46.5
20680.02	64
19241.13	88.5
28183.87	41
39420.01	35.5
47068.13	50
37033.67	86
45691	59.5
50147.07	62
26511.84	50.5
18715.12	44
19114.28	13
15293.88	24
22904.42	16
19384.62	33.5
21590.78	43

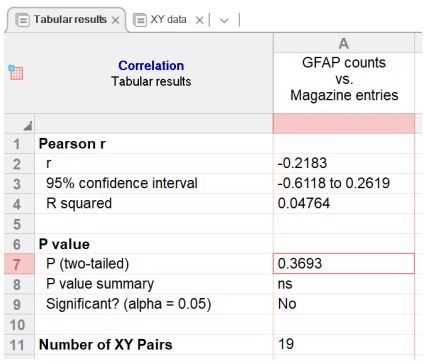

Correlation Tabular results	A GFAP counts vs. Magazine entries
Pearson r	
r	-0.2183
95% confidence interval	-0.6118 to 0.2619
R squared	0.04764
P value	
P (two-tailed)	0.3693
P value summary	ns
Significant? (alpha = 0.05)	No
Number of XY Pairs	19

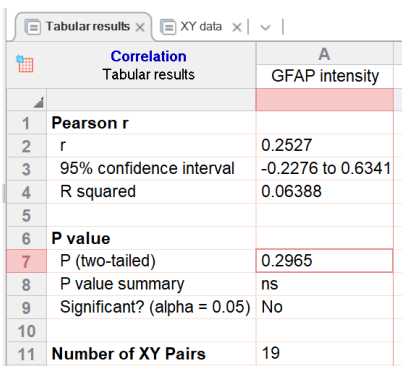

Correlation Tabular results	A GFAP intensity
Pearson r	
r	0.2527
95% confidence interval	-0.2276 to 0.6341
R squared	0.06388
P value	
P (two-tailed)	0.2965
P value summary	ns
Significant? (alpha = 0.05)	No
Number of XY Pairs	19

Day 8 – astrocytes devaluation correlation:

GFAP counts	Devaluation ratio
102	0.185777521
109.25	-0.005004853
119.7142857	0.104825661
80.33333333	-0.003425579
86	0.011355519
94.625	0.311403943
87.75	0.192894942
76.75	0.108748198
88.75	0.108409181
92.375	0.021380108
79.25	0.331418963
46	0.09258178
104	0.154256126
101.625	0.03454085
115.5	0.227865157
96.125	0.134799505
95.25	0.310066527
92.57142857	0.024525852
65.83333333	0.104147617

GFAP intensity	Devaluation ratio
44205.16	0.185777521
40463.05	-0.005004853
61095.99	0.104825661
17212.96	-0.003425579
20680.02	0.011355519
19241.13	0.311403943
28183.87	0.192894942
39420.01	0.108748198
47068.13	0.108409181
37033.67	0.021380108
45691	0.331418963
50147.07	0.09258178
26511.84	0.154256126
18715.12	0.03454085
19114.28	0.227865157
15293.88	0.134799505
22904.42	0.310066527
19384.62	0.024525852
21590.78	0.104147617

Tabular results | XY data

	Correlation Tabular results	A GFAP counts vs. Devaluation ratio
1	**Pearson r**	
2	r	0.07144
3	95% confidence interval	-0.3956 to 0.5091
4	R squared	0.005104
5		
6	**P value**	
7	P (two-tailed)	0.7713
8	P value summary	ns
9	Significant? (alpha = 0.05)	No
10		
11	**Number of XY Pairs**	19

Tabular results | XY data

	Correlation Tabular results	A GFAP intensity
1	**Pearson r**	
2	r	0.01340
3	95% confidence interval	-0.4435 to 0.464
4	R squared	0.0001795
5		
6	**P value**	
7	P (two-tailed)	0.9566
8	P value summary	ns
9	Significant? (alpha = 0.05)	No
10		
11	**Number of XY Pairs**	19

Day 8 – astrocytes magazine entries correlation:

GFAP counts	Magazine entries
102	71
109.25	36.5
119.7142857	19.5
80.33333333	32.5
86	40
94.625	27
87.75	83.5
76.75	41
88.75	60.5

GFAP intensity	Magazine entries
44205.16	71
40463.05	36.5
61095.99	19.5
17212.96	32.5
20680.02	40
19241.13	27
28183.87	83.5
39420.01	41
47068.13	60.5

92.375	56	37033.67	56
79.25	50	45691	50
46	58.5	50147.07	58.5
104	61.5	26511.84	61.5
101.625	22.5	18715.12	22.5
115.5	14	19114.28	14
96.125	35.5	15293.88	35.5
95.25	34	22904.42	34
92.57142857	23	19384.62	23
65.83333333	41.5	21590.78	41.5

Tabular results | XY data

	Correlation Tabular results	A GFAP counts vs. Magazine entries
1	**Pearson r**	
2	r	-0.3568
3	95% confidence interval	-0.6979 to 0.1162
4	R squared	0.1273
5		
6	**P value**	
7	P (two-tailed)	0.1337
8	P value summary	ns
9	Significant? (alpha = 0.05)	No
10		
11	**Number of XY Pairs**	19

Tabular results | XY data

	Correlation Tabular results	A GFAP intensity
1	**Pearson r**	
2	r	0.3337
3	95% confidence interval	-0.1421 to 0.684
4	R squared	0.1113
5		
6	**P value**	
7	P (two-tailed)	0.1627
8	P value summary	ns
9	Significant? (alpha = 0.05)	No
10		
11	**Number of XY Pairs**	19

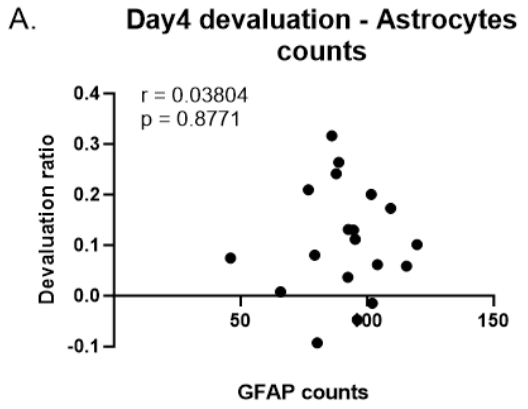

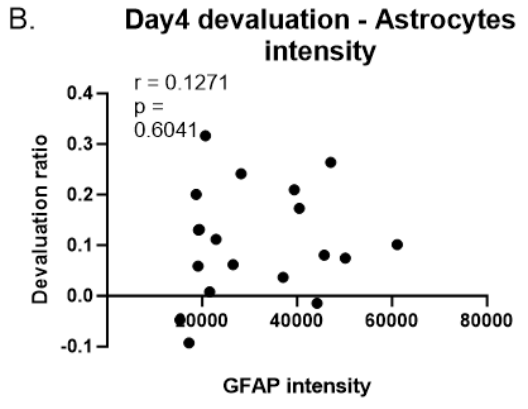

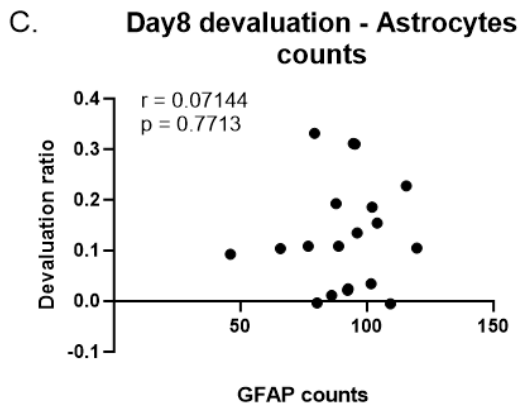

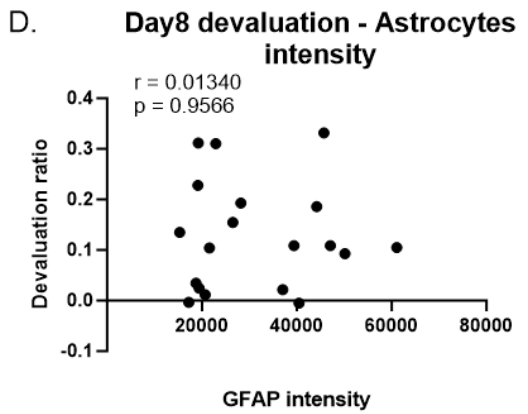

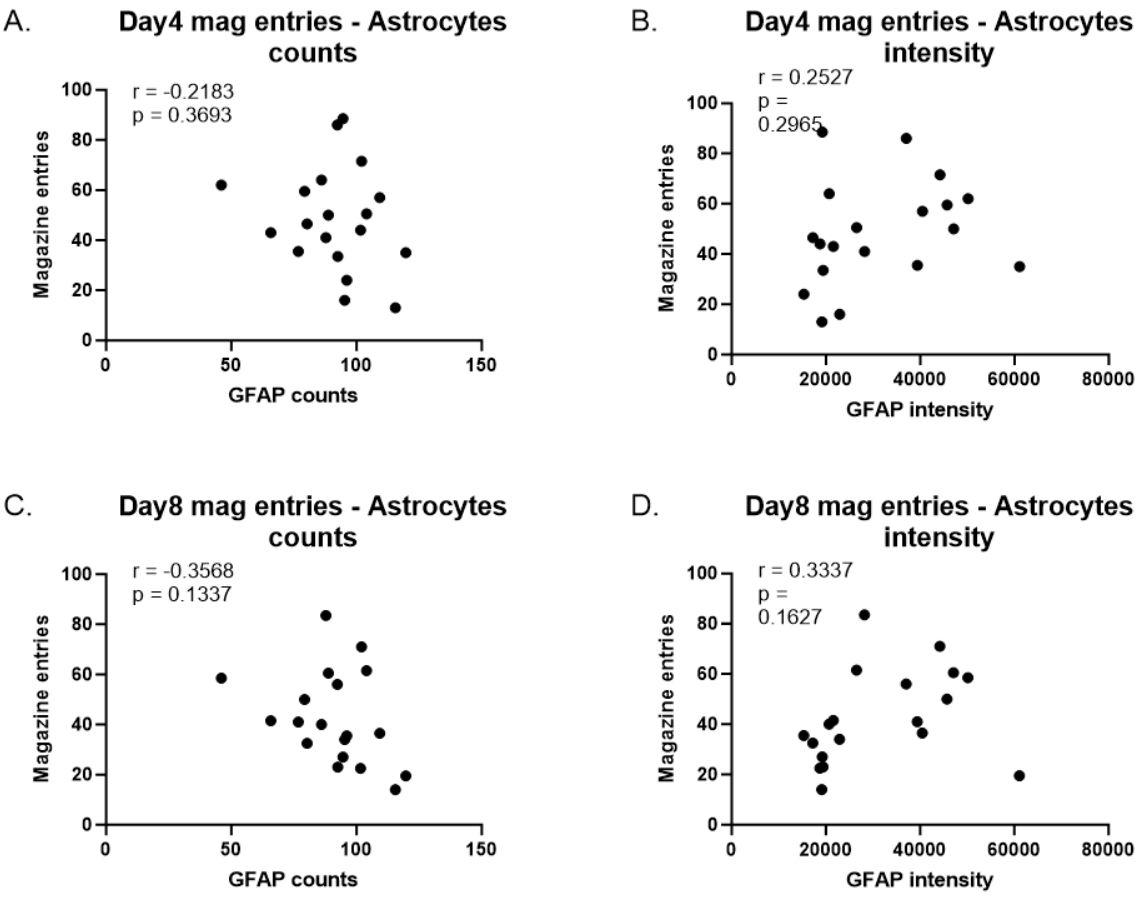

NeuN expression:

CA1

Saline	LPS
24539.59	20073.73
27291.53	23840.18
24114.48	21779.84
23684.38	28525.07
28465.84	23451.44
22954.32	29817.88
30711.73	36888.2
36615.24	27891.18
35734.71	42002.01

DG

Saline	LPS
34543.66	29836.81
46107.61	41852.37
44605.74	34834.04
35510.31	45466.65
46164.93	25803.12
47805.05	49809.79
40672.58	65788.14
57986.32	53116.26
43759.7	63796.75

Mann-Whitney test	
Table Analyzed	NeuN-intensity-CA1
Column B	LPS
vs.	vs.
Column A	Saline
Mann Whitney test	
P value	0.8633
Exact or approximate P value?	Exact
P value summary	ns
Significantly different (P < 0.05)?	No
One- or two-tailed P value?	Two-tailed
Sum of ranks in column A,B	88 , 83
Mann-Whitney U	38
Difference between medians	
Median of column A	27292, n=9
Median of column B	27891, n=9
Difference: Actual	599.7
Difference: Hodges-Lehmann	-574.7

Mann-Whitney test	
Table Analyzed	NeuN-intensity-DG
Column B	LPS
vs.	vs.
Column A	Saline
Mann Whitney test	
P value	0.8633
Exact or approximate P value?	Exact
P value summary	ns
Significantly different (P < 0.05)?	No
One- or two-tailed P value?	Two-tailed
Sum of ranks in column A,B	83 , 88
Mann-Whitney U	38
Difference between medians	
Median of column A	44606, n=9
Median of column B	45467, n=9
Difference: Actual	860.9
Difference: Hodges-Lehmann	1180

c-Fos expression:

		cFOS counts CA1		cFOS intensity CA1		cFOS counts DG		cFOS intensity DG	
Saline	LPS	Saline	LPS	Saline	LPS	Saline	LPS	Saline	LPS
34543.66	29836.81	55.71429	53.25	16763.92	16547.57	46.125	54	16374.35	16246.63
46107.61	41852.37	48.125	40.25	14934.05	14432.57	61.5	71.375	16695.15	15439.18
44605.74	34834.04	73	76.16667	18159.21	16517.77	59.85714	61.28571	17097.07	16775.27
35510.31	45466.65	49.125	44	18866.51	16229.46	85.71429	54.16667	17398.88	16353.96
46164.93	25803.12	51.875	52.33333	21010.5	19895.4	50.25	61.125	21737.11	20470.71
47805.05	49809.79	50.75	75.125	20683.38	19274.61	52	66.25	21260.07	20525.65
40672.58	65788.14	76.5	51.33333	16274.9	19914.63	65.375	69.16667	18441.38	21825.01
57986.32	53116.26	88.83333	43.5	18090.02	17196.87	63.16667	63.125	19159.94	22860.76
43759.7	63796.75	46	84.875	19922.42	21537.41	63.71429	62.14286	16740.23	26070.74

Mann-Whitney test	
Table Analyzed	cFOS-counts-CA1
Column B	LPS
vs.	vs.
Column A	Saline
Mann Whitney test	
P value	0.7304
Exact or approximate P value?	Exact
P value summary	ns
Significantly different (P < 0.05)?	No
One- or two-tailed P value?	Two-tailed
Sum of ranks in column A,B	90 , 81
Mann-Whitney U	36
Difference between medians	
Median of column A	51.88, n=9
Median of column B	52.33, n=9
Difference: Actual	0.4583
Difference: Hodges-Lehmann	-2.464

Mann-Whitney test	
Table Analyzed	cFOS-intensity-CA1
Column B	LPS
vs.	vs.
Column A	Saline
Mann Whitney test	
P value	0.6665
Exact or approximate P value?	Exact
P value summary	ns
Significantly different (P < 0.05)?	No
One- or two-tailed P value?	Two-tailed
Sum of ranks in column A,B	91 , 80
Mann-Whitney U	35
Difference between medians	
Median of column A	18159, n=9
Median of column B	17197, n=9
Difference: Actual	-962.3
Difference: Hodges-Lehmann	-501.5

Mann-Whitney test	
Table Analyzed	cFOS-counts-DG
Column B	LPS
vs.	vs.
Column A	Saline
Mann Whitney test	
P value	0.5457
Exact or approximate P value?	Exact
P value summary	ns
Significantly different (P < 0.05)?	No
One- or two-tailed P value?	Two-tailed
Sum of ranks in column A,B	78 , 93
Mann-Whitney U	33
Difference between medians	
Median of column A	61.50, n=9
Median of column B	62.14, n=9
Difference: Actual	0.6429
Difference: Hodges-Lehmann	2.286

Mann-Whitney test	
Table Analyzed	cFOS-intensity-DG
Column B	LPS
vs.	vs.
Column A	Saline
Mann Whitney test	
P value	0.7962
Exact or approximate P value?	Exact
P value summary	ns
Significantly different (P < 0.05)?	No
One- or two-tailed P value?	Two-tailed
Sum of ranks in column A,B	82 , 89
Mann-Whitney U	37
Difference between medians	
Median of column A	17399, n=9
Median of column B	20471, n=9
Difference: Actual	3072
Difference: Hodges-Lehmann	400.9

A. **cFOS cells CA1**

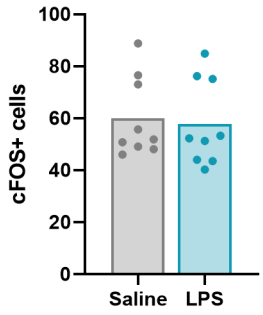

B. **cFOS intensity CA1**

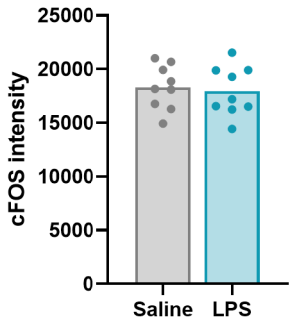

C. **cFOS cells DG**

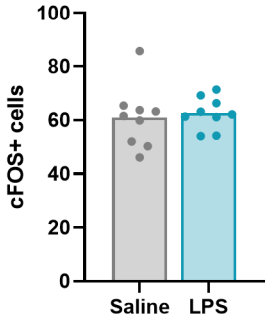

D. **cFOS intensity DG**

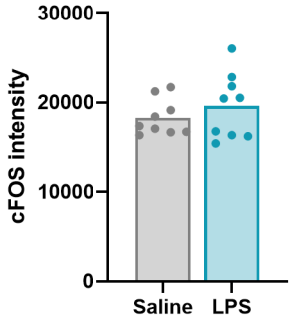

c-Fos/NeuN expression:

Saline	LPS
0.041882	0.041579
0.036163	0.028927

Saline	LPS
0.06196	0.032804
0.036699	0.028273

0.049981	0.046653	0.03179	0.034392
0.052004	0.043531	0.053774	0.035303
0.036717	0.034978	0.053591	0.026411
0.04066	0.042763	0.049306	0.023735
0.034954	0.041258	0.022081	0.028581
0.044472	0.030465	0.041091	0.027536
0.034743	0.031209	0.015583	0.030288

Unpaired t test	
Table Analyzed	CFOS colc
Column B	LPS
vs.	vs.
Column A	Saline
Unpaired t test	
P value	0.2899
P value summary	ns
Significantly different (P < 0.05)	No
One- or two-tailed P value?	Two-tailed
t, df	t=1.095, df
How big is the difference?	
Mean of column A	0.04129
Mean of column B	0.03793
Difference between means (B -	-0.003357
95% confidence interval	-0.009859
R squared (eta squared)	0.06966
F test to compare variances	
F, DFn, Dfd	1.044, 8, 8
P value	0.9533
P value summary	ns
Significantly different (P < 0.05)	No
Data analyzed	
Sample size, column A	9
Sample size, column B	9

Unpaired t test	
Table Analyzed	cFOS coloc DG
Column B	LPS
vs.	vs.
Column A	Saline
Unpaired t test	
P value	0.0571
P value summary	ns
Significantly different (P < 0.05)?	No
One- or two-tailed P value?	Two-tailed
t, df	t=2.050, df=16
How big is the difference?	
Mean of column A	0.04065
Mean of column B	0.02970
Difference between means (B - A) ± SEM	-0.01095 ± 0.005341
95% confidence interval	-0.02227 to 0.0003724
R squared (eta squared)	0.2080
F test to compare variances	
F, DFn, Dfd	16.44, 8, 8
P value	0.0007
P value summary	***
Significantly different (P < 0.05)?	Yes
Data analyzed	
Sample size, column A	9
Sample size, column B	9

Appendix G: DREADDs experiment:

This experiment employed males (34) and females (34) C57BL/6J mice together in the same cohort. Mice received bilateral hippocampal injections of AAVs to cause astrocyte specific DREADDs expression. Specifically:

pAAV-GFAP-hM3D(Gq)-mCherry (AAV5) at a titre of 7 x 10^{12} vg/mL

pAAV-GFAP104-mCherry (AAV5) at a titre of 1 x 10^{13} vg/mL

Behavioural procedures were conducted as described for Experiment 5, except that all mice received either CNO (3mg/Kg) or vehicle 30 minute prior to each training session. CNO/Vehicle was not administered on the test days. CNO was dissolved in Saline+DMSO mixture, therefore Vehicle contained Saline+DMSO to the same concentration. The experimental timeline, (surgery, behavioural procedures and tissue collection) were conducted identically to those described for Experiment 5.

The effect of dorsal hippocampus astrocytic reactivity on goal-directed behaviours:

LPS induced neuroinflammation in the hippocampus caused sex specific effects in C57BL6/J mice. With a view of understanding these effects, we proceeded with selective excitation of glial cells in the hippocampus. One common consequence of invivo and invitro LPS treatment appears to be glutamate excitotoxicity(Bakaeva et al., 2021; Qu et al., 2022). Briefly, glutamate excitotoxicity refers to excessive glutamate release at the synapses, triggered by an external stimulus, which continues to excite the post-synaptic neurons. This uncontrolled excitation of synapses eventually leads to synaptic loss and neuronal death. Astrocytes have been reported to play an important role in synaptic transmission, by forming a tripartite synapse(Chung et al., 2015). Astrocytes express glutamate transporters, which clears excessive glutamate from the synaptic cleft, recycles the glutamate to provide neurons when needed. Continuous activation of astrocytes results in an inability to clear up the excessive glutamate secreted at the synaptic cleft, thus accelerating excitotoxicity(Haroon et al., 2017). This has been witnessed in Alzheimer's disease leading to neuronal degeneration(Nanclares et al., 2021). In our intrahippocampal injection paradigm, we witnessed persistent activation of astrocytes starting 3 days after LPS injections and continuing to persist throughout the experimental span. It is therefore possible that the continuous activation of astrocytes in the brain might impact some changes to the neuronal excitation. Since astrocytes play a key role in synaptic maintenance, and because we noticed continuous activation of astrocytes in the brain, we speculated that the observed effects in both male and female cohorts could have been an effect of continuous activation of astrocytes. For this reason, we chose to excite astrocytes in the brain, with a specific hM3D(Gq)-DREADDs specific for astrocytes.

The experimental timeline mentioned in Figure 36, follows the LPS cohort's timeline, with the LPS being replaced by AAV injections. Animals received either pAAV-GFAP-hM3D(Gq)-mCherry (AAV5) which when activated, excites the astrocytes and a relevant control, pAAV-GFAP104-mCherry (AAV5) expressed in astrocytes. After a week's recovery time, animals were taken for outcome devaluation. Animals received CNO or Vehicle throughout the training days at the concentration of 3mg/kg. The animals were roughly split into three groups, (i) pAAV-GFAP104-mCherry receiving CNO (mCherry-CNO), (ii) pAAV-GFAP-hM3D(Gq)-mCherry receiving Vehicle (DREADDs-VEH) and (iii) pAAV-GFAP-hM3D(Gq)-mCherry receiving CNO (DREADDs-CNO). The following sections detail the effect of astrocytic excitation on goal-directed actions.

Slight differences in the lever press rates and magazines entries amongst all groups on training days 1-4:

Since the animals received CNO and vehicle treatments on the training days, it was mandatory to check for lever press rates and magazine entries made by all groups. Figure 61A shows the lever press rates of all animals during the training days 1-4. There was a significant main effect of training days ($p<0.0001$, $F_{(1.707, 99.01)}=358.7$), indicating

that all animals progressively learned to press levers throughout the 4 days of training. There was a significant main effect of treatment groups (p=0.0219, $F_{(2, 58)}$=4.696) suggesting that there were slight differences in the treatment groups on the level of acquisition of lever press. Additionally, there was a significant interaction between the training days and treatment groups (p=0.0229, $F_{(6, 174)}$=2.524), therefore the main effect of treatment groups received a post-hoc Bonferroni analysis. On training day 2, there was a significant difference between DREADDs-VEH and DREADDs-CNO (p=0.0022), which is evident from the figure that the DREADDs-VEH groups was pressing levers more than the other two groups. Additionally, on training day 4, there was a significant difference between DREADDs-VEH and mCherry-CNO (p=0.0433), on the same day the difference between DREADDs-VEH and DREADDs-CNO was also almost significant (p=0.0686).

Checking for changes in magazine entries, overall, it looked like all animals were making the same level of magazine entries throughout the 4 days of training (Figure 61B). There was a main effect of training days (p<0.0001, $F_{(2.299, 133.3)}$=55.68) showing that there was some differences in the entries made by these animals throughout the training days. Additionally, there was a significant interaction between training days and treatment groups (p=0.0470, $F_{(6, 174)}$=2.181). Therefore the simple effect of training days received a post-hoc Bonferroni analysis. It was seen that on day 2 of training, DREADDs-CNO group was making significantly more entries to the magazine compared to the mCherry-CNO group (p=0.0009) and DREADDs-VEH group (p=0.0075). This was evident from the graph, however, these differences seemed to fade on the last two days of training, indicating that after a initial difference, all animals started making similar entries to the magazine irrespective of the treatment groups. Overall, these results indicate that during lever press training, CNO seemed to decrease lever press rates of the animals, but do not have an effect on magazine entries.

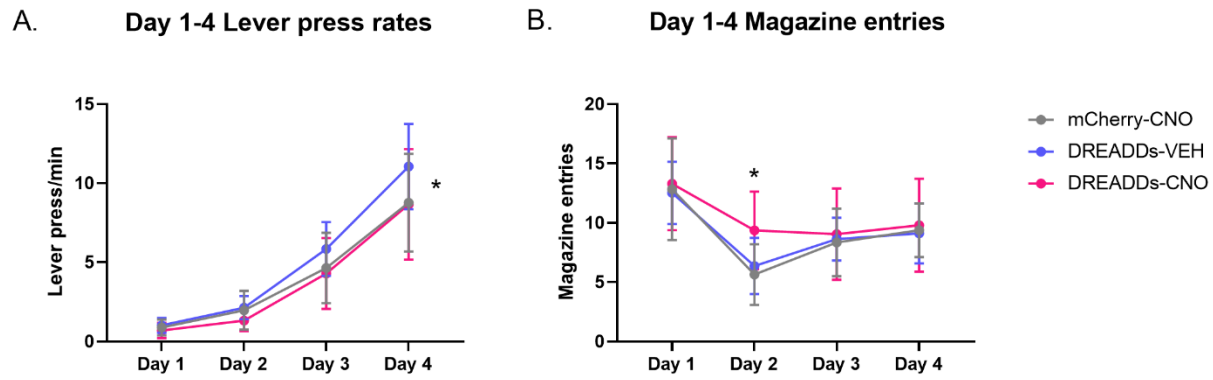

Lever press rates for all animals during training days 1-4 (A). Magazine entries made by mice during training days 1-4 (B) (mCherry-CNO – 23, DREADDs-VEH – 20, DREADDs-CNO - 19; Analysis: Two-way ANOVA) All values represent the Mean±SEM.

Slight differences in the lever press rates and magazines entries amongst all groups on training days 5-8:

Lever press rates were calculated for the next 4 days of training – Days 5-8. The figure 63A showed that there was not much difference amongst the groups in their lever press rates. This was supported by a two-way ANOVA which showing a significant main effect of training days ($p<0.0001$, $F_{(2.153, 124.9)}=18.49$), confirming that all animals progressively learnt to press levers. The treatment factor was almost significant ($p=0.0581$, $F_{(2, 58)}=2.898$), suggesting there might be subtle differences in the lever press rates between different groups. However, there was no significant interaction between the training days and treatment groups ($p=0.2629$, $F_{(6, 174)}=1.293$).

Checking for magazine entries made on the training days 5-8, from the Figure 63B, it can be inferred that all animals were making similar magazine entries throughout the training days. This was supported by a two-way ANOVA showing a significant main effect on training days, ($p<0.0001$, $F_{(2.699, 156.6)}=8.203$) and a significant interaction of training days and treatment groups ($p=0.0424$, $F_{(6, 174)}=2.230$). However, a post-hoc Bonferroni analysis revealed no differences amongst the groups on different training days. Overall, these data suggest that the lever press rates and magazine entries remained the same for all groups, across all the training days.

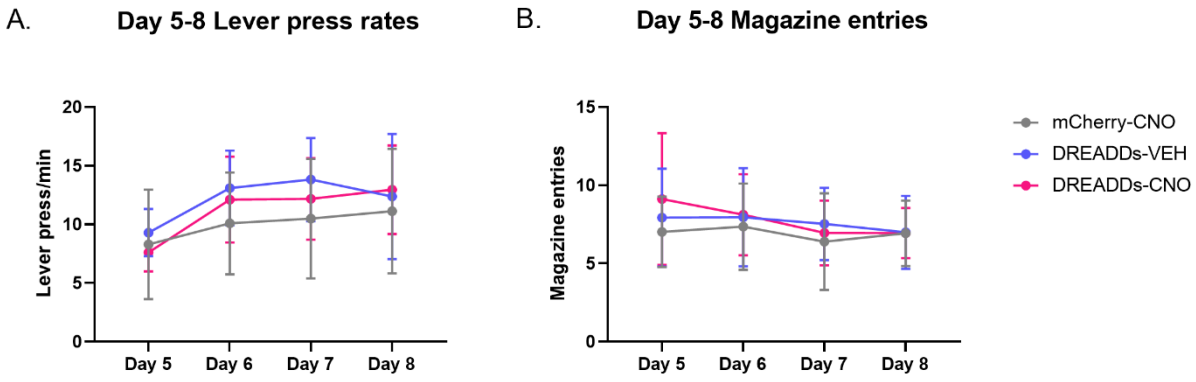

Figure 63: Lever press rates for all animals during training days 5-8 (A). Magazine entries made by mice during training days 5-8 (B) (mCherry-CNO – 23, DREADDs-VEH – 20, DREADDs-CNO - 19; Analysis: Two-way ANOVA) All values represent the Mean±SEM.